2017-11

Investigating the Mechanistic Mode of Action of Novel Cu(II) Complexes as Potential Chemotherapeutics Drugs

Garret Rochford
Technological University Dublin

Recommended Citation

Rochford, G. (2017) *Investigating the mechanistic mode of action of novel Cu(II) complexes as potential chemotherapeutics drugs*. Doctoral thesis, DIT, 2017. doi.org/10.21427/j6jb-dq08

Investigating the mechanistic mode of action of novel Cu(II) complexes as potential chemotherapeutics drugs

Garret Rochford, M.Sc.

Thesis submitted to the Dublin Institute of Technology for the award of Doctor of Philosophy

November 2017

School of Biological Sciences,

Dublin Institute of Technology,

Kevin Street,

Dublin 8

Supervisor: Prof. Orla Howe, DIT

Co-Supervisor: Assoc. Prof. Andrew Kellett, DCU

Advising Supervisor: Prof. Kevin Kavanagh, MU

Abstract

A new class of Cu(II) phenanthroline-phenazine complexes (developed in Dublin City University) have recently been reported to have the highest DNA binding constants of any copper therapeutic complex and at a similar level to Actinomycin. These new complexes show great clinical potential with their high activity against a range of *in-vitro* mammalian cell lines including those with cisplatin resistance however the underlying biological mechanism of their action has yet to be explored in-depth.

The biological data generated in this project has examined the activity of the Cu(II) phenanthroline-phenazine complexes in selected mammalian cells lines *in-vitro* and demonstrated that the Cu(II) complexes are highly active against cisplatin resistant (SKOV-3 and A2780/ Cis) cells. The use of γH2AX a DNA DSB marker demonstrated a high number of foci in cisplatin resistant (SKOV-3) cells compared to the cisplatin sensitive (MCF-7) cells. The strong detection of mitochondrial outer membrane potential (MoMP) decay in resistant (SKOV-3 and A2780/ Cis) cells after exposure to the Cu(II) phenanthroline-phenazine complexes was complemented by the potential disruption of mitochondrial protein homeostasis, with resultant mitochondrial toxicity and apoptosis induction detected by gene expression studies. The work was then complemented by the untargeted whole cell quantitative LFQ proteomics method. Proteomics of both resistant (SKOV-3) and sensitive (MCF-7) cell lines demonstrated increased production of metal sequestration by metallothioneins (Metallothionein-2, -1X) and, heat shock (HSP70) and ribosomal proteins (40S and others) however, metabolic proteins (glycolysis/ gluconeogenesis, fatty acid synthesis and purine metabolism related) tended to dominate the repertoire of the resistant cells. This

evidence suggests the response of the cell to the Cu(II) phenanthroline-phenazine complexes is associated with its energy status.

Parallel *in-vivo* studies using the *G. mellonella* model was carried out with the Cu(II) phenanthroline-phenazine complexes to examine the *in-vivo* biological mechanistic response to the Cu(II) complexes. The Cu(II) complexes presented a superior toxicity profile when compared to cisplatin and through high-resolution LFQ proteomics it was determined that the *in-vivo* response was characterised by metabolic enzymes (glycolysis/ gluconeogenesis and purine metabolism related) and detoxification processes (GST). Both *in-vitro* and *in-vivo* data generated in this project demonstrated that the mitochondria and associated metabolic factors in addition to the DNA interactions inducing apoptosis play a vital role in the mechanism of action of the Cu(II) complexes. However, this is not withstanding the fact that this work also provided clues to other associated mechanisms of action which warrants further investigation. This work demonstrated for the first time the molecular mode of action of this class of novel Cu(II) phenanthroline-phenazine complexes in both *in-vitro* and *in-vivo* biological models. The strong activity of these Cu(II) complexes against cisplatin resistant cells has the potential to offer a novel and alternative therapeutic option to the challenge of cisplatin refractory cancers, which is a high priority in clinical oncology.

Declaration

I certify that this thesis which I now submit for examination for the award of Doctor of Philosophy, is entirely my own work and has not been taken from the work of others, save and to the extent that such work has been cited and acknowledged within the text of my work.

This thesis was prepared according to the regulations for postgraduate study by research of the Dublin Institute of Technology and has not been submitted in whole or in part for another award in any other third level institution.

The work reported on in this thesis conforms to the principles and requirements of the DIT's guidelines for ethics in research.

DIT has permission to keep, lend or copy this thesis in whole or in part, on condition that any such use of the material of the thesis be duly acknowledged.

Signature:  Date: 20/07/2018_____

Acknowledgement

This PhD has been without a doubt the most challenging undertaking of my life, with highs, lows and unforgettable experiences. The broad scope of my project has introduced me to areas of biology and chemistry that will inspire me in my future career. The complexity of this project has been tempered by my fantastic supervisory team, without which I would not have succeeded.

First and foremost I would like to thank my supervisor Prof. Orla Howe for her amazing support and direction she gave me throughout the project. I always got a great boost after our chats especially when I was feeling snowed under and finding it difficult to focus. You always helped me to see the big picture. I would like to thank my co-supervisor Assoc. Prof. Andrew Kellett, who has been a fantastic support throughout both my M.Sc. and Ph.D. projects. I always found our discussion fascinating even if I didn't understand all the chemistry. I would also like to thank my advising supervisor Prof. Kevin Kavanagh for expanding the scope of the project and giving me the opportunity to work in Maynooth University. Your knowledge and experience put me at ease working in a completely new area.

I would like to thank the FOCAS Research Institute, School of Biological Sciences and the Medical Mycology lab, MU for facilitating my project. Sincere thanks to all the staff in FOCAS and the RESC for making life in the lab run so smoothly. Special thanks to Prof. Michael Devereux and Dr. Alan Casey for the interesting discussions, perspectives and support throughout the project. Life as a Ph.D. student would not be the same without the encouragement and camaraderie of the following people. To Dr. Jane Bryant for all her advice and help in the lab. To Dr. Lisa White, Dr. Adrian Maguire,

Dr. Dáire O'Donnell, Damien Traynor, Lucie Causeret, Megan O'Shaughnessy, Aisling Crowley, Neha Chaudhary and others for helping me to maintain my morale and allowing me to relax. You all made me look forward to work every day even when things weren't going well. I would like to thank Dr. Niall Browne, Ronan Maguire, Amie Maher, Gerard Sheehan and Anatte Margalit in the Maynooth Lab for their help and making my time there an enjoyable one. I would also like to thank Dr. Creina Slator and Dr. Zara Molphy in DCU for their help.

I would like to express my deepest gratitude to my parents, Barbara and Donal, my brother, Conor and my granny, Mary for their love and support throughout the project. I would especially like to the thank Catherine for being a bedrock of support from my undergraduate to Ph.D.

Publications

Biological response mechanisms of contrasting mammalian cell lines to novel copper(II) phenanthrene-phenazine complexes: An omics approach (in-preparation)
Garret Rochford, Padraig Doolan, Zara Molphy, Michael Devereux, Kevin Kavanagh, Andrew Kellett and Orla Howe
Contribution: *in-vitro* cytotoxicity, LFQ proteomics, data analysis and primary author of manuscript

Mitochondrial function and signalling is a mechanisms for cellular therapeutic resistance (in-preparation)
Garret Rochford, Zara Molphy, Kevin Kavanagh, Michael Devereux, Andrew Kellett, and Orla Howe
Contribution: *in-vitro* cytotoxicity, gene expression, mitochondrial assay, data analysis and primary author of manuscript

***In-vivo* evaluation of *Galleria mellonella* larvae to novel copper(II) phenanthroline-phenazine complexes.** *J. Inorg. Biochem*. 2018, 186, pp. 135-146.
Garret Rochford, Zara Molphy, Niall Browne, Carla Surlis, Michael Devereux, Malachy McCann, Andrew Kellett, Orla Howe and Kevin Kavanagh
Contribution: mortality assay, haemocyte count, gene expression, proteomics (2D-PAGE and LFQ), all data analysis and primary author of manuscript

Water soluble and photo-stable silver(I) dicarboxylate complexes containing 1,10-phenanthroline ligands: antimicrobial and anticancer chemotherapeutic potential, DNA interactions and antioxidant activity. *J. Inorg. Biochem.* 2016, 159, pp. 120-132. doi: 10.1016/j.jinorgbio.2016.02.024
Laura Thornton, Vidya Dixit, Letícia O. N. Assad, Thales P. Ribeiro, Daniela D. Queiroz, Andrew Kellett, Alan Casey, John Colleran, Marcos D. Pereira, **Garret Rochford**, Malachy McCann, Denis O'Shea, Rita Dempsey, Siobhán McClean, Agnieszka Foltyn-Arfa Kia, Maureen Walsh, Bernie Creaven, Orla Howe, and Michael Devereux
Contribution: double strand DNA break assay (γH2AX) (flow cytometry)

Regulating Bioactivity of Cu^{2+} Bis-1,10-phenanthroline Artificial Metallonucleases with Sterically Functionalized Pendant Carboxylates. *J. Med. Chem.* 2013, 56 (21), pp. 8599-8615. doi: 10.1021/jm401465m.

Andreea Prisecaru, Vickie McKee, Orla Howe, **Garret Rochford**, Malachy McCann, John Colleran, Milan Pour, Niall Barron, Nicholas Gathergood, and Andrew Kellett.

Contribution: *in-vitro* cytotoxicity and double strand DNA break assay (γH2AX) (flow cytometry and confocal microscopy)

Conferences & Presentations

Novel phenanthroline-phenazine copper(II) complexes induce immune priming through genomic and proteomic downstream affects in Galleria mellonella larvae: A mechanistic study, 13th European Biological Inorganic Chemistry Conference (EuroBIC 13), Budapest, Hungary, August 2016 (Oral and poster).

Novel phenanthroline-phenazine copper(II) complexes induce immune priming through genomic and proteomic downstream affects in Galleria mellonella larvae: A mechanistic study, 7th meeting of the Irish Institute of Metal Based Drugs, Dublin Institute of Technology, Ireland, 25th November 2016 (Poster).

Novel phenanthroline-phenazine copper(II) complexes induce immune priming through genomic and proteomic downstream affects in Galleria mellonella larvae: A mechanistic study, 6th Annual Graduate Research Symposium, Dublin Institute of Technology, November 2015 (1st prize for best oral presentation)

γ-H2AX: An effective biomarker of metallo-drug evaluation. 6th meeting of the Irish Institute of Metal-based drugs, RCSI. 1st November 2013 (Oral).

Statement of Ethical Approval

No ethical approval was required to undertake any part of this project

List of Tables:

List of Figures:

significant ($p < 0.05$) difference between highest exposed concentration of the test complexes/ cisplatin and the negative control. N=8.

Fig. 2.4 Immuno-detection of γH2AX recorded through mean fluorescence intensity of MCF-7 cells exposed to Cu-Phen (**1**), Cu-DPQ-Phen (**2**), Cu-DPPZ-Phen (**3**), Cu-DPPN-Phen (**4**) and cisplatin at their respective IC_{25} concentration for both 24 and 48 h. * indicated significant ($p < 0.05$) (N=3) increase in MFI in comparison to the negative control.

Fig. 2.5 Immuno-detection of γH2AX recorded through mean fluorescence intensity of SKOV-3 cells exposed to Cu-Phen (**1**), Cu-DPQ-Phen (**2**), Cu-DPPZ-Phen (**3**), Cu-DPPN-Phen (**4**) and cisplatin at their respective IC_{25} concentration for both 24 and 48 h. * indicated significant ($p < 0.05$) (N=3) increase in MFI in comparison to the negative control.

Fig. 2.6 Immuno-detection of γH2AX recorded through % positive cells. MCF-7 cells exposed to Cu-Phen (**1**), Cu-DPQ-Phen (**2**), Cu-DPPZ-Phen (**3**), Cu-DPPN-Phen (**4**) and cisplatin at their respective IC_{25} concentration for both 24 and 48 h. * indicated significant increase ($p < 0.05$) (N=3) in % positive cells in comparison to the negative control.

Fig 2.7 Immuno-detection of γH2AX recorded through % positive cells. SKOV-3 cells exposed to Cu-Phen (**1**), Cu-DPQ-Phen (**2**), Cu-DPPZ-Phen (**3**), Cu-DPPN-Phen (**4**) and cisplatin at their respective IC_{25} concentration for both 24 and 48 h. * indicated significant increase ($p < 0.05$) (N=3) in % positive cells in comparison to the negative control.

Fig. 2.8 MCF-7 cells exposed to the IC_{25} 24 h concentrations of cisplatin, Cu-Phen (**1**), Cu-DPQ-Phen (**2**), Cu-DPPZ-Phen (**3**) and Cu-DPPN-Phen (**4**) in comparison to the negative control. γH2AX foci determined using primary antibody stain with fluorescent FITC secondary label and propidium iodide used as a nuclear counter stain.

Fig. 2.9 MCF-7 cells exposed to the IC_{25} 48 h concentrations of cisplatin, Cu-Phen (**1**), Cu-DPQ-Phen (**2**), Cu-DPPZ-Phen (**3**) and Cu-DPPN-Phen (**4**) in comparison to the negative control. γH2AX foci determined using primary antibody stain with fluorescent FITC secondary label and propidium iodide used as a nuclear counter stain.

Fig. 2.10 SKOV-3 cells exposed to the IC_{25} 24 h values of cisplatin, Cu-Phen (**1**), Cu-DPQ-Phen (**2**), Cu-DPPZ-Phen (**3**) and Cu-DPPN-Phen (**4**) in comparison to the negative control. γH2AX foci determined using primary antibody stain with fluorescent FITC secondary label and propidium iodide used as a nuclear counter stain.

Fig. 2.11 SKOV-3 cells exposed to the IC_{25} 48 h values of cisplatin, Cu-Phen (**1**), Cu-DPQ-Phen (**2**), Cu-DPPZ-Phen (**3**) and Cu-DPPN-Phen (**4**) in comparison to the negative control. γH2AX foci determined using primary antibody stain with fluorescent FITC secondary label and propidium iodide used as a nuclear counter stain.

Fig. 2.12 Gene expression of HT-29 cells at 24 h following exposure to cisplatin, Cu-Phen (**1**) and Cu-DPQ-Phen (**2**). Error bars represent 95 % Confidence interval (N=3). Relative expression of target genes calculated in relation to the geometric mean of the

third replicates from each condition removed from the analysis due to lack of clustering.

Fig. 3.9 Hierarchical clustering of SSDA proteins and statistically significant proteins with less than a 1.5 fold change in the MCF-7 cell line after 48 h exposure to Cu-Phen (**1**) and Cu-DPQ-Phen (**2**) in relation to the control. Hierarchical clustering generated from mean Log(2) transformed values of LFQ abundance with samples clustered through columns.

Fig. 3.10 GO analysis of biological process in MCF-7 cells exposed to Cu-Phen (**1**) and Cu-DPQ-Phen (**2**) with respect to the negative control after 48 h incubation. Process containing more than 6 proteins was of greater interest for the analysis.

Fig. 3.11 GO analysis of molecular process in MCF-7 cells exposed to Cu-Phen (**1**) and Cu-DPQ-Phen (**2**) with respect to the negative control after 48 h incubation. Process containing more than 6 proteins was of greater interest for the analysis.

Fig. 3.12 KEGG analysis of significantly upregulated protein in purine metabolism. Pyruvate kinase (2.7.1.40) (red).

Fig. 3.13 KEGG analysis of significantly upregulated proteins in glycolysis/ gluconeogenesis. Phosphoglycerate kinase (2.7.2.3) (green) and pyruvate kinase (2.7.1.40) (red).

Fig. 3.14 STRING based protein interaction analysis of statistically significant protein with fold changes ≥ 1.5 in the MCF-7 cell after 48 h exposure to Cu-Phen (**1**) and Cu-DPQ-Phen (**2**) compared to the negative control. The STRING analysis demonstrated that there is not a strong clustering of proteins identified.

Fig. 3.15 Principle component analysis (PCA) of whole cell lysate proteome of SKOV-3 cells exposed to Cu-Phen (**1**) and Cu-DPQ-Phen (**2**) for 24 h in comparison to a negative control. PCA of three replicates for the negative control and three replicates of both test exposures. Enclosures define the different experimental conditions. Red X denotes the third replicates from each condition removed from the analysis due to lack of clustering.

Fig. 3.16 Hierarchical clustering of SSDA proteins and statistically significant proteins with less than a 1.5 fold change in the SKOV-3 cell line after 24 h exposure to Cu-Phen (**1**) and Cu-DPQ-Phen (**2**) in relation to the control. Hierarchical clustering generated from mean Log(2) transformed values of LFQ abundance with samples clustered through columns.

Fig. 3.17 GO analysis of biological process in SKOV-3 cells exposed to Cu-Phen (**1**) and Cu-DPQ-Phen (**2**) with respect to the negative control after 24 h incubation. Process containing more than 2 proteins was of greater interest for the analysis.

Fig. 3.18 GO analysis of molecular process in SKOV-3 cells exposed to Cu-Phen (**1**) and Cu-DPQ-Phen (**2**) with respect to the negative control after 24 h incubation. Process containing more than 2 proteins was of greater interest for the analysis.

Fig. 3.19 KEGG analysis of significantly upregulated proteins in glycolysis/

gluconeogenesis. Phosphoglycerate kinase (2.7.2.3) (green).

Fig. 3.20 STRING based protein interaction analysis of statistically significant protein with fold changes ≥ 1.5 in the SKOV-3 cell after 24 h exposure to Cu-Phen (**1**) and Cu-DPQ-Phen (**2**) compared to the negative control. The STRING analysis demonstrated that there is not a strong clustering of proteins identified.

Fig. 3.21 Principle component analysis (PCA) of whole cell lysate proteome of SKOV-3 cells exposed to Cu-Phen (**1**) and Cu-DPQ-Phen (**2**) for 48 h in comparison to a negative control. PCA of three replicates for the negative control and three replicates of both test exposures. Enclosures define the different experimental conditions. Red X denotes the third replicates from each condition removed from the analysis due to lack of clustering.

Fig. 3.22 Hierarchical clustering of SSDA proteins and statistically significant proteins with less than a 1.5 fold change in the SKOV-3 cell line after 48 h exposure to Cu-Phen (**1**) and Cu-DPQ-Phen (**2**) in relation to the control. Hierarchical clustering generated from mean Log(2) transformed values of LFQ abundance with samples clustered through columns.

Fig. 3.23 GO analysis of biological process in SKOV-3 cells exposed to Cu-Phen (**1**) and Cu-DPQ-Phen (**2**) with respect to the negative control after 48 h incubation. Process containing more than 25 proteins was of greater interest for the analysis.

Fig. 3.24 GO analysis of biological process in SKOV-3 cells exposed to Cu-Phen (**1**) and Cu-DPQ-Phen (**2**) with respect to the negative control after 48 h incubation. Process containing more than 20 proteins was of greater interest for the analysis.

Fig. 3.25 KEGG analysis of significantly upregulated proteins in glycolysis/ gluconeogenesis. Glucose-6-phosphate isomerase (5.3.1.9) (red), 6-phosphofructokinase (2.7.1.11) (orange), fructose-bisphosphate aldolase (4.1.2.13) (yellow), triose-phosphate isomerase (5.3.1.1) (grey), glyceraldehyde-3-phosphate dehydrogenase (1.2.1.12) (pink), glyceraldehyde-3-phosphate dehydrogenase (NAD(P)+) (1.2.1.59) (wine), bisphosphoglycerate mutase (5.4.2.4) (purple), phosphoglycerate kinase (2.7.2.3) (brown) and L-lactate dehydrogenase (1.1.1.27) (blue).

Fig. 3.26 KEGG analysis of significantly upregulated proteins in the pentose phosphate pathway. Glucose-6-phosphate isomerase (5.3.1.9) (orange), 6-phosphofructokinase (2.7.1.11) (brown) and fructose-bisphosphate aldolase (4.1.2.13) (yellow).

Fig. 3.27 KEGG analysis of significantly upregulated proteins in fatty acid biosynthesis pathway. Fatty acid synthase (FASN) (red).

Fig. 3.28 KEGG analysis of significantly upregulated proteins in purine metabolism. Nucleoside diphosphate kinase (2.7.4.6) (red).

Fig. 3.29 STRING based protein interaction analysis of statistically significant protein with fold changes ≥ 1.5 in the SKOV-3 cell after 48 h exposure to Cu-Phen (**1**) and Cu-DPQ-Phen (**2**) compared to the negative control. The dashed red oval highlights proteins that may have regulatory role.

Fig. 3.30 Venn diagram illustrating the number of protein commonly upregulated in each of the cell lines and timepoints with all proteins abundances in each experimental condition of ≥ 1.5 fold change. Proteins related to the 4 major comparisons are displayed in **Table 3.10**.

Fig. 4.1 Detection of changes in % MMP (ΔΨ) decay in A2780 and A2780/ Cis cells at 24 h after exposure to IC_{50} concentration of Cu-Phen (**1**), Cu-DPQ-Phen (**2**), Cu-DPPZ-Phen (**3**), Cu-DPPN-Phen (**4**), doxorubicin and cisplatin with H_2O_2 used as a positive control. All treatments have been normalized to the negative control. Baseline represents the negative control and no loss of mitochondrial membrane potential. Statistical significance set at 0.05 with Bonferroni correction performed on two-way ANOVA. N=8.

Fig. 4.2 Detection of changes in % MMP (ΔΨ) decay in MCF-7 cell at 24 h after exposure to IC_{50} concentration of Cu-Phen (**1**), Cu-DPQ-Phen (**2**), Cu-DPPZ-Phen (**3**), Cu-DPPN-Phen (**4**) and cisplatin with H_2O_2 used as a positive control. All treatments have been normalized to the negative control. Baseline represents the negative control and no loss of mitochondrial membrane potential. Statistical significance set at 0.05 with Bonferroni correction performed on two-way ANOVA. N=7.

Fig. 4.3 Gene expression of A2780 cells at 24 h following exposure to doxorubicin, cisplatin, Cu-Phen (**1**) and Cu-DPQ-Phen (**2**), Cu-DPPZ-Phen (**3**) and Cu-DPPN-Phen (**4**). Error bars represent 95 % Confidence interval (N=4).

Fig. 4.4 Gene expression of A2780/ Cis cells at 24 h following exposure to doxorubicin, cisplatin, Cu-Phen (**1**) and Cu-DPQ-Phen (**2**), Cu-DPPZ-Phen (**3**) and Cu-DPPN-Phen (**4**). Error bars represent 95 % Confidence interval (N=4).

Fig. 4.5 Mitochondrial related gene expression of MCF-7 cells at 48 h following exposure to cisplatin, Cu-Phen (**1**) and Cu-DPQ-Phen (**2**). Error bars represent 95 % Confidence interval (N=3).

Fig. 4.6 Mitochondrial related gene expression of SKOV-3 cells at 48 h following exposure to cisplatin, Cu-Phen (**1**) and Cu-DPQ-Phen (**2**). Error bars represent 95 % Confidence interval (N=3).

Fig. 5.1 Inoculation procedure for *G. mellonella* larvae. Twenty µl was injected into last left pro-leg. Image adapted from Cotter *et al.* (2000).

Fig. 5.2 Living (**A**) (normal colour) and dead (**B**) (melanised) *G. mellonella*. Image adapted from Kavanagh & Fallon (Kavanagh and Fallon 2010).

Fig. 5.3 Characteristic changes (**A-D**) in response to test inoculation.

Fig. 5.4 Piercing point (anterior portion) of the *G. mellonella* larvae for haemocyte extraction indicated by the black arrow.

Fig 5.5 Heatmap representation of **Table 5.4** showing the mean larval mortality (%) after 4, 24, 48 and 72 h inoculations with Cu-Phen (**1**), Cu-DPQ-Phen (**2**) and Cu-

DPPZ-Phen (**3**).

Fig. 5.6 Changes in haemocyte count 24 h post inoculation with Cu-Phen (**1**) and Cu-DPQ-Phen (**2**) and Cu-DPPZ-Phen (**3**). In addition to the Cu(II) phenanthroline-phenanzine complex series the solvent, sham-inoculated and undisturbed controls were used for comparison.

Fig. 5.7 Relative expression of (IMPI) and transferrin after 24 h exposure to LD_{50} value of Cu-Phen (**1**), Cu-DPQ-Phen (**2**) and Cu-DPPZ-Phen (**3**). Gene expression is displayed relative to the undisturbed control with the solvent control used to determine significance ($p < 0.05$) (N=4).

Fig. 5.8 2D PAGE gel of separated haemolymph proteins from *G. mellonella* inoculated, (**a**) reference gel (control), (**b**) Cu-Phen (**1**), (**c**) Cu-DPQ-Phen (**2**) and (**d**) Cu-DPPZ-Phen (**3**). Circled spots excised and identified through LC/ MS and descriptions displayed in **Table 5.7**

Fig. 5.9 Principle component analysis (PCA) of haemolymph proteomic profiles of larvae inoculated with Cu-Phen (**1**), Cu-DPQ-Phen (**2**) and Cu-DPPZ-Phen (**3**) versus the solvent control. PCA of four replicates for the solvent control and three replicates for each of the test exposures. Enclosures define the different experimental conditions.

Fig. 5.10 Hierarchical clustering of haemolymph profiles of larvae inoculated with Cu-Phen (**1**), Cu-DPQ-Phen (**2**) and Cu-DPPZ-Phen (**3**) versus the solvent control. Heat map generated using mean protein expression values of statistically significant differentially abundant proteins. Four replicates for the solvent control and three replicates for each of the test exposures. Samples are clustered through columns.

Fig. 5.11 Volcano plots highlighting proteins altered in abundance in haemolymph of *G. mellonella* larvae following inoculation with Cu-Phen (**1**) (**A**), Cu-DPQ-Phen (**2**) (**B**) and Cu-DPPZ-Phen (**3**) (**C**). Plots represent protein intensity differences ($-\log_2$ mean intensity difference (difference)) and significance in differences (-log P-value) based on a two sided t-test. Points above the curve are considered statistically significant ($p < 0.05$). Points above the line and to the right are present at higher levels of abundance in the test exposure and have a fold change ≥ 1.5. Points above the line and to the left are present at lower levels of abundance in the test exposure and have a fold change ≥ 1.5. Proteins annotated represent an example of differentially expressed proteins following inoculation with the test complex in comparison to the solvent control. Volcano plots are based on post imputated data.

Fig. 5.12 Bar chart showing the different number of proteins present in a test exposure that is associated with selected biological processes **(A)** and molecular functions (**B**). Comparative bar charts represent level 4 ontology.

Fig. 5.13 KEGG analysis of the metabolism of selected xenobiotics by cytochrome P450. Glutathione S-transferase (2.5.1.18) (pink) is shown to be significantly upregulated in all test exposures.

Fig. 5.14 KEGG analysis of significantly upregulated proteins in glycolysis/ gluconeogenesis (highlighted: blue, green, grey, orange and pink) between all test

List of abbreviations:

2D-PAGE	2 Dimensional-Polyacrylamide Gel Electophoresis
ABCC2	ATP-binding cassette sub-family C member 2
ADP	Adenosine diphosphate
AICAR	phosphoribosylaminoimidazolecarboxamide formyltransferase
AMP	Adenosine MonoPhosphate
ARE	Antioxidant Response Element
ATCC	American Type Culture Collection
ATM	Ataxia Telangietasia Mutated
ATOX1	Antioxidant Protein 1
ATP	Adenosine Triphosphate
ATP7A/ B	Adenosine Triphosphate 7A/ B
BAC	Bacterial Artificial Chromosome
BAK	BCL-2 homologous antagonist killer
BCL-2	B-Cell Lymphoma protein 2
BCRP	Breast Cancer Resistance Protein
BER	Base Excision Repair
BIRC5	Baculoviral IAP repeat-containing protein 5
BRD4	BRD4 - Bromodomain-containing protein 4
CART	cytarabine, asparaginase, daunorubicin and thioguanine
CBP	CREB-Binding Protein
cDNA	complementary DNA
ChIP	Chromatin Immunoprecipitation
CHOP	CCAAT/Enhancer-Binding Protein Homologous Protein
cIAP	Inhibitor of Apoptosis
CLPP	ATP-dependent Clp protease proteolytic subunit
COAP	cyclophosphamide, vincristine, cytarabine and prednisolone
COX	Cyclo Oxygenase
Ct	Critical threshold
CTR1	Copper Transporter 1
CypD	Peptidylprolyl isomerase D
Da	Dalton
DDP	diamminedichloridoplatinum(II)
DEPC	Diethylpyrocarbonate
DIABLO	direct IAP binding protein with low pI
DMSO	Dimethyl Sulphoxide
DNA	Deoxyribose Nucleic Acid
DPPN	benzo[i]dipyrido[3,2-a:2′,3′-c]phenazine)
DPPZ	dipyrido[3,2-a:2′,3′-c]phenazine
DPQ	dipyrido[3,2-*f*:2′,3′-h]quinoxaline
DRP1	Dynamin-Related Protein
DSB	Double Stranded Break
dsDNA	double stranded DNA

ECACC	European Collection of Authenticated Cell Cultures
EGFR	Epidermal Growth Factor Receptor
ER	Estrogen Receptor
ERK	Extracellular Signal–Regulated Kinases
ESI	Electro-Spray Ionization
EST	Expressed Sequence Tag
ETC	Eletron Transport Chain
FADH	Flavin adenine dinucleotide
FASN	Fatty Acid Synthase
FDA	Federal Drug Administration
FDR	False Discovery Rate
FITC	Fluorescein Isothiocynate
FL-1	Fluorescent Line-1
FMNH	Flavin mononucleotide
FMS-like	FMS-like tyrosine kinase 3 ligand
GADD45	Growth Arrest and DNA Damage-inducible 45
GCL	Glutamate–cysteine ligase
GDP	Guanine Diphosphate
gH2AX	gamma phosphorylated histone 2AX
GO	Gene Ontology
GST	Glutathione S-transferase
GTP	Guanine Triphosphate
H2DCFDA	2',7'-dichlorodihydrofluorescein diacetate
H4	Histone 4
HAT	Histone Acetyltransferase
HDAC	Histone Deacetylase
HIF-1	Hypoxia Inducible Factor-1
HLA	Human Leukocyte Antigen
HMOX	Heme Oxygenase
HRR	Homologous Recombination
HSP	Heat-Shock Protein
IAA	Iodoacetamide
IC	Inhibitory Concentration
ICP	Inductivly Coupled Plasma
IL-6	Interleukin-6
IMPI	Inhibitor of Metalloprotinase Inhibitor
iTRAQ	isobaric Tag for Relative and Absolute Quantitation
JAK/ STAT3	Janus Kinase/ Signal Transducer and Activator of Transcription 3
JMJD2	JmjC-containing protein
JNK	c-Jun N-terminal kinases
KEGG	Kyoto Encyclopedia of Genes and Genomes
LD	Lethal Dose

LFQ	Label-Free Quantitative
LON1	Lon protease homolog 1
LRP	Lung Resistance Protein
LTQ	Linear Trap Quadrupole
MALDI	Matrix-Assisted Laser Desorption Ionization
MAPK	Mitogen Activated Protein Kinase
Mdm2	Mouse double minute 2 homolog
MFI	Mean Fluorescent Intensity
MFN(1)	Mitofusin-1
miRNA	micro-RNA
MLH1	DNA Mismatch Repair protein MIh1
MMP	Mitochodnrial Membrane Potential
MMR	Miss Match Repair
mRNA	messenger RNA
MRP2	Multi-Drug Resistance 2
MS	Mass Spectrometry
MSH2	MutS protein homolog 2
MutS	Mismatch Repair
NAD	Nicotinamide Ninucleotide
NADP(H)	Nicotinamide adenine dinucleotide phosphate
NaN	Number not Assigned
NCI	National Cancer Institute
NER	Nucleotide Excision Response
NF-kB	Nuclear Factor-kappa B
NHEJ	Non-Homologous End Joining
NIH	National Institute of Health
NKX3.1	High Purity NK3 Homeobox 1
NQO1	NAD(P)H dehydrogenase (quinone 1)
Nrf-2	Nuclear factor (erythroid-derived 2)-like 2
Keap1	Kelch-like ECH-associated protein 1
OPA1	Dynamin-like 120 kDa protein
p300	protein 300
PARP	Poly ADP-Ribose Polymerase
PBS	Phosphate Buffered Saline
PCA	Principle Component Analysis
PEP	Posterior Error Probability
PKC	Protein Kinase C
PKK	Protein Kinase C-associated kinase
POLH	DNA Ploymerase eta
POMP	Purinethol, Oncovin, methotrexate, and prednisone
PTM	Post-Translation Modification
RNS	Reactive Nitrogen Species
ROOH	Hydroperoxy

ROOR	Organic Peroxide
ROS	Reactive Oxygen Species
RPMI-1640	Roswell Park Memorial Institute-1640
RT	Room Temperature
RT-qPCR	Reverse Transcriptase-quantitative Polymerase Chain Reaction
SAICAR	phosphoribosylaminoimidazolesuccinocarboxamide synthase
SAPK	Stress-Activated Protein Kinase
SILAC	Stable Isotope Labelling with amino acids in cell culture
SMAC	Second Mitochondria-derived Activator of Caspases
SMC1	Structural maintenance of chromosomes protein 1
SOD	Superoxide Dismutase
SPG7	paraplegin matrix AAA peptidase subunit
SSDA	Statistical Significant Differentially Abundant
SWI/SNF	SWItch/Sucrose Non-Fermentable
TEMED	Tetramethylethylenediamine
TFAM	Transcription Factor A
TFB(1)M	Transcription factor B1, mitochondrial
TIFF	Tagged Image File Format
TLS	Translesion synthesis
TMT	Tandem Mass Tag
TNFR	Tumour Necrosis Factor Receptor
TP53	Tumour Protein 53
VDAC	Voltage Dependent Anion Channel
XAF1	XIAP-associated factor 1
XIAP	X-linked inhibitor of apoptosis protein
YME1L1	ATP-dependent metalloprotease YME1L1

Table of contents:

Chapter 1: General Introduction

1.1 The Pharmaceutical Industry

Pharmacology is the branch of medicinal chemistry with biology studying the users, effects and modes of actions of drugs (synthetic, natural or endogenous) on the body. Many of the disciplines can be described through the region of the body they target such as: neuropharmacology, psychopharmacology and cardiovascular pharmacology among others, with the other major disciplines concerning the use of molecular and epidemiological analysis on the targeting and development of drugs (Rang and Hill 2013). The development of pharmaceuticals can trace its origins back to 1550 BC with the earliest known compendium of medical conditions and herbal derived remedies (Wreszinski 1937; Rang and Hill 2013). These earliest records of the use of remedies and medicines developed into a more formalised structure in the 19th and 20th century where the modern pharmaceutical industry was born. The pharmaceutical industry today is one of the largest and most powerful industries in the world with revenues from sales in 2015 exceeding 1 trillion dollars and projected sales to reach 1.6 trillion dollars by 2020 (Arlington 2017). Ireland has a well-established pharmaceutical industry with over 75 companies and annual sales exceeding 39 billion euros producing an accumulated total of 40 FDA approved drugs to date (Fanning 2017). While many aspects of the study of pharmacology overlap, the development of pharmaceuticals can be broadly divided into pharmaceuticals and biopharmaceuticals. The development of biopharmaceuticals occurred after the identification of antibody structure and the establishment of hybridoma technology. The use of antibodies in therapy is referred to as immunotherapy and is implemented by identifying disease targets that when bound by the therapeutic antibody, have either an agonist or antagonist function, thereby ameliorating the disease (Breedveld 2000). Biopharmaceuticals also descripbes a large array of biological products produced from recombinant DNA technologies such as

blood clotting factors, hormones, interferon and interleukin based products. Traditional pharmaceuticals are often described as “small molecules”, typically 900 Daltons in size which readily diffuse across the cell membrane to reach intracellular sites in the cell (Ganellin *et al.* 2013). Small molecules are developed through organic and inorganic synthetic medicinal chemistry and are targeted towards different cellular processes and biological molecules such as DNA or proteins in specific cellular and metabolic pathways.

1.1.1 Pharmaceutical drug design process

The pharmaceutical drug development and approval process can take between 12-15 years and encompasses different stages, many of which overlap (FDA 2015). Broadly, the process can be described under three phases: discovery, development and commercialization (**Fig. 1.1**). The discovery phase usually describes the therapeutic concept, target selection, target validation, lead compound identification and optimization. The developmental phase usually includes preclinical development, clinical development and regulatory approval. The final commercialization phase often overlaps with the development phase, sharing clinical development, regulatory approval and finally product production (Hait 2010). The first development stage of drugs is often associated with the Research and Development divisions of pharmaceutical companies and as medicinal chemistry research projects in 3rd level academic Institutions. In the developmental stage the production of a small molecule drug is subjected to multiple iterations in design and may produce tens of thousands of compounds for initial screening to identify a small number of select candidates with the most potent therapeutic effect. The selected lead compounds then progress on to the clinical trial phase which can also take up to 7 years. These 2 phases can be laborious

and time consuming with only the possibility of one FDA approved drug at the end of the process (FDA 2015). **Figure 1.1** illustrates the drug develop and approval process over time to lead to an FDA-approved medicine.

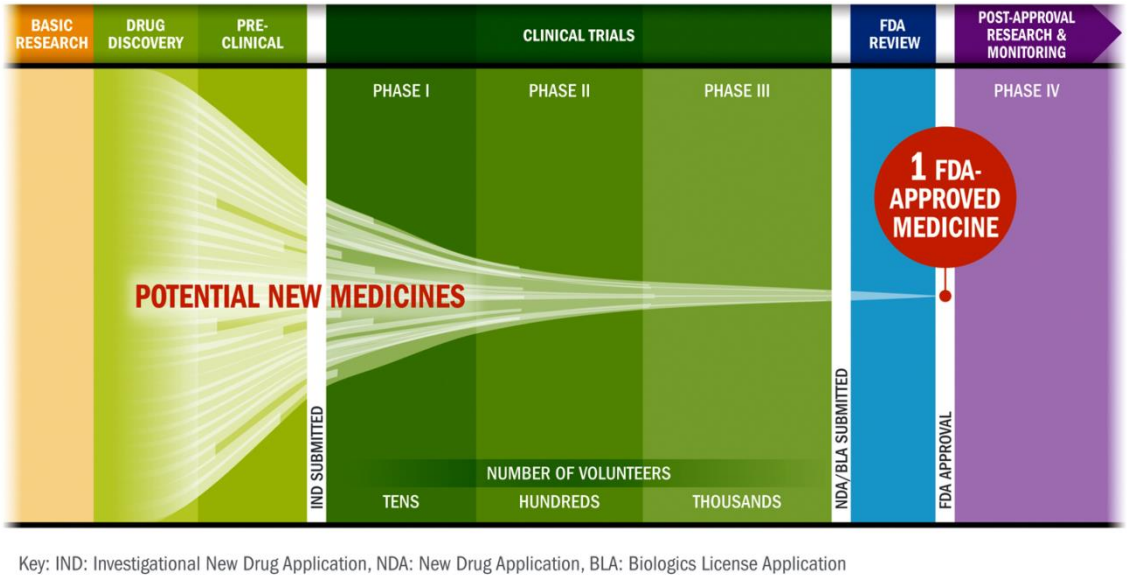

Fig. 1.1 Drug development and approval process. Image adapted from FDA, (2015).

The mechanism of evaluating the functional and therapeutic characteristics of lead compounds involves both *in-vitro* and *in-vivo* assessments. *In-vitro* models are the primary driver of research in cellular biology and were first identified by Gey and Colleagues (Scherer *et al.* 1953). Subsequent efforts were placed in the development of synthetic culture media and growth factors which preserved the differentiated cellular phenotype (Levintow and Eagle, 1961). There are now several tissue and cell culture repositories maintained around the world (Geraghty *et al.* 2014). The most prominent for Ireland is the European funded ECACC for Public Health England, established in 1985 and over 40,000 accessible cell lines, representing 45 different species, 50 tissue types, 300 HLA types, 450 monoclonal antibodies and at least 800 genetic disorders (ECACC 2017). Additionally, the American Tissue Culture Collection (ATCC) is also available with a range of cell lines (ATCC 2017).

The vast collections of cell lines representing different tissue phenotypes has provided the essential platform to understand cellular systems and their response to novel drugs under development. Therefore the screening process of drug development relies heavily on *in-vitro* mammalian cell culturing. The *in-vivo* models are subsequently utilised after *in-vitro* mammalian cell lines have identified and characterised the candidate drug along with an established *in-vitro* efficacy. *In-vitro* mammalian cell line models have limitations such as: the testing of only a single cell type in an experiment, monolayer growth in comparison to 3 dimensional growth patterns, the use of artificial cell culture media to maintain cell growth and the loss of certain interactions between different cell types which effects cell growth. The *in-vivo* testing can utilise multiple species such as mice, rat, dog, chicken and monkeys all of which can be used along with different models of the human tumour process in anticancer pharmaceutical development. The combination of circulatory, immune, detoxification, excretion, musculo-skeletal and nervous systems provides the most comprehensive assessment of both the ability of the organism to tolerate and the efficacy of the developmental therapeutic. While some *in-vivo* animal models can emulate certain human tumours, genetic engineering methods such as GEM, tumour xenograft and PDX can also be used to emulate human tumours for the purposes of novel pharmaceutical evaluations (Liu *et al.* 2017). The use of invertebrate models such as *Drosophila melanogaster* and *Caenorhabditis elegans* has been central to the study of developmental biology and genetics (Wilson-Sanders 2011). Other models such as *Galleria mellonella* has also proved to be a valuable normal tissue invertebrate model for evaluating potential utility and targets of therapeutic agents (Cotter *et al.* 2000; Kavanagh and Reeves 2004; Renwick and Kavanagh 2007; Rowan *et al.* 2009; Kavanagh and Fallon 2010; Browne and Kavanagh 2013; Browne *et al.* 2014) and the development of models for neurological conditions (Thompson and

Marsh 2003; Neri 2011). Both the *in-vitro* and *in-vivo* stages in the discovery phase provide the critical pre-clinical data which is required to advance the candidate drug onto the clinical phase where human testing can begin.

1.1.2 Development of chemotherapeutic drugs

Chemotherapeutic drugs have been used for decades to treat a range of malignancies along with their more recent use in non-cancerous complex diseases. The designs have ranged from synthetic chemicals, natural product extracts to humanised monoclonal antibody therapies designed through recombinant DNA technologies. Chemotherapy was originally coined by Paul Ehrlich in the early 1900s, and is broadly defined as compounds that kill fast growing malignant and neoplastic cells. Chemotherapy originates in the use of nitrogen mustard to treat patients for non-Hodgkin's lymphoma in 1942 (Krumbhaar and Krumbhaar 1919; Gilman 1946). The nitrogen mustard predecessor, sulphur mustard (mustard gas), was originally utilised as a chemical warfare agent in World War I effecting troops with disabling skin blisters and subsequently had a high degree of carcinogenicity. Nitrogen mustard was later found to result in temporary regression of lymphoid tumours. The optimism generated by the discovery of the therapeutic properties of nitrogen mustards Methyl-Bis(Beta-Chloroethyl)amine Hydrochloride and Tris(Beta-Chloroethyl)amine Hydrochloride in 1946 (Goodman *et al.* 1945) led to the development of cyclophosphamide, another DNA alkylating agent (Gross and Wulf 1959). The increasing nutritional research from 1937 onwards had shown that deficiencies in folic acid produced the same regressive effect in bone marrow as had been demonstrated in lymphoid tissue with nitrogen mustard, precipitating the synthesis of antifolate drugs such as aminopterin and methotrexate in 1948 (Farber *et al.* 1948).

The founding of the National Cancer Institute (NCI) in 1937 permitted the eventual formulation of a systematic drug screening programme commencing after the identification of the thiopurine drugs, such as 5-Fluorouracil (Heidelberger *et al.* 1957), which inhibit adenine metabolism and are still widely used today. In the 1960s, the Food and Drug Administration (FDA) approved the use of alkylating agents, antifolates, fluoridated pyrimadines and vinca alkaloids in combination to treat a variety of solid and haematological tumours. The earliest reported combination regimens was POMP (6-mercaptopurine, vincristin, methotrexate and prednisone) (Rodriguez *et al.* 1973) for treating acute adult leukemia and this was followed by several others, such as COAP (cyclophosphamide, vincristine, cytarabine and prednisolone) and CART (cytarabine, asparaginase, daunorubicin and thioguanine) providing higher success rates in acute lymphocytic leukemia and solid tumours (Spiers *et al.* 1975). In 1965, cisplatin a platinum based drug was discovered serendipitously to inhibit cell division in *E.coli* and was later found to erradicate transplanted sarcomas in mice (Rosenberg *et al.* 1965). This was superior to mustard gas because treated cells could recover, meaning that the DNA targeting effects of mustard gas were more severe to cells. However, the FDA did not approve its use for treatment of metastatic testicular and ovarian cancer until 1978 with further platinum analogues such as carboplatin, nedaplatin (Japan) and oxaliplatin approved for use in 1986, 1995 and 1996, respectively (Monneret 2011). Cisplatin was later found to have a broad range of activity across multiple solid tumours, cementing its position as one of the most indispensable chemotherapeutic agents today. Since the 1980s a rapid increase in the use of molecular biology with advanced cell culture systems has allowed indentifications and characterisation of novel therapeutic agents resulting in faster discoveries of novel chemotherapeutic drugs. In 1989, the NCI

introduced the Developmental Therapeutics Programme; a 60-cell line panel, to identify novel drug mechanisms of action by using the known biological mechanisms from key cell line phenotypes, thereby accelerating their development (Shoemaker 2006). The introduction of the DTP NCI programme also assisted in the maturation of hybridoma technology which culminated in the development of the first monoclonal antibody therapy (Imatinib), and the subsequent hugely expanded range of other monoclonal therapies targeting multiple tumour types. The completion of the human genome project in 2003 (Human Genome Sequencing Consortium 2004) along with improvements in protein isolation, modifications and profiling has led to specific targeting of synthetic small molecules with modifications designed to specific molecules of known cell signalling pathways, particularly related to cell growth and development. This capability to target specific signal transduction events in the cell has permitted a refinement of drug activity and a reduction in adverse effects and toxicity to healthy cells, improving patient outcomes (Sever and Brugge 2015).

Throughout the development of chemotherapies, DNA has remained one of the most sought after pharmaceutical sites to target. The initial development of alkylating agents such as cyclophosphamide and nitrogen mustard was complemented with folic acid and adenine metabolism inhibitors, all of which affect DNA replication. The discovery of cisplatin was shown to bind DNA specifically at guanine and purine nucleobases leading to DNA strand crosslinking, oxidative lesions and subsequently, damage. DNA is widely considered to be the main target of therapeutic action of cisplatin although recently, additional non-DNA mechanisms have also been proposed (St Germain *et al.* 2010; Florea and Büsselberg 2011; Koch *et al.* 2013; Shaloam and Tchounwou 2014). What is clear is that cisplatin led to significant improvements in survival rates from

many solid tumours and has resulted in one of the few curative treatments for germline cancers (i.e. testicular) and opened up a new area in the development of medicinal inorganic therapeutics.

1.2 Cisplatin and platinum derivatives

1.2.1 Cisplatin discovery

The platinum based compound, cisplatin was first described by Michele Peyrone in 1844 (Peyrone 1844) (**Fig. 1.2**), however its pharmacological properties would remain unknown until Barnett Rosenberg's serendipitous discovery.

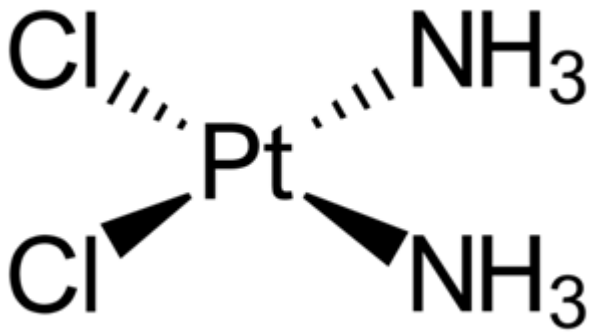

Fig. 1.2 Molecular structure of cisplatin.

During the 1960s, Rosenberg began a series of experiments examining the effect of electrical currents on *Escherichia coli* and discovered throughout the experiments, that cell division was being inhibited and an escalation in filamentous growth was occurring (**Fig. 1.3**) (Rosenberg *et al.* 1967).

The causative agent of the bacterial cell division inhibition and filamentous growth was determined to be $(NH_4)_2PtCl_6$ under electrolysis conditions. Additionally Loretta Van Camp demonstrated that stock preparations of $(NH_4)_2PtCl_6$ underwent photochemical change and became enhanced in bacterial medium. Both *cis*-$[Pt(NH_3)_2Cl_4]$ and *cis*-$[Pt(NH_3)_2Cl_2]$ inhibited cell division *in-vitro* and were subsequently tested *in-vivo* for antitumor activity, with *cis*-$[Pt(NH_3)_2Cl_2]$ demonstrating superior activity (Rosenberg *et al.* 1967).

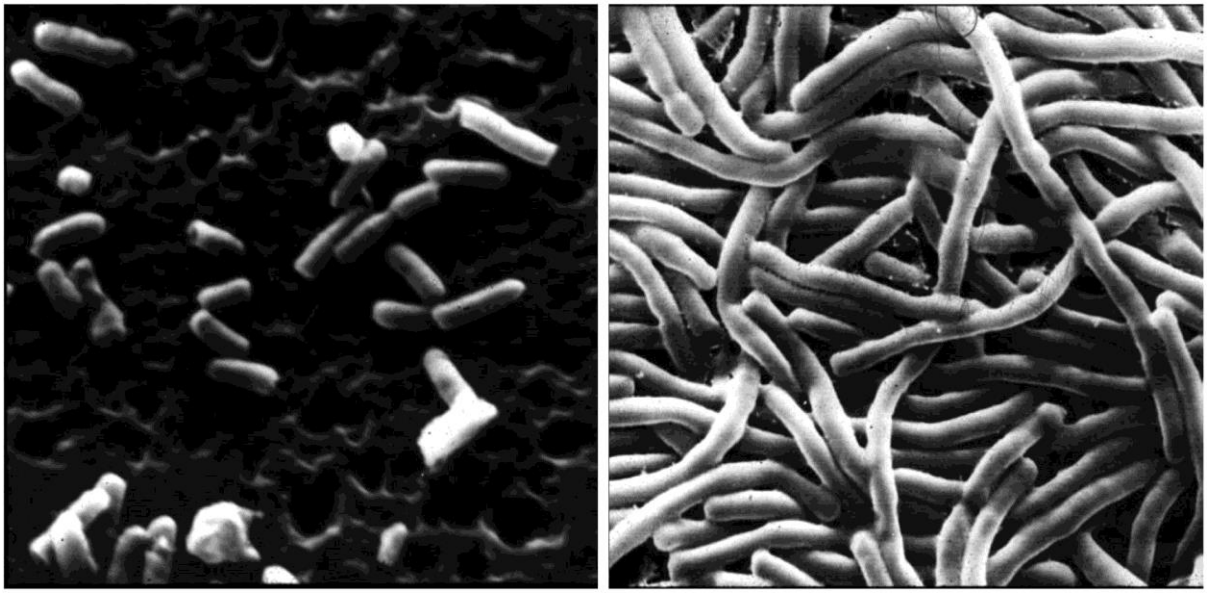

A **B**

Fig. 1.3 Filamentous growth of *E. coli* (**B**) after exposure to platinated nutrient broth. Non-filamentous growth shown in image **A** adapted from Rosenberg *et al.* (1967).

The more active *cis*-[$Pt(NH_3)_2Cl_2$] was examined for its antitumour capability in S180 murine sarcomas and after an initial 8 day growth period it was discovered that a single 8 mg/kg dose resulted in successful regression of the tumours after 8 days (**Fig. 1.4**) (Rosenberg and Van Camp 1970).

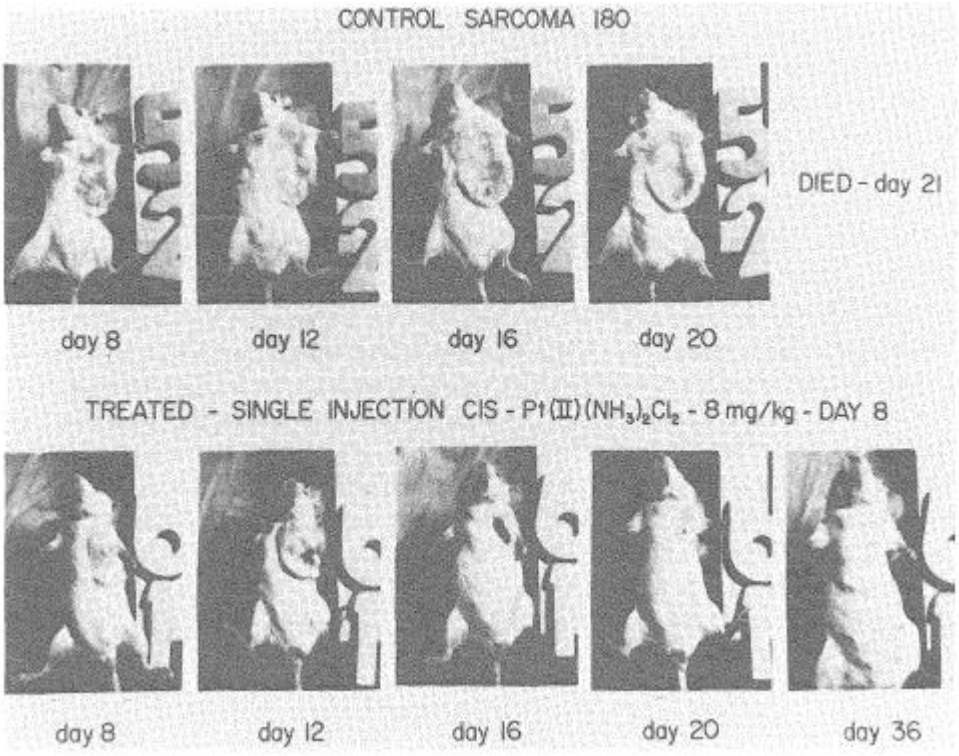

Fig. 1.4 *In-vivo* study of effects of *cis*-[$Pt(NH_3)_2Cl_2$] on the progression of S180 sarcoma tumours in mice. Image adapted from Rosenberg and Van Camp, (1970).

This key finding led to clinical trials beginning in 1971 and its later approval for use against testicular and ovarian adenocarcinoma in 1978. While it was initially approved for use against two solid tumours its approval was later incorporated into combination therapies for treating bladder, lung, head and neck, gastric and triple negative breast cancers making it the backbone of many therapeutic regimes (Chabner 2010).

Since its discovery, *cis*-DDP (cisplatin) has remained the only stereoisomer (**Fig. 1.5**) to have biological activity and as such has had hundreds of analogoes developed. The *trans* isomer (*trans*-DDP) was also investigated by Rosenberg (Rosenberg *et al.* 1967) with two other series of investigation by Cleare and Hoeschele (1973a, 1973b), demonstrating its lack of significant biological activity.

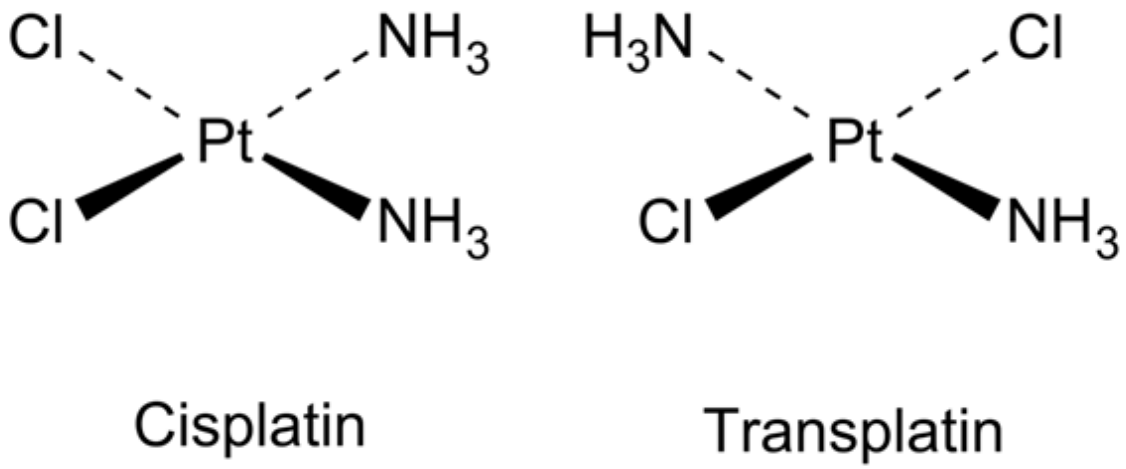

Fig. 1.5 Cis-trans isomerism structure of cisplatin.

Its inactivity was explained by its weaker inhibition of DNA replication and poor capability of forming DNA adducts as effectively as cisplatin, greatly reducing its *in-vitro* and *in-vivo* capability (Kalinowska-Lis *et al.* 2008). However, the extensive literature examining platinum based drugs has provided a new motivation to examine the effects of the *trans* isomer on DNA and its effect on other regulatory elements (Coluccia and Natile 2007; Kalinowska-Lis *et al.* 2008). This is due to transplatin's ability to produce relevant *in-vitro* cytotoxicity when the amine ligands are substituted by aromatic N- donor heterocycles, branched aliphatic amines, or imino ligands (Coluccia and Natile 2007). Multiple type of ligands coordinated by platinum have been investigated for their cytotoxic capability and clinical efficacy such as aminoether, planar amines, carboxylato, non-planar heterocyclic, aliphatic, 2-phenylindole, ketoimine and sulphonamide ligands (Tomé *et al.* 2013; Pérez *et al.* 2014; Silva *et al.* 2014).

The primary mechanism through which cisplatin yields its cytotoxicity in the cell is thought to be through DNA binding and damage (Basu and Krishnamurthy 2010), although more recent evidence suggests that non DNA effects may have an equally important role (Messori and Merlino 2016). The binding of DNA with cisplatin occurs following hydrolysis and the formation of the charged platinum complex, $[Pt(NH_3)_2(H_2O)Cl]^+$. The complex interacts with DNA through the N7 position of either guanine or the adenine base. The remaining chloride is displaced through further hydrolysis allowing platinum to bind the second nucleotide base. The intra strand binding of the cisplatin-DNA adduct results in destacking of the nucleotide bases leading to the DNA helix becoming 'kinked' (**Fig. 1.6**). The 'kinked' DNA is then recognised by nuclear high-mobility group proteins which bind the lesion and prevent DNA repair from occurring (Takahara *et al.* 1995; Basu and Krishnamurthy 2010).

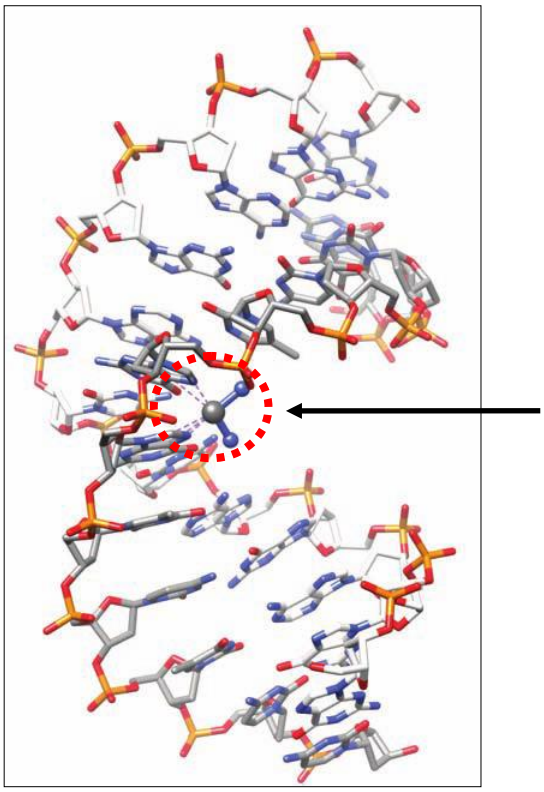

Fig. 1.6 Cisplatin forming a 1,2-intrastrand d(ApG) crosslink in DNA. Other forms of adduct formation produce less pharmacological active effects. Image adapted from Gelasco and Lippard, (1998) and Turel and Kljun, (2011).

The formation of cisplatin-DNA adducts results in cell cycle arrest and cellular apoptosis activation. The activation of p53 remains central to the cascade of signal transductions which result in apoptosis (**Fig. 1.7**) (Basu and Krishnamurthy 2010). The outcome of cell death occurs through a complex series of interactions primarily emanating from the activation of p53 after platinum adduct formation followed by high-mobility group proteins locating to the platinated site and subsequently an inability to complete DNA repair. The inherent inability of DNA repair in some prokaryotic (Beck and Brubaker 1973) and eukaryotic (Fraval *et al.* 1978) cells was shown in 1973 and 1978, respectively, and both demonstrated accelerated cisplatin activity with mechanistic activity that was strongly related to DNA repair capacity. The activation of

p53 can precipitate the activation of cell cycle arrest through Growth Arrest and DNA Damage-inducible 45 (GADD45), p21 and Mouse double minute 2 homolog (Mdm2), and the activation of apoptosis through direct action of the Caspase cascade specifically with Caspase-6 and -7. Apoptosis can also be signalled with P53 induction of BCL-X protein where cytochrome c is released from the mitochondrial to activate Caspase-9 and then Caspase-3 (Basu and Krishnamurthy 2010; Dasari and Tchounwou 2014).

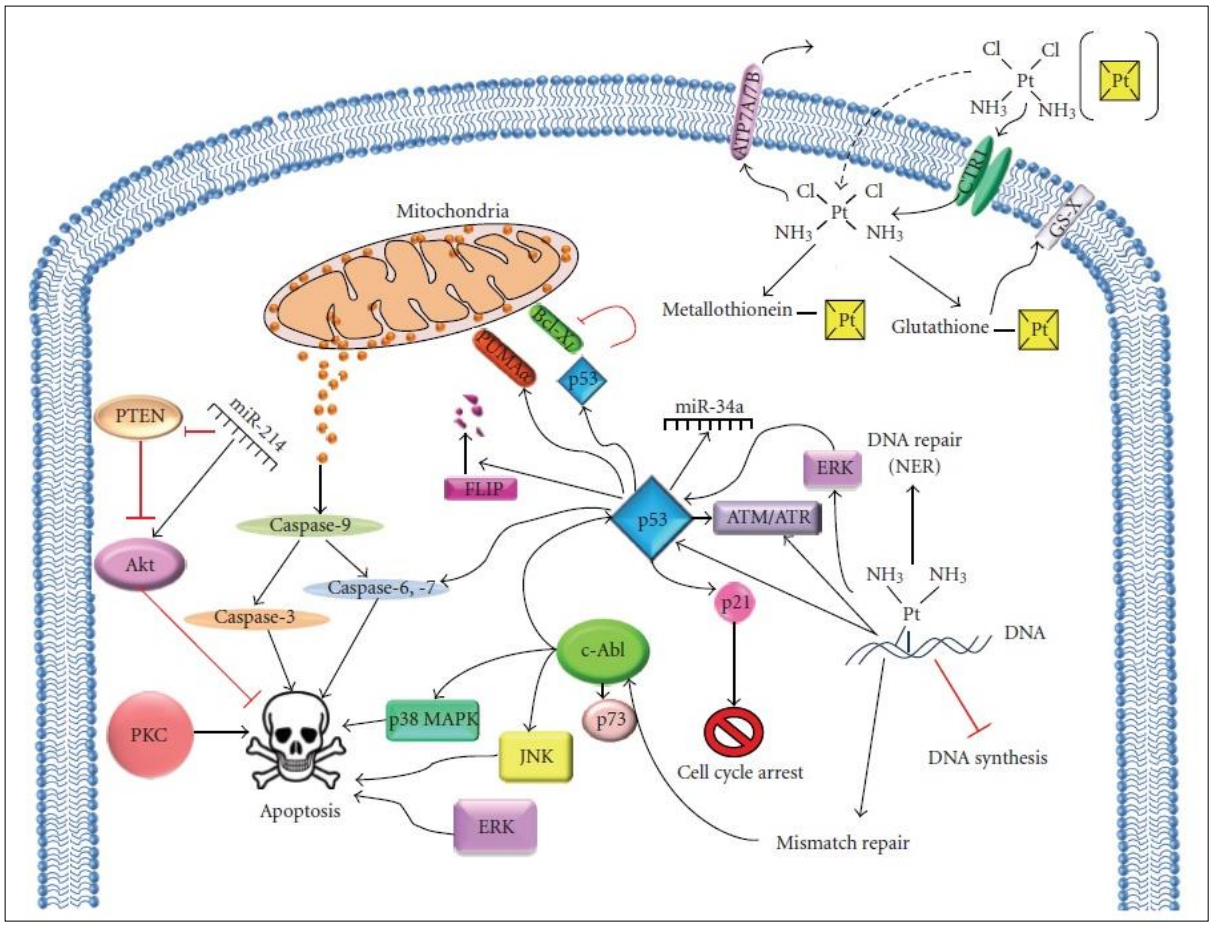

Fig. 1.7 Overview of the cellular response to cisplatin-induced DNA damage. Image adapted from Basu and Krishnamurthy, (2010).

Estimates of the percentage of cisplatin bound to DNA typically record less than 5 % which has concentrated efforts in studying its interaction with proteins (Gullo *et al.*

1980; Eastman 1983, 1986; Messori and Merlino 2016). While the action of cisplatin has been widely associated with DNA interaction, cisplatin has a potent affinity for intracellular proteins rich in thiol and histidine residues. Indeed the interaction between cisplatin and proteins play a determinant role in the pharmacokinetics of cisplatin through cellular transport, uptake, biodistribution and toxicity profile changes (Knipp *et al.* 2007; Casini *et al.* 2012). Major functional classes of protein have been shown to interact with cisplatin such as: haemoglobin (Lammering *et al.* 1999), serum albumin (Barnes and Lippard 2004), transferrin (Khalaila *et al.* 2005; Zhao *et al.* 2005), glutathione (Kasherman *et al.* 2009), and metallothioneins (Knipp *et al.* 2007; Karotki and Vašák 2009) among others.

Due to the irreversible nature of cisplatin binding to DNA and its ability to effect healthy tissue, the possibility of mutations and secondary tumours due to these effects is increased (Sakai *et al.* 2008; Dertinger *et al.* 2014). Furthermore, as described above, the pervasive nature of cisplatin protein interaction and consequent disruption in cellular function remains one of the key factors limiting prolonged use of this therapeutic. While cisplatin displays ototoxicity, gastrotoxicity and myelosuppression, nephrotoxicity remains one of the biggest rate limiting factors in its prolonged use. The kidney absorbs (particularly in the proximal convoluted tubule) cisplatin at higher concentrations than any other tissue in the body. With the accelerated uptake, a potentiation of the multitude of apoptotic signals results from activation of the endoplasmic reticulum, p53, Reactive Oxygen Species (ROS), mitochondrial cytochrome c release and TNFR (Karasawa and Steyger 2015). The majority of patients undergoing cisplatin therapy experience some form of renal dysfunction monitored through serum creatinine and blood urea nitrogen levels, an increase of which indicate a deterioration of renal clearance (Akcay *et al.*

2010). The uncoordinated binding of cisplatin to sulphur residues on circulating proteins is typically addressed by diuretics and administration of sulphur containing agents which provide a decoy molecule to bind the platinum agent and limit the damage of biologically produced sulphur rich proteins (Kröning *et al.* 2000; Peres and Cunha Júnior 2013; Rosic *et al.* 2017). Carboplatin and oxaliplatin, analogues of cisplatin, have a lower protein binding capability and consequently have become more common in oncology treatment than cisplatin.

1.2.2 Platinum derivatives

Carboplatin is one of the most successful analogues generated to-date and one of the few widely accepted for the treatment of ovarian, lung, head and neck cancers. Carboplatin differs from cisplatin in that it contains a bidentate carboxylate ligand in place of the two chloride ligands. This alteration results in slower DNA binding kinetics and diminished protein-carboplatin complexation. The combination of these features result in reduced nephrotoxicity compared to cisplatin (Dasari and Tchounwou 2014a). Oxaliplatin is another commonly used platinum analogue with a high degree of activity against colon cancer and typically used as part of a combination therapy of leucovorin and 5-fluorouracil (André *et al.* 2004; Mayer 2012). This analogue stands alongside several other modified platinum coordinated ligands currently undergoing clinical trials. Carboplatin differs from cisplatin with a bidentate carboxylate in place of the two chloride ligands (**Fig. 1.8**) and oxaliplatin contains the bidentate ligand, 1,2-diaminocyclohexane in place of the monodentate amine ligands (**Fig. 1.8**).

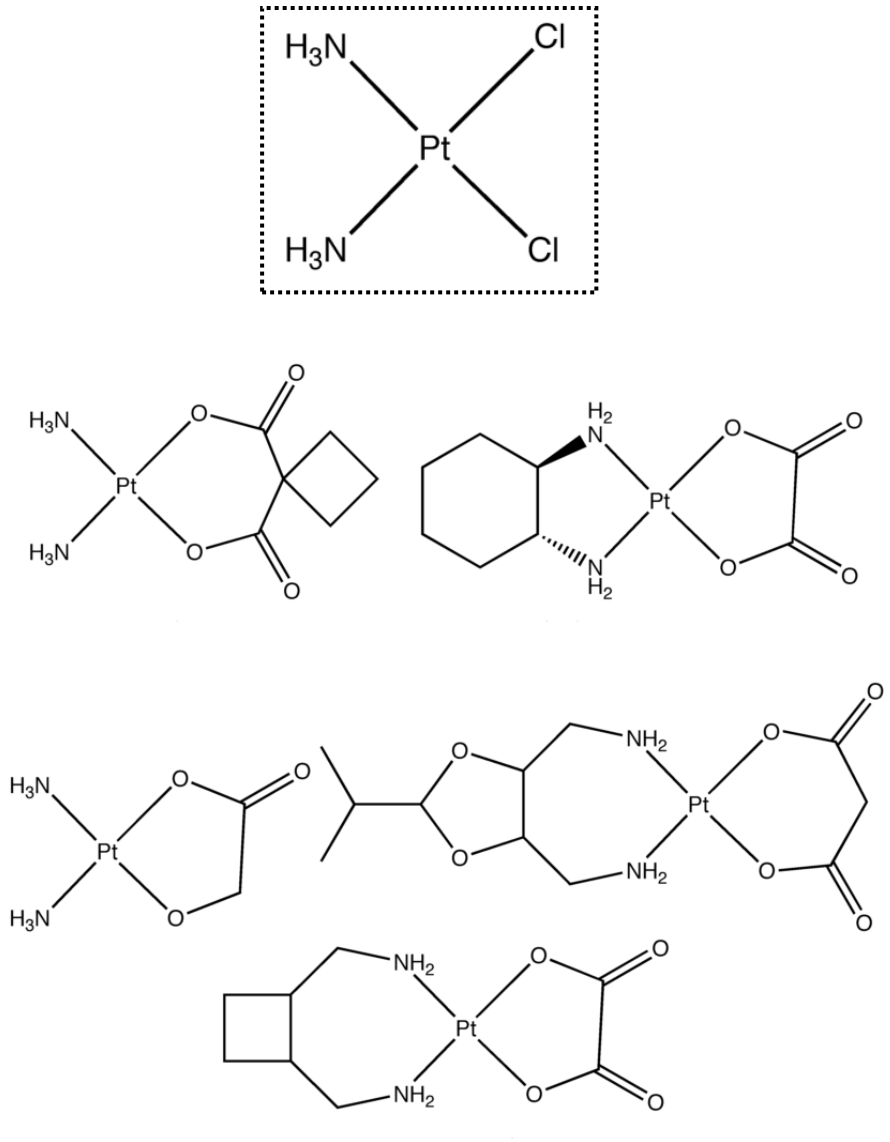

Fig. 1.8 Molecular structures of cisplatin (top, in dashed box) and its clinical platinum derivatives: carboplatin (middle left), oxaliplatin (middle right), nedaplatin (lower left), heptaplatin (lower right) and lobaplatin (bottom). Images adapted from Hannon, (2007).

Alongside the worldwide approved carboplatin and oxaliplatin, the additional platinum agents; Nedaplatin (Japan) (**Fig. 1.8**), Lobaplatin (China) (**Fig. 1.8**) and Heptaplatin (**Fig. 1.8**) have gained single market approval (Wheate *et al.* 2010) with the hope that international approval will follow. Nedaplatin contains the same amine carrier ligands as cisplatin but with a bidentate five-membered ring structure providing the same DNA

binding capability as cisplatin but decreased renal and gastrointestinal toxicities (Kameyama *et al.* 1990; Niioka *et al.* 2007; Shimada *et al.* 2013). Lobaplatin contains a lactic acid leaving group and forms mainly GG and AG intra-strand cross links and is believed to influence the expression of *c*-myc, a key transcription factor in the regulation of cell proliferation (McKeage 2001). Heptaplatin development sought to maintain the properties of cisplatin while emulating the reduced toxicities of carboplatin while not demonstrating platinum cross-resistance. A combinatorial phase III study showed that heptaplatin with 5-fluorouracil responded similarly to cisplatin tolerable toxicities (Choi *et al.* 2004; Lee *et al.* 2009). The 'traditional' mono platinum based drug design are being increasingly joined by variants such as the oral delivery candidate, satraplatin [$Pt(NH_3)_2$(cyclohexylamine)$Cl(COOCH_3)_2$] (Lovejoy and Lippard 2009), and the current state-of-art polyplatinum(II) compounds, TriplatinumNC-A and TriplatinumNC derived from the parent BBR3464 complex have shown promising activity in phase I and II clinical trials (Farrell 2015). Investigations are continuing on the monofunctional platinum complex with the recent evaluation of *N*-heterocyclic ligated phenanthriplatin. This has been reported to have promising activity exceeding cisplatin and oxilaplatin and an NCI-60 cell panel suggesting a different mechanism of action to the clinical complex (Park *et al.* 2012).

1.2.3 Cellular resistance mechanisms to cisplatin

Due to the ubiquitous and widespread success of cisplatin and platinum-related therapies, a considerable body of literature describing the numerous cisplatin resistance mechanisms exists. Cisplatin therapy has demonstrated a high degree of effectiveness against testicular germ cell cancer, with a durable complete remission rate of greater than 80 % (Feldman *et al.* 2008; Winter and Albers 2011). In contrast, rates of

resistance to cisplatin therapeutic regimes are considerable increased in ovarian, lung, prostate and colorectal cancer patients (Giaccone 2000; Köberle *et al.* 2010). The resistance mechanism are part of four main categories: pre-target (cellular transport mechanisms), on-target (acting on the site of DNA adduct formation), post-target (intracellular response to DNA adduct formation) and off-target (effects unrelated to DNA adduct formation) (Galluzzi *et al.* 2012). At the pre-target stage the expression level of the copper transporter 1 (CTR1) has been shown to have a strong effect on the active transport of cisplatin into the cytoplasm with lower expression levels resulting in lower intracellular accumulation of cisplatin and the consequently protective effect (Holzer and Howell 2006). Overexpression of the efflux transporters Adenosine Triphosphate 7A/ B (ATP7A/B) and Multi-Drug Resistance 2 (MRP2) also function to reduce the intracellular accumulation of cisplatin (Aida *et al.* 2005; Yamasaki *et al.* 2011). Prior to DNA adduct formation the upregulated expression of glutathione S transferase (Chen and Kuo 2010) and metallothioneins (Notta and Koropatnick 2006) can result in inactivation through increased antioxidant capacity, the capture of superoxide and hydroxyl radicals through the presence of cysteine residues and heavy metal sequestration. On-target resistance at the DNA platinum adduct site can take many forms. The increased action of the Nucleotide Excision Repair (NER) process has been noted through multiple studies to increase the tendency for cisplatin resistance by allowing the DNA integrity to be maintained (Bellmunt *et al.* 2006; Olaussen *et al.* 2006; Jun *et al.* 2008; Kim *et al.* 2008). The increase in Translesion Synthesis (TLS) which encompasses a process, which allows for platinum adduct regions to be bypassed by DNA Polymerase H (POLH) (Ceppi *et al.* 2009; Shachar *et al.* 2009) and the catalytic subunits of the TLS DNA polymerase ζ (Roos *et al.* 2009; Shachar *et al.* 2009). In addition to the increased action of NER and TLS, deficiencies in Mismatch

Repair (MMR) proteins such as Methylation-dependent Silencing 1 (MLH1) (Gifford *et al.* 2004) and MutS protein Homologue 2 (MSH2) (Kamal *et al.* 2010) often show mutated or depressed activity. A large number of intracellular proteins associated with resistance to apoptosis are involved post-target such as BAX-like proteins, B-Cell Lymphoma 2 (BCL-2) like proteins, Baculoviral IAP repeat-containing protein 5 (BIRC5), calpains, caspases, Mitogen Activated Protein Kinase (MAPKs), p53 and XIAP-associated factor 1 (XAF1) (Galluzzi *et al.* 2012). BCL-2 protein family can act in both a pro-apoptotic (BAX) and anti-apoptotic (BCL-2) manner. Deficiencies in BCL-2 associated X protein (BAX)/BCL-2 homologous antagonist killer (BAK) has been shown to confer resistance in *in-vitro* models (Kroemer *et al.* 2007; Tajeddine *et al.* 2008) and overexpression in BCL-2 and B-cell Lymphoma extra-large (BCL-X_L) has been shown to increases resistance *in-vitro* with clinical data being currently collected (Michaud *et al.* 2009; Jain and Meyer-Hermann 2011). With regards to caspase initiated apoptosis, modification of the activation cascade has been shown *in-vitro* to increase the resistance profile to cisplatin (Janson *et al.* 2010). The overexpression of BIRC5 proteins; X-linked inhibitor of apoptosis protein (XIAP), cytoplasmic Inhibitor of Apoptosis 1/ 2 (cIAP1/ 2) was shown to be associated with chemoresistance and poor prognosis (Altieri 2008; Ryan *et al.* 2009). Drug development approaches are currently being evaluated for BIRC5 inhibition (Groner and Weiss 2014; Hagenbuchner *et al.* 2016). In relation to apoptosis, XAF1 is another protein that antagonises IAP activity and was reported to be at highly expressed and associated with improved progression-free survival in bladder cancer patients (Plenchette *et al.* 2007; Pinho *et al.* 2009). The MAPKs such as c-Jun N-terminal Kinases (JNKs), Extracellular signal–Regulated Kinases (ERKs) and Stress Activated Protein Kinases (SAPK) have demonstrated chemoresistant and chemosensitive properties with experimental data leading to

uncertainty of the clinical data (Brozovic and Osmak 2007; Haagenson and Wu 2010; St Germain *et al.* 2010; Li and Melton 2012; Kong *et al.* 2015). Similar to MAPK related proteins, p53, which is a highly deterministic protein in terms of cell fate has been associated with both sensitivity and resistance to cisplatin therapy (Liang *et al.* 2011; di Pietro *et al.* 2012; Chee *et al.* 2013). Mechanisms of resistance not related to the site of cisplatin action have been associated with a cell death process such known as autophagy and this has been associated with cisplatin resistance (Ren *et al.* 2010; Yu *et al.* 2011; Xia *et al.* 2014), overexpression of Epidermal Growth Factor Receptor (EGFR) (Hsu *et al.* 2009; Mandic *et al.* 2009; Ahsan *et al.* 2010; Rho *et al.* 2011) and the association of Heat-Shock Proteins (HSPs) in cisplatin resistant profiles (Shen *et al.* 2012; Stope *et al.* 2016). Due to the complex nature of cisplatin resistance and the heterogeneity of the cells within the tumour mass in patients, proteomic approaches alone have been unable to completely describe the changes generating the different response profiles. The analysis of glycosylation states of protein, a Post Translational Modification (PTM), is allowing a greater insight into the functions of proteins during resistance development, particularly the action of intracellular detoxification proteins (Ferreira *et al.* 2015). Extensive efforts have been placed on the understanding of biological resistance mechanisms and the development platinum analogues to cisplatin which do not elicit cross-resistance. In this effort the development of alternative metal-based drugs present the most likely viable alternative to overcoming the inherent drawback of platinum therapy.

1.3 Non-platinum based coordination compounds

Due to the success of cisplatin and its platinum related FDA approved analogues in addition to multitude of other related compounds in the developmental pipeline, attention has been focused on the development of a non-platinum based DNA coordination chemotherapeutic. This is primarily to provide a new repertoire of metal-based drugs to help treat tumours resistant to platinum based therapeutics or to help alleviate platinum based toxicities and adverse reactions commonly present after prolonged treatment regimes. Multiple transition metals (copper, ruthenium, gold, silver, iron, cobalt and titanium) and metalloids (gallium and arsenic) have formed the coordination centre of multiple ligand types and chemistries. **Table 1.1** provides an overview of metal-based drugs currently in development.

1.3.1 Ruthenium

Ruthenium complexes have been designed in both the transition states ruthenium(II) and ruthenium(III) with Ru(II) capable of forming both penta- or hexa-coordination and Ru(III) capable of forming only hexa-coordination. The use of Ru(III) has been demonstrated *in-vivo* to be reduced to Ru(II) in hypoxic conditions, typical of the tumour environment (Spreckelmeyer *et al.* 2014). Ru(II) additionally, has recorded lower systematic toxicity than platinum-based compounds with Ru(II) complexes binding to iron-binding proteins such as transferrin and albumin, leading to increased accumulation in cells and upregulation of iron selective transport proteins and potentially redusing the overall therapeutic dose required (Guo *et al.* 2013). Ruthenium(II) has three lead complexes to-date: RM175, RAPTA-C and RDC-11, and Ru(III) have two lead complexes to-date: KP1019 and NAMI-A. RM175, [Ru(biphenyl)(en)Cl]PF_6, a lead compound from the Ru(II)-arene complex family binds

DNA through aromatic ligand intercalation or covalent metal ion binding (Hayward *et al.* 2005). Hydrolysis reactions of [Ru(η^6-*p*-cym)(acac)Cl] (*p*-cym = *para*-cymene) in DNA binding occur through loss of the chloride ligand and the resulting species binding to guanine and adenine (Fernández *et al.* 2004). The ruthenium complex KP1019, [Ru $(HIn)_2Cl_4](H_2In)$ (HIn = indazole) which has a III transition state also binds DNA and induces apoptosis through the intrinsic mitochondrial pathway (Hartinger *et al.* 2006). This complex demonstrated activity against tumour cell lines which were known to over-express multi-drug resistance proteins (multidrug resistance protein 1 MRP1, breast cancer resistance protein BCRP, and lung resistance protein LRP) (Hartinger *et al.* 2006). Phase I trials began in 2003 with no dose-limiting toxicity detected (Dittrich *et al.* 2005). More recently, conjugations of Ru(III)-indazole complexed with PARP-1 have been reported to disrupt the DNA repair process (Wang *et al.* 2014). Alternative modes of interaction have been observed with arene-ligated and water soluble phosphine Ru(II) complexes, [Ru(η^6-*p*-cym)(1,3,5-triaza-7-phospha-adamantane)Cl_2] (RAPTA-C) capable of interacting with the cysteine peptidase, cathepsin B resulting in the degradation of the extracellular matrix which then helps to slow down metastases (Casini *et al.* 2008; Ang *et al.* 2011). The [Ru(2-phenyl- pyridine)$(NCMe)_2$phen]PF6 (phen is 1,10-phenanthroline) (RDC-11) belongs to RDC family of organometallic Ru(II) compounds have been shown to induce apoptosis through activation of the pro-apoptotic protein CHOP (CCAAT/Enhancer-Binding Protein Homologous Protein) which induces the unfolding stress response in the endoplasmic reticulum (Meng *et al.* 2009). Another Ru(III) complex which is involved with the inhibition of the extracellular membrane along with other cellular functions is NAMI-A (*trans*-$[Ru(HIm)(DMSO)Cl_4](H_2Im)$ (Him=imidazole; DMSO=dimethylsulfoxide). Unusually, NAMI-A did not demonstrate strong *in-vitro* or *in-vivo* activity, it did however show

strong inhibition of metastases (Sava *et al.* 2003; Gava *et al.* 2006). As a result of this capability clinical trials began in 1999 with the phase I trials demonstrating a low toxicity of the complex but had no significant benefit to non-small cell lung cancer patients. Phase II clinical trials proceeded but combined with gemcitabine and ultimately demonstrated no significant efficacy beyond the use of gemcitabine alone (Leijen *et al.* 2015). Ruthenium complexes represent a highly customizable chemistry with partially filled 4d electronic sub-shell allowing for the tuning of reduction potential, ligand affinity, substitution rates and altering metal centrochirality and planar chirality, all the features allowing for strong future development.

1.3.2 Gold

In 1985, the phosphine ligated Au(I) complex, auranofin unexpectedly demonstrated decrease in the incidence of cancer in patients being treated for rheumatoid arthritis (Fries *et al.* 1985). Later their activity was linked to thioredoxin reductase inhibition, which is typically elevated in cancer cells (Bruijnincx and Sadler 2008a). The new intracellular target of phosphine ligated Au(I) prompted a more intensive study of the redox potential along with their strong binding affinity for thiol and sulphur containing proteins (Hayashi *et al.* 2014; Abbehausen *et al.* 2016; Al-Jaroudi *et al.* 2017; Milaeva *et al.* 2017; Reddy *et al.* 2017; Tavares *et al.* 2017). In relation to the study of adduct formation between gold(III) compounds/ ions, Glišić *et al.* has studied the oxidation mechanism of amino acids (glycine, methionine, histidine, cysteine etc.) using mass spectrometry (Glišić, Rychlewska and Djuran 2012). Au(III) complexes are another major group of cytotoxic active gold complexes. When Au(III) complexes were initially synthesised their square planar geometry and similar isoelectronic point to Pt led to the belief that their mode of interaction in the cell would be similar to Pt(II) complexes that

target DNA. However subsequent investigation failed to demonstrate a strong interaction between DNA and Au(III) complexes (Ronconi *et al.* 2006; Milacic and Dou 2009). More recently the interaction of Au(III) complexes and the newly discovered telomeric G-quadruplex DNA therapeutic targets have shown to be of increased interest (Gratteri *et al.* 2015; Bertrand *et al.* 2017). Au(III) complexes have been bound to multiple ligand types such as: multidendate, bipyridine, hydroxo and amino-quinoline. The multidendate ligands: $[Au(en)Cl_2]Cl$, $[Au(dien)\ Cl]Cl_2$, $[Au(cyclam)][ClO_4]_2Cl$, $[Au(terpy)Cl]Cl_2$, and $[Au(phen)Cl_2]Cl$ demonstrated high cytotoxicity in A2780 ovarian adenocarcinoma cells and in addition overcame the cisplatin resistant variant (Gabbiani *et al.* 2007). The complexes were shown to have a high rate of hydrolysis and interestingly no renal tubular necrosis in *in-vivo* studies (Casini *et al.* 2010). The functionalised bipyridine complexes with the general formula $[Au(N\text{-}N)Cl_2][PF_6]$ (where N-N = 2,2'- bipyridine, 4,4'-dimethyl-2,2'-bipyridine, 4,4'-dimethoxy-2,2'-bipyridine, and 4,4'-diamino-2,2'-bipyridine) have demonstrated moderate cytotoxicity in A2780/ Cis cells which indicates that the cross resistant phenotypes typical of platinum cross resistance may not be effecting the activity of these Au(III) complexes (Rabik *et al.* 2007; Casini *et al.* 2010). A group of Au(III) ligated hydroxyl and amino-quinoline ligands have also demonstrated anti-proliferative potency exceeding cisplatin in many cases. Investigations using supercoiled pBR322 plamid DNA have again demonstrated a weak interaction however strong interactions have been detected with cytochrome *c* suggesting a very different mechanism of action to that of Pt(II) complexes (Martín-Santos *et al.* 2015). Overall the Au complexes have shown a large degree of instability in aqueous solution due to their very rapid hydrolysis at physiological conditions which poses developmental challenges for the future, however their strong protein thiol binding and activity against platinum cross-resistant cells

makes them promising future developmental therapeutic candidates (Lazarevi *et al.* 2017).

1.3.3 Silver

Silver is a well known antimicrobial agent. However for chemotherapeutics use, the development of Ag(I) complexes have not demonstrated the same degree of success as other transition metals. In spite of this disadvantage silver has a number of advantages as the coordination centre of potential chemotherapeutics. While toxicity from silver is well known in bacteria, for humans it is uncommon which provides for the ability to use its capacity for coordination with a lower possibility of systemic toxicity (Hadrup and Lam 2014). Silver's anticancer capability differs from platinum based-drugs in terms of DNA interaction, mitochondrial targeting, inhibition of thioredoxin reductase and potential antioxidant capability (Pellei *et al.* 2012), similarly to the features observed with gold(III) complexes (Hickey *et al.* 2008; Banti *et al.* 2012, 2014). Three primary design formats have been in use for Ag(I) complexes; N-hetercyclic carbenes, phosphines and N-heterocycles. N-hetercyclic carbene Ag(I) complexes while having a better response than cisplatin in certain *in-vitro* situations, the *in-vivo* situation presents a number of problems such as rapid clearance from the system. Ubiquitous chloride ions can abstract Ag in solution and sulphur rich proteins can inactivate the complexes (Medici *et al.* 2016). The use of phosphine ligands on Ag(I) complexes has been beneficial mostly in antimicrobial development. The development of N-heterocycles has typically been associated with other metal centres due to Ag(I) being more limiting. Positive activity has been observed in MCF-7 (breast adenocarcinoma) and HeLa (cervical cancer) along with an antioxidant effect and purified DNA interaction studies suggesting intercalation or electrostatic interactions are likely (Banti *et al.* 2015).

Recently a series of polynuclear Ag(I) dicarboxylate complexes with variable length linker chains demonstrated good cytotoxicity against MCF-7 and SKOV-3 (ovarian adenocarcinoma) cells, in addition no ROS generation or significant increase in the DNA double stranded break marker γH2AX was detected (Thornton *et al.* 2016). Overall, while the low or absent nature of the systemic toxicity with Ag(I) has provided a strong developmental incentive, challenges such as rapid clearance, Ag abstraction and sulphur rich protein inactivation in *in-vivo* environments have frustrated extensive assessment of this transition metal as a potential chemotherapeutic drug.

1.3.4 Iron

Iron is a trace element and is an essential component in a number of cellular processes such as oxygen transport, DNA synthesis, oxidation phosphorylation and cell cycle progression. All of these processes can be involved in carcinogenesis (Coombs *et al.* 2012; Gasche 2013). The use of iron in the form of organometallic ferrocifen rings has been used in the clinic to treat certain forms of oestrogen receptor (ERα+) breast cancer cells. The ferrocifen ring has been incorporated into the existing organic drug tamoxifen by replacing one phenyl ring in the tamoxifen structure. The modified tamoxifen/ ferrocifen is highly active against breast cancer cells that are ERα-ve (ERβ+ve) as well as cells that are ERα+ve (Vessières *et al.* 2006; Lange *et al.* 2008; Rafique *et al.* 2010). The activity of ferrocene has also been integrated with chloroquine in the development of antiparasitic agents (Blackie and Chibale 2008). The chelation of iron is currently used for the treatment of β-thallassemia patients, where abnormal levels of intestinally absorbed iron occur with the subsequent increase in DNA, protein, and lipid oxidation (Cappellini *et al.* 2008). Data have shown that desferrioxamine is capable of reducing the incidences of neuroblastoma and leukemia (Desoize 2004). More recently, iron

depletion therapies have been proposed for multiple cancers (Kovacevic and Richardson 2012; Keeler and Brookes 2013; Richardson *et al.* 2013; Torti and Torti 2013).

1.3.5 Cobalt

Cobalt(II) has been combined with acetylsalicylic acid which has been shown to inhibit Cyclooxygenase-1 and -2 (COX-1, -2) enzymes. COX1/ 2 are enzymes involved in prostanoid synthesis, including thromboxane and prostaglandins. COX-1 is constitutively expressed while COX-2 is inducible. While acetylsalicylic acid also inhibits COX-1 and COX-2 enzymes independent of cobalt the coordination with cobalt through cobalt-alkyne complexes was shown to increase enzyme inhibition and anticancer activity (Ott *et al.* 2004; Bruijnincx and Sadler 2008b; Algra *et al.* 2012). Co(III) complexes have also been explored as prodrugs which are reduced to Co(II) in hypoxic environments releasing their cytotoxic ligand that is destined for DNA alkylation or matrix metalloproteinase inhibition (Ahn *et al.* 2006; Failes *et al.* 2007; Lu *et al.* 2011).

1.3.6 Gallium

The metalloid gallium has been known to accumulate in tumour tissue and as such it has been used as a radio tracer using gamma cameras to diagnose lymphomas and osteomyelitis (Bryan 2010; Bleeker-Rovers *et al.* 2011). Gallium shares multiple similarities with iron such as similar ionic radius, ionization potential and electron affinities (Chitambar 2012). These similarities allow gallium to bind with transferrin, which can potentially allow gallium complexes to be transported via transferrin receptors in a similar fashion to ruthenium complexes (Chitambar and Antholine 2013). Gallium nitrate was the first gallium compound to be brought to phase I and phase II

clinical trials, with moderate success against non-Hodgkin's lymphoma and advanced bladder cancer, however long intravenous infusions to prevent nephrotoxicity complicated the success of the formulation (Chitambar 2012). Gallium(III) complexes of 8-hydroxyquinoline have also been shown to interfere with the cellular transport of iron with its competitive binding to transferrin and thereby inhibiting the supply of iron to fast dividing cells. Independently, gallium(III) complexes have also been shown to interfere with the activity of ribonucleotide reductase, which results in an inhibition of DNA synthesis (Deally *et al.* 2012). Anti-tumour activity has also been recorded in phosphinoarylbisthiolato gallium(III) complexes (Fischer-Fodor *et al.* 2014). They showed strong activity against cisplatin-resistant A2780/ Cis cells and demonstrated an ability to bind DNA in the 7-methylguanine and 8-oxoguanine positions, oxidizing the pyrimidine bases and resulting in apoptosis (Fischer-Fodor *et al.* 2014). In addition to gallium nitrate, the gallium complex KP46 was also successfully brought to clinical trials with further studies being planned (Valiahdi *et al.* 2009). Owing to the success of the clinical trial data on gallium compounds and complexes there is a strong incentive to investigate the in-depth biological mechanism of action of gallium complexes (Mikuš *et al.* 2014).

1.3.7 Titanium

In the 1990s, Titanium in the form of titanocene dichloride entered clinical trial as an anticancer agent, however high toxicity related to Reactive Oxygen Species (ROS) production rendered it unsuitable soon afterwards (Christodoulou *et al.* 1998; Lümmen *et al.* 1998). Many parallels with cisplatin had been observed with this agent in relation to the *cis*-dichloride composite and its hydrolyzation with water to form a variety of species. The active component of the drug is still unclear and information regarding its

DNA binding has not yet been elucidated (Strohfeldt et al. 2007; Deally et al. 2012; Melendez 2012). More recently the ligand isopropoxide supported by pyrrolyl Schiff base ligands have been coordinated to Ti(IV) and shown cytotoxic activity towards HCT-116 (colon), PC-3 (prostate) and MCF-7 (breast) cells, exceeding cisplatin (Lin *et al.* 2014).

1.3.8 Arsenic

The arsenic treatment, arsenic trioxide (As_2O_3) was approved by the FDA in 2000 for the treatment of acute promyelocytic leukemia demonstrating increased rates of survival (Douer *et al.* 2003; Wang and von Recum 2011). More recently darinaparsin (S-dimethylarsino-glutathione) has been approved for use in treating T-cell lymphoma with evidence suggesting that the Nuclear factor (erythroid-derived 2)-like 2-Kelch-like ECH-associated protein 1 (Nrf2-Keap1) pathway is important in the difference between the mechanism of action of the two arsenicals (Matulis *et al.* 2009; Barry *et al.* 2013).

Table 1.1 Overview of metal-based drugs in development.

Metals	Advantages	Disadvantages	Therapeutic Potential
Platinum: cisplatin, carboplatin, oxaliplatin Multiple ligands and polyplatinum complexes	• Highly established clinical therapeutic, • Known toxicities. • Well established co-treatment regiments.	• High renal toxicity. • Cross-resistance of platinum therapies.	• Strong potential for the development of new platinum therapies which do not suffer cross-resistance and maintain therapeutic effect.
Ruthenium: (RM175, RAPTA-C, RDC-11) (Ru(II)) (KP1019, NAMI-A) (Ru(III))	• Overcoming therapeutic resistance in *in-vitro* cells expressing multi-drug resistance protein. • Strong DNA intercalator (known chemistry).	• Failure to demonstrate benefit in phase II trials over present therapy (NAMI-A).	• Highly customizable chemistry: ligand affinity, centro and planar chirality. • Low toxicity in previous clinical trials.
Gold: phosphine ligated Au(I) Au(III) complexes	• Similar square planar geometry and isoelectric point to Pt. • Low renal tubular necrosis in *in-vivo* studies.	• Rapid hydrolysis and instability in aqueous solution.	• New studies assessing protein inhibition potential. • Strong thiol protein binding and activity against platinum resistance cells.
Silver: Ag(I) multiple ligands	• Known antimicrobial properties. • Low systemic toxicity in humans.	• Different anticancer properties to platinum complexes. • Rapid biological clearance. • Detoxification by sulphur rich proteins.	• Strong possibilities in antimicrobial development • Greater knowledge of mechanism of action would allow for more targeted development
Iron: Fe(II) and Fe(III)	• Complex biological processes for and transport and utilisation (reducing systemic toxicities). • Modified tamoxifen/ ferrocifen treating ERα-ve and ERα+ve.	• Failure to demonstrate significant anticancer activity with multiple ligand types	• Therapies focusing principally on iron depletion.
Cobalt: Co(II)	• Co(II) combined with acetylsalicylic acid inhibiting COX-1, -2 enzymes. • Increased enzyme inhibition.	• Limited number of ligand types tested.	• Potential as pro drug (Co(III) → Co(II)) releasing cytotoxic agent intracellularly, reducing systemic toxicity.
Gallium (metalloid): Ga(III)	• Competitive binding of iron. • Similar chemistry to Iron • Strong therapeutic activity against cisplatin resistance cells.	• Nephrotoxicity has been difficult to overcome in clinical trials.	• Multiple complexes brought to clinical trial.
Titanium: Ti(IV)	• Cytotoxicity exceed cisplatin in many tumour cell lines	• Toxicities related to high ROS activity.	• Mechanism of action unclear, hindering development.
Arsenic (metalloid):	• Present in current T-cell lymphoma therapies. • As_2O_3 in treatment of acute promyelocytic leukemia.	• Short plasma half-life and narrow therapeutic windows.	• Promising development in haematological malignancies
Copper: Cu(I) and Cu(II) Multiple ligands	• Well known targeting effects (DNA, ROS and enzymatic inhibition). • High activity against cisplatin resistance cancer.	• Can become easily oxidized.	• Clinical trials presently in Casiopeinas® family.

1.4 Overview of copper in physiology, pathophysiology and coordination therapeutics

Copper plays an essential role in the structure and activity of multiple functional protein classes, such as haemoglobin formation, xenobiotics and carbohydrate metabolism, catecholamine biosysnthesis, cross-linkage of collagen, elastin in addition to pivotal roles in detoxification and oxidative phosphorylation based proteins (Festa and Thiele 2011). Antioxidant proteins such as cytochrome *c* oxidase, superoxide dismutase, ferroxidases, monoamine oxidase, and dopamine β-monooxygenase, are involved in neutralizing ROS or molecular oxygen and rely on copper for their functional integrity. Owing to the biological importance of copper, the cell employs specific copper-efflux transporters Adenosine Triphosphate 7A/B (ATP7A) and (ATP7B), in addition to the multidrug efflux pumps belonging to the ATP-Binding Cassette (ABC) superfamily (P-glycoprotein (Pgp, ABCB1) and multi- drug resistance protein 2 (MRP2, ABCC2) (Safaei *et al.* 2004; Fontaine and Mercer 2007; Crisponi *et al.* 2010; Kalayda *et al.* 2012). Copper enters the body through CTR1 protein on the apical membrane surface of enterocytes cells where it is typically converted from $Cu^{2+} \rightarrow Cu^{+}$ and bound to Antioxidant Protein 1 (ATOX1). ATOX1 is bound for the Golgi apparatus which permits the export of Cu^{+} through the basolateral membrane located ATP7A after which it is bound to albumin, α2-macroglubulin and ceruloplasmin in the bloodstream. The transport of copper from hepatocytes to other target cells occurs after extracellular intake of copper at the CTR1 protein on the hepatocyte, intracellular transport with ATOX1 and importing into the Golgi apparatus through the ATP7B for incorporation into cupro-proteins (Kaplan and Lutsenko 2009; Bandmann *et al.* 2014). Due to the essential physiological requirements of copper, pathologies are associated with deficiencies or excesses. Wilson's disease is one of the best known pathologies of

copper excess where copper primarily accumulate in the liver and brain, inducing liver failure and is being increasingly associated with chronic neurological disorders such as Alzheimer's and Parkinson's disease (Bandmann *et al.* 2014). Wilson's disease is caused by autosomal recessive mutation in the ATP7B gene, encoding the copper-transporting P-type ATPase protein. The subsequent mutated phenotype results in the intracellular accumulation of the copper, resulting in increased oxidative stress, free radical formation and mitochondrial dysfunction independent of oxidative stress (Gu *et al.* 2000; Zischka *et al.* 2011; Bandmann *et al.* 2014). Menkes disease is an X-linked recessive disorder resulting in copper deficiency. It is caused by a mutation of the ATP7A copper transporter which results in a failure to adequately absorb copper and resulting in deficiencies in cupro-proteins (Crisponi *et al.* 2010). Penicillamine is the current treatment standard for copper chelation therapy and results in the binding of copper and enhanced excretion via the kidneys (Peisach and Blumberg 1969). Recently trientine and 8-hydroxyquinolines have shown superior chelation capability to penicillamine through their copper excretion via bile in contrast penicillamine's less stable excretion through urine (Říha *et al.* 2013).

1.4.1 Copper coordinated complexes

From a biological perspective, the endogenous nature of copper in the body is hypothesised to reduce the systemic toxicities that are common with many other non-essential metals utilised in metallodrugs. In addition, the variety of N-, S-, or O-containing ligands and the range of oxidative states permit copper to form multiple planar and non-planar molecular structures in addition to its ability to coordinate biologically active aromatic ligands, which have applications in anticancer therapeutics (Trudu *et al.* 2015). The essential nature of copper in the cell and its complex

homeostasis through specific transporters and trafficking proteins (Gupta and Lutsenko 2009; Wee *et al.* 2013) holds a strong potential for the utilisation of it as a therapeutic substance, specifically as an agent to target DNA. Prior to research into copper based therapeutics copper was known to bind to DNA with higher affinity than many other divalent cation, which promoted DNA oxidation. The binding of copper to DNA and subsequent conformational modification of polynucleotides, proteins structures and membranes was shown to be dependent on the electron affinity and geometry of the copper ion, providing a strong basis for the development of redox active therapeutic designs. At present the biological targets of copper complex focus strongly on DNA interaction, ROS induction and protein inhibition (Trudu *et al.* 2015). The discovery of the first synthetic chemical nuclease $[Cu(Phen)_2]^{2+}$ in 1979 by Sigman *et al.*, sparked intensive effort toward the development of novel artificial metallonucleases with DNA cleavage capability (Sigman *et al.* 1979). The $[Cu(phen)_2]^{2+}$ complex predominately binds DNA in the minor groove and in its reduced form abstracts a hydrogen atom primarily from the C1′ deoxyribose position resulting in strand damage (Sigman *et al.* 1993). The $[Cu(phen)_2]^{2+}$ nuclease binds both nucleic acids and proteins without specificity inducing a general toxicity, and is thus considered a "promiscuous" agent. Accordingly, manipulation of this chemotype represents an interesting developmental challenge. In addition to the development of the $[Cu(Phen)_2]^{2+}$ chemotype, a multitude of other coordination chemistries are presently under investigation such as: thiosemicarbazones (Palanimuthu *et al.* 2013; Sîrbu *et al.* 2017), conjugated Schiff bases (Creaven *et al.* 2009; Chakraborty *et al.* 2010), Imidazol (and other organic ligands) (McGinley *et al.* 2013), phosphine (Kaeser *et al.* 2013; Małecki *et al.* 2015; Villarreal *et al.* 2017) and phenanthroline (Palanimuthu *et al.* 2013; Prisecaru *et al.* 2013; Fan *et al.* 2017).

The therapeutic development of copper complexes has progressed to a more advanced stage with the Casiopeinas® family with the general formula $[Cu(N\text{-}N)(A\text{-}A)]NO_3$, where N-N represent neutral aromatic diamine donors (phenanthroline or bipyridine) and A-A stands for uninegative N-O or O-O donor ligands (aminoacidates or acetylacetonate) being used presently in phase I clinical trials. The progress to this stage of development has come about through the demonstration of their cytoxicity activity against medulloblastoma, glioma and colorectal adenocarcinoma cell lines (Carvallo-Chaigneau *et al.* 2008; Mejia and Ruiz-Azuara 2008; Serment-Guerrero *et al.* 2011). Their mechanism of action is not fully understood, however they are believed to exert their biological effects through DNA binding in intercalative and non-intercalative methods at high affinities, degrading nucleic acids through the generation of ROS, depleting the antioxidant systems, and inducing mitochondrial toxicity (Trejo-Solís *et al.* 2005).

1.4.2 Cu(II) phenanthroline complexes

The activity of copper phenanthroline complexes with different secondary ligands such as acetylacetonate and glycinate groups (Galindo-Murillo *et al.* 2015) to the aromatic ligands have shown strong cytotoxicity profiles against cancer cell lines (Kellett *et al.* 2011a; Kellett *et al.* 2011b; Kellett *et al.* 2012; Prisecaru *et al.* 2012; Prisecaru *et al.* 2013), of which endogenous reactive oxygen species was found to accompany nuclease activity (Kellett *et al.* 2011a; Kellett *et al.* 2012b; Prisecaru *et al.* 2012). Research conducted by the supervision team and extended research collaborators was published on *bis*-phenanthroline copper(II) phthalate complexes (Kellett et al. 2011). They were identified as the first such compounds in their class with “self-activating” nuclease

capability along with avid DNA binding properties. They demonstrated a broad spectrum of cytotoxic activity complemented by lack of induced cytotoxicity in the cell with negative expression of p53 tumour suppressor gene. These results showed toxicity being mediated in the reaction was of a different mechanistic pathway to that of Cisplatin. The research team then demonstrated that analysis of dinuclear Cu^{2+} and Mn^{2+} *bis*-phenanthroline octanedioate compounds could exhibit rapid and potent nano and picomolar *in-vitro* cytotoxicity against human-derived colorectal cancer lines (HT-29, SW480 and SW620) and were less cytotoxic towards non-cancerous normal human keratinocyte cells (HaCaT) (Kellett et al. 2011). Both Cu^{2+} and Mn^{2+}complexes displayed greater *in-vivo* drug tolerance compared to cisplatin when examined using the insect *Galleria mellonella*. The mechanism of action with regards to potent generation of intracellular reactive oxygen species and the O_2–dependent cleavage of supercoiled pUC18 DNA was also identified (McCann *et al.* 2012). The activity of bleomycin as mentioned earlier has helped to promote the development of redox-active metal-based drug DNA oxidants. This work led to further studies of square-planar copper(II) complexes (where Phen = 1,10-phenanthroline) incorporating *o*-phthalate and Phen that showed that a broad spectrum of chemotherapeutic potential over 24 and 96 h interval generated through hydroxyl related ROS mediating DNA scission from the reduction of Cu(II) to Cu(I) (**Fig. 1.9**). The copper complexes compared well with the clinical agent cisplatin on MCF-7 (breast adenocarcinoma), DU145 (prostate carcinoma), HT-29 (colonic adenocarcinoma) and the intrinsically cisplatin resistant SKOV-3 (ovarian adenocarcinoma) cells (Kellett *et al.* 2012).

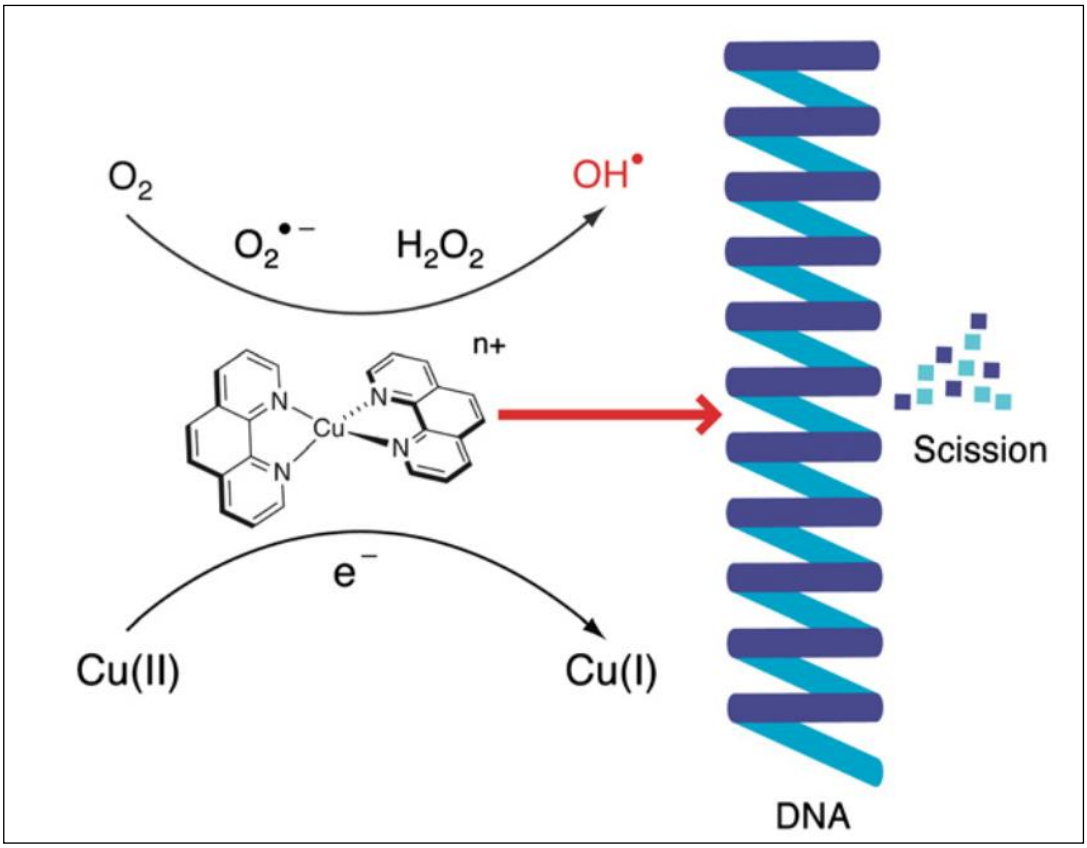

Fig. 1.9 ROS generation and DNA toxicity by the synthetic artificial metallonuclease $[Cu(1, 10\text{-phen})_2]^{2+}$. Image adapted from Kellett *et al.* (2012).

The activity of copper(II) complexes with Phen and 1,10-phenanthroline-5,6-dione showed an enhanced superoxide dismutase and catalase mimetic activity in cell lines (McCann *et al.* 2012). These exposures were also carried out using *in-vivo* studies in *Galleria mellonella* and *Mus musculus* (Swiss mice). The data demonstrated a greater tolerance to the compounds than the equivalent use of cisplatin (McCann *et al.* 2012). Advancements from these complexes took the form of a di-copper cytotoxin, $Cu(II)(\mu\text{-terephthalate})(Phen)_4]^{2+}$. This complex was proven to be a powerful, non-sequence-specific, minor-groove oxidizer of duplex DNA which is capable of operating independently of exogenous reagents. The compound also shows exceptional *in-vitro* cytotoxicity towards cisplatin resistant ovarian cancer cells, producing intracellular

reactive oxygen species upon nano-molar exposure (Prisecaru *et al.* 2012). Phen ligated to Cu(II) was further demonstrated in 2013 with the production of a family of sterically functionalized pendant carboxylates complexes. These adaptions to the ligand structure resulted in a 10-fold increase in dsDNA binding and a reduced incidence of bovine serum albumin binding. The substances recorded increased cytoselectivity between human cancer cells, bacteria, and fungal cells. With only a small percentage of the cells showing evidence of dsDNA cleavages indicated as γH2AX foci the Cu(II) *bis*-phen complex could only be described as a non-selective cytotoxin with "promiscuous" activity (Prisecaru *et al.* 2013). The study by Slator *et al.*, (2016). was the most in-depth to our knowledge on the biological mechanistic activity of Cu(II) phenanthroline-based metallodrugs where the [Cu(*o*-phthalate)(phenanthroline)] complex was examined. Through the use of the COMPARE algorithm on the National Cancer Institute's (NCI) Development Therapeutics Program, 60 human cell line screen panel, competitive fluorescence binding, intracellular oxidation, ROS scavenging, mitochondrial membrane depolarization, annexin V and caspase 3, 7, 8 and 9, a mechanism of action was constructed of this copper complex. Caspase 8 and 9 were activated in this study indicating that both the intrinsic and extrinsic apoptotic pathways were implicated along with mild induction of annexin V, an apoptotic marker. The generation of superoxide was shown to play a role in DNA oxidation along with depolarization of the mitochondrial membrane potential resulting in caspase mediated apoptosis. The NCI-60 cell line panel indicated a differential mode of action to the clinical therapeutics cisplatin and bleomycin, while showing a similar mode of action to that of topoisomerase I inhibitors (Slator *et al.* 2016).

1.4.3 Cu(II) phenanthroline-phenazine complex development

Cu-phenanthroline chemotype $[Cu(phen)_2]^{2+}$, was capable of binding nucleic acids and proteins but was however unable to be directed towards specific intracellular targets limiting its capability. With the identification of the highly ordered intercalative DNA properties of the dipyridophenazine ligand bound to ruthenium(II), its ligating to the Cu-phenanthroline chemotype provided an opportunity to assess its intercalative properties and mechanism of action in the cell.

The identification of the Λ-$[Ru(phen)_2dppz]^{2+}$ ruthenium "light switch" complex (Niyazi *et al.* 2012) (**Fig. 1.10**) has generated considerable interest into the nature of its DNA intercalative properties, with crystal structures of ruthenium complexed Λ-$[Ru(phen)_2dppz]^{2+}$ showing two intercalation modes and specific ordering of water in the DNA minor groove (Niyazi *et al.* 2012; Hall *et al.* 2013). The "light switch" properties of Λ -$[Ru(phen)_2dppz]^{2+}$ upon nucleotide binding have applications in both biosensors (Barsan *et al.* 2008) and therapeutics (Yu *et al.* 2012). Given the excellent intercalative properties of phenazine ligands when present within Ru(II) complexes, their incorporation into Cu(II) phenanthroline chemical nucleases presented us with a good opportunity to advance the current state-of-art.

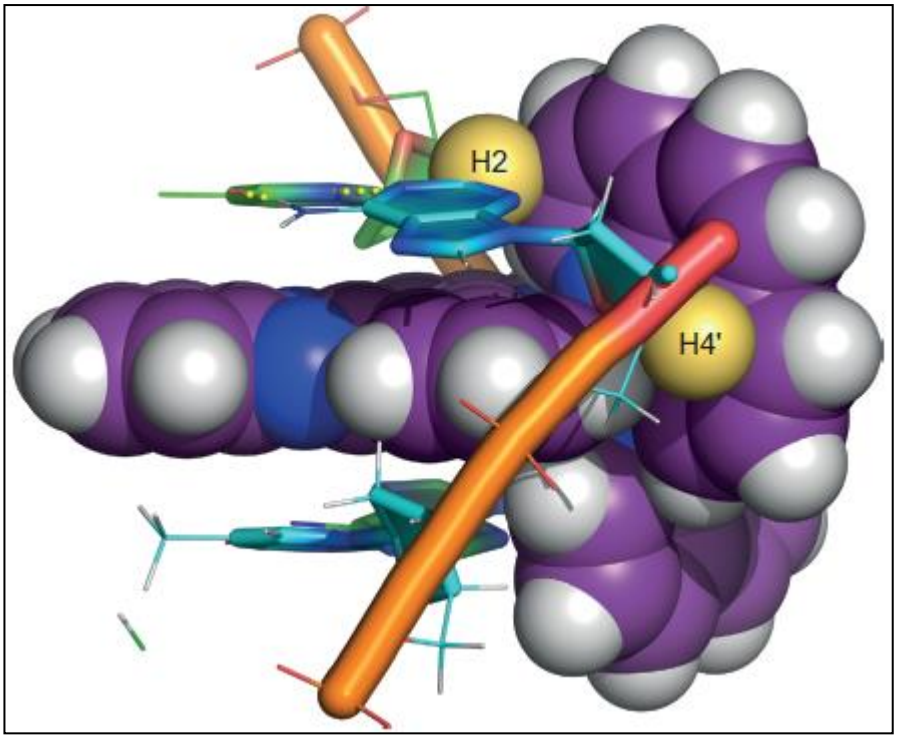

Fig 1.10 Space-filled model of a ruthenium(II) complex of dipyridophenazine (DPPZ) intercalating with DNA acquired from crystallographic data. Image adapted from Niyazi *et al.* (2012).

The Cu(II) chemical nucleases of $[Cu(phen)(N,N')]^{2+}$ carrying designer phenazine type-intercalators (where *N,N′* represents phen = 1,10-phenanthroline, DPQ = dipyrido[3,2-*f*:2′,3′-*h*]quinoxaline, DPPZ = dipyrido[3,2-*a*:2′,3′-*c*]phenazine, DPPN = benzo[*i*]dipyrido[3,2-*a*:2′,3′-*c*]phenazine) (**Fig. 1.11**) were synthesised and examined in order to identify how the systematic extension of the ligated phenanthrene ligand influences nucleotide binding affinity, base selectivity, oxidative chemical nuclease activity, and cytotoxicity within human cancer cells. Examination of their DNA binding constants revealed the highest activity of currently known Cu(II) phenanthrene compounds with thermal melting experiments indicated intercalation through both minor and major groove of the DNA and comparable activity in SKOV3 cells to doxorubicin (Molphy *et al.* 2014).

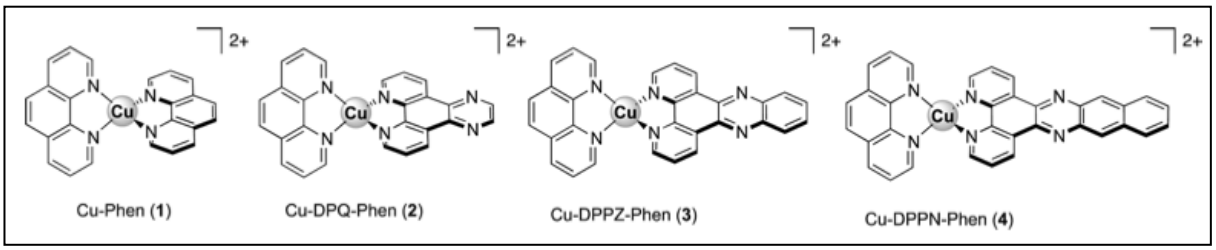

Fig. 1.11 Molecular Structure of the Cu(II) phenanthroline-phenazine complex series. Image adapted from Molphy *et al*. (2014).

The use of pUC19 DNA showed strong nuclease ability, with an enhanced activity in G-C rich regions of DNA. This finding has led to possibility that the complexes mode of action may include the targeting of cytosine-phosphate-guanine (CpG) islands, which are found in the promoter regions of many mammalian genes. The subsequent study investigation of their DNA properties demonstrated 8-oxo-2′-deoxyguanosine (8-oxo-dG) lesions, generated from the metal-hydroxo or free hydroxyl radicals (•OH) species produced from hydrogen peroxide (Molphy *et al.* 2015). The work to date on Cu(II) phenanthroline-phenazine complexes has established their cytotoxic, DNA-binding and the ROS DNA cleavage properties. However, an in-depth biological mechanistic study of these complexes was required to elucidate their mechanism of action and this has therefore formed the basis of the research reported herein. Three candidate Cu(II) complexes were selected for this study from the initial biological screen on the basis of their potential chemotherapeutic activity. These were, dipyrido[3,2-*f*:2′,3′-*h*]quinoxaline (DPQ), dipyrido[3,2-*a*:2′,3′-*c*]phenazine (DPPZ) and benzo[*i*]dipyrido[3,2-*a*:2′,3′-*c*]phenazine (DPPN) present as a π-backbone extension of the aromatic phenanthroline ligand to the $[Cu(Phen)_2]^{2+}$ scaffold (**Fig. 1.9**). Their structures are illustrated in **Figure 1.11** with the Cu-phenanthroline scaffold represented as Cu-Phen (**1**), the single

phenazine π-backbone extension of DPQ represented as Cu-DPQ-Phen (**2**), the double phenazine π-backbone extension of DPPZ represented as Cu-DPPZ-Phen (**3**) and the triple phenazine π-backbone extension of DPPN represented as Cu-DPPN-Phen (**4**). The numbered nomenclature of the Cu-complexes presented in **Figure 1.11** are referred to in this manner throughout this thesis.

1.5 Biological mechanistic approaches to screening novel therapeutics

1.5.1 Approaches to biological evaluation

The data generated on the evaluation of Cu(II) coordinated complex as detailed above has extensively involved *in-vitro* mammalian cell models such as MCF-7, HT-29, SKOV-3 and PC-3 among several other cancerous immortalized tumour cell lines. The *in-vitro* mammalian cell models form the bedrock to allow therapeutic development not just for Cu(II) complexes and other metal-based drugs as well as the vast majority of pharmaceutical and biopharmaceutical development. *In-vivo* models are utilised typically after initial validation in *in-vitro* models to assess the activity of the therapeutic at the system level and in turn provide potential information regarding mechanism of action, clinical efficacy and toxicity.

To-date the mechanistic investigations of Cu(II) complexes and indeed many other metal-based drugs has focused on the production of ROS (with species delineation), DNA binding and damage (through DNA nuclease assays and *in-vitro* γH2AX immunofluorescent detection), depolarization of the mitochondrial membrane potential, and the production of known markers of apoptosis.

1.5.2 *In-vitro* and *in-vivo* models in therapeutic evaluation

The key challenge for the design and testing of novel therapeutics is the ability to evaluate the capability of the compound in a biological environment that closely resembles human physiology. *In-vitro* and *in-vivo* models are commonly used for the purpose of pre-clinical evaluation. The use of *in-vitro* mammalian cell lines forms the foundation of pharmaceutical evaluation with the *in-vivo* methodology commonly used to progress the stage of evaluation to more human-like physiological response. One of

the most common approaches (used in this study) is the identification of active pharmaceutical candidates through the use of *in-vitro* phenotypic screens. Phenotypic screening utilises the different properties of the tissue of origin to evaluate the response of the drug candidate. This approach has been extensively utilised over the last few decades since the isolation of the first immortal cell lines and has been formalised based on tissues and cell lines by the NCI (NCI-60 Therapeutics Development Program) (Shoemaker 2006), NIH (LINCS project) (Yu *et al.* 2016), Broad institute (drug sensitivity study) (Barretina *et al.* 2012), and the Wellcome Trust Sanger Institute (Garnett *et al.* 2012). With the use of phenotypic screening the effects of novel therapeutics can be determined by the selective cytotoxicity, inhibition of proliferation and decrease in the overall cancer cell size. These characteristic changes allow for the initial screening of the activity of the novel compound thereby permitting a more detailed mechanistic evaluation (Liu *et al.* 2017). The evaluation of Cu(II) complexes has utilised *in-vitro* mammalian cell lines to identify functional activity through cytotoxicity screening and mechanism of action studies of Cu(II) complexes. HT-29 (colon carcinoma) (Kellett *et al.* 2011a; Kellett *et al.* 2011b; Kellett *et al.* 2012), MCF-7 (breast adenocarcinoma) (Kellett *et al.* 2011b; Kellett *et al.* 2012), PC-3 (prostate carcinoma) (Prisecaru *et al.* 2013) and SKOV-3 (ovarian adenocarcinoma) (Kellett *et al.* 2012; Prisecaru *et al.* 2012; Prisecaru *et al.* 2013; Molphy *et al.* 2014; Thornton *et al.* 2016; Slator *et al.* 2017) have been extensively utilised in previous Cu(II) complex and other metal-based screening and mechanistic evaluation as part of the Dublin Institute of Technology – Dublin City University – Maynooth University collaboration. In addition to their extensive prior use in this study, these four cell lines are members of the NCI-60 therapeutics development program, included in this panel due to their diverse phenotypic characteristics in the specific tissue type. In 2015 SKOV-3 cells

were found to provide poor genetic fidelity to their tissue of origin and atypical growth pattern when transplanted as subcutaneous xenografts. SKOV-3 cells however have maintained a strong presence in published to date in ovarian cancer research and in particular their use a model in testing cisplatin senstivity and resistance (Elias *et al*. 2015). *In-vivo* models typically involve the use of mice, rats, dogs or monkeys to evaluate the mortality endpoints and other toxicity profiles such as hepatic, cardiovascular and nephrotoxicity. Along with *in-vivo* mortality, each of these toxicity profiles allows for the collection of potential adverse effects in humans. In addition to these assays, advanced methods of simulating the studied tumour in an *in-vivo* environment such as cell line xenografts, patient-derived xenografts and genetically engineered mice are being utilised to provide a more faithful testing platform for evaluating the efficacy of novel therapeutics (Liu *et al.* 2017). *In-vivo* evaluation of novel therapeutics has many advantages, however the resources required to regularly examine the efficacy of developmental therapeutic candidates is seldom readily accessible in the academic setting. *Galleria mellonella* larvae represent a new model for pre-mammalian *in-vivo* assessment of novel metal-based drugs. With insects being one of the most ubiquitous groups of invertebrates on the planet (Elzinga 2004), their use in the evaluation of new therapeutics is being increasingly recognised as a valuable initial screening step for the later evaluation in *in-vivo* mammalian models (e.g. *Mus musculus*). At the point of evolutionary divergence of invertebrates and vertebrates, a shared innate immune response was supplemented by an adaptive immune response in the vertebrates system (Cooper and Alder 2006; Bailey *et al.* 2013; Viljakainen 2015). The similarities of the innate immune system in the two branches of life have continued to be comparable (Kavanagh and Reeves 2004; Renwick *et al.* 2007; Kelly and Kavanagh 2011; Browne *et al.* 2013). This comparability allows insects to be used in

therapeutic evaluation of novel drugs and coupled with their lower financial and ethical drawbacks provide a good opportunity to be a predictive platform for subsequent mammalian studies (Kemp and Massey 2007; Cook and McArthur 2013). *G. mellonella* along with their similar innate immune system to mammals represent a basic normal tissue model whose results can later leed to refinement and targeting of specific biological process in mammalian testing. While they are not a replacement for mammalian *in-vivo* models they do offer a rapidly deployable screening system which can inform therapeueitc development. In addition to the biological similarities of both *in-vivo* models, international funding agencies are increasingly adopting an approach of Replacement, Reduction and Refinement (3R) policy whenever possible to augment the use of *in-vivo* animal models and implement valid and ethically acceptable screening systems (Kilkenny *et al.* 2010).

1.5.3 *In-vitro* mechanistic evaluation (ROS, γH2AX, apoptosis and mitochondrial related toxicity)

1.5.3.1 Cellular viability and ROS

The physiological state of the cell has for decades been the basis for the evaluation of bio-molecular processes and has been the mainstay of pharmacological assessment of novel targets and treatment approaches. Viability assays such as tetrazolium salts rely on the metabolic capability of the cell to produce a reduction environment that can be measured. The MTT assay produces a formazan product from the substrate 3-(4,5-dimethylthiazol-2yl)-2,5-diphenyl tetrazolium bromide primarily through mitochondrial action in the cell. The production of this product occurs due to the activity of

mitochondrial enzymes NADPH, FADH, FMNH, NADH and other cytochromes (Mosmann 1983; Vega-Avila and Pugsley 2011).

ROS are a collection of heterogeneous group of diatomic oxygen from free and non-free radical species. The activities of enzyme-catalysed reactions are a major contributor to the presence of ROS. With this in mind, the physiological production of ROS is counteracted by antioxidant enzymes such as catalase, superoxide dismutase and glutathione. The examination of the presence of ROS species provides important support information about the state of the cell and activity mechanisms of the test agents (Dada and Sznajder 2011). The fluorescent dye 2′,7′-dichlorodihydrofluorescein diacetate (H_2DCFDA) is a reduced form of fluorescein commonly used to indicate the presence of ROS in cells evaluating this mechanistic quality of novel therapeutics (Gibson 2013). The use of the MTT cell viability assay along with ROS identification coupled with selection of tissue specific mammalian cell lines provides the opportunity to assess the potential cytoselectivity properties of novel therapeutics. A range of cell lines have been characterised through the MTT and 2′,7′-dichlorodihydrofluorescein diacetate assay as part of the ongoing collaboration between Dublin Institute of Technology – Dublin City University – Maynooth University (Kellett *et al.* 2011a; Kellett *et al.* 2011b; Kellett *et al.* 2012; Prisecaru *et al.* 2012; Prisecaru *et al.* 2013; Molphy *et al.* 2014).

The production of ROS is a regulated process related to mitochondrial function. ROS generation in the mitochondria primarily takes the form of superoxide ($O_2^{-\cdot}$), which is converted to H_2O_2 by either spontaneous dismutation or through the enzyme Superoxide Dismutase (SOD). The activity of Fenton chemistry can drive the production of $OH^{\cdot}$ in

the presence of metal ions (Craig and Marszalek 2002). Mitochondrial ROS production occurs at different stages of the oxidative phosphorylation pathway. The main production of $O_2^{-\cdot}$ occurs in complex III during the Q cycle at the Q_O site in the form of $QH^{\cdot}$ (Turrens 1997; St-Pierre *et al.* 2002; Muller *et al.* 2003). The majority of $O_2^{-\cdot}$ from the Q_O is made facing the intermembrane space (St-Pierre *et al.* 2002), which has led to the suggestion that $O_2^{-\cdot}$ species may transit through the Voltage-Dependent Anion Channel (VDAC) (Han *et al.* 2003), and subsequently identified to have a role in apoptosis (Shoshan-Barmatz *et al.* 2010). A central component to homeostatic balance is the regulation of free radical chemistry in the cell. Free radicals can be generated by multiple processes leading to the production of a chemical species with one or more unpaired electrons. ROS represents the primary speciation method with Reactive Nitrogen Species (RNS) also contributing. ROS are primarily produced in the mitochondria and by Nicotinamide Adenine Dinucleotide Phosphate (NADPH) oxidases. In addition to being a by-product of cellular metabolism, ROS has also been shown to contribute to the immune response (Dan Dunn *et al.* 2015). The Electron Transport Chain (ETC) is known to have a strong influence on the production of ROS with Quinlan and co-workers showing the 2-oxoacid dehydrogenase and pyruvate dehydrogenase complex have a strong contribution to this process (Quinlan *et al.* 2014). ROS production in the cytosol in addition to the mitochondrial derived can stimulate additional production through the redox sensitive Protein Kinase C (PKC) isoforms and the Src family of kinases following activation with angiogenesis II signalling (Nazarewicz *et al.* 2013; Kröller-Schön *et al.* 2014; Quinlan *et al.* 2014).

1.5.3.2 Mitochondrial dysfunction and apoptosis

Apoptosis is a major form of regulated cell death in the body and has functions ranging from tissue formation at embryonic stages to immune cell effector function (Green 2011). The process of apoptosis has numerous links to pathogenic processes and has implication for drug action and therapeutic responses (Hassan *et al.* 2014; Baig *et al.* 2016; Delbridge *et al.* 2016). Apoptosis forms one of the 'Hallmarks' of cancer and as such the targeting with therapeutics has been of considerable interest (Hanahan and Weinberg 2000; Hanahan *et al.* 2011). The process of programmed cell death (apoptosis) is usually described through both the intrinsic and extrinsic pathways (**Fig. 1.12**). Both these pathways provide the primary means through which apoptosis occurs in the cell. The mitochondria is one of the primarily driver of cellular energy, central to this is the maintenance of its membrane potential, which permits the proton gradients to be maintained. The loss of the mitochondrial membrane potential which can be brought about through a variety of mitochondrial stressors, induces the release of Secondary Mitochondria-derived Activators of Caspases (SMAC) and cytochrome *c* which results in the oligomerization of Apoptotic protease activating factor-1 (Apaf-1) and the formation of the apoptosome. The apoptosome cleaves pro-caspases to activate the initiator caspase, caspase 9, ultimately resulting activation of the effector caspase, caspase 3 (Ichim and Tait 2016). This process constitutes the intrinsic apoptotic process which can also be inhibited through the action of the BCL-2 and XIAP family of proteins. The extrinsic pathways of apoptosis operate through the activation of cell surface receptor activation. The Tumor Necrosis Factor-1 (TNF-1) and Fas receptor are both capable of activating apoptosis through ligand binding and the subsequent cleavage of pro-caspase 8 and 10 resulting the activation of the effector caspases, caspase 3 and 7 resulting in apoptosis (Ichim and Tait 2016). Both the intrinsic and extrinsic pathways

of apoptosis share common components and are capable of effecting each other through activation of the pro-apoptotic factors BAX, BH3 interacting-domain death agonist (BID) and BCL-2 homologous Antagonist Killer (BAK) (Ichim and Tait 2016). The activation of apoptosis as a mechanism of triggering cell death in relation to the therapeutic action of metal based drugs such as cisplatin (Kim *et al.* 2004; Zhang *et al.* 2008; Michaud *et al.* 2009; Gumulec *et al.* 2014), has been a prominent research goal in drug development. The investigation of different copper coordination complexes has also extensively utilised apoptosis as a means to investigate the mechanism and therapeutic utility of novel metal-based drugs (Thati *et al.* 2007; Filomeni *et al.* 2009; Idan Valencia-Cruz *et al.* 2013; Zuo *et al.* 2013; Montagner *et al.* 2015; Fan *et al.* 2017). Autophagy is another form of cell death not described until the 1990s has shown increased interest in its use as an endpoint for metal-based drug mechanistic assessment (Slator *et al.* 2017). Many metal-based therapeutics and other small molecules under evaluation are capable of generating both ROS and RNS species which ultimately trigger different forms of cell death which has become important to differentiate, especially in relation to cancer treatment (Li *et al.* 2012; Gibson 2013). The activity of the mitochondrial has important roles in the generation of oxidative radicals and a fundamental position in intrinsic apoptosis. To this end the monitoring of caspases indicative of both intrinsic and extrinsic apoptotic process (**Fig. 1.12**) have previously been examined through the use of fluorescent inhibitors specific for each of the cysteine endoproteases (Slator *et al.* 2016, 2017). In addition to the apoptotic markers the assessment of mitochondrial health through membrane permeability assessment using either 5,5′,6,6′-tetrachloro-1,1′,3,3′-tetraethylbenzimidazolocarbo-cyanine iodide (JC-1) or Rhodamine 123, which are fluorescent cationic dyes sensitive to the proton gradient in the mitochondria and accumulate after the collapse of the membrane potential (Slator

et al. 2016, 2017). The assessment of the activation of specific apoptotic markers provides an avenue into the mechanism of action of metal-based drugs and additionally an evaluation of their mechanism of action in cisplatin resistant cell lines.

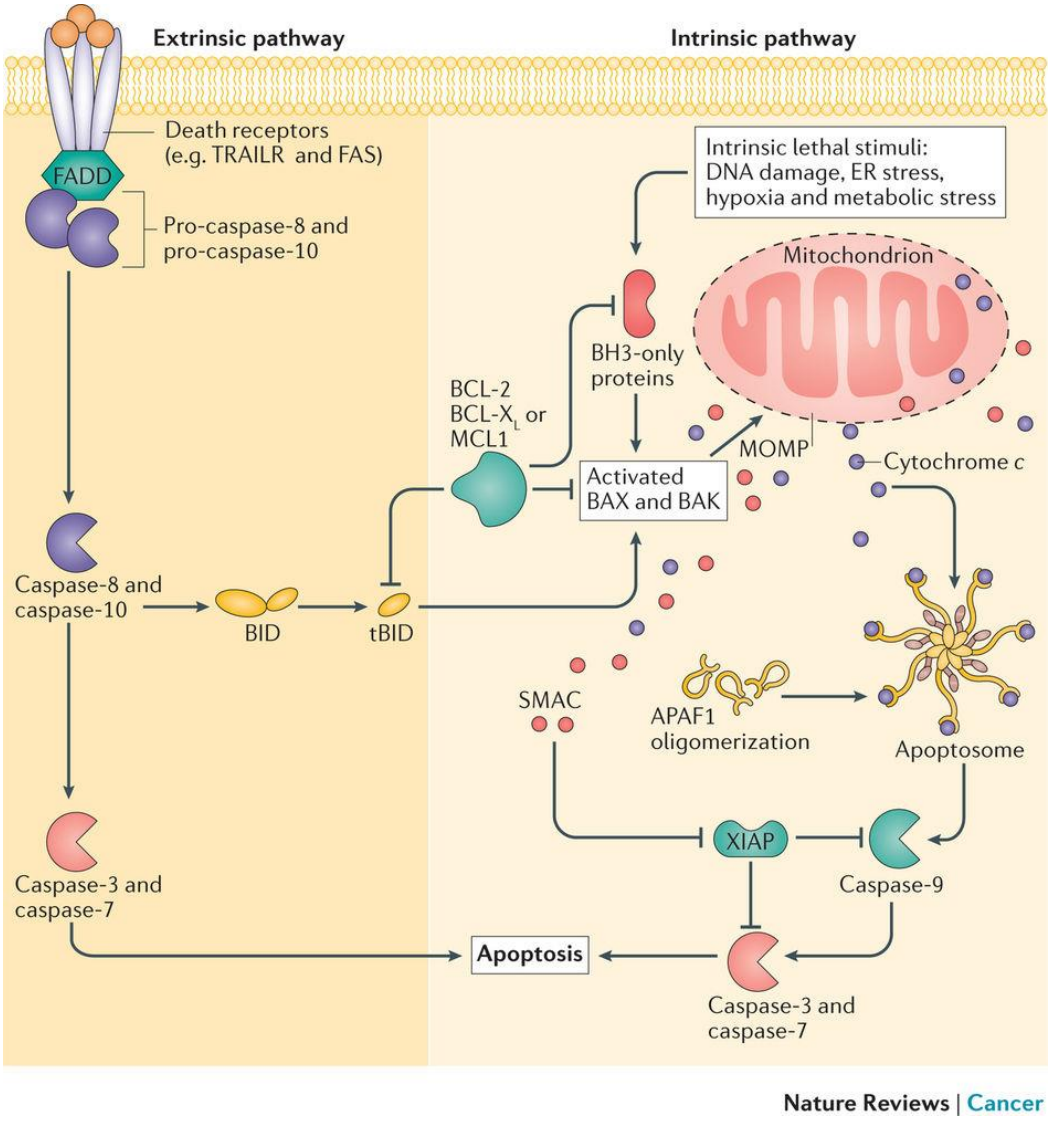

Fig. 1.12 Overview of intrinsic and extrinsic apoptosis pathways. Image adapted from Ichim and Tait, (2016).

1.5.3.3 DNA binding and damage

The integrity of DNA is a central part of cellular homeostasis and is managed through a complex molecular choreography of interacting repair enzymes which respond to a variety of DNA damage and forms a central focus in the mechanism of action of many

drugs. The discovery and subsequent development of cisplatin, a DNA interacting drug has provided a strong developmental objective for using other transition metal-based coordination compounds to target DNA integrity and subsequently disrupt cellular survival. Many metal-based drugs function through the generation of oxidative species. The kinetic properties of copper metal-based drugs are believed to operate under Fenton-like conditions where the catalytic cycle of Cu^{+}/Cu^{2+} produces different oxidative species (Molphy *et al*., 2014). The oxidative species generated are believed to induce oxidative DNA base modification, primarily through the formation of 8-oxo-G which precipitates a modification in the interstrand cross-linking and subsequent disruption of DNA integrity (Cadet *et al*., 2017). Biological nucleases such as endonuclease and exonucleases function by hydrolyzing internal bonds within the polynucleotide chain thereby separating the polynucleotide chain. Restriction endonucleases have been extensively used in recombinant DNA technologies. Due to the crucial activity that nucleases play in DNA integrity and manipulation, there has been considerable interest in the development of metal based drugs targeting this process as an alternative to the current nuclease active drug, bleomycin and the binding activity of cisplatin. The development of a synthetic "self-activating" metal-based drugs with this capability was a significant development in this level of DNA targeting in metal based drugs (Kellett *et al*. 2011b; Kellett *et al*. 2012). The analysis of the nuclease activity takes place initially against purified plasmid DNA and subsequently the effects on DNA in the cell are established in culture. Through the use of γH2AX fluorescent assays the visualisation of Double Stranded Breaks (DSB) formation can take place which further supports the characterisation of the nuclease capability of novel metal agents.

Copper complexes have been demonstrated to have nuclease cleaving abilities. With this process resulting in double strand DNA damage formation (Kellett *et al.* 2012; Prisecaru *et al.* 2013), subsequent DNA repair mechanism become active. The detection of DSB formation is an important metric in the effectiveness of nuclease active therapeutics. The fluorescent detection of γH2AX foci has been established as a strong indicator of the repair of DSB in DNA (Thompson 2012). The immunodetection of γH2AX foci through flow cytometry and confocal microscopy has been part of a biological evaluation of previous Cu(II) phenanthroline complexes as part of the Dublin Institute of Technology – Dublin City University – Maynooth University collaboration (Kellett *et al.* 2012; Prisecaru *et al.* 2013).

1.5.3.4 Utilisation of *G. mellonella* for the evaluation of the Cu(II) complex series

The use of the mortality assays has been a common tool for the evaluation of the tolerance and toxicity of metal-based drugs in *G. mellonella* for several years (Rowan *et al.* 2009; Kellett *et al.* 2011a; Biot *et al.* 2012; McCann *et al.* 2012; McCann *et al.* 2013; McGinley *et al.* 2013; Browne *et al.* 2014). The analysis of the cellular immune response through the measurement of the insect haemocyte count and sub populations provides a useful metric of the organism's immunogenic response to metal-based drugs. Previously the measurement of haemocytes have been used to evaluate immune response to silver SBC3 (Browne *et al.* 2014), in addition to other studies using the Lepidoptera species as model for human related infections (Cotter *et al.* 2000a; Coyle *et al.* 2004; Kavanagh and Reeves 2004; Renwick and Kavanagh 2007; Rowan *et al.* 2009; Kavanagh and Fallon 2010; Browne and Kavanagh 2013; Browne *et al.* 2014). Furthermore, expanding on the investigation of the immune response with humoral elements and in particular the examination of Inducible Metalloproteinase Inhibitor

(IMPI) and transferrin gene expression and proteomic analysis has expanded the evaluative capacity of activation of the immune system (Bergin *et al.* 2006; Mowlds and Kavanagh 2008; Mowlds *et al.* 2008; Kelly and Kavanagh 2011; Browne *et al.* 2014).

The publication of the *G. mellonella* transcriptome in by Vogel *et al*, (2011) permitted the production of a cDNA library which could then be used to develop a proteomics database based on known protein homology and the opening to the application of Label Free Quantitative (LFQ) proteomics. The application of LFQ proteomics in the Lepidoptera model has permitted a higher resolution evaluation of the mechanism of action of novel Cu(II) complexes and in other settings such as the effects of food preservatives (Maguire *et al.* 2017) and effects of secondary metabolites of entomopathogenic fungi (Mc Namara *et al.* 2017).

1.6 Thesis synopsis

The development of chemotherapeutic drugs has produced a large repertoire of available therapeutics for a range of malignancies, despite this achievement resistance continues to be an ongoing issue in particular to the highly successful metal-based drug, cisplatin. The copper(II) complexes described in this PhD thesis represent a rationally designed suite of copper(II) coordinated phenanthroline-phenazine complexes capable of therapeutic action *in-vitro* Additionally, their biological profile of activity has been examined in the *G. mellonella in-vivo* model, developing ideas and targets for future *in-vivo* mammalian work. These complexes have been synthesised and characterised by Molphy *et al*. (2014) and (2015), under the project supervision team and have demonstrated promising chemotherapeutic potential, exceeding that of the existing chemotherapeutic drugs. Overall Molphy *et al.* (2014) and (2015) has demonstrated the DNA intercalative, oxidative, redox properties and *in-vitro* activity of this series of Cu(II) complexes. While this information provides a high level assessment of the activity of the complexes in the cell, it is not capable of examining wider non-targeted changes at the genomic and proteomic levels which can provide a more comprehensive assessment of the mechanism of action.

The biological investigations in this project sought to advance the existing mechanistic evaluation of Cu(II) complexes through using traditional mechanistic evaluations with contemporary molecular methodologies of gene expression and proteomics. The fusion of these two approaches has enabled an in-depth elucidation of the pathways associated with ROS induction, apoptosis, mitochondrial toxicity, drug sensitivity and resistance pathways. This project also sought to utilise the highly versatile *in-vivo* Lepidoptera model, *G. mellonella* as a pre-mammalian screen of the activity of the novel Cu(II)

complexes and identify further therapeutic targets for evaluation in *in-vivo* mammalian models. These approaches overall will expand the biological scope of the evaluations of developmental inorganic chemotherapeutics and identify key biological pathways and targets for future therapeutic development.

Chapter 2: Screening of novel Cu(II) phenanthroline-phenazine complexes in *in-vitro* mammalian cell models

2.1 Introduction

The work in this chapter describes the initial *in-vitro* exposure of Cu(II) phenanthroline-phenazine complexes to a group of phenotypically diverse mammalian cancer cell lines. The cell viability was assessed through the MTT tetrazolium dye (3-(4,5-dimethylthiazol-2-yl)-2,5-diphenyltetrazolium bromide) which measured the activity of NAD(P)H-dependent cellular oxidoreductase enzymes. The MTT assay was followed up using characterisation tests such as Reactive Oxygen Species (ROS) production in the HeLa cell line, DNA Double Strand Break (DSB) formation using γH2AX foci examination in both MCF-7 and SKOV-3 cell lines and activation of inflammatory and apoptotic markers using Reverse Transcriptase quantitative-Polymerase Chain Reaction (RT-qPCR) gene expression across all the cell lines.

The following cell lines representing different tumour types were subjected to the MTT viability assay to establish the active concentration of the Cu(II) phenanthroline-phenazine complexes for subsequent screening and characterisation experiments: MCF-7 (breast adenocarcinoma) (Le Bivic *et al.* 1988), HT-29 (colonic carcinoma) (Davis *et al.* 1998), PC-3 (grade IV prostate adenocarcinoma) (Tai *et al.* 2011), OE-33 (oesophageal adenocarcinoma) (Timme *et al.* 2013), HeLa (cervical carcinoma) (Masters 2002), SKOV-3 (cisplatin resistance, original ovarian origin and widly used in ovarian research) (O'Connor *et al.* 1997; O'Neill *et al.* 1999), A2780 (ovarian adenocarcinoma) (ECACC Cat. No. 93112519) and the cisplatin resistant variant (A2780/ Cis) (Espina *et al.* 2017).

The HT-29, MCF-7, PC-3 and SKOV-3 cell lines are part of the NCI developmental therapeutics program, which provided a strong case for their use in evaluating the

mechanistic characteristics of these novel chemotherapeutic drugs. Additionally, comparability of therapeutic activity between different cell lines derived from various tissues has been an ongoing challenge in medicinal chemistry. With this challenge, the use of the ovarian cancer cell lines, A2780 and its cisplatin resistance variant (A2780/ Cis) provided a better platform for comparing the action of novel therapeutics against known resistant variants of the same cell line.

The measurement of apoptosis through fluorescent detection of specific apoptotic markers has previously been performed with copper and manganese complexes (Slator *et al.* 2016, 2017). The apoptotic activity along with inflammation and DNA damage can also be monitored by qRT-PCR by assessing changes in gene expression. Inflammation was measured through the expression of Interleukin-6 (IL-6) and Nuclear Factor-κB (NF-κB). IL-6 and NF-κB are often synergistic in their response with activation of NF-κB in-turn leading to the upregulation of IL-6 (Aggarwal *et al.* 2006). Poly (ADP-ribose) polymerase 1 (PARP1) is a key protein involved in the repair of single strand breaks through Base Excision Repair (BER) (Kraus and Hottiger 2013). The artificial nuclease capacity of Cu(II) phenanthroline-phenazine complexes makes the measurement of PARP1 an important marker of DNA damage, this was utilised in this study. Apoptosis is a key process in controlled cell death and its measurement is an important process for the *in-vitro* mechanistic assessment of copper complexes. The genes used in this study are involved in regulating the switch into apoptosis (B-cell Lymphoma 2 (BCL-2) and Bcl-2 associated X protein (BAX)), the initiation of apoptosis (Caspase 9) and its execution (Caspase 3 and Second Mitochondrial-derived Activator of Caspases (SMAC)). BCL-2 and BAX are part of the BCL-2 family of regulatory apoptotic proteins. BCL-2 functions in an anti-apoptotic manner while BAX

is pro-apoptotic (Gross 2016). Pro-apoptotic BAX is responsible for forming the mitochondrial membrane transition pores that permeabilising the membrane and releasing cytochrome *c* into the cytosol.

Cytochrome *c* is known to recruits Apoptotic Protease Activating Factor 1 (APAF-1) and initiator Caspase 9 to form the apoptosome. This results in the activation of the apoptotic executioner Caspase 3 (Würstle *et al.* 2012; McIlwain *et al.* 2013). The breakdown of the mitochondrial membrane also releases SMAC, potentiating the activation of caspases and inhibiting Inhibitors of Apoptosis (IAP's) activity (Du *et al.* 2000). The action of XIAP, IAP1 and IAP2 functions in inhibiting the pro-apoptotic activity of caspases. XIAP, IAP1 and IAP2 all contain ubiquitin-ligase that counteracts the cysteine-aspartic protease activity of caspases which promotes a strong inhibition of apoptosis (Estornes and Bertrand 2014). In addition to the inhibition of caspases, IAP's have been demonstrated to have a pro-survival strategy activating NF-κB (Bertrand *et al.* 2008). The measurement of IAP activity provided information regarding the inhibition of apoptosis and whether cell survival was related to apoptosis inhibition or another mechanism after cellular exposure to the Cu(II) phenanthroline-phenazine complexes.

The objective of this work was to conduct an *in-vitro* screen of the Cu(II) complexes on a range of cell lines. This initial viability screen also established the IC_{25}/ IC_{50} of each complex that was applied to the further mechanistic studies of ROS induction, γH2AX DNA DSB formation and gene expression of selected markers indicative of a range of cellular mechanisms including inflammation, DNA damage, and apoptosis induction.

2.2 Material and Methods

2.2.1 Mammalian cell culture conditions and maintenance

The MCF-7, HT-29, OE-33, PC-3, SKOV-3, HeLa, A2780 and A2780/ Cis cell lines were obtained from the Radiation and Environmental Science Centre (RESC), FOCAS Research Institute cell bank or commercially obtained through ATCC or ECACC. Each cell line was stored at -80 ˚C in a cryovial containing 1 ml of cells in 10 % DMSO (Sigma, Ireland) (cat# 276855). Each vial was thawed slowly and placed into 20 ml of Roswell Park Memorial Institute (RPMI-1640) media (Sigma, Ireland) (Cat# R8758) supplemented with 12 % Foetal Bovine Serum (Sigma, Ireland) (Cat# F2442) and 2 % L-glutamine 200mM (Sigma, Ireland) (Cat# G7513) (Appendix 1.1.1) in a T75 cell culture flask (Sigma, Ireland) (Cat# CLS3276). Cells were incubated for 24 h at 37 °C and in 5 % CO_2 atmosphere to allow adherence to the base of the flask and enter the log growth phase. Cells were monitored each day until 85-90 % cell confluency was reached and they were then subcultured for routine maintenance or experimentation.

Subculturing involved first removing the cell culture media from the monolayer of cells, then adding 10 ml of trypsin solution (Thermo, Ireland) (Cat# 15090046) (Appendix 1.1.2) : EDTA (Sigma, Ireland Cat# E9884) (1:1) to remove any dead or detached cells from the population. The remaining 10 ml of trypsin solution was added and the cells were incubated at 37 °C for 1-2 min approximately to remove cells from their monolayer on the base of the flask. Cells were placed in 10 ml of fresh culture media to deactivate the trypsin enzyme and produce the 20 ml single cell stock suspension. This stock cell suspension was used to seed different cell densities in T75 stock flasks to maintain the cells in culture. The stock cell solution was also used for subsequent

experiments described below. Cells were stored in liquid nitrogen as described in appendix 1.1.3 when not in use.

2.2.2 The MTT viability assay

2.2.2.1 Cell counting and plating

One ml of cell suspension was placed into 20 ml of isoton electrolyte solution (BD, Ireland) to conduct a cell count and determine the required volume of cell suspension for plating. A Beckman COULTERTM Z1 coulter®(Beckman-Coulter, USA) particle counter was used to count the number of cells per ml in solution. Cells were subcultured at different densities according to their morphology and growth characteristics and determined by pre-optimisation experiments. A lower number of cells were plated for 48 h analyses compared to 24 h to allow for cell growth through the mammalian cell cycle.

MCF-7, OE-33, SKOV-3, HeLa, A2780 and A2780/ Cis cells were plated at 5×10^2 cells into each well for the 24 h exposure and 2.5×10^2 into the 48 h exposure on a clear 96-well plate (Thermo Fisher Scientific, Ireland) (Cat# 167008). The HT-29 cell line was plated with 10^3 cells for 24 h and 8×10^2 cells for 48 h. The PC-3 cell line was plated at 2.5×10^2 cells for 24 h and 1.25×10^2 cells for 48 h experiment. The 96-well plate set-up is illustrated in Appendix 1.1.4 with all exposures (μM) performed in triplicate with independent stock cultures (independent experiments) to ensure *in-vitro* statistical validity.

2.2.2.2 Drug exposure

MCF-7, OE-33, SKOV-3, HeLa, HT-29, SKOV-3, A2780 and A2780/ Cis cell lines were exposed to Cu-Phen (**1**) (Appendix 1.1.4), Cu-DPQ-Phen (**2**) (Appendix 1.1.4), Cu-DPPZ-Phen (**3**) (Appendix 1.1.4), Cu-DPPN-Phen (**4**) (Appendix 1.1.4), cisplatin (Sigma, Ireland) (Cat# P4394) (Appendix 1.1.5) and doxorubicin (Sigma, Ireland) (Cat# D2975000) (Appendix 1.1.6). Cu(II) phenanthroline-phenazine complexes nomenclature refers to the Cu(II) chemical nucleases of $[Cu(phen)(N,N')]^{2+}$ carrying designer phenazine type-intercalators (where *N,N′* represents phen = 1,10-phenanthroline, DPQ = dipyrido[3,2-*f*:2′,3′-*h*]quinoxaline, DPPZ = dipyrido[3,2-*a*:2′,3′-*c*]phenazine, DPPN = benzo[*i*]dipyrido[3,2-*a*:2′,3′-*c*]phenazine). The Cu(II) phenanthroline-phenazine complexes and cisplatin were dissolved in DMSO (ACS grade) prior to subsequent dilution in aqueous cell culture media (200 µM). Cu-Phen (**1**) and Cu-DPQ-Phen (**2**) was dissolved completly while Cu-DPPZ-Phen (**3**) and Cu-DPPN-Phen (**4**) required additional agitation to fully dissolve prior to subsequent dilution. Cisplatin fully dissolved in DMSO prior to subsequent dilution. Doxorubicin was dissolved in aqueous cell culture media (20 µM). Cu-Phen (**1**), Cu-DPQ-Phen (**2**), Cu-DPPZ-Phen (**3**) and Cu-DPPN-Phen (**4**) (Appendix 1.1.4) exposures were made with a stock of 10 µM in supplemented RPMI-1640 media and diluted further to produce a range of 0.25-10 µM (Appendix 1.1.7) for MCF-7, OE-33, SKOV-3, HeLa, HT-29 and SKOV-3 cells set up as in the 96-well plate template detailed in Appendix 1.1.8. Cells were treated with cisplatin at a range of 0.5-200 µM (Appendix 1.1.9) in MCF-7, OE-33, SKOV-3, HeLa, HT-29 and SKOV-3 cells and was set up as in the 96-well plate template detailed in Appendix 1.1.10. Cells were treated with the Cu(II) phenanthroline-phenazine complexes at a range of 0.156-10 µM (Appendix 1.1.11), doxorubicin at a range of 0.312-20 µM (Appendix 1.1.11) and cisplatin at a range of

3.125-200 µM (Appendix 1.1.12) in the following 96-well template: Cu(II) phenanthroline-phenazine complexes (Appendix 1.1.13), cisplatin (Appendix 1.1.14) and doxorubicin (Appendix 1.1.15). Cisplatin and doxorubicin are included as clinical controls due to their ability to induce their therapeutic activity primarily through DNA intrastrand crosslinking and interaction, respectively (Fornari *et al.* 1994; Jamieson and Lippard 1999). Following 24 h incubation at 37 °C and 5 % CO_2, the cell culture media was replaced with the prepared solutions. All plates were then incubated for 24 or 48 h before methylthiazolyldiphenyl-tetrazolium bromide (MTT) (Sigma, Ireland) (Cat# M5655) (5 mg/ ml) was applied. Each exposure was performed on 3 separate plates. The triplicate plates were additionally performed 3 independent times to ensure statistical validity.

2.2.2.3 MTT viability

After the 24 and 48 h drug exposure a working solution of methylthiazolyldiphenyl-tetrazolium bromide (MTT) (Sigma, Ireland) (Cat# M5655) (5 mg/ ml) (Appendix 1.1.16) was prepared and 100 µl of the solution was added to each well of the 96-well plates after the exposed cell culture media was then removed. All plates were incubated for 3 h and afterwards each well was washed (×3) with sterilised PBS (Sigma, Ireland) (Cas# 806544). After the final wash, 100 µl of DMSO (ACS grade) was added to each well and the plates were placed on a plate shaker for 15 min to allow the coloured formazan crystals to develop. The plate was then read on the 1420 Multilabel Counter Victor^{3}V spectrophotometer (PerkinElmer, USA) at 595 nm wavelength after 15 min on a plate shaker (see Appendix 1.1.17 for MTT assay working protocol).

Based on the set-up of the 96-well plate template (Appendix 1.1.8, 1.1.10, and 1.1.13-1.1.15) the absorbance data was analysed accordingly. The mean of each of the exposed concentrations was taken using the 3 independent 96-well plates along with the mean of the unexposed cells (Negative). Based on this experiment the highest absorbance was observed in the negative controls due to these cells containing the highest degree of viability compared to the compound exposed cells. The mean absorbance from the exposed cells was calculated based on the 5 replicates wells within each plate compared to the negative wells (unexposed cells). This same analysis was performed for each of the three plates in each independent experiment and an average of the 3 plates per triplicate experiment was calculated along with the standard deviation (S.D.).

2.2.2.4 Statistical analysis of data

The mean and standard deviation was calculated as described above. The standard deviation was used to measure the variability of the data set and provide information regarding the precision of the experiment. See Appendix 3 for raw data. Using Microsoft® Excel (Microsoft Corporation, USA) and the statistical package GraphPad Prism (Ver. 5.0) (GraphPad, USA), the IC_{25} and IC_{50} concentration was calculated for each cell line, time-point, complex exposure and control. The IC_{25} and IC_{50} concentration was calculated for each cell lines/ exposed to a complex or clinical drug compared to the control, per timepoint. The IC_{25} and IC_{50} concentration represents the concentration of the test exposure which produces a 25 % and 50 % inhibition of cell growth respectively. The IC_{25} rather than the IC_{50} concentration was used for subsequent chemical exposures due to the complex and high toxicity elicited by the Cu(II) phenantholine-phenazine complexes. The lower level of inhibition produced in the experimental conditions also allowed for a more sensitive investigation of early

mechanistic effects on the cellular environments. Standard deviation instead of standard error of the mean was used as a descriptive statistic in this experiment due to the better representation of variability in the data set and less random nature in describing the sampling process. Standard deviation has also been previously used in the publications of *in-vitro* cytotoxicity data. Statistical analysis to compare the changes between the Cu(II) phenantholine-phenazine complexes and either cisplatin or doxorubicin (A2780 and A2780/ Cis) was performed using one-way ANOVA with Tukey's post-hoc test.

2.2.3 Fluorescent detection of Reactive Oxygen Species (ROS)

The HeLa cell line was used to measure ROS generation owing to its common use in antioxidant investigations in the published literature. ROS production was investigated after exposure to Cu-Phen (**1**), Cu-DPQ-Phen (**2**), Cu-DPPZ-Phen (**3**), Cu-DPPN-Phen (**4**), cisplatin and the positive control hydrogen peroxide (H_2O_2) using the fluorescent 2',7'-dichlorodihydrofluorescein diacetate (H_2DCFDA) (Thermo, Ireland) (Cat# D399) dye. HeLa cells were sub-cultured from an 80-90 % confluency stock into 96-well plates at a cell density of 1×10^4 cells/ ml and incubated for 24 h to allow sufficient time for the cells to attach and grow. On the day of the experiment H_2DCFDA was dissolved in DMSO (ACS grade) at a concentration of 1 mM stock and then further diluted to 10 µM working solution in 12 % foetal bovine serum supplemented RPMI-1640 cell culture media. The working solution of H_2DCFDA dye (10 µM) was incubated with the cells for 30 min in the dark at 37 °C in a 5 % CO_2 atmosphere. After 30 min the H_2DCFDA working solution was removed and 20 µM of each of the Cu(II) phenanthroline-phenazine complexes and cisplatin with doubling dilution as in the template 96-well plate detailed in Appendix 1.2.1. A negative control of 12 % foetal bovine serum supplemented RPMI-1640 cell culture media was used for normalization

of ROS expression. Hydrogen peroxide (Sigma, Ireland) (Cat# 95321) at 0.312 µM was used as a positive control (value experimentally optimized). All 96-well plates were covered in tin foil and incubated as described above. Fluorescent measurements were taken after 15 min, 30 min, 1 h, 2 h, 3 h, 4 h and 5 h at an excitation wavelength of 495 nm and emission of 529 nm. The production of ROS was expressed relative to the negative control. An unpaired t-test was performed on the average of the normalized fluorescent measurements of both the negative control and the highest exposed concentration of either the test complexes or cisplatin. A p-value of 0.05 was used to establish statistical significance. Each normalized average was calculated from 7 measurements representing 15 min to 5 h (N=7).

2.2.4 Immuno-detection of γH2AX foci with flow cytometry

2.2.4.1 Cell preparation, exposure and immune-staining

MCF-7 and SKOV-3 cell lines were selected due to their sensitivity and resistance respectively to the Cu(II) complexes and cisplatin as determined by their initial MTT cytotoxicity screen. SKOV-3 and MCF-7 cells were subcultured at 1×10^5 cells per T25 flask (Sigma, Ireland) (Cat# CLS430639) and were incubated for 24 h to allow for attachment and growth. After the 24 h attachment and growth period the MCF-7 and SKOV-3 cells were exposed to their respective IC_{25} values over 24 and 48 h. Cells were subcultured as previously described in section 2.2.1 to generate the cell suspensions which were then pelleted by centrifugation at 120 g for 10 min. The supernatant was decanted and 200 µl of 2 % paraformaldehyde (Sigma, Ireland) (Cat# F8775) fixative solution (Appendix 1.3.1) was added and incubated for 10 min. A second centrifugation was performed at 120 g for 5 min, the supernatant removed and the cell pellet re-suspended in ice-cold 70 % ethanol (Sigma, Ireland) (Cat# 51976). The cells were

centrifuged as above for 5 min with the supernatant being discarded and the cells re-suspended in 200 µl 0.25 % Triton X-100 (Sigma, Ireland) (Cat# T8787) working solution (Appendix 1.3.2). A final centrifugation (as above) was conducted with the cell pellet then exposed to 200 µl of blocking solution (2 % BSA (Sigma, Ireland) (Cat# A9418) in PBS) and incubated for 30 min (Appendix 1.3.3). A separate aliquot of the unstained cells was placed in a new tube prior to the addition of the primary antibody and used as the auto fluorescent control.

Blocking solution was removed as before through centrifugation and pellet was re-suspended in 100 µl of the primary antibody (Milipore, Ireland) (Anti-phospho-Histone H2A.X (Ser 139), clone JBW301) (Cat# 05-636) (Lot# 2068177)) (1:500) (Appendix 1 1.6) for 1 h at room temperature. A separate aliquot of the biological negative control was put into a new tube and was stained only with the primary antibody. Another aliquot was taken from the biological negative control and was stained only with the secondary antibody. The secondary antibody (Milipore, Ireland) (goat anti-mouse IgG Antibody, Alexa fluor 488 FITC conjugate)) (1:200) (Appendix 1.6) was applied after (×3) PBS washes for 1 h in the dark. Three wash steps as before were performed and the final pellet was re-suspended in 1 ml of PBS. The samples were centrifuged as before and re-suspended in a working solution of the counterstain, propidium iodide (PI) (1µg/ µl) (Sigma, Ireland) (Cat# P4864) (Appendix 1.3.6) for 10 min at room temperature. Three wash steps were performed with the final pellet being re-suspended in 1 ml blocking solution.

2.2.4.2 Detection of γH2AX foci by flow cytometry

Flow cytometry utilises the properties of the scattering of light and detection of fluorescence in specific spectral ranges to resolve information about the cells in sheath fluid passing by a detector in single file (Telford *et al.* 2012). The BD Accuri C6 (BD Biosciences, USA) flow cytometer was used to detect foci formation in cells staining positive for γH2AX fluorescence and was resolved in the FL-1 FITC band (excited at 495 nm and emission at 519 nm). The unstained auto fluorescent sample for both the MCF-7 and SKOV-3 cells was used to acquire the region of the scatter plot to be gated for the experimental samples. Gating is a principle in flow cytometry which uses defined regions in the scatter plot to examine populations of cells with common characteristics. Both primary and secondary only stained samples were used to set the positive fluorescent detection limit (to determine if either the primary or secondary antibodies erroneously contribute to positive detection) for the subsequent stained experimental samples (stained with both primary and secondary antibodies). Once the gated regions were set, 1×10^4 cells were acquired for each of the samples. Mean Fluorescent Intensity (MFI) and % positive cells were recorded from the experimentally determined positive gated region. An increase in the MFI is represented by a log scale shift to the right in the FL-1 channel histogram and the y-axis representing the number of cells expressing this level of fluorescence. Percentage positive is a measure of the number of cells expressing γH2AX foci with respect to the total number of measured cells in the gated region. Biological samples were performed on three independent occasions to ensure statistically validity.

2.2.4.3. Statistical processing of flow cytometry data

MFI data for each sample was subtracted from the auto fluorescent MFI value and an average and standard deviation was recorded for each experimental condition (N=3). Percentage positive data was processed similarly to the MFI data. MFI and % positive results were graphed using GraphPad Prism (Ver. 5.0) and unpaired t-tests were performed between test complex exposure (N=3) and the negative control (N=3) with *p* value set at 0.05.

2.2.5 Immunodetection of γH2AX foci with confocal microscopy

2.2.5.1 Cytospin slide preparation

Aliquots of 100 µl cell suspension stained with γH2AX and PI (as described above) were deposited onto glass slides by cytospin at 120 rpm for 5 min. Glass slides and cover slips (Thermo, Germany) (26x76mm, 0.8-1.0mm) were boiled in ethanol prior to use to produce a clean surface. A No. 0 clover slip (Thermo, Ireland) (0.085-0.13 mm thick) was applied to the slides using mounting media and was sealed with clear nail varnish.

2.2.5.2 Confocal microscope image acquisition

The slides were read using the LSM© 510 Meta Confocal Microscope (Zeiss, Germany) with the negative control used to establish the minimum laser gain, amplitude and offset setting along with the positive control to establish the upper limits to resolve saturation of the images (electronic and image setting are detailed in Appendix 1.3.7). Each image represented a random field of view on each slide. All images were taken at 620x magnification with both argon and Helium-Neon lasers simultaneously scanning. Images were captured in TIFF format and processed with ImageJ (Open source)

software. ImageJ was used to split each TIFF image into its 4 component channels (green (γH2AX foci), red (propidium iodide), merged and brightfield).

2.2.6 qRT-PCR analysis of cellular process

2.2.6.1 Molecular targets

The molecular gene targets of inflammation, DNA damage, apoptosis and inhibition of apoptosis were identified by the chosen pathway that is described in the introduction of this chapter. Early stage inflammation, DNA damage, apoptosis related genes and endogenous inhibitors of caspase action all represent a suite of functions which can characterise the state of the cell after exposure to Cu(II) phenanthroline-phenazine complexes, cisplatin and doxorubicin. See **Table 2.1** contains the gene target and housekeeping reference genes with their primer sequences. These primer sets (forward and reverse) were designed *in-house* using Primer3PLUS programme and were synthesised by Sigma, Ireland.

Table 2.1 List of oligonucleotide sequences and genes used for the gene expression analysis.

Primer name	Oligonucleotides (5'-3')
Actin F*	ACTCTTCCAGCCTTCCTTCC
Actin R*	GTTGGCGTACAGGTCTTTGC
Tubulin F*	GCTTCTTGGTTTTCCACAGC
Tubulin R*	CGTTCTTCAGGTTCGACCTC
IL-6 F	GATGCAATAACCACCCCTGACCC
IL-6 R	CAATCTGAGGTGCCCATGCTAC
NF-KB F	TCTGTGTTTGTCCAGCTTCG
NF-KB R	GCTTCTGACGTTTCCTCTGC
PARP1 F	GATGGGTTCTCTGAGCTTCG
PARP1 R	TCTGCCTTGCTACCAATTCC
Casp 9 F	TCCAGATTGACGACAAGTGC
Casp 9 R	CCTACAAGTCGTGACAGGGA
Casp 3 F	TTTGTTTGTGTGCTTCTGAG
Casp 3 R	TATAAGAACCGCTTTAAGT
SMAC F	GCTCCGTCAGAAAACACAGG
SMAC R	CACAGACAGTCATGCCAACC
BCL-2 F	AAGCGGTCCCGTGGATAGA
BCL-2 R	TCCGGTATTCGCAGAAGTCC
BAX F	AGGATGCGTCCACCAAGAAG
BAX R	CCAGTTGAAGTTGCCGTCAGA
XIAP F	GCACGGATCGTTACTTTTGGACA
XIAP R	GTGGAAGCACTTCACTTTATCGCC
IAP1 F	TGAATACACCTGTGGTTAAATCTGC
IAP1 R	TTTCATCTTCAGCATTAAGAAGTGC
IAP2 F	TTAGGTTTGATAATGAATGGACAGC
IAP2 R	TTATAATATCCCCATCCCATACAGG

* Represent primers of references genes used to establish the relative expression of the target genes.

F refers to forward primer while R refers to reverse primer.

2.2.6.2 Mammalian cell sample preparation

HT-29, PC-3, OE-33, HeLa, MCF-7, SKOV-3, A2780 and A2780/ Cis cell lines were exposed (1×10^4 cells) to their respective IC_{25} values for 24 and 48 h after allowing 24 h for attaching and growth in the T25 flask. Cu-Phen (**1**), Cu-DPQ-Phen (**2**), Cu-DPPZ-Phen (**3**) (A2780 and A2780/ Cis only), Cu-DPPN-Phen (**4**) (A2780 and A2780/ Cis only)**,** cisplatin and doxorubicin (A2780 and A2780/ Cis only) along with a negative control were incubated in triplicate T25 flasks. The A2780 and A2780/ Cis were only examined at 24 h due to resource constraints. Following the required timepoint, the T25

flask was subcultured as previously described in section 2.2.1. The cell suspension was centrifuged at 400 g for 5 min with the cell pellet re-suspended in 5 ml of PBS as a wash step. Cells were centrifuged again (as before) and the pellet re-suspended in 1 ml of Tri-Reagent (Sigma, Ireland) (Cat# T9424). The 1 ml cell suspension in Tri-Reagent was allowed to stand for 2 min prior to storage at -80 ˚C in a 1.5 ml eppendorf tube (Thermo, USA) (Cat# AM12450).

2.2.6.3 RNA extraction from samples

Prior to the thawing of any samples all workspaces and equipment were treated with RNase Away (Thermo, Ireland) (Cat# 10328011) to eradicate any environmental RNAses and minimise RNA contamination and degradation. Two hundred µl of chloroform (ACS grade) (Sigma, Ireland) (Cat# 288306) was added to each of the samples for 5 min. Samples were centrifuged at 11,300 g for 15 min at 4 °C to separate the contents into 3 distinct phases. The upper phase (clear) containing the RNA was carefully transferred to a separate Eppendorf (taking care not to disturb the lower protein phase). To the upper aqueous phase 0.5 ml of 2-propanol (ACS grade) (Sigma, Ireland) (Cat# 278475) was added, tubes were gently inverted and incubated at room temperature for 10 min and then centrifuged at 4 °C for 10 min at 11,300 g. The supernatant was removed without disturbing the RNA pellet. The pellet was washed once with 1 ml of 75 % ethanol (Sigma, Ireland) (Cat# 51976) and re-suspended in 30 µl of 0.1 % dietylpyrocarbonate (DEPC) (ACS grade) (Sigma, Ireland) (Cat# 40718) treated water.

2.2.6.4 RNA quantification

The purity and concentration of the RNA samples was measured using the MaestroNano™ spectrophotometer (MaestroGen, USA). After an initial blank with 0.1 % DEPC treated water the absorbance ratios (A260/A280 and A260/A230) of the samples was recorded to allow for the cDNA synthesis step. Impurities and contamination were noted from the spectrophotometer readings. RNA qualification using 1.5 % agrose gel was not performed.

2.2.6.5 cDNA synthesis

cDNA was synthesised from the extracted mRNA per cell line sample using the qScript cDNA synthesis kit (Quanta Biosciences, USA) (Cat# 733-1173). Based on the RNA concentrations previously obtained from the NanoDrop, a standardised value of 150 ng was chosen based on the smallest measured concentration. All subsequent samples were normalised to this concentration in a 5 µl volume. cDNA synthesis reactions was made and detailed in Appendix 1.4.1. Each reaction was prepared in a separate PCR reaction tube and placed into the Thermocycler (Techne, UK) for 5 min at 22 °C, 30 min at 42 °C, 5 min at 85 °C followed by samples being held at 4 °C prior to the quantitative real-time PCR.

2.2.6.6 Quantitative real-time PCR

Synthesised cDNA serve as the template for the quantitative real time PCR with the primers sets for each gene target. SYBR Green I (Thermo, Ireland) (Cat# 4309155) was used as the reaction probe for the following reaction. Master mix was made up for each gene target (20 µl per reaction) with 6 µl PCR-grade water, 1 µl forward primer (10 µM), 1 µl reverse primer (10 µM) and 10 µl SYBR green MM 2x for each reaction. The

final 2 µl of the normalized sample was added to 18 µl of the working master mix. cDNA sample was normalized prior to qPCR step. A master mix for each primer was made up for the required number of wells. The master mix was also incubated with PCR-grade water to establish that there was no fluorescent signal in the absence of a DNA template.

The samples and master mix were placed in 96 well PCR plates. The reaction for each sample was performed in duplicate. The PCR plate was sealed and centrifuged at 290 g for 2 min before being placed in the 7500 fast Real-Time PCR System (Applied Biosystems, USA). Details of the PCR-cycle programme are detailed in **Table 2.2** below:

Table 2.2 Thermal cycle PCR parameters.

Pre-incubation (1 cycle)	95 °C, 5 min, ramp 4.4 °C
Quantification (45 cycles)	95 °C 10 s ramp 4.4 °C, 60 °C 10 s ramp 2.2 °C, 72 °C 10 s ramp 4.4 °C
Melting curve (1 cycle)	95 °C 5 s ramp 4.4 °C, 65 °C 1 min ramp 2.2 °C, 97 °C continuous ramp 0.11 °C acquisition 10 per °C
Cooling (1 cycle)	40 °C 10 s ramp 1.5 °C

2.2.6.7 Statistical analysis of gene expression data

The expression levels of each target and reference genes was measured using the Ct (cycle threshold) (Kurnik 2007) generated from the 7500 fast Real-Time PCR system (Applied Biosystems, USA). The experiment was performed 3 times (N=3) for all target and reference genes with the exception of A2780 and A2780/ Cis cells which was performed 4 times (N=4). For each PCR plate the water negative for each gene was used to confirm that no autofluorescence was contributing to the final value. The individual Ct values were recorded in Microsoft Excel™ along with average and standard deviation for each cDNA sample. The Ct values are related to the amount of

amplicon present in the reaction mix. The lower the Ct value the greater the level of amplicon present in the sample (Livak and Schmittgen 2001). The geometric mean of both actin and tubulin reference genes was used to establish a more stable normalization factor which has been shown to produce more consistent amplification gene expression data (Vandesompele *et al.* 2002). Target genes were compared to the geometrically averaged reference genes. Each sample and target gene Ct value of the reference gene was subtracted from the Ct value of the target gene. The delta change of target gene in relation to the reference Ct value is then subtracted from the biological negative control for that sample. This second delta value was then normalized using the following logarithmic formula: $2^{-\Delta Ct1(test)-\Delta Ct2(control)}$ (Livak and Schmittgen 2001). The average Ct value for both reference and target gene was calculated along with a standard deviation. Both standard deviations were subjected to error propagation with the final standard deviation being normalized in a manner as stated in the formula above (Nordgård *et al.* 2006). Both the positive and negative error bars reflects a 95 % confidence interval around the mean normalized gene expression value.

2.3 Results

2.3.1 MTT cytotoxicity

To examine the broad-spectrum of chemotherapeutic activities of these metal complexes, a range of characterisation experiments was conducted on a range of human cancer cell lines. The *in-vitro* cell lines; HT-29 (colorectal adenocarcinoma) (**Table 2.3)**, MCF-7 (breast adenocarcinoma) (**Table 2.3)**, PC-3 (prostatic adenocarcinoma) (**Table 2.3)**, OE-33 (oesophageal carcinoma) (**Table 2.3)**, SKOV-3 (ovarian adenocarcinoma) (**Table 2.3)**, HeLa (cervical adenocarcinoma) (**Table 2.3**) along with the cisplatin sensitive, A2780 (ovarian carcinoma) (**Table 2.3)** and its cisplatin resistant variant A2780/Cis (**Table 2.3**) were used to evaluate the activity of the tested complex using the MTT viability assay. **Figure 2.1** represents a heatmap of the data from **Table 2.3**. For comparison purposes, the IC_{50} concentration for each of the cell lines and timepoints was calculated and is presented in **Table 2.4** with a heatmap of the data presented in **Figure 2.2**. One-way ANOVA with Tukey's post-hoc test was used to compare the statistical significances of the changes between each of the Cu(II) phenantholine-phenazine complexes and either cisplatin or doxorubicin (A2780 and A2780/ Cis) (**Table 2.4 – 2.5**).

In all cases Cu-Phen (**1**), Cu-DPQ-Phen (**2**), Cu-DPPZ-Phen (**3**), Cu-DPPN-Phen (**4**) and cisplatin showed increased activity after 48 h of exposure when compared to 24 h indicating a time-dependent cytotoxic response. Cisplatin was tested over a greater range of 0.5-200 µM compared to Cu-Phen (**1**), Cu-DPQ-Phen (**2**), Cu-DPPZ-Phen (**3**) and Cu-DPPN-Phen (**4**) (0.25-10 µM).

Cisplatin showed variable level of activity accross the range of tested cell lines and timepoints. In HT-29 cells there was a small decrease in the toxicity over the two timepoints. The MCF-7 cells saw an unchanged level of activity after both exposed timepoints possibly indicating some resistance in response. The PC-3 cell lines showed a large resistance to toxicity induced by the platinum agent, markedly decreasing after 48 h of exposure. OE-33 cells showed a relatively unchanged level of toxicity while SKOV-3 cells displayed an indicative profile of platinum resistance as observed in prior studies (Beaufort *et al.* 2015). HeLa cells demonstrated rapid toxicity increasing over the two timepoints. Cisplatin displayed differential activity in both A2780 and A2780/Cis cell lines (**Table 2.3**), with the resistant variant demonstrating a higher concentration in relation to the sensitive variant at 24 h (> 200 μM vs. 63.10 μM). The IC_{25} concentration increased at 48 h with the resistant and sensitive characteristics remaining similar to the 24 h timepoint (33.22 μM vs. 3.85 μM). The chemotherapeutic, doxorubicin was also exposed to both the A2780 and A2780/ Cis cells. Both these cell lines are known to be sensitive to this clinical drug. For both cell lines, doxorubicin displayed time-dependant increase in toxicity from 24 to 48 h (A2780 24 h 1.13 μM → A2780 48 h 0.61 μM) (A2780/ Cis 24 h 1.473 μM → A2780/ Cis 48 h 0.655 μM), as with cisplatin. Both cell lines demonstrate no appreciable difference between the responses to doxorubicin when the standard deviation is taken into account.

Cu-Phen (**1**), Cu-DPQ-Phen (**2**), Cu-DPPZ-Phen (**3**) and Cu-DPPN-Phen (**4**) in **Table 2.3** all show very active IC_{25} concentrations values of <10 μM with the exception of OE-33 cells. Cu-Phen (**1**) represents the fundamental architecture upon which the phenazine π backbone is extended such as in Cu-DPQ-Phen (**2**), Cu-DPPZ-Phen (**3**) and Cu-DPPN-Phen (**4**). Here, Cu-Phen (**1**) is shown to have significant activity of <5 μM

exceeding the activity of cisplatin in PC-3 (4.87 μM 24 h, 2.12 μM 48 h), OE-33 (1.76 μM 24 h, 1.32 μM 48 h) and cisplatin resistant SKOV-3 (2.56 μM 24 h, 1.87 μM 48 h) cells. Cu-Phen (**1**), significantly exceeded the activity of cisplatin in A2780 and A2780/ Cis cells, along with the clinical drug doxorubicin in A2780 cells (0.39 μM vs. 1.13 μM, 0.83 μM vs. 1.473 μM). Cu-DPQ-Phen (**2**), Cu-DPPZ-Phen (**3**) and Cu-DPPN-Phen (**4**) represent phenazine π-backbone extended ligands of the Cu-Phen (**1**) architecture with the increasing phenazine chain lengths going from DPQ → DPPZ → DPPN. In most cases the extension of the phenazine complex by a single aromatic ring to Cu-DPQ-Phen (**2**) does not provide an increase in toxicity in the cell lines: HT-29, MCF-7, OE-33, SKOV-3 and HeLa, with the exception of PC-3 cells at 24 h (3.91 μM) but not at 48 h (4.41 μM). Additionally, both A2780 (except at 48 h) and A2780/ Cis cells demonstrate increased activity of Cu-DPQ-Phen (**2**) in comparison to Cu-Phen (**1**) (A2780 24 h: 0.34 μM vs. 0.39 μM) (A2780/ Cis 24 h: 0.72 μM vs. 0.83 μM, A2780/ Cis 48 h: 0.43 μM vs. 0.44 μM). Exposure to Cu-DPPZ-Phen (**3**) yields increased toxicity across all the different cell lines over 24- and 48-h with significant increases observed in PC-3, OE-33, SKOV-3, HeLa, A2780 and A2780/ Cis cells in comparison to cisplatin. With Cu-DPPZ-Phen (**3**) many of the IC_{25} concentrations are reduced to ≤1 μM after 24 h. Cu-DPPZ-Phen (**3**) (except in the case of the MCF-7 cells) provide a significant increase over the chemotherapeutic activity of cisplatin and doxorubicin in the A2780/ Cis cell line. The activity of Cu-DPPN-Phen (**4**) in the HT-29, MCF-7, PC-3, OE-33 and HeLa cells showed a significant decrease in activity compared to the activity of cisplatin over 24- and 48- h. The activity of Cu-DPPN-Phen (**4**) at both 24- and 48- h in the A2780 and A2780/ Cis cell line in contrast to the other cell lines demonstrated a significant increase in activity in comparison to cisplatin and in the case of doxorubicin, A2780 48 h and A2780/ Cis 24 h. The IC_{25} values (except in the case of

the A2780 and A2780/ Cis cells) of Cu-Phen (**1**), Cu-DPQ-Phen (**2**) and Cu-DPPZ-Phen (**3**) show superior activity for all cell lines at both 24- and 48- h in comparison to Cu-DPPN-Phen (**4**). In contrast the A2780 and A2780/ Cis cell only demonstrated superior toxicity to the Cu-DPPN-Phen (**4**) complex at 24 h in the A2780 (Cu-Phen (**1**)), 48 h in the A2780 (Cu-Phen (**1**), Cu-DPQ-Phen (**2**), Cu-DPPZ-Phen (**3**)), in the A2780/ Cis cells at 24 h (Cu-Phen (**1**) and Cu-DPQ-Phen (**2**)) and at 48 h in A2780/ Cis (Cu-Phen (**1**), Cu-DPQ-Phen (**2**), Cu-DPPZ-Phen (**3**)). Both known cisplatin sensitive cell lines (MCF-7 and A2780) demonstrate higher toxicity towards the Cu(II) phenanthroline-phenazine complexes in comparison to both known cisplatin resistant cell lines (SKOV-3 and A2780/ Cis). In general the activity of the copper complexes is similar with Cu-Phen (**1**) and Cu-DPQ-Phen (**2**) showing a high degree of homology. Some improvements in cytotoxic response are seen for the Cu-DPPZ-Phen (**3**) complex while activity recedes with the introduction of Cu-DPPN-Phen (**4**), possibility due to its larger size and lipophilicity.

Table 2.3 IC_{25} values for HT-29, MCF-7, PC-3, OE-33, SKOV-3, HeLa, A2780 and A2780/ Cis cells when exposed to Cu-Phen (**1**), Cu-DPQ-Phen (**2**), Cu-DPPZ-Phen (**3**) and Cu-DPPN-Phen (**4)**, cisplatin and doxorubicin over 24 and 48 h.

Compound	IC_{25} (μM) ± S.D.															
	HT-29		MCF-7		PC-3		OE-33		SKOV-3		HeLa		A2780		A2780/ Cisplatin	
	24 h	48 h	24 h	48 h	24 h	48 h	24 h	48 h	24 h	48 h	24 h	48 h	24 h	48 h	24 h	48 h
Cisplatin	1.21± 1.09	4.75± 3.96	0.45±0 .07	0.45± 0.50	>200	19.07± 5.29	4.19± 0.65	4.71± 0.08	21.52± 4.54	3.99± 0.72	2.97± 1.14	0.87± 0.16	63.10±1 3.91‡	3.85±0.3 6	>200	33.22±10. 04
Doxorubicin	N.P.	N.P	N.P.	N.P.	N.P.	N.P.	N.P.	N.P.	N.P.	N.P.	N.P.	N.P.	1.13±0. 25	0.61±0.0 1	1.473±0. 16	0.655±0.0 3
Cu-Phen (**1**)	2.71± 0.99	1.41± 0.27	0.97±0 .10	0.71± 0.07	4.87± 0.03***	2.12±0 .30***	1.76± 0.32**	1.32± 0.03***	2.56±0 .12***	1.87± 0.33***	1.71± 0.19	1.16± 0.21	0.39±0. 07***	0.12±0.0 1***	0.83±0.0 03***ÞÞ	0.44±0.02 ***
Cu-DPQ-Phen (**2**)	2.62± 0.53	1.54± 0.36	1.27±0 .40*	0.87± 0.07	3.91± 0.37***	4.41±0 .05***	2.24± 0.94**	1.35± 0.14***	2.51±0 .09***	1.98± 0.38**	1.85± 0.34	1.17± 0.12	0.34±0. 09***	0.13±0.0 3***	0.72±0.0 2***ÞÞ Þ	0.43±0.02 ***
Cu-DPPZ-Phen (**3**)	0.92± 0.29	0.61± 0.11	0.63±0 .007	0.47± 0.04	1.06± 0.11***	0.98±0 .16***	1.04± 0.05***	0.53± 0.06***	1.61±0 .74***	0.95± 0.28***	0.96± 0.07**	0.59± 0.04	0.31±0. 04***	0.12±0.0 3***	0.39±0.0 7***ÞÞ Þ	0.42±0.03 ***
Cu-DPPN-Phen (**4**)	3.89± 0.55**	1.51± 0.18	1.37±0 .32**	0.69± 0.19	7.54± 2.05***	4.50±0 .45***	>10***	1.32± 0.19***	5.71±0 .92***	3.04± 0.06	4.51± 0.33*	2.18± 0.82*	0.36±0. 10‡***	0.00046 ±0.0003 5‡***Þ	0.53±0.0 2***ÞÞ Þ	0.30±0.01 ***

IC_{25} values represent the mean ± standard deviation (N=3).
‡ denotes reduced number of replicates.
* denotes $p < 0.05$ in comparison to cisplatin.
** denotes $p < 0.01$ in comparison to cisplatin.
*** denotes $p < 0.001$ in comparison to cisplatin.
Þ denotes $p < 0.05$ in comparison to doxorubicin.
ÞÞ denotes $p < 0.01$ in comparison to doxorubicin.
ÞÞÞ denotes $p < 0.001$ in comparison to doxorubicin.
N.P. indicates test not performed.

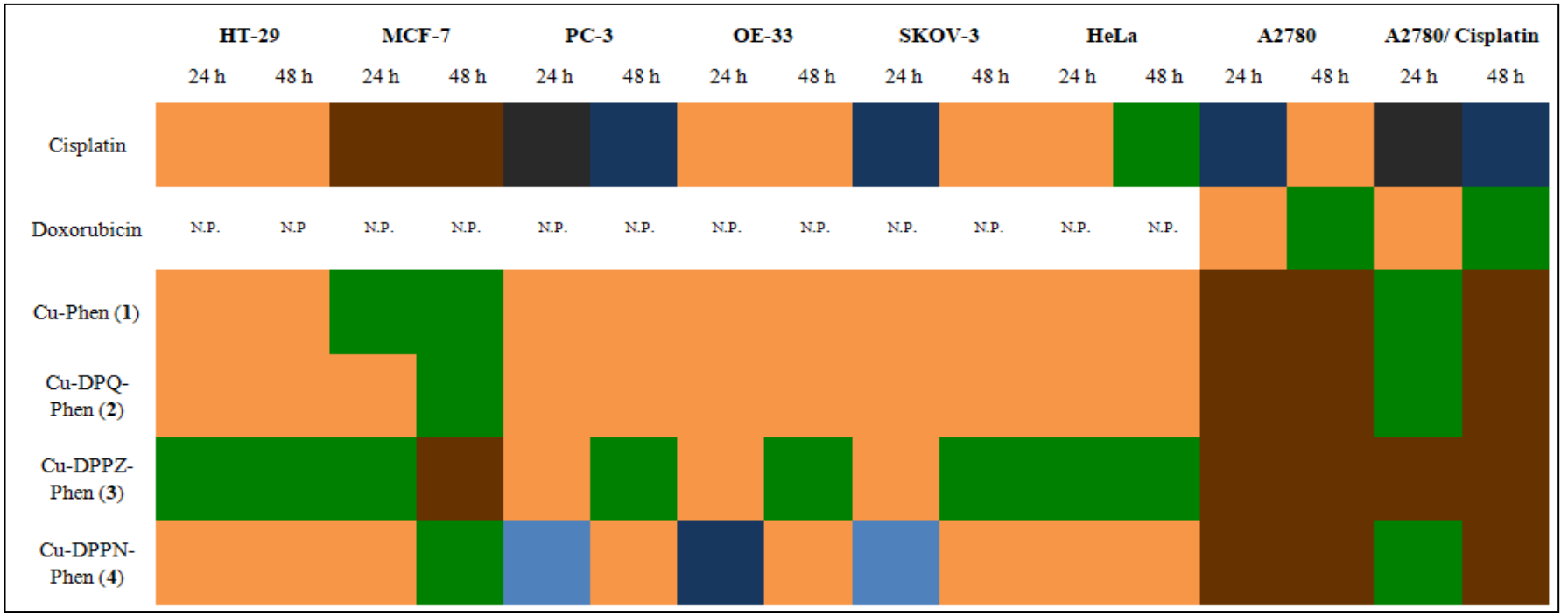

Fig. **2.1** Heatmap representing the results of IC_{25} values generated from the tested cell lines using the MTT assay (**Table 2.3**). Details of the concentrations range and its relation to the colour is displayed in the legend (right). N.P. indicates test not performed.

Table 2.4 IC_{50} values for HT-29, MCF-7, PC-3, OE-33, SKOV-3, HeLa, A2780 and A2780/ Cis cells when exposed to Cu-Phen (**1**), Cu-DPQ-Phen (**2**), Cu-DPPZ-Phen (**3**) and Cu-DPPN-Phen (**4**), cisplatin and doxorubicin over 24 and 48 h.

Compound	IC_{50} (μM) ± S.D.															
	HT-29		MCF-7		PC-3		OE-33		SKOV-3		HeLa		A2780		A2780/ Cisplatin	
	24 h	48 h	24 h	48 h	24 h	48 h	24 h	48 h	24 h	48 h	24 h	48 h	24 h	48 h	24 h	48 h
Cisplatin	1.32± 1.09	3.33± 2.56	0.53 ± 0.09	6.60± 6.98	90.14 ±61.60	41.13± 11.34	11.19 ±1.02	4.99± 0.06	53.44± 4.35	8.47± 1.62	7.28± 3.04	2.00± 0.10	>200	9.84±0.30	>200	64.52±18.48
Doxorubicin	N.P.	N.P.	N.P.	N.P.	N.P.	N.P.	N.P.	N.P.	N.P.	N.P.	N.P.	N.P.	2.20±0.23	0.64±0.01	2.35±0.06	0.91±0.05
Cu-Phen (**1**)	3.37± 0.69*	1.67± 0.07	1.78 ± 0.15***	1.13± 0.09	5.13± 0.02*	2.89±0 .59***	2.61± 0.57***	1.65± 0.04***	3.05±0 .09***	2.40± 0.27***	2.30± 0.14**	1.45± 0.18*	0.56±0.08***ÞÞÞ	0.14±0.07***ÞÞ	1.07±0.13***ÞÞÞ	0.54±0.35***
Cu-DPQ-Phen (**2**)	3.12± 0.43	2.02± 0.38	2.03 ± 0.48***	1.4±0 .25	4.80± 0.52*	4.61±0 .03***	2.77± 1.04***	1.91± 0.15***	2.92±0 .07***	2.40± 0.15***	2.30± 0.29**	1.43± 0.10*	0.62±0.02***ÞÞÞ	0.14±0.05***ÞÞ	1.14±0.05***ÞÞÞ	0.52±0.01***
Cu-DPPZ-Phen (**3**)	1.21± 0.23	0.78± 0.09	1.01 ± 0.02	0.66± 0.02	1.46± 0.18*	1.26±0 .18***	2.70± 1.16***	0.76± 0.05***	1.87±0 .80***	1.11± 0.30***	1.19± 0.04**	0.71± 0.04***	0.43±0.04***ÞÞÞ	0.19±0.03***Þ	0.97±0.07***ÞÞÞ	0.49±0.02***
Cu-DPPN-Phen (**4**)	4.86± 0.82***	2.69± 0.67	2.60 ± 0.04***	1.21± 0.32	12.34 ±4.53*	8.29±1 .02***	>10	2.77± 0.31***	7.45±2 .91***	4.88± 0.84**	6.98± 0.30	3.30± 0.30***	0.09±0.09***ÞÞÞ	0.001±0.001***ÞÞ	1.13±0.13***ÞÞÞ	0.43±0.02***

IC_{25} values represent the mean ± standard deviation (N=3).
* denotes $p < 0.05$ in comparison to cisplatin.
** denotes $p < 0.01$ in comparison to cisplatin.
*** denotes $p < 0.001$ in comparison to cisplatin.
Þ denotes $p < 0.05$ in comparison to doxorubicin.
ÞÞ denotes $p < 0.01$ in comparison to doxorubicin.
ÞÞÞ denotes $p < 0.001$ in comparison to doxorubicin.
N.P. indicates test not performed.

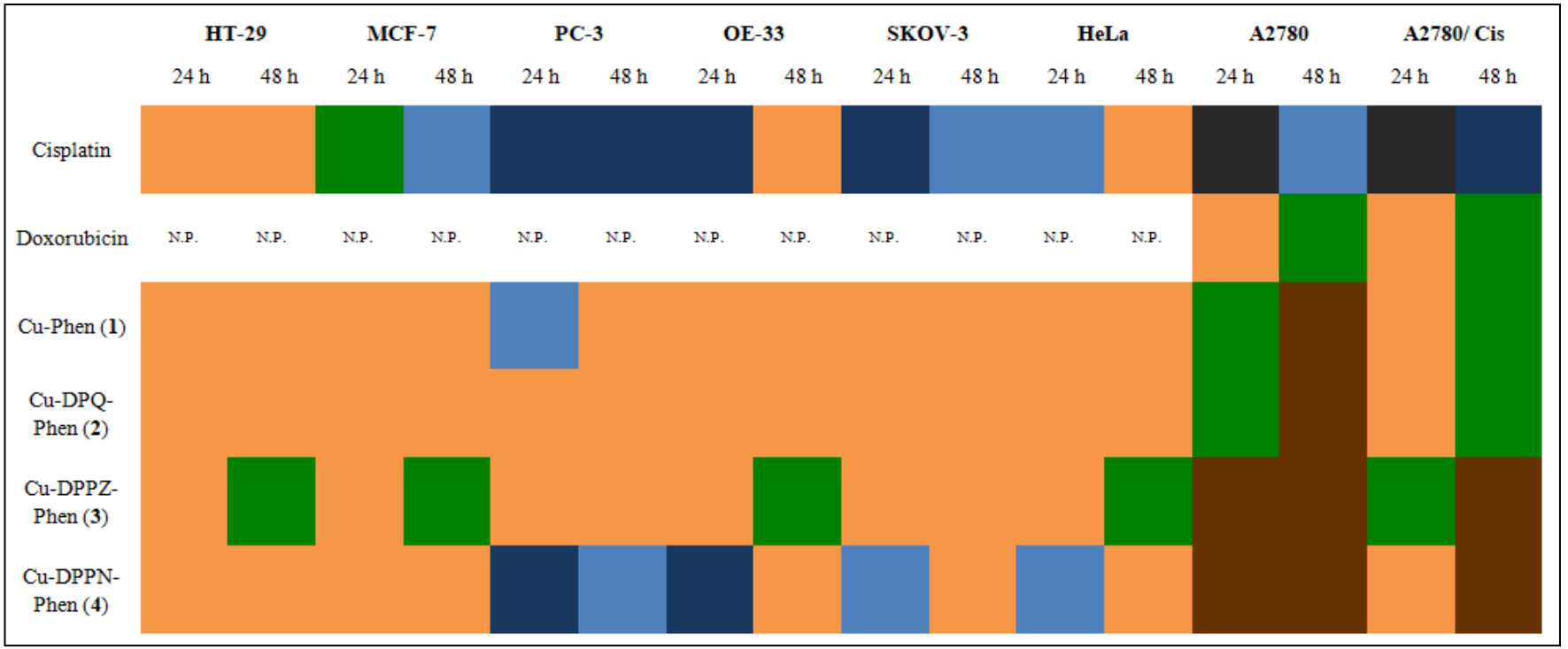

Fig. 2.2 Heatmap representing the results of IC_{50} values generated from the tested cell lines using the MTT assay (**Table 2.4**). Details of the concentrations range and its relation to the colour is displayed in the legend (right). N.P. indicates test not performed.

2.3.2 Fluorescent detection of Reactive Oxygen Species

ROS production was assessed through the fluorescent dye, 2′7′-dichlorofluorescein diacetate (H_2DCFDA). HeLa cells were assessed for the presence of ROS at a doubling concentration of cisplatin (0.195-50 µM) (**Fig. 2.3 E**), Cu-Phen (**1**), Cu-DPQ-Phen (**2**), Cu-DPPZ-Phen (**3**), Cu-DPPN-Phen (**4**) (**1-4**: 0.078-20 µM) (**Fig. 2.3 A-D**) over a 5 h period. Hydrogen peroxide (H_2O_2) was used as a positive control. The negative control remained unexposed to any of the drugs and was used to establish the relative increase in endogenous ROS generation. H_2O_2 showed a strong time-dependent increase in ROS generation in all experiments accross the 5 h exposure period. Exposure to Cu-Phen (**1**) (0.078-20 µM) (**Fig. 2.3 A**) produced a significant time-dependent increase in ROS generation at 20 µM and down to 0.312 µM. Exposure to Cu-DPQ-Phen (**2**) (0.078-20 µM) (**Fig. 2.3 B**) produced a smaller (than Cu-Phen (**1**)) but significant overall increase in ROS generation as the concentration was increased however over the increasing timepoints, ROS generation decreased slightly, potentially due to ETC impairment or cell death. Exposure to Cu-DPPZ-Phen (**3**) (0.078-20 µM) (**Fig. 2.3 C**) produced a significant but smaller (than Cu-Phen (**1**)) time-dependent increase in ROS generation at 20 µM. Smaller changes in ROS generation were observed in all lower exposed concentrations with relatively little change over the time course. Exposure to Cu-DPPN-Phen (**4**) (0.078-20 µM) (**Fig. 2.3 D**) produced a significant but small time-dependent increase in ROS generation at 20 µM and below. Smaller changes in ROS generation were observed in all lower exposed concentrations with a small increase over the timepoints. Overall the exposure to Cu-Phen (**1**) demonstrated an increase in ROS production over the timeperiod while Cu-DPQ-Phen (**2**), Cu-DPPZ-Phen (**3**) and Cu-DPPN-Phen (**4**) ROS production decreased or stayed that same over the timeperiod.

Cisplatin demonstrated a concentration-dependent significant increase in ROS at 50 µM exposure when compared to the negative control.

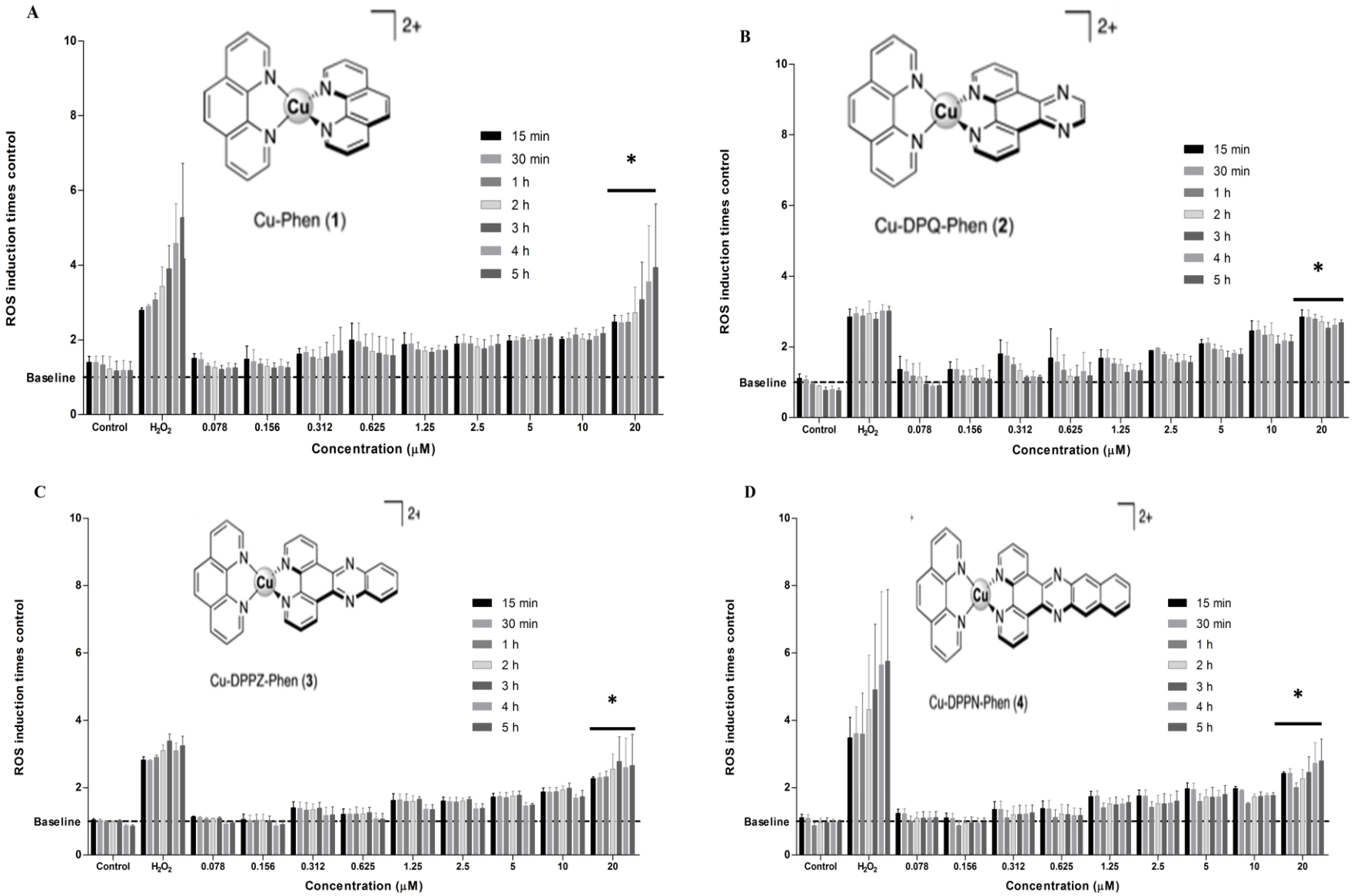
A
B
C
D
ROS induction times control
Concentration (μM)
Control
H2O2
0.078
0.156
0.312
0.625
1.25
2.5
5
10
20
Baseline
15 min
30 min
1 h
2 h
3 h
4 h
5 h
*
Cu-Phen (1)
Cu-DPQ-Phen (2)
Cu-DPPZ-Phen (3)
Cu-DPPN-Phen (4)
Cu
2+

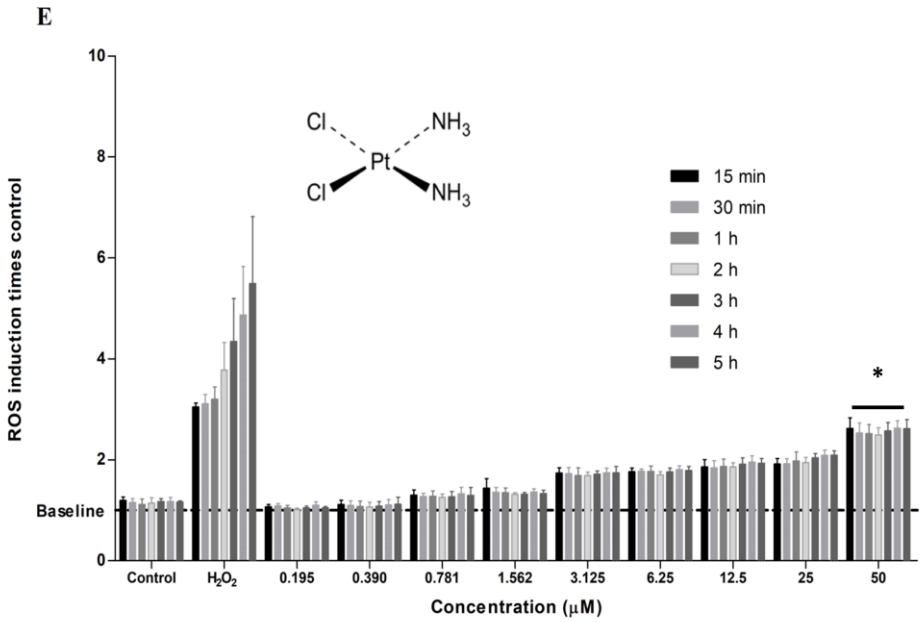

Fig. 2.3 (A-E) Fluorescent detection of ROS using DCF/DA in HeLa cells after exposure to Cu-Phen (**1**), Cu-DPQ-Phen (**2**), Cu-DPPZ-Phen (**3**), Cu-DPPN-Phen (**4**) and cisplatin over a period of 5 h. H_2O_2 used as positive control. * Statistically significant ($p < 0.05$) difference between highest exposed concentration of the test complexes/ cisplatin and the negative control. N=8.

2.3.3 Immuno-detection of γH2AX foci using flow cytometry

2.3.3.1 Immuno-detection of γH2AX foci in MCF-7 and SKOV-3 cells

The γH2AX foci formation in the MCF-7 and SKOV-3 cells was examined by flow cytometry after exposure to IC_{25} concentrations to assess the impact of lower Inhibitory Concentrations (IC) of the Cu(II) phenanthroline-phenazine complexes and cisplatin in relation to the unexposed negative control over both 24 and 48 h. γH2AX foci was expressed as Mean Fluorescent Intensity (MFI) for MCF-7 (**Fig. 2.4**) and SKOV-3 cells (**Fig. 2.5**). γH2AX foci was also expressed through % positive cells in MCF-7 (**Fig. 2.6**) and SKOV-3 cells (**Fig. 2.7**).

Foci formation in the MCF-7 cells (**Fig. 2.4**) indicates that exposure to cisplatin, a known DNA damaging agent, produces a characteristic increase in fluorescence in comparison to the negative control. Exposure to the IC_{25} concentration of Cu-Phen (**1**), Cu-DPQ-Phen (**2**), Cu-DPPZ-Phen (**3**) and Cu-DPPN-Phen (**4**) result in increased foci formation with respect to the negative control. A significant increase ($p \leq 0.05$) was seen in the 24 h exposure of Cu-Phen (**1**) and Cu-DPQ-Phen (**2**), additionally a significant increase ($p \leq 0.05$) was seen with both 24 and 48 h exposures to Cu-DPPN-Phen (**4**) in comparison to the negative control. In the SKOV-3 cell line at both 24 and 48 h, γH2AX foci formation measured through MFI (**Fig. 2.5**) showed a significant increase ($p \leq 0.05$) after incubation with Cu-Phen (**1**), Cu-DPQ-Phen (**2**) and Cu-DPPN-Phen (**4**) while a non-significant ($p \leq 0.05$) increase occurs after exposure to Cu-DPPZ-Phen (**3**). The positive control, cisplatin demonstrated a marginal increase in γH2AX foci formation over the negative control. With the exception of Cu-DPPZ-Phen (**3**) all

other Cu(II) phenanthroline-phenazine complexes induced higher foci formation than the cisplatin exposure at both timepoints.

Similarly to the measurement of γH2AX foci through MFI, the MCF-7 % positive cells (**Fig. 2.6**) for γH2AX foci formation indicate double stranded DNA damage in a similar pattern to the MFI results (**Fig. 2.4**). Cisplatin demonstrates increased foci formation as previously described. Exposures to Cu-Phen (**1**), Cu-DPQ-Phen (**2**), Cu-DPPZ-Phen (**3**) and Cu-DPPN-Phen (**4**) all show significantly increased ($p \leq 0.05$) incidences of foci formation after both 24 and 48 h exposures. The incidence of γH2AX foci formation measured through % positive cells (**Fig. 2.7**) in the SKOV-3 cell lines after exposure to Cu-Phen (**1**), Cu-DPQ-Phen (**2**), Cu-DPPZ-Phen (**3**), Cu-DPPN-Phen (**4**) and cisplatin at both timepoints produces a measurement profile similar to the MFI (**Fig. 2.5**). A significant increase ($p \leq 0.05$) is observed in the % positive cells after exposure to Cu-Phen (**1**), Cu-DPQ-Phen (**2**), Cu-DPPZ-Phen (**3**) and Cu-DPPN-Phen (**4**) at both timepoints. The positive control, cisplatin induced double stranded DNA damage at both timepoints. All Cu(II) phenanthroline-phenazine complexes and cisplatin produced a decreased % positive response at 48 h in relation to their 24 h result.

Overall the MCF-7 cell measurement of γH2AX foci formation through both MFI and % positive show a similar pattern of results between both analysis methods. The SKOV-3 cell measurement of γH2AX foci formation through both MFI and % positive show a similar pattern of results. The exposure of Cu-DPPZ-Phen (**3**) produced lower foci formation in comparison to Cu-Phen (**1**), Cu-DPQ-Phen (**2**) and Cu-DPPN-Phen (**4**) when represented through both MFI and % positive cells.

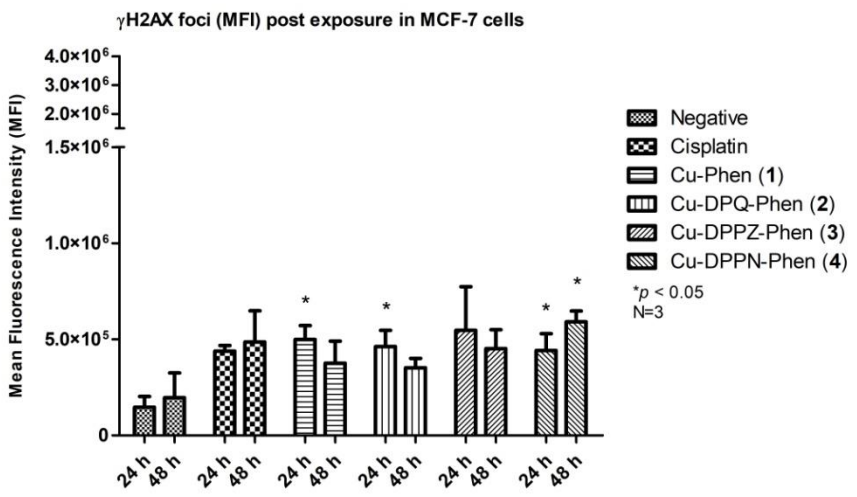

Fig. 2.4 Immuno-detection of γH2AX recorded through mean fluorescence intensity of MCF-7 cells exposed to Cu-Phen (**1**), Cu-DPQ-Phen (**2**), Cu-DPPZ-Phen (**3**), Cu-DPPN-Phen (**4**) and cisplatin at their respective IC_{25} concentration for both 24 and 48 h. * indicated significant ($p < 0.05$) (N=3) increase in MFI in comparison to the negative control.

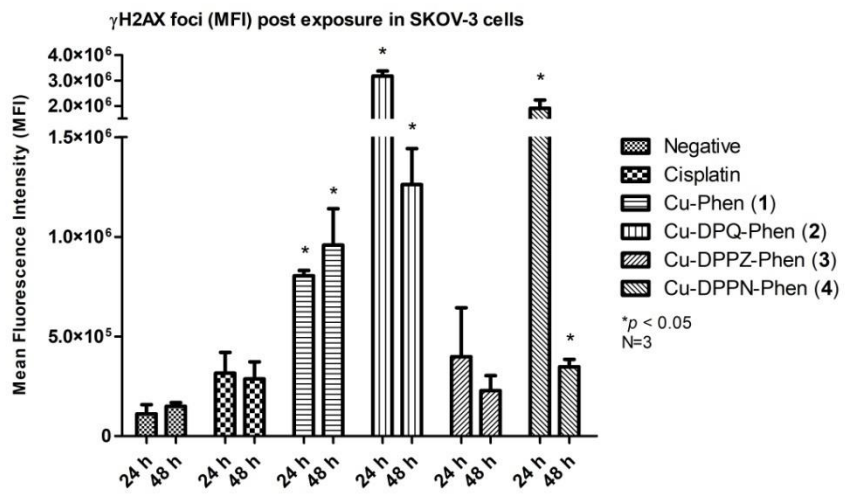

Fig. 2.5 Immuno-detection of γH2AX recorded through mean fluorescence intensity of SKOV-3 cells exposed to Cu-Phen (**1**), Cu-DPQ-Phen (**2**), Cu-DPPZ-Phen (**3**), Cu-DPPN-Phen (**4**) and cisplatin at their respective IC_{25} concentration for both 24 and 48 h. * indicated significant ($p < 0.05$) (N=3) increase in MFI in comparison to the negative control.

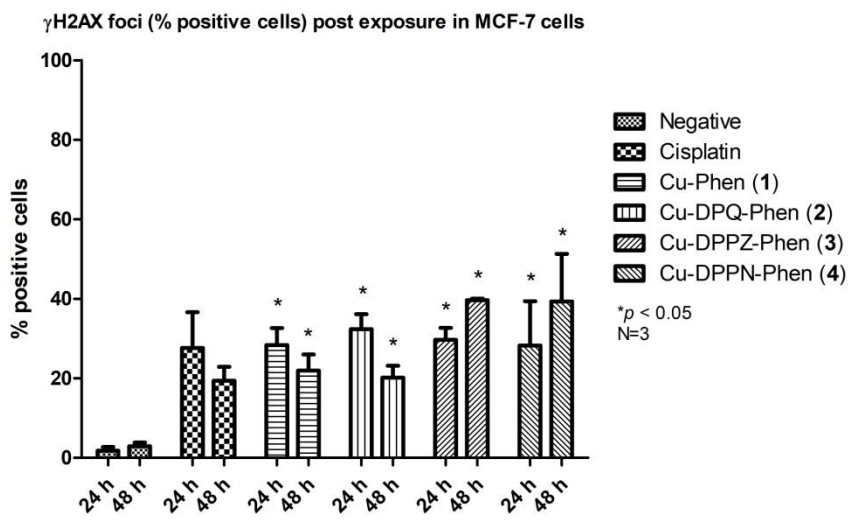

Fig. 2.6 Immuno-detection of γH2AX recorded through % positive cells. MCF-7 cells exposed to Cu-Phen (**1**), Cu-DPQ-Phen (**2**), Cu-DPPZ-Phen (**3**), Cu-DPPN-Phen (**4**) and cisplatin at their respective IC_{25} concentration for both 24 and 48 h. * indicated significant increase ($p < 0.05$) (N=3) in % positive cells in comparison to the negative control.

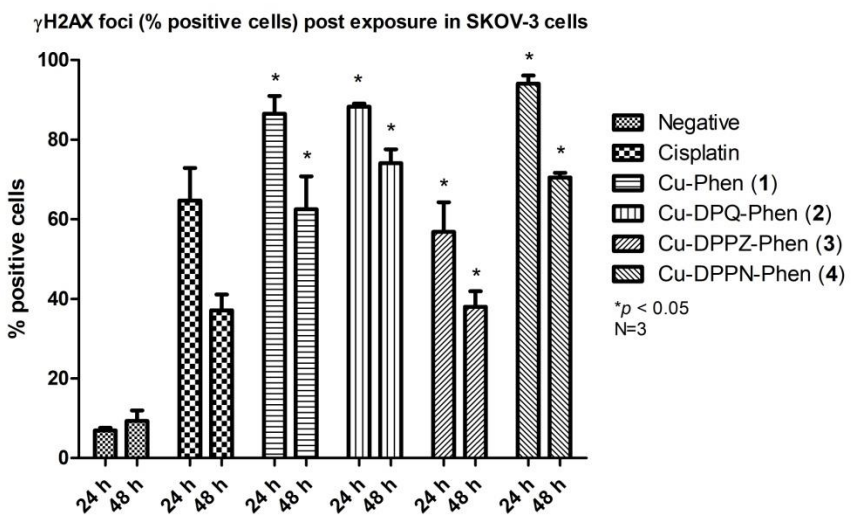

Fig 2.7 Immuno-detection of γH2AX recorded through % positive cells. SKOV-3 cells exposed to Cu-Phen (**1**), Cu-DPQ-Phen (**2**), Cu-DPPZ-Phen (**3**), Cu-DPPN-Phen (**4**) and cisplatin at their respective IC_{25} concentration for both 24 and 48 h. * indicated significant increase ($p < 0.05$) (N=3) in % positive cells in comparison to the negative control.

2.3.4 Immuno-detection of γH2AX foci using confocal microscopy

MCF-7 (**Fig. 2.8-2.9**) and SKOV-3 cells (**Fig. 2.10-2.11**) were analysed for the presence of γH2AX foci using confocal microscopy after both 24- and 48- h exposures to the IC_{25} concentrations of cisplatin, Cu-Phen (**1**), Cu-DPQ-Phen (**2**), Cu-DPPZ-Phen (**3**) and Cu-DPPN-Phen (**4**). γH2AX foci were determined using both a primary and a FITC labelled secondary antibody. Propidium iodide (PI) was used as a nuclear counterstain. A merged green and red channel image was displayed along with a brightfield image to give a non-fluorescent context to the images. The overlapping of primary stain (green) with the counterstain (red) on the merged image produced a yellow colour.

Figure 2.8 shows the production of γH2AX foci in MCF-7 cells following 24- and 48-h respectively exposure of IC_{25} values of cisplatin, Cu-Phen (**1**), Cu-DPQ-Phen (**2**), Cu-DPPZ-Phen (**3**) and Cu-DPPN-Phen (**4**). The negative control indicates no appreciable increase in γH2AX foci while the positive control, cisplatin indicates an appreciable increase. Cisplatin, Cu-Phen (**1**) and Cu-DPQ-Phen (**2**) exposures produce more concentrated foci formation, while Cu-DPPN-Phen (**4**) tends to be more diffuse. Cu-DPPZ-Phen (**3**) induces no detectable foci formation, however a smaller number of cells were intact for confocal analysis. Overall, while strong foci formation was found in specific cells, the number of cells displaying foci formation was small after the 24 h exposure to cisplatin and the Cu(II) phenanthroline-phenanzine complex series. **Figure 2.9** shows the production of γH2AX foci in MCF-7 cells following 48 h exposure of IC_{25} values of cisplatin, Cu-Phen (**1**), Cu-DPQ-Phen (**2**), Cu-DPPZ-Phen (**3**) and Cu-DPPN-Phen (**4**). The negative control indicates no appreciable increase in γH2AX foci while the positive control, cisplatin indicates a strong increase in specific cells. Cu-Phen (**1**) induces diffuse foci formation in a smaller number of cells, similarly to the cisplatin

exposure. Cu-DPQ-Phen (**2**) and Cu-DPPN-Phen (**4**) produce more concentrated foci in the cells, with Cu-DPPN-Phen (**4**) inducing γH2AX foci in a larger number of cells. Exposure to Cu-DPPZ-Phen (**3**) induced a small number of foci in the observed cells, although only a small number of cells remained intact for confocal analysis. Overall, while strong foci formation was found in specific cells, the number of cells displaying foci formation was small after the 48 h exposure to cisplatin and the Cu(II) phenanthroline-phenanzine complex series.

Figure 2.10 shows the production of γH2AX foci in SKOV-3 cells following 24- and 48- h exposure of IC_{25} values of cisplatin, Cu-Phen (**1**), Cu-DPQ-Phen (**2**), Cu-DPPZ-Phen (**3**) and Cu-DPPN-Phen (**4**). The negative control indicates a very small increase in γH2AX foci while the positive control, cisplatin indicates a strong increase in most cells. Cu-Phen (**1**), Cu-DPQ-Phen (**2**), Cu-DPPZ-Phen (**3**) and Cu-DPPN-Phen (**4**), all show a strong increase in both diffuse and concentrated foci formation in cells. Cu-Phen (**1**), Cu-DPQ-Phen (**2**) and Cu-DPPN-Phen (**4**) demonstrated the strongest increases in foci formation while exposure to Cu-DPPZ-Phen (**3**) induced an appreciable smaller number of foci. Overall, an strong level of foci formation was observed after exposures to cisplatin, Cu-Phen (**1**), Cu-DPQ-Phen (**2**), Cu-DPPZ-Phen (**3**) and Cu-DPPN-Phen (**4**) in SKOV-3 cells at 24 h. **Figure 2.11** shows the production of γH2AX foci in SKOV-3 cells following 48 h exposure of IC_{25} values of cisplatin, Cu-Phen (**1**), Cu-DPQ-Phen (**2**), Cu-DPPZ-Phen (**3**) and Cu-DPPN-Phen (**4**). The negative control indicates a very small increase in γH2AX foci while the positive control, cisplatin induces a stronger increase in a small number of cells. Cu-Phen (**1**), Cu-DPQ-Phen (**2**), Cu-DPPZ-Phen (**3**) and Cu-DPPN-Phen (**4**), all show a strong increase in both diffuse and concentrated foci formation in cells. Cu-Phen (**1**), Cu-DPQ-Phen (**2**) and Cu-DPPN-

Phen (**4**) demonstrated the strongest increases in foci formation while exposure to Cu-DPPZ-Phen (**3**) induced an appreciable smaller and more diffuse number of foci formation. Overall, an intense level of foci formation was observed after exposures to cisplatin, Cu-Phen (**1**), Cu-DPQ-Phen (**2**), Cu-DPPZ-Phen (**3**) and Cu-DPPN-Phen (**4**) in SKOV-3 cells at 48 h.

Between both MCF-7 and SKOV-3 cells a strong difference in both the concentration of foci and the number of cells present with foci was observed. MCF-7 cells demonstrated both a smaller number of cells with induced foci and a smaller number of foci formation per cell when compared to the fluorescence induction profile of the SKOV-3 cells.

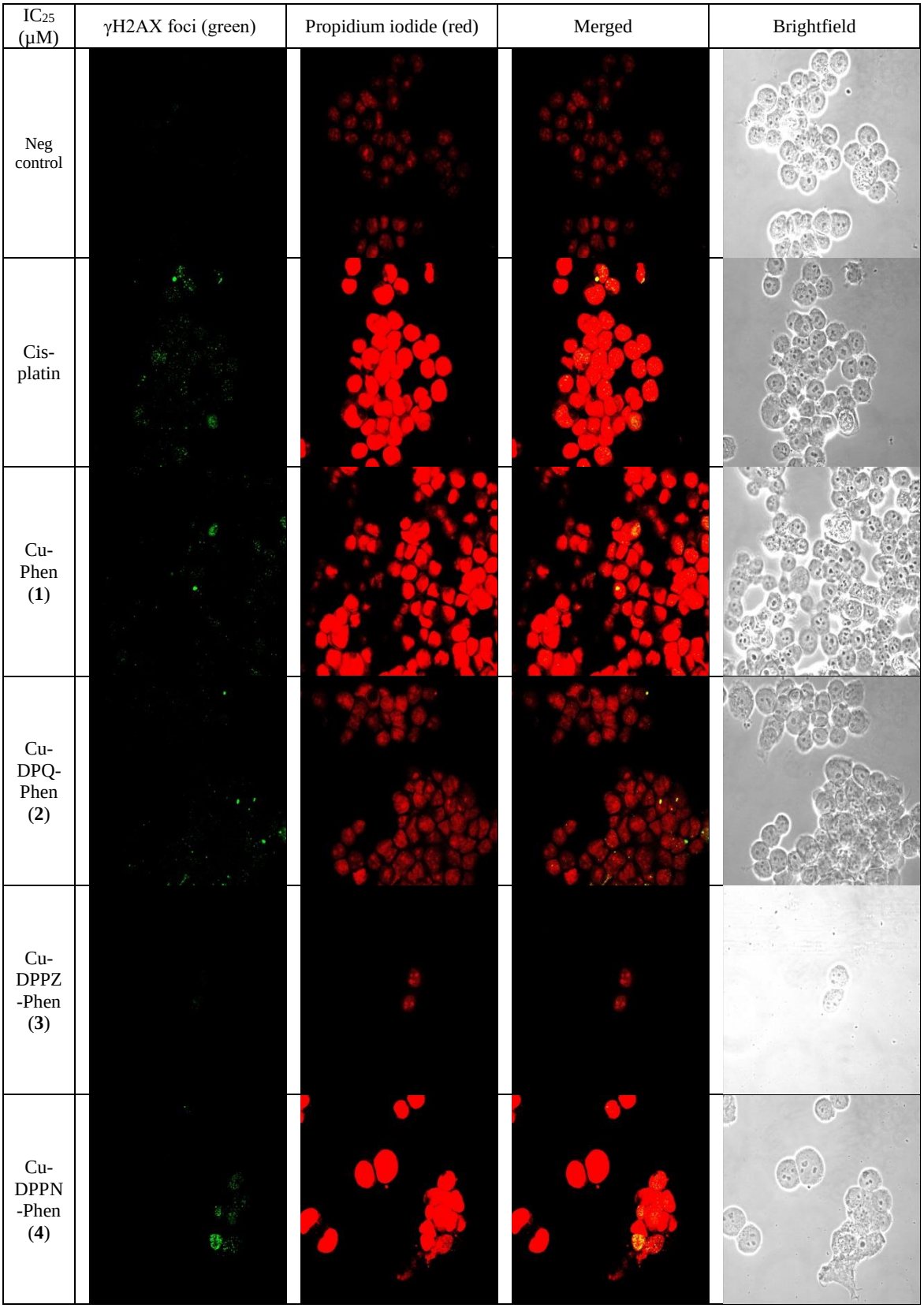

Fig. 2.8 MCF-7 cells exposed to the IC_{25} 24 h concentrations of cisplatin, Cu-Phen (**1**), Cu-DPQ-Phen (**2**), Cu-DPPZ-Phen (**3**) and Cu-DPPN-Phen (**4**) in comparison to the negative control. γH2AX foci determined using primary antibody stain with fluorescent FITC secondary label and propidium iodide used as a nuclear counter stain.

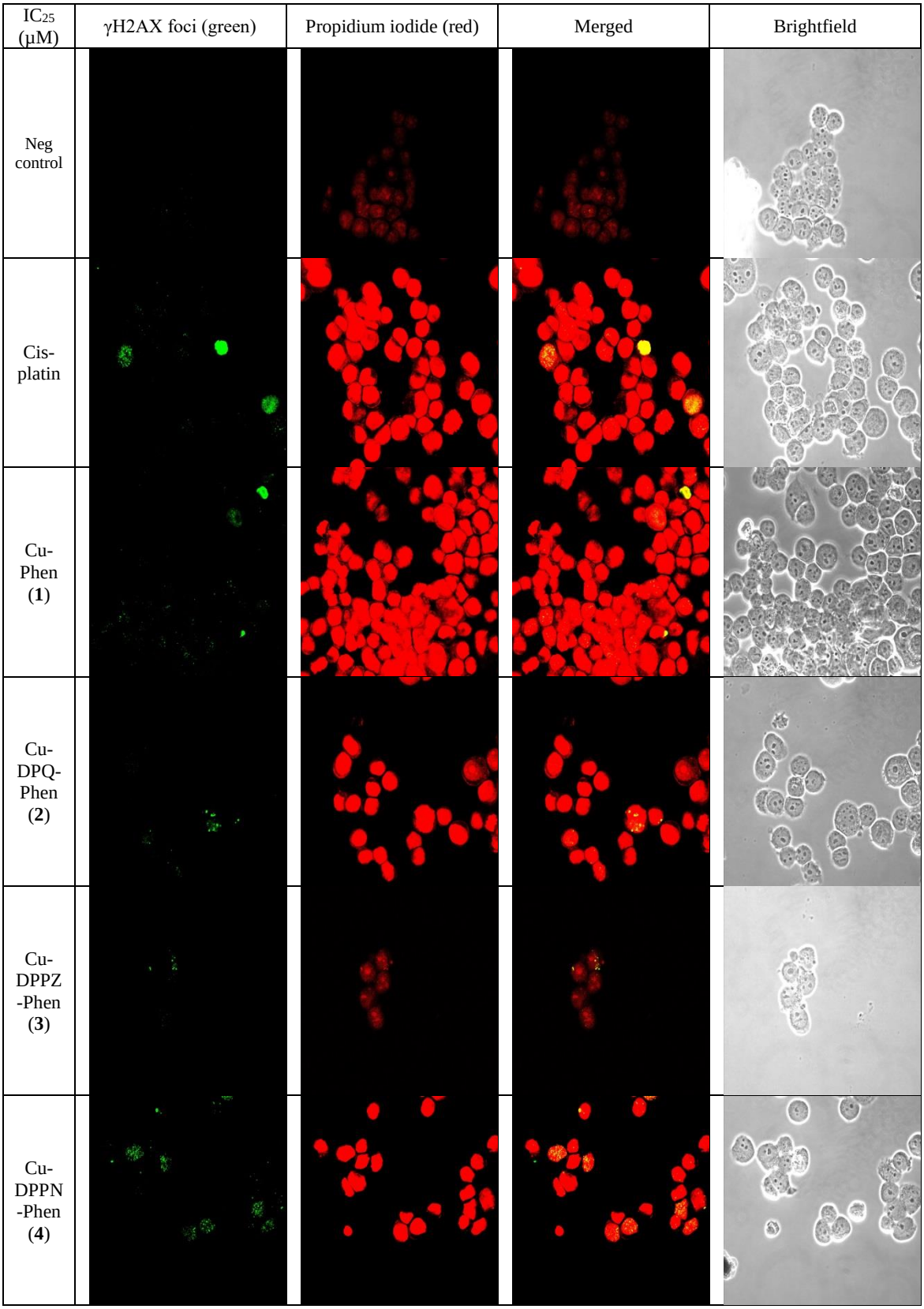

Fig. 2.9 MCF-7 cells exposed to the IC_{25} 48 h concentrations of cisplatin, Cu-Phen (**1**), Cu-DPQ-Phen (**2**), Cu-DPPZ-Phen (**3**) and Cu-DPPN-Phen (**4**) in comparison to the negative control. γH2AX foci determined using primary antibody stain with fluorescent FITC secondary label and propidium iodide used as a nuclear counter stain.

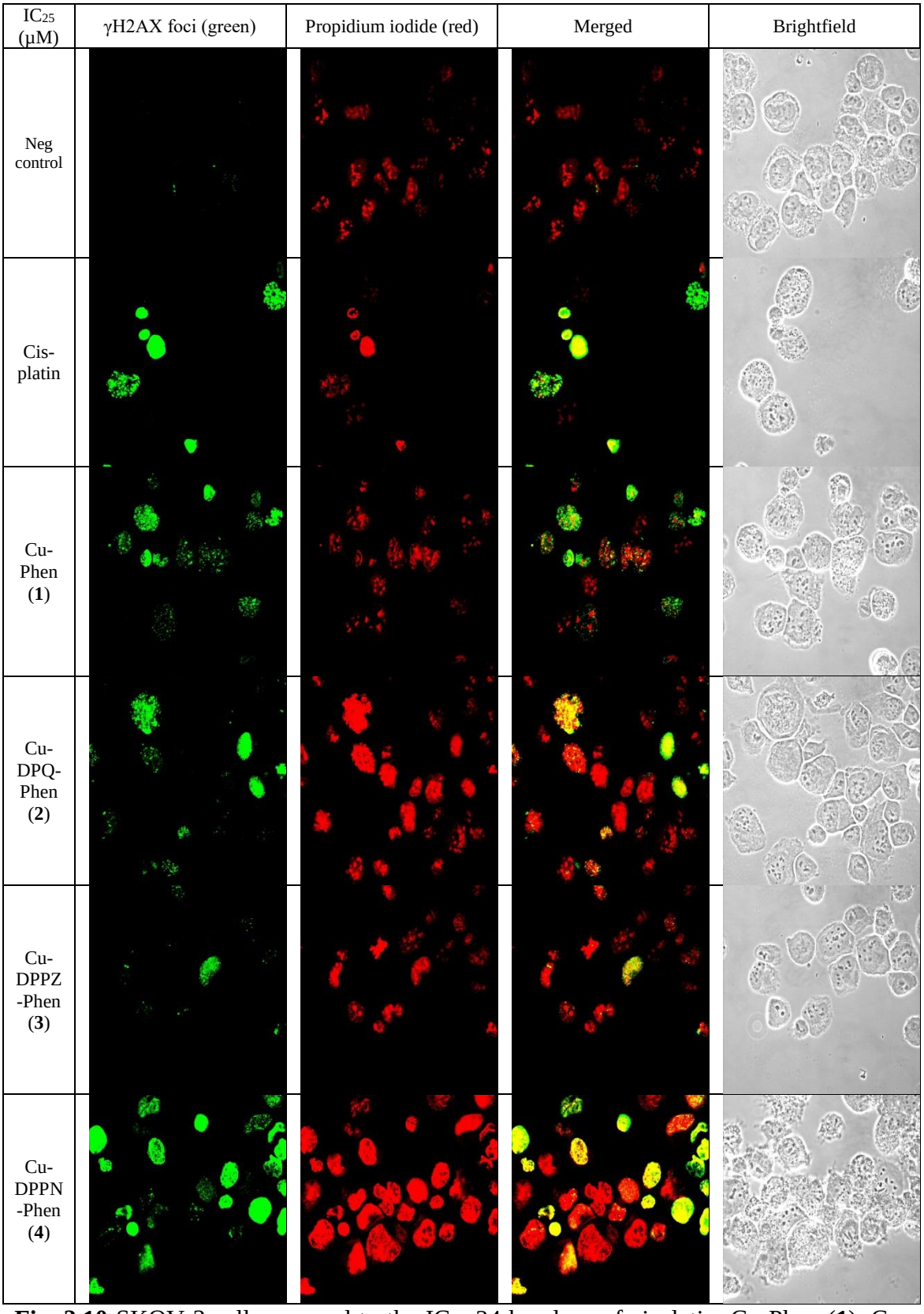

Fig. 2.10 SKOV-3 cells exposed to the IC_{25} 24 h values of cisplatin, Cu-Phen (**1**), Cu-DPQ-Phen (**2**), Cu-DPPZ-Phen (**3**) and Cu-DPPN-Phen (**4**) in comparison to the negative control. γH2AX foci determined using primary antibody stain with fluorescent FITC secondary label and propidium iodide used as a nuclear counter stain.

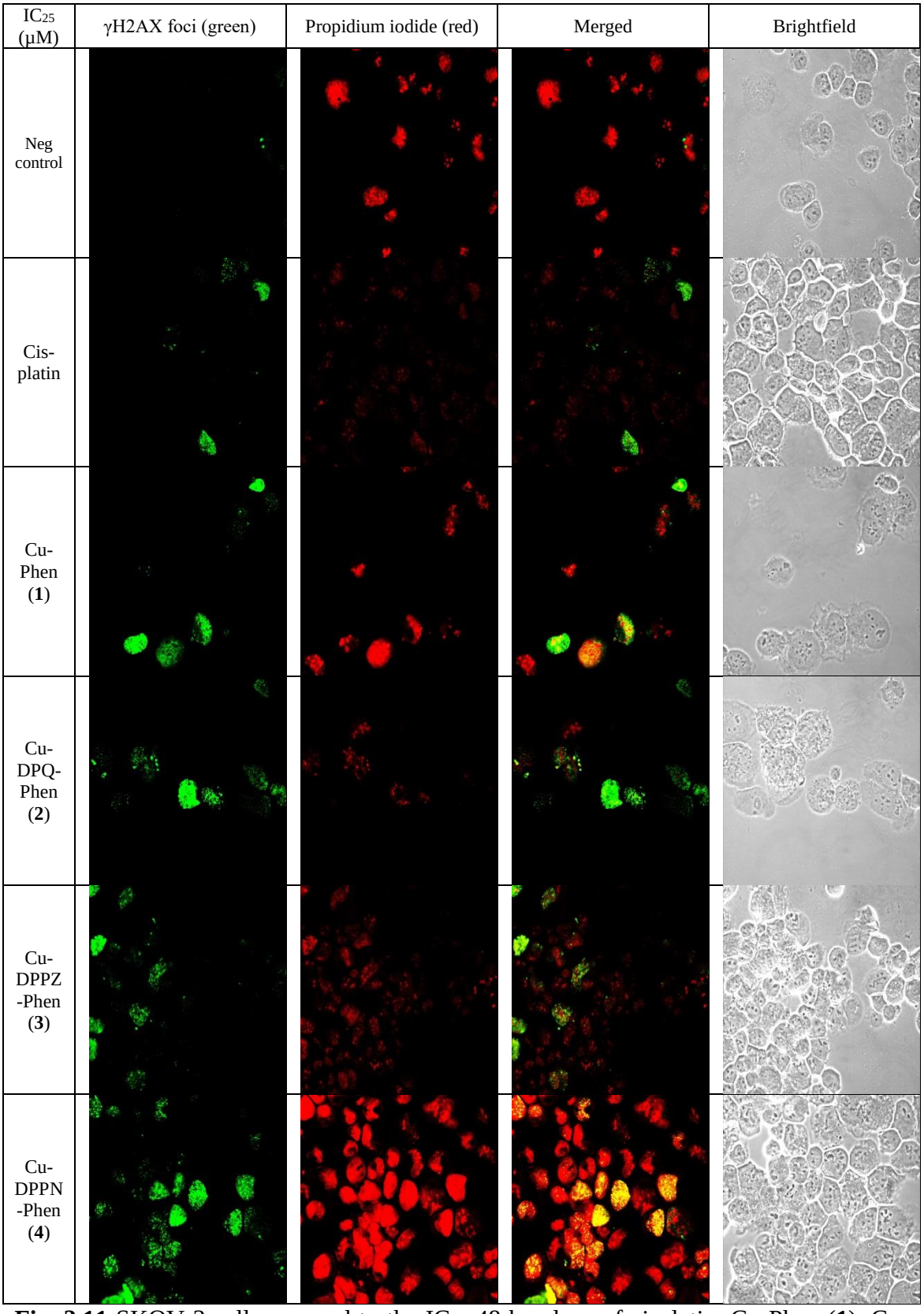

Fig. 2.11 SKOV-3 cells exposed to the IC_{25} 48 h values of cisplatin, Cu-Phen (**1**), Cu-DPQ-Phen (**2**), Cu-DPPZ-Phen (**3**) and Cu-DPPN-Phen (**4**) in comparison to the negative control. γH2AX foci determined using primary antibody stain with fluorescent FITC secondary label and propidium iodide used as a nuclear counter stain.

2.3.5 qRT-PCR analysis of cellular processes

The differences in gene expression between the two timepoints of each of the cell lines will be discussed separately. The level of activity of each target was assessed by the relative expression of the specific mRNA representative of the cDNA of the target gene being assayed. The expression of the target gene was made in relation to geometric mean expression level of the two reference genes, actin and tubulin. The standard deviation of the means calculated from both the reference gene and target gene was error propagated and subsequently Log(2) transformed to produce a 95 % confidence interval range around the log(2) transformed mean double delta Ct value. Grouped columns in **Figure 2.12** to **Figure 2.25** display the log(2) transformed mean expression value relative to the biological negative control with the broken line at y = 1 indicating negative expression below and positive expression above.

Figure 2.12 and **Figure 2.13** shows the expression of genes outlined in **Table 2.1** relative to the geometric mean of the references genes, actin and tubulin in the HT-29 cell line at 24- and 48- h exposures respectively. Twenty four hours after exposure to cisplatin the HT-29 cells demonstrate a strong apoptotic initiator (Caspase 9) and executioner (Caspase 3) activity and a moderate increase in SMAC activity this was contrasted with a strong activity of the apoptotic inhibitor XIAP and low activity of IAP1 and IAP2. Gene expression at 48 h after exposure to cisplatin presents a different profile with only the elevation of SMAC presenting. Exposure to Cu-Phen (**1**) at 24 h activates a strong executioner caspase (Caspase 3) but not the initiator (Caspase 9). The apoptosis related SMAC and anti-apoptotic IAP2 are also strongly upregulated. At 48 h exposure, Cu-Phen (**1**) initiates an inflammatory response (IL-6) with low level of Caspases 9 and 3 but is characterised by an anti-apoptotic response of high XIAP and

moderately elevated IAP1 and IAP2. Exposure to Cu-DPQ-Phen (**2**) at 24 h initiates a low level inflammatory (IL-6) and apoptotic response (Caspase 3 and SMAC)**.** The 48 h response of HT-29 to Cu-DPQ-Phen (**2**) is characterised by a strong inflammatory (IL-6) and anti-apoptotic (XIAP and IAP2) response.

Figure 2.14 and **Figure 2.15** shows the expression of genes outlined in **Table 2.1** relative to the geometric mean of the references genes, actin and tubulin in the PC-3 cell line at 24- and 48- h exposure respectively. Twenty four hours after exposure to cisplatin an early stage inflammatory response (IL-6) with a small increase in the initiator caspase (Caspase 9) and executioner (Caspase 3) is observed. At 48 h the inflammatory response (IL-6 and NF-kB) was increased with a small upregulation of caspase activity and a larger increase in IAP2. The profile of activity of Cu-Phen (**1**) is similar to the profile of cisplatin at 24 h with increased activity of IAP2. In contrast, the effects of Cu-Phen (**1**) at 48 h demonstrated no appreciable increase in the measured processes except for a mild increase in the anti-apoptotic gene (XIAP). Exposure to Cu-DPQ-Phen (**2**) at 24 h again produces a similar profile to that of cisplatin and Cu-Phen (**1**) with increased activation of Caspase 3 and IAP2. At 48 h exposure to Cu-DPQ-Phen (**2**) continues with an upregulated inflammatory process (IL-6) but had no upregulated apoptotic markers and a small upregulation of IAP2. The error bars represent a 95 % confidence interval and was large for some of the MCF-7 24 h measurements indicating a larger amout of variability in the measurement on that target gene in the experimental condition.

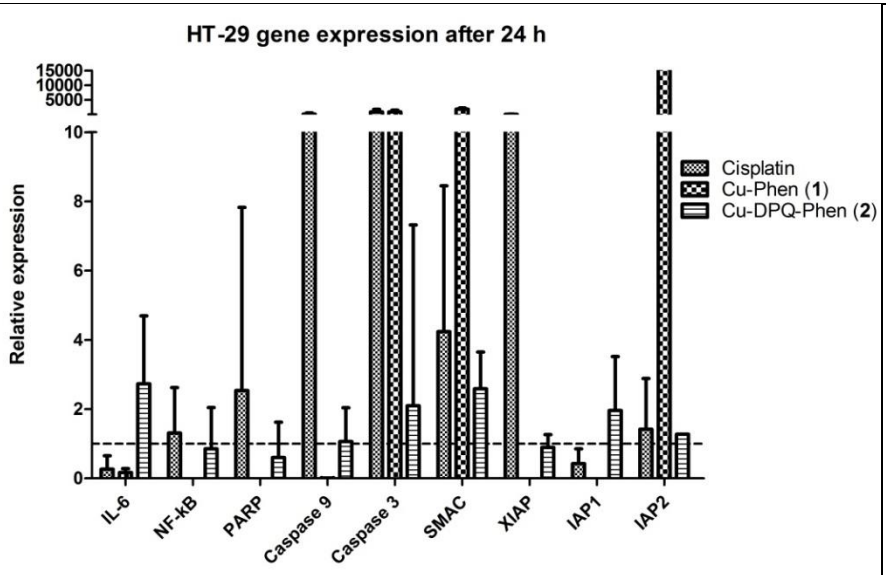

Fig. 2.12 Gene expression of HT-29 cells at 24 h following exposure to cisplatin, Cu-Phen (**1**) and Cu-DPQ-Phen (**2**). Error bars represent 95 % Confidence interval (N=3). Relative expression of target genes calculated in relation to the geometric mean of the references genes, actin and tubulin.

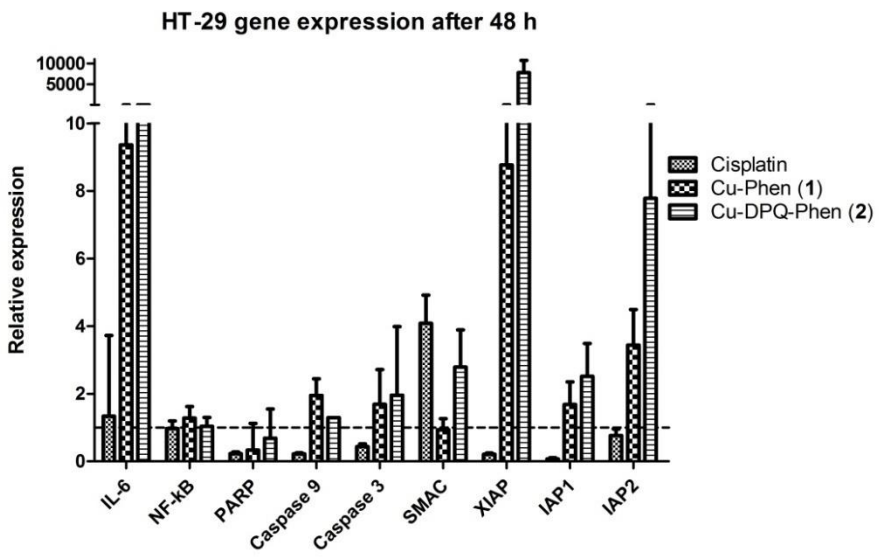

Fig. 2.13 Gene expression of HT-29 cells at 48 h following exposure to cisplatin, Cu-Phen (**1**) and Cu-DPQ-Phen (**2**). Error bars represent 95 % Confidence interval (N=3). Relative expression of target genes calculated in relation to the geometric mean of the references genes, actin and tubulin.

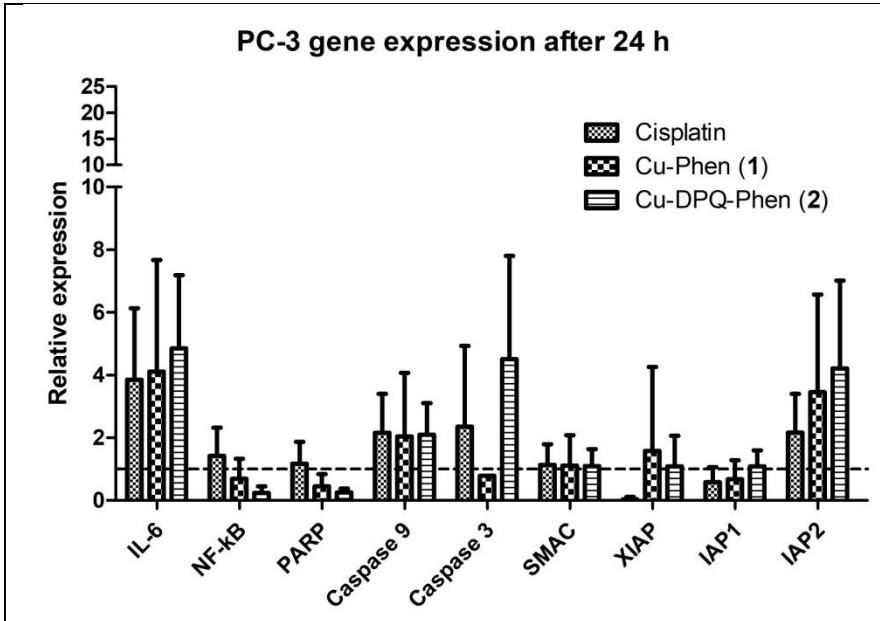

Fig. 2.14 Gene expression of PC-3 cells at 24 h following exposure to cisplatin, Cu-Phen (**1**) and Cu-DPQ-Phen (**2**). Error bars represent 95 % Confidence interval (N=3). Relative expression of target genes calculated in relation to the geometric mean of the references genes, actin and tubulin.

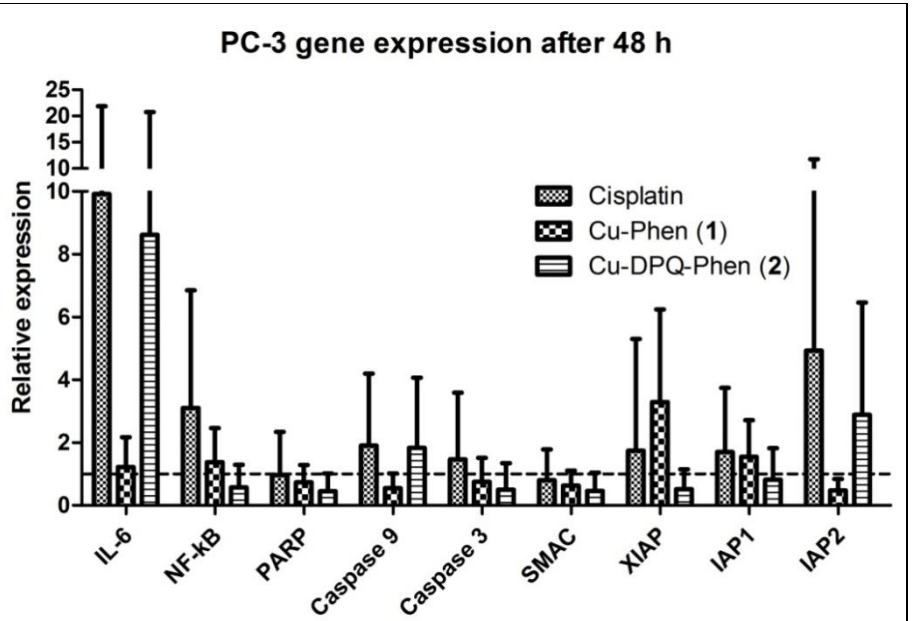

Fig. 2.15 Gene expression of PC-3 cells at 48 h following exposure to cisplatin, Cu-Phen (**1**) and Cu-DPQ-Phen (**2**). Error bars represent 95 % Confidence interval (N=3). Relative expression of target genes calculated in relation to the geometric mean of the references genes, actin and tubulin.

Figure 2.16 and **Figure 2.17** shows the expression of genes outlined in **Table 2.1** relative to the geometric mean of the references genes, actin and tubulin in the OE-33 cell line in 24- and 48- h exposures respectively. 24 h after exposure to cisplatin a large upregulation was observed in the expression of inflammatory genes (IL-6 and NF-kB), single strand DNA break (PARP), executioner Caspase 3 and IAP1. This is in contrast to the 48 h profile of the cisplatin exposure which showed no upregulation of inflammatory, DNA damage and apoptotic processes genes with only the anti-apoptotic XIAP upregulated. Exposure to Cu-Phen (**1**) at 24 h produces a small inflammatory (NF-kB) response. This profile changes after the 48 h exposure with an upregulation of apoptotic (Caspase 9, Caspase 3 and SMAC) and anti-apoptotic (XIAP) markers. Exposure to Cu-DPQ-Phen (**2**) after 24 h showed a large upregulation of apoptotic (Caspase 3) and anti-apoptotic (XIAP) response with a low level activity of apoptotic (Caspase 9 and SMAC) and anti-apoptotic (XIAP) factors at 48 h.

Figure 2.18 and **Figure 2.19** shows the expression of genes outlined in **Table 2.1** relative to the geometric mean of the references genes, actin and tubulin in the HeLa cell line in 24- and 48- h exposures respectively. Exposure to cisplatin at 24 h induced the expression of the inflammatory marker (IL-6) with a small increase in NF-κB. Apoptotic marker, Caspase 3 was upregulated with moderate upregulation of anti-apoptotic factors (XIAP, IAP1 and IAP2). In contrast, at 48 h cisplatin exposure induced no upregulation in any of the measured processes. Exposure to Cu-Phen (**1**) at 24 h resulted in the upregulation of Caspase 9 and SMAC with a progressively larger increase in anti-apoptotic factor, the largest increase occured in IAP2. In contrast, the 48 h exposure of Cu-Phen (**1**) produces no appreciable upregulation in any of the measured processes. Exposure to Cu-DPQ-Phen (**2**) at 24 h induced a small upregulation in

inflammatory markers (IL-6 and NF-kB) and a large increase in anti-apoptotic factors (IAP1 and IAP2). Again in contrast, the 48 h exposure of Cu-DPQ-Phen (**2**) induced no appreciable upregulation in any of the measured processes.

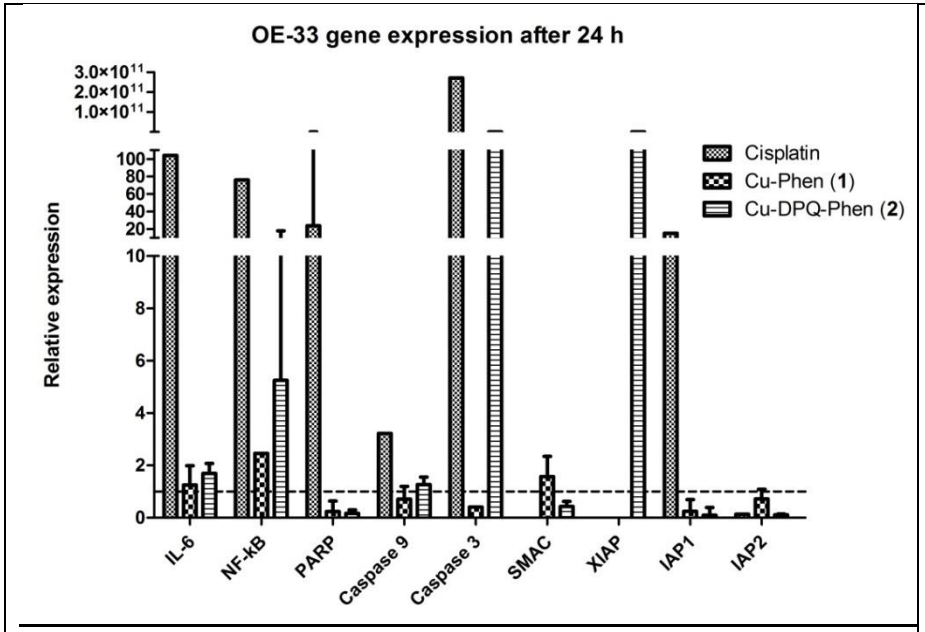

Fig. 2.16 Gene expression of OE-33 cells at 24 h following exposure to cisplatin, Cu-Phen (**1**) and Cu-DPQ-Phen (**2**). Error bars represent 95 % Confidence interval (N=3). Relative expression of target genes calculated in relation to the geometric mean of the references genes, actin and tubulin.

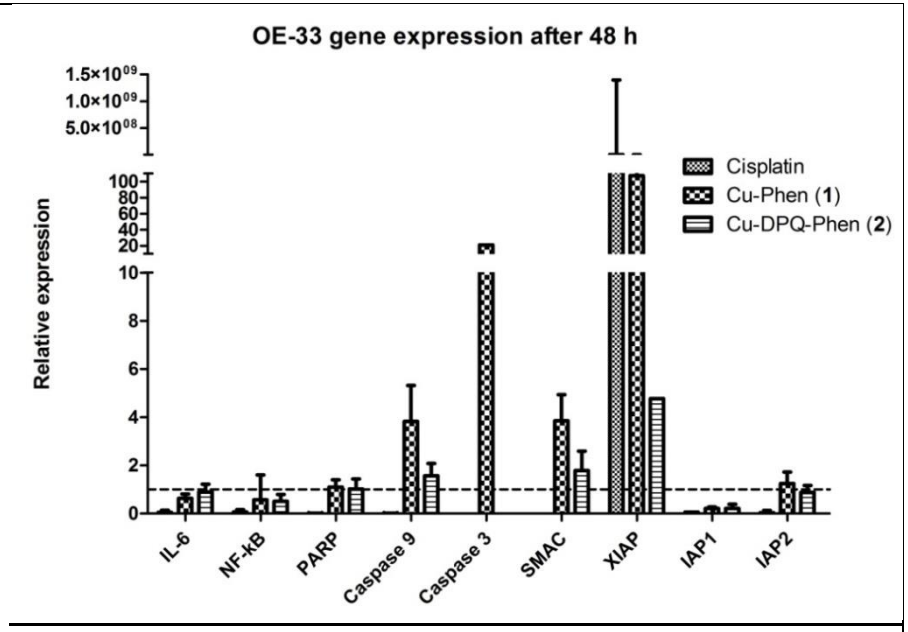

Fig. 2.17 Gene expression of OE-33 cells at 48 h following exposure to cisplatin, Cu-Phen (**1**) and Cu-DPQ-Phen (**2**). Error bars represent 95 % Confidence interval (N=3). Relative expression of target genes calculated in relation to the geometric mean of the references genes, actin and tubulin.

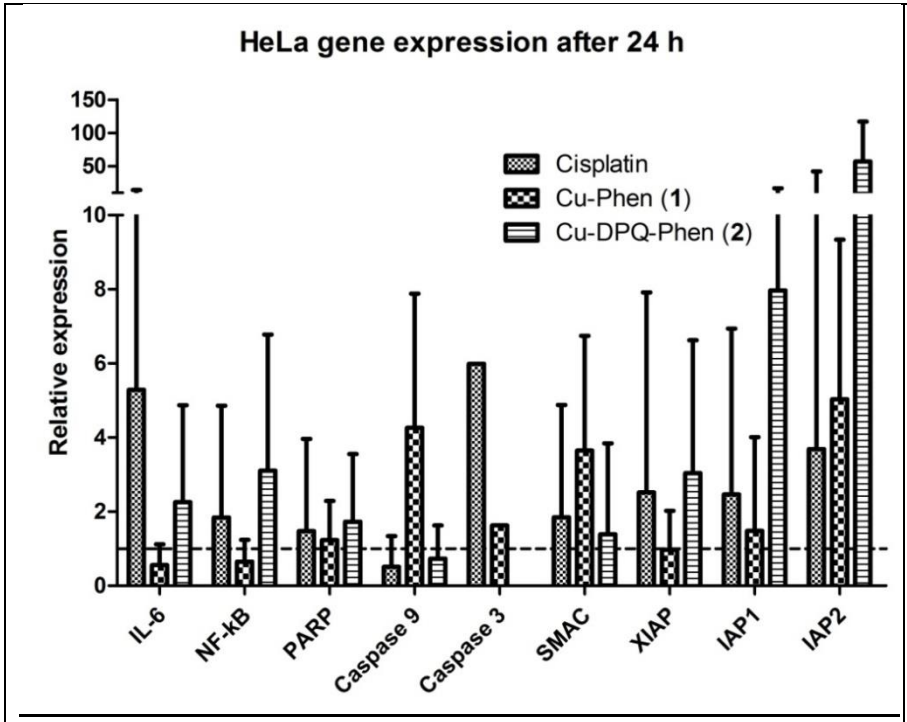

Fig. 2.18 Gene expression of HeLa cells at 24 h following exposure to cisplatin, Cu-Phen (**1**) and Cu-DPQ-Phen (**2**). Error bars represent 95 % Confidence interval (N=3). Relative expression of target genes calculated in relation to the geometric mean of the references genes, actin and tubulin.

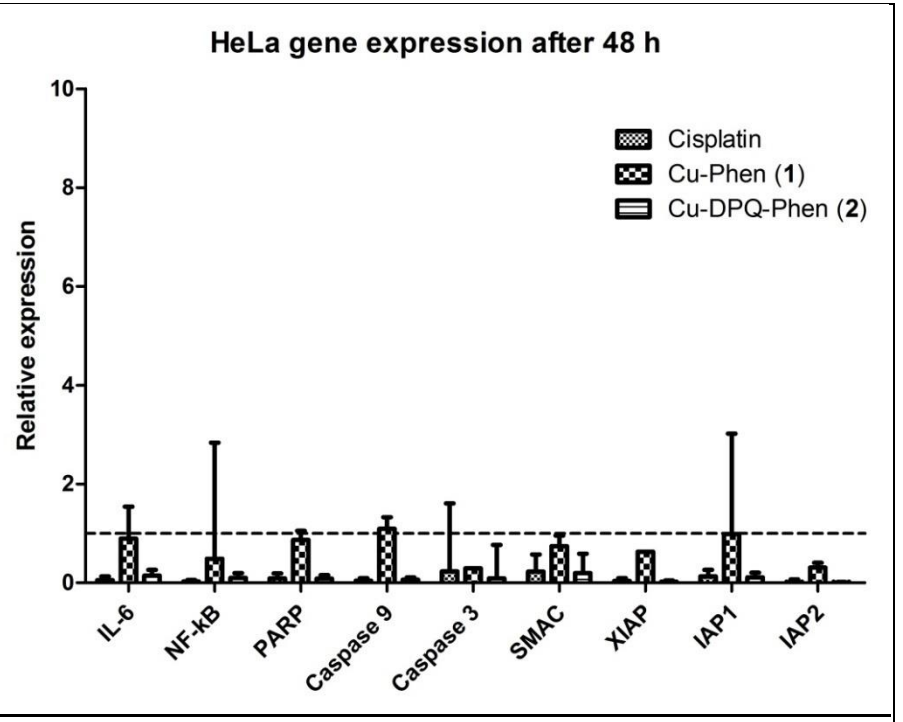

Fig. 2.19 Gene expression of HeLa cells at 48 h following exposure to cisplatin, Cu-Phen (**1**) and Cu-DPQ-Phen (**2**). Error bars represent 95 % Confidence interval (N=3). Relative expression of target genes calculated in relation to the geometric mean of the references genes, actin and tubulin.

Figure 2.20 and **Figure 2.21** shows the expression of genes outlined in **Table 2.1** relative to the geometric mean of the references genes, actin and tubulin in the MCF-7 cell line in 24- and 48- h exposures respectively. MCF-7 cells after exposure to cisplatin after 24 h produced an increase in the early stage inflammatory marker, NF-κB and no appreciable up regulation of any other measured process. At 48 h the exposure to cisplatin induced an increase in the anti-apoptotic gene IAP1. Cu-Phen (**1**) exposure over 24 h induced a similar upregulation of the early stage inflammatory marker, NF-kB and a small increase in the anti-apoptotic gene IAP2. At 48 h an increase in the apoptotic factor BAX was observed along with other process. Exposure to Cu-DPQ-Phen (**2**) for 48 h resulted in a similar upregulation of NF-κB to cisplatin and Cu-Phen (**1**). A small increase of Caspase 9 and XIAP was observed at 24 h with no other appreciable increase observed in any other process at 24 h. After Cu-DPQ-Phen (**2**) was exposed for 48 h BAX expression was induced, similarly to the exposure to Cu-Phen (**1**) indicating apoptotic induction in the MCF-7 cells.

Figure 2.22 and **Figure 2.23** shows the expression of genes outlined in **Table 2.1** relative to the geometric mean of the references genes, actin and tubulin in the SKOV-3 cell line in 24- and 48- h exposures respectively. Exposure to cisplatin after 24 h induced a small increase in the apoptotic gene, Caspase 3 and BAX. No other gene demonstrated an appreciable increase in expression. In contrast, at 48 h, cisplatin did not induce Caspase 3 and BAX expression, with only a small increase in BCL-2. Cu-Phen (**1**) induced a small increase in the early stage inflammatory marker, IL-6 and an equally small increase in the apoptotic genes, Caspase 9 and BAX. At 48 h a small increase in the early stage inflammatory marker, IL-6 and NF-kB was coupled with a small increase in PARP and the apoptotic related genes, SMAC and BCL-2. Exposure to Cu-DPQ-

Phen (**2**) induced a moderate to large increase in Caspase 3 and BAX respectively. At 48 h a increase in the early stage inflammatory marker, IL-6 was observed, with no increase seen in the apoptotic process.

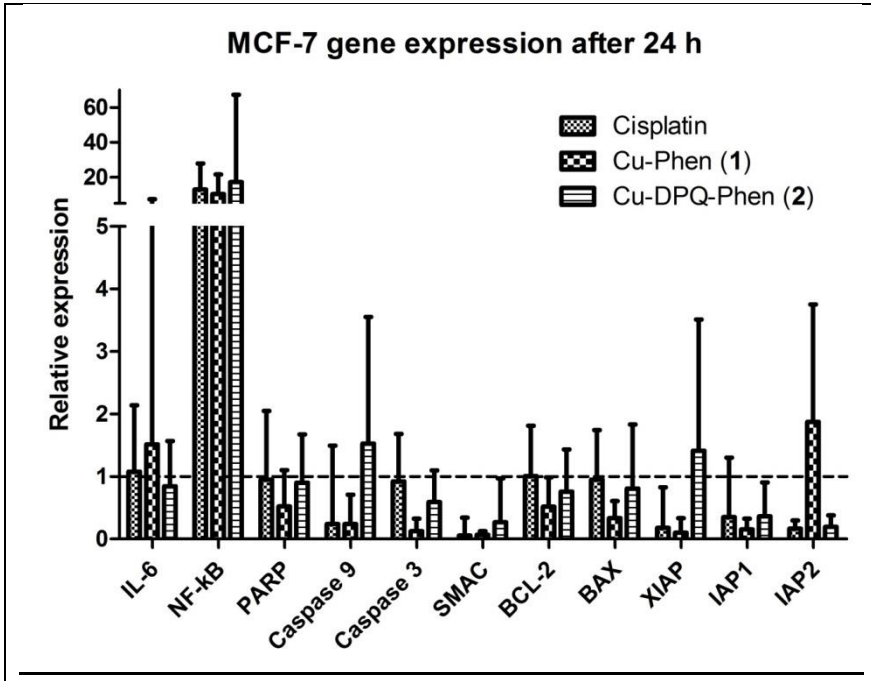

Fig. 2.20 Gene expression of MCF-7 cells at 24 h following exposure to cisplatin, Cu-Phen (**1**) and Cu-DPQ-Phen (**2**). Error bars represent 95 % Confidence Interval (N=3). Relative expression of target genes calculated in relation to the geometric mean of the references genes, actin and tubulin.

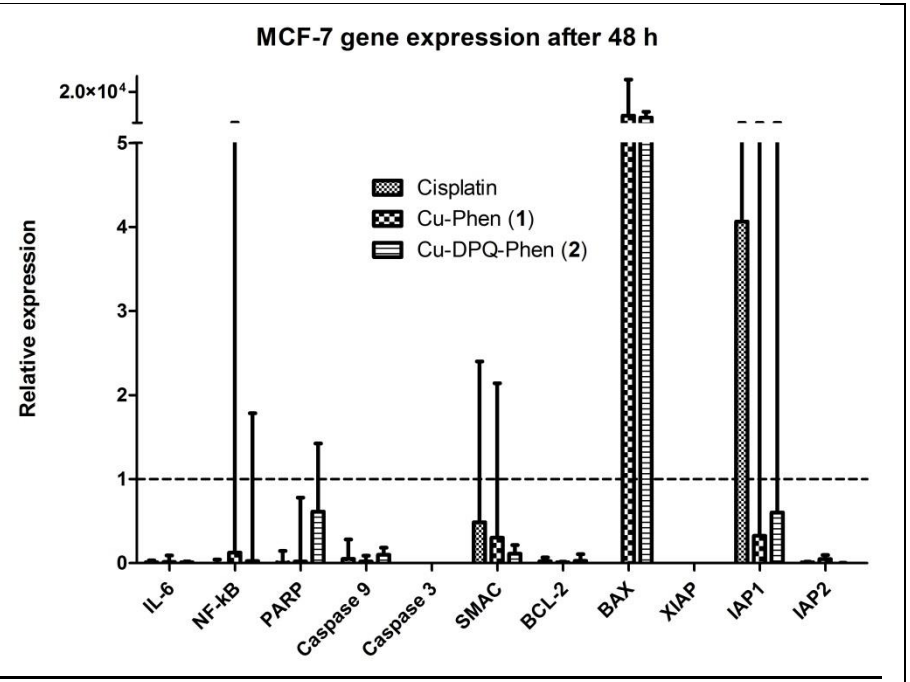

Fig. 2.21 Gene expression of MCF-7 cells at 48 h following exposure to cisplatin, Cu-Phen (**1**) and Cu-DPQ-Phen (**2**). Error bars represent 95 % Confidence Interval (N=3). Relative expression of target genes calculated in relation to the geometric mean of the references genes, actin and tubulin.

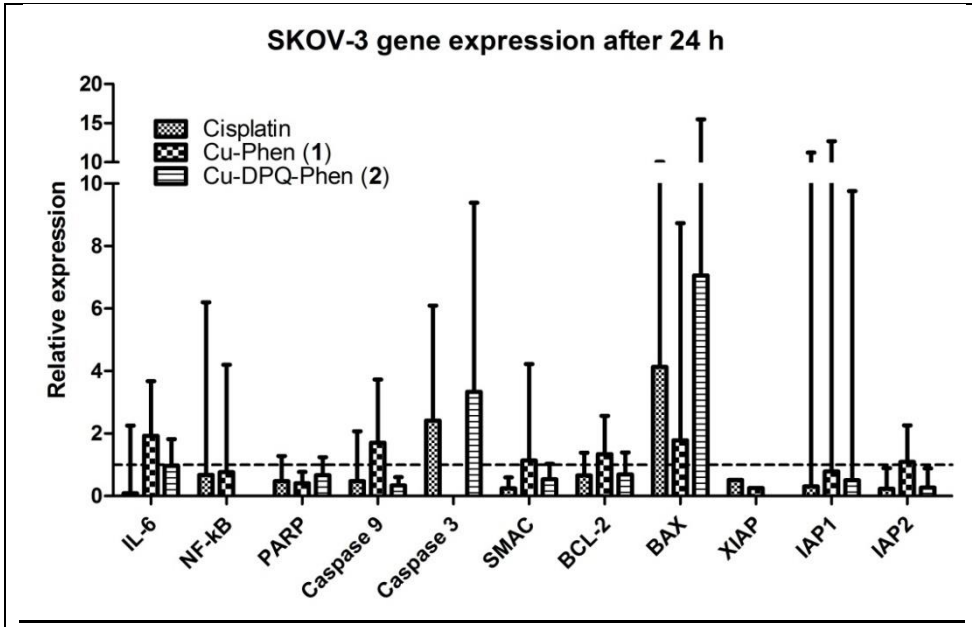

Fig. 2.22 Gene expression of SKOV-3 cells at 24 h following exposure to cisplatin, Cu-Phen (**1**) and Cu-DPQ-Phen (**2**). Error bars represent 95 % Confidence Interval (N=3). Relative expression of target genes calculated in relation to the geometric mean of the references genes, actin and tubulin.

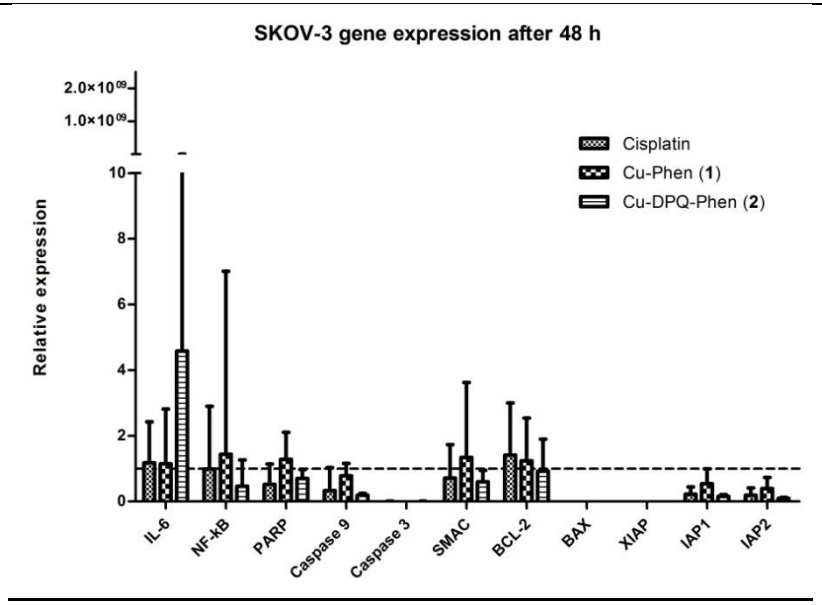

Fig. 2.23 Gene expression of SKOV-3 cells at 48 h following exposure to cisplatin, Cu-Phen (**1**) and Cu-DPQ-Phen (**2**). Error bars represent 95 % Confidence Interval (N=3). Relative expression of target genes calculated in relation to the geometric mean of the references genes, actin and tubulin.

Figure 2.24 shows the expression of genes outlined in **Table 2.1** relative to the geometric mean of the references genes, actin and tubulin in the A2780 cell line. Exposure to doxorubicin upregulated apoptotic processes, such as Caspase 9, BCL-2 and BAX. XIAP, an inhibitor of apoptosis was also upregulated. Cisplatin induced a large increase in the expression of the anti-apoptotic gene, XIAP. Cu-Phen (**1**) exposure induced a moderate increase in the expression of the apoptotic related genes, Caspase 9, BCL-2 and BAX. A large increase in the anti-apoptotic, XIAP was observed. Cu-Phen (**1**) induces a moderate increase in the expression of the apoptotic related genes, Caspase 9, BCL-2 and BAX. A large increase in the anti-apoptotic, XIAP was observed. Exposure to Cu-DPQ-Phen (**2**) shows no appreciable increase in any of the apoptotic process. Cu-DPPZ-Phen (**3**) induced a small increase in the apoptotic gene BAX. Exposure to Cu-DPPN-Phen (**4**) induced only a small increase in the expression of the anti-apoptotic gene, XIAP. All other genes were either not detected or not increased in expression.

Figure 2.24 shows the expression of genes outlined in **Table 2.1** after a 24 h exposure, relative to the geometric mean of the references genes, actin and tubulin in the A2780/ Cis cell line. Exposure to doxorubicin induced a decrease or undetectable change in the apoptotic genes and related processes. Cisplatin exposure induced a strong increase in the apoptotic related factor, BCL-2. Exposure to Cu-Phen (**1**) induced a decrease or undetectable change in the apoptotic related genes. Cu-DPQ-Phen (**2**) induced a strong apoptotic activation of Caspase 3 while Cu-DPPZ-Phen (**3**) induced a strong increase in the apoptotic factors, Caspase 9 and BAX. The exposure to Cu-DPPN-Phen (**4**) induced a large response across all of the measured processes. Apoptosis related factors showed increases in Caspase 9, Caspase 3, BCL-2 and BAX.

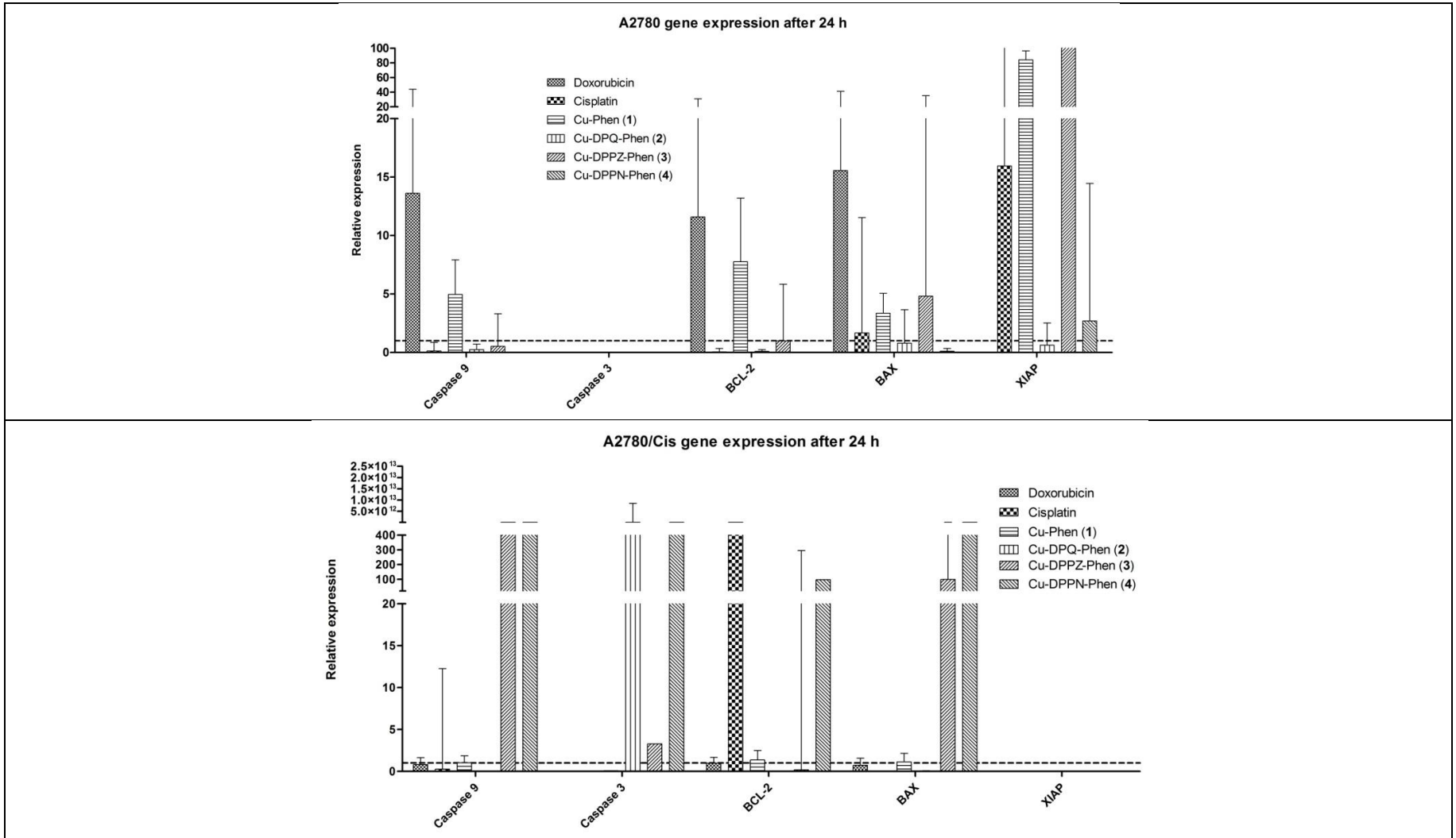

Fig. 2.24 Gene expression of A2780 and A2780/ Cis cells at 24 h following exposure to doxorubicin, cisplatin, Cu-Phen (**1**) and Cu-DPQ-Phen (**2**), Cu-DPPZ-Phen (**3**) and Cu-DPPN-Phen (**4**). Error bars represent 95 % Confidence Interval (N=4). Relative expression of target genes calculated in relation to the geometric mean of the references genes, actin and tubulin.

2.4 Discussion

The experimental work detailed in this Chapter describes the fundamental evaluation of the Cu(II) phenanthroline-phenazine complex series and compares them to the clinical therapeutics, cisplatin and doxorubicin. A range of cell lines derived from different solid tumours were used to evaluate the activity of the drugs across a broad range of phenotypes. A range of sensitivities was detected in all of the cell lines to cisplatin and the Cu(II) phenanthroline-phenazine complex series, demonstrating the potential of anti-cancer activity. ROS (H_2DCFDA), DNA DSB formation (γH2AX), inflammation and the apoptosis (gene expression) were used to provide a screen of the mechanisms of action which will be expanded on in subsequent chapters.

Throughout viability testing the novel Cu(II) complexes were shown to exert time-dependent, superior toxicity in comparison to cisplatin and doxorubicin (except where N.P. is indicated). Overall a viability profile with the following cadence was demonstrated, with some exceptions: Cu-DPPZ-Phen (**3**) (greatest toxicity) > Cu-Phen (**1**) > Cu-DPQ-Phen (**2**) > Cu-DPPN-Phen (**4**) (lowest toxicity). The extension of the phenazine ligand generally resulted in increased loss of cell viability. In particular, Cu-DPPZ-Phen (**3**) demonstrated the lowest viability at both 24- and 48- h in the tested cell lines, with Cu-DPPN-Phen (**4**) demonstrating the highest viability. With the exception of the cisplatin sensitive MCF-7 cell line one or more of the Cu(II) complex series exceeded the activity of cisplatin in all cell lines thereby demonstrating their further developmental potential. A key finding of this investigation through multiple cell lines was the demonstration of the superior inhibition of viability of the Cu(II) complex series to cisplatin in all the cisplatin resistant cell lines (PC-3, SKOV-3 and A2780/ Cis). The activity of the Cu(II) complex series in SKOV-3 cells was previously demonstrated with

a similar result profile in the study by Molphy *et al*. (2014). The results from the Cu(II) complexes in the cisplatin resistant cell lines may indicate that they have a different mechanism of action to cisplatin, which is a key therapeutic objective in inorganic medicinal chemistry. Many of the sensitive cell lines demonstrated very little difference between the response to cisplatin and the Cu(II) complexes.

ROS generation as a therapeutic characteristic has proven to be a strong developmental objective in metal-based drugs (Cadet *et al.* 2017). The previous study by Molphy *et al.* (2015), demonstrated that Cu-DPQ-Phen (**2**), Cu-Phen (**1**) and Cu-DPPZ-Phen (**3**) resulted in the production of metal-hydroxo or free hydroxyl radicals (˙OH) as the predominant oxidative species and in-turn produced DNA oxidation of 8-oxo-2′-deoxyguanosine (8-oxo-dG) lesion with strong evidence that singlet oxygen generation is the causative factor (Frelon *et al*. 2003). These conditions were however examined on purified pUC19 plasmid DNA and not *in-vitro*. Here the *in-vitro* studies on HeLa cells demonstrated moderate ROS production after exposure to Cu-Phen (**1**) but weaker production after exposure to Cu-DPQ-Phen (**2**), Cu-DPPZ-Phen (**3**) and Cu-DPPN-Phen (**4**). Cu-Phen (**1**) has been previously demonstrated as a chemical nuclease, capable of abstracting hydrogen (•H) from the pentose ring of DNA in the presence of both exogenous reductant (Cu(II) → Cu(I)) and oxidant (O_2 or H_2O_2) (Sigman *et al.* 1979; Chen *et al.* 2001; Santini *et al.* 2014). The results of the weaker ROS production from the phenazine π-backbone extended ligands demonstrate that the toxicity in the cells may not be entirely a result of ROS generation.

One of the primary developmental objectives in inorganic medicinal chemistry is the establishment of an alternative DNA interacting metal-based drug, with the hope of

emulating and expanding of the therapeutic success of the platinum-based cisplatin. The study by Molphy *et al.* (2014), established that the Cu(II) phenanthroline-phenazine complexes bound to calf thymus DNA as follows: Cu-DPQ-Phen (**2**) ~ Cu-DPPZ-Phen (**3**) (strongest) > Cu-DPPN-Phen (**4**) > Cu-Phen (**1**) (weakest) and additionally was found to interact with DNA through intercalation of both the minor and major grooves. In all tested cell lines, the lowest viability was observed after exposure to Cu-DPPZ-Phen (**3**) with the highest being Cu-DPPN-Phen (**4**). This published data suggests that the intercalation capability of the Cu(II) phenanthroline-phenazine complexes may not have sole responsibility for inducing the toxicity in the cell. In this study both MCF-7 and SKOV-3 cells induced the production of γH2AX foci after exposure to cisplatin, Cu-Phen (**1**), Cu-DPQ-Phen (**2**), Cu-DPPZ-Phen (**3**) and Cu-DPPN-Phen (**4**), however at different intensities. MCF-7 cells demonstrated γH2AX foci formation but with a low % of cells effected, while SKOV-3 cells demonstrated γH2AX foci formation with a much higher % cell affected. Based on the lower viability values of the MCF-7 compared to SKOV-3 cells when exposed to the Cu(II) phenanthroline-phenazine complex series, the lower percentage of γH2AX foci formation of effected cells may have a greater role in the toxicity of the cisplatin sensitive, MCF-7 cells in comparison to the higher percentage of γH2AX foci cisplatin resistant, SKOV-3 cells.

Apoptosis, as a means through which programmed cell death occurs, is a common feature of the mechanism of action of cisplatin (Dasari and Tchounwou 2014). Due to its investigation in relation to cisplatin, the Cu(II) complex, [Cu(*o*-phthalate)(phenanthroline)] has also been studied both from the intrinsic and extrinsic apoptosis perspective (Slator *et al.* 2016).

The cisplatin sensitive cell lines: HT-29, MCF-7, OE-33, HeLa and A2780 generally responded to the exposure of cisplatin and the Cu(II) phenanthroline-phenanzine complexes with the upregulation of both apoptotic and anti-apoptotic process over both 24- and 48- h timepoints. In addition to apoptosis, a mild to strong upregulation in the anti-apoptotic genes was observed in the HT-29, OE-33, HeLa and MCF-7 cells demonstrating that the apoptotic process may not have sole responsibility for cell death after exposure to Cu-Phen (**1**). Exposure to Cu-DPQ-Phen (**2**) was characterised by a time-dependent inflammatory response coupled to a time-dependent apoptotic response in the HT-29, OE-33 and MCF-7 cell lines. The response to cisplatin was characterised by a strong apoptotic activation in contrast to the more complex response to the Cu(II) phenanthroline-phenanzine complexes. The cisplatin resistant cells: PC-3, SKOV3 and A2780/ Cis responded to the cisplatin exposure with a similar exposure to the cisplatin sensitive cells lines however the response to the Cu(II) phenanthroline-phenanzine complexes was more complex. The response of both SKOV-3 and A2780/ Cis to Cu-Phen (**1**) showed no upregulation of apoptotic and anti-apoptotic processes, indicating that these may not be part of its resistance mechanism. In contrast, SKOV-3 cells exposure to Cu-DPQ-Phen (**2**) demonstrated an apoptotic response at 24 h which was lost at 48 h, similarly to the SKOV-3 exposure to Cu-Phen (**1**). Exposure of Cu-DPQ-Phen (**2**) in the A2780/ Cis cells induced a strong executioner caspase response but no other apoptotic marker. The upregulation of IAP's has been a well documented resistance factor in therapeutics and is a potential factor in these results (Li *et al.* 2001; Nomura *et al.* 2005; Zhang *et al.* 2008; Del Bello *et al.* 2013). The activation of apoptotic markers was observed following Cu-DPPZ-Phen (**3**) and Cu-DPPN-Phen (**4**) exposures with progressive expansion of apoptosis signature, as the phenazine π-backbone was extended.

Table 2.5 Summary of Chapter 2 results

<table>
<tr><th>Cisplatin response profile</th><th>Cell line</th><th>Viability/ MTT assay</th><th>Gene expression (apoptosis)</th><th>DNA DSB formation (γH2AX)</th><th>ROS</th></tr>
<tr><td rowspan="2">Sensitive</td><td>MCF-7</td><td>Mild activity of complexes 1-4 compared to cisplatin</td><td rowspan="2">Apoptotic process not prominent feature of response to complexes 1-4</td><td>Low DNA DSB formation with complexes 1-4</td><td rowspan="6">N.P</td></tr>
<tr><td>A2780</td><td>Strong activity of complexes 1-4 compared to cisplatin</td><td>N.P.</td></tr>
<tr><td rowspan="3">Resistant</td><td>PC-3</td><td rowspan="3">Far superior activity of complexes 1-4 compared to cisplatin</td><td>Mild inflammatory response</td><td></td></tr>
<tr><td>SKOV-3</td><td rowspan="2">Apoptotic process featured more prominently in response to complexes 1-4</td><td>High DNA DSB formation with complexes 1-4</td></tr>
<tr><td>A2780/ Cis</td><td rowspan="3">N.P</td></tr>
<tr><td rowspan="3">Mixed responses</td><td>OE-33</td><td>Stronger activity of complexes 1-4 compared to cisplatin</td><td rowspan="3">Mild IAP and inflammatory gene expression markers</td></tr>
<tr><td>HT-29</td><td>lower overall activity of complexes 1-4 compared to cisplatin</td></tr>
<tr><td>HeLa</td><td>Stronger activity of complexes 1-4 compared to cisplatin</td><td>Moderate ROS generation</td></tr>
<tr><td colspan="6"></td></tr>
<tr><td colspan="6">Further in-vitro mechanistic investigations carried out in Chapter 3 and 4</td></tr>
<tr><td colspan="3">Cisplatin sensitive cells (MCF-7 and A2780)</td><td colspan="3">Cisplatin resistance cells (SKOV-3 and A2780/ Cis)</td></tr>
<tr><td colspan="6">Label free Quantitative proteomic (MCF-7 and SKOV-3 only)
Mitochondrial membrane potential decay
Mitochondrial related gene expression</td></tr>
</table>

N.P. Not Performed

The work described in this chapter and summarised in **Table 2.5** identified the activity and initial characterisation of the mechanisms of action of the novel Cu(II) phenanthroline-phenazine complexes with the clinical drugs, cisplatin and doxorubicin in a series of tumorigenic cell lines. The MCF-7, A2780 cells were shown to be sensitive to cisplatin while SKOV-3, A2780/ Cis cells were shown to be resistant. The Cu(II) phenanthroline-phenazine complexes strongly exceeded the activity of cisplatin

in the resistant cells. Intracellular ROS generation was found to vary between mild to moderate levels of generation. DNA DSB formation indicated by γH2AX foci was found weakly positive in the MCF-7 compared to SKOV-3 cells. Both the MCF-7 and SKOV-3 have demonstrated good comparative profiles through cell viability/ toxicity and DNA DSB assays. Additionally, they have demonstrated using gene expression that the process of apoptosis was not a prominent feature of the MCF-7 and A2780 cell lines while the apoptotic process featured more prominently in the SKOV-3 and A2780/ Cis cells.

The contrasting results between the MCF-7 and SKOV-3 cells demonstrated that a proteomic level evaluation (Chapter 3) of both these cell lines would give new insights into their responses. The evaluation of MCF-7 and SKOV-3 cells for mitochondrial related gene expression along with A2780 and A2780/ Cis cells (Chapter 4) allowed for a more detailed investigation of their mechanism of action.

Chapter 3: *In-vitro* mammalian cell proteomic responses to novel Cu(II) phenanthroline-phenazine complexes

3.1 Introduction

Mass spectrometry based proteomics has emerged in the past two decades due to advances in chromatographic and mass spectrometric detection technology and has greatly benefitted research into intracellular signalling, biomarker discovery, infection classification and characterisation and recently, drug target evaluation (Dias *et al.* 2016). With the sequencing of the first cancer genome in 2008 (Ley *et al.* 2008), a large quantity of tumorigenic information was acquired which aided in drug target selection and prognostic evaluation. Similarily to genomic sequencing technologies, the exapansion of modern proteomic technologies has opened up a new avenue into evaluating response of the cell at protein level to therapeutic action.

Mass spectrometry and Two Dimensional (2D)-gel based analysis platforms are the two main methodologies used for quantitative proteomics. Two-dimensional gel electrophoresis utilises polyacrylamide gels to separate proteins by pH and size, with comparisons between gel spots revealing relative fold changes in protein expression. The spots of interest can then be excised, chemically digested and identified using LC/MS and protein sequence alignment (Dias *et al.* 2016). Mass spectrometry based quantitative proteomics is accomplished using several peptide spectral identification methods. The use of chemical labelling such as isobaric Tags for Relative and Absolute Quantification (iTRAQ), Tandem Mass Tags (TMT) and dimethyl labelling are used to label different biological samples to measure the relative abundance of peptides.

Over the past few decades the development of metal-based drugs has occurred through the evaluation of purified biomolecules extracts. The results from these investigations have been further enhanced using stratified experiments in *in-vitro* mammalian models

with successful candidates progressing to murine models. Many metal-based drugs including copper-based coordinated complexes are designed to target DNA and as such the evaluation of their capabilities has been restricted to non-cell-based assays and only later *in-vitro* evaluation. Additionally, ROS production has been classified as a major contributing factor towards their therapeutic effects on the cell. While this reductionist approach is valuable in defining the potential mechanism of action, it is limited by an inability to take into account other contributing factors contributing to the observed cellular effects. The effects of metal-based drugs, principally cisplatin on proteins, and in particular their preponderance to form adducts in sulphur rich sequences have been the subject of studies (Florea and Büsselberg 2011; Trudu *et al.* 2015). Recently, a more concerted effort has been placed on establishing the interaction of metal-based drugs with proteins on the overall therapeutic outcome of the cell and also resistance profiles (Mena *et al.* 2013; Moraleja *et al.* 2014; Giner Martínez-Sierra *et al.* 2015; Kullmann *et al.* 2015). Examination of platinum and other metal content in the cell utilising ICP-MS and ESI LTQ technologies investigate the degree to which platinum content is forming DNA adducts, (Harrington *et al.* 2010; Corte-Rodríguez *et al.* 2015), the interaction of platinum with other proteins (Timerbaev *et al.* 2012; Moraleja *et al.* 2014) and effects on the cellular metalloproteome (Timerbaev *et al.* 2012). The interaction of a metal complex with epigenetic regulators such as histone deacetylases (HDAC), BRD4 and JMJD2 has also gained prominence (Leung *et al.* 2016). Copper complexes have demonstrated DNA double strand break (γH2AX) (Kellett *et al.* 2012; Prisecaru *et al.* 2013) and topoisomerase-like activity (Slator *et al.* 2016) as part of their mechanism of action. The addition of proteomics to these mechanistic studies will provide new insight into protein interaction and potential epigenetic effects which provide a more comprehensive analysis of the *in-vitro* mechanistic effects. The proteomic evaluation of

organogold(III) (Gamberi *et al.* 2014) and titanium dioxide (Vuong *et al.* 2016) demonstrated changes in multiple protein functional classes such as stress response, metabolic, transport and protein synthetic process. The analysis of these individual protein expression changes in addition to wider changes across functional classifications give significant information regarding the response of the cell to the therapeutics. Proteomic approaches to mechanism of action studies can also be integrated into transcriptomic and metabolomics data sets (Cho *et al.* 2012; Wilmes *et al.* 2013) to produce a highly integrated assessment of the potential success of a candidate therapeutic and also can identify alternative drug targets not previously envisaged in the initial workup.

The work described in this chapter uses label free quantitative proteomics to identify and assess the quantitative changes in proteins following treatment with Cu(II) phenanthroline-phenazine complexes in cisplatin sensitive and resistant cell lines. This comparison will help identify potential mechanisms of action resulting from changes in the cellular proteome and identify additional biological targets for evaluation of Cu(II) phenanthroline-phenazine complexes.

3.2 Material and methods

3.2.1 Cell preparation, exposure and processing

The cisplatin sensitive, MCF-7 and cisplatin resistant, SKOV-3 cells were chosen for the LFQ proteomics study due to their differential response to cisplatin and their sensitivity to Cu-Phen (**1**) and Cu-DPQ-Phen (**2**). Both cell lines were subcultured into T25 flasks at a density of 1×10^5 cells. After 24 h cells were exposed to their respective IC_{25} concentrations (as in the gene expression and γH2AX studies in Chapter 2) of Cu-Phen (**1**) and Cu-DPQ-Phen (**2**) for a 24- and 48- h timepoints. While both Cu-DPPZ-Phen (**3**) and Cu-DPPN-Phen (**4**) demonstrated good toxicity in Chapter 2, an increased variability in results, cost and complexity of processing the generated data excluded them from analysis in this chapter. After 24- and 48- h, 500 µl of cell lysis buffer (Sigma, Ireland) (6 M Urea, 2 M Thiourea, 0.1 M Tris-HCl (pH 8.0)) (Appendix 1.5.1) (Cat# U5378, Cat# T8656, Cat# T3038 respectively) was added to each flask and left to incubate for 1 h. Lysed cellular components were then transferred to an Eppendorf tube (Thermo, USA) (Cat# 90410) and were incubated for a further 3 h on a rotary mixer. Following this the samples were centrifuged at 6000 g. The supernatant was then transferred to a new tube and stored at -20 ˚C until required.

3.2.2 In-solution digestion protocol using ProteaseMAX

The samples were thawed on the day of the digestion procedure. The Bradford assay (BioRad, USA) (Cat# G-250) (Appendix 1.5.2) was used to determine the concentration of protein in each sample. Sixty µg of protein in 25 µl of cell lysis buffer was removed and subjected to the in-solution protein digestion protocol using ProteaseMAX (Promega, USA) (Cat# V2071) (Appendix 1.5.3). Samples were re-suspended in sample re-suspension buffer with the proteolytic inhibitors; Aprotinin (Sigma, Ireland) (10

mg/mL) (Cat# A6106), Leupeptin (Sigma, Ireland) (Cat# L5793), Pepstatin (Sigma, Ireland) (Cat# P5318) and TLCK (Sigma, Ireland) (Cat# T7254) added. One hundred and twenty five µl of ammonium bicarbonate (50 mM) (Sigma, Ireland) (Cat# 09830) was added to the sample along with 1 µl of DTT (0.5 M) (Sigma, Ireland) (Cat# D0632). Samples were incubated at 56 °C for 20 min. Once samples had cooled 2.7 µl of IAA (0.55 M) (Sigma, Ireland) (Cat# I4386) was added, followed by incubation at room temperature for 15 min in the dark. A working solution of ProteaseMAX (1 % (w/v stock) (Promega, USA) (Cat# V2071) and sequence grade Trypsin (0.5 µg/µl) (Promega, USA) (Cat# V5111) (Appendix 1.5.3) was added to each of the samples with a subsequent overnight incubation at 37 °C. Following the overnight incubation the samples were acidified with 1 µl of TFA (Sigma, Ireland) (Cat# 8.08260), vortexed and incubated at room temperature for 5 min and subsequently centrifuged at 13,000 g for 10 min at room temperature. See Appendix 1.5.3 for further details of in-solution protein digestion. Following the in-solution digestion protocol one of the aliquots from each biological sample was subjected to the C18 spin columns (Thermo, USA) (Cat# 89870) (Appendix 1.5.4 and 1.5.5) which used reverse phase chromatography to enrich the hydrophobic peptides before mass spectrometric analysis.

3.2.3 Sample clean-up using C18 spin-columns

C18 spin-columns (Thermo, USA) (Cat# 89870) were used to enrich the hydrophobic peptides and desalt the eluted peptides prior to mass spectrometric analysis. Samples were mixed with the sample buffer 1 (Appendix 1.5.4). Two hundred µl of activation solution (Appendix 1.5.4) was added to each of the columns to rinse and wet the separating resin. Columns were centrifuged at 1500 g for 1 min and flow-through was discarded. This process was repeated once. Two hundred µl of equilibrium solution

(Appendix 1.5.4) was added to each of the columns and centrifuged at 1500 g for 1 min and flow-through was discarded. This process was repeated once. Samples (10-150 µl; up to 30 µg) were loaded to the top of the resin bed and the columns were placed in new receiver tubes. Samples were centrifuged at 1500 g for 1 min, the flow-through was recovered and re-applied to the column. This step was repeated twice more to ensure complete sample binding. The columns were transferred into new receiver tubes and 200 µl of wash buffer (Appendix 1.5.4) was added. The columns were centrifuged at 1500 g for 1 min and the flow-through was discarded. This step was repeated twice more to remove high levels of contaminants. The columns were placed in new receiver tubes and 25 µl of elution buffer (Appendix 1.5.4) was applied to the top of the resin bed. The columns were centrifuged at 1500 g for 1 min. This step was repeated twice more using the same receiver tube to collect a total ~75 µl of eluant. The resulting samples were dried out in a SpeedyVac (Thermo, USA) at medium heat for 1 h. Samples were stored at -20 °C until loading onto the Q Exactive™ (Thermo, USA). The constituents and procedure for the C18 reverse phase chromatography columns is detailed in Appendix 1.5.4-1.5.5.

3.2.4 Q Exactive analysis

Dried samples were re-suspended in 32 µl of Q Exactive buffer (Appendix 1.5.5) on day of analysis. Samples were placed in a sonication bath for 5 min to aid peptide re-suspension. Samples were subsequently centrifuged at 13,000 g for 5 min at RT to pellet any insoluble material. The supernatant was transferred to LC MS/ MS vials (Thermo, Ireland) (Cat# 60180-508). A peptide mix was separated on a Dionex Ultimate 3000 (RSLC nano, Thermo, USA)) chromatography system with increasing gradient of acetonitrile on a Biobasic C18 Picofrit TM column (100 mm length, 75 mm

ID), using a 180 min reverse phase gradient at a flow rate of 250 nl min^{-1}. High resolution MS scan (300-2000 Da) was performed using the Orbitrap to select the 15 most intense ions prior to MS/ MS. Each sample was run 3 times for technical comparison and a 3 h blank was run between each biological sample.

3.2.5 Computational and statistical processing of LC-MS data

Label free LC-MS data analysis was performed on Progenesis QI for Proteomics (Nonlinear Dynamics, USA) package with subsequent identification using Proteome Discoverer (Thermo Fischer Scientific, USA). Spectral files were aligned in Progenesis QI for Proteomics using retention time from the LC and m/z peak height, from the peptides in the replicate samples to produces consensus peak ion intensity. Differential analysis was performed on the peak height at the specific retention time between biological samples. The experimental comparison was divided up into 4 separate analyses as follows as outlined in **Table 3.1**.

Table 3.1 Set-up for the LFQ proteomics experimental conditions.

Experimental designation	Experimental condition
(A)	MCF-7 24 h exposure to Cu-Phen (**1**) and Cu-DPQ-Phen (**2**) in comparison to the negative control
(B)	MCF-7 48 h exposure to Cu-Phen (**1**) and Cu-DPQ-Phen (**2**) in comparison to the negative control
(C)	SKOV-3 24 h exposure to Cu-Phen (**1**) and Cu-DPQ-Phen (**2**) in comparison to the negative control
(D)	SKOV-3 48 h exposure to Cu-Phen (**1**) and Cu-DPQ-Phen (**2**) in comparison to the negative control

Ion intensity peaks were identified after meeting the following criteria: ANOVA p-value ≤ 0.05, minimum fold-change between experimental groups of 1.5 and a ≥ 2 peptides contributing to the protein identification. Proteins which meet the inclusion

criteria were identified using the software, Proteome Discoverer. Proteins were identified through a consensus workflow comparing the results of both the SEQUEST and MASCOT algorithms and using the following identification parameters: peptide mass tolerance at 20 ppm with the fragment tolerance set at 0.02 Da, up to 2 missed cleavages, a static modification of cysteine carboxymethylation and dynamic modification of methionein oxidation, MASCOT ion score was set at a minimum of 40, and SEQUEST HT XCorr was set at minimum 1.5 and FDR for PSMs and peptides set for strict at 0.01 and relaxed at 0.05. See appendix 1.5.6 for further details. Principle Component Analysis (PCA) uses orthogonal transformation to convert a set of potentially correlated variables into a smaller number of uncorrelated variables (principle components). This statistical procedure is used to reduce a large set of variable into a smaller set while preserving the trends and patterns present in the original dataset. PCA was performed on each of the experimental designs to establish the protein abundance variation between the different experimental exposures and examine the variation within each experimental group. Tight clustering indicated similar protein abundance while dispersed data points indicated dissimilar protein abundance. Dispersion of the data points on the x-axis (Component 1) represented the largest difference in protein abundance while dispersion of data points on the y-axis (Component 2) represented the next largest difference in protein abundance. Proteins with statistical significant expression and ≥ 1.5 fold change between the test exposure and the negative control were labelled, Statistically Significant Differentially Abundant (SSDA) proteins. Proteins with statistically significant changes in relation to the negative control but < 1.5 protein fold change were included and tabulated separately. Statistically significant changes in protein abundance between both Cu-Phen (**1**) and Cu-DPQ-Phen (**2**) treated cells were not included in the analysis. All fold changes were

calculated based on mean normalized abundances of the test exposures with the negative control. Hierarchical clustering was performed on all statistically significant proteins with log(2) transformed raw abundance values processed in Perseus software package (ver. 1.5.0.31).

The Blast2GO suite (www.blast2GO.com) of software tools was used to assign annotation, enzyme code, KEGG and Gene Ontology mapping on SSDA proteins. GO mapping for biological processes and molecular functions was graphed at level 4 ontology. Due to the different number of proteins detected in each of the experimental conditions, arbitrary thresholds were used to discuss the results of the GO analysis. Proteins of interest in both MCF-7 48 h and SKOV-3 48 h exposures were further analysed using Pathway Studio which used supervised text mining of published journal article along with the production of directional specific regulation proteins networks and their associated cell processes. Pathway Studio analysis was performed by Dr. Padraig Doolan in the National Institute for Cellular Biotechnology, Dublin City University, as part of ongoing collaboration efforts.

3.3 Results

3.3.1 (A) MCF-7 24 h exposure to Cu-Phen (1) and Cu-DPQ-Phen (2) in comparison to the negative control

The cell lysate from the MCF-7 cell line was extracted after a 24 h exposure to Cu-Phen (**1**) and Cu-DPQ-Phen (**2**) along with a negative control for comparison. A total of 42 Statistically Significant Differentially Abundant (SSDA) proteins (**Table 3.2**) were found to meet the following criteria: containing ≥ 2 unique peptide from the identified protein, showed a significant change (ANOVA) in comparison to the negative control, had ≥ 1.5 fold change in relation to the negative control (a fold change of < 1.5 was also included if the same protein was expressed at ≥ 1.5 fold change in another exposure). A total of 159 proteins (**Table 3.3**) were found to be statistically significant but had a < 1.5 fold change in protein expression in relation to the negative control. Principle component analysis (PCA) (**Fig. 3.1**) was used to visualise the variation in protein abundance across individual replicates. In each of the exposed (Cu-Phen (**1**) and Cu-DPQ-Phen (**2**)) and unexposed cells (negative control), a single replicates was excluded from the subsequent analysis. Both the negative control and Cu-Phen (**1**) exposed cells showed close clustering, indicating a similar protein expression pattern. This is in contrast to the separation observed in the negative control and Cu-DPQ-Phen (**2**). Cu-Phen (**1**) and Cu-DPQ-Phen (**2**) treated cells show closer clustering to each other through both component 1 and 2. Hierarchical clustering was generated through the mean of the Log(2) transformed LFQ abundances (**Fig. 3.2**) and indicated a closer clustering of both Cu-Phen (**1**) and Cu-DPQ-Phen (**2**) results, similarly to the PCA in **Figure 3.1**. **Table 3.2** represents a diverse functional classification of proteins with roles in metal based detoxification and signalling (metallothioneins), heat shock

signalling (HSP's), DNA modification (histones), ribosomal related (60S, 40S etc.) and metabolic related proteins which are the principle focus of this analysis. **Table 3.3** additionally, detailed further proteins in these classes at lower fold changes in relation to the negative control. Many of the functional processes these proteins are associated with are similar to **Table 3.2**. Gene Ontology (GO) biological process (**Fig. 3.3**) indicated a large increase in biosynthetic, primary metabolic, organic substance metabolic and nitrogen compound metabolic processes. The processes containing more than 25 proteins were of greater interest for the analysis. GO molecular process analysis revealed large numbers of proteins associated with binding of ions, small molecules, organic cyclic compounds, heterocyclic compounds and drugs. The processes containing more than 20 proteins formed the main focus of the analysis. KEGG analysis highlighted several pathways with associated proteins (**Table 3.2**). While additional KEGG pathways were identified but not included in this chapter the pathways presented below represent pathways that were highlighted across multiple experimental conditions and in many cases contained multiple protein identification within the same pathways. Fatty acid biosynthesis: fatty-acid synthase (FASN) (**Fig. 3.5**). Glycolysis/ gluconeogenesis: 6-phosphofructokinase (2.7.1.11) and L-lactate dehydrogenase (1.1.1.27) (**Fig. 3.6**). Nucleoside diphosphate kinase B and purine nucleoside phosphorylase are associated with purine metabolism but had a low fold change after both exposures. STRING protein network analysis (**Fig. 3.7**) demonstrates putative associations between heat shock, ribosomal and metabolic proteins.

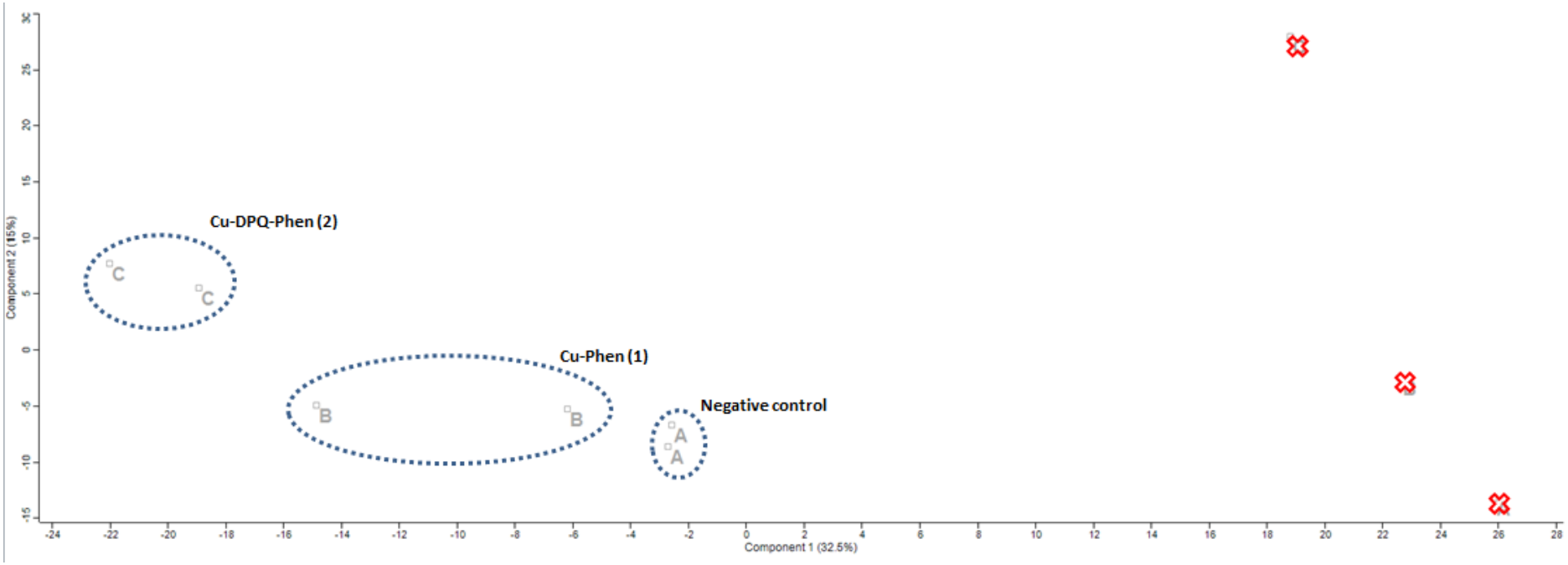

Fig. 3.1 Principle component analysis of whole cell lysate proteome of MCF-7 cells exposed to Cu-Phen (**1**) and Cu-DPQ-Phen (**2**) for 24 h in comparison to the negative control. PCA of three replicates for the negative control and three replicates (N=3) of both test exposures. Enclosures define the different experimental conditions. Red X denotes the third replicates from each condition removed from the analysis due to lack of clustering.

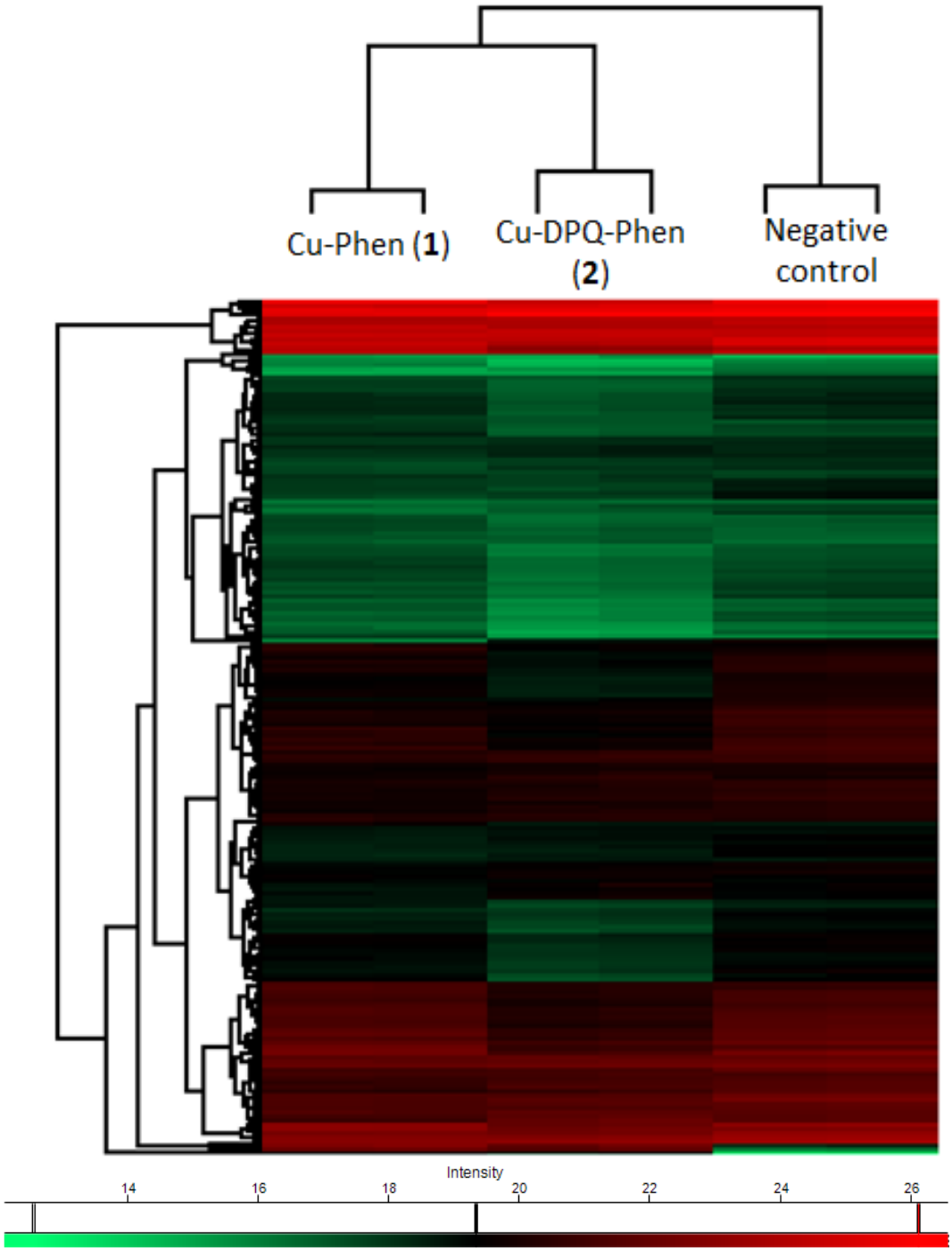

Fig. 3.2: Hierarchical clustering of SSDA proteins and statistically significant proteins with less than a 1.5 fold change in the MCF-7 cell line after 24 h exposure to Cu-Phen (**1**) and Cu-DPQ-Phen (**2**) in relation to the control. Hierarchical clustering generated from mean Log(2) transformed values of LFQ abundance with samples clustered through columns (N=2).

Table 3.2 Statistically significant differentially abundant (SSDA) proteins (42) after exposure of Cu-Phen (**1**) and Cu-DPQ-Phen (**2**) in the MCF-7 cell line after 24h incubation.

Protein description	Accession	Peptide count	Anova (p)	Cu-Phen (**1**) (fold change)	Cu-DPQ-Phen (**2**) (fold change)
Metallothionein-1F	P04733	2	2.09E-04	121.17	85.66
Metallothionein-1X	P80297	4	8.01E-06	74.59	75.32
Metallothionein-2	P02795	3	1.66E-04	25.65	21.78
Protein NDRG1	Q92597	2	3.55E-04	3.60	1.00
BAG family molecular chaperone regulator 3	O95817	2	1.63E-03	2.27	1.10
Thioredoxin reductase 1, cytoplasmic	Q16881	3	3.97E-03	2.21	1.54
60S ribosomal protein L14	P50914	2	2.36E-02	1.96	2.47
L-lactate dehydrogenase A chain	P00338	10	6.11E-05	1.95	0.95
Ubiquitin-60S ribosomal protein L40	P62987	3	3.16E-04	1.89	1.23
Sequestosome-1	Q13501	4	2.80E-06	1.86	1.17
cAMP-dependent protein kinase type I-alpha regulatory subunit	P10644	2	3.46E-03	1.73	1.68
Golgin subfamily B member 1	Q14789	2	1.70E-02	1.72	1.43
26S protease regulatory subunit 6A	P17980	6	1.19E-02	1.69	1.40
ATP-dependent 6-phosphofructokinase, platelet type	Q01813	2	4.08E-03	1.64	1.32
Paxillin	P49023	2	4.67E-04	1.62	0.89
Ras GTPase-activating protein-binding protein 1	Q13283	2	7.22E-03	1.60	1.05
60 kDa heat shock protein, mitochondrial	P10809	8	1.04E-03	1.58	1.08
Clathrin heavy chain 1	Q00610	3	1.24E-04	1.55	0.89
Bcl-2-associated transcription factor 1	Q9NYF8	2	5.01E-03	1.54	1.13
Serum albumin	P02768	3	6.01E-05	1.54	0.63
DNA replication licensing factor MCM3	P25205	2	8.22E-03	1.52	1.83
Transaldolase	P37837	2	2.92E-02	1.50	1.58
Annexin A4	P09525	2	3.19E-02	1.36	1.56
T-complex protein 1 subunit alpha	P17987	2	1.46E-02	1.27	1.61
Heat shock protein HSP 90-alpha	P07900	16	2.68E-03	1.26	1.58
60S ribosomal protein L28	P46779	4	6.07E-03	1.14	1.83
Heat shock protein beta-8	Q9UJY1	3	6.69E-04	1.14	1.70
Ubiquitin carboxyl-terminal hydrolase 14	P54578	4	1.44E-03	1.12	1.62
Actin-related protein 2	P61160	2	1.09E-03	1.11	1.61
Histone H3.1	P68431	4	1.01E-04	1.05	2.27
Adenosylhomocysteinase	P23526	3	1.14E-02	1.04	1.54
Heat shock protein HSP 90-beta	P08238	16	7.64E-03	1.01	1.61
Fatty acid synthase	P49327	3	3.25E-03	0.97	1.51
Proteasome subunit alpha type-5	P28066	2	1.23E-02	0.95	1.62
Protein LSM14 homolog B	Q9BX40	2	2.78E-03	0.87	1.64

60S ribosomal protein L32	P62910	3	5.98E-03	0.86	1.57
40S ribosomal protein S25	P62851	4	6.49E-05	0.83	2.08
60S ribosomal protein L8	P62917	4	1.25E-02	0.82	1.94
60S ribosomal protein L23a	P62750	3	1.62E-04	0.80	1.70
D-3-phosphoglycerate dehydrogenase	O43175	2	4.85E-03	0.79	1.52
60S ribosomal protein L35a	P18077	4	6.92E-04	0.74	1.58
Histone H2A type 1-B/E	P04908	4	1.10E-04	0.62	1.95

Relative fold changes are given for each test exposure in comparison to the negative control.

Fold changes of < 1.5 were included when expression in other test exposure was ≥ 1.5 fold change.

Proteins (highlighted in grey) involved in metal based detoxification and signalling (metallothioneins), heat shock signalling (HSP's), DNA modification (histones), ribosomal related (60S, 40S etc.) and metabolic related proteins are the principle focus of this analysis.

Table 3.3 Statistically significant proteins (159) with fold changes < 1.5 fold change after exposure of Cu-Phen (**1**) and Cu-DPQ-Phen (**2**) in the MCF-7 cell line after 24 h incubation.

Protein description	Accession	Peptide count	ANOVA (p)	Cu-Phen (**1**) (fold change)	Cu-DPQ-Phen (**2**) (fold change)
Heat shock 70 kDa protein 1B	P0DMV9	17	3.13E-03	1.49	1.31
Nuclear migration protein nudC	Q9Y266	2	3.32E-03	1.48	0.97
Glucose-6-phosphate 1-dehydrogenase	P11413	9	9.15E-05	1.47	1.17
Fructose-bisphosphate aldolase A	P04075	19	1.94E-04	1.43	0.84
6-phosphogluconate dehydrogenase, decarboxylating	P52209	2	2.21E-03	1.41	0.74
Heterogeneous nuclear ribonucleoprotein A0	Q13151	2	4.87E-03	1.41	0.90
Ubiquitin carboxyl-terminal hydrolase 5	P45974	2	9.08E-03	1.40	0.87
LIM and SH3 domain protein 1	Q14847	2	6.83E-04	1.39	0.70
Guanine nucleotide-binding protein subunit beta-2-like 1	P63244	5	3.05E-05	1.31	0.84
Isocitrate dehydrogenase [NADP], mitochondrial	P48735	2	1.98E-03	1.28	0.72
Stress-70 protein, mitochondrial	P38646	8	1.37E-03	1.28	0.72
Nucleosome assembly protein 1-like 1	P55209	2	8.52E-03	1.26	0.71
Protein disulfide-isomerase A3	P30101	6	1.93E-03	1.26	0.81
Chromobox protein homolog 5	P45973	3	1.79E-03	1.26	0.76
Elongation factor Tu, mitochondrial	P49411	4	7.31E-04	1.25	0.83
Transcriptional repressor p66-alpha	Q86YP4	2	7.35E-05	1.25	0.71
Small glutamine-rich tetratricopeptide repeat-containing protein alpha	O43765	2	3.01E-03	1.23	0.66
Translationally-controlled tumor protein	P13693	3	1.89E-02	1.23	0.76
Calreticulin	P27797	2	5.14E-03	1.22	0.68
DnaJ homolog subfamily B member 1	P25685	3	1.51E-03	1.22	0.73
Thioredoxin domain-containing protein 5	Q8NBS9	3	8.59E-05	1.18	0.37
Protein disulfide-isomerase	P07237	2	2.28E-04	1.18	0.36
Endophilin-B2	Q9NR46	3	1.84E-03	1.17	0.74
10 kDa heat shock protein, mitochondrial	P61604	8	3.33E-03	1.16	0.77
S-adenosylmethionine synthase isoform type-2	P31153	2	8.16E-03	1.16	0.70
Serine/arginine-rich splicing factor 2	Q01130	2	9.69E-03	1.16	0.76
Poly(rC)-binding protein 2	Q15366	6	2.05E-05	1.15	0.68
Calcyclin-binding protein	Q9HB71	6	2.69E-03	1.14	0.77
Phosphoglycerate mutase 1	P18669	7	4.44E-04	1.11	0.68
40S ribosomal protein S12	P25398	3	5.15E-03	1.11	0.72
40S ribosomal protein S9	P46781	2	1.00E-02	1.10	0.71
Galectin-1	P09382	3	9.59E-04	1.09	0.46
Ras-related protein Rap-1b	P61224	3	1.76E-03	1.07	0.70
Cysteine-rich protein 2	P52943	2	2.00E-02	1.06	0.69
ATP synthase subunit beta, mitochondrial	P06576	7	6.93E-04	1.06	0.65
N-alpha-acetyltransferase 10	P41227	2	5.79E-04	1.05	0.68
Glyceraldehyde-3-phosphate dehydrogenase	P04406	20	1.67E-03	1.04	0.67

Proteasome subunit alpha type-1	P25786	5	2.38E-04	1.04	1.46
78 kDa glucose-regulated protein	P11021	14	4.95E-04	1.03	0.68
Cofilin-1	P23528	7	6.34E-05	1.02	0.61
40S ribosomal protein S3	P23396	3	2.63E-03	1.02	0.61
Heterogeneous nuclear ribonucleoprotein D0	Q14103	4	7.47E-04	1.02	0.59
Destrin	P60981	3	3.27E-04	1.02	0.60
Poly(rC)-binding protein 1	Q15365	7	1.05E-02	1.02	0.78
Acidic leucine-rich nuclear phosphoprotein 32 family member A	P39687	2	3.05E-03	1.02	0.61
Alpha-enolase	P06733	21	1.84E-03	1.00	0.77
Ubiquitin-40S ribosomal protein S27a	P62979	2	4.55E-04	0.98	0.66
40S ribosomal protein S23	P62266	2	1.67E-03	0.98	0.66
Peroxiredoxin-6	P30041	5	4.36E-02	0.97	1.44
26S protease regulatory subunit 8	P62195	5	1.52E-03	0.95	1.45
Voltage-dependent anion-selective channel protein 2	P45880	4	1.16E-02	0.95	0.58
Eukaryotic initiation factor 4A-III	P38919	2	1.79E-02	0.94	1.41
Prefoldin subunit 2	Q9UHV9	2	1.31E-02	0.94	0.52
Transgelin-2	P37802	7	7.37E-05	0.93	0.67
Lysine--tRNA ligase	Q15046	2	1.75E-02	0.93	0.62
60S ribosomal protein L13	P26373	5	5.40E-04	0.92	1.40
Myosin light polypeptide 6	P60660	6	9.12E-04	0.92	0.66
rRNA 2'-O-methyltransferase fibrillarin	P22087	2	4.55E-03	0.92	0.47
Heterogeneous nuclear ribonucleoprotein A/B	Q99729	7	7.62E-04	0.92	0.54
High mobility group protein B1	P09429	4	1.23E-04	0.92	0.52
mRNA export factor	P78406	3	3.98E-02	0.91	0.61
Serine/threonine-protein phosphatase PP1-alpha catalytic subunit	P62136	2	3.43E-03	0.91	0.58
Histone H4	P62805	4	1.26E-02	0.91	1.40
Protein CDV3 homolog	Q9UKY7	2	6.12E-03	0.90	0.62
Aspartate aminotransferase, cytoplasmic	P17174	2	1.72E-03	0.90	1.39
Splicing factor U2AF 65 kDa subunit	P26368	2	1.45E-03	0.90	0.57
Non-POU domain-containing octamer-binding protein	Q15233	10	5.59E-06	0.89	0.72
Serine/arginine-rich splicing factor 1	Q07955	2	3.35E-03	0.89	0.56
Voltage-dependent anion-selective channel protein 1	P21796	3	2.41E-03	0.89	0.59
Hematological and neurological expressed 1-like protein	Q9H910	5	5.32E-04	0.89	1.40
Na(+)/H(+) exchange regulatory cofactor NHE-RF1	O14745	5	9.72E-03	0.88	0.67
Chloride intracellular channel protein 1	O00299	11	1.88E-03	0.88	0.64
Heat shock protein beta-1	P04792	7	3.20E-02	0.88	1.28
Heterogeneous nuclear ribonucleoproteins A2/B1	P22626	9	6.08E-03	0.88	1.25
Acyl-CoA-binding protein	P07108	2	4.15E-04	0.88	0.54
Serine/threonine-protein phosphatase 2A 65 kDa regulatory subunit A alpha isoform	P30153	3	2.41E-03	0.87	1.38
Endoplasmic reticulum resident protein 29	P30040	3	3.40E-03	0.87	0.58
Fructose-1,6-bisphosphatase 1	P09467	4	7.77E-03	0.87	0.52
Serpin H1	P50454	4	3.09E-03	0.86	0.66
Lupus La protein	P05455	3	5.26E-04	0.85	0.52

Inorganic pyrophosphatase	Q15181	5	3.05E-04	0.83	0.53
Adenylyl cyclase-associated protein 1	Q01518	2	5.65E-03	0.83	0.57
40S ribosomal protein S16	P62249	3	7.02E-03	0.81	1.22
T-complex protein 1 subunit eta	Q99832	7	4.73E-03	0.81	1.11
Ubiquitin carboxyl-terminal hydrolase 10	Q14694	2	1.31E-02	0.80	0.45
Alpha-actinin-4	O43707	12	1.65E-02	0.80	1.19
Prohibitin	P35232	6	1.52E-03	0.79	1.29
RNA-binding protein EWS	Q01844	2	5.07E-03	0.79	0.59
6-phosphogluconolactonase	O95336	2	6.65E-03	0.79	1.19
Neuroblast differentiation-associated protein AHNAK	Q09666	6	1.88E-02	0.79	0.61
Keratin, type II cytoskeletal 80	Q6KB66	2	3.94E-02	0.78	1.31
Hepatoma-derived growth factor	P51858	3	1.24E-02	0.78	0.59
Peptidyl-prolyl cis-trans isomerase A	P62937	16	5.21E-04	0.78	0.66
Myosin-9	P35579	6	4.03E-03	0.77	0.86
60S ribosomal protein L9	P32969	2	6.31E-03	0.77	1.34
60S ribosomal protein L34	P49207	3	4.93E-03	0.77	1.26
60S ribosomal protein L5	P46777	2	1.55E-03	0.77	0.59
Desmoplakin	P15924	3	3.17E-03	0.77	0.45
Tubulin beta-3 chain	Q13509	16	1.12E-02	0.77	1.03
Macrophage migration inhibitory factor	P14174	6	3.44E-03	0.77	1.26
Plakophilin-3	Q9Y446	3	4.65E-02	0.77	1.26
Proteasome subunit alpha type-2	P25787	3	2.73E-02	0.76	1.22
Nuclear mitotic apparatus protein 1	Q14980	4	3.17E-02	0.75	1.19
Coronin-1B	Q9BR76	5	1.50E-03	0.75	1.13
40S ribosomal protein S8	P62241	4	4.56E-03	0.75	1.21
Zinc finger protein 185	O15231	2	7.29E-03	0.74	0.55
60S ribosomal protein L21	P46778	4	6.48E-04	0.74	1.16
Heterogeneous nuclear ribonucleoprotein K	P61978	10	3.24E-03	0.73	0.97
60S ribosomal protein L10a	P62906	2	1.66E-02	0.73	0.60
4F2 cell-surface antigen heavy chain	P08195	3	9.42E-03	0.71	1.22
40S ribosomal protein S21	P63220	10	5.03E-03	0.71	1.10
Guanine nucleotide-binding protein G(I)/G(S)/G(T) subunit beta-2	P62879	2	9.21E-04	0.71	0.66
Transitional endoplasmic reticulum ATPase	P55072	16	1.16E-02	0.71	0.85
60S acidic ribosomal protein P2	P05387	3	3.72E-03	0.71	0.42
Cold-inducible RNA-binding protein	Q14011	4	6.55E-03	0.70	1.04
RNA-binding protein 4	Q9BWF3	4	4.57E-03	0.70	0.61
60S ribosomal protein L6	Q02878	4	1.38E-03	0.69	1.31
Heterogeneous nuclear ribonucleoprotein Q	O60506	5	2.01E-03	0.69	0.57
RuvB-like 2	Q9Y230	3	6.89E-03	0.69	1.22
Proliferating cell nuclear antigen	P12004	3	2.09E-03	0.69	1.15
S-formylglutathione hydrolase	P10768	4	5.36E-03	0.68	0.63
60S ribosomal protein L24	P83731	4	5.82E-04	0.68	1.05
Sialic acid synthase	Q9NR45	4	4.65E-04	0.67	0.59
Emerin	P50402	2	1.13E-02	0.66	0.45

40S ribosomal protein S6	P62753	4	1.02E-02	0.65	1.31
Heterogeneous nuclear ribonucleoprotein H2	P55795	3	2.32E-04	0.65	0.48
Anterior gradient protein 2 homolog	O95994	4	3.38E-03	0.65	0.64
Annexin A11	P50995	4	1.06E-03	0.64	0.83
Histone H2B type 3-B	Q8N257	3	5.63E-03	0.64	0.66
Flap endonuclease 1	P39748	2	2.06E-03	0.64	0.72
Nucleophosmin	P06748	11	1.13E-03	0.64	1.18
Rab GDP dissociation inhibitor beta	P50395	6	8.30E-03	0.64	1.17
Mitochondrial import receptor subunit TOM34	Q15785	2	6.60E-03	0.62	1.12
Hematological and neurological expressed 1 protein	Q9UK76	4	8.27E-04	0.62	0.86
Eukaryotic translation initiation factor 4H	Q15056	2	3.06E-03	0.62	1.02
Tubulin beta chain	P07437	11	1.72E-02	0.62	0.82
Serine/arginine-rich splicing factor 5	Q13243	4	1.11E-02	0.62	0.88
Acidic leucine-rich nuclear phosphoprotein 32 family member B	Q92688	2	2.56E-02	0.61	0.71
Methionine aminopeptidase 1	P53582	2	1.29E-02	0.61	0.98
40S ribosomal protein S7	P62081	6	7.53E-03	0.61	1.16
Structural maintenance of chromosomes protein 1A	Q14683	2	3.39E-03	0.60	0.68
Cytochrome c oxidase subunit 6B1	P14854	5	3.52E-03	0.59	0.86
Ladinin-1	O00515	3	3.01E-02	0.58	1.08
Gelsolin	P06396	3	1.02E-02	0.58	0.77
Importin subunit alpha-1	P52292	5	3.00E-03	0.57	0.64
Phosphatidylethanolamine-binding protein 1	P30086	3	3.46E-05	0.56	0.57
Ubiquitin fusion degradation protein 1 homolog	Q92890	2	1.03E-02	0.54	0.94
Polypyrimidine tract-binding protein 1	P26599	4	9.65E-04	0.53	0.74
Poly(U)-binding-splicing factor PUF60	Q9UHX1	4	3.85E-03	0.52	0.52
RNA-binding protein 3	P98179	4	1.14E-02	0.51	0.86
Histone H2B type 1-D	P58876	15	1.20E-03	0.50	1.17
Tubulin beta-6 chain	Q9BUF5	5	1.68E-04	0.49	0.85
Ribosome biogenesis regulatory protein homolog	Q15050	2	7.88E-06	0.45	0.67
tRNA-splicing endonuclease subunit Sen34	Q9BSV6	2	2.23E-03	0.43	0.86
CUGBP Elav-like family member 1	Q92879	2	4.30E-04	0.42	0.96
Purine nucleoside phosphorylase	P00491	2	3.51E-03	0.38	0.59
Annexin A5	P08758	2	2.17E-03	0.32	0.52
Rac GTPase-activating protein 1	Q9H0H5	2	1.77E-03	0.30	0.44
Nucleoside diphosphate kinase B	P22392	3	1.07E-04	0.09	0.73

Relative fold changes are given for each test exposure in comparison to the negative control.

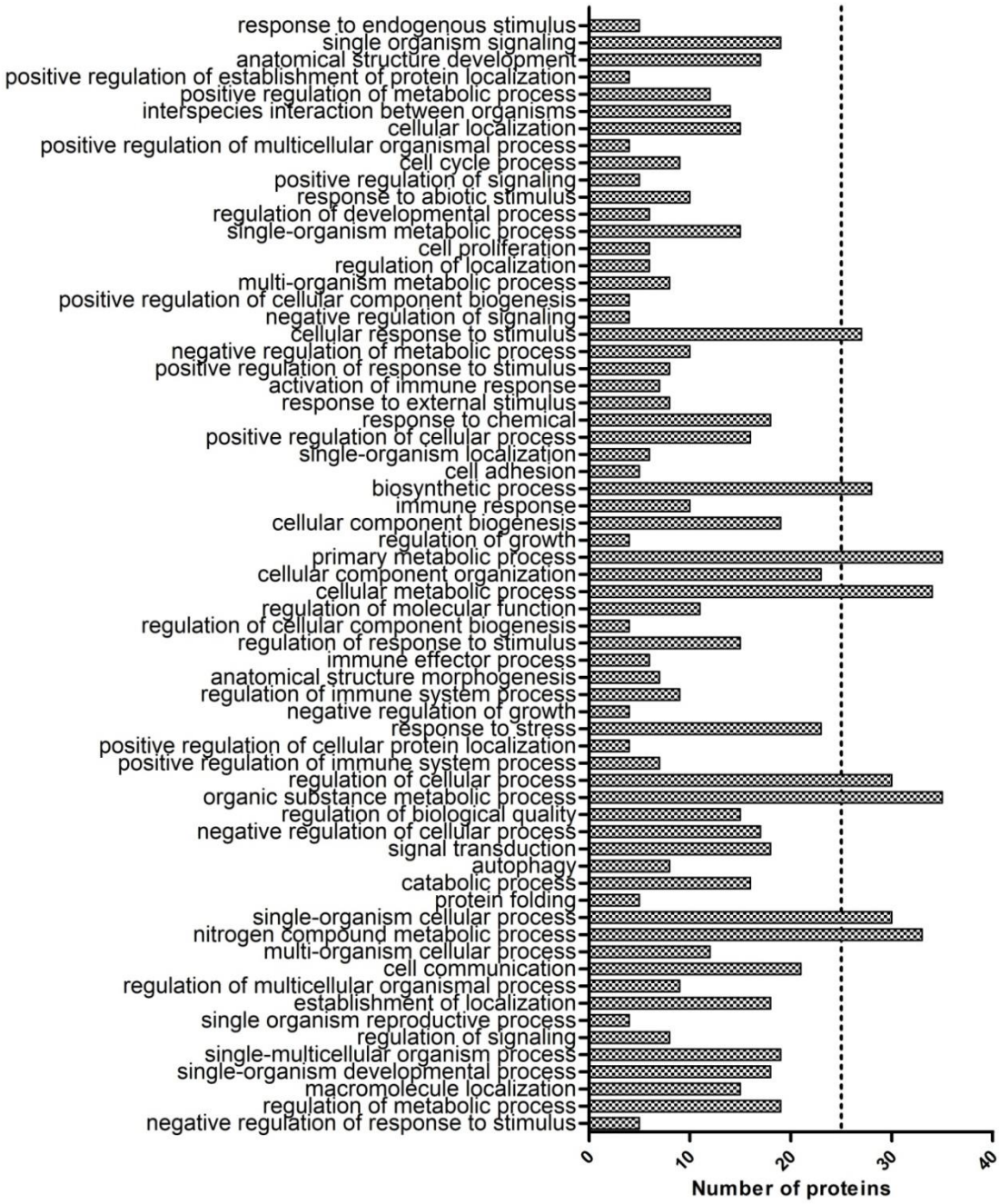

Fig. 3.3 GO analysis of biological process in MCF-7 cells exposed to Cu-Phen (**1**) and Cu-DPQ-Phen (**2**) with respect to the negative control after 24 h incubation. Process containing more than 25 proteins was of significant interest for the analysis.

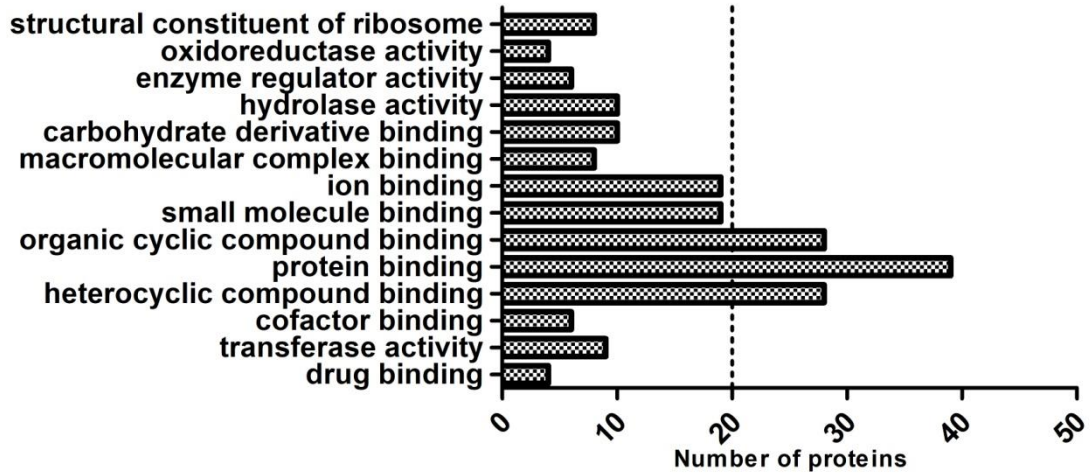

Fig. 3.4 GO analysis of molecular process in MCF-7 cells exposed to Cu-Phen (**1**) and Cu-DPQ-Phen (**2**) with respect to the negative control after 24 h incubation. Process containing more than 20 proteins was of greater interest for the analysis.

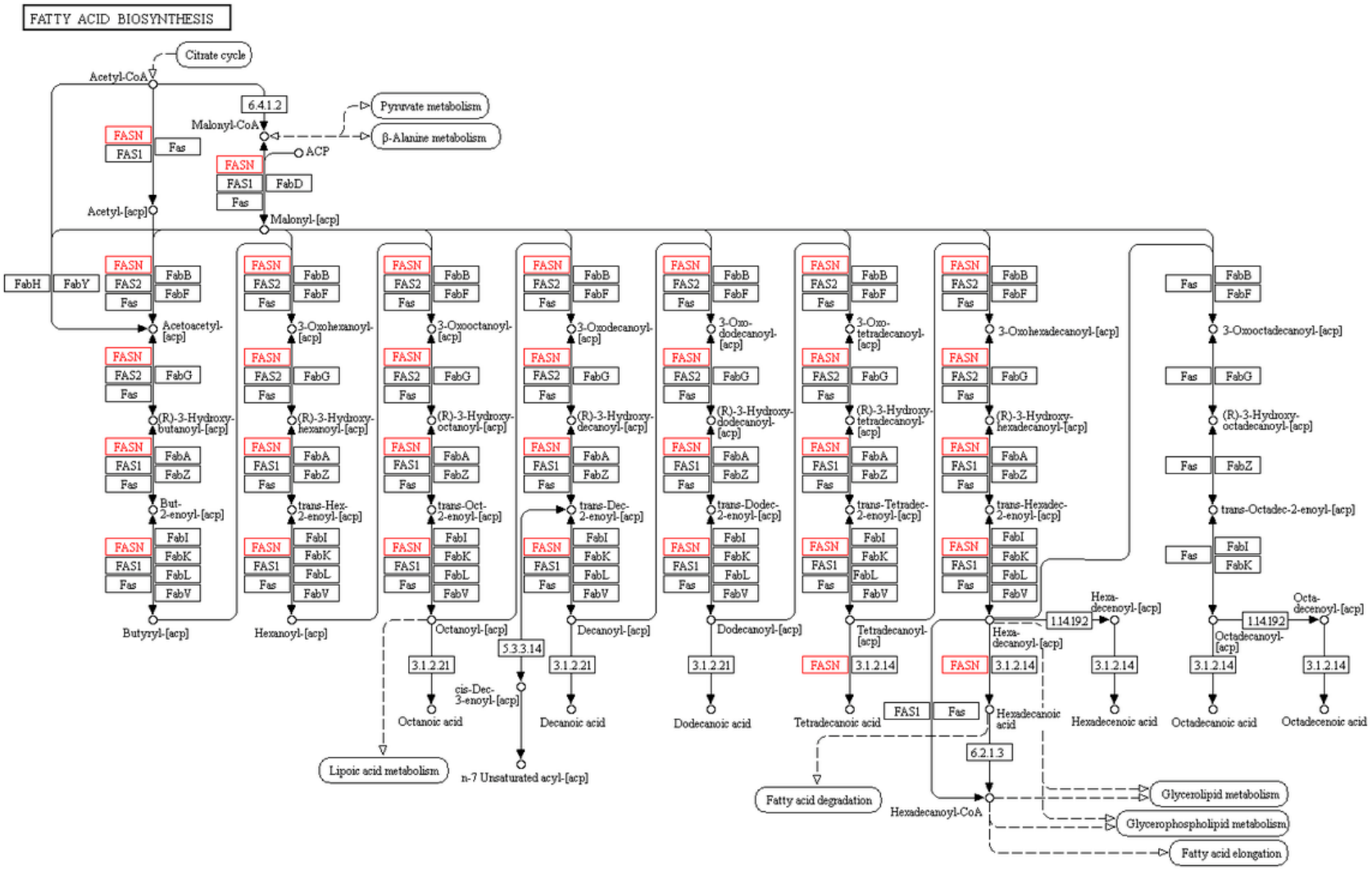

Fig. 3.5 KEGG analysis of significantly upregulated proteins in fatty acid biosynthesis. Fatty acid synthase (FASN) (red).

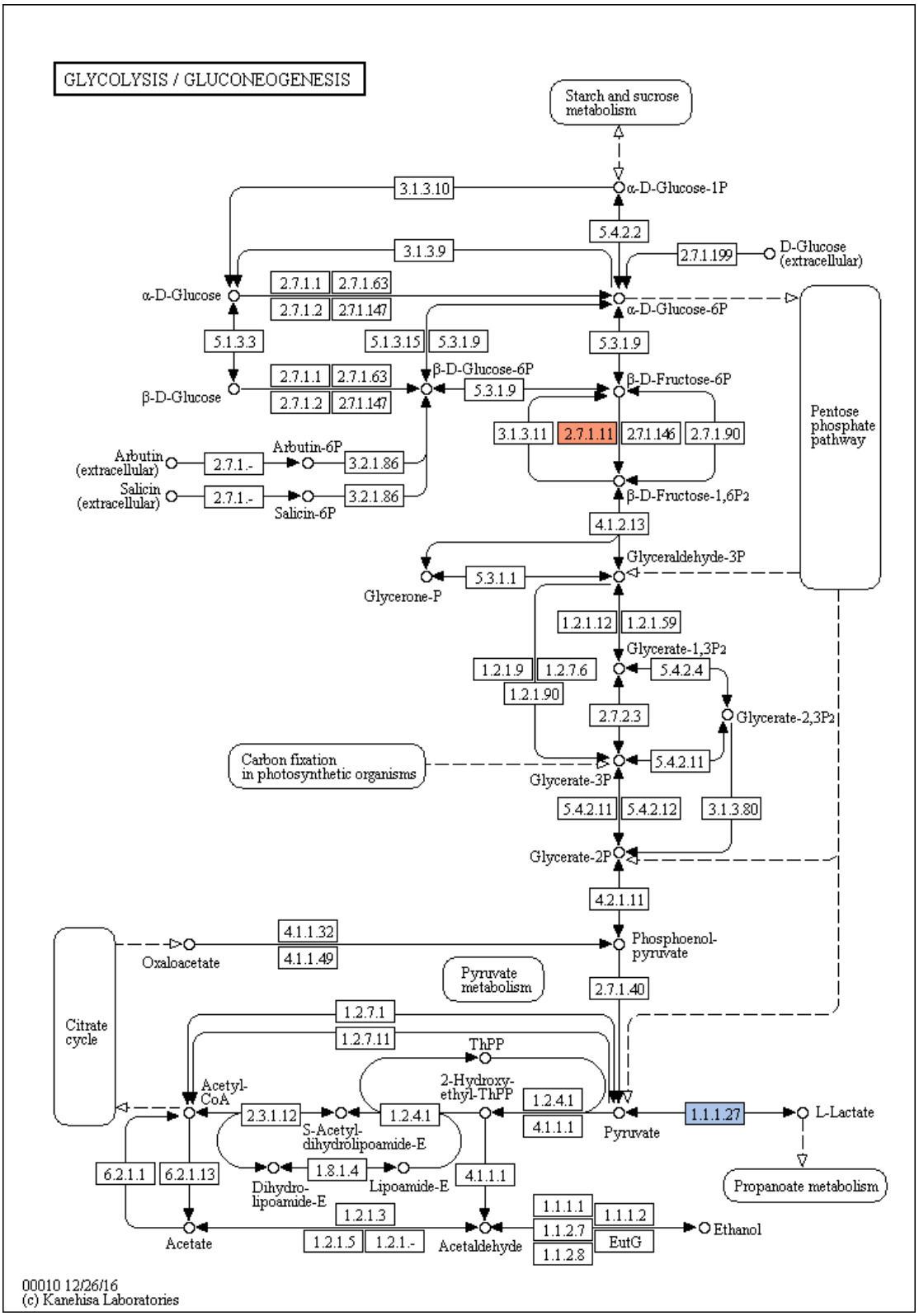

Fig. 3.6 KEGG analysis of significantly upregulated proteins in glycolysis/ gluconeogenesis. 6-phosphofructokinase (2.7.1.11) (orange) and L-lactate dehydrogenase (1.1.1.27) (blue).

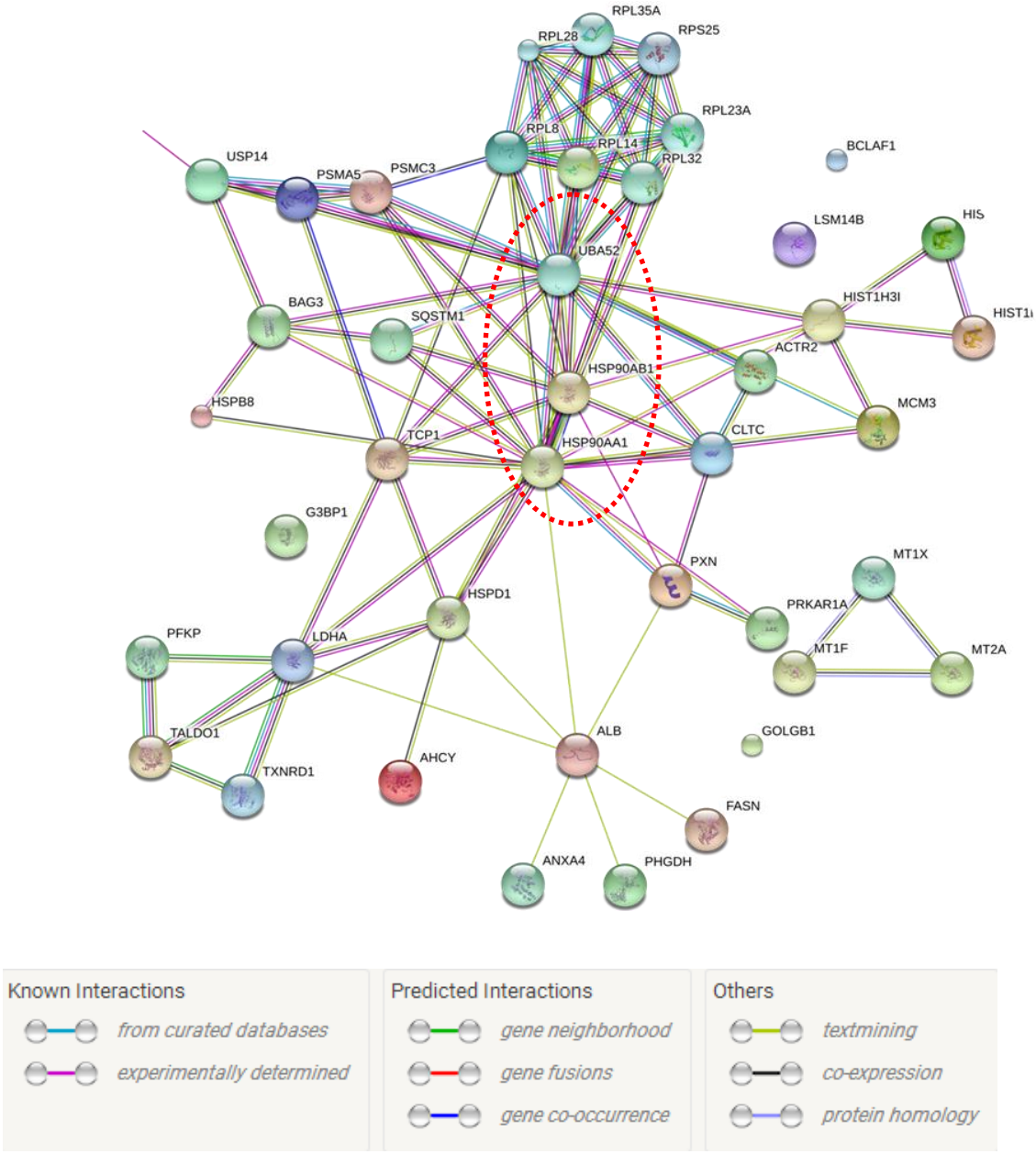

Fig. 3.7 STRING based protein interaction analysis of statistically significant protein with fold changes ≥ 1.5 in the MCF-7 cell after 24 h exposure to Cu-Phen (**1**) and Cu-DPQ-Phen (**2**) compared to the negative control. The dashed red oval highlights proteins that may have regulatory role.

3.3.2 (B) MCF-7 48 h exposure to Cu-Phen (1) and Cu-DPQ-Phen (2) in comparison to the negative control

Cell lysates from MCF-7 cells were extracted after a 48 h exposure to Cu-Phen (**1**) and Cu-DPQ-Phen (**2**) along with a negative control for comparison. A total of 12 Statistically Significant Differentially Abundant (SSDA) proteins (**Table 3.4**) were found to meet the following criteria: containing ≥ 2 unique peptide from the identified protein, showed a significant change (ANOVA) in comparison to the negative control, had ≥ 1.5 fold change in relation to the negative control (a fold change of < 1.5 was also included if the same protein was expressed at ≥ 1.5 fold change in another exposure). A total of 5 proteins (**Table 3.5**) were found to be statistically significant but were < 1.5 fold change in protein expression in relation to the negative control. PCA (**Fig. 3.8**) was used to visualise the variation in protein abundance across individual replicates. In each of the exposure and negative control a single replicate was excluded from the subsequent analysis. Both the negative control and Cu-DPQ-Phen (**2**) treatments showed close clustering, indicating a similar protein profile while Cu-Phen (**1**) was largely separated from the other 2 by component 2. Hierarchical clustering was generated through the mean of the Log(2) transformed LFQ abundances (**Fig 3.9**) and indicates the separation of both complexes from the negative control, similarly to the PCA in **Figure 3.8**. **Table 3.4** represents significant differentially abundant proteins with multiple functional classes from metal detoxification and signalling (metallothionein), cytoskeletal (Tubulin), metabolic (Pyruvate kinase) and ribosomal (40S). **Table 3.5** additionally, detailed further proteins at lower differentially abundant to the negative control. Gene Ontology (GO) biological process (**Fig. 3.10**) indicated a large increase in biosynthetic, primary metabolic, organic substance metabolic and

nitrogen compound metabolic processes. Processes that contained more than 6 proteins were of greater interest in the analysis. GO molecular process (**Fig. 3.11**) analysis revealed increased numbers of proteins associated with binding of ions, small molecules, organic cyclic compounds and heterocyclic compounds. Processes that contained more than 6 proteins were of greater interest in the analysis. KEGG analysis highlighted 2 pathways with associated proteins (**Table 3.4**). While additional KEGG pathways were identified but not included in this chapter the pathways presented below represent pathways that were highlighted across multiple experimental conditions and in many cases contained multiple protein identification within the same pathways. Purine metabolism (**Fig. 3.12**) highlighted the following proteins: pyruvate kinase (2.7.1.40). Glycolysis/ gluconeogenesis (**Fig. 3.13**): phosphoglycerate kinase (2.7.2.3) and pyruvate kinase (2.7.1.40). STRING protein interaction network (**Fig. 3.14**) showed associations between tubulin and ribosomal proteins with connection to metabolic enzymes.

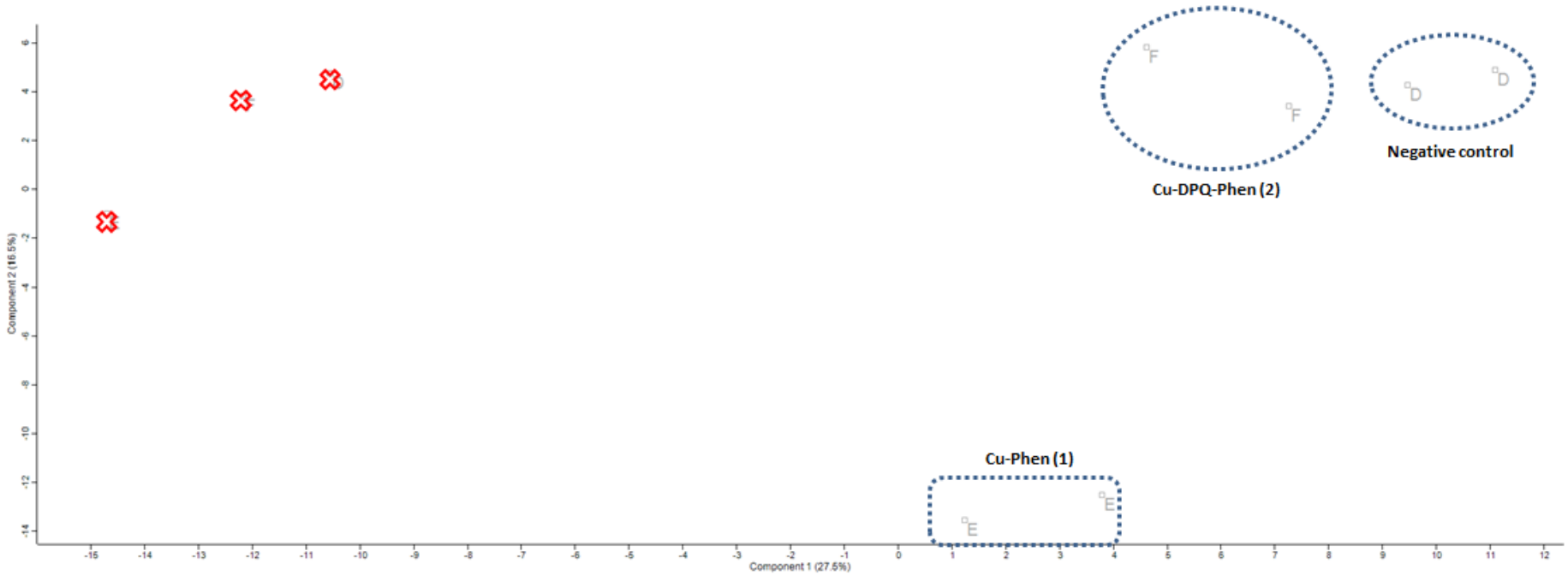

Fig. 3.8 Principle component analysis (PCA) of whole cell lysate proteomes of MCF-7 cell exposed to Cu-Phen (**1**) and Cu-DPQ-Phen (**2**) for 48 h in comparison to a negative control. PCA of three replicates for the negative control and three replicates of both test exposures. Enclosures define the different experimental conditions. Red X denotes the third replicates from each condition removed from the analysis due to lack of clustering.

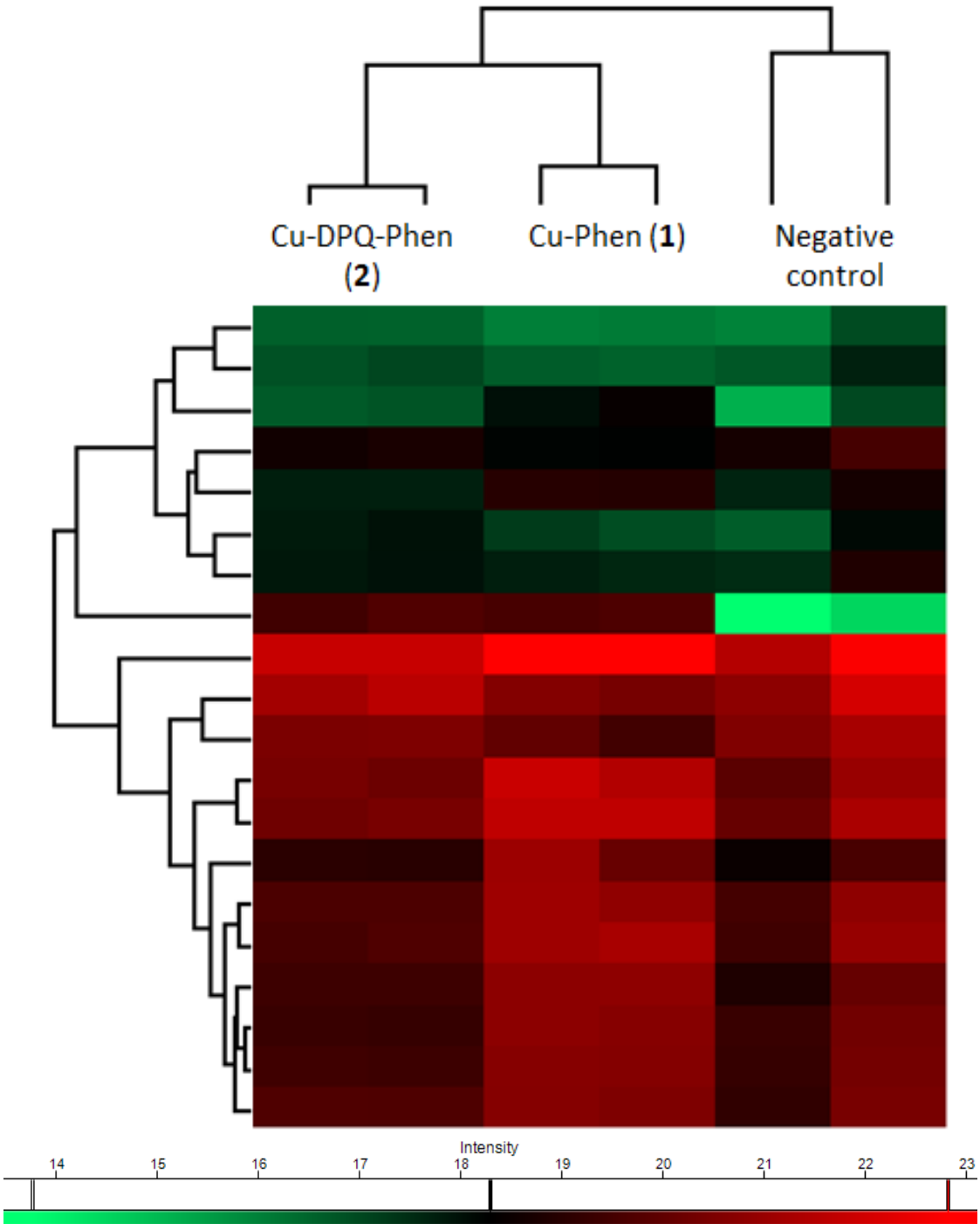

Fig. 3.9 Hierarchical clustering of SSDA proteins and statistically significant proteins with less than a 1.5 fold change in the MCF-7 cell line after 48 h exposure to Cu-Phen (**1**) and Cu-DPQ-Phen (**2**) in relation to the control. Hierarchical clustering generated from mean Log(2) transformed values of LFQ abundance with samples clustered through columns.

Table 3.4 Statistically significant differentially abundant (SSDA) proteins (12) after exposure of Cu-Phen (**1**) and Cu-DPQ-Phen (**2**) in the MCF-7 cell line after 48 h incubation.

Protein description	Accession	Peptide count	Anova (p)	Cu-Phen (**1**) (fold change)	Cu-DPQ-Phen (**2**) (fold change)
Metallothionein-2	P02795	3	2.35E-05	42.56	58.51
40S ribosomal protein S7	P62081	2	1.41E-02	3.60	1.97
Filamin-A	P21333	3	3.55E-02	2.61	1.36
60S acidic ribosomal protein P0	P05388	2	2.98E-02	2.15	1.21
Tubulin beta-4A chain	P04350	2	9.25E-04	1.95	1.20
Phosphoglycerate kinase 1	P00558	3	1.64E-04	1.92	1.01
Tubulin beta chain	P07437	2	3.02E-04	1.87	1.15
Tubulin beta-3 chain	Q13509	3	3.29E-05	1.78	1.08
GTP-binding nuclear protein Ran	P62826	2	1.31E-05	1.72	1.30
Annexin A2	P07355	2	1.36E-03	1.61	1.07
Pyruvate kinase PKM	P14618	5	1.50E-02	1.59	1.02
Ubiquitin-40S ribosomal protein S27a	P62979	2	9.22E-03	0.89	1.85

Relative fold changes are given for each test exposure in comparison to the negative control.

Fold changes of < 1.5 were included when expression in other test exposure was ≥ 1.5 fold change.

Proteins (highlighted in grey) involved in metal detoxification and signalling (metallothionein), cytoskeletal (Tubulin), metabolic (Pyruvate kinase) and ribosomal (40S) were the principle focus of this analysis.

Table 3.5 Statistically significant proteins (5) with fold changes <1.5 fold change after exposure of Cu-Phen (**1**) and Cu-DPQ-Phen (**2**) in the MCF-7 cell line after 48 h incubation.

Protein description	Accession	Peptide count	Anova (p)	Cu-Phen (**1**) (fold change)	Cu-DPQ-Phen (**2**) (fold change)
Plectin	Q15149	2	3.14E-02	0.76	1.33
Protein RCC2	Q9P258	2	1.98E-02	0.71	1.14
Proteasome subunit alpha type-1	P25786	2	2.83E-02	0.68	1.06
Cold-inducible RNA-binding protein	Q14011	2	1.72E-02	0.52	0.92
Serum albumin	P02768	3	1.54E-02	0.45	0.93

Relative fold changes are given for each test exposure in comparison to the negative control.

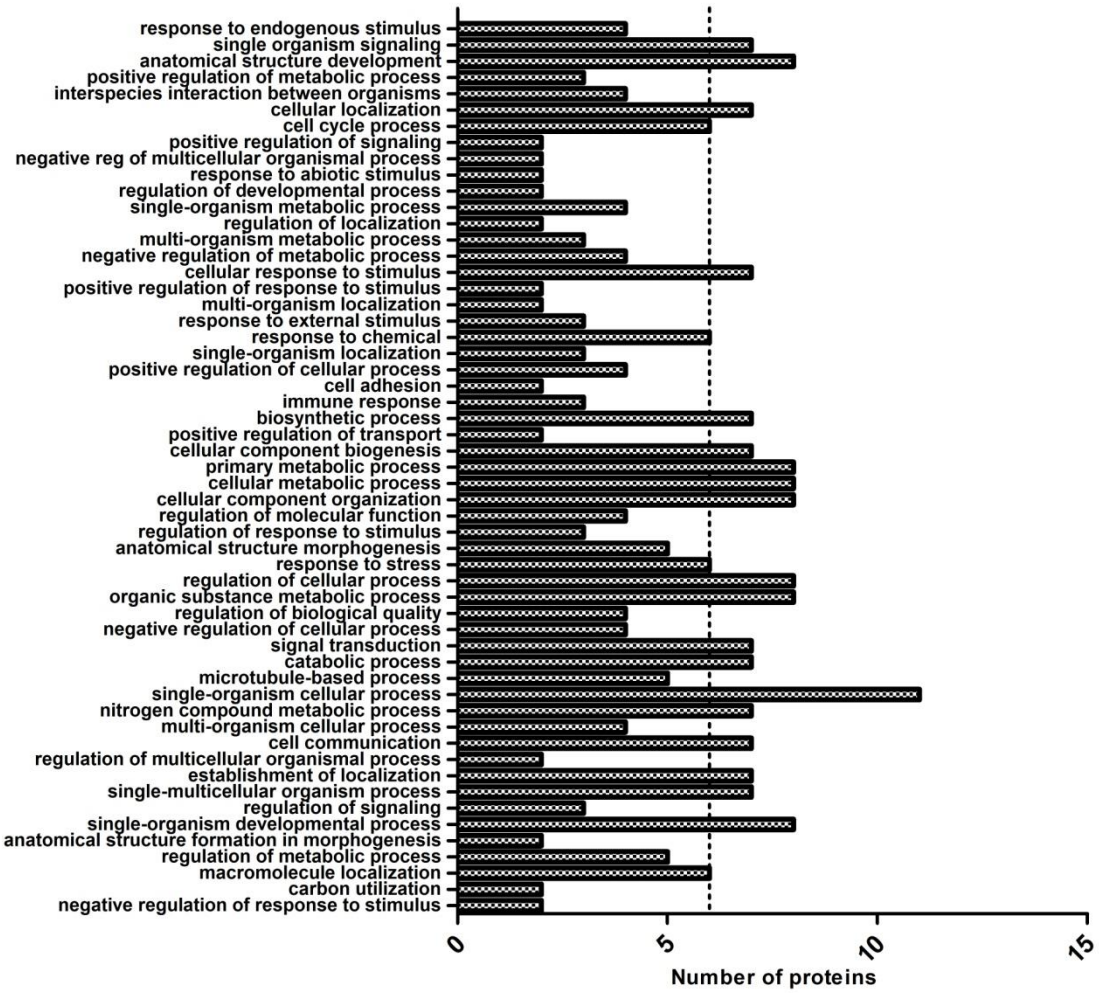

Fig. 3.10 GO analysis of biological process in MCF-7 cells exposed to Cu-Phen (**1**) and Cu-DPQ-Phen (**2**) with respect to the negative control after 48 h incubation. Process containing more than 6 proteins was of greater interest for the analysis.

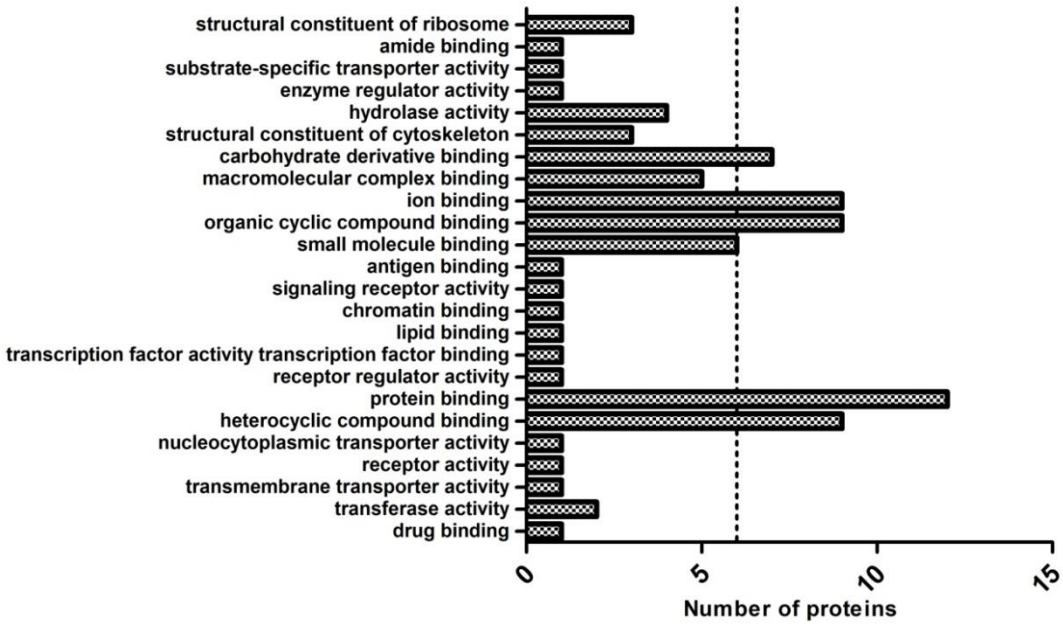

Fig. 3.11 GO analysis of molecular process in MCF-7 cells exposed to Cu-Phen (**1**) and Cu-DPQ-Phen (**2**) with respect to the negative control after 48 h incubation. Process containing more than 6 proteins was of greater interest for the analysis.

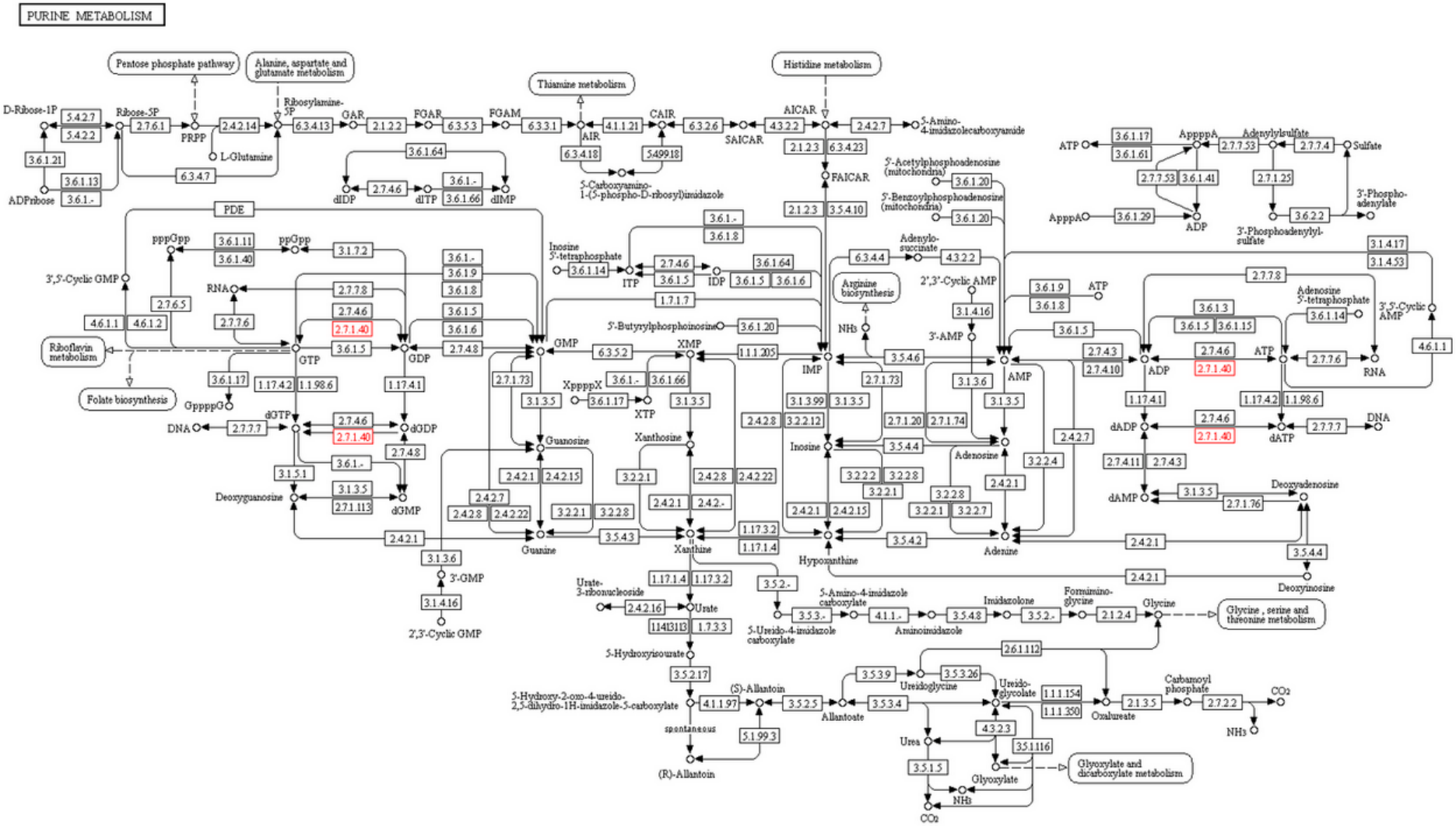

Fig. 3.12 KEGG analysis of significantly upregulated protein in purine metabolism. Pyruvate kinase (2.7.1.40) (red).

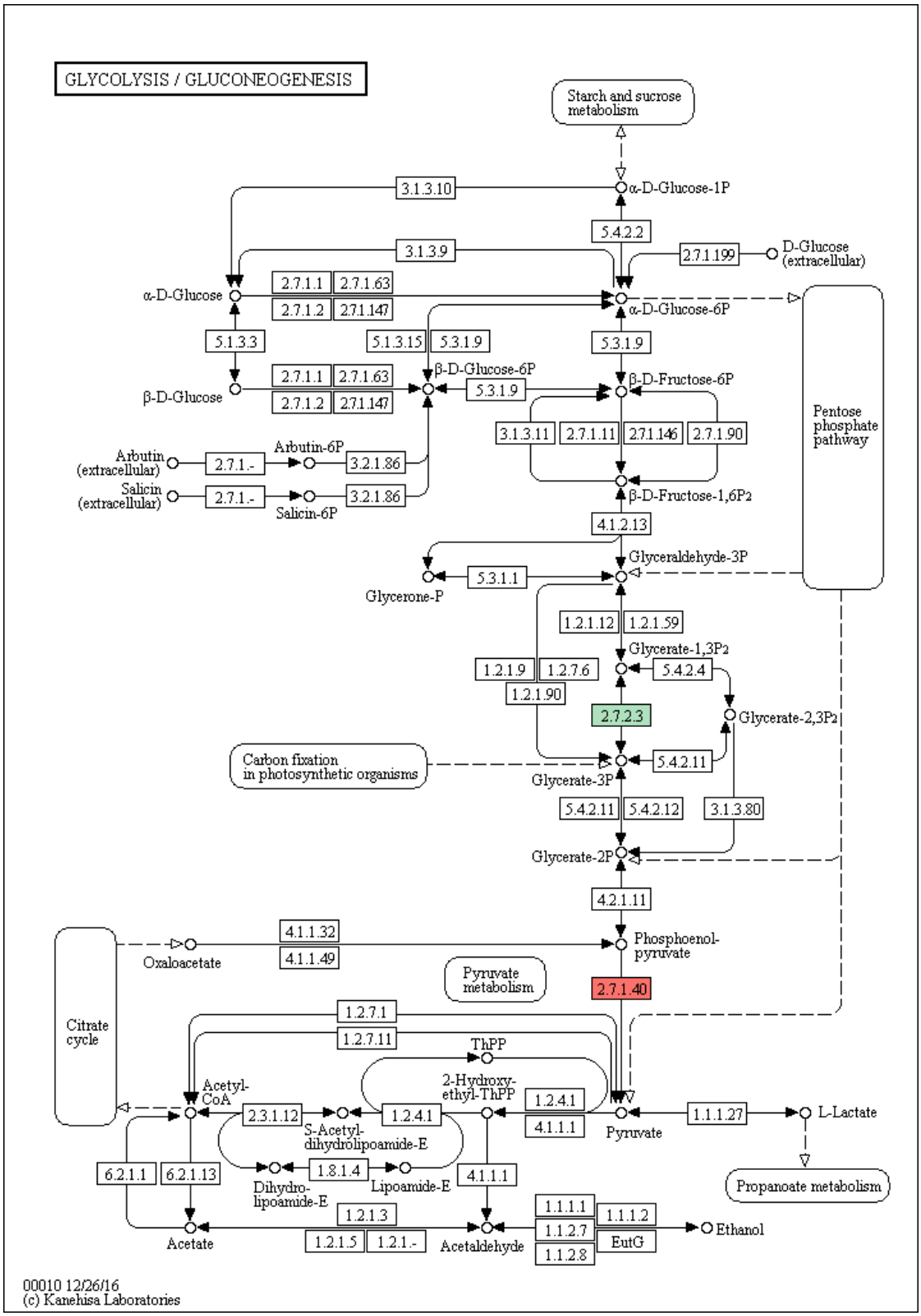

Fig. 3.13 KEGG analysis of significantly upregulated proteins in glycolysis/ gluconeogenesis. Phosphoglycerate kinase (2.7.2.3) (green) and pyruvate kinase (2.7.1.40) (red).

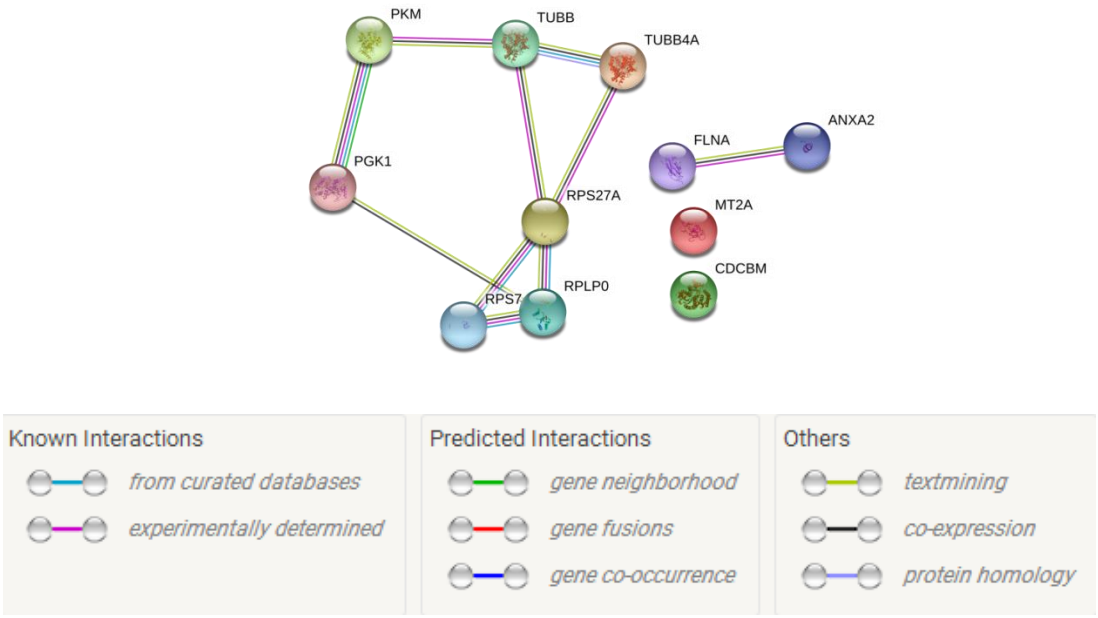

Fig. 3.14 STRING based protein interaction analysis of statistically significant protein with fold changes ≥ 1.5 in the MCF-7 cell after 48 h exposure to Cu-Phen (**1**) and Cu-DPQ-Phen (**2**) compared to the negative control. The STRING analysis demonstrated that there is not a strong clustering of proteins identified.

3.3.3 (C) SKOV-3 24 h exposure to Cu-Phen (1) and Cu-DPQ-Phen (2) in comparison to the negative control

Cell lysates from SKOV-3 cells were extracted after a 24 h exposure to Cu-Phen (**1**) and Cu-DPQ-Phen (**2**) along with a negative control for comparison. A total of 7 Statistically Significant Differentially Abundant (SSDA) proteins (**Table 3.6**) were found to meet the following criteria: containing ≥ 2 unique peptide from the identified protein, showed a significant change (ANOVA) in comparison to the negative control, had ≥ 1.5 fold change in relation to the negative control (a fold change of < 1.5 was also included if the same protein was expressed at ≥ 1.5 fold change in another exposure). A total of 26 proteins (**Table 3.7**) were found to be statistically significant but were < 1.5 fold change in protein expression in relation to the negative control. PCA (**Fig. 3.15**) was used to visualise the variation in protein abundance across individual replicates. In each of the complex exposures and negative control, a single replicate was excluded from the subsequent analysis due to lack of clustering. PCA showed separation of the negative control, Cu-Phen (**1**) and Cu-DPQ-Phen (**2**) with Cu-Phen (**1**) being separated more strongly by component 2. However hierarchical clustering using Log(2) transformed LFQ abundances (**Fig. 3.16**) of the all protein showed an absence of profile clustering in both Cu-Phen (**1**) and Cu-DPQ-Phen (**2**), indicating their similar protein expression pattern. **Table 3.6** contains significantly differentially abundant proteins from multiple functional classes of which include metal detoxification and signalling (metallothioneins), signalling and chaperones (heat shock proteins) and metabolic (phosphoglycerate kinase 1). **Table 3.7** contains lower differentially abundant protein in relation to the negative control. Gene Ontology (GO) biological process (**Fig. 3.17**) indicates proteins associated with the following functions: primary metabolic, organic substance metabolic and nitrogen compound metabolic processes. Processes that

contained more than 2 proteins were of greater interest in the analysis. GO molecular process. (**Fig. 3.18**) indicated proteins associated with the following functions: heterocyclic compound, organic cyclic compound, small molecule, protein and ion binding. Processes that contained more than 2 proteins were of greater interest in the analysis. KEGG analysis demonstrated involvement of phosphoglycerate kinase (2.7.2.3) in Glycolysis/ gluconeogenesis (**Fig. 3.19**) pathway. Additionally, nucleoside diphosphate kinase A was upregulated ≤ 1.5 fold change, a protein involved in purine metabolism. While additional KEGG pathways were identified but not included in this chapter the pathways presented below represent pathways that were highlighted across multiple experimental conditions and in many cases contained multiple protein identification within the same pathways. STRING protein interaction network described only two interactions between heat shock protein and metabolic proteins and between two metallothionein proteins.

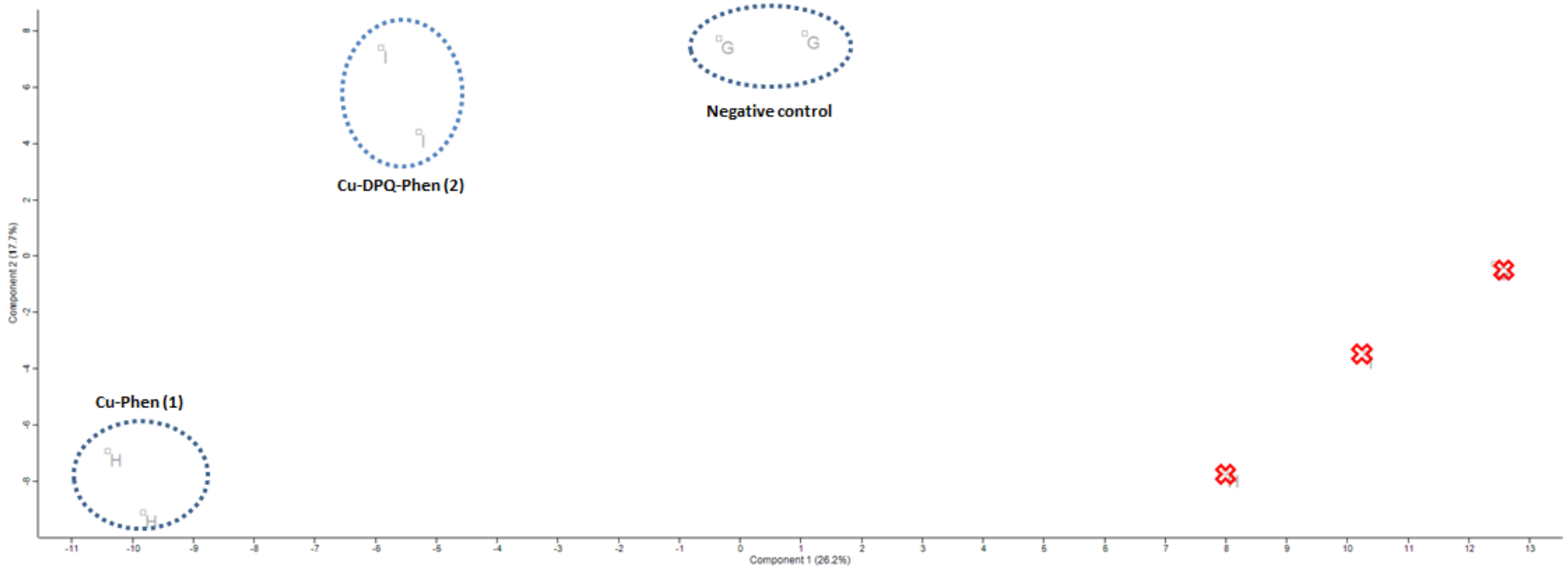

Fig. 3.15 Principle component analysis (PCA) of whole cell lysate proteome of SKOV-3 cells exposed to Cu-Phen (**1**) and Cu-DPQ-Phen (**2**) for 24 h in comparison to a negative control. PCA of three replicates for the negative control and three replicates of both test exposures. Enclosures define the different experimental conditions. Red X denotes the third replicates from each condition removed from the analysis due to lack of clustering.

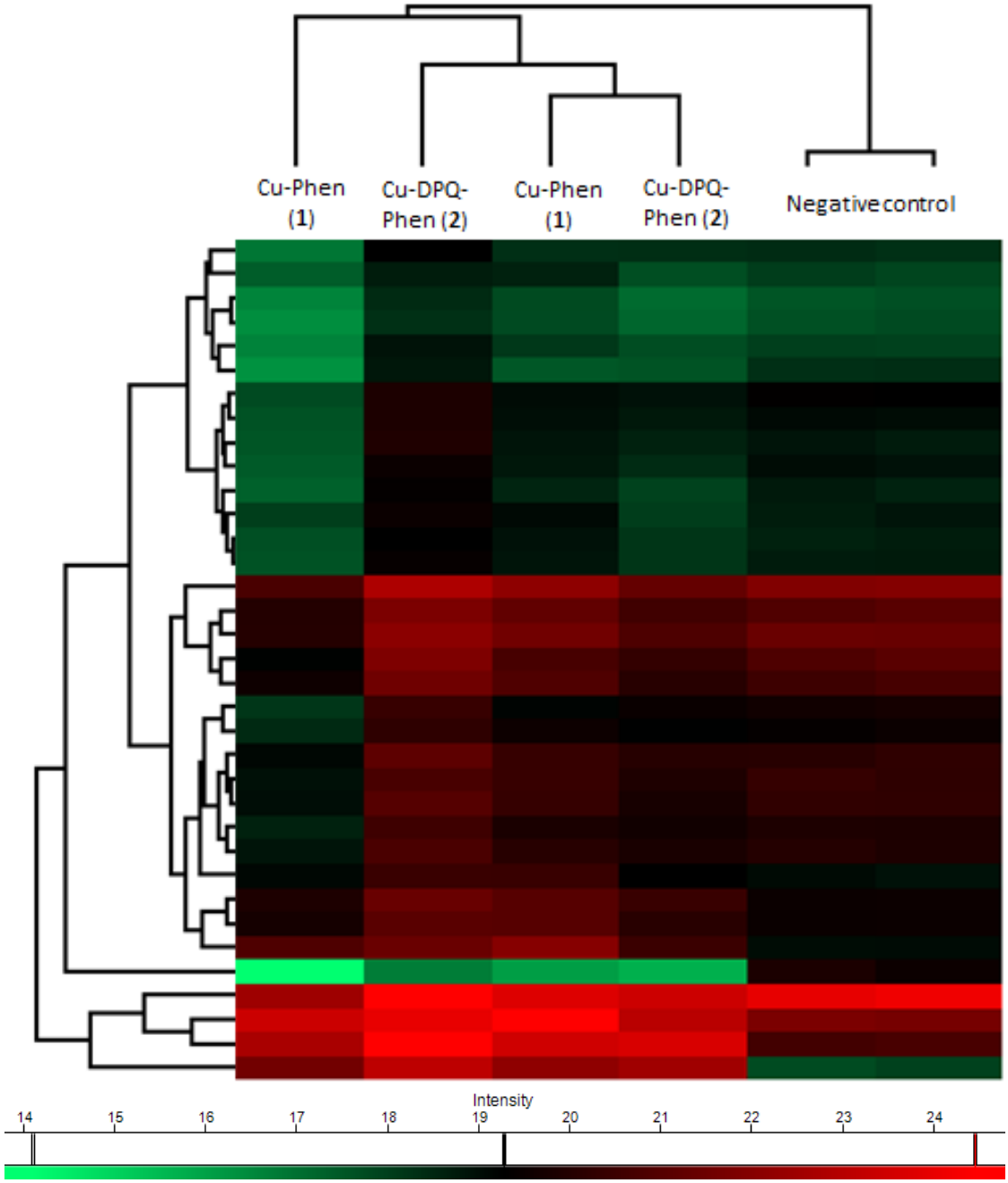

Fig. 3.16 Hierarchical clustering of SSDA proteins and statistically significant proteins with less than a 1.5 fold change in the SKOV-3 cell line after 24 h exposure to Cu-Phen (**1**) and Cu-DPQ-Phen (**2**) in relation to the control. Hierarchical clustering generated from mean Log(2) transformed values of LFQ abundance with samples clustered through columns.

Table 3.6 Statistically significant differentially abundant (SSDA) proteins (7) after exposure of Cu-Phen (**1**) and Cu-DPQ-Phen (**2**) in the SKOV-3 cell line after 24 h incubation.

Protein description	Accession	Peptide count	Anova (p)	Cu-Phen (**1**) (fold change)	Cu-DPQ-Phen (**2**) (fold change)
Metallothionein-1X	P80297	5	2.82E-03	14.72	17.63
Metallothionein-2	P02795	5	3.97E-03	4.77	5.87
Heat shock 70 kDa protein 6	P17066	9	6.25E-04	4.56	2.04
Heat shock 70 kDa protein 1B	P0DMV9	11	2.07E-03	4.04	1.92
Tumor protein D54	O43399	2	1.04E-02	1.68	1.47
Ubiquitin-40S ribosomal protein S27a	P62979	2	7.84E-03	1.60	1.19
Phosphoglycerate kinase 1	P00558	4	5.27E-03	1.50	1.00

Relative fold changes are given for each test exposure in comparison to the negative control.

Fold changes of < 1.5 were included when expression in other test exposure was ≥ 1.5 fold change.

Proteins (highlighted in grey) involved in metal detoxification and signalling (metallothioneins), signalling and chaperones (heat shock proteins) and metabolic (phosphoglycerate kinase 1) were the principle focus of this analysis.

Table 3.7 Statistically significant proteins (26) with fold changes < 1.5 fold change after exposure of Cu-Phen (**1**) and Cu-DPQ-Phen (**2**) in the SKOV-3 cell line after 24 h incubation.

Protein description	Accession	Peptide count	ANOVA (p)	Cu-Phen (**1**) (fold change)	Cu-DPQ-Phen (**2**) (fold change)
60S ribosomal protein L24	P83731	2	1.65E-02	0.90	0.65
60S ribosomal protein L29	P47914	2	2.50E-02	0.74	0.55
Talin-1	Q9Y490	2	1.24E-03	0.68	0.59
Heterogeneous nuclear ribonucleoproteins A2/B1	P22626	3	3.69E-03	0.67	0.64
Ezrin	P15311	2	3.13E-02	0.67	0.64
Elongation factor 2	P13639	6	5.24E-03	0.66	0.76
Polypyrimidine tract-binding protein 1	P26599	2	5.94E-03	0.65	0.62
Triosephosphate isomerase	P60174	2	2.54E-02	0.64	0.68
GMP synthase [glutamine-hydrolyzing]	P49915	3	2.27E-02	0.63	0.70
Nucleophosmin	P06748	6	1.98E-02	0.63	0.61
60S ribosomal protein L4	P36578	2	5.83E-05	0.62	0.58
Myosin-9	P35579	3	5.94E-04	0.59	0.61
Tubulin beta-4A chain	P04350	2	9.56E-03	0.58	0.59
ATP synthase subunit beta, mitochondrial	P06576	2	5.63E-03	0.58	0.76
40S ribosomal protein S7	P62081	2	2.34E-02	0.58	0.57
Stress-70 protein, mitochondrial	P38646	2	7.22E-03	0.57	0.70
Carbonyl reductase [NADPH] 1	P16152	2	1.07E-03	0.57	0.58
Alpha-actinin-1	P12814	2	1.11E-02	0.56	0.65
Thioredoxin-like protein 1	O43396	2	1.19E-02	0.52	0.76
Nucleoside diphosphate kinase A	P15531	2	1.15E-02	0.52	0.54
Plectin	Q15149	5	2.14E-03	0.51	0.66
Keratin, type I cytoskeletal 17	Q04695	4	1.17E-03	0.48	0.55
Importin subunit alpha-1	P52292	2	5.04E-03	0.47	0.59
Histone H2B type 1-D	P58876	7	3.12E-03	0.46	0.58
Histone H1.3	P16402	3	1.11E-02	0.45	0.67
Tubulin alpha-1B chain	P68363	2	2.75E-03	0.03	0.05

Relative fold changes are given for each test exposure in comparison to the negative control.

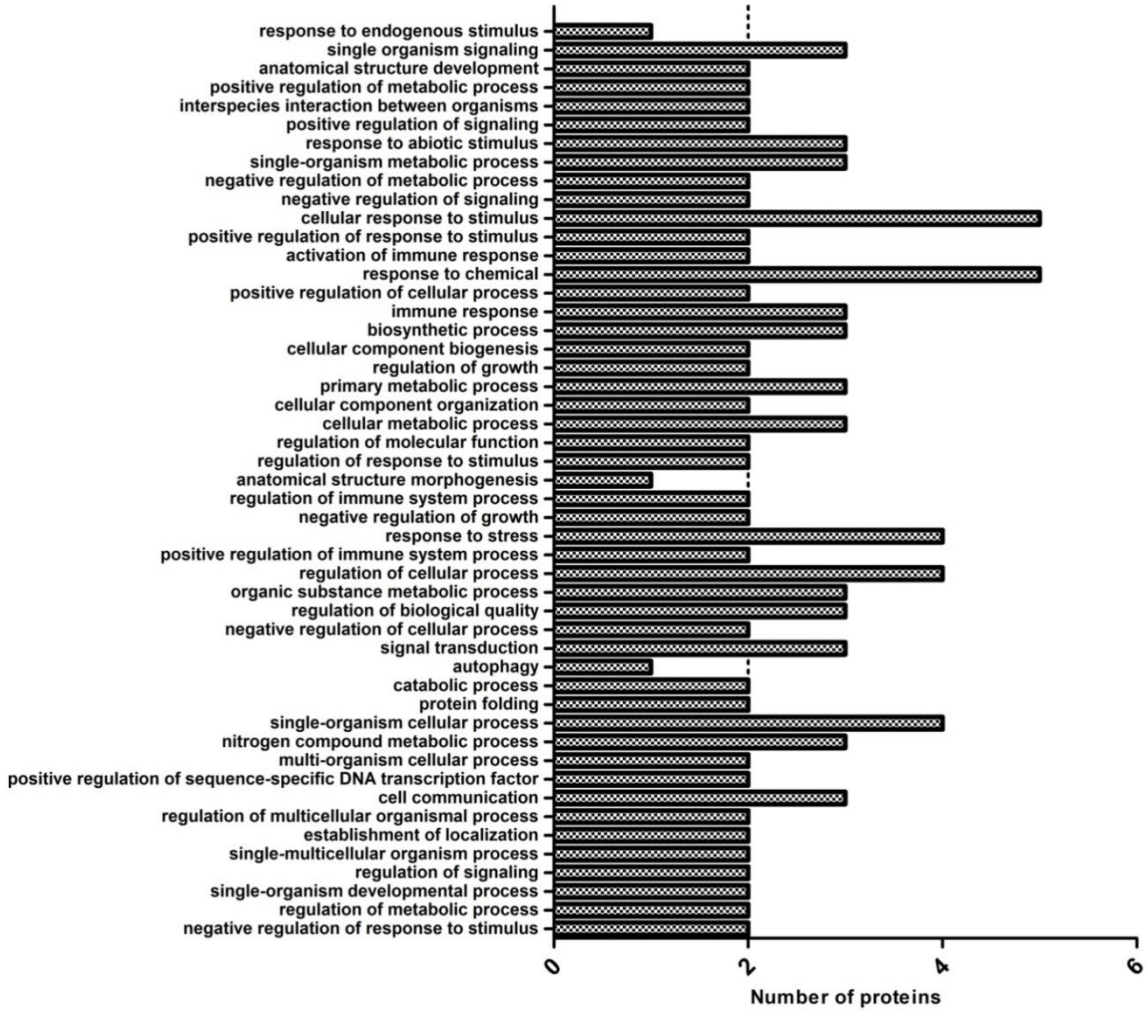

Fig. 3.17 GO analysis of biological process in SKOV-3 cells exposed to Cu-Phen (**1**) and Cu-DPQ-Phen (**2**) with respect to the negative control after 24 h incubation. Process containing more than 2 proteins was of greater interest for the analysis.

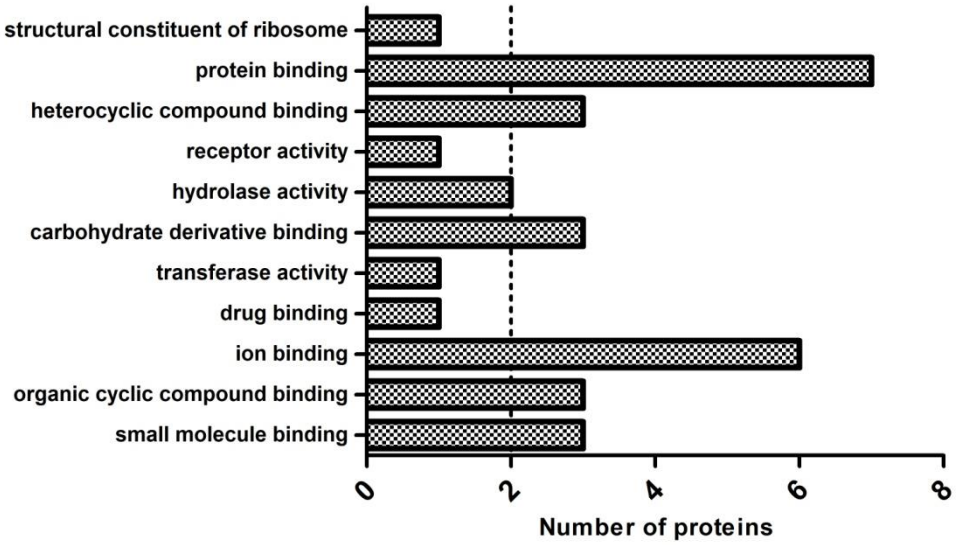

Fig. 3.18 GO analysis of molecular process in SKOV-3 cells exposed to Cu-Phen (**1**) and Cu-DPQ-Phen (**2**) with respect to the negative control after 24 h incubation. Process containing more than 2 proteins was of greater interest for the analysis.

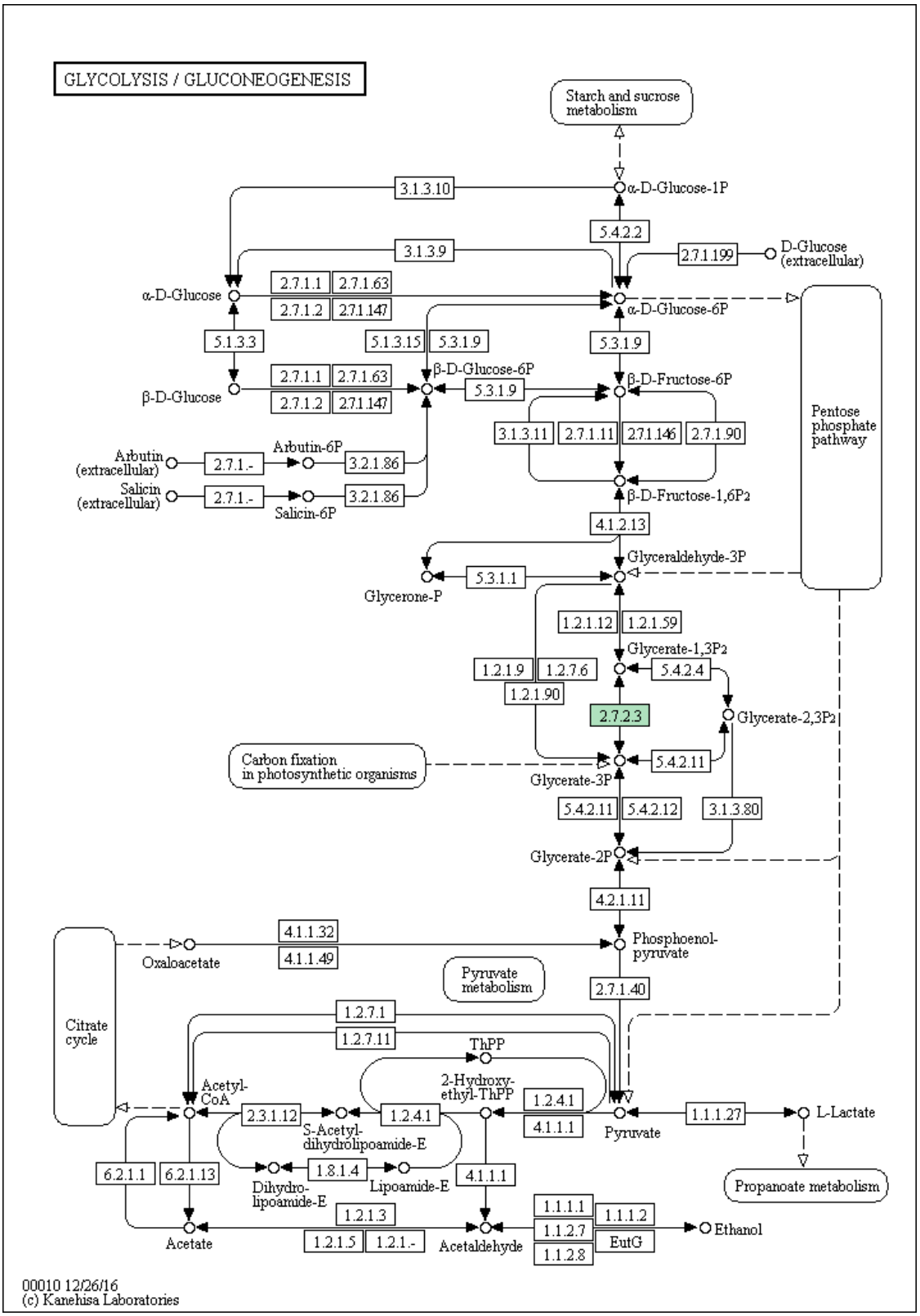

Fig. 3.19 KEGG analysis of significantly upregulated proteins in glycolysis/ gluconeogenesis. Phosphoglycerate kinase (2.7.2.3) (green).

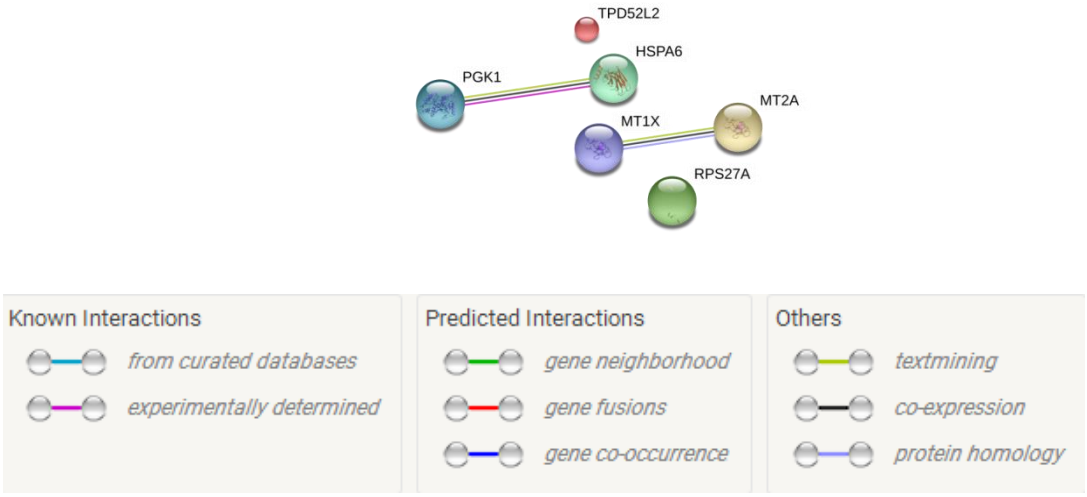

Fig. 3.20 STRING based protein interaction analysis of statistically significant protein with fold changes ≥ 1.5 in the SKOV-3 cell after 24 h exposure to Cu-Phen (**1**) and Cu-DPQ-Phen (**2**) compared to the negative control. The STRING analysis demonstrated that there is not a strong clustering of proteins identified.

3.3.4 (D) SKOV-3 48 h exposure to Cu-Phen (1) and Cu-DPQ-Phen (2) in comparison to the negative control

Cell lysates from SKOV-3 cells were extracted after a 48 h exposure to Cu-Phen (**1**) and Cu-DPQ-Phen (**2**) along with a negative control for comparison. A total of 44 Statistically Significant Differentially Abundant (SSDA) proteins (**Table 3.8**) were found to meet the following criteria: containing ≥ 2 unique peptide from the identified protein, showed a significant change (ANOVA) in comparison to the negative control, had ≥ 1.5 fold change in relation to the negative control (a fold change of < 1.5 was also included if the same protein was expressed at ≥ 1.5 fold change in another exposure). A total of 90 proteins (**Table 3.9**) were found to be statistically significant but were < 1.5 fold change in protein expression in relation to the negative control. PCA (**Fig. 3.21**) was used to visualise the variation in protein abundance across individual replicates. Both Cu-Phen (**1**) and Cu-DPQ-Phen (**2**) show separation from each other primarily through component 2 while the negative control and Cu-DPQ-Phen (**2**) show close clustering indicating a similar protein expression profile. Hierarchical clustering (**Fig. 3.22**) indicates separation of all experimental conditions with the negative control and Cu-DPQ-Phen (**2**) showing closer association than Cu-Phen (**1**), similarly to PCA in **Figure 3.21.** In each of the complex exposures and negative control, a single replicate was excluded from the subsequent analysis due to lack of clustering. PCA shows separation of the negative control, Cu-Phen (**1**) and Cu-DPQ-Phen (**2**) with Cu-Phen (**1**) being separated more strongly by component 2. However hierarchical clustering using Log(2) transformed LFQ abundances (**Fig. 3.22**) of the all protein showed the absence of profile clustering in both Cu-Phen (**1**) and Cu-DPQ-Phen (**2**), indicating their similar protein expression pattern. **Table 3.8** indicates significant differentially abundant proteins with multiple functional protein classes in relation to the negative control.

Protein functional classes, such as detoxification and signalling (e.g. metallothioneins), metabolic (e.g. glucose-6-phosphate isomerase), transcription factor related (e.g.pre-mRNA-processing factor), ribosomal (e.g. 40S) and chaperones/ signalling (e.g. heat-shock proteins) among others. **Table 3.9** also detailed significant lower differentially expressed proteins with multiple protein functional classes in comparison to the negative control. GO analysis of biological processes (**Fig. 3.23**) indicated a large number of proteins associated with the following processes: cellular metabolic, organic substance metabolic and nitrogen compound metabolic processes. Processes that contained more than 25 proteins were of greater interest to the analysis. GO analysis of molecular processes (**Fig. 3.24**) indicated a large number of proteins associated with the following processes: small molecule, organic cyclic compound, heterocyclic, ion and protein binding. Processes that contained more than 20 proteins were of greater interest in the analysis. KEGG analysis highlighted several pathways containing identified protein. While additional KEGG pathways were identified but not included in this chapter the pathways presented below represent pathways that were highlighted across multiple experimental conditions and in many cases contained multiple protein identification within the same pathways. Glycolysis/ gluconeogenesis (**Fig. 3.25**): glucose-6-phosphate isomerase (5.3.1.9), 6-phosphofructokinase (2.7.1.11), fructose-bisphosphate aldolase (4.1.2.13), triose-phosphate isomerase (5.3.1.1), glyceraldehyde-3-phosphate dehydrogenase (1.2.1.12), glyceraldehyde-3-phosphate dehydrogenase (NAD(P)+) (1.2.1.59), bisphosphoglycerate mutase (5.4.2.4), phosphoglycerate kinase (2.7.2.3) and L-lactate dehydrogenase (1.1.1.27). Pentose phosphate pathway (**Fig. 3.26**): glucose-6-phosphate isomerase (5.3.1.9), 6-phosphofructokinase (2.7.1.11) and fructose-bisphosphate aldolase (4.1.2.13). Fatty acid biosynthesis (**Fig. 3.27**): fatty-acid synthase (FasN). Purine metabolism (**Fig. 3.28**): nucleoside-diphosphate kinase

(2.7.4.6). STRING protein interaction network (**Fig. 3.29**) demonstrated strong clustering of multiple processes to the large number of glucose and metabolic related proteins.

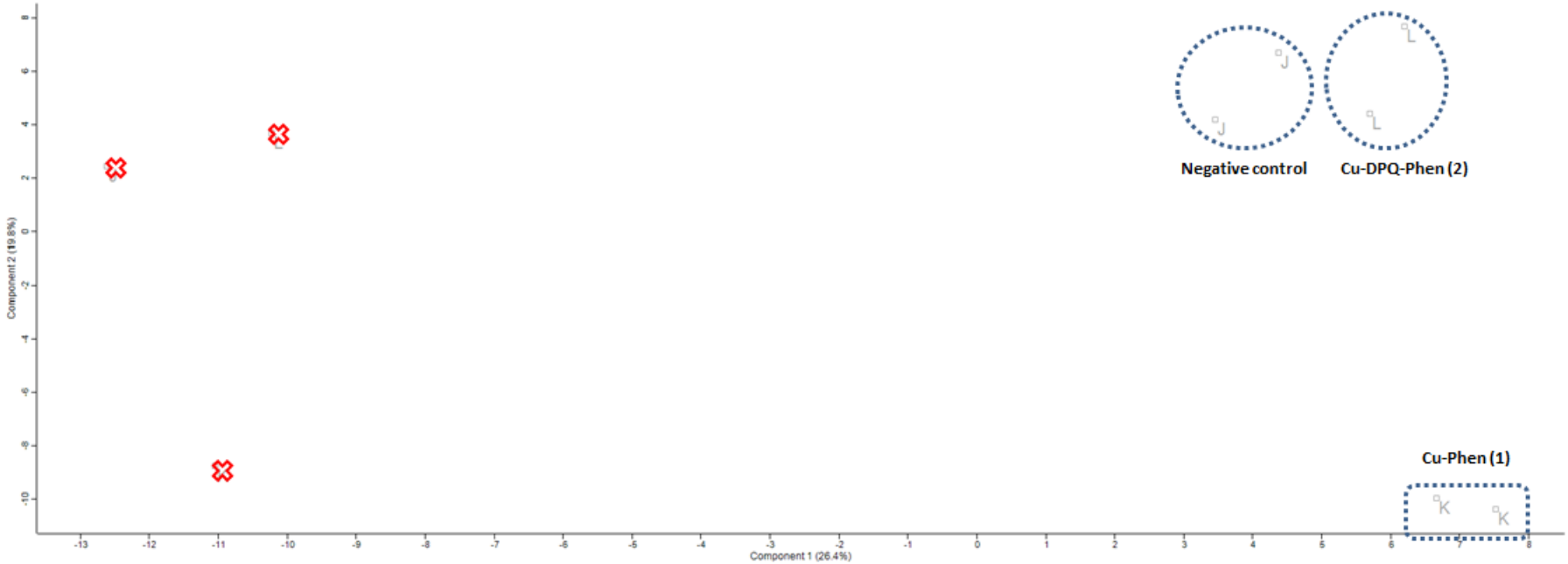

Fig. 3.21 Principle component analysis (PCA) of whole cell lysate proteome of SKOV-3 cells exposed to Cu-Phen (**1**) and Cu-DPQ-Phen (**2**) for 48 h in comparison to a negative control. PCA of three replicates for the negative control and three replicates of both test exposures. Enclosures define the different experimental conditions. Red X denotes the third replicates from each condition removed from the analysis due to lack of clustering.

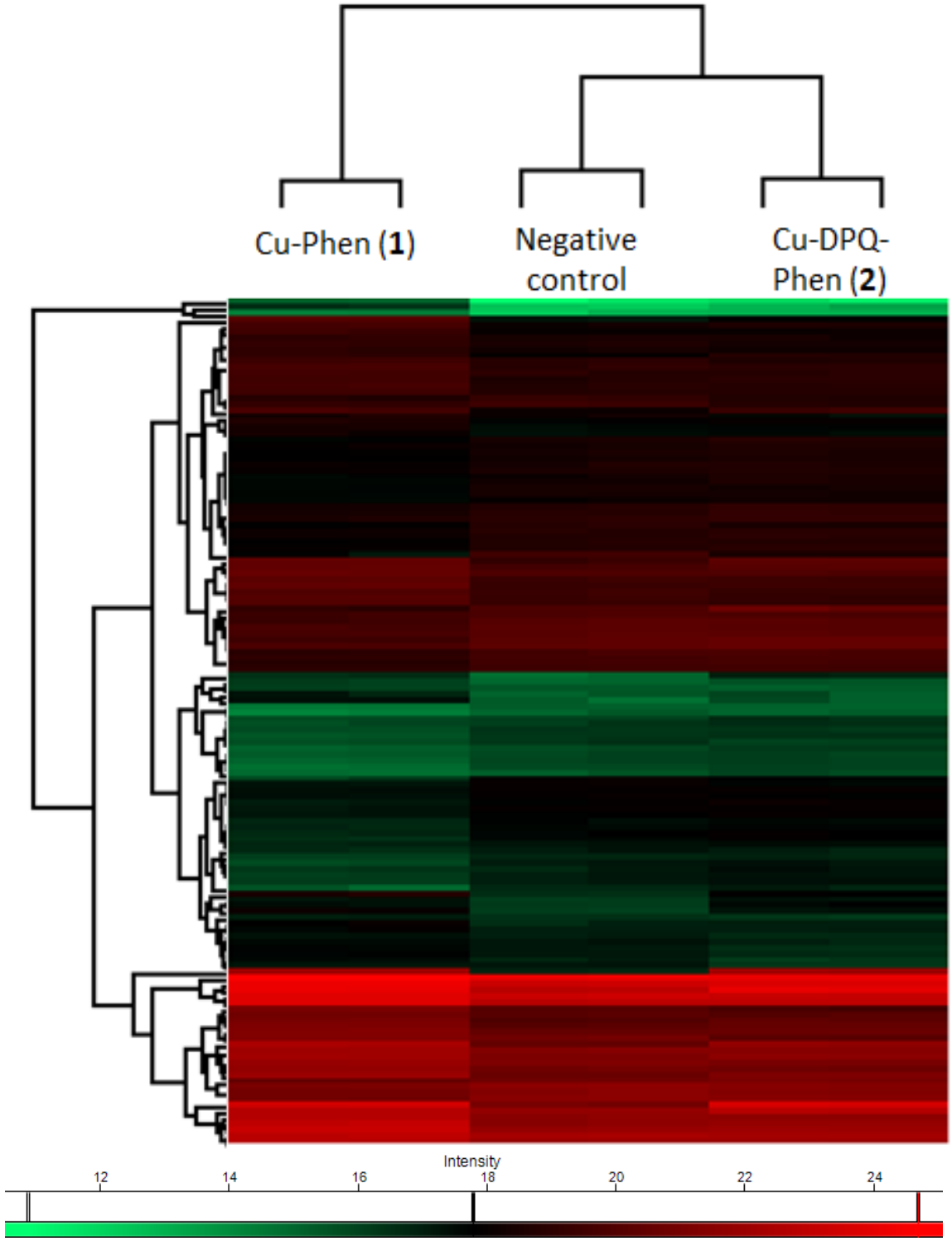

Fig. 3.22 Hierarchical clustering of SSDA proteins and statistically significant proteins with less than a 1.5 fold change in the SKOV-3 cell line after 48 h exposure to Cu-Phen (**1**) and Cu-DPQ-Phen (**2**) in relation to the control. Hierarchical clustering generated from mean Log(2) transformed values of LFQ abundance with samples clustered through columns.

Table 3.8 Statistically significant differentially abundant (SSDA) proteins (44) after exposure of Cu-Phen (**1**) and Cu-DPQ-Phen (**2**) in the SKOV-3 cell line after 48 h incubation.

Protein description	Accession	Peptide count	Anova (p)	Cu-Phen (**1**) (fold change)	Cu-DPQ-Phen (**2**) (fold change)
Metallothionein-1X	P80297	5	1.37E-05	32.12	32.12
Fructose-bisphosphate aldolase C	P09972	2	1.26E-03	14.89	1.57
Prolyl 4-hydroxylase subunit alpha-2	O15460	2	7.00E-03	13.75	1.29
Protein NDRG1	Q92597	6	2.28E-04	6.51	1.29
Metallothionein-2	P02795	5	3.17E-04	4.92	5.45
Procollagen-lysine,2-oxoglutarate 5-dioxygenase 2	O00469	2	1.88E-02	4.43	1.25
Rab GDP dissociation inhibitor alpha	P31150	2	2.08E-03	3.66	2.21
Importin subunit beta-1	Q14974	3	1.12E-03	3.39	2.10
Tubulin beta chain	P07437	3	1.84E-04	3.27	2.09
Cathepsin Z	Q9UBR2	2	3.59E-02	2.96	1.12
Pre-mRNA-processing factor 19	Q9UMS4	2	1.39E-03	2.71	3.48
Alpha-actinin-1	P12814	3	3.31E-03	2.64	2.26
L-lactate dehydrogenase A chain	P00338	10	1.41E-03	2.52	1.09
Glucose-6-phosphate isomerase	P06744	3	7.17E-04	2.46	1.20
Neutral alpha-glucosidase AB	Q14697	5	1.30E-03	2.36	0.96
Phosphoglycerate kinase 1	P00558	16	2.69E-05	2.30	1.01
Alpha-actinin-4	O43707	2	3.30E-05	2.26	1.37
Histone H2B type 1-K	O60814	11	2.95E-04	2.21	2.12
ATP-dependent 6-phosphofructokinase, platelet type	Q01813	2	1.31E-02	2.03	1.05
40S ribosomal protein S7	P62081	4	1.30E-03	2.02	1.82
Calponin-3	Q15417	2	3.54E-03	1.96	2.42
Tubulin beta-3 chain	Q13509	4	1.21E-03	1.96	1.23
Proteasome subunit alpha type-1	P25786	2	1.36E-04	1.95	0.99
Nucleoside diphosphate kinase A	P15531	2	1.86E-03	1.95	1.97
Fatty acid synthase	P49327	2	2.86E-03	1.94	1.34
Nucleoside diphosphate kinase B	P22392	2	1.64E-03	1.93	1.66
Phosphoglycerate mutase 1	P18669	6	6.96E-04	1.90	0.95
Macrophage migration inhibitory factor	P14174	8	1.52E-04	1.83	1.00
Triosephosphate isomerase	P60174	7	1.52E-04	1.83	1.15
Heat shock 70 kDa protein 1B	P0DMV9	9	4.30E-05	1.77	1.21
Fructose-bisphosphate aldolase A	P04075	12	1.73E-04	1.75	0.88
Protein disulfide-isomerase	P07237	2	8.61E-04	1.73	0.68
Nucleophosmin	P06748	8	2.53E-05	1.66	1.74
Endoplasmin	P14625	7	1.39E-04	1.64	0.83
Tubulin beta-2A chain	Q13885	14	1.97E-03	1.64	1.19
Hematological and neurological expressed 1-like protein	Q9H910	2	2.40E-03	1.62	0.89
Phosphoserine aminotransferase	Q9Y617	3	1.57E-03	1.61	1.01

Alanine--tRNA ligase, cytoplasmic	P49588	2	3.74E-03	1.59	0.90
Ubiquitin-like modifier-activating enzyme 1	P22314	2	4.57E-03	1.59	1.08
Microtubule-associated protein 1B	P46821	2	2.50E-03	1.56	1.04
Tubulin beta-6 chain	Q9BUF5	5	3.77E-03	1.56	1.00
Myosin-9	P35579	4	1.42E-03	1.53	1.30
Protein BRICK1	Q8WUW1	2	2.41E-02	1.52	0.96
Glyceraldehyde-3-phosphate dehydrogenase	P04406	6	3.50E-06	1.51	0.95

Relative fold changes are given for each test exposure in comparison to the negative control.

Fold changes of < 1.5 were included when expression in other test exposure was ≥ 1.5 fold change.

The proteins (highlighted in grey) relate to detoxification and signalling (e.g. metallothioneins), metabolic (e.g. glucose-6-phosphate isomerase), transcription factor related (e.g.pre-mRNA-processing factor), ribosomal (e.g. 40S) and chaperones/ signalling (e.g. heat-shock proteins) were the principle focus of this analysis.

Table 3.9 Statistically significant proteins (90) with fold changes <1.5 fold change after exposure of Cu-Phen (**1**) and Cu-DPQ-Phen (**2**) in the SKOV-3 cell line after 48 h incubation.

Protein description	Accession	Peptide count	ANOVA (p)	Cu-Phen (**1**) (fold change)	Cu-DPQ-Phen (**2**) (fold change)
Actin-related protein 2	P61160	2	2.82E-02	1.49	0.91
Serine/threonine-protein phosphatase 2A 65 kDa regulatory subunit A alpha isoform	P30153	4	2.02E-03	1.48	0.76
Macrophage-capping protein	P40121	2	1.31E-02	1.47	0.89
Transitional endoplasmic reticulum ATPase	P55072	9	1.14E-03	1.44	0.92
Vinculin	P18206	4	4.92E-04	1.44	0.91
Adenosylhomocysteinase	P23526	2	3.65E-02	1.44	0.89
Protein disulfide-isomerase A3	P30101	4	1.09E-04	1.42	0.79
78 kDa glucose-regulated protein	P11021	9	1.60E-04	1.40	0.81
40S ribosomal protein S28	P62857	2	7.48E-04	1.38	0.91
Cytidine deaminase	P32320	4	8.69E-03	1.37	0.86
Thioredoxin domain-containing protein 5	Q8NBS9	2	1.10E-02	1.35	0.82
PDZ and LIM domain protein 1	O00151	2	5.87E-03	1.35	0.83
Protein AHNAK2	Q8IVF2	2	6.30E-03	1.34	0.56
Nuclear mitotic apparatus protein 1	Q14980	2	3.33E-02	1.31	0.83
Alpha-enolase	P06733	11	2.68E-03	1.31	0.85
Protein kinase C delta-binding protein	Q969G5	2	3.45E-03	1.31	0.79
Epidermal growth factor receptor kinase substrate 8-like protein 2	Q9H6S3	2	1.34E-03	1.31	0.77
Gelsolin	P06396	2	6.48E-04	1.31	0.66
Major vault protein	Q14764	2	3.31E-03	1.28	0.75
Pyruvate kinase PKM	P14618	9	4.21E-04	1.27	0.81
Pyridoxal kinase	O00764	3	2.14E-03	1.26	0.78
Protein disulfide-isomerase A6	Q15084	2	1.25E-03	1.26	0.60
Tubulin beta-4A chain	P04350	3	1.39E-04	1.21	0.58
WASH complex subunit CCDC53	Q9Y3C0	2	3.53E-03	1.10	0.73
Annexin A11	P50995	2	6.30E-03	1.09	0.70
Prohibitin	P35232	2	4.58E-02	1.07	0.54
Sorting nexin-3	O60493	2	2.35E-05	0.88	0.49
Vasodilator-stimulated phosphoprotein	P50552	2	1.13E-02	0.77	1.31
Histone H4	P62805	2	5.86E-03	0.72	0.56
Prelamin-A/C	P02545	8	3.53E-04	0.71	1.07
60S ribosomal protein L30	P62888	4	1.09E-02	0.70	1.10
Proteasome subunit alpha type-6	P60900	2	6.70E-03	0.67	1.06
Voltage-dependent anion-selective channel protein 1	P21796	4	2.03E-02	0.66	0.65
14-3-3 protein zeta/delta	P63104	3	1.41E-02	0.66	0.88
Poly(rC)-binding protein 2	Q15366	4	1.34E-03	0.65	1.14
Nucleosome assembly protein 1-like 4	Q99733	2	1.95E-03	0.65	1.02
40S ribosomal protein S14	P62263	3	1.21E-03	0.65	1.11

T-complex protein 1 subunit epsilon	P48643	6	2.33E-04	0.65	1.05
60S ribosomal protein L3	P39023	2	3.78E-02	0.64	1.15
Elongation factor 2	P13639	11	5.64E-04	0.64	0.80
Splicing factor 3B subunit 2	Q13435	3	2.42E-05	0.63	0.93
Ubiquitin-40S ribosomal protein S27a	P62979	3	2.93E-05	0.63	1.02
GTP-binding nuclear protein Ran	P62826	3	2.46E-03	0.63	0.94
60S acidic ribosomal protein P0	P05388	2	3.31E-02	0.63	0.94
T-complex protein 1 subunit zeta	P40227	3	5.18E-04	0.62	1.01
Plectin	Q15149	16	6.09E-04	0.62	0.88
Heterogeneous nuclear ribonucleoprotein K	P61978	4	6.34E-04	0.61	0.97
LIM and SH3 domain protein 1	Q14847	3	9.70E-03	0.61	1.14
Importin subunit alpha-1	P52292	5	9.15E-04	0.61	0.84
Eukaryotic translation initiation factor 6	P56537	2	2.61E-02	0.61	0.76
Ran-binding protein 3	Q9H6Z4	2	2.10E-04	0.61	1.01
ATP-dependent RNA helicase DDX1	Q92499	3	1.30E-02	0.61	1.25
Far upstream element-binding protein 1	Q96AE4	4	3.29E-04	0.60	0.99
Nucleolin	P19338	4	3.70E-03	0.60	0.81
Eukaryotic translation initiation factor 5	P55010	2	7.02E-04	0.60	0.81
60S ribosomal protein L7	P18124	2	2.12E-02	0.59	1.22
Ran GTPase-activating protein 1	P46060	2	5.10E-03	0.59	0.95
60S ribosomal protein L13	P26373	2	3.79E-04	0.58	1.03
Apoptotic chromatin condensation inducer in the nucleus	Q9UKV3	3	2.48E-03	0.58	1.24
Probable ATP-dependent RNA helicase DDX17	Q92841	2	2.39E-03	0.58	0.94
Scaffold attachment factor B1	Q15424	2	3.96E-03	0.58	0.88
Protein S100-A6	P06703	3	3.69E-03	0.56	0.98
DNA replication licensing factor MCM7	P33993	2	8.95E-03	0.56	0.84
Elongation factor 1-alpha 2	Q05639	6	1.75E-05	0.56	0.87
KH domain-containing, RNA-binding, signal transduction-associated protein 1	Q07666	2	5.80E-04	0.56	1.09
60S ribosomal protein L15	P61313	2	4.63E-03	0.54	0.71
Stathmin	P16949	4	2.79E-04	0.54	0.85
Heterogeneous nuclear ribonucleoprotein A0	Q13151	2	2.18E-03	0.53	1.05
Probable ATP-dependent RNA helicase DDX5	P17844	4	2.83E-03	0.53	0.87
Splicing factor, proline- and glutamine-rich	P23246	5	5.12E-05	0.53	0.96
Histone H1.3	P16402	3	2.06E-03	0.53	0.98
Chromobox protein homolog 3	Q13185	3	1.03E-03	0.52	0.70
Serum albumin	P02768	2	5.02E-05	0.52	1.02
60S ribosomal protein L22	P35268	2	1.16E-03	0.52	1.09
Cold-inducible RNA-binding protein	Q14011	2	3.01E-03	0.51	0.90
ATP-dependent RNA helicase DDX3X	O00571	4	3.93E-03	0.51	0.97
Polyadenylate-binding protein 1	P11940	5	2.93E-03	0.50	0.84
Heterogeneous nuclear ribonucleoprotein D0	Q14103	2	1.59E-02	0.50	0.89
Proliferation-associated protein 2G4	Q9UQ80	4	1.69E-04	0.50	1.05
Heterogeneous nuclear ribonucleoprotein A1	P09651	5	3.16E-03	0.50	1.47

Serine/arginine-rich splicing factor 1	Q07955	2	4.16E-04	0.49	0.90
Proteasome subunit alpha type-7	O14818	2	1.47E-03	0.49	0.96
Nuclear migration protein nudC	Q9Y266	2	2.72E-04	0.47	1.12
Bcl-2-associated transcription factor 1	Q9NYF8	2	1.62E-03	0.47	1.05
Matrin-3	P43243	2	2.53E-03	0.46	1.01
DnaJ homolog subfamily A member 1	P31689	2	6.53E-04	0.45	1.05
Histone H1.5	P16401	3	3.50E-04	0.41	1.07
60S ribosomal protein L29	P47914	2	7.11E-04	0.35	0.98
Eukaryotic translation initiation factor 5A-1	P63241	2	1.16E-02	0.32	1.06
Heterogeneous nuclear ribonucleoprotein D-like	O14979	2	2.45E-03	0.24	0.75

Relative fold changes are given for each test exposure in comparison to the negative control.

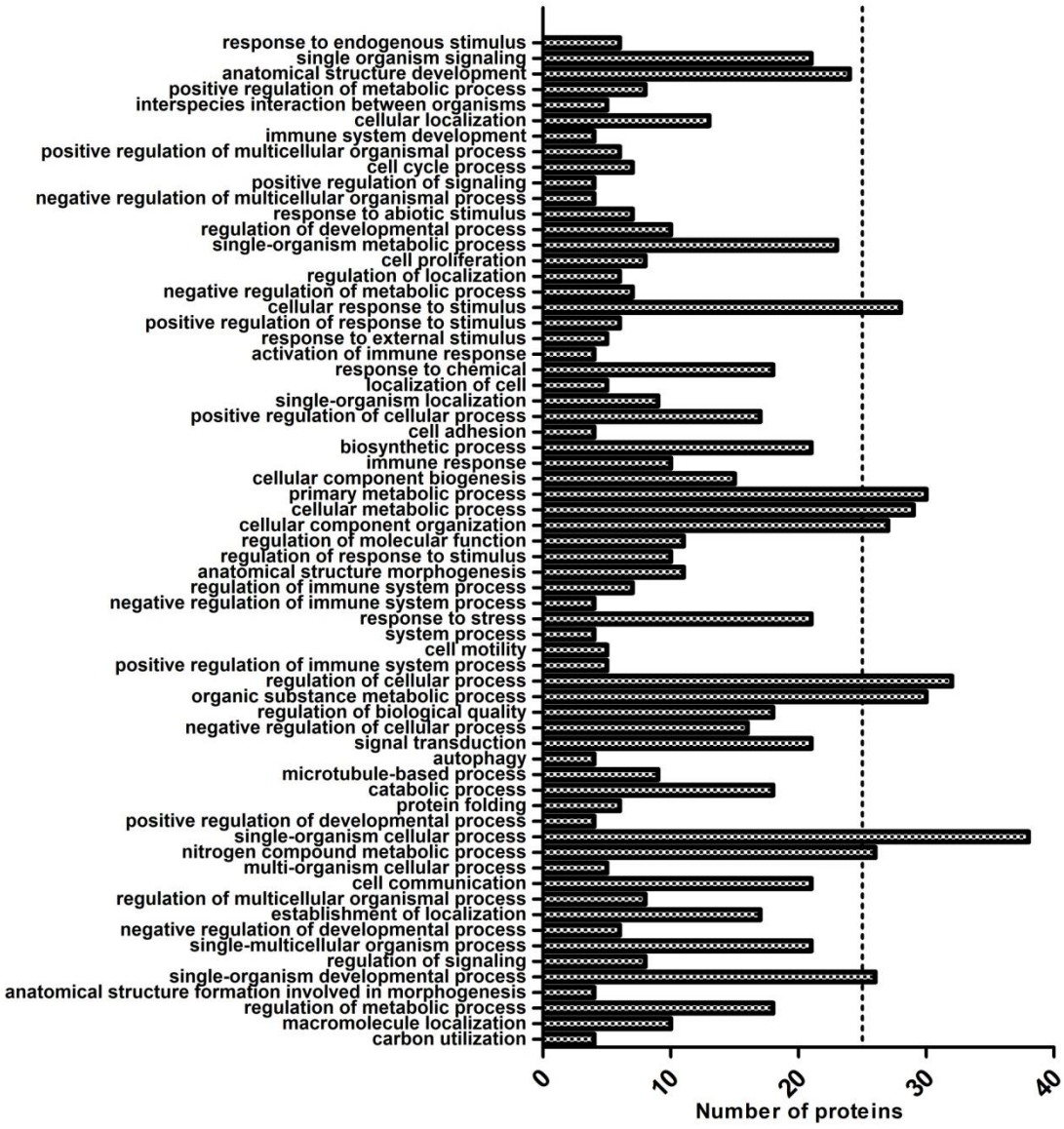

Fig 3.23 GO analysis of biological process in SKOV-3 cells exposed to Cu-Phen (**1**) and Cu-DPQ-Phen (**2**) with respect to the negative control after 48 h incubation. Process containing more than 25 proteins was of greater interest for the analysis.

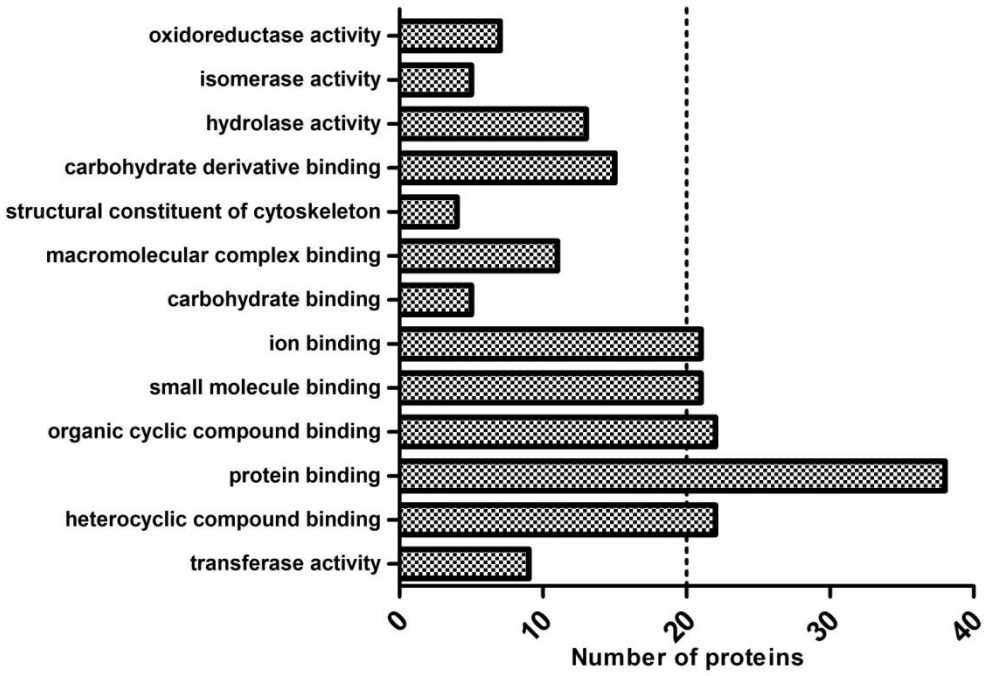

Fig 3.24 GO analysis of biological process in SKOV-3 cells exposed to Cu-Phen (**1**) and Cu-DPQ-Phen (**2**) with respect to the negative control after 48 h incubation. Process containing more than 20 proteins was of greater interest for the analysis.

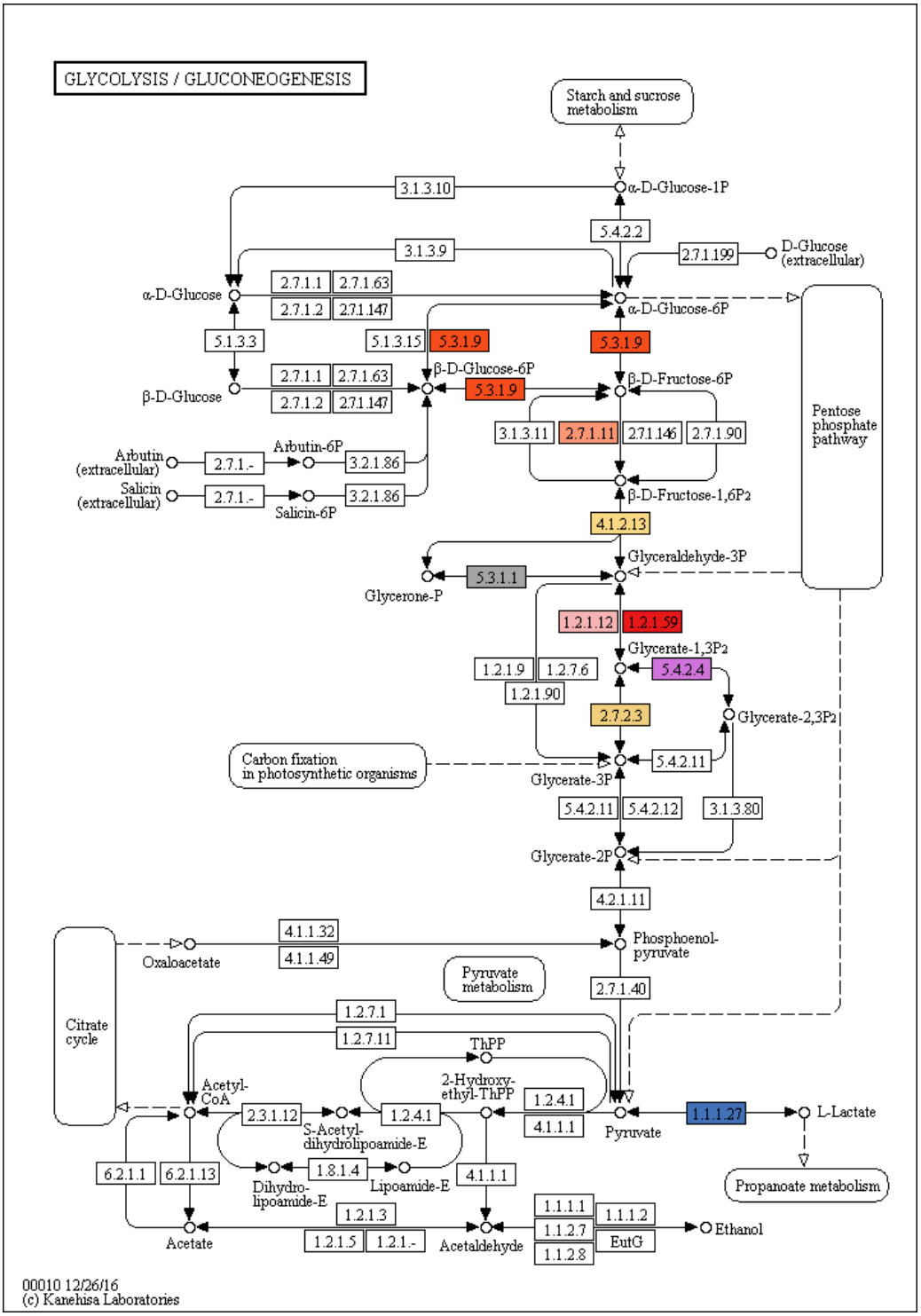

Fig. 3.25 KEGG analysis of significantly upregulated proteins in glycolysis/ gluconeogenesis. Glucose-6-phosphate isomerase (5.3.1.9) (red), 6-phosphofructokinase (2.7.1.11) (orange), fructose-bisphosphate aldolase (4.1.2.13) (yellow), triose-phosphate isomerase (5.3.1.1) (grey), glyceraldehyde-3-phosphate dehydrogenase (1.2.1.12) (pink), glyceraldehyde-3-phosphate dehydrogenase (NAD(P)+) (1.2.1.59) (wine), bisphosphoglycerate mutase (5.4.2.4) (purple), phosphoglycerate kinase (2.7.2.3) (brown) and L-lactate dehydrogenase (1.1.1.27) (blue).

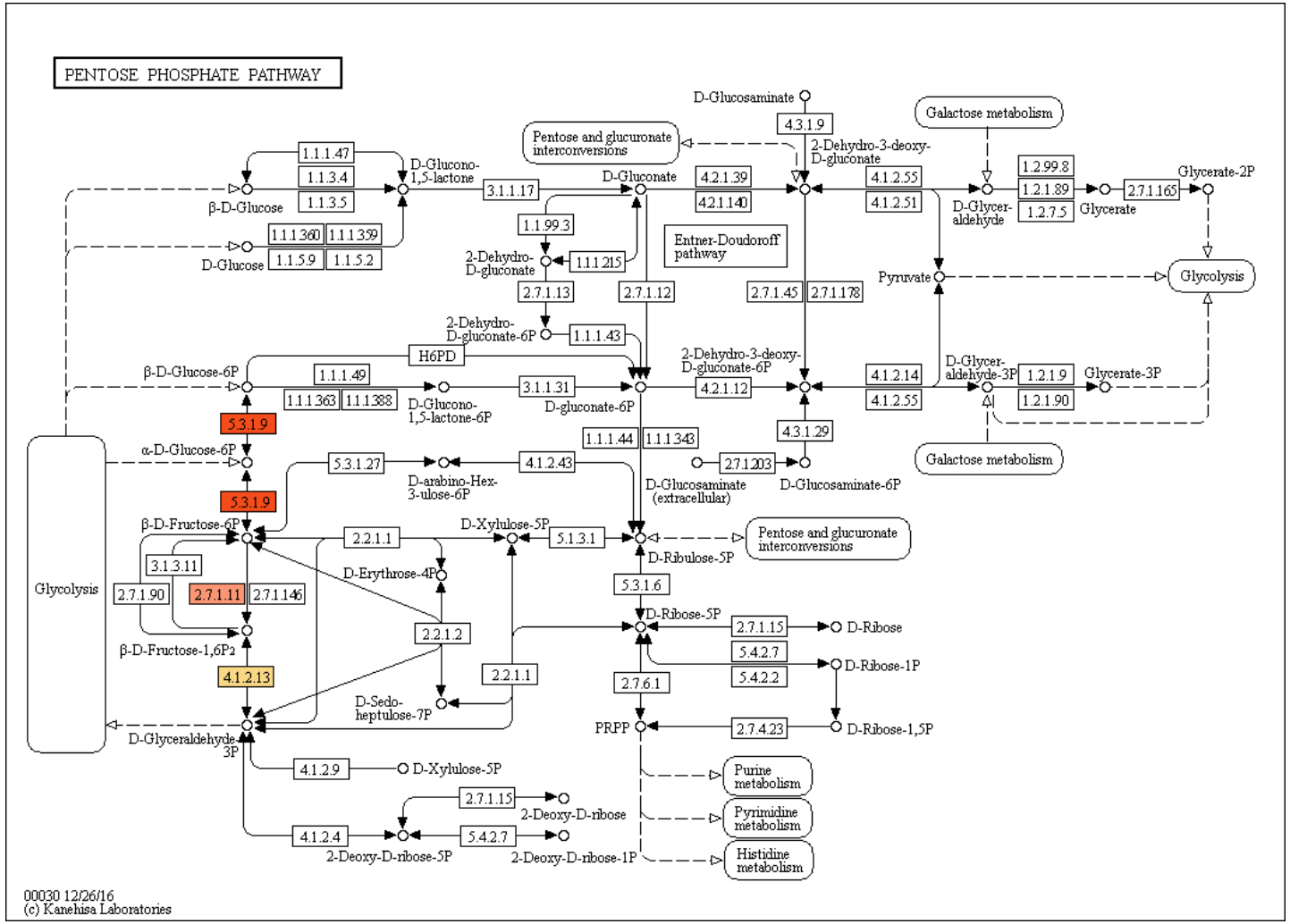

Fig. 3.26 KEGG analysis of significantly upregulated proteins in the pentose phosphate pathway. Glucose-6-phosphate isomerase (5.3.1.9) (orange), 6-phosphofructokinase (2.7.1.11) (brown) and fructose-bisphosphate aldolase (4.1.2.13) (yellow).

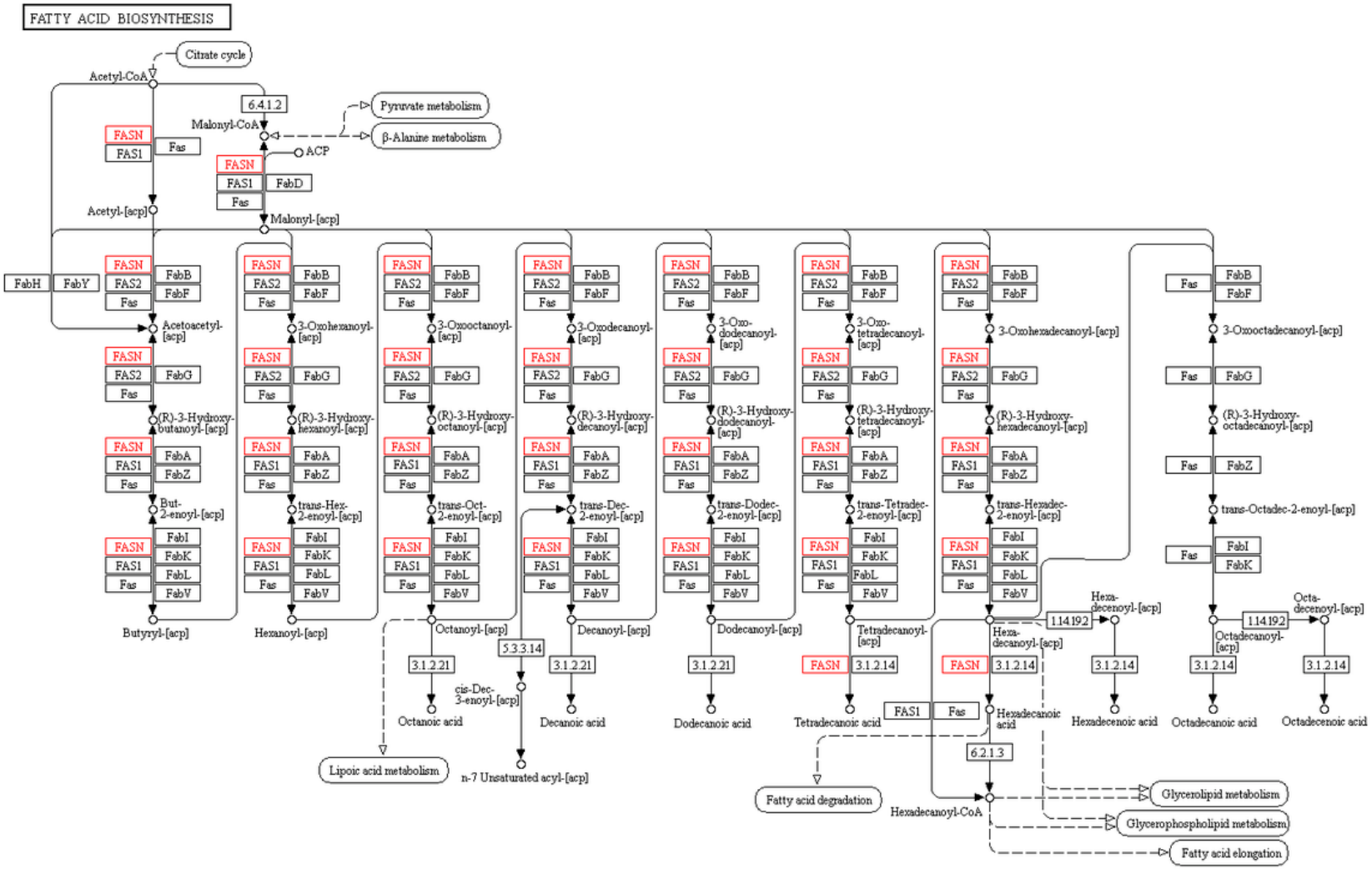

Fig. 3.27 KEGG analysis of significantly upregulated proteins in fatty acid biosynthesis pathway. Fatty acid synthase (FASN) (red).

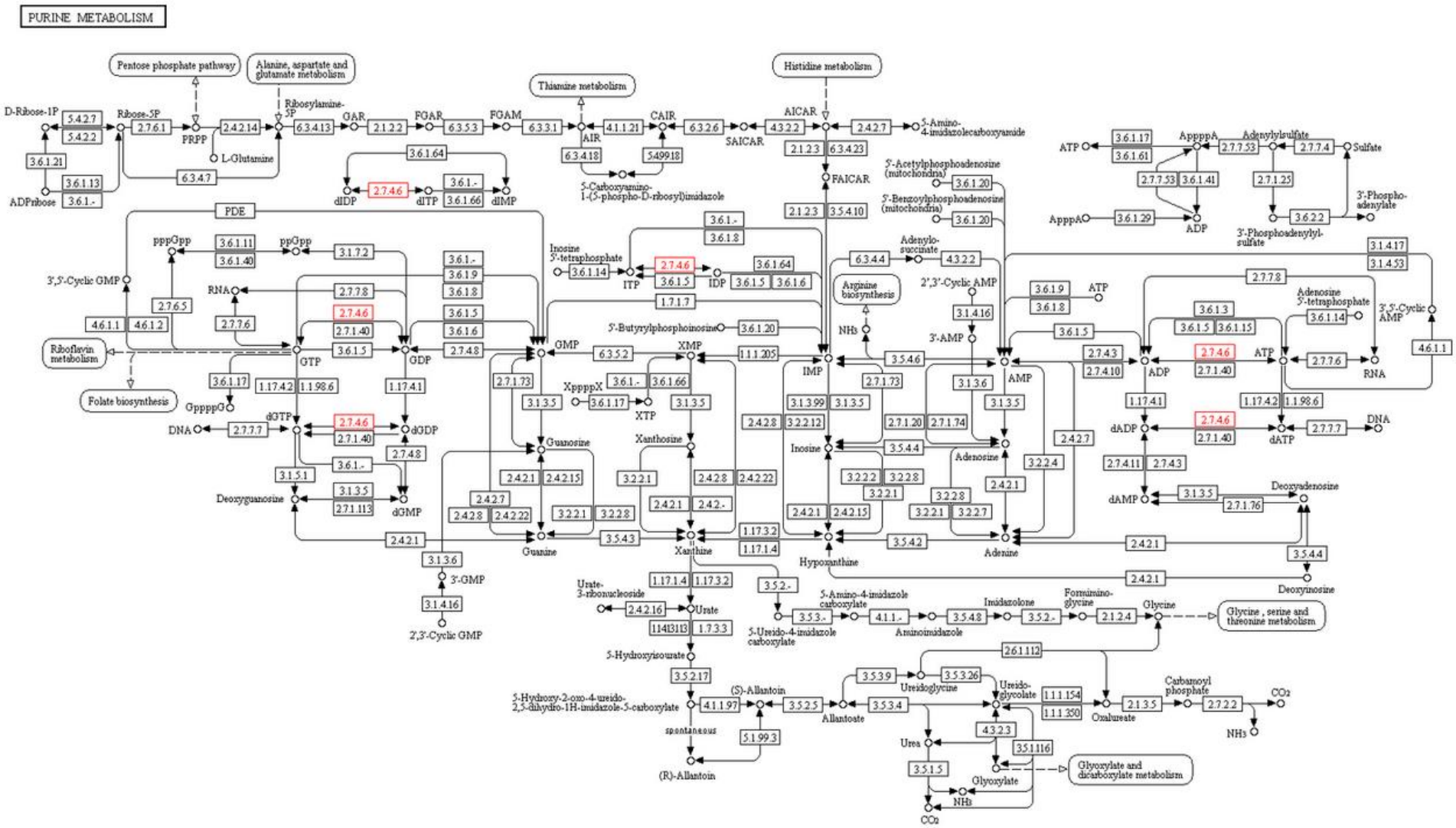

Fig. 3.28 KEGG analysis of significantly upregulated proteins in purine metabolism. Nucleoside diphosphate kinase (2.7.4.6) (red).

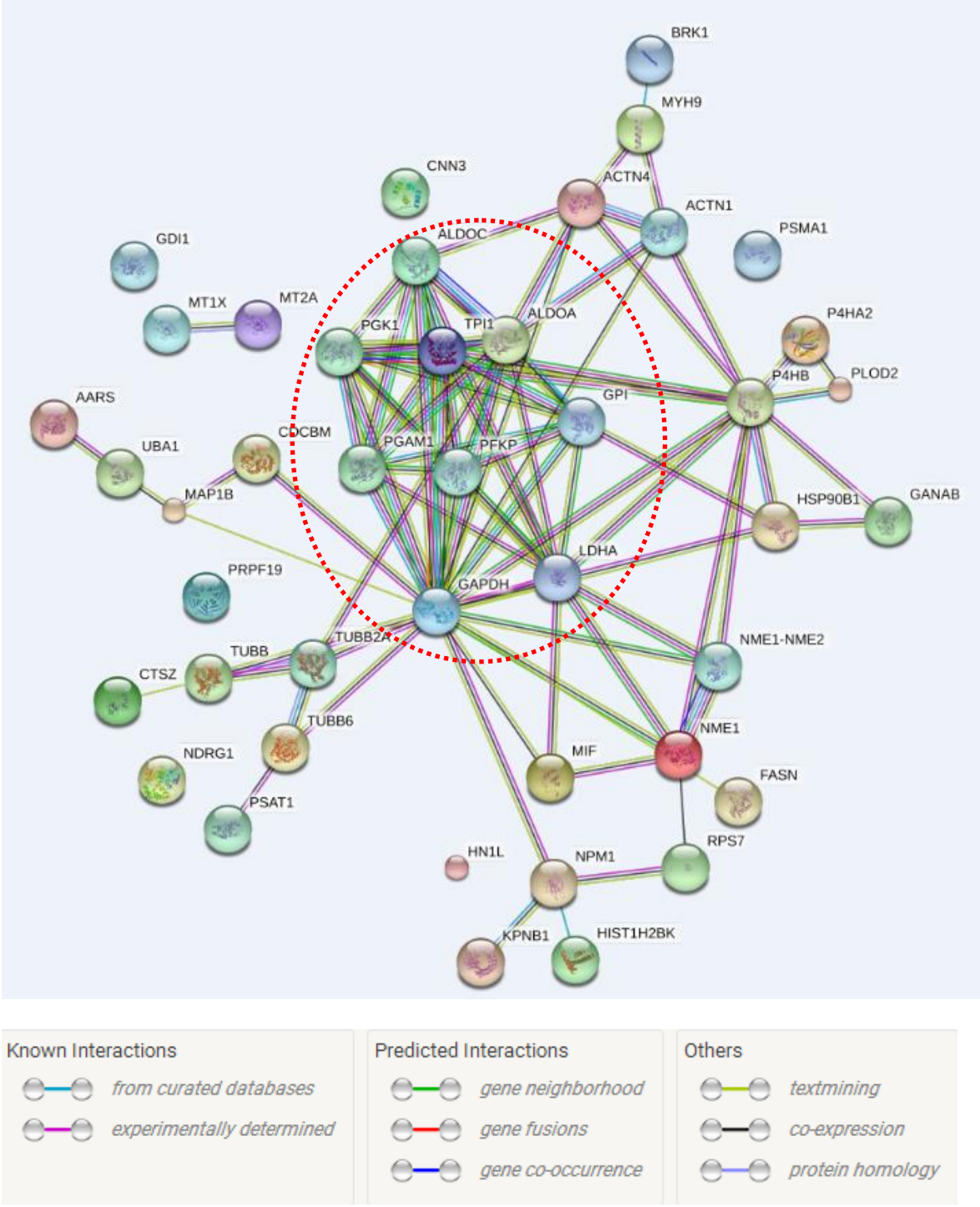

Fig. 3.29 STRING based protein interaction analysis of statistically significant protein with fold changes ≥ 1.5 in the SKOV-3 cell after 48 h exposure to Cu-Phen (**1**) and Cu-DPQ-Phen (**2**) compared to the negative control. The dashed red oval highlights proteins that may have regulatory role.

Commonly upregulated proteins from four experimental conditions

Multiple proteins observed at ≥ 1.5 fold change were commonly upregulated throughout the experimental conditions. **Table 3.10** and **Figure 3.30** detail the commonly expressed proteins in each of the experimental conditions.

Table 3.10. Common upregulated proteins (SSDA) with fold change ≥ 1.5 between both cell lines and Cu-Phen (**1**) and Cu-DPQ-Phen (**2**) exposures.

MCF-7 24 h + SKOV-3 24 h	MCF-7 48 h + SKOV-3 48 h	MCF-7 24 h + MCF-7 48 h	SKOV-3 24 h + SKOV-3 48 h
P02795 (Metallothionein-2) P80297 (Metallothionein-1X)	P02795 (Metallothionein-2) P00558 (Phosphoglycerate kinase 1)	P02795 (Metallothionein-2)	P02795 (Metallothionein-2) P80297 (Metallothionein-1X) P00558 (Phosphoglycerate kinase 1) P0DMV9 (Heat shock 70 kDa protein 1B)
Commonly upregulated in all: P02795 (Metallothionein-2)			

Proteins detailed in table above are reflected in the Venn diagram (**Fig. 3.30**) along with number of commonly expressed proteins among the experimental conditions.

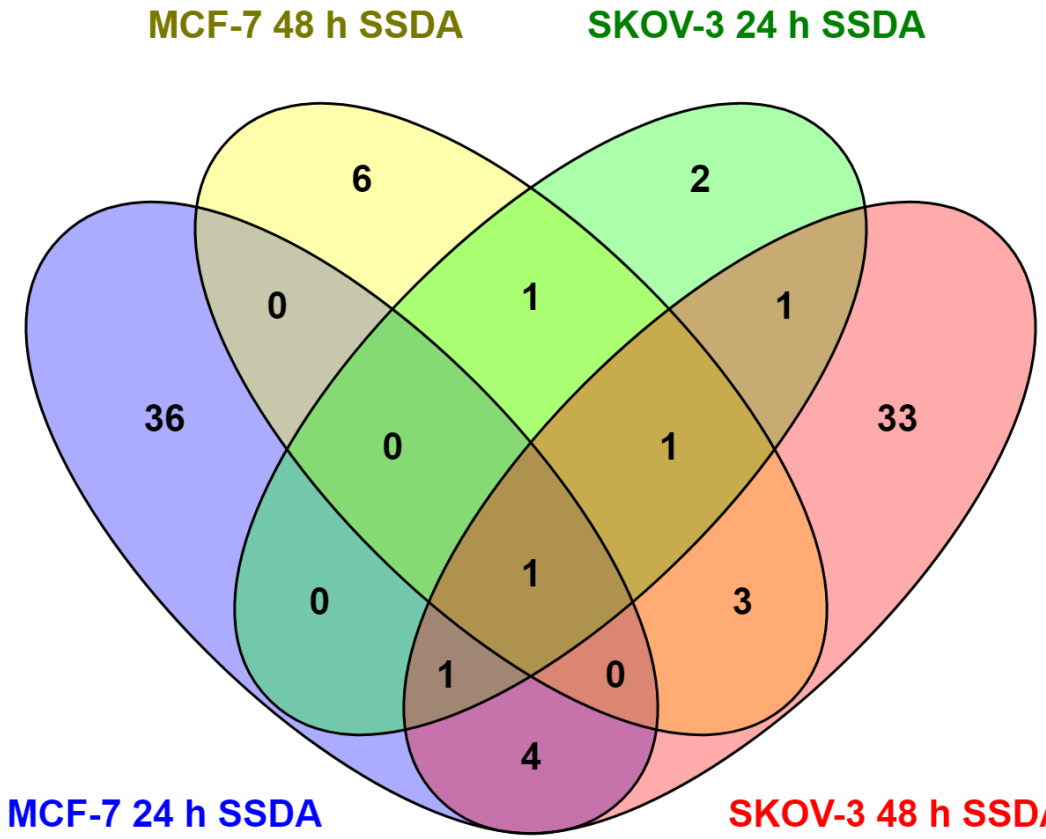

Fig. 3.30 Venn diagram illustrating the number of protein commonly upregulated in each of the cell lines and timepoints with all proteins abundances in each experimental condition ≥ 1.5 fold change. Proteins related to the 4 major comparisons are displayed in **Table 3.10**.

3.4 Discussion

The work outlined in this Chapter describes the whole-cell proteomic response of the MCF-7 and SKOV-3 cell lines at both 24- and 48- h to Cu-Phen (**1**) and Cu-DPQ-Phen (**2**) in comparison to the negative control. Both cisplatin sensitive MCF-7 and cisplatin resistant SKOV-3 cell lines were used in this study as in Chapter 2.

Overall, across the experimental conditions upregulation of metabolic, heat shock, cytoskeletal, ribosomal and metal chelation (metallothioneins) proteins were a common characteristic feature of the mechanistic response of the cells to the Cu(II) phenanthroline-phenazine complex series. With the MCF-7 24 h exposure, differences were observed between the abundance levels of proteins between both exposures to Cu-Phen (**1**) and Cu-DPQ-Phen (**2**). Cu-Phen (**1**) tended to illicit higher abundance changes in the metabolic and ribosomal proteins while Cu-DPQ-Phen (**2**) induced higher abundance changes in heat shock and related proteins. This trend continued at the 48 h exposure although there were less proteins detected. An increased abundance in cytoskeletal proteins was also detected in the Cu-Phen (**1**) exposure in contrast to lower abundance detected after exposre to Cu-DPQ-Phen (**2**).

Cisplatin resistant SKOV-3 cells at 24 h exposure were similar to the MCF-7 cells at 24 h in regards to the higher upregulation of heat-shock, ribosomal and metabolic proteins after exposure to Cu-Phen (**1**). This same functional protein expression portfolio was also present in the SKOV-3 48 h exposure, however, a large increase in the amount of cytoskeletal and RNA binding proteins were identified in the 48 h exposure with the highest abundance changes occurring after exposure to Cu-DPQ-Phen (**2**).

STRING analysis provided a means to assess the clustering and potential functional interactions in each of the experiments. In the two larger networks (MCF-7 24 h and SKOV-3 48 h) both metabolic and heat shock-related proteins were shown to be a strong focal point for potential mechanistic interactions. The two smaller networks (MCF-7 48 h and SKOV-3 24 h) did not form around a common functional protein class but contained elements of ribosomal, cytoskeletal and heat shock protein as potential mechanistic interactions. Overall, the experimental conditions, metallothionein-2 was observed to be upregulated in all cases. Metallothioneins are typically stimulated through metal ions, cytokines and growth factors and normally function in the control of oxidative stress and promote factors to reduce cellular stress. Metallothioneins have also been associated with drug resistance, tumour survival and cell proliferation through NF-κB and p53 regulatory proteins (Notta and Koropatnick 2006; Ruttkay-Nedecky *et al.* 2013). Metallothioneins have previously been associated with mediating cisplatin resistance (Andrews *et al.* 1987), but more recent studies have established reactivity's between the protein and platinum and ruthenium complexes (Casini *et al.* 2009; Karotki and Vašák 2009). With a growing body of knowledge regarding its interaction with therapeutics directly and cellular regulatory functions, there is a strong possibility that the protein interacts with the novel Cu(II) complexes and assists in the cellular mechanistic response. The metal chelators remained the most prominent of all upregulated proteins in terms of fold changes in relation to the negative control, demonstrating the importance of copper sequestration and potential other regulatory functions. It is however not clear as to what degree the level of copper sequestration has on the mechanism of action in the cell and the subsequent toxicity. Interestingly, across all the experimental conditions there were no appreciable increases in specific drug detoxification proteins, typical of many xenobiotic exposures. Overall, both cell lines

share common increases in heat shock and ribosomal proteins, however, metabolic related proteins tended to dominate the response of the cisplatin resistant cell line, indicating that they may be playing a stronger role in cellular resistance mechanisms.

Chapter 4: In-vitro mammalian cell mechanisms of action: mitochondrial effects and gene expression

4.1 Introduction

The work described in the 2 preceding Chapters have detailed the results of screening assays and proteomics evaluations of the Cu(II) phenanthroline-phenanzine complexes. The work in Chapter 2 and Chapter 3 detailed the process of apoptosis and the proteomics expression response respectively of both the MCF-7 and SKOV-3 cells after exposure to the Cu(II) phenanthroline-phenazine complexes. Both these preceding chapters identified apoptosis and metabolic enzymes as potentially playing a part in the mechanism of action of the Cu(II) phenanthroline-phenazine complexes. Therefore the work detailed this Chapter 4 explores the role of the mitochondria as a target for the action of Cu(II) phenanthroline-phenazine complexes.

The MCF-7 and SKOV-3 cell lines were used as well as A2780 and its cisplatin and doxorubicin resistant variant, A2780/ Cis representing a sensitive and resistant cisplatin profile respectively in each cell lines set. The A2780 (ovarian adenocarcinoma) and cisplatin and doxorubicin variant, A2780/ Cis have been widely used to examine the cisplatin mechanisms of resistance and evaluation of other metal-based drugs (Gamberi *et al.* 2014; Bashford and Cooper 2016). An additional advantage to their inclusion in this research is that both the sensitive and resistant variants are derived from the same cell and as such will have a similar gene and protein expression profile, unlike the MCF-7 and SKOV-3 cell lines previously used.

Mitochondria-related gene expression and associated signalling involves multiple processes, all of which may contribute to the mechanism of action of the Cu(II) phenanthroline phenazine complexes. Heme Oxygenase (HMOX-1) is a member of the phase II antioxidant enzymes and is primarily involved in the removal of iron based

porphyrin, heme from the non-protein moiety of haemoglobin (Tebay *et al.* 2015). Nuclear factor (erythroid-derived 2)-like 2 (Nrf-2) is closely involved with the induction of HMOX-1 through the Antioxidant Response Element (ARE) transcription region. In addition to the involvement of HMOX-1, another suite of antioxidant enzymes such as NAD(P)H quinine oxidoreductase 1 (NQO1), glutamate-cystein ligase (GCL) and glutathione S-transferases (GST) (Kansanen *et al.* 2012, 2013) play a role in antioxidant response by activation of their ARE transcription region. Nrf-2 also forms part of the transcriptional regulation of Transcription factor B1/2, mitochondrial (TFB1M) and (TFB2M) which in turn regulates the transcription of the general mitochondrial transcription factor, Transcription Factor A (TFAM) (Gleyzer *et al.* 2005; Litonin *et al.* 2010; Shi *et al.* 2012).

The genes ATP-dependent Clp protease proteolytic subunit (CLPP), Lon protease homolog 1 (LON1), paraplegin matrix AAA peptidase subunit (SPG7) and ATP-dependent metalloprotease YME1L1 (YME1L1) are involved in the regulation of mitochondrial quality control. Both LON and CLPP are present in the mitochondrial matrix and are involved in the proteolysis of oxidised proteins from ROS damage and misfolded protein due to damage respectively. Both CLPP and LON are potential targets for degenerative conditions (Cole *et al.* 2015; Quirós *et al.* 2015; Bota and Davies 2016). In addition to LON and CLPP, SPG7 and the AAA metalloprotease, YME1L1 are embedded in the inner mitochondrial forming components of the permeability transition pore complex with functions in both protein quality control and the maintenance of the respiratory chain complexes (Shanmughapriya *et al.* 2015; Hartmann *et al.* 2016).

Dynamin-Related Protein (DRP1), Mitofusin-1/-2 (MFN1), (MFN2) and Dynamin-like 120 kDa protein (OPA1) are involved in the control of mitochondrial fission and fusion. The process of mitochondrial fission is largely controlled by DRP1, which is translocated to the outer membrane of the mitochondria to bring about fission (Reddy 2014). The process of mitochondrial fusion involves OPA1 in concert with MFN1 and MFN2 which regulate mitochondrial fusion from the inner mitochondrial membrane and is essential for the cristae remodelling which also has a regulatory function in oxidative phosphorylation (Patten *et al.* 2014; Reddy 2014).

In addition to examining the relative changes in gene expression related to apoptosis and mitochondrial function, measurement of the changes in the mitochondrial membrane potential ($\Delta\Psi$) should help complement the mechanistic assessment of the Cu(II) complexes. Rhodamine 123 is a cell-permeable, monovalent cationic, fluorescent dye which accumulates in energized mitochondria, a feature which allows the detection of depolarization of the mitochondrial membrane potential ($\Delta\Psi$) (Chalovich and Eisenberg 2005). The dye, 5,5′,6,6′-tetrachloro-1,1′,3,3′-tetraethylbenzimidazolcarbocyanine iodide (JC-1) also performs the same function (Cossarizza *et al.* 1993). The loss of the mitochondrial membrane potential ($\Delta\Psi$) is a key indicator of the loss of mitochondrial function and toxicity. Coupled to the role the mitochondrial plays in intrinsic apoptosis the measurement of mitochondrial membrane potential is an important way to assess the activity of novel metal-based drugs, such as in cisplatin (Choi *et al.* 2015) and copper complexes (Slator *et al.* 2016).

The genes above control the regulation of protein quality, misfolding and regulation of mitofission/ mitofusion have been associated with neurodegenerative, metabolic

syndromes and cancer (Quirós *et al.* 2015). In addition, the regulation of mitochondria function has a direct effect on the activation of apoptosis and as such, cell survival. The connection between apoptosis, mitochondrial related gene expression and mitochondrial membrane potential ($\Delta\Psi$) provide a strong framework for the evaluation of the mechanism of action of the novel Cu(II) phenanthroline-phenazine complexes.

4.2 Material and methods

4.2.1 Detection of mitochondrial membrane potential decay (ΔΨ)

4.2.1.1 Cell preparation

The A2780, A2780/ Cis, MCF-7 and SKOV-3 cell lines were used to assess whether changes in mitochondrial membrane potential due to their can explain their drug sensitivity profile. The loss of the mitochondrial membrane potential is a strong indicator of loss of mitochondrial function and mitochondrial toxicity. Cells were prepared as described previously in section 2.2.1.

4.2.1.2 Subculturing and compound exposure

Cells were subcultured and seeded into clear 96-well plates as described in section 2.2.2.1. The 88 wells in each plate were inoculated with 1×10^4 cells as shown in the template in Appendix 1.7.1. Cells were incubated at 37 °C in 5 % CO_2 atmosphere for 24 h to allow for attachment and growth. A2780 cells were exposed to the following IC_{50} concentrations of the clinical controls and Cu(II) phenanthroline-phenazine complexes: cisplatin (200 µM) (Sigma, Ireland) (*cis*-Diamineplatinum(II) dichloride, CAS: 15663-27-1) (Cat# P4394), doxorubicin (2.20 µM) (Doxorubicin hydrochloride, CAS: 25316-40-9) (Cat# D2975000), Cu-Phen (**1**) (0.56 µM), Cu-DPQ-Phen (**2**) (0.62 µM), Cu-DPPZ-Phen (**3**) (0.43 µM) and Cu-DPPN-Phen (**4**) (0.09 µM) (**Table 2.4**). A2780/ Cis cells were exposed to the following IC_{50} concentrations of the clinical controls and Cu(II) phenanthroline-phenazine complexes: cisplatin (200 µM), doxorubicin (2.35 µM), Cu-Phen (**1**) (1.07 µM), Cu-DPQ-Phen (**2**) (1.14 µM), Cu-DPPZ-Phen (**3**) (0.97 µM) and Cu-DPPN-Phen (**4**) (1.13 µM) (**Table 2.4**). MCF-7 cells were exposed to the following IC_{50} concentrations of the clinical control and Cu(II) phenanthroline-phenazine complexes: cisplatin (0.53 µM), Cu-Phen (**1**) (1.78 µM), Cu-

DPQ-Phen (**2**) (2.03 µM), Cu-DPPZ-Phen (**3**) (1.01 µM) and Cu-DPPN-Phen (**4**) (2.60 µM) (**Table 2.4**). SKOV-3 cells were exposed to the following IC_{50} concentrations of the clinical control and Cu(II) phenanthroline-phenazine complexes: cisplatin (53.44 µM), Cu-Phen (**1**) (3.05 µM), Cu-DPQ-Phen (**2**) (2.92 µM), Cu-DPPZ-Phen (**3**) (0.76 µM) and Cu-DPPN-Phen (**4**) (7.45 µM) (**Table 2.4**). The clinical controls and Cu(II) phenanthroline-phenazine complexes were made up at the concentrations described above in 12 % supplemented (Cat# F2442) (Sigma, Ireland) RPMI-1640 (Sigma, Ireland) (Cat# R8758) cell culture media and were double diluted using cell culture media as per the 96-well plate template in Appendix 1.7.1. Doubling dilutions of each of the compounds was used to examine the response of different concentrations of the compounds within the biologically relevant IC_{50} concentrations. Hydrogen peroxide (Hydrogen peroxide solution, 30 % w/w), (Sigma, Ireland) (Cat# H1009) was used as a positive control at 10 µM (value experimentally determined).

4.2.1.3 Rhodamine 123 dye application and fluorescent measurement

Rhodamine 123 (1 mg/ml) (Sigma, Ireland) (Cat# R8004) was dissolved in ethanol and made up to a concentration of 10 µg/ml in PBS. Upon completion of the 24 h exposure to either cisplatin, doxorubicin, Cu-Phen (**1**), Cu-DPQ-Phen (**2**), Cu-DPPZ-Phen (**3**) and Cu-DPPN-Phen (**4**), the exposed cell culture media was removed and the cells washed 3 times with PBS. After the final wash, 100 µl of the rhodamine 123 working solution was placed on the cells. The 96-well plates were quickly wrapped in tin foil as the dye is photosensitive and they were incubated at 37 ˚C in 5 % CO_2 atmosphere for 30 min. The rhodamine 123 working solution was removed and the cells washed twice with PBS. Cells were covered with 100 µl PBS after the final wash prior to measurement. Fluorescence was measured on the SpectraMax M3 Multi-Mode Microplate Reader

(Molecular Devices, USA) with an excitation of 485 nm and emission wavelength of 530 nm. Fluorescence of the IC_{50} concentration exposed cells was displayed relative to the negative control (cell culture media). The mean and standard deviation from 8 replicate wells (N=8) were used to represent the relative change between the exposed cells and the negative control. Two-way ANOVA with Bonferroni correction was performed between MCF-7/ SKOV-3 and A2780/A2780/Cis to establish statistically significant ($p < 0.05$) changes after exposure to test complexes.

4.2.2 Gene expression analysis of molecular targets

4.2.2.1 Primer design and synthesis of molecular targets

Mitochondrial-related gene transcription factors, mitochondrial proteases and mitochondrial fission/ fusion regulation genes all represent a suite of functions which can characterise the state of the cell after exposure to the Cu(II) phenanthroline-phenazine complexes, cisplatin and doxorubicin. Forward and reverse primer sequences per molecular target were designed in-house using Primer3PLUS programme and were synthesised by Sigma. The primer sequence for each target and reference genes are detailed in **Table 4.1**.

Table 4.1 List of primers and oligonucleotide sequence used to examine mitochondrial-related gene expression in MCF-7, SKOV-3, A2780 and A2780/ Cis mammalian cell lines after exposure to Cu-Phen (1), Cu-DPQ-Phen (2), Cu-DPPZ-Phen (3), Cu-DPPN-Phen (4), doxorubicin and cisplatin for 24 h (A2780 and A2780/ Cis) and 48 h (MCF-7 and SKOV-3).

Primer name	Oligonucleotides (5'-3')
Actin F*	ACTCTTCCAGCCTTCCTTCC
Actin R*	GTTGGCGTACAGGTCTTTGC
Tubulin F*	GCTTCTTGGTTTTCCACAGC
Tubulin R*	CGTTCTTCAGGTTCGACCTC
HMOX1 F	CAGGGCCATGAACTTTGTCC
HMOX1 R	GAGAGGGACACAGTGAGAGG
TFAM F	GGGATCTTGCTATGTTGCCC
TFAM R	TTATGGTCAAGCATGGTGGC
TFB1M F	AGTCGCCTCTCTGTTATGGC
TFB1M R	ATGGCTGCTCTATCTTGGGC
TFB2M F	ACCAAGTAGACCTCCACACC
TFB2M R	GTTTTGTCACTTTCGAGCGC
NRF-2 F	ACCAAAACCACCCTGAAAGC
NRF-2 R	AGGCCAAGTAGTGTGTCTCC
CLPP F	CCTTGTTATCGCACAGCTCC
CLPP R	TCGGGTTGAGGATGTACTGC
LON F	GAAGGAAAGTTCGTCTCGCC
LON R	CTCATGGATCTGGGCAAACG
SPG7 F	ATATCGAGGCCAAGGACAGG
SPG7 R	GGCCAGACGGAAAACATACC
YME1L1 F	CTTTTCCGGAGCAGAGTTGG
YME1L1 R	CACTTCTTCTTTCAGGCCCC
DRP1 F	CCAATTATGCCAGCCAGTCC
DRP1 R	CTCACAATCTCGCTGTTCCC
MFN1 F	GGAAGAGGCCAGTTTTGCC
MFN1 R	GCATTTCCACCAGCTCAAGG
MFN2 F	CTTGTGTGTGTCCATCTCGC
MFN2 R	AGCATCCTTTCTACCACCCC
OPA1 F	CCCGCTTTATGACAGAACCG
OPA1 R	GTCCTCCGCAAAGTCATTCC

* Represent primers of references genes used to establish the relative expression of the target genes.

4.2.2.2 Gene expression of molecular targets

A2780 and A2780/ Cis (10^5 cells) were exposed in T25 flasks after an initial 24 h attachment and growth period to their respective IC_{25} concentrations of cisplatin, doxorubicin, Cu-Phen (**1**), Cu-DPQ-Phen (**2**), Cu-DPPZ-Phen (**3**) and Cu-DPPN-Phen (**4**) for 24 h. The MCF-7 and SKOV-3 (1×10^5 cells) were exposed in T25 flasks after

an initial 24 h attachment and growth period to their respective IC_{25} concentrations of cisplatin, Cu-Phen (**1**), Cu-DPQ-Phen (**2**), Cu-DPPZ-Phen (**3**) and Cu-DPPN-Phen (**4**) for 48 h. Cells were incubated in triplicate for their required timepoint in T25 flasks and subcultured and Tri-reagent extracted as described in section 2.2.6.2.

4.2.2.3 Processing of RNA sample to qRT-PCR analysis

RNA extraction from samples performed as described in section 2.2.6.3. RNA concentration established as described in section 2.2.6.4. RNA concentration standardised as described in section 2.2.6.5. Quantitative real time PCR was performed as described in section 2.2.6.6. Relative expression of target genes was determined as described in section 2.2.6.7.

4.3 Results

4.3.1 Detection of mitochondrial membrane potential decay (ΔΨ)

Rhodamine 123 is a cationic non-toxic cell dye which is actively sequestered from active mitochondria. Loss of mitochondrial membrane potential is a key indicator of the loss of mitochondrial function and toxicity. Cells were normalized against a negative control with mitochondrial membrane potential decay represented a positive potential above the negative control baseline. The A2780, A2780/ Cis, MCF-7 and SKOV-3 cells were exposed to the IC_{50} concentrations of the Cu-Phen (**1**), Cu-DPQ-Phen (**2**), Cu-DPPZ-Phen (**3**), Cu-DPPN-Phen (**4**), cisplatin and doxorubicin (for A2780 and A2780/ Cis) for 24 h. Hydrogen peroxide (H_2O_2) was used as a positive control.

4.3.1.1 Changes in mitochondrial membrane potential (MMP) in the A2780 and A2780/ Cis cells

Exposure to the IC_{50} concentration of Cu-Phen (**1**), Cu-DPQ-Phen (**2**), Cu-DPPZ-Phen (**3**), Cu-DPPN-Phen (**4**), cisplatin and doxorubicin over 24 h induced different intensities of MMP decay relative to the negative control baseline in A2780 cells (**Fig. 4.1**). Both cisplatin and doxorubicin induced similar levels of MMP decay while Cu-Phen (**1**), Cu-DPQ-Phen (**2**), Cu-DPPZ-Phen (**3**) and Cu-DPPN-Phen (**4**) induced higher levels of decay with Cu-Phen (**1**) and Cu-DPQ-Phen (**2**) inducing the highest level of MMP decay. H_2O_2 induced an increase in MMP decay. Exposure to the IC_{50} concentration of Cu-Phen (**1**), Cu-DPQ-Phen (**2**), Cu-DPPZ-Phen (**3**), Cu-DPPN-Phen (**4**), cisplatin and doxorubicin over 24 h induced different intensities of MMP decay relative to the negative control baseline in A2780/ Cis cells (**Fig. 4.1**). Exposure to doxorubicin induced a higher level of MMP decay than cisplatin. Exposure to the IC_{50} concentration of Cu-Phen (**1**), Cu-DPQ-Phen (**2**), Cu-DPPZ-Phen (**3**) and Cu-DPPN-

Phen (**4**) induced MMP decay with the highest levels observed after exposure to Cu-DPQ-Phen (**2**) and Cu-DPPZ-Phen (**3**). H_2O_2 induced an increase in MMP decay.

Between both A2780 and A2780/ Cis cells, differences between levels of MMP decay remain relatively unchanged after exposure to cisplatin. However, significant increases in the level of MMP decay were observed after exposure to Cu-DPQ-Phen (**2**) and Cu-DPPZ-Phen (**3**) in A2780/ Cis cells and in contrast, a significant decrease was observed in levels of MMP decay after exposure to Cu-Phen (**1**). Generally exposure to the clinical controls and Cu(II) phenanthroline-phenanzine complexes resulted in an increase in MMP decay in the cisplatin and doxorubicin resistant, A2780/ Cis cells.

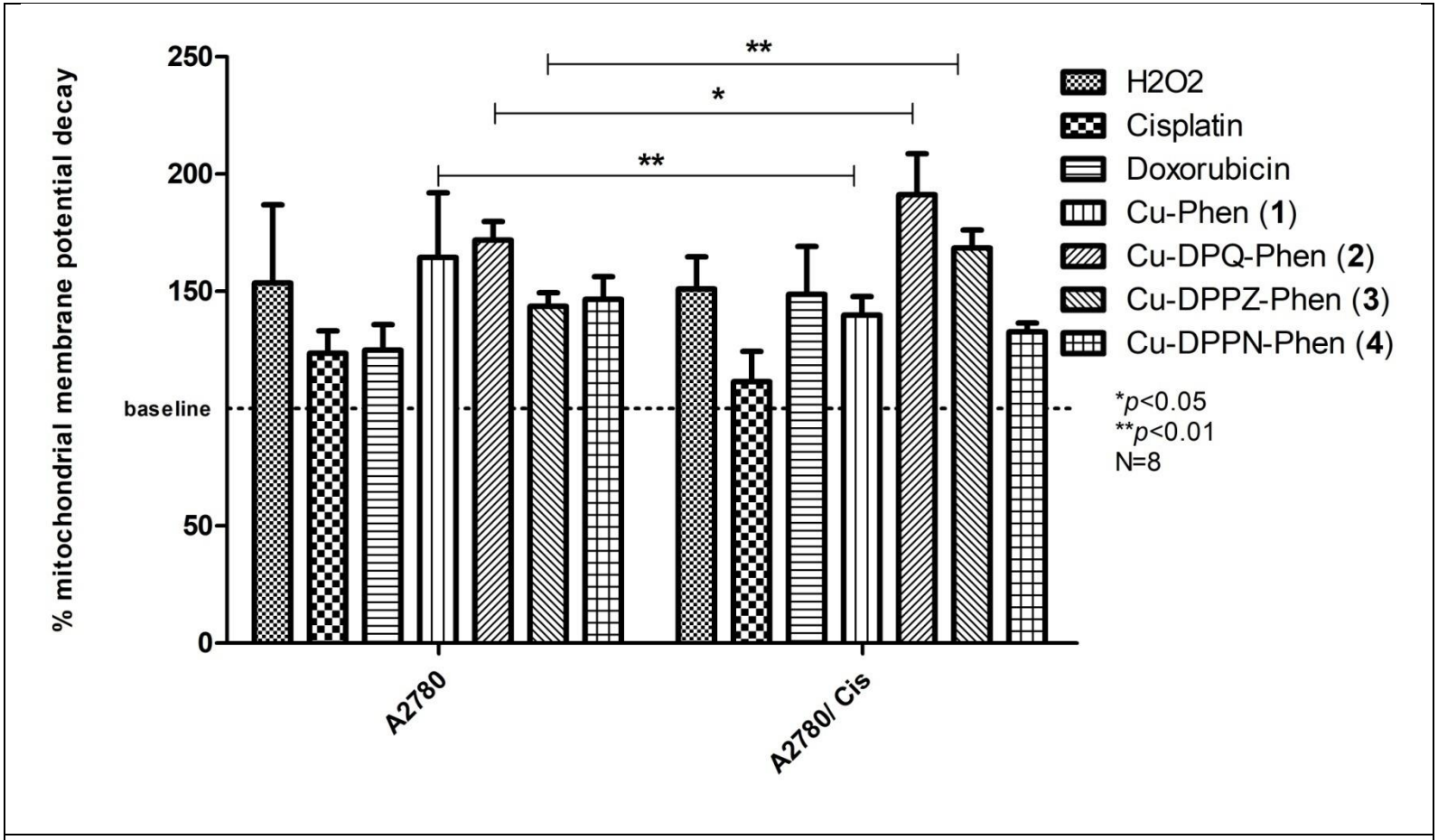

Fig. 4.1 Detection of changes in % MMP (ΔΨ) decay in A2780 and A2780/ Cis cells at 24 h after exposure to IC_{50} concentration of Cu-Phen (**1**), Cu-DPQ-Phen (**2**), Cu-DPPZ-Phen (**3**), Cu-DPPN-Phen (**4**), doxorubicin and cisplatin with H_2O_2 used as a positive control. All treatments have been normalized to the negative control. Baseline represents the negative control and no loss of mitochondrial membrane potential. Statistical significance set at 0.05 with Bonferroni correction performed on two-way ANOVA. N=8.

4.3.1.2 Changes in mitochondrial membrane potential (MMP) ($\Delta\Psi$) in the MCF-7 and SKOV-3 cells

Exposure to the IC_{50} concentration of Cu-Phen (**1**), Cu-DPQ-Phen (**2**), Cu-DPPZ-Phen (**3**), Cu-DPPN-Phen (**4**) and cisplatin over 24 h induced different intensities of MMP decay relative to the negative control baseline in MCF-7 cells (**Fig. 4.2**). Exposure to the IC_{50} concentration of Cu-Phen (**1**), Cu-DPQ-Phen (**2**), and Cu-DPPN-Phen (**4**) induced similar levels of MMP decay while Cu-DPPZ-Phen (**3**) induced a much smaller change relative to the negative control baseline. Cisplatin and H_2O_2, both induced MMP decay at similar levels to Cu-Phen (**1**), Cu-DPQ-Phen (**2**), and Cu-DPPN-Phen (**4**) exposure. Exposure to the IC_{50} concentration of Cu-Phen (**1**), Cu-DPQ-Phen (**2**), Cu-DPPZ-Phen (**3**), Cu-DPPN-Phen (**4**) and cisplatin over 24 h induced different intensities of MMP decay relative to the negative control baseline in SKOV-3 cells (**Fig. 4.2**). Exposure to the IC_{50} concentration Cu-Phen (**1**), Cu-DPQ-Phen (**2**), Cu-DPPZ-Phen (**3**) and Cu-DPPN-Phen (**4**) induced MMP decay with the lowest recorded after exposure to Cu-Phen (**1**) relative to the negative control baseline. Both cisplatin and H_2O_2 induced MMP decay strongly above the negative control baseline.

Exposure to Cu-DPPZ-Phen (**3**) in the cisplatin resistant SKOV-3 cell line induced a significant increase in MMP decay compared to the MCF-7 cells. Exposure to Cu-DPQ-Phen (**2**) resulted in non-significant increase in MMP decay while a significant increases in MMP decay occured after exposure to Cu-DPPZ-Phen (**3**) in A2780/ Cis compared to A2780 cells. Across all tested cell lines exposure to Cu-Phen (**1**), Cu-DPQ-Phen (**2**), Cu-DPPZ-Phen (**3**) and Cu-DPPN-Phen (**4**) induced increases in MMP decay. With the exception of Cu-Phen (**1**) the level of MMP decay was increased or marginally changed in the cisplatin resistant SKOV-3 cells after exposure to cisplatin and the

Cu(II) phenanthroline-phenazine complexes in comparison to the cisplatin sensitive, MCF-7 cells.

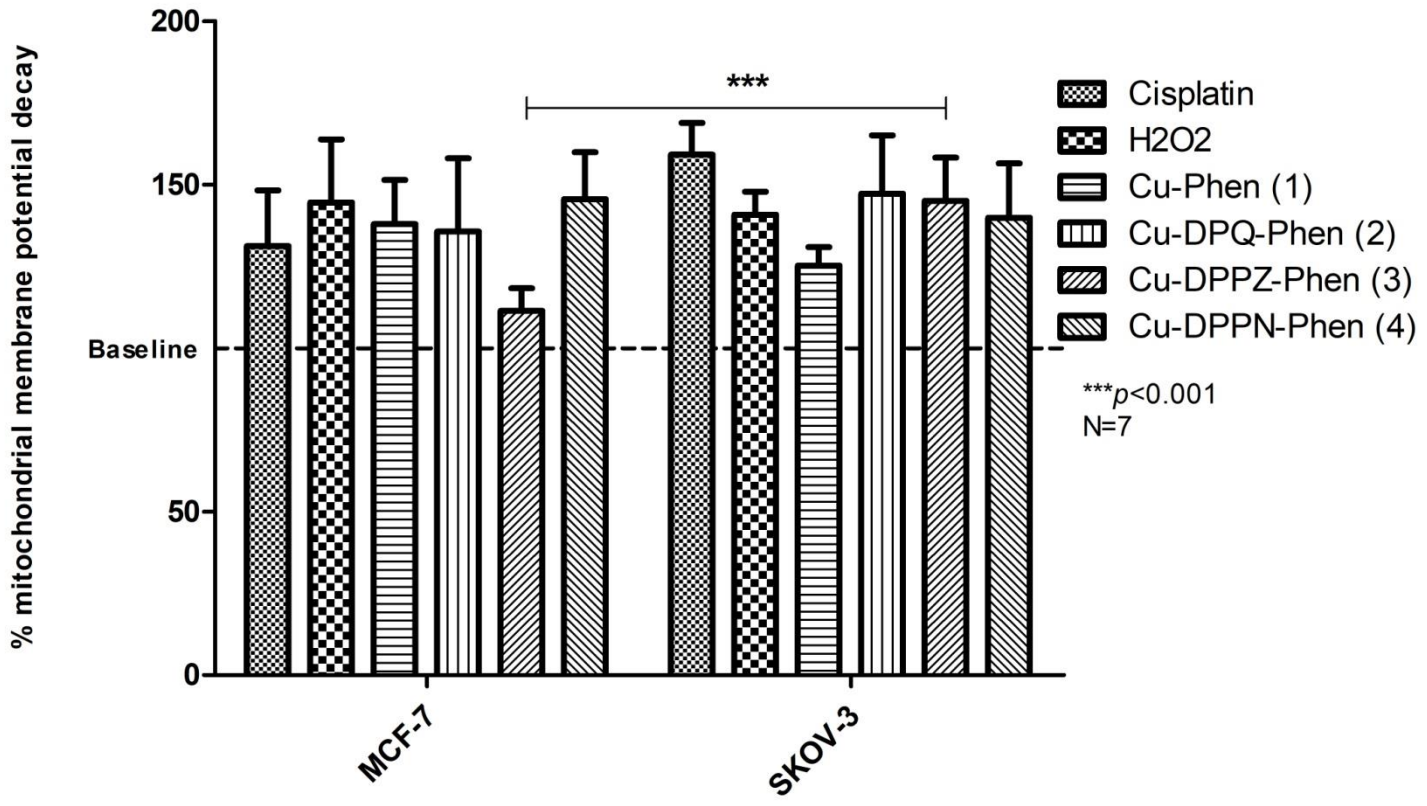

Fig. 4.2 Detection of changes in % MMP (ΔΨ) decay in MCF-7 cell at 24 h after exposure to IC_{50} concentration of Cu-Phen (**1**), Cu-DPQ-Phen (**2**), Cu-DPPZ-Phen (**3**), Cu-DPPN-Phen (**4**) and cisplatin with H_2O_2 used as a positive control. All treatments have been normalized to the negative control. Baseline represents the negative control and no loss of mitochondrial membrane potential. Statistical significance set at 0.05 with Bonferroni correction performed on two-way ANOVA. N=7.

4.3.2 Gene expression analysis

The level of activity of each gene target was assessed by the relative expression of the specific mRNA representative of the cDNA of the target gene being assayed. The expression of the target gene was made in relation to geometric mean expression level of the two housekeeping genes, actin and tubulin. The standard deviation of both the reference gene mean and target gene mean were error propagated and subsequently Log(2) transformed to produce a 95 % confidence interval range around the log(2) transformed mean double delta Ct value. Grouped columns in **Fig. 4.3-4.6** display the log(2) transformed mean expression value relative to the biological negative control with the broken line at y = 1 indicating negative expression below and positive expression above.

Figure 4.3 shows the expression of genes outlined in **Table 4.1** relative to the geometric mean of the references genes, actin and tubulin in the A2780 cell line. Exposure to doxorubicin resulted in a marginal increase in the antioxidant enzyme, HMOX with a larger increase observed in the mitochondrial transcription regulators, TFAM, TFB1M and NRF-2. Mitochondrial protease regulators show no increased activity or were undetected. Regulators of the mitochondrial fission/ fusion process demonstrated progressive increases. Exposure to cisplatin resulted in only a moderate upregulation in the serine protease, CLPP, and a small increase in dynamin fusion, OPA1. Exposure to Cu-Phen (**1**) resulted in an upregulation in the antioxidant, HMOX. Similarly to doxorubicin the mitochondrial related transcription factors, TFAM, TFB2M and NRF-2 are upregulated after exposure. Mitochondrial related protease genes show no increase or were undetectable. Again, similarly to doxorubicin but at a lower magnitude a stepwise increase was observed in the expression of fission/ fusion

regulation genes from DRP1, MFN1, MFN2 to OPA1. Exposure to Cu-DPQ-Phen (**2**) showed no appreciable increase in any of the process with the exception to the serine protease, CLPP, which recorded a small increase. Exposure to Cu-DPPZ-Phen (**3**) resulted in a large increase in the fission/ fusion processes, OPA1 but also an increasing trend, although still negative when compared to the biological negative in DRP1, MFN1 and MFN2. Exposure to Cu-DPPN-Phen (**4**) resulted in no detectable or downregulated gene expression across all the measured processes. The error bars representing a 95 % confidence interval demonstrated a high degree of variability particularly in the target genes representing mitochondrial related transcription.

Figure 4.4 shows the expression of genes outlined in **Table 4.1** after a 24 h exposure, relative to the geometric mean of the references genes, actin and tubulin in the A2780/ Cis cell line. Exposure to doxorubicin induced a small to moderate upregulation in the antioxidant enzyme, HMOX and mitochondrial transcription factor, TFAM. The largest increase was observed in the serine-threonine kinase regulators of mitochondrial oxidative stress response, DRP1 with no other genes showing appreciable upregulation. Exposure to cisplatin induced a slight increase in the mitochondrial transcription related, TFB1M and NRF-2. A large increase was recorded in the serine-threonine kinase regulators of mitochondrial oxidative stress response, DRP1 and a small increase in MFN1, MFN2 and OPA1. Exposure to Cu-Phen (**1**) induced a small increase in the mitochondrial transcription factors, TFB1M and TFB2M. A moderate increase was observed with the protease and structural gene, LON and YME1L1, which respond to oxidatively damaged protein and an AAA metallo-protease respectively. Similarly to doxorubicin and cisplatin a large increase was observed in the gene DRP1 and a small increase in MFN1. Exposure to Cu-DPQ-Phen (**2**) induced a strong increase in the

antioxidant enzyme, HMOX and the mitochondrial transcription factors, TFB1M and TFB2M. A moderate to small increase was recorded with the mitochondrial protease and structural related genes, CLPP, LON and SPG7. Again, similarly to the previous exposures of cisplatin, doxorubicin and Cu-Phen (**1**), a large increase was recorded in the serine threonine kinase; DRP1. Exposure to Cu-DPPZ-Phen (**3**) induced a strong increase in the transcription regulator; NRF-2 demonstrated a strong increase in contrast to previous exposures. Again, DRP1 showed a strong increase, as with previous exposures. The exposure to Cu-DPPN-Phen (**4**) induced a large response across all of the measured processes. A strong increase in the antioxidant enzyme, HMOX and the mitochondrial transcription factors, TFB1M and TFB2M and NRF-2 were demonstrated. A strong increase was recorded with the mitochondrial protease and structural related genes, CLPP, LON, SPG7 and YME1L1. Finally, similarly to the other exposures a strong increase was recorded in the activity of DRP1 and in addition MFN1, MFN2 and OPA1 were strongly upregulated.

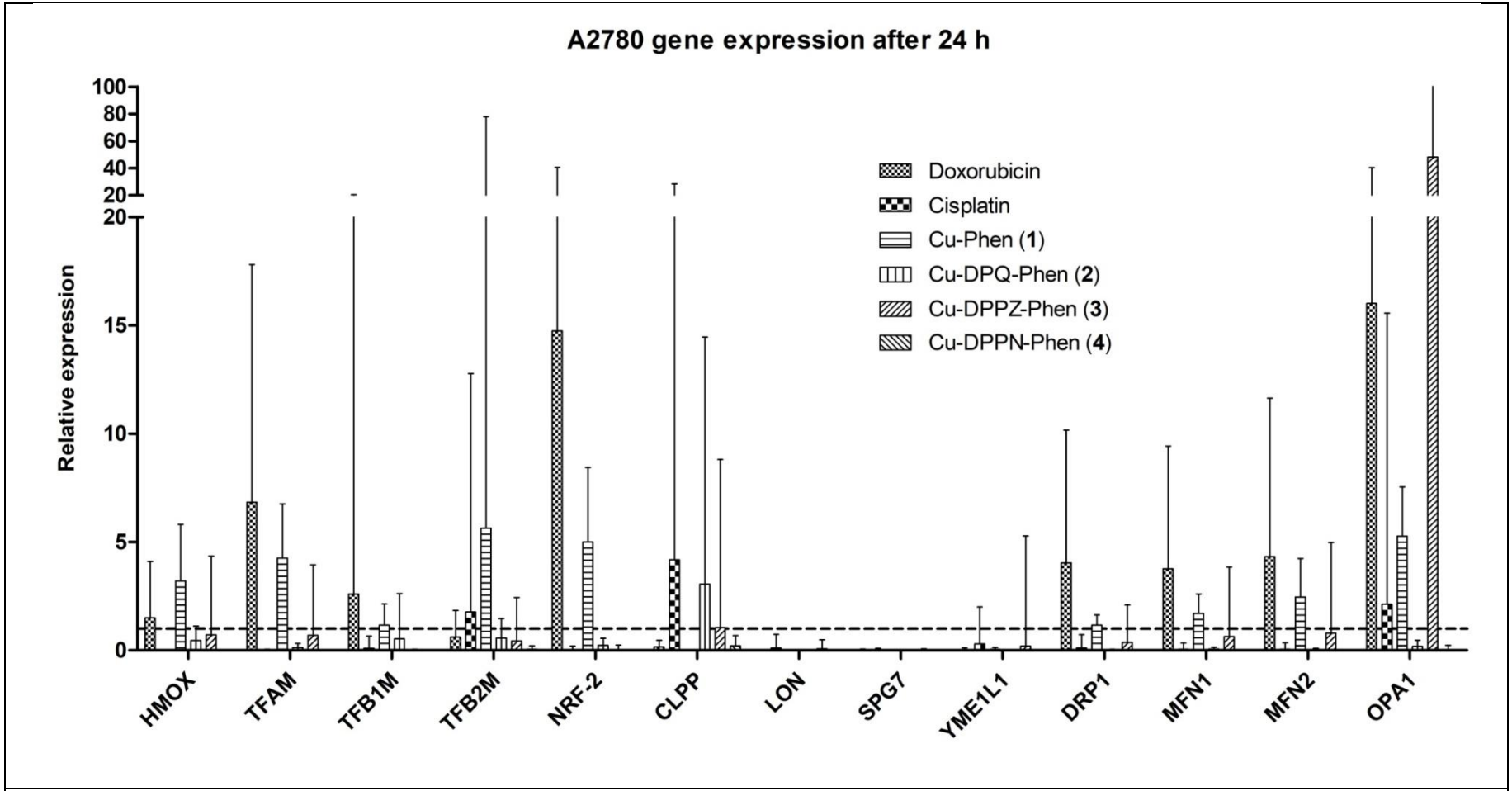

Fig. 4.3 Gene expression of A2780 cells at 24 h following exposure to doxorubicin, cisplatin, Cu-Phen (**1**) and Cu-DPQ-Phen (**2**), Cu-DPPZ-Phen (**3**) and Cu-DPPN-Phen (**4**). Error bars represent 95 % Confidence interval (N=4).

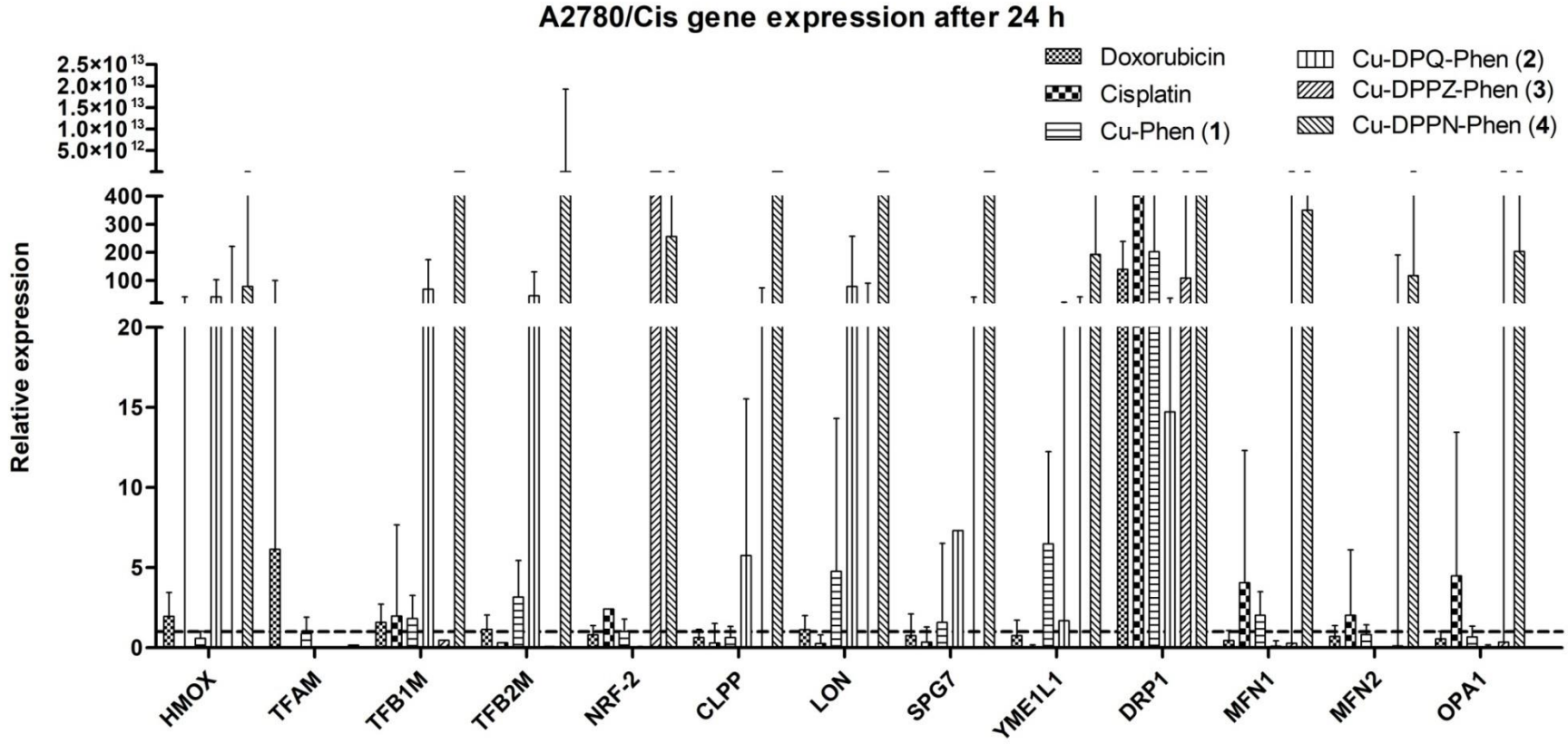

Fig. 4.4 Gene expression of A2780/ Cis cells at 24 h following exposure to doxorubicin, cisplatin, Cu-Phen (**1**) and Cu-DPQ-Phen (**2**), Cu-DPPZ-Phen (**3**) and Cu-DPPN-Phen (**4**). Error bars represent 95 % Confidence interval (N=4).

Figure 4.5 shows the expression of genes outlined in **Table 4.1** relative to the geometric mean of the references genes, actin and tubulin in the MCF-7 cell line. Exposure to cisplatin induced the expression of the mitochondrial transcription regulator, TFAM and the mitochondrial serine protease, CLPP. Exposure to Cu-Phen (**1**) induced expression of the phase I enzyme, HMOX. Expression of all other mitochondrial related processes was either downregulated or not detected. Exposure to Cu-DPQ-Phen (**2**) induces upregulation of the serine protease, CLPP. Expression of all other mitochondrial related processes was either downregulated or not detected.

Figure 4.6 shows the expression of genes outlined in **Table 4.1** relative to the geometric mean of the references genes, actin and tubulin in the SKOV-3 cell line. Exposure to cisplatin resulted in a large increase in mitochondrial related transcription from TFAM and TFB1M. Exposure to cisplatin also showed a large increase in the AAA Metallo-protease; YME1L1 along with increases in the fission/ fusion genes; MFN1, MFN2 and to a lesser extent OPA1. Exposure to Cu-Phen (**1**) did not demonstrate the same increase in mitochondrial related transcription from TFAM but did show similar expression levels in YME1L1 and MFN2 to that of cisplatin. Exposure to Cu-DPQ-Phen (**2**) only induced an appreciable increase in the serine protease, CLPP and no other measured processes.

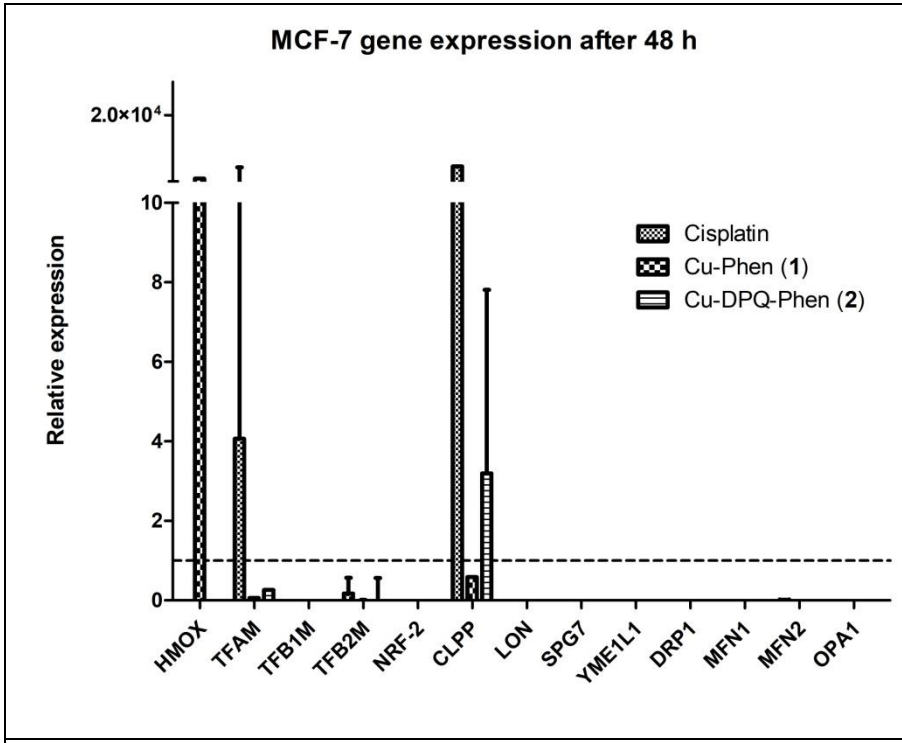

Fig. 4.5 Mitochondrial related gene expression of MCF-7 cells at 48 h following exposure to cisplatin, Cu-Phen (**1**) and Cu-DPQ-Phen (**2**). Error bars represent 95 % Confidence interval (N=3).

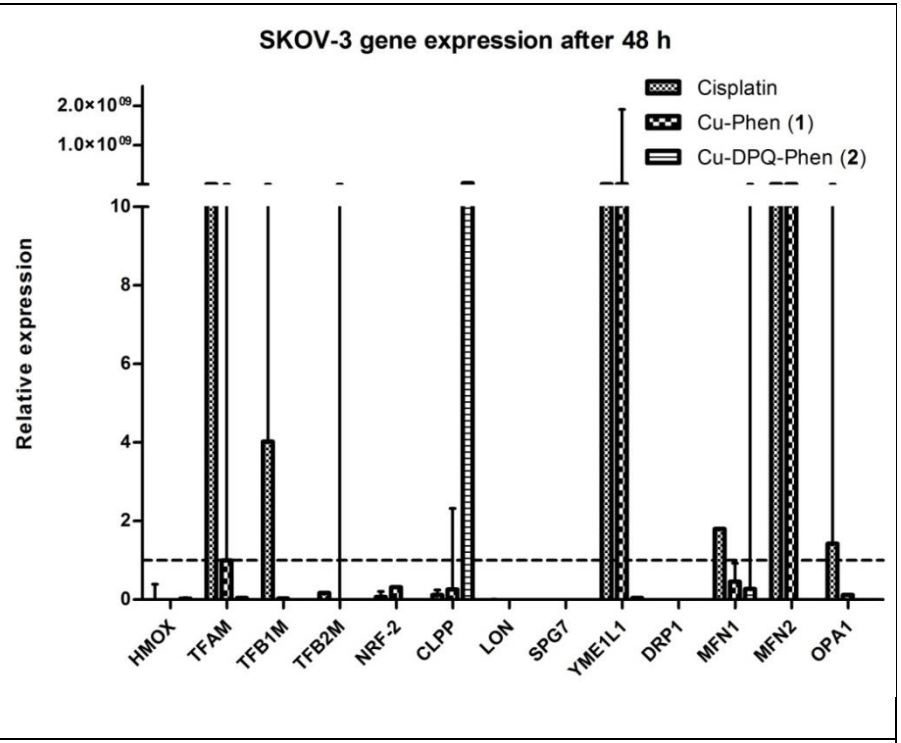

Fig. 4.6 Mitochondrial related gene expression of SKOV-3 cells at 48 h following exposure to cisplatin, Cu-Phen (**1**) and Cu-DPQ-Phen (**2**). Error bars represent 95 % Confidence interval (N=3).

4.4 Discussion

The work described in this Chapter examines the decay of the mitochondrial membrane potential ($\Delta\Psi$) and alterations in gene expression related to mitochondrial transcription, mitochondrial protease function and mitochondrial fission/ fusion. Both mitochondrial membrane potential and mitochondrial related gene expression are closely associated with the apoptotic process described in Chapter 2 and as such facilitate a more complete picture of the mechanism of action of the Cu(II) phenanthroline-phenazine complexes. Chapter 2 identified the cisplatin sensitive cells, MCF-7 and A2780 and the cisplatin resistant cells, SKOV-3 and A2780/ Cis as being strongly susceptible to the activity of Cu(II) phenanthroline-phenazine complexes exceeding the activity of the clinical therapeutics and demonstrating evidence of apoptosis through the apoptosis molecular targets in Chapter 2. The evaluation of mitochondrial membrane potential changes and mitochondrial related gene expression in this Chapter helped to examine the mitochondrial contribution to the mechanism of action.

The mitochondrial membrane potential has previously been used to examine mitochondrial toxicity of [Cu(*o*-phthalate)(phenanthroline)] and di-manganese(II) complexes (Slator *et al*. 2016, 2017). The result of the Mitochondrial Membrane Potential (MMP) decay assay indicated that all of the tested cell lines demonstrated different degree of MMP decay after exposure to cisplatin, doxorubicin (A2780 and A2780/ Cis) (A2780 and A2780/ Cis) and the Cu(II) phenanthroline-phenazine series in the A2780, A2780/ Cis, MCF-7 and SKOV-3 cells. The A2780 and A2780/ Cis demonstrated contrasting activity in terms of MMP decay with a general increase of MMP after exposure to most of the Cu(II) phenanthroline-phenazine complexes in the A2780/ Cis cells. The profile of increase MMP decay after exposure to Cu(II)

phenanthroline-phenazine complexes was demonstrated similarly SKOV-3 cells in comparison to the MCF-7 cells. The increased MMP decay in resistant phenotypes after exposure to the Cu(II) phenanthroline-phenazine complexes in comparison to the relatively unchanged cisplatin values may potentially indicate that the breakdown of the mitochondrial membrane potential has a role in the mechanisms of action of the Cu(II) phenanthroline-phenazine complexes. The intrinsic apoptotic pathway is initiated through a breakdown in mitochondrial function. The results of Chapter 2 demonstrated a profile of apoptosis activation after exposure to the Cu(II) phenanthroline-phenazine complexes. With the breakdown of the mitochondrial membrane potential demonstrated in this Chapter and the activation of apoptosis demonstrated in Chapter 2, there is a strong association which may contribute to the mechanism of action of the Cu(II) phenanthroline-phenazine complexes.

The mitochondrial related gene expression panel was examined through antioxidant enzyme production, HMOX, while mitochondrial related transcription was monitored through TFAM, TFB1M, TFB2M and NRF-2. Mitochondrial protease genes were monitored through CLPP, LON, SPG7 and YME1L1. The process of fission/ fusion of the mitochondria were monitored through DRP1, MFN1, MFN2 and OPA1.

The A2780 and A2780/ Cis cells demonstrated contrasting gene expression profiles with the antioxidant and mitochondrial related transcription along with the protease, CLPP characterising the gene expression response. The cisplatin and doxorubicin resistant, A2780/ Cis is characterised by the upregulation of mitochondrial transcription, proteases and the mitochondrial fission regulator, DRP1. The activity of transcription factors and fission/ fusion regulators are known to be involved in drug resistance

mechanisms (Chiang *et al.* 2009; Thomas and Jacobson 2012; Kashatus *et al.* 2015; Cai *et al.* 2016). Doxorubicin interacts with DNA through intercalation, similarly to the proposed interaction mechanism of the Cu(II) phenanthroline-phenazine complexes (Molphy *et al.* 2014, 2015). The Cu-DPPZ-Phen (**3**) exposure which is known to have the highest DNA binding constant produced a similar gene expression profile to doxorubicin. Cu-DPPN-Phen (**4**) with a much lower DNA binding capability induces no change in any target genes. Large error bars in the A2780 24 h exposures demonstrated that a high degree of variability particularly in mitochondrial related trandcription. This may have been due to changing rates of transcription of these genes at the time point. In A2780/ Cis cells, exposures to both doxorubicin and cisplatin were shown to strongly upregulate DRP1 in addition to all of the Cu(II) phenanthroline-phenazine complexes. DRP1 is strongly associated with mitochondrial membrane impairment and resulting loss of the oxidative phosphorylation pathway and in the cases of low expression, a drug resistance factor (Bras *et al.* 2007; Thomas and Jacobson 2012). The MCF-7 and SKOV-3 cells present contrasting gene expression profiles with MCF-7 cells demonstrating antioxidant and the mitochondrial protease, CLPP being upregulated after exposure to Cu-Phen (**1**) and Cu-DPQ-Phen (**2**). The response of the cisplatin resistant SKOV-3 cells to Cu-Phen (**1**) and Cu-DPQ-Phen (**2**) is characterised by a protease and mitochondrial related transcription response. The increase in protease activity which is present in the SKOV-3 cells after exposure to the Cu(II) phenanthroline-phenazine complexes, has been associated with HSP proteins and protein unfolding in the mitochondria (Jovaisaite *et al.* 2014).

The work detailed in this Chapter utilised the cisplatin sensitive and resistant cell lines to examine the differences in mitochondrial related effects both at the membrane

potential and the mitochondrial related gene expression. The A2780 and its cisplatin and doxorubicin resistant variant, A2780/ Cis were included in this Chapter due to their identical lineage and similar genomic expression profile, allowing them to be differentiated by only their resistant features. Overall both the sensitive (MCF-7 and A2780) and resistant (SKOV-3 and A2780/ Cis) cells demonstrated some degree of impairment of the mitochondrial membrane potential, with the resistant cells generally demonstrating higher levels of mitochondrial membrane potential decay. Gene expression analysis demonstrated that mitochondrial related transcription factors and proteases may be involved in the mechanism of action of Cu-Phen (**1**) and Cu-DPQ-Phen (**2**) in A2780/ Cis cisplatin resistant cells. The cisplatin resistant SKOV-3 cells were also characterised by an increase in mitochondrial related transcription factors and proteases, both of which are involved in the control of oxidatively and misfolded protein damage in the mitochondria. In addition to the transcription and proteases gene expression profile the resistant A2780/ Cis cells demonstrated strong upregulation of the mitochondrial fission regulator, DRP1 in all exposures. Upregulation of DRP1 has been shown to protect from damage-induced fission events in the mitochondria and may provide a common mechanism of action between both clinical controls and the Cu(II) phenanthroline-phenazine complexes.

Chapter 5: *In-vivo* evaluation of response of *Galleria mellonella* larvae to novel copper(II) phenanthroline-phenazine complexes

The work outlined in the following chapter appears in-part in the article entitled "*In-vivo* evaluation of response of *Galleria mellonella* larvae to novel copper(II) phenanthroline-phenazine complexes" published in *J. Inorg. Biochem.* 2018, 186, pp. 135-146.

5.1 Introduction

Insects represent one of the most phenotypically diverse classes of organism, with habitats occupying every ecological niche across the planet, apart from the sea (Elzinga 2004). Additionally, insects such as *Drosophila melanogaster* have been pivotal in the study of genetics and developmental biology (Jennings 2011). The insect innate immune system is one of the key features of an insect's ability to inhabit such a wide variety of habitats. While vertebrates have developed a strong adaptive immune response over millions of years of evolution, much of their innate immune systems shows structural and functional similarities to the insect immune system (Kavanagh and Reeves 2004; Renwick *et al.* 2007; Kelly and Kavanagh 2011; Browne and Kavanagh 2013). In many cases insect models can provide comparable immunological response to higher mammals and therefore are useful option to assess new therapeutics without the financial implications and have a lower ethical threshold (Kemp and Massey 2007; Cook and McArthur 2013).

Insects also provide a powerful tool for the evaluation of potential novel drug and other immunological based therapeutic candidates. The larvae of the greater wax moth (*Galleria mellonella*) provide a useful opportunity to study the toxicological profile of the copper complex studied in the *in-vitro* mammalian cell lines in Chapter 2. The physical size of the larvae allows for an easy inoculation procedure and the effects of the exposure can be measured visually, cellularly and at a molecular level with alterations in gene and protein expression. The amenable nature of *G. mellonella* to pharmacodynamics studies allows investigation into the larval immune response when exposed to or inoculated with active copper complexes (Kavanagh and Fallon 2010).

G. mellonella larvae were first used to examine the pathogenic properties of wild-type and lipopolysaccharide deficient mutants of *Pseudomonas aeruginosa* (Dunphy *et al.* 1986) and in studies incorporating *Proteus mirabilis, Escherichia coli* and *Bacillus cereus* (Walters and Ratcliffe 1983; Paterson *et al.* 1987; Cotter *et al.* 2000). The similarity of the immune response to that of mammals centres on structural and passive barriers as well as cellular and humoral responses. Haemocytes are responsible for the cellular immune response in *G. melleonlla* larvae and many other invertebrates. Haemocytes perform similar functions to polymorphonuclear cells in mammals and can be functionally sub-catagorised. Sub-categories of haemocytes identified are believed to perform different function such as phagocytosis, encapsulation and nodule formation (Matha and Acek 1984). Research has shown that the production of superoxide in larval haemocytes originates from NADPH oxidase complex which contains two proteins, 67-kDa and 47-kDa, which have significant regional homology to human derived $p67^{phox}$ and $p47^{phox}$ proteins found in neutrophils (Bergin *et al.* 2005; Renwick *et al.* 2007).

The cellular insect immune response is characterised by lectin-mediated phagocytosis and oxidative burst, similarly to the vertebrate system (Bergin *et al.* 2005; Browne *et al.* 2013). The humoral element of the insect immune response centres on the production of antimicrobial peptides (AMPs) which provide a competent defence mechanism for the insect. To this end, two common AMP genes; inducible metalloproteinase inhibitor (IMPI) and transferrin are typically up regulated during in larval immune responses. IMPI was the first metalloproteinase inhibitor characterised in invertebrates and was purified from *G. mellonella*. It functions by inhibiting the action of enzymes secreted by pathogenic microbes (Clermont *et al.* 2004; Vertyporokh and Wojda 2016). Transferrin was identified in *D. melanogaster* after bacterial infection and has also shown increases

in expression. These increases have also been seen in sham inoculations and are believed to be caused by a priming effect (Yoshiga *et al.* 1999). For many pathogens iron is an important growth factor, its sequestration from the mammalian system has been strongly associated with improved survival (Iglesias-Osma *et al.* 1995). With such homology present it is likely that it functions in the invertebrate model in the same way (Kelly and Kavanagh 2011). The immunogenicity of therapeutics is an important characteristic in the evaluation and development process. The *G. mellonella* model provides a basic platform to assess potential immunogenic response in later higher mammal testing. The evaluation of the proteomic response provides another vital avenue into the evaluation of the larval immune response to infection and foreign agents. Presently multiple proteins have been observed in haemolymph, some of which can be described as non-specific responses. Ferritin subunit is a protein commonly observed in protein responses. Its importance in iron homeostasis is mirrored in the mammalian response to infection. Prophenoloxidase is a common protein in insects which is directly involved in melanin synthesis, a key defence strategy in insects. Juvenile hormone binding protein is also another common protein seen after the *G. mellonella* exposure to an environmental stressor (Banville *et al.* 2012). It is important in regulating growth of the insect and can also function as protection from non-specific esterase action (Kramer and Childs 1977; Zalewska *et al.* 2009). Arginine kinase is another protein involved in the transfer of phosphates from ATP. These examples above represent a small list of proteins found to have significant homology to other organisms, and from this, their functionality is determined. The type of functionalities of these proteins is usually associated with antimicrobial or metabolic function. With the publishing of the *G. mellonella* transcriptome by Vogel *et al* (2011), the capability of high throughput proteomics such as Label-Free Quantification (LFQ) has permitted a

larger scale assessment of the proteomics response of the larvae to experimental conditions such as responses to food preservatives (Maguire *et al.* 2017).

With the host/ pathogen evaluation platform well established in the *G. mellonella* model, there remains an important opportunity to explore the capacity of the Lepidoptera model for metal-based drugs as an initial pre-screening *in-vivo* model. To this effect a group of studies have previously used *G. mellonella* to evaluate the *in-vivo* activity of a variety of metal-based drugs (Kavanagh and Fallon 2010; Kellett *et al.* 2011b; McCann *et al.* 2012). Cu(II) *bis*-phen complexes showed tolerance exceeding that of cisplatin in the *G. mellonella* model (Kellett et al. 2011) with phendione modifications to the copper(II) showing well tolerated exposures in both the larval model and Swiss mice (McCann *et al.* 2012). Multiple copper and other metal-based complexes have been developed as part of the Kellett group, Dublin City University and have established good biological potential not just according to the chemical activity of the novel complexes on DNA integrity and radical species of oxygen and nitrogen production but also due to the ability of *G. mellonella* to biologically tolerate them.

To date, the work on *G. mellonella* has stemmed from a host-pathogenicity or infection-treatment model. This has provided invaluable information regarding the response of the larvae to certain infection that pertain to humans and how these infections are altered by certain novel metal-based drugs and microbiologically derived agents. This study will examine the effects of the novel Cu(II) phenanthroline-phenazine complex series on larvae through mortality assays, gene expression and high resolution LFQ proteomics. While in the absence of a antimicrobial derived focus, this study, given the promising activity of Cu(II) phenanthroline-phenazine complexes (Molphy *et al.* 2014,

2015), will provide valuable insight into the *in-vivo* activity of these novel series of Cu(II) complexes and identify therapeutic targets and mode of action information for further development in mammalian models.

5.2 Material and Methods

5.2.1 *Galleria mellonella in-vivo* toxicity assay and cuticle changes

In-vivo cytotoxicity testing of Cu-Phen (**1**), Cu-DPQ-Phen (**2**), Cu-DPPZ-Phen (**3**) and Cu-DPPN-Phen (**4**) and cisplatin were performed on *G. mellonella* larvae in the 6th developmental stage sourced from the Meal Worm Company, (Sheffield, UK). The phenazine ligands: DPQ, DPPZ and DPPN were in addition, separately exposed to the larvae. All larvae were stored in the dark at 15 °C in wood shaving prior to testing. Thirty three larvae (average weight 0.3±0.05 g) with no cuticle decolouration were used for each experiment. Thirty three larvae were allocated for each toxicity experiment. All solutions were prepared fresh before use as detailed in Appendix 1.6.1. Larvae were inoculated (20 µl) by injection (BD Ultra-Fine™ Insulin Syringe) into their haemocoel through the last pro-leg (**Fig. 5.1**) (Cotter *et al.* 2000). Solvent control (8.92 % DMSO) (Sigma, Ireland) (Cat# 276855) was also inoculated in the same manner along with sham-inoculations and undisturbed controls. Larval toxicity after exposure was monitored at 4, 24, 48 and 72 h.

Visual changes were recorded throughout the course of the experiment. The onset of melanisation, characterised by the larvae turning brown/ black was recorded after the inoculations. The onset of melanisation occurred due to the insect immune response driven by the cleavage of prophenoloxidase to active phenoloxidase. The chemical cleavage of prophenoloxidase is driven generalised damage to the organisms where it responds to limit the growth of a potential pathogen within the haemocoel (Kavanagh and Reeves 2004). Dead larvae usually appeard black (**Fig. 5.2**) however this did not always occur. Other characteristic changes were also recorded (**Fig. 5.3**).

Fig. 5.1 Inoculation procedure for *G. mellonella* larvae. Twenty µl was injected into last left pro-leg. Image adapted from Cotter *et al.* (2000).

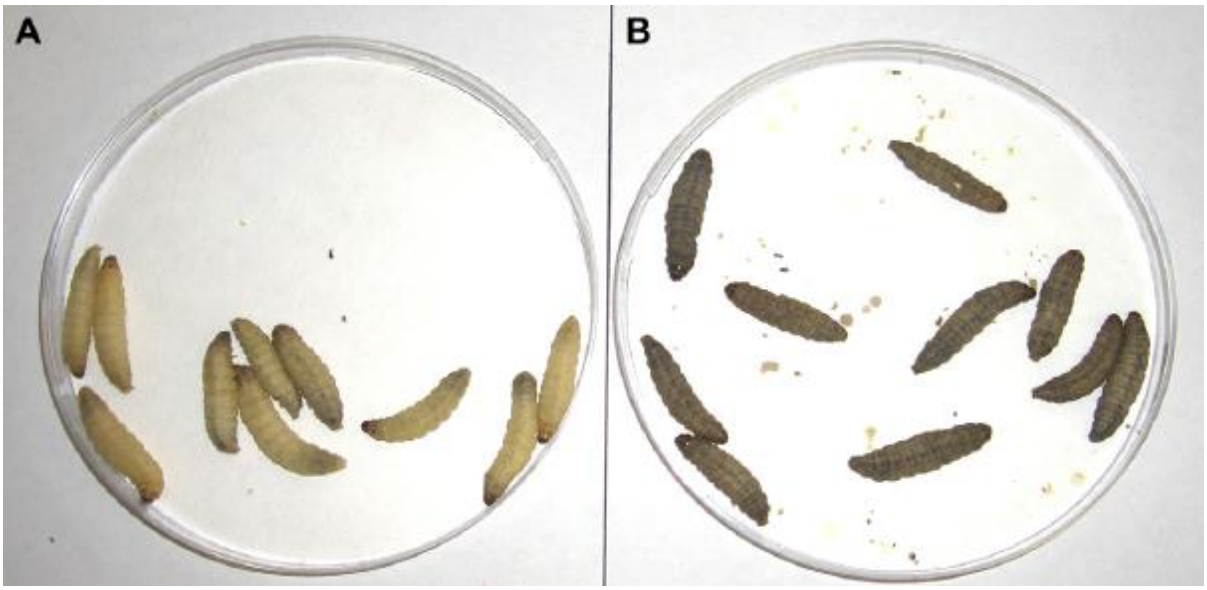

Fig. 5.2 Living (**A**) (normal colour) and dead (**B**) (melanised) *G. mellonella*. Image adapted from Kavanagh & Fallon (Kavanagh and Fallon 2010).

Melanisation (mild)	Melanisation (moderate)	Orange discolouration of cuticle	Paralysis
A	B	C	D

Fig. 5.3 Characteristic changes (**A-D**) in response to test inoculation

5.2.1.1 Measurement of haemocyte count

Haemocyte count was measured 24 h post inoculation with the LD_{50} value of Cu-Phen (**1**) (8.94 µg), Cu-DPQ-Phen (**2**) (11.47 µg) and Cu-DPPZ-Phen (**3**) (25.05 µg) along with a solvent control (8.94 % DMSO in MilliQ water), sham-inoculated and undisturbed control. Five larvae representing each condition were bled through the anterior region of the head (**Fig. 5.4**), with the inoculation and bleeding performed on 4 separate occasions (N=4). The extracted haemolymph was diluted 1:10 with mercaptoethanol (0.37 %) (ACS grade) (Sigma, Ireland) (Cat# M6250). Cell counts were performed using a haemocytometer.

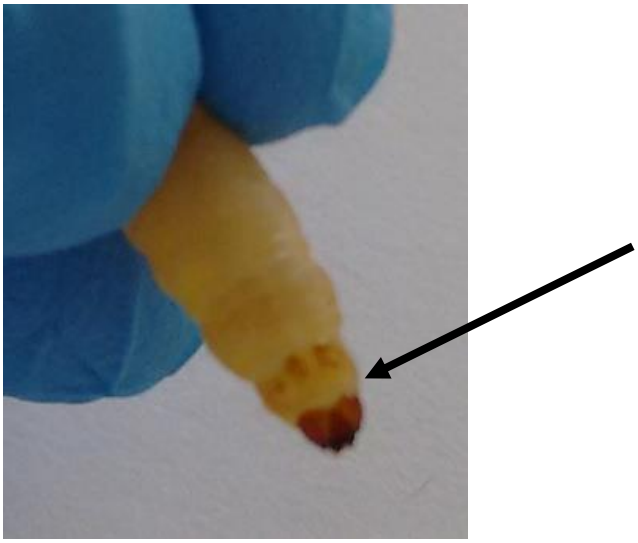

Fig. 5.4 Piercing point (anterior portion) of the *G. mellonella* larvae for haemocyte extraction indicated by the black arrow.

5.2.2 Measurement of immune related gene expression by Quantitative Real Time – PCR (qRT-PCR)

5.2.2.1 Sample preparation

Larvae were inoculated with Cu-Phen (**1**) (8.94 µg), Cu-DPQ-Phen (**2**) (11.47 µg) and Cu-DPPZ-Phen (**3**) (25.05 µg) along with solvent, sham-inoculation and undisturbed controls for 24 h. After 24 h, 3 larvae representing each experimental condition were immersed in liquid nitrogen in a sterile mortar and ground-up with a sterile pestle into a fine powder. The mortar was allowed to warm for a few minutes before 1 ml of tri-reagent (Sigma, Ireland) (Cat# T9424) was added to the powdered remains. The mixture was carefully transferred to an RNase free Eppendorf. The sample was allowed to stand for 2 min before being centrifuged at 2000 g for 2 min. Here, all the insoluble material from the sample was pelleted. The supernatant was transferred to a new Eppendorf and stored at -80 ˚C.

5.2.2.2 RNA extraction to qRT-PCR

RNA extraction was performed as described in section 2.2.6.3. RNA quantification was performed as described in 2.2.6.4. cDNA synthesis of RNA templates was performed as described in section 2.2.6.5. Quantitative real-time PCR was performed as described in section 2.2.6.6. Primer sequences were designed and obtained from the medical mycology lab in Maynooth University. Both forward and reverse primers for each target and reference gene are detailed in **Table 5.2**. Each probe and primer was mixed with molecular grade water to check for autofluorescence. The samples and master mix were placed in 96-well PCR plates. Assay was performed in quadruplicate. PCR plate was sealed and centrifuged at 1200 g for 2 min before being placed in the 7500 Fast Real-

Time PCR System (Applied Biosystems, USA). Thermal cycling parameters are detailed in **Table 5.1** below.

Table 5.1 Thermal cycling parameters

Pre-incubation (1 cycle)	95 °C, 10 min, ramp 4.4°C
Quantification (45 cycles)	95 °C 10 sec ramp 4.4 °C, 60 °C 30 sec ramp 2.2 °C, 72 °C 30 sec ramp 4.4 °C
Melting curve (1 cycle)	95 °C 5 sec ramp 4.4 °C, 65 °C 1 min ramp 2.2°C, 97 °C continuous ramp 0.11 °C acquisition 5 per °C
Cooling (1 cycle)	37 °C 11 sec ramp 2.2 °C

Table 5.2 Forward and reverse primer sequences for genes related to immune activity in *G. mellonella*.

Primer name	Oligonucleotides (5'-3')	Fragment size (base pair (bp))
S7e F* S7e R*	ATGTGCCAATGCCCAGTTG GTGGCTAGGCTTGGGAAGAAT	131
transferrin F transferrin R	CCCGAAGATGAACGATCAC CGAAAGGCCTAGAACGTTTG	535
IMPI F IMPI R	ATTTGTAACGGTGGACACGA CGCAAATTGGTATGCATGG	409

*Represents primers of reference gene, S7e (ribosomal related).

5.2.2.3 Statistical analysis of gene expression data

The expression levels of each target and reference gene was measured using Ct values (Cycle threshold) (Kurnik 2007). For each PCR plate the water negative for each gene was used to confirm that autofluorescence was not contributing to the final reading. The individual Ct values were recorded in Microsoft Excel™ (Microsoft Corporation, USA) along with average and standard deviation for each cDNA sample. The Ct values are related to the amount of amplicon present in the reaction mix. The lower the Ct value the greater the level of amplicon present in the sample. For each sample and target gene the Ct value of the reference gene (S7e) (Browne 2014) was subtracted from the Ct value of the target gene. The delta change of target gene in relation to the S7e Ct value

is then subtracted from the biological negative control for that sample. The second delta value is then normalized using the following logarithmic formula: $2^{-\Delta Ct1(test)-\Delta Ct2(control)}$. The average Ct value for both reference and target gene was calculated along with the standard deviation. Both standard deviations were subjected to error propagation with the final standard deviation being normalized in a manner as stated in the formula above (Nordgård *et al.* 2006). Both positive and negative range reflects a 95 % confidence interval around the mean normalized gene expression value.

5.2.3 2D SDS-PAGE analysis of protein expression

5.2.3.1 Sample collection, Bradford assay and protein precipitation

Larvae were inoculated with the LD_{50} value of Cu-Phen (**1**) (8.94 µg), Cu-DPQ-Phen (**2**) (11.47 µg) and Cu-DPPZ-Phen (**3**) (25.05 µg) along with a solvent control (8.94 % in MilliQ water) for 24 h. Haemolymph (~100 µl) was collected from 5 larvae in a similar manner to the haemocyte density count. Haemolymph was collected into pre-chilled eppendorf and a 1/10 dilution with PBS was performed. The collection of haemolymph (5 larvae each) was performed on 3 separate occasions for each of the experimental conditions. The sample was centrifuged at 1500 g for 5 min in order to pellet the collected haemocytes. The supernatant was transferred to a new Eppendorf and further diluted 1:10. Protein was quantified using the Bradford assay (Bio-Rad Munich, Germany) (Cat# G-250) (Appendix 1.5.2). Protein concentration was diluted to 200 µg per sample. Following the Bradford assay an acetone (Sigma, Ireland) (Cat# V800023) precipitation was performed at a ratio of 1:4 sample to acetone. The acetone was ice-cold before being added to the protein samples. Protein/ acetone solution was then incubated -20 °C for 1 h. Following the 1 h incubation samples were spun for 30 min, 13,000 g at 4 °C. Pelleted samples were then re-suspended in 100 µl of IEF buffer

(appendix 1.7.2) and 2 µl of DTT (Sigma, Ireland) Cat# 43815) and ampholytes (pH 4-7) were added. Samples were mixed and 150 µl of IEF buffer was added on top of the samples along with 1 µl of bromoplenol blue. Samples were let stand for 15 min at room temperature.

5.2.3.2 1D gel set-up

One dimensional IEF gel strips pH 4-7 (Thermo, Ireland) (Cat# ZM0012) were removed from the freezer and gel strip retainers with lids were rinsed with deionised water and dried prior to use. Two hundred and fifty µl of the sample was added to the positive end of the coffin and pH strip was peeled apart carefully. The coffin was gently tilted as the strip was laid down into the coffin allowing the strip to be evenly submerged. A Pasteur pipette was used to cover the pH strip with Plus One dry strip cover fluid (GE Healthcare, Ireland). Isoelectric focusing was performed on the EttanIPGphore II (Amersham Biosciences, USA) using the following programme (**Table 5.3**). Resulting gel strips were stored at -70 °C before 2D gel electrophoresis.

Table 5.3 EttanIPGphore II electrical separation parameters.

Step 1	50 Volts, step and hold for 10 h
Step 2	250 Volts, step and hold for 15 min
Step 3	8000 Volts, gradient for 5 h
Step 4	8000 Volts, step and hold for 8 h

5.2.3.3 2D-PAGE set-up (separating gel)

Equilibrium buffer X2 (Appendix 1.7.3) was thawed and brought to 37°C and place 10 ml in individual test tubes. DTT (Sigma, Ireland) (Cat# D0632) (1 g) was added to each 10 ml of equilibrium buffer and 1D gel strips were immerse in individual test tubes. IAA (Sigma, Ireland) (Cat# I4386) (0.25 g) was added with 1 µl of bromophenol blue (Sigma, Ireland) (Cat# B8026) to each tube and was then sealed with parfilm and

protected from light with tin foil. The tubes were placed horizontally on a plate rocker for 20 min to incubate. Separating gel (Appendix 1.7.4) was made up with the TEMED (Sigma, Ireland) (Cat# T9281) excluded until later polymerization. A 1 ml solution of 200 µl 5X Solubilisation Buffer (Appendix 1.7.5), 800 µl deionised water, 10 µl of marker + 190 µl 5X solubilisation buffer was boiled at 95 °C for 5 min. A 1 % agrose gel in 1X running buffer (appendix 1.7.6) + and 1 µl of bromophenol blue was produced with the solution being heated in a microwave for 1 min. TEMED was added to the separating gel and the gel was set in a pre-cleaned plate of approximately 1.5 mm thickness. The 1D gel strips were taken out of IAA with a tweezers and washed in 10X electrode running buffer (Appendix 1.7.6). The gel strip was orientated facing away from the glass and plastic side against glass. The positive side was placed to the left and a straw was used to push the strip down to the surface of the set gel. A Pasteur pipette was used to cover the top of the strip with blue (tipped with bromophenol blue) agrose gel and was subsequently allowed to set. Each plate was then connected to the electrophoresis rig with Vaseline around the corners to prevent drying. The chambers were filled with 10 X running buffer to the top and the chambers on the outside were filled with 1 X running buffer (Appendix 1.7.6). The electrophoresis rig was run at 30 V overnight. After the electrophoresis run, the gel is carefully removed with a plastic wedge and a mark placed in the gel to aid in later orientation. The gels were placed in Coomassie Brilliant Blue stain (Appendix 1.7.7) for 1 h followed by Coomassie Destain (Appendix 1.7.8) for 1 h.

5.2.3.4 Progenesis SameSpot analysis and protein spot picking

Each gel was scanned using a Hewlett Packard scanjet 5100c scanner (HP, USA) and images were orientated with Microsoft Office™ Powerpoint (Microsoft Corporation,

USA) and analysed using Progenesis SameSpot (Nonlinear Dynamics, USA) software. Progenesis software allows for the analysis of protein expression changes between replicates with significance determined through ANOVA. A table of protein spots was built with an annotated gel image to provide a final check on gel alignment before spot excision. Important spots were identified using the Progenesis SameSpot. The truncated pipette tip was used produce a clean circular cut in the desired gel. The 2D gel was rinsed with water for 2 h and placed on a light box to visualise the proteins spots. The required spot was cut with the tip and placed into a labelled Eppendorf.

5.2.3.5 In-gel digestion of excised protein spots

Ammonium bicarbonate/ acetonitrile (Sigma, Ireland) (Cat# 09830/Cat# 271004) (100 µl) (1:1 v/ v) 10 mM was added to the Eppendorf, sample was incubated and stored at room temperature for 10 min. Acetonitrile (500 µl) was added to gel spots until gel became white and shrunk, following this acetonitrile was removed (samples were then stored at -20 °C). The sample was saturated with Trypsin (0.5 µg/µl) (Promega, USA) (Cat# V5111) making sure the spot was covered and incubated for 2 h in the fridge. Ammonium bicarbonate (10 µl) buffer was added to the spot pieces and left at 37 °C for 24 h. Trypsin digestion similar to (Shevchenko *et al.* 2006) was performed. Following 24 h digestion the sample was centrifuge and 50 µl of the supernatant was removed and place into a labelled tube. To the gel piece, 100 µl of extraction buffer (1:2 v/ v 5 % formic acid/ acetonitrile) (Sigma, Ireland) was added to each tube and incubated at 37 °C for 15 min. The supernatant was removed with a small pipette tip to avoid aspirating pieces of the remaining gel. The supernatant was placed into a separate Eppendorf and dried down in a vacuum centrifuge. The samples were re-dissolved with 20 µl of 0.1 % (v/ v) formic acid then vortexed for 5 min and placed in a sonication bath for 5 min.

Each sample was centrifuged at 10,000 g for 15 min and transferred to a spin filters and repeated. The eluant was placed into acetonitrile washed vials and the lid labelled to ensure that no keratin contamination occurred.

5.2.3.6 LC/MS analysis of protein spots

The fragmented protein samples were eluted by Agilent 6340 Ion trap LC/ MS (Waters, USA). A run table was produced with blanks dividing up each sample and a BSA standard to check the performance of the instrument prior to sample injection. All samples were run for 20 min and the resulting data was analysed using the Mascot search engine (http://www.matrixscience.com).

5.2.3.7 Statistical analysis of LC/ MS protein spots identifications

Three independent gels from 3 individual biological experiments were used to examine each experimental condition. Protein fold changes between 2D gels were determined with the Progenesis SameSpot software. Their significance was determined through ANOVA testing and choice of picking for LC/ MS analysis made accordingly. A MASCOT score above 67 was deemed to be a significant match ($p \leq 0.05$) (MASCOT 2017). MASCOT programme search parameters are detailed in Appendix 1.6.9. A mass error tolerance of 1 Dalton was allowed for a maximum of no more than two missed cleavages. Protein sequences were verified by blasting the protein sequences on the Uniprot (www.uniprot.org) and NCBI (www.ncbi.nlm.nih.gov) websites.

5.2.4 Label Free Quantification of larval haemolymph protein using Q Exactive LC/ MS

5.2.4.1 Protein preparation and processing for Q Exactive analysis

Samples for Q Exactive analysis were processed from the same haemolymph extracts for 2D PAGE analysis detailed in section 5.2.3.1. An additional replicate was included from each experimental condition for Q Exactive analysis bringing the total number of independent replicates to 4. Samples were normalized to 100 µg and stored at -20 °C prior to the in-solution digestion protocol using ProteaseMAX (Promega, USA) (Cat# V2071). The protein samples were digested as described in the in-solution digestion protocol using ProteaseMAX in section 3.2.2. Samples were cleaned-up using the reverse phase C18 spin-column. The protocol is described in section 3.2.3.

5.2.4.2 Q Exactive analysis

Dried samples were re-suspended in 32 µl of Q Exactive buffer (Appendix 1.3.4) on day of analysis. Samples were placed in a sonication bath for 5 min to aid peptide re-suspension. Samples were subsequently centrifuged at 13,000 g for 5 min at room temperature to pellet any insoluble material. The supernatant was transferred to LC MS/MS vials. Peptide mix was separated on a Dionex Ultimate 3000 (Thermo Fisher Scientific, USA) chromatrgraphy system with increasing gradient of acetonitrile on a Biobasic C18 Picofrit TM column (100 mm length, 75 mm ID), using a 60 min reverse phase gradient at a flow rate of 250 nl min^{-1}. High resolution MS scan (300-2000 Da) was performed using the Orbitrap to select the 15 most intense ions prior to MS/MS. A 1 h blank was run between each experimental condition.

5.2.4.3 Computational identification of ion peaks

MS/ MS ion peaks were identified using MaxQuant (open source,ver. 1.2.2.5, http://maxquant.org/) through the use of the incorporated Andromeda search engine (Cox *et al.* 2011) and correlated against a 6-frame translation of the EST contigs identified for *G. mellonella* (Vogel *et al.* 2011). The following search parameters were set for identification of proteins in MaxQuant: First peptide tolerance was set at 20 ppm, second peptide tolerance was set at 4.5 ppm, cysteine carbamidomethylation set as a fixed modification, N-acetylation of proteins and oxidation of methionine as a variable modification, and a maximum of 2 missed cleavage sites allowed. Search results were challenged with a target decoy database and False Discovery Rate (FDR) was set to 1 % for both peptide and proteins. Identified peptides contained a minimum of 7 amino acids and proteins were only considered identified when 2 or more unique constituent peptides were observed.

5.2.4.4 Statistical and visual processing of identified proteins

Identified proteins were processed using Perseus (open source, ver. 1.5.6, http://www.perseus-framework.org). LFQ intensities were subjected to log(2) transformation. Proteins were only processed when they were present in at least 3 of 4 biological replicates. Proteins that contained LFQ intensity values of zero (NaN) were included in the results when they were absent in 1 group and present in at least 3 replicates of another group. Subsequently, replicate samples that were missing from one group were imputated based on Gaussian distribution using the value for each dataset, which was calculated as being a 1.75 downshift from the mean value and a 0.25 width downshift for the standard deviation. Unpaired t-tests between the solvent control and each of the test complexes were performed with a *p*-value of 0.05 set with FDR

correction (Benjamini-Hochberg). Principle Component Analysis (PCA) was performed on each of the experimental designs to establish the protein abundance variation between the different experimental exposures and examine the variation within each experimental group. Tight clustering indicated similar protein abundance while dispersed data points indicated dissimilar protein abundance. Dispersion of the data points on the x-axis (Component 1) represented the largest difference in protein abundance while dispersion of data points on the y-axis (Component 2) represented the next largest difference in protein abundance. Hierarchical clustering and volcano plots were generated between each of the test complexes and the solvent control from the imputated dataset. Proteins with statistical significant expression ($p \leq 0.05$) and ≥ 1.5 fold change between the test exposure and the negative control were referred to as Statistically Significant Differentially Abundant (SSDA) proteins. The Blast2GO suite (BioBam Bioinformatics, Spain) of software tools was used to assign annotation, enzyme code, KEGG and Gene Ontology mapping on SSDA proteins. GO mapping for biological processes and molecular functions was graphed at level 4 ontology.

5.3 Results

5.3.1 *Galleria mellonella in-vivo* toxicity assay and cuticle changes

G. mellonella larvae were exposed to Cu-Phen (**1**)**,** Cu-DPQ-Phen (**2**), Cu-DPPZ-Phen (**3**) and cisplatin and the level of toxicity was assessed by the mean mortality (%) over 72 h (**Table 5.4 – 5.5**). No mortality (data not shown) was recorded at any timepoint after incubation of solvent (8.94% DMSO in MilliQ water), sham inoculated and undisturbed controls. The results of the individual larval responses to the inoculated doses and timepoints are detailed **Table 5.4 – 5.5**. In the case of Cu-Phen (**1**) (**Table 5.4**), the onset of toxicity occurs rapidly with inoculation in excess of 10 µg at 24 h and after, with inoculation dose of under 10 µg producing no appreciable increase in mortality over the subsequent timepoints.

The inoculation of the larvae with Cu-DPQ-Phen (**2**) (**Table 5.4**) produced a different effect in comparison to inoculation with Cu-Phen (**1**). At the 4 h timepoint mortality was not observed until 20 µg in comparison to 10 µg with Cu-Phen (**1**). Mortality increases at both 24 and 48 h and increases marginally again at 72 h with toxicity beginning to appear at 8 µg. Cu-Phen (**1**) and Cu-DPQ-Phen (**2**) differ in terms of their toxicity to the larvae both in relation to the dose administration and the rate of increase in mortality with Cu-Phen (**1**) producing a superior toxicity profile in all cases in comparison to Cu-DPQ-Phen (**2**).

Inoculation of larvae with Cu-DPPZ-Phen (**3**) (**Table 5.4**) produces a different profile to that of Cu-Phen (**1**) and Cu-DPQ-Phen (**2**). Mortality was restricted to the 12-30 µg range until the 72 h timepoint where it was observed at 40 % in the 10 µg inoculation. The inoculation with Cu-DPPZ-Phen (**3**) also showed very little increase in the level of mortality over time in contrast to Cu-Phen (**1**) and Cu-DPQ-Phen (**2**). Cu-DPPZ-Phen

(**3**) was injected in micro-suspension which may partially explain the profile of early toxicity followed by a very marginal increase in mortality over time. **Figure 5.5** presents the results from **Table 5.4** as a heatmap.

Table 5.4 Mean larval mortality (%) after 4, 24, 48 and 72 h inoculations with Cu-Phen (**1**), Cu-DPQ-Phen (**2**) and Cu-DPPZ-Phen (**3**) at the required doses.

		Larval dose (µg)	**30**	**20**	**12**	**10**	**8**	**6**	**4**	**2**
Cu-Phen (**1**)	4 hr	% Mortality	100	86	46	6	0	0	0	0
		µmol	0.054	0.036	0.021	0.018	0.014	0.010	0.007	0.003
		mg kg^{-1}	99.99	66.66	39.99	33.33	26.66	19.99	13.33	6.66
Cu-DPQ-Phen (**2**)	4 hr	% Mortality	100	40	0	0	0	0	0	0
		µmol	0.048	0.032	0.019	0.016	0.013	0.009	0.006	0.003
		mg kg^{-1}	99.99	66.66	39.99	33.33	26.66	19.99	13.33	6.66
Cu-DPPZ-Phen (**3**)	4 hr	% Mortality	100	100	76	0	0	0	0	0
		µmol	0.046	0.030	0.018	0.015	0.012	0.009	0.006	0.003
		mg kg^{-1}	99.99	66.66	39.99	33.33	26.66	19.99	13.33	6.66
Cu-Phen (**1**)	24 hr	% Mortality	100	100	100	83	16	0	0	0
		µmol	0.054	0.036	0.021	0.018	0.014	0.010	0.007	0.003
		mg kg^{-1}	99.99	66.66	39.99	33.33	26.66	19.99	13.33	6.66
Cu-DPQ-Phen (**2**)	24 hr	% Mortality	100	100	73	36	0	0	3	0
		µmol	0.048	0.032	0.019	0.016	0.013	0.009	0.006	0.003
		mg kg^{-1}	99.99	66.66	39.99	33.33	26.66	19.99	13.33	6.66
Cu-DPPZ-Phen (**3**)	24 hr	% Mortality	100	100	80	0	0	0	0	0
		µmol	0.048	0.030	0.018	0.015	0.012	0.009	0.006	0.003
		mg kg^{-1}	99.99	66.66	39.99	33.33	26.66	19.99	13.33	6.66
Cu-Phen (**1**)	48 hr	% Mortality	100	100	100	83	16	0	0	0
		µmol	0.054	0.036	0.021	0.018	0.014	0.010	0.007	0.003
		mg kg^{-1}	99.99	66.66	39.99	33.33	26.66	19.99	13.33	6.66
Cu-DPQ-Phen (**2**)	48 hr	% Mortality	100	100	73	36	0	0	3	0
		µmol	0.048	0.032	0.019	0.016	0.013	0.009	0.006	0.003
		mg kg^{-1}	99.99	66.66	39.99	33.33	26.66	19.99	13.33	6.66
Cu-DPPZ-Phen (**3**)	48 hr	% Mortality	100	100	80	0	0	0	0	0
		µmol	0.048	0.030	0.018	0.015	0.012	0.009	0.006	0.003
		mg kg^{-1}	99.99	66.66	39.99	33.33	26.66	19.99	13.33	6.66
Cu-Phen (**1**)	72 hr	% Mortality	100	100	100	83	20	0	0	0
		µmol	0.054	0.036	0.021	0.018	0.014	0.010	0.007	0.003
		mg kg^{-1}	99.99	66.66	39.99	33.33	26.66	19.99	13.33	6.66
Cu-DPQ-Phen (**2**)	72 hr	% Mortality	100	100	73	50	30	0	0	0
		µmol	0.048	0.032	0.019	0.016	0.013	0.009	0.006	0.003
		mg kg^{-1}	99.99	66.66	39.99	33.33	26.66	19.99	13.33	6.66
Cu-DPPZ-Phen (**3**)	72 hr	% Mortality	100	100	80	40	0	0	3	0
		µmol	0.048	0.030	0.018	0.015	0.012	0.009	0.006	0.003
		mg kg^{-1}	99.99	66.66	39.99	33.33	26.66	19.99	13.33	6.66

Cu(II) phenanthroline-phenazine complexes inoculated in 20 µl solution.

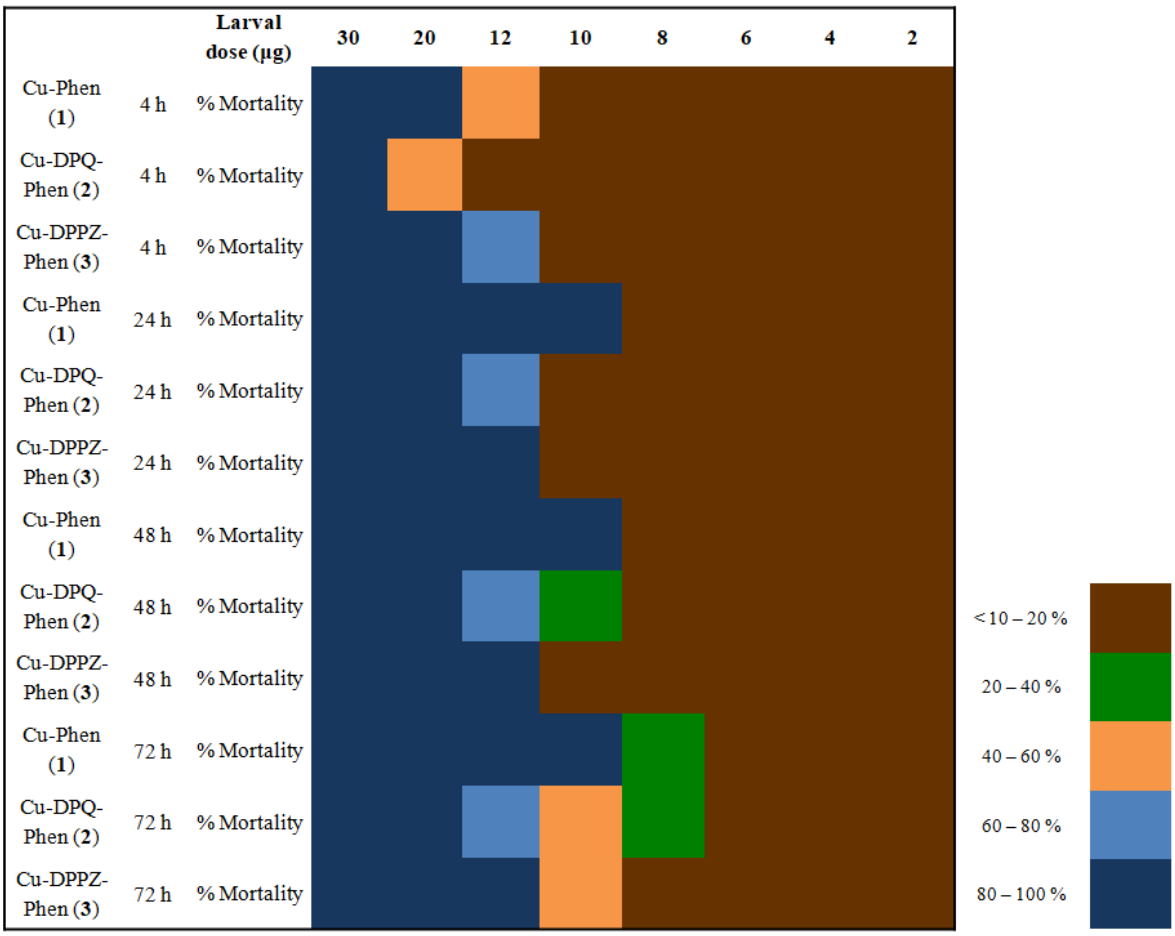

Fig 5.5 Heatmap representation of **Table 5.4** showing the mean larval mortality (%) after 4, 24, 48 and 72 h inoculations with Cu-Phen (**1**), Cu-DPQ-Phen (**2**) and Cu-DPPZ-Phen (**3**).

The pharmacological reference drug, cisplatin produced far lower levels of toxicity (**Table 5.5**) than Cu-Phen (**1**), Cu-DPQ-Phen (**2**) and Cu-DPPZ-Phen (**3**) over 3 timepoints. An additional high dose inoculation (100 µg) was performed to demonstrate maximal toxicity which was previously demonstrated by (McCann *et al.* 2012). Cu-Phen (**1**), Cu-DPQ-Phen (**2**) and Cu-DPPZ-Phen (**3**) exceed the toxicity of cisplatin over a 72 h period. The DPQ and DPPZ ligands independent of the Cu-Phen scaffold complex was administered at a range of 2-10 µg but no mortality was observed at any dose or timepoint due to lack of solubility in the required solution.

Table 5.5 Mean larval mortality (%) after 24, 48 and 72 h inoculation with 20 µl of cisplatin at required doses.

Cisplatin	Larval dose (µg)	100	10	8	6	4	2
24 h	% Mortality µmol mg kg^{-1}	86 0.333 333.33	0 0.033 33.33	0 0.026 26.66	0 0.019 19.99	0 0.013 13.33	0 0.006 6.66
48 h	% Mortality µmol mg kg^{-1}	86 0.333 333.33	6 0.033 33.33	0 0.026 26.66	0 0.019 19.99	0 0.013 13.33	0 0.006 6.66
72 h	% Mortality µmol mg kg^{-1}	90 0.333 333.33	6 0.033 33.33	0 0.026 26.66	0 0.019 19.99	0 0.013 13.33	0 0.006 6.66

The LD_{50} values (**Table 5.6**) from Cu-Phen (**1**), Cu-DPQ-Phen (**2**) and Cu-DPPZ-Phen (**3**) decrease over the increasing timepoints with Cu-Phen (**1**) showing superior toxicity to Cu-DPQ-Phen (**2**) and Cu-DPPZ-Phen (**3**) at all timepoints. All complexes demonstrated time-dependent toxicity. Mild orange discoloration was observed after exposure Cu-Phen (**1**) at 24 h with no other remarkable colour changes apparent except for melanisation being apparent in some larvae at death.

Table 5.6 Calculated LD_{50} values and the representation of cuticle presentation post exposure.

	LD_{50} (µg) ± S.D.			
	4 h	24 h	48 h	72 h
Cu-Phen **(1)**	12.62±0.008	8.94±0.006	8.94±0.006	8.56±0.75
Cu-DPQ-Phen **(2)**	21.53±0.007	11.47±0.006	10.69±0.005	9.88±0.017
Cu-DPPZ-Phen **(3)***	26.07±0.312	25.05±0.312	25.05±0.312	16.81±0.236
	Treatment images after 24 h exposure			
Exposure	Control (24 h)	Cu-Phen (**1**) (24 h)	Cu-DPQ-Phen (**2**) (24 h)	Cu-DPPZ-Phen (**3**) (24 h)*
Cuticle response				
Comment	Cuticle unchanged	Mild orange discoloration	Unremarkable cuticle changes	Unremarkable cuticle changes

* Cu-DPPZ-Phen (**3**) injected in micro-suspension.

5.3.2 Measurement of haemocyte count

Haemocytes count (**Fig. 5.6**) was performed from the haemolymph extracted from 5 larvae per treatment (LD_{50} value at 24 h). This procedure was replicated × 4 for statistical validity. No significant changes were observed between any of the controls and test complex exposures.

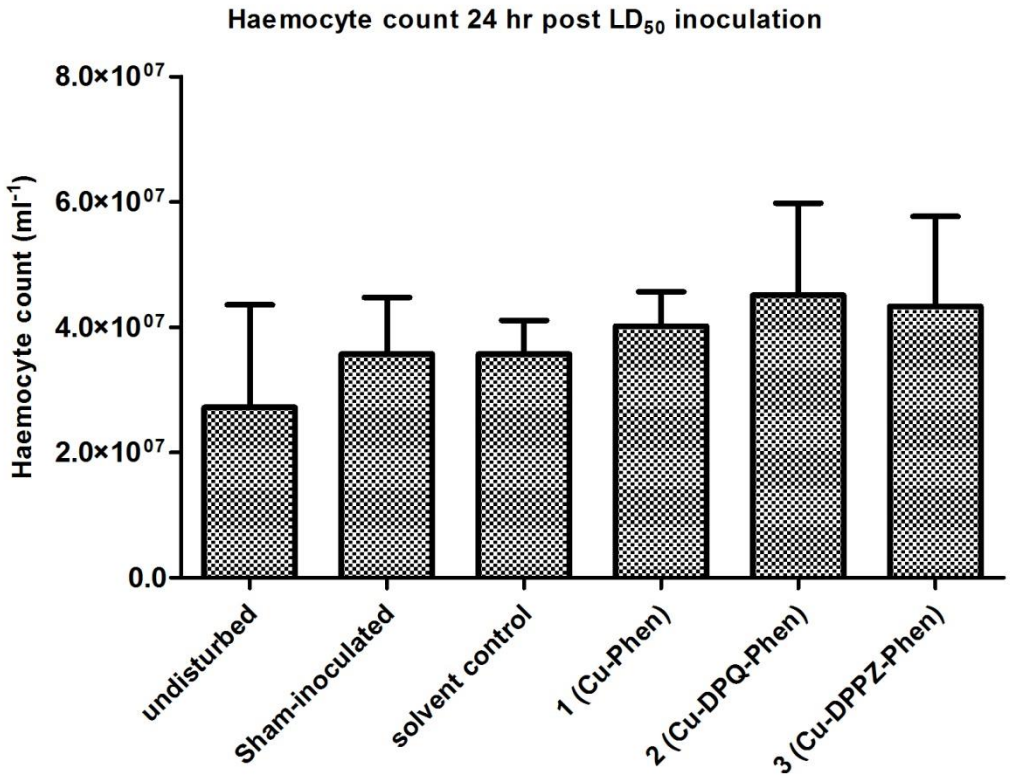

Fig. 5.6 Changes in haemocyte count 24 h post inoculation with Cu-Phen (**1**) and Cu-DPQ-Phen (**2**) and Cu-DPPZ-Phen (**3**). In addition to the Cu(II) phenanthroline-phenanzine complex series the solvent, sham-inoculated and undisturbed controls were used for comparison.

5.3.3 Measurement of IMPI and Transferrin by qRT-PCR

Larvae were exposed to the 24 h LD_{50} value of Cu-Phen (**1**) (8.94 µg), Cu-DPQ-Phen (**2**) (11.47 µg) and Cu-DPPZ-Phen (**3**) (25.05 µg). Solvent control, sham-inoculation and undisturbed control were utilised as previously described. Both transferrin and IMPI were normalised against the expression of S7e reference gene and all larval treatments were compared to the undisturbed control. Both sham-inoculation and undisturbed controls produced similar expression levels (data not shown). **Fig. 5.7** demonstrates the expression of both genes. A significant decrease in IMPI expression was observed in Cu-Phen (**1**), Cu-DPQ-Phen (**2**) and Cu-DPPZ-Phen (**3**) treated larvae in comparison to the solvent control. In all LD_{50} complex exposures there was a significant decrease in transferrin activity with respect to the solvent control.

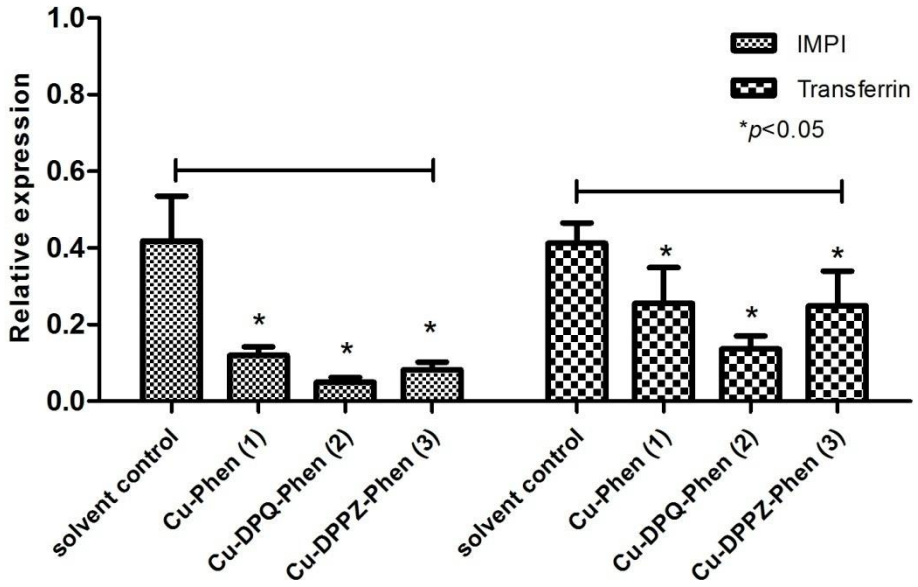

Fig. 5.7 Relative expression of (IMPI) and transferrin after 24 h exposure to LD_{50} value of Cu-Phen (**1**), Cu-DPQ-Phen (**2**) and Cu-DPPZ-Phen (**3**). Gene expression is displayed relative to the undisturbed control with the solvent control used to determine significance ($p < 0.05$) (N=4).

5.3.4 2D SDS-PAGE analysis of protein expression

2D PAGE gels were produced by separating proteins on the basis of size after IEF 1D gel strips separated proteins based on a pH gradient. Progenesis SameSpot (Nonlinear Dynamics, USA) software was used to compare the density of protein spots across the different exposures and in relation to the solvent control (**Table 5.7**), spots were then excised from the reference gel (**Fig. 5.8 (a)**) and subsequent LC/MS identification. **Table 5.7** details 10 protein spots which had a ≥ 1.5 fold change in expression between the control (reference gel) and test exposures with Cu-Phen (**1**), Cu-DPQ-Phen (**2**) and Cu-DPPZ-Phen (**3**). The location of the spots is shown in **Fig. 5.8 (a)**. **Table 5.7** displays the spots 1-10 identifications based on LC/MS (Mascot) analysis. Asterisks denote significant changes ($p \leq 0.05$) in protein abundance as determined by ANOVA compared to the solvent control.

Spots 2, 7, 3, 6, 8 and 9 have all been identified to function in the immune response as well as other capabilities. Spot 2 represents apolipophorin-III. Apolipophorin-III is a pattern recognition receptor, a fundamental component of the innate immune response in mammals and insects involved in recognition of foreign antigens. A significant increase in apolipophorin-III was observed when exposed to Cu-Phen (**1**) but is significantly decreased upon inoculation with Cu-DPQ-Phen (**2**) or Cu-DPPZ-Phen (**3**) relative to the solvent control. Spot 7 represents apolipophorin which is a precursor of apolipophorin-III and is involved in the transport of lipids and activation of the innate immune response. A non-significant decrease was observed upon exposure to all the test complexes relative to the solvent control. Spot 3 was identified as storage protein 1, a close analogue of arylophorin which functions in amino acid storage and immune functioning. A significant increase in arylophorin was observed when the larvae were

exposed to all of the test complexes relative to the solvent control. Spot 6 represents transferrin precursor, the precursor to transferrin, which is involved in iron storage and transport. A non-significant decrease was observed in all exposure to the test complexes relative to the solvent control. Both spot 8 and 9 represent two subunits of ferritin. Ferritin is found in all eukaryotic cells and functions in iron storage, transport and antioxidant activity and is commonly elevated in response to infection. A non-significant decrease was seen in both these subunits following exposure to the test complexes relative to the solvent control.

Spots 1, 4, 5 and 10 relates to the proteins identified to have metabolic, adaptor and signaling functions. Spot 1 was identified as 27 kDa hemolymph protein which is secreted and functions in signaling. Significant decreases in this protein were seen after inoculation with all of the complex series relative to the solvent control. Spot 4 represents a phosphotidylserine receptor (GL24169) identified through homology to *Drosophila melanogaster* in Flybase (www.flybase.org). A significant increase was observed with this protein in response to all the test complexes with the strongest increase observed with Cu-DPPZ-Phen (**3**) relative to the solvent control. Spot 5 was identified as juvenile hormone binding protein which is involved in the regulation of embryogenesis and reproduction. A non-significant decrease was seen with this protein in response to inoculation with all the test complexes, the strongest of which was seen in Cu-DPQ-Phen (**2**) relative to the solvent control. Spot 10 represents imaginal disc growth factor (partial) which is important in regulating cell proliferation and growth. In all exposure the protein was non-significantly decreased relative to the solvent control with the greatest amplitude of the response with the exposure to Cu-DPQ-Phen (**2**).

Table 5.7 Protein identifications from MASCOT analysis after spot picking from reference gel (**a**), trypsin digestion and LC/MS analysis.

Spot No.	Protein identity	Organism	Mr	PI	Score	Sequence Coverage (%)	Accession no.	Solvent control (relative fold change)	Cu-Phen (**1**) (relative fold change)	Cu-DPQ-Phen (**2**) (relative fold change)	Cu-DPPZ-Phen (**3**) (relative fold change)
1 (53)*	27 kDa hemolymph protein	*Galleria mellonella*	26374	5.17	258	16	P83632	1	-1.86	-6.35	-4.34¥
2 (65)*	Apolipophorin-III	*G. mellonella*	20498	8.59	184	18	P80703	1	+1.25	-3.65¥	-3.28¥
3 (11)*	Storage protein 1	*Omphisa fuscidentalis*	83261	8.21	73	1	ABO27097	1	+1.72	+3.36	+2.52
4 (60)*	GL24169 (phosphotidylserine receptor) (Flybase)	*Drosophilia persimilis*	46763	9.25	70	3	XP_002013494	1	+3.30	+3.12	+4.57
5 (45)	Juvenile hormone binding protein	*G. mellonella*	27469	6.84	346	33	AAN06604	1	-1.13	-2.24	-1.56¥
6 (23)	Transferrin precursor	*G. mellonella*	77212	6.76	951	37	AAQ63970	1	-1.35	-1.66	-1.53¥
7 (4)	Apolipophorin, partial	*G. mellonella*	168310	6.25	549	10	AAT76806	1	-1.00	-2.11	-2.01
8 (48)	32 kDa ferritin subunit	*G. mellonella*	26727	5.69	85	4	AAL47694	1	-1.54	-2.40	-1.50
9 (56)	26 kDa ferritin subunit	*G. mellonella*	23932	6.22	186	9	AAG41120	1	-1.48	-1.85	-2.45
10 (34)	Imaginal disc growth factor, partial	*Biston betularia*	22111	4.97	80	14	ADO33018	1	-1.19	-1.98¥	-1.65¥

Fold changes of proteins are presented relative to solvent control.
*indicates statistically significant ($p \leq 0.05$) fold changes using ANOVA (N=3).
¥ Denotes proteins and expression profile expressed in both 2D PAGE and LFQ proteomics (**Table 4.8-4.10**).

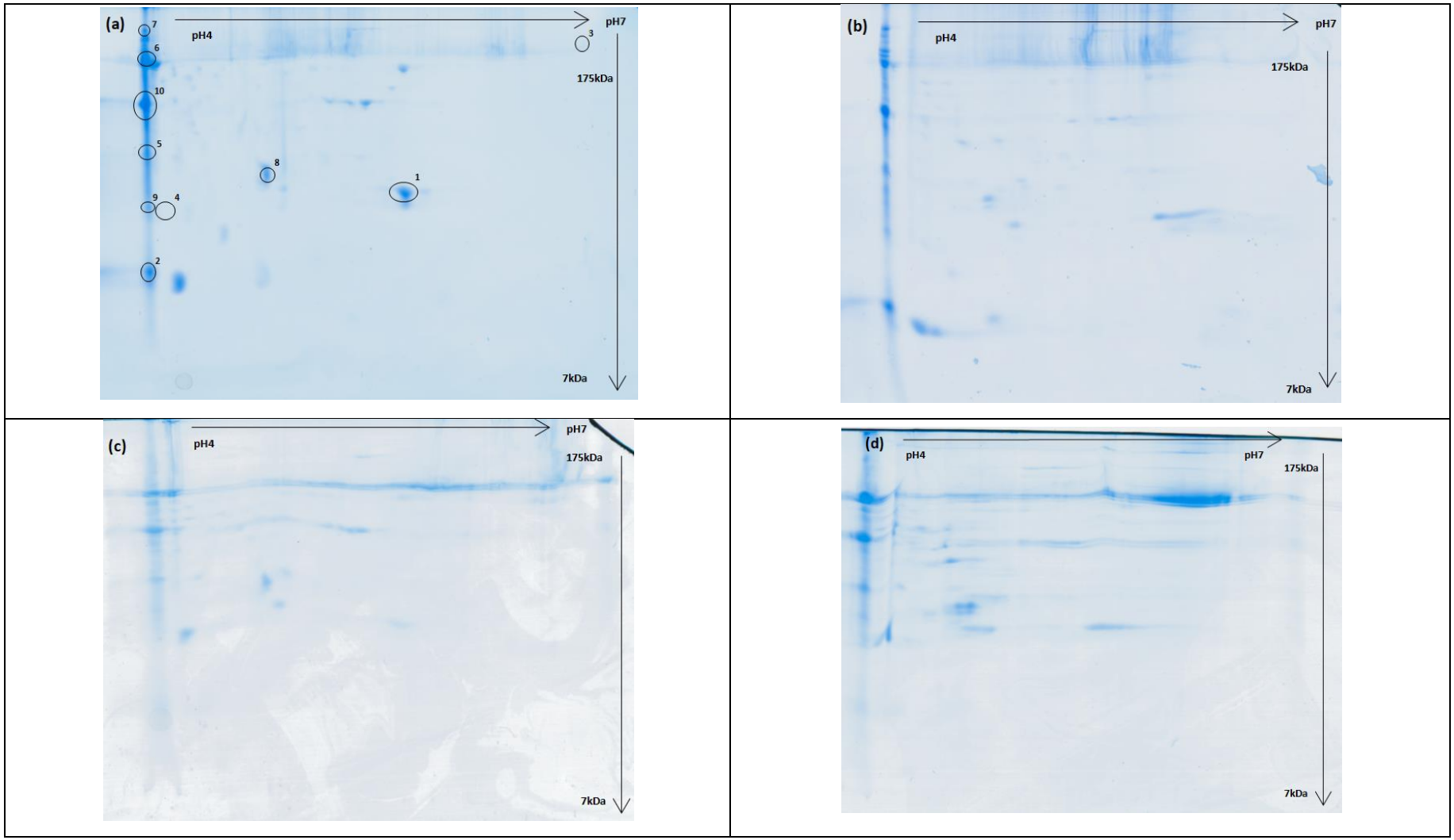

Fig. 5.8 2D PAGE gel of separated haemolymph proteins from *G. mellonella* inoculated, (**a**) reference gel (control), (**b**) Cu-Phen (**1**), (**c**) Cu-DPQ-Phen (**2**) and (**d**) Cu-DPPZ-Phen (**3**). Circled spots excised and identified through LC/ MS and descriptions displayed in **Table 5.7**.

5.3.5 LFQ proteomics between Cu(II) complex exposures and control

The haemolymph of larvae was extracted after the 24 h exposure to the LD_{50} value of the complex series in order to assess the difference in protein abundance between the treated and control larvae. **Table 5.8** displays statistically significant proteins which were ≥ 1.5 fold change in relation to the solvent control after exposure to Cu-Phen (**1**). **Table 5.9** displays statistically significant proteins which were ≥ 1.5 fold change in relation to the solvent control after exposure to Cu-DPQ-Phen (**2**). **Table 5.10** displays statistically significant proteins which were ≥ 1.5 fold change in relation to the solvent control after exposure to Cu-DPPZ-Phen (**3**). A total of 299 proteins were detected with 2 or more peptides. One hundred and four proteins were found to be significantly altered in abundance or uniquely detected across the 4 conditions (**Table 5.11**). Nine proteins were found to be absent or below the limit of detection following exposure to Cu-DPQ-Phen (**2**). Twelve proteins were found to be absent or below the detection limit following exposure to Cu-Phen (**1**). Four proteins were found to be absent or below the limit of detection after exposure to Cu-DPQ-Phen (**2**) and Cu-DPPZ-Phen (**3**). One protein was found to be absent or below the limit of detection after exposure to Cu-Phen (**1**) and Cu-DPPZ-Phen (**3**). Twenty three proteins were found to be absent or below the limit of detection after exposure to Cu-Phen (**1**) and Cu-DPQ-Phen (**2**). Principle component analysis (PCA) (**Fig. 5.9**) was used to visualise the variation in protein abundance across the individual replicates. The proteomes of larvae exposed to the solvent control and Cu-DPPZ-Phen (**3**) showed clustering that was widely separated by component 1, however Cu-Phen (**1**) and Cu-DPQ-Phen (**2**) were closely clustered. Hierarchical clustering (**Fig. 5.10**) similarly reflected the PCA analysis. Four replicates were included for the solvent control and one replicate was removed from each of the test exposures due to lack of clustering with the parent group. Volcano plots (**Fig. 5.11**

(A), (B) and **(C)**) show the increasing number of significantly up regulated proteins in the following pattern: Cu-Phen (**1**) < Cu-DPQ-Phen (**2**) < Cu-DPPZ-Phen (**3**). In the case of Cu-DPPZ-Phen (**3**) exposure, a greater number of antimicrobial proteins were observed to be significantly downregulated while a greater number of metabolic proteins and proteins containing calcium binding sites were up regulated. Gene Ontology (GO) terms were categorised by both biological processes (**Fig. 5.12 (A)**) and molecular function (**Fig. 5.12 (B)**) with categorisations being performed at level 4 ontology. The biological process analysis (**Fig. 5.12 (A)**) does not show any major changes in larvae inoculated with the different complexes. Protein groups such as precursor metabolites, organonitrogen and cellular nitrogen associated proteins were more prominent in terms of observed proteins. An overall increase was observed in the number of proteins recorded after exposure to Cu-DPQ-Phen (**2**) and Cu-DPPZ-Phen (**3**) with the number of proteins increasing as the ligated phenazine π-backbone was extended. However, the number of proteins associated with each GO process proportionally increased in comparison to Cu-Phen (**1**). Interestingly, proteins associated with sulphur compounds and cellular aldehyde processes were only present after exposure to Cu-DPPZ-Phen (**3**). Analysis of molecular functions (**Fig. 5.12 (B)**) also showed a similar trend of increasing number of proteins involved in the functionally categorised processes as the Cu(II) series progressed from Cu-Phen > Cu-DPQ-Phen > Cu-DPPZ-Phen. Proteins associated with coenzyme binding, oxidoreductases acting on CH-OH and peptidase activity was only associated with exposure of Cu-Phen (**1**), while all other protein groups were co-expressed by all three test complexes. Glutathione S-transferase (GST) highlighted in the KEGG analysis (**Fig. 5.13**), exhibited an increased relative abundance following exposure to Cu-Phen (**1**), Cu-DPQ-Phen (**2**) and Cu-DPPZ-Phen (**3**) in comparison to the control. KEGG

glycolysis/ gluconeogenesis analysis (**Fig. 5.14**) of all three complex exposures showed an upregulation of several proteins: fructose bisphosphate, triose phosphate isomerase, glyceraldehydes-3-phosphate dehydrogenase and phosphopyruvate hydratase (enolase). KEGG analysis of purine metabolism (**Fig. 5.15**) showed increased relative abundance of 6 proteins after exposure to all test complexes: phosphoribosylaminoimidazolesuccinocarboxamide synthase (SAICAR), phosphoribosylaminoimidazolecarboxamide formyltransferase (AICAR), IMP cyclohydrolase, nucleoside-diphosphate kinase, nucleoside-triphosphate phosphatise and purine-nucleoside phosphorylase.

Table 5.8 Identities and relative expression values for proteins that were identified as being significantly higher and lower in abundance in the larvae inoculated with the LD_{50} dose of Cu-Phen (**1**) compared to the negative control.

Protein annotation	Peptides	Sequence coverage [%]	PEP	Mean LFQ intensity	Rel. Exp. in Cu-Phen (**1**)
chitin deacetylase 1	35	63.3	0.00E+00	1.65E+10	6.88
dihydropteridine reductase	30	61.4	0.00E+00	1.28E+10	6.24
elongation factor 1-alpha	25	61.5	0.00E+00	1.19E+10	6.19
cholinesterase 1-like	25	44.7	0.00E+00	1.65E+10	6.10
translationally controlled tumor	12	39.9	0.00E+00	7.06E+09	5.64
D-arabinitol dehydrogenase 1-like	16	51.2	5.65E-214	7.10E+09	5.13
glutathione S-transferase-like	6	18.2	1.55E-174	6.28E+09	5.16
N-acetylneuraminate lyase-like	25	46.4	0.00E+00	7.30E+09	5.24
fibrous sheath CABYR-binding	13	32.3	2.53E-295	3.95E+09	5.18
multifunctional ADE2	13	55.4	3.04E-161	2.24E+09	5.06
glutathione S-transferase 1-like	22	59.5	1.54E-196	6.86E+09	5.01
esterase FE4-like	16	53.8	3.02E-224	5.71E+09	5.11
cellular retinoic acid binding	12	22.2	0.00E+00	3.05E+09	5.17
triosephosphate isomerase	21	26.2	0.00E+00	4.94E+09	4.92
lambda-crystallin homolog	8	26.1	2.51E-101	8.00E+09	4.89
trans-1,2-dihydrobenzene-1,2-diol dehydrogenase-like	4	47.2	9.89E-277	3.41E+09	4.69
Tubulin alpha chain	23	46	1.36E-254	5.29E+09	4.68
tubulin beta chain	18	59.1	0.00E+00	1.00E+10	4.43
fructose-bisphosphate aldolase isoform X1	30	50.6	0.00E+00	1.24E+10	4.59
immune-related Hdd1	14	45.1	3.38E-215	3.57E+09	4.64
L-threonine ammonia-lyase-like	4	28.4	6.93E-31	1.89E+09	4.08
arginine partial	5	9.8	8.02E-110	1.78E+09	4.02
PREDICTED: uncharacterized protein LOC106129042	15	58.8	2.50E-224	3.61E+09	3.89
aliphatic nitrilase	19	45.1	4.19E-244	3.41E+09	3.61
glutamine synthetase 2 cytoplasmic-like	7	37	1.13E-44	1.07E+09	3.49
Purine nucleoside phosphorylase	12	61.5	1.32E-146	8.16E+08	3.61
enolase	5	16.7	1.12E-97	3.61E+09	3.39
heat shock 90	20	41.9	1.36E-241	1.91E+09	3.49
Profilin	21	32	4.84E-263	1.73E+09	3.18
homeobox 2-like isoform X4	9	48.1	4.28E-288	2.65E+09	3.14
glyceraldehyde-3-phosphate partial	3	15.2	3.72E-92	1.67E+09	3.15
D-3-phosphoglycerate dehydrogenase	5	36.2	4.27E-39	9.54E+08	3.05
Peptidyl-prolyl cis-trans isomerase	9	29.1	6.27E-93	2.15E+09	3.03
circadian clock-controlled -like	9	35.5	6.41E-171	1.95E+09	3.01
15-hydroxyprostaglandin dehydrogenase [NAD(+)]-like	29	44.9	0.00E+00	5.33E+10	2.70
probable salivary secreted peptide	19	45.3	0.00E+00	4.41E+09	2.71
cytosolic malate partial	19	28.2	7.32E-209	4.09E+09	2.90
glutathione S-transferase 1-1-like	24	38	0.00E+00	4.14E+10	2.81
cysteine ase inhibitor precursor	14	32	3.26E-82	1.01E+09	2.54
isocitrate partial	6	38	2.66E-52	5.87E+08	2.50
proliferation-associated 2G4	26	61.8	0.00E+00	5.31E+10	2.48
ecdysteroid-regulated 16 kDa -like	7	34.3	2.22E-85	6.68E+08	2.96
gustatory receptor candidate 59	13	31.2	7.71E-149	1.49E+09	2.19
chemosensory	11	46.5	4.67E-148	1.45E+09	2.78
uncharacterized protein Dmoj_GI19595	6	31.1	1.29E-32	7.59E+08	2.25
cytosolic non-specific dipeptidase	5	36	2.31E-38	8.00E+08	2.23
aldehyde dehydrogenase mitochondrial-like	6	21.3	2.40E-48	2.21E+08	2.61
leukotriene A-4 hydrolase isoform X2	11	37.9	2.32E-85	1.68E+09	2.06
N-acetylneuraminate lyase-like	18	30.9	3.56E-168	1.06E+09	2.03
ejaculatory bulb-specific 3-like	14	57.3	0.00E+00	2.05E+10	2.13
Peptidoglycan recognition	5	8.1	3.31E-26	1.69E+08	2.02
Selenium-binding 1	6	24.8	7.89E-90	9.73E+08	2.05
heat shock	8	57.7	3.46E-179	1.07E+10	1.98
bifunctional purine biosynthesis PURH	16	29.2	1.29E-152	4.27E+09	1.75

ejaculatory bulb-specific 3-like	15	76.3	0.00E+00	1.80E+10	1.63
aminopeptidase	5	20.9	3.12E-31	2.17E+08	1.65
superoxide dismutase [Mn] mitochondrial	11	30.9	4.34E-90	1.12E+09	-1.52
seroin-like isoform X2	2	57.7	1.94E-07	4.54E+08	-2.06

Proteins shaded in grey at the end of the table were significantly downregulated in abundance upon inoculation with Cu-Phen (**1**).

Peptides matched to the annotated protein, sequence coverage, PEP (Posterior Error Probability) and mean LFQ intensities, with a t-test probability of $p \leq 0.05$ (N=4).

Table 5.9 Identities and relative expression values for proteins that were identified as being significantly higher in abundance in the larvae inoculated with the LD_{50} dose of Cu-DPQ-Phen (**2**) in comparison to the negative control.

Protein annotation	Peptides	Sequence coverage [%]	PEP	Intensity	Rel. Exp. in Cu-DPQ-Phen (**2**)
aldehyde dehydrogenase mitochondrial-like	35	63.3	0.00E+00	1.65E+10	7.16
lambda-crystallin homolog	25	61.5	0.00E+00	1.19E+10	6.76
Selenium-binding 1	30	61.4	0.00E+00	1.28E+10	6.62
tubulin beta chain	25	44.7	0.00E+00	1.65E+10	6.37
D-arabinitol dehydrogenase 1-like	16	53.8	3.02E-224	5.71E+09	5.80
cytoplasmic A3a	12	39.9	0.00E+00	7.06E+09	5.74
N-acetylneuraminate lyase-like	6	18.2	1.55E-174	6.28E+09	5.69
elongation factor 1-alpha	16	51.2	5.65E-214	7.10E+09	5.57
serine cytosolic isoform X1	23	46	1.36E-254	5.29E+09	5.48
D-3-phosphoglycerate dehydrogenase	13	32.3	2.53E-295	3.95E+09	5.27
multifunctional ADE2	30	50.6	0.00E+00	1.24E+10	5.13
15-hydroxyprostaglandin dehydrogenase [NAD(+)]-like	22	59.5	1.54E-196	6.86E+09	5.05
glutamine synthetase 2 cytoplasmic-like	12	22.2	0.00E+00	3.05E+09	5.00
cytosolic malate partial	25	46.4	0.00E+00	7.30E+09	4.97
triosephosphate isomerase	21	26.2	0.00E+00	4.94E+09	4.96
glutathione S-transferase-like	13	55.4	3.04E-161	2.24E+09	4.65
probable enoyl- mitochondrial	14	45.1	3.38E-215	3.57E+09	4.61
glyceraldehyde-3-phosphate partial	18	59.1	0.00E+00	1.00E+10	4.60
glutathione S-transferase 1-1-like	15	58.8	2.50E-224	3.61E+09	4.60
Tubulin alpha chain	4	47.2	9.89E-277	3.41E+09	4.60
N-acetylneuraminate lyase-like	6	14.9	2.86E-59	1.49E+09	4.34
probable phosphoserine aminotransferase	18	55.3	2.12E-160	8.79E+08	4.23
trans-1,2-dihydrobenzene-1,2-diol dehydrogenase-like	19	45.1	4.19E-244	3.41E+09	4.17
fructose-bisphosphate aldolase isoform X1	4	28.4	6.93E-31	1.89E+09	4.14
thioredoxin	7	22.6	3.62E-44	1.78E+09	3.87
tubulin alpha chain	9	76.9	1.73E-39	2.54E+09	3.85
bifunctional purine biosynthesis PURH	5	9.8	8.02E-110	1.78E+09	3.70
N-acetylneuraminate lyase-like	3	15.2	3.72E-92	1.67E+09	3.69
ejaculatory bulb-specific 3-like	5	16.7	1.12E-97	3.61E+09	3.68
cholinesterase 1-like	20	41.9	1.36E-241	1.91E+09	3.64
immune-related Hdd1	19	28.2	7.32E-209	4.09E+09	3.58
superoxide dismutase [Mn] mitochondrial	9	48.1	4.28E-288	2.65E+09	3.53
small heat shock	5	24.4	2.12E-30	1.17E+09	3.46
dihydropteridine reductase	9	29.1	6.27E-93	2.15E+09	3.40
heat shock 90	21	32	4.84E-263	1.73E+09	3.36
aminopeptidase	13	31.2	7.71E-149	1.49E+09	3.34
L-threonine ammonia-lyase-like	18	30.9	3.56E-168	1.06E+09	3.30
leukotriene A-4 hydrolase isoform X2	11	46.5	4.67E-148	1.45E+09	3.26
ecdysteroid-regulated 16 kDa -like	6	38	2.66E-52	5.87E+08	3.23
uncharacterized protein LOC106129042	24	38	0.00E+00	4.14E+10	3.23
15-hydroxyprostaglandin dehydrogenase [NAD(+)]-like	15	41.8	3.49E-289	2.84E+09	3.22
aliphatic nitrilase	26	61.8	0.00E+00	5.31E+10	3.19
rab GDP dissociation inhibitor alpha	13	27.1	5.92E-159	9.52E+08	3.15
Peptidyl-prolyl cis-trans isomerase	9	35.5	6.41E-171	1.95E+09	3.12
cellular retinoic acid binding	29	44.9	0.00E+00	5.33E+10	3.06
enolase	19	45.3	0.00E+00	4.41E+09	2.95
fibrous sheath CABYR-binding	11	37.9	2.32E-85	1.68E+09	2.89
ejaculatory bulb-specific 3-like	6	31.1	1.29E-32	7.59E+08	2.72
argininosuccinate synthase	14	32	3.26E-82	1.01E+09	2.66
takeout-like	13	22.1	2.70E-95	9.39E+08	2.33
high mobility group D	4	9	1.77E-90	1.11E+09	2.27
actin	14	57.3	0.00E+00	2.05E+10	2.22
heat shock	16	29.2	1.29E-152	4.27E+09	2.20

uncharacterized oxidoreductase TM_0325-like	8	28.4	1.92E-235	3.18E+08	2.18
isopentenyl-diphosphate Delta-isomerase 1	6	21.3	2.40E-48	2.21E+08	2.13
staphylococcal nuclease domain-containing 1	11	21.4	8.04E-45	4.95E+08	2.13
glutathione S-transferase omega 1	7	44.3	2.06E-108	6.78E+08	2.07
arginine partial	15	76.3	0.00E+00	1.80E+10	2.04
Serpin-2	9	21.5	1.83E-109	1.26E+09	2.00
proliferation-associated 2G4	5	20.9	3.12E-31	2.17E+08	1.98
Purine nucleoside phosphorylase	12	61.5	1.32E-146	8.16E+08	1.96
uncharacterized protein Dmoj_GI19595	8	57.7	3.46E-179	1.07E+10	1.91
fumarylacetoacetase	8	33.3	2.71E-34	1.54E+08	1.57
chitin deacetylase 1	5	8.1	3.31E-26	1.69E+08	1.52
probable salivary secreted peptide	7	50.7	5.52E-50	2.31E+09	-1.72
gloverin-like	2	57.7	1.94E-07	4.54E+08	-2.50
Peptidoglycan recognition	11	30.9	4.34E-90	1.12E+09	-4.02
apolipophorins isoform X2*	1	13.8	1.22E-06	1.18E+09	-4.15

Proteins shaded in grey at the end of the table were significantly down-regulated in abundance upon inoculation with Cu-DPQ-Phen (**2**).

* Denotes protein also expressed in 2D PAGE analysis with a similar profile. Imaginal disc growth factor also detected in LFQ proteomics (down regulated with a fold change of -0.72 relative to the solvent control) and also present in 2D PAGE analysis in **Table 4.4**. Relative expression changes of proteins up regulated and down regulated after Cu-DPQ-Phen (**2**) exposure. Peptides matched to the annotated protein, sequence coverage, PEP and mean LFQ intensities, with a t-test probability of $p \leq 0.05$ (N=4).

Table 5.10 Identities and relative expression values for proteins that were identified as being significantly higher in abundance in the larvae inoculated with the LD_{50} dose of Cu-DPPZ-Phen (**3**) in comparison to the negative control.

Protein annotation	Peptides	Sequence coverage [%]	PEP	Intensity	Rel. exp. in Cu-DPPZ-Phen (**3**)
aldehyde dehydrogenase mitochondrial-like	35	63.3	0.00E+00	1.65E+10	8.05
Selenium-binding 1	30	61.4	0.00E+00	1.28E+10	7.80
lambda-crystallin homolog	25	61.5	0.00E+00	1.19E+10	7.55
tubulin beta chain	25	44.7	0.00E+00	1.65E+10	7.41
D-arabinitol dehydrogenase 1-like	16	53.8	3.02E-224	5.71E+09	6.85
elongation factor 1-alpha	16	51.2	5.65E-214	7.10E+09	6.63
15-hydroxyprostaglandin dehydrogenase [NAD(+)]-like	22	59.5	1.54E-196	6.86E+09	6.49
cytoplasmic A3a	12	39.9	0.00E+00	7.06E+09	6.40
N-acetylneuraminate lyase-like	6	18.2	1.55E-174	6.28E+09	6.38
serine cytosolic isoform X1	23	46	1.36E-254	5.29E+09	6.36
multifunctional ADE2	30	50.6	0.00E+00	1.24E+10	6.19
cytosolic malate partial	25	46.4	0.00E+00	7.30E+09	6.16
D-3-phosphoglycerate dehydrogenase	13	32.3	2.53E-295	3.95E+09	6.04
glutathione S-transferase-like	13	55.4	3.04E-161	2.24E+09	5.99
Tubulin alpha chain	4	47.2	9.89E-277	3.41E+09	5.90
triosephosphate isomerase	21	26.2	0.00E+00	4.94E+09	5.87
muscle-specific 20	17	45.4	2.07E-216	3.37E+09	5.73
glutamine synthetase 2 cytoplasmic-like	12	22.2	0.00E+00	3.05E+09	5.41
probable enoyl- mitochondrial	14	45.1	3.38E-215	3.57E+09	5.31
glutathione S-transferase 1-1-like	15	58.8	2.50E-224	3.61E+09	5.22
glyceraldehyde-3-phosphate partial	18	59.1	0.00E+00	1.00E+10	5.04
peroxiredoxin- mitochondrial	8	28.5	9.37E-84	2.46E+09	4.96
fructose-bisphosphate aldolase isoform X1	4	28.4	6.93E-31	1.89E+09	4.94
15-hydroxyprostaglandin dehydrogenase [NAD(+)]-like	15	41.8	3.49E-289	2.84E+09	4.88
tubulin alpha chain	9	76.9	1.73E-39	2.54E+09	4.85
thioredoxin	7	22.6	3.62E-44	1.78E+09	4.81
superoxide dismutase [Mn] mitochondrial	9	48.1	4.28E-288	2.65E+09	4.70
trans-1,2-dihydrobenzene-1,2-diol dehydrogenase-like	19	45.1	4.19E-244	3.41E+09	4.70
glutathione S-transferase 1-like	7	37	1.13E-44	1.07E+09	4.67
bifunctional purine biosynthesis PURH	5	9.8	8.02E-110	1.78E+09	4.56
rab GDP dissociation inhibitor alpha	13	27.1	5.92E-159	9.52E+08	4.55
N-acetylneuraminate lyase-like	3	15.2	3.72E-92	1.67E+09	4.53
probable phosphoserine aminotransferase	18	55.3	2.12E-160	8.79E+08	4.46
aminopeptidase	13	31.2	7.71E-149	1.49E+09	4.39
heat shock 90	21	32	4.84E-263	1.73E+09	4.33
enolase	19	45.3	0.00E+00	4.41E+09	4.32
L-threonine ammonia-lyase-like	18	30.9	3.56E-168	1.06E+09	4.27
arginine partial	15	76.3	0.00E+00	1.80E+10	4.24
tropomyosin-1 isoform X1	7	30.1	2.10E-145	8.84E+08	4.22
actin	14	57.3	0.00E+00	2.05E+10	4.22
aliphatic nitrilase	26	61.8	0.00E+00	5.31E+10	4.19
troponin T	7	33.2	6.39E-37	6.43E+08	4.18
annexin B9 isoform X4	8	31.1	8.55E-124	4.82E+08	4.15
Peptidyl-prolyl cis-trans isomerase	9	35.5	6.41E-171	1.95E+09	4.13
dihydropteridine reductase	9	29.1	6.27E-93	2.15E+09	4.13
aldehyde dehydrogenase mitochondrial-like	8	22.5	3.21E-67	5.23E+08	4.05
cholinesterase 1-like	20	41.9	1.36E-241	1.91E+09	4.02
Purine nucleoside phosphorylase	12	61.5	1.32E-146	8.16E+08	3.97
small heat shock	5	24.4	2.12E-30	1.17E+09	3.97
troponin I	8	30.2	2.15E-110	5.84E+08	3.97
takeout-like	13	22.1	2.70E-95	9.39E+08	3.97
muscle-specific 20	9	19.1	1.46E-47	5.54E+08	3.78
cellular retinoic acid binding	29	44.9	0.00E+00	5.33E+10	3.77

argininosuccinate synthase	14	32	3.26E-82	1.01E+09	3.74
high mobility group D	4	9	1.77E-90	1.11E+09	3.74
uncharacterized protein Dmoj_GI19595	8	57.7	3.46E-179	1.07E+10	3.65
heat shock	16	29.2	1.29E-152	4.27E+09	3.64
Profilin	6	24.8	7.89E-90	9.73E+08	3.64
asteroid	8	32.5	7.54E-44	7.85E+08	3.62
immune-related Hdd1	19	28.2	7.32E-209	4.09E+09	3.57
antichymotrypsin-2-like isoform X2	9	21.5	1.83E-109	1.26E+09	3.56
ejaculatory bulb-specific 3-like	5	16.7	1.12E-97	3.61E+09	3.52
fibrous sheath CABYR-binding	11	37.9	2.32E-85	1.68E+09	3.46
aminoacrylate peracid reductase	5	36	2.31E-38	8.00E+08	3.35
staphylococcal nuclease domain-containing 1	11	21.4	8.04E-45	4.95E+08	3.16
ubiquitin carboxyl-terminal hydrolase isozyme L3	5	21.7	3.36E-37	3.91E+08	3.14
leukotriene A-4 hydrolase isoform X2	11	46.5	4.67E-148	1.45E+09	3.13
PREDICTED: uncharacterized protein LOC106129042	24	38	0.00E+00	4.14E+10	3.13
cytosolic non-specific dipeptidase	7	34.3	2.22E-85	6.68E+08	3.10
S-Adenosyl-L-homocysteine partial	2	10.2	1.22E-15	2.61E+08	3.08
C-1-tetrahydrofolate cytoplasmic isoform X2	4	77.3	8.26E-30	4.02E+08	3.03
glutathione S-transferase omega 1	7	44.3	2.06E-108	6.78E+08	2.92
troponin C	7	24.6	4.42E-81	3.70E+08	2.88
uncharacterized oxidoreductase TM_0325-like	8	28.4	1.92E-235	3.18E+08	2.82
phosphoglycerate mutase 1	7	14.1	6.98E-83	3.63E+08	2.82
probable transaldolase	9	20.7	1.44E-106	5.93E+08	2.78
ejaculatory bulb-specific 3-like	6	31.1	1.29E-32	7.59E+08	2.77
cytosolic non-specific dipeptidase	8	34.2	6.01E-34	3.70E+08	2.77
circadian clock-controlled -like	7	20.4	6.28E-38	2.91E+08	2.70
ecdysteroid-regulated 16 kDa -like	6	38	2.66E-52	5.87E+08	2.64
4-coumarate-- ligase 1-like	5	19.3	2.35E-30	4.16E+08	2.62
isopentenyl-diphosphate Delta-isomerase 1	6	21.3	2.40E-48	2.21E+08	2.55
uncharacterized oxidoreductase TM_0325-like	7	20.3	4.02E-72	3.15E+08	2.48
glutathione-specific gamma-glutamylcyclotransferase 2	6	15.6	1.85E-37	2.78E+08	2.37
fumarylacetoacetase	8	33.3	2.71E-34	1.54E+08	2.35
proliferation-associated 2G4	5	20.9	3.12E-31	2.17E+08	2.35
seroin-like isoform X2	5	18.9	1.55E-139	3.06E+09	2.28
ATPase inhibitor	3	11.6	8.88E-08	2.49E+08	2.28
acyl- -binding homolog	4	27.1	2.52E-23	1.13E+09	1.99
glyceraldehyde-3-phosphate partial	19	54.2	0.00E+00	1.32E+10	1.86
multiple inositol polyphosphate phosphatase 1-like	5	22.1	1.51E-20	3.77E+08	1.86
nucleoside diphosphate kinase	10	51.2	1.90E-115	2.79E+09	1.83
elongation factor 1-beta	7	34.2	1.98E-101	4.50E+08	1.76
hydroxypyruvate isomerase	15	36.3	9.02E-162	2.50E+09	1.76
Proactivator polypeptide	6	16.9	4.40E-13	2.33E+08	1.74
phosphotriesterase-related -like	8	23.3	1.23E-46	2.62E+08	1.71
glyoxalase domain-containing 4	4	16	5.06E-25	1.01E+08	1.67
L-threonine 3- mitochondrial	6	34.1	2.48E-11	1.50E+08	1.66
Prostaglandin reductase 1	7	27.6	2.55E-53	4.96E+08	1.57
chitin deacetylase 1	5	8.1	3.31E-26	1.69E+08	1.55
chitinase EN03 (imaginal disc growth)*	22	53.8	0.00E+00	1.39E+11	-1.50
probable salivary secreted peptide	7	50.7	5.52E-50	2.31E+09	-1.77
vanin 2 isoform X1	7	25.4	3.05E-50	5.24E+08	-1.79
homeobox 2-like isoform X4	33	67.9	0.00E+00	1.58E+10	-2.15
apolipophorins isoform X2*	6	36.9	2.42E-38	2.00E+10	-2.24
chymotrypsin-like elastase family member 2A	7	17.7	1.17E-41	4.45E+08	-2.30
serine protease 42-like	3	40.2	5.25E-24	4.10E+08	-2.41
probable salivary secreted peptide	3	14.5	7.38E-170	1.63E+09	-2.80
gloverin-like	2	57.7	1.94E-07	4.54E+08	-2.96
Peptidoglycan recognition	11	30.9	4.34E-90	1.12E+09	-3.28

Proteins shaded in grey at the end of the table were significantly down-regulated in abundance upon inoculation with Cu-DPPZ-Phen (**3**).

* Denotes protein also expressed in 2D PAGE analysis with a similar profile. Transferrin (-0.6 fold change), juvenile like binding hormone (-0.76 fold change) and 27 kDa hemolymph protein (-0.62 fold change) were also detected in exposure to Cu-DPPZ-Phen (**3**) relative to the solvent control and were also present in the 2D PAGE analysis in **Table 5.4**. Relative expression changes of proteins up regulated and down regulated after Cu-DPPZ-Phen (**3**) exposure. Peptides matched to the annotated protein, sequence coverage, PEP and mean LFQ intensities, with a t-test probability of $p \leq 0.05$ (N=4).

Table 5.11 Statistically significant differentially abundant (SSDA) proteins between exposure to Cu-Phen (**1**), Cu-DPQ-Phen (**2**) and Cu-DPPZ-Phen (**3**) in comparison to the negative control.

Protein annotation	**Relative expression to solvent control**		
	Cu-Phen (**1**)	Cu-DPQ-Phen (**2**)	Cu-DPPZ-Phen (**3**)
aldehyde dehydrogenase mitochondrial-like	2.19	7.16	8.05
Selenium-binding 1	2.02	6.62	7.8
lambda-crystallin homolog	4.89	6.76	7.55
tubulin beta chain	4.64	6.37	7.41
D-arabinitol dehydrogenase 1-like	5.24	5.8	6.85
elongation factor 1-alpha	6.19	5.57	6.63
15-hydroxyprostaglandin dehydrogenase [NAD(+)]-like	2.96	5.05	6.49
cytoplasmic A3a	1.28	5.74	6.4
N-acetylneuraminate lyase-like	5.17	5.69	6.38
serine cytosolic isoform X1	0.63	5.48	6.36
multifunctional ADE2	5.13	5.13	6.19
cytosolic malate partial	2.81	4.97	6.16
D-3-phosphoglycerate dehydrogenase	3.05	5.27	6.04
glutathione S-transferase-like	5.18	4.65	5.99
Tubulin alpha chain	4.68	4.6	5.9
triosephosphate isomerase	4.92	4.96	5.87
glutamine synthetase 2 cytoplasmic-like	3.61	5	5.41
probable enoyl- mitochondrial	1.09	4.61	5.31
glutathione S-transferase 1-1-like	2.78	4.6	5.22
glyceraldehyde-3-phosphate partial	3.14	4.6	5.04
fructose-bisphosphate aldolase isoform X1	4.59	4.14	4.94
superoxide dismutase [Mn] mitochondrial	-1.52	3.53	4.7
trans-1,2-dihydrobenzene-1,2-diol dehydrogenase-like	4.69	4.17	4.7
bifunctional purine biosynthesis PURH	1.75	3.7	4.56
aminopeptidase	1.39	3.34	4.39
heat shock 90	3.39	3.36	4.33
enolase	3.49	2.95	4.32
L-threonine ammonia-lyase-like	4.08	3.3	4.27
arginine partial	4.02	2.04	4.24
aliphatic nitrilase	3.61	3.19	4.19
dihydropteridine reductase	6.24	3.4	4.13
Peptidyl-prolyl cis-trans isomerase	3.03	3.12	4.13
cholinesterase 1-like	6.1	3.64	4.02
Purine nucleoside phosphorylase	3.49	1.96	3.97
cellular retinoic acid binding	5.01	3.06	3.77
argininosuccinate synthase	1.28	2.66	3.74
uncharacterized protein Dmoj_GI19595	2.25	1.91	3.65
immune-related Hdd1	4.43	3.58	3.57
ejaculatory bulb-specific 3-like	2.05	3.68	3.52
fibrous sheath CABYR-binding	5.16	2.89	3.46
leukotriene A-4 hydrolase isoform X2	2.13	3.26	3.13
PREDICTED: uncharacterized protein LOC106129042	3.89	3.23	3.13
ecdysteroid-regulated 16 kDa -like	2.54	3.23	2.64
isopentenyl-diphosphate Delta-isomerase 1	-1.01	2.13	2.55
heat shock	1.98	2.2	2.4
proliferation-associated 2G4	2.61	1.98	2.35
seroin-like isoform X2	-2.06	1.37	2.28
actin	1.63	4.22	1.99
nucleoside diphosphate kinase	-0.66	0.79	1.83
chitin deacetylase 1	6.88	1.52	1.55
contig19736_1_exp_NA	1.43	-1.62	-1.82
homeobox 2-like isoform X4	3.15	-1.33	-2.15
probable salivary secreted peptide	2.9	-1.72	-2.8
gloverin-like	0.92	-2.5	-2.96
Peptidoglycan recognition	2.03	-4.02	-3.28
glutathione S-transferase 1-like	5.11	-	4.67
Profilin	3.18	-	3.64

aminoacrylate peracid reductase	-0.69	-	3.35
cytosolic non-specific dipeptidase	2.23	-	3.1
circadian clock-controlled -like	3.01	-	2.7
4-coumarate-- ligase 1-like	1.16	-	2.62
multiple inositol polyphosphate phosphatase 1-like	1.14	-	1.86
isocitrate partial	2.7	-	1.48
esterase FE4-like	5.06	-	-1.18
thioredoxin	-	3.87	4.81
rab GDP dissociation inhibitor alpha	-	3.15	4.55
probable phosphoserine aminotransferase	-	4.23	4.46
small heat shock	-	3.46	3.97
takeout-like	-	2.33	3.97
high mobility group D	-	2.27	3.74
staphylococcal nuclease domain-containing 1	-	2.13	3.16
glutathione S-transferase omega 1	-	2.07	2.92
fumarylacetoacetase	-	1.57	2.35
hydroxypyruvate isomerase	-	1.1	1.76
apolipophorins isoform X2*	-	-4.15	-0.72
chitinase EN03 (imaginal disc growth)*	-	-0.72	-1.5
translationally controlled tumor	5.64	-	-
cysteine ase inhibitor precursor	2.71	-	-
gustatory receptor candidate 59	2.5	-	-
chemosensory	2.48	-	-
Serpin-2	-	2.00	-
muscle-specific 20	-	-	5.73
peroxiredoxin- mitochondrial	-	-	4.96
tropomyosin-1 isoform X1	-	-	4.22
troponin T	-	-	4.18
annexin B9 isoform X4	-	-	4.15
troponin I	-	-	3.97
asteroid	-	-	3.62
antichymotrypsin-2-like isoform X2	-	-	3.56
ubiquitin carboxyl-terminal hydrolase isozyme L3	-	-	3.14
S-Adenosyl-L-homocysteine partial	-	-	3.08
C-1-tetrahydrofolate cytoplasmic isoform X2	-	-	3.03
troponin C	-	-	2.88
phosphoglycerate mutase 1	-	-	2.82
probable transaldolase	-	-	2.78
ATPase inhibitor	-	-	2.28
acyl- -binding homolog	-	-	1.99
Proactivator polypeptide	-	-	1.74
phosphotriesterase-related -like	-	-	1.71
L-threonine 3- mitochondrial	-	-	1.66
Prostaglandin reductase 1	-	-	1.57
vanin 2 isoform X1	-	-	-1.79
chymotrypsin-like elastase family member 2A	-	-	-2.3
serine protease 42-like	-	-	-2.41

Relative fold changes are given for each test exposure in comparison to the solvent control.
- denotes level of expression that was either absent or not detected.
Shaded proteins were of particular interest and made a strong contribution to the discussion.
Fold changes of < 1.5 were included when expression in other test exposures was ≥ 1.5 fold change.
* Denotes protein also expressed in 2D PAGE analysis with a similar expression profile.

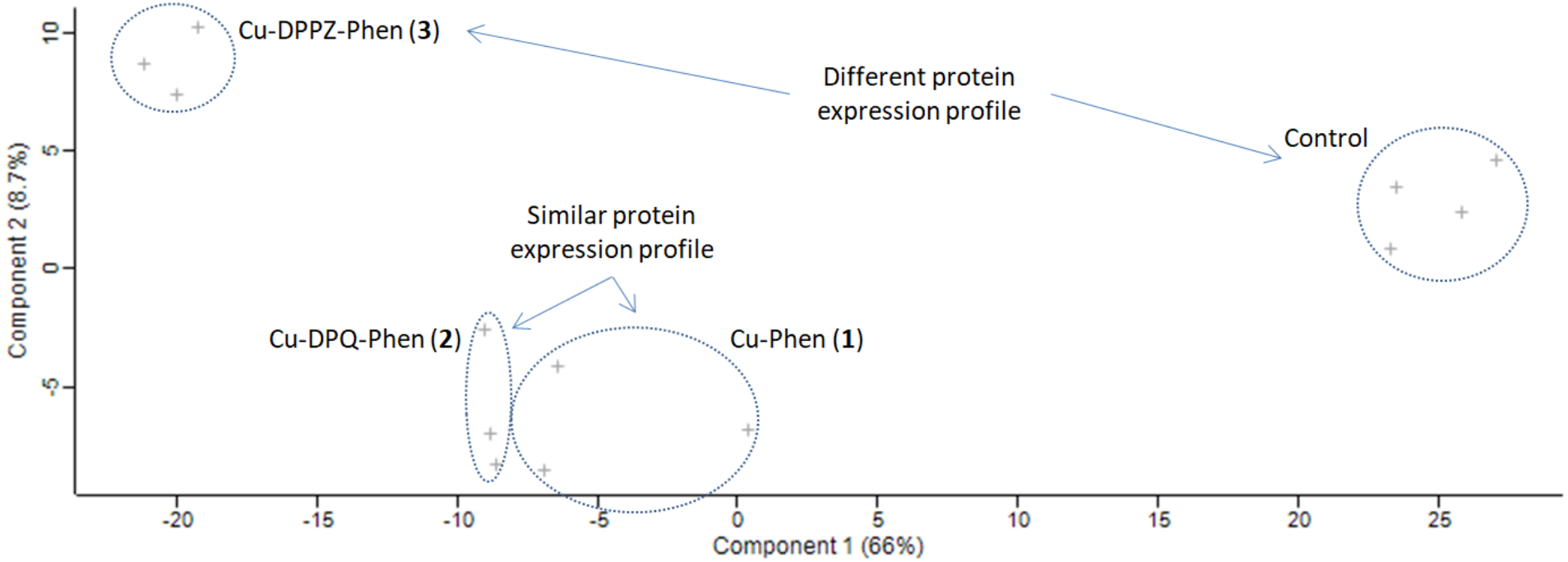

Fig. 5.9 Principle component analysis (PCA) of haemolymph proteomic profiles of larvae inoculated with Cu-Phen (**1**), Cu-DPQ-Phen (**2**) and Cu-DPPZ-Phen (**3**) versus the solvent control. PCA of four replicates for the solvent control and three replicates for each of the test exposures. Enclosures define the different experimental conditions.

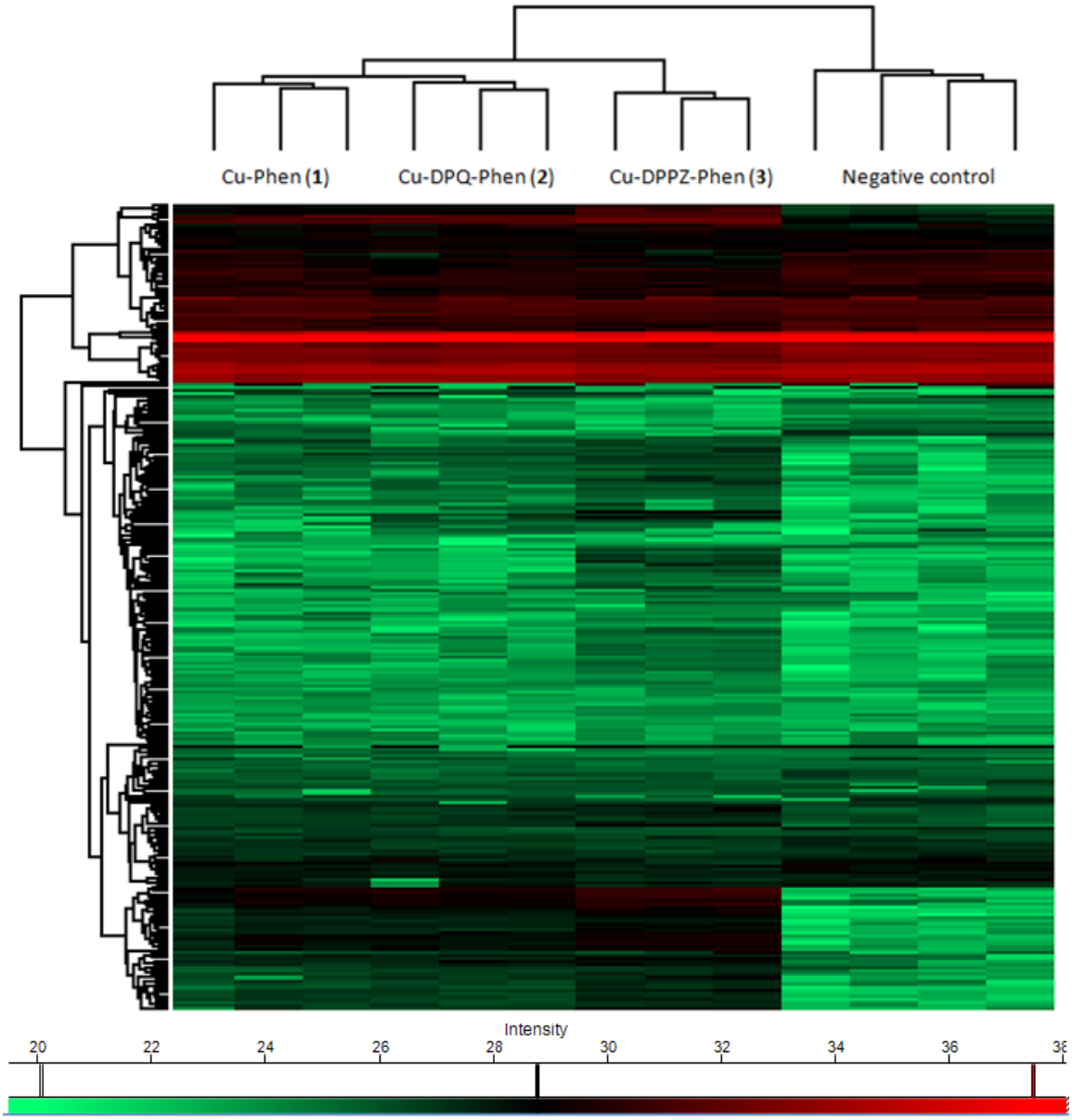

Fig. 5.10 Hierarchical clustering of haemolymph profiles of larvae inoculated with Cu-Phen (**1**), Cu-DPQ-Phen (**2**) and Cu-DPPZ-Phen (**3**) versus the solvent control. Heat map generated using mean protein expression values of statistically significant differentially abundant proteins. Four replicates for the solvent control and three replicates for each of the test exposures. Samples are clustered through columns.

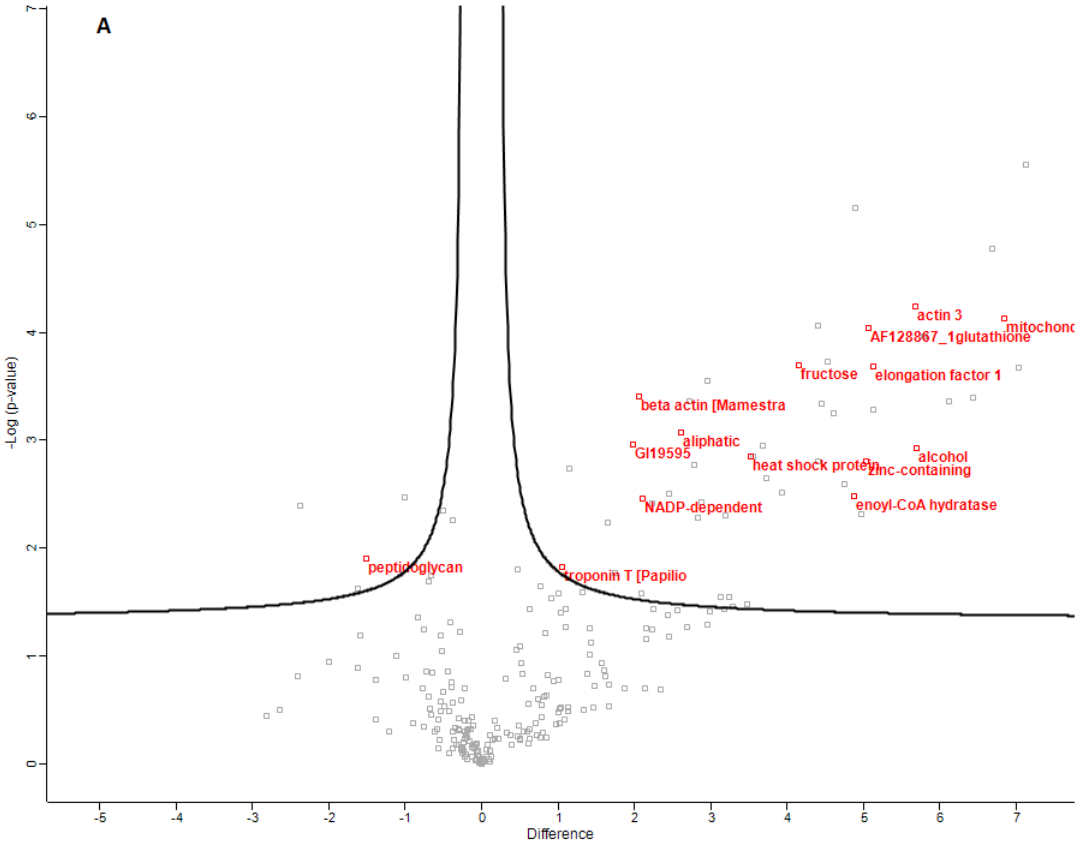
A
-Log (p-value)
Difference
actin 3
mitochond
AF128867_1glutathione
fructose
elongation factor 1
beta actin [Mamestra
aliphatic
GI19595
heat shock protein
alcohol
zinc-containing
NADP-dependent
enoyl-CoA hydratase
peptidoglycan
troponin T [Papilio

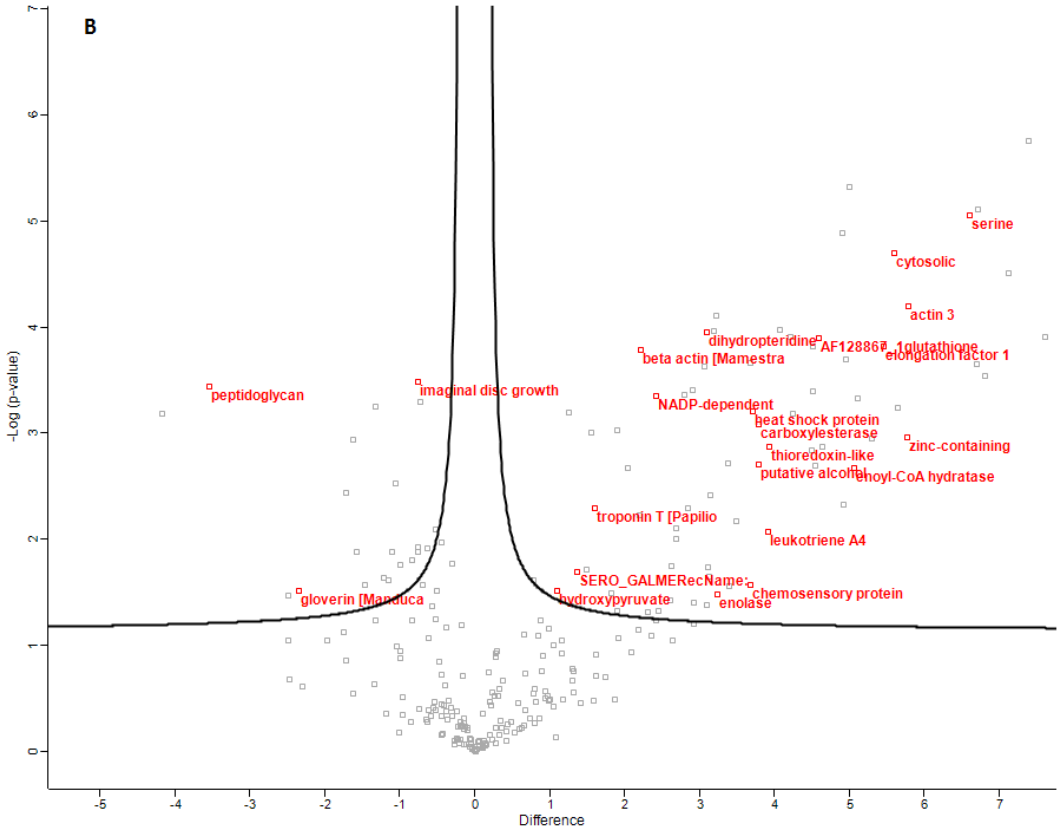
B
-Log (p-value)
Difference
serine
cytosolic
actin 3
dihydropteridine
AF128867_1glutathione
elongation factor 1
beta actin [Mamestra
peptidoglycan
imaginal disc growth
NADP-dependent
heat shock protein
carboxylesterase
zinc-containing
thioredoxin-like
putative alcohol
enoyl-CoA hydratase
troponin T [Papilio
leukotriene A4
SERO_GALMERecName:
gloverin [Manduca
hydroxypyruvate
enolase
chemosensory protein

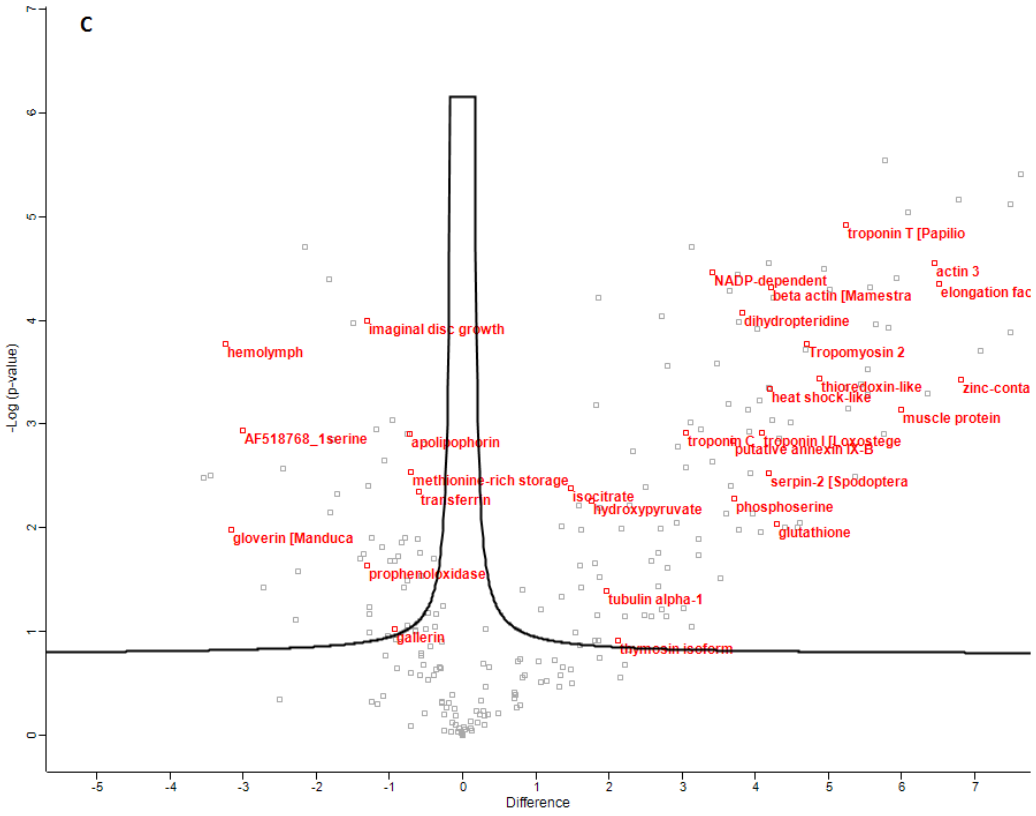

Fig. 5.11 Volcano plots highlighting proteins altered in abundance in haemolymph of *G. mellonella* larvae following inoculation with Cu-Phen (**1**) (**A**), Cu-DPQ-Phen (**2**) (**B**) and Cu-DPPZ-Phen (**3**) (**C**). Plots represent protein intensity differences ($-\log_2$ mean intensity difference (difference)) and significance in differences (-log P-value) based on a two sided t-test. Points above the curve are considered statistically significant ($p < 0.05$). Points above the line and to the right are present at higher levels of abundance in the test exposure and have a fold change ≥ 1.5. Points above the line and to the left are present at lower levels of abundance in the test exposure and have a fold change ≥ 1.5. Proteins annotated represent an example of differentially expressed proteins following inoculation with the test complex in comparison to the solvent control. Volcano plots are based on post imputated data.

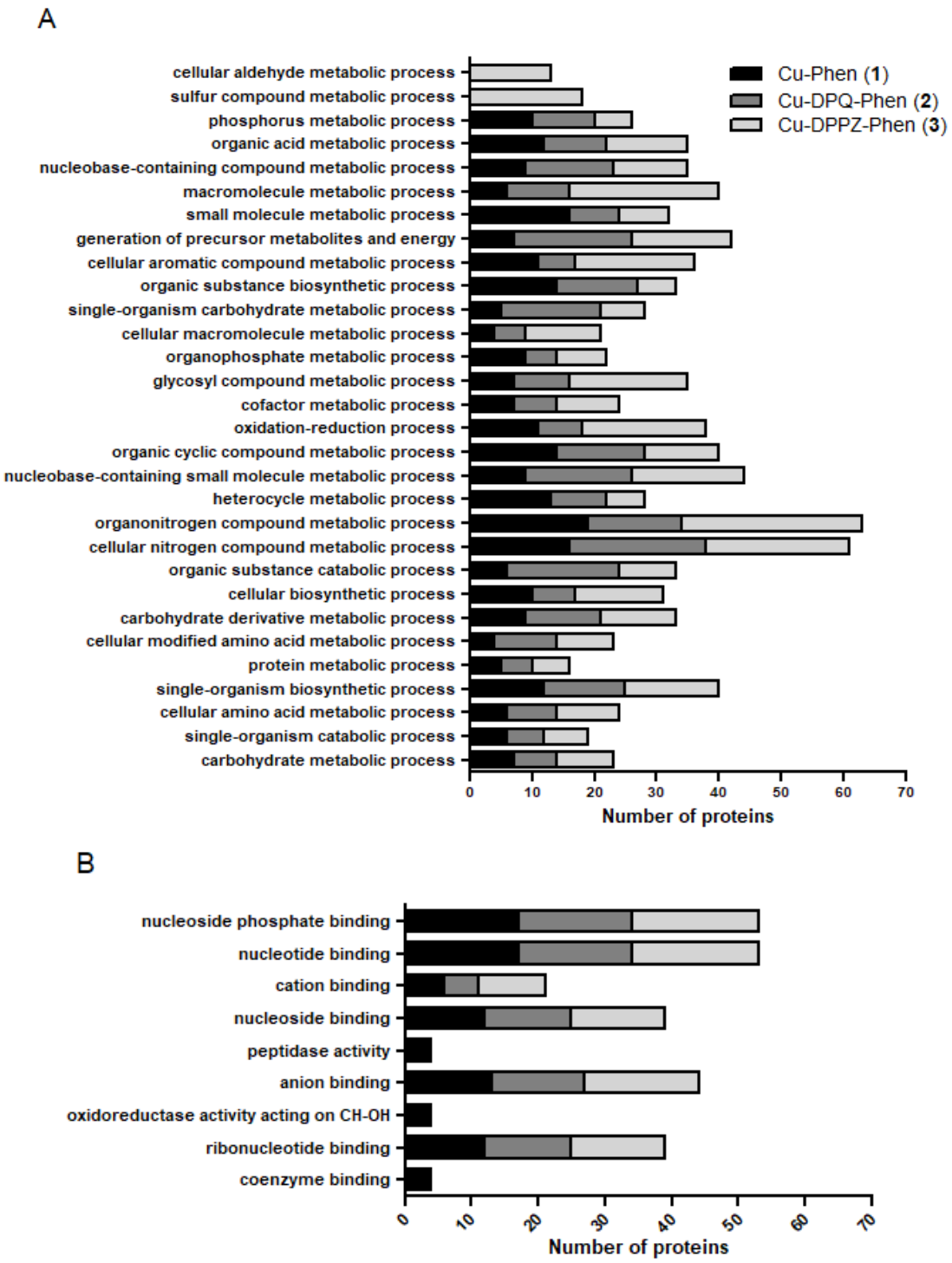

Fig. 5.12 Bar chart showing the different number of proteins present in a test exposure that is associated with selected biological processes **(A)** and molecular functions (**B**). Comparative bar charts represent level 4 ontology.

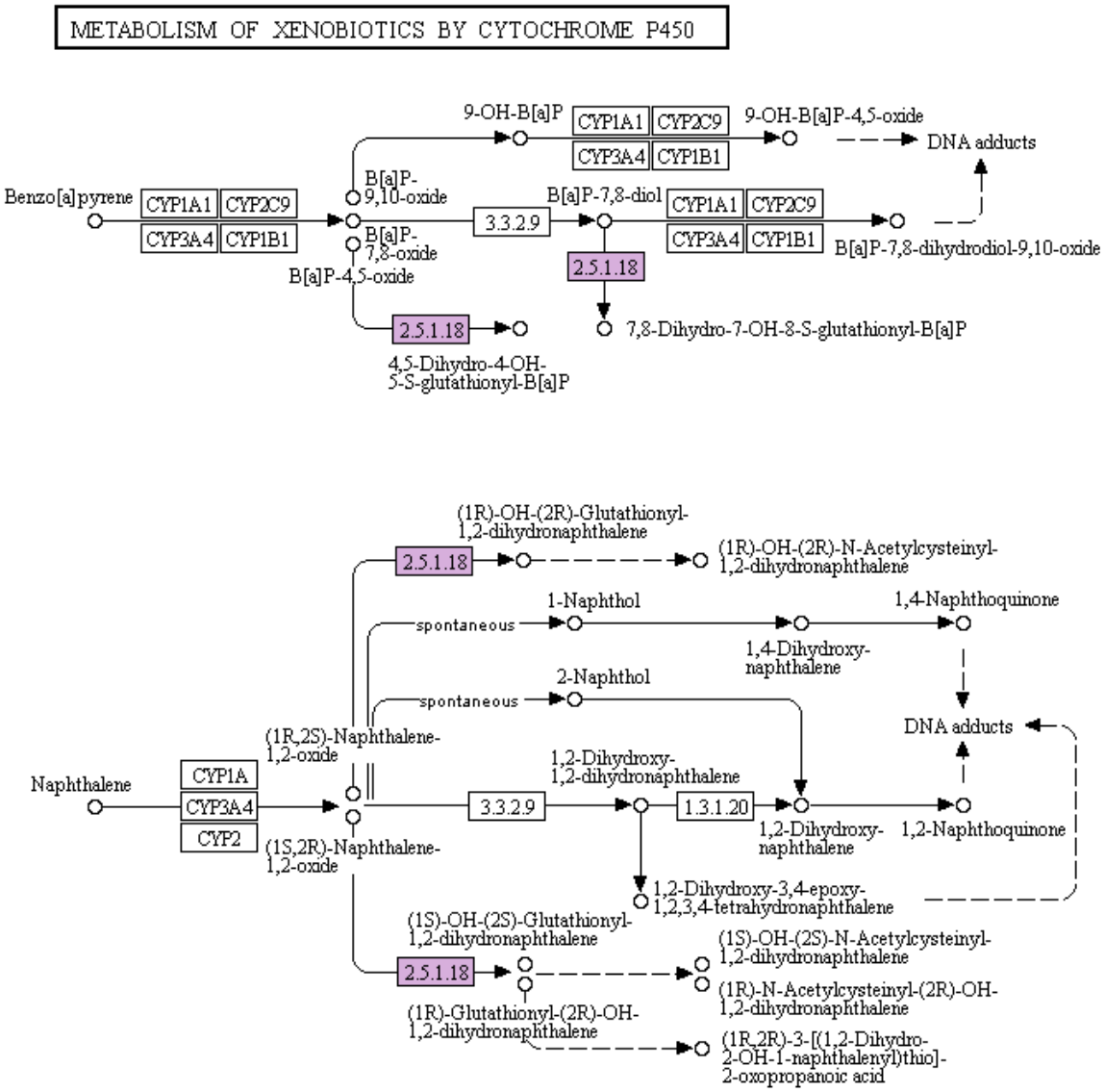

Fig. 5.13 KEGG analysis of the metabolism of selected xenobiotics by cytochrome P450. Glutathione S-transferase (2.5.1.18) (pink) is shown to be significantly upregulated in all test exposures.

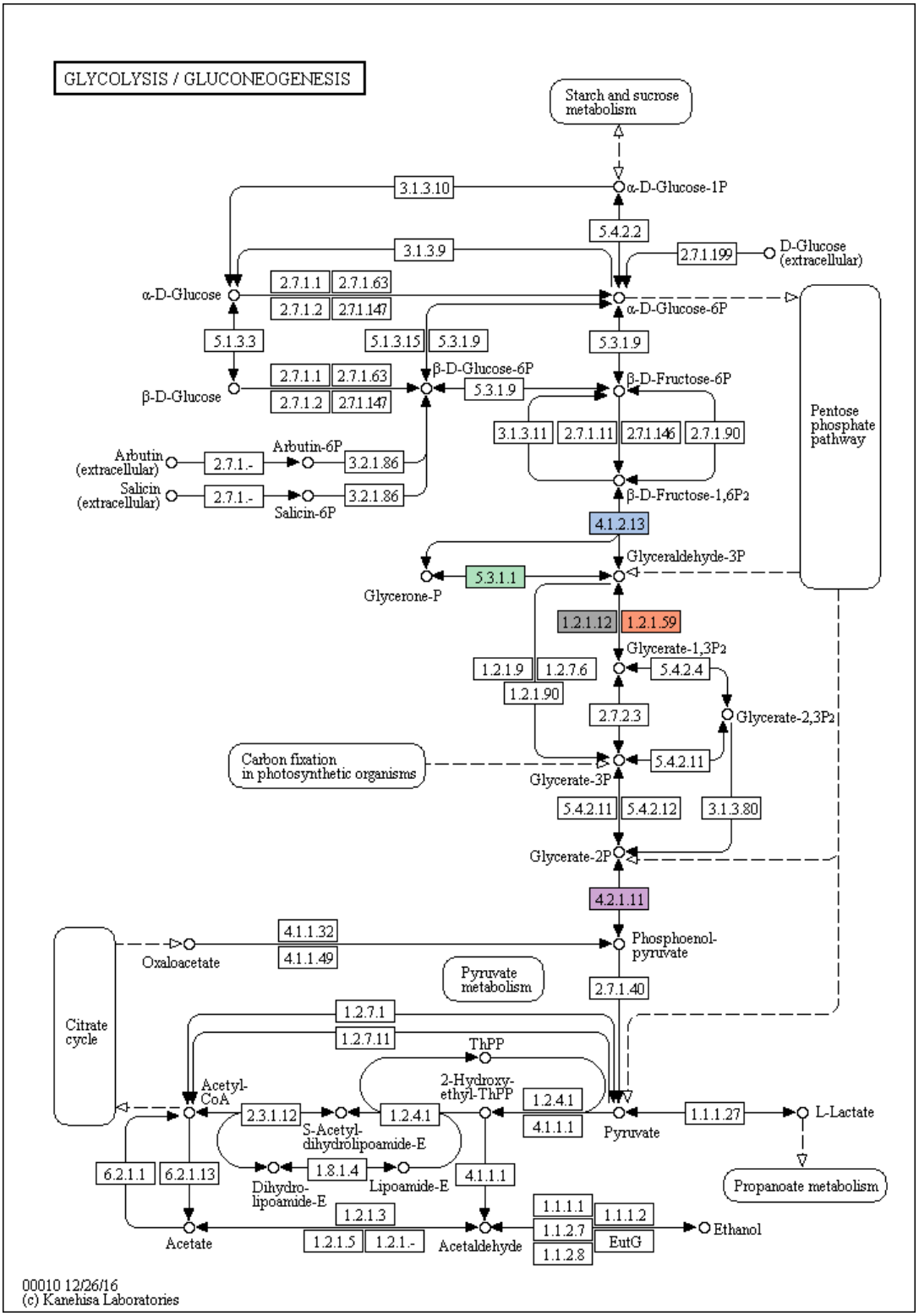

Fig. 5.14 KEGG analysis of significantly upregulated proteins in glycolysis/ gluconeogenesis (highlighted: blue, green, grey, orange and pink) between all test exposures. Cu-DPQ-Phen (**2**) shows no upregulation of 4.2.1.11 (phosphopyruvate hydratase) (pink).

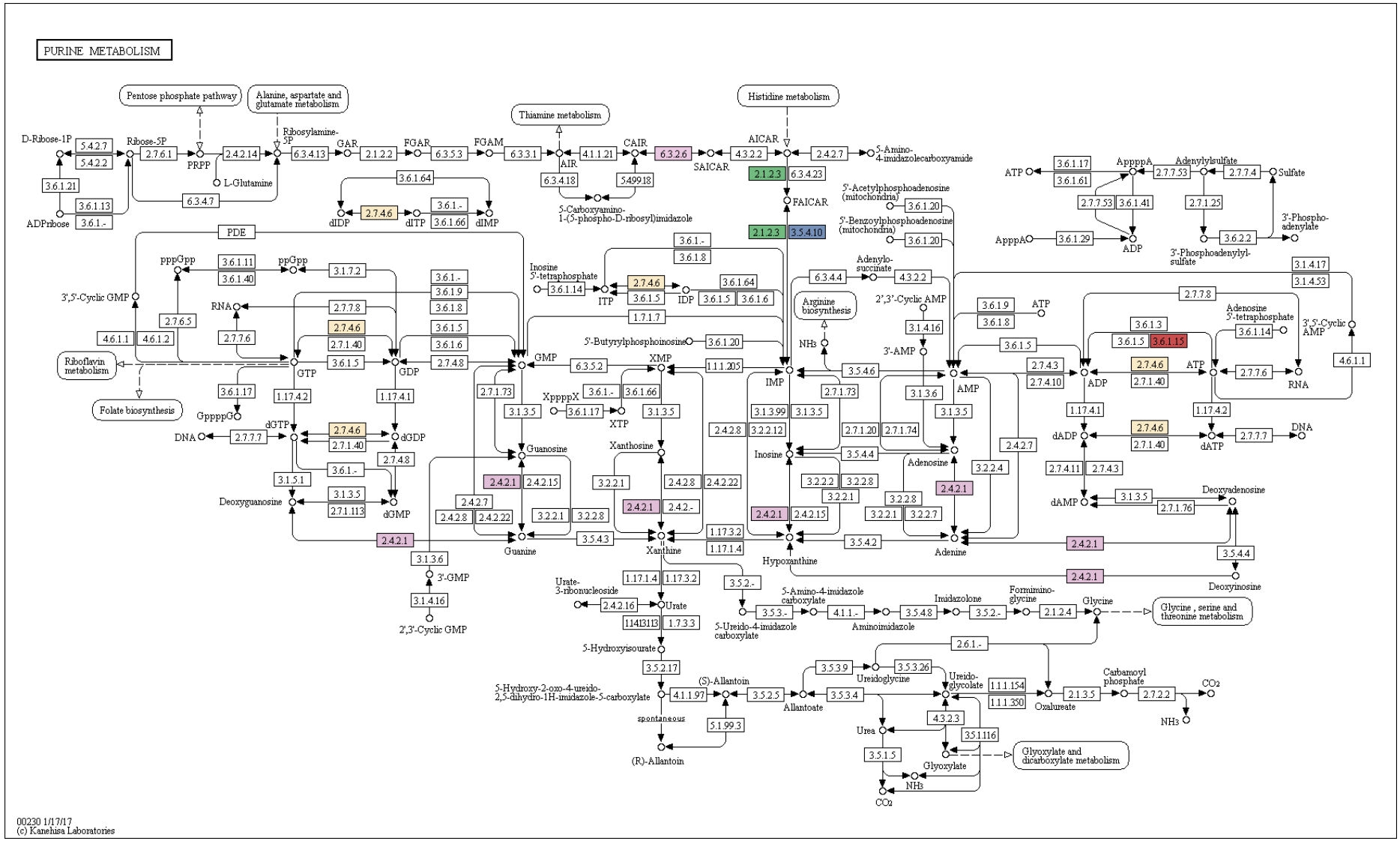

Fig. 5.15 KEGG analysis of significantly upregulated proteins in purine metabolism (highlighted: pink, yellow, blue and red).

5.4 Discussion

The aim of this study was to assess the response of *G. mellonella* larvae to novel copper phenanthroline-phenazine complexes as a means to determine their biological mode of action and therefore developmental potential. Larval mortality decreased as the ligated phenazine ligand in the $[Cu(Phen)(N,N')]^{2+}$ model was extended (Cu-Phen (**1**) > Cu-DPQ-Phen (**2**) > Cu-DPPZ-Phen (**3**)). The mortality assay demonstrates that the complex series had superior toxicity at all timepoints to cisplatin with the exception of Cu-DPPZ-Phen (**3**) which, in comparison to Cu-Phen (**1**) and Cu-DPQ-Phen (**2**) was relatively non-toxic. Previous studies have confirmed the enhanced toxicity of copper complexes in comparison to platinum agents in *G. mellonella* larvae (McCann *et al.* 2012). *G. mellonella* in this study function essentially as a 'normal tissue' model in the investigation of basic *in-vivo* biological responses and provide information regarding the potential effects and targeting information for mammalian *in-vivo* models.

Immune priming often plays a large role in the larval response to foreign bodies, either chemical or pathological and alterations in the larval haemocyte density is one of the earliest markers of the invertebrate immune response (Browne 2014). Both controls and complex series induced a non-significant increase in the haemocyte response after complex exposure, which indicates that the novel Cu(II) complex series does not elicit a generalised cellular immune response. The non-stimulation of a non-specific immune response was also shown with the evaluation of the antimicrobial effects of 1,3-dibenzyl-4,5-diphenyl-imidazol-2-ylidene silver(I) acetate (SBC3) in *G. mellonella* post infection with *Staphylococcus aureus* and *Candida albicans* (Browne *et al.* 2014). In contrast, other studies have shown a priming of the larval immune response with biologically derived echinocandines producing a resistance to subsequent infection

(Kelly and Kavanagh 2011). The priming of the immune response has been previously observed through amplification of immune-related genes (Volkoff *et al.* 2003; Bergin *et al.* 2006; Wojda and Jakubowicz 2007). This study in contrast shows significant decreases in IMPI and transferrin gene expression after exposure to the metallo-agents compared to the solvent control. Transferrin is typically increased following infection and based on functional homology with mammalian systems, sequesters biologically active iron from circulation to prevent it from being used as a microbial growth factor. IMPI was first identified in *G. mellonella* and is responsible for breaking down metal based proteases released by microbial pathogens (Wedde *et al.* 1998). Significantly, across the complex series there is no increase in either of these antimicrobial factors, indicating that at a cellular and mRNA level, the Cu(II) complexes are not indicating a larval immune response in a similar fashion to carbene silver(I) acetate (SBC3) exposure (Browne *et al.* 2014). In contrast, the larval exposure to caspofungin induces an immune priming reaction (Kelly and Kavanagh 2011).

In this study, LFQ proteomics produced a high resolution analysis of the larval response to the complex series with the possibility of gaining an insight into the potential response in the mammalian system. Two-dimensional polyacrylamide gel electrophoresis (2D-PAGE) confirms many of the downregulated proteins using the LFQ proteomics method (**Table 5.7**) and supports the decrease in the immune related genes and the non-significant increase in the larval haemocyte response. 2D-PAGE analysis showed that imaginal disc growth factor and apolipophorin was downregulated in larvae treated with either Cu-DPQ-Phen (**2**) or Cu-DPPZ-Phen (**3**). Additionally, transferrin, juvenile like binding hormone and 27 kDa hemolymph protein was downregulated after exposure of larvae to Cu-DPPZ-Phen (**3**). All larvae were exposed

to the 24 h LD_{50} value of the 3 complexes but have a different number of proteins significantly altered in abundance.

GST is a family of phase II detoxification enzymes that catalyses the conjugation of glutathione to a wide variety of endogenous and exogenous electrophilic compounds by making the exogenous molecule more hydrophilic, which aids in its elimination (Enayati *et al.* 2005; Bartolini *et al.* 2015). Studies have shown GST abundance to be elevated during oxidative stress in the mammalian system (Board and Menon 2013). Evidence has also linked the GST isozymes to anti-cancer drug resistance (Townsend and Tew 2003). The action of copper N-(2-hydroxy acetophenone) glycinate has shown promise in overcoming doxorubicin generated GST and MDR (Majumder *et al.* 2006). KEGG analysis of the metabolism of xenobiotics by cytochrome P450 (**Fig. 5.13**) highlighted the involvement of GST in detoxification of benzo-[a]-pyrene and napthalene both of which contain polycyclic aromatic rings which are present in the phenazine ligand in Cu-DPQ-Phen (**2**) and Cu-DPPZ-Phen (**3**). The upregulation of GST is also involved in the detoxification of cyclophosphamide and ifosfamide which are key therapeutic alkylating agents. Cu-Phen (**1**), Cu-DPQ-Phen (**2**) and Cu-DPPZ-Phen (**3**) have previously been shown to have nuclease cleaving ability (Molphy *et al.* 2014), and potentially interact with DNA through intercalation properties at the minor groove as seen with the ruthenium complex Λ-$[Ru(phen)_2dppz]^{2+}$ (Niyazi *et al.* 2012).

Cu-DPQ-Phen (**2**) and Cu-DPPZ-Phen (**3**) have previously been shown to generate excellent SOD mimetic activity with a progressive Fenton reaction matching the cadence of the chemical nuclease capacity against pUC19 DNA (Molphy *et al.* 2014). Mitochondrial aldehyde dehydrogenase and mitochondrial superoxide dismutase have been shown to be closely associated with oxidative stress (McCord and Fridovich 1988;

Daiber 2004). The upregulation of activity of these proteins in both the Cu-DPQ-Phen (**2**) and Cu-DPPZ-Phen (**3**) treated larvae may be associated with increased oxidative stress. Aldehyde dehydrogenase in mammalian cells has been associated with tolerance to increased organic nitrates (Chen *et al.* 2002), which are known to produce oxidative stress. The upregulation of both aldehyde dehydrogenase and superoxide dismutase in the Cu-DPQ-Phen (**2**) and Cu-DPPZ-Phen (**3**) treated larvae rather than just the upregulation of aldehyde dehydrogenase in the Cu-Phen (**1**) may indicate that oxidative stress plays a stronger mechanistic role in the secondary phenazine ligands despite the lower LD_{50} value. Isocitrate dehydrogenase is only upregulated in Cu-Phen (**1**) exposure while malate dehydrogenase is only upregulated in Cu-DPQ-Phen (**2**) and Cu-DPPZ-Phen (**3**) treated larvae. These dehydrogenase are closely linked to the TCA cycle and have an effect on NAD+/ NADH ratio, which has been the subject of renewed interest due to its capacity to alter/ ameliorate effects on aging and other complex disease phenotypes (Yang and Sauve 2016). An additional dehydrogenase present at increased levels of abundance in all exposures is 15-hydroxylprostaglandin dehydrogenase[NAD(+)] which has been shown to suppress eicosanoids such as prostaglandins and liposin, previously demonstrated to have anticancer properties (Tuncer and Banerjee 2015).

KEGG analysis of glycolysis/ gluconeogenesis (**Fig. 5.14**) indicated upregulation of fructose bisphosphate, triose phosphate isomerase, glyceraldehydes-3-phosphate dehydrogenase and phosphopyruvate hydratase (enolase) after exposure to all complexes. Previous studies have shown enolase to become up regulated in response to cellular stress (Ji *et al.* 2016). Based on the study conducted by Molphy *et al.* (2014), Cu(II) phenanthroline-phenazine complexes showed chemical nuclease activity in

pUC19 plasmid DNA. Chemical nuclease action on larval DNA may have contributed to cellular stress and related alterations in carbohydrate metabolism. Other proteins highlighted during this analysis were fructose-bisphosphate aldolase, triose-phosphate isomerase, glyceraldehyde-3-phosphate dehydrogenase. Glyceraldehyde-3-phosphate dehydrogenase is involved in the conversion of glyceraldehydes-3-phosphate to D-glycerate. The non-enzymatic elimination of phosphate groups from glyceraldehyde-3-phosphate can lead to the production of the cytotoxic methylglyoxal which is known to be a progenitor of advanced glycation end-products (Allaman *et al.* 2015).

Purine metabolism from KEGG analysis (**Fig. 5.15**) indicated increased abundance of regulatory enzymes SAICAR, AICAR and other purine support enzymes. Changes in purine metabolism as a result of cellular stress states have promoted increased interest recently as a potential therapeutic target for new drug development (Chitrakar *et al.* 2017). Among some of the new studies is evidence for the formation of a dynamic multi-enzyme complex (purinosome) proximal to the mitochondria and microtubules (Pedley and Benkovic 2017). The formation of this multimeric protein complex has been associated with the depletion of purines and the upregulation of heat shock 90 protein (HSP90) which aids in higher order protein structure (Chitrakar *et al.* 2017). Based on the KEGG analysis, HSP90 was observed at higher levels of abundance in larvae treated with all test complexes highlighting the potential involvement of the newly described purinosome in the mechanistic response to nuclease active drugs due to accelerated DNA breakdown from the cleavage activity of the metal complexes.

The GO analysis performed at level 4 ontology showed that for each of the grouped biological processes the percentage of proteins involved was largely unchanged between

the complex series when the total number of proteins was taken into account. The number of proteins in the following groups was markedly elevated: cellular nitrogen compound metabolic process, organonitrogen compound metabolic process, heterocyclic metabolic process, organic cyclic compound metabolic process, organic substance biosynthetic process and small molecule metabolic process associated proteins. The increased abundance of proteins associated with the complex series and in particular, Cu-DPQ-Phen (**2**) and Cu-DPPZ-Phen (**3**) are accompanied by a broad upregulation in detoxification and degradation pathways. The increased abundance of nitrogen containing, heterocyclic and small molecule related metabolism most likely reflects the cellular detoxification response to the complexes which peaks upon administration with Cu-DPQ-Phen (**2**) and Cu-DPPZ-Phen (**3**). The GO analysis of molecular function at level 4 ontology showed an elevated group of proteins indicative of DNA binding by all the test complexes; nucleotide binding and nucleoside phosphate binding. The upregulated activity of these groups of proteins may reflect an increased association with DNA damage and potential repair complexes. Radical hydroxyl attack is believed to be an effect of these complexes owing to their previously established Fenton chemistry (Molphy *et al.* 2014). The groups of protein associated with co-enzyme binding and oxidoreductase action on CH-OH were associated only with Cu-Phen (**1**) and with none of the other test complexes. Oxidoreductase and co-enzyme binding may be associated with the energy status of the organisms, with specific regard to the mitochondria where electron transfer plays a critical role in the homeostasis of respiratory complexes (Jungwirth *et al.* 2012).

Concluding remarks

Since the immune system of *G. mellonella* bears structural and functional similarities to the innate immune system of mammals, these larvae provide a vital pre-mammalian *in-vivo* screening method in which to evaluate system wide changes in response to metallo-drugs (Kellett *et al.* 2011b; McCann *et al.* 2012; Browne *et al.* 2014). For that reason, these insects were employed in this study to establish the *in-vivo* toxicity, immune related gene expression and proteomic effects induced by the novel Cu(II) phenanthroline-phenazine complex series without the necessity of mammalian testing. The immunogenicity of a therapeutic lead is an important consideration in the future development process. This model provides a basic analysis of the innate and humoral response and informs development and testing at the mammalian *in-vivo* level.

This investigation showed that the extension of the phenazine π-backbone within the complex scaffold resulted in a decrease in both mortality and immune response in the larval model with the trend following Cu-Phen < Cu-DPQ-Phen < Cu-DPPZ-Phen. Interestingly, this trend in reactivity is in contrast to previous studies performed where enhanced nuclease activity, DNA binding and thermal melting stability were governed by the extended phenazine π-framework (Devereux *et al.* 2005; Slator *et al.* 2016).

The label free quantitation (LFQ) mass spectrometry method produced a high resolution assessment of the proteomic changes occurring in the larvae in response to test complexes allowing for gene ontology (GO) analysis of both biological and molecular functions to be performed. The results indicated a prominent metabolic and detoxification response which may provide an opportunity to develop drug targeting to

this region but also to utilise the larval model to evaluate future therapeutic and targeting improvements.

Overall, the analysis of these changes provides an additional evaluative tool for the synthetic process in medicinal inorganic chemistry. The results presented here highlight the detoxification, stress induction and metabolic proteins which have characterised the larval response to the complex series and provide a valuable insight into their likely effect in mammals.

Chapter 6: General Discussion

The development of metal-based drugs as alternative cancer therapeutics to cisplatin is a promising area of pharmaceutical development. The success of the platinum based drug cisplatin proved to be one of the major breakthroughs in chemotherapeutic treatment with therapeutic activity across a large range of solid tumours, significantly improving patient survival rates over recent decades. However, the many associated side effects, toxicities and cellular drug resistance have limited the long-term use in cancer patients. This limitation has accelerated the development of alternative metal-based drugs utilising different transition metals and ligands with the goal of meeting or exceeding the therapeutic activity of cisplatin, reducing or eliminating the adverse side-effects and removing the possibility of drug resistance, common to platinum therapies. The novel copper(II) phenanthroline scaffolds utilising phenazine π-backbone extensions has permitted customizable DNA intercalation capability along with the potent nuclease activity of copper(II) phenanthroline making them a strong therapeutic candidate. However, the biological modes of action of these drugs were unknown and therefore this study explored these mechanisms underlying their potential therapeutic response in cancer cells.

The research used a range of *in-vitro* mammalian cells lines representing tumourigenic tissues; members of the NCI-60 therapeutic developmental panel and platinum resistant cell lines established the therapeutic cytotoxic values over both 24- and 48- h. The use of cisplatin sensitive and resistant cell lines allowed for the identification of activity of the Cu(II) phenanthroline-phenazine complexes that far exceeded cisplatin in specific cisplatin resistant SKOV-3, and A2780/ Cis cell lines. The activity profile of the Cu(II) phenanthroline-phenazine complexes across the range of cell lines demonstrated strong activity in the Cu-Phen (**1**) and Cu-DPQ-Phen (**2**) complexes. **Figure 6.1** provides a

summary of the biological effect of the Cu(II) phenanthroline-phenazine complexes in both cisplatin sensitive and resistant cell lines. The Cu(II) complexes demonstrate a greater capacity to initiate DNA DSB formation, MoMP decay, mitochondrial related proteases transcription, mitochondrial fission/ fusion processes, increased apoptosis and increased expression of metabolic related proteins. Interestingly the DNA DSB marker γH2AX demonstrated higher levels of DSB formation in the cisplatin resistant, SKOV-3 (**Fig. 6.1**). This coupled with the increased activity of apoptosis in the resistant cell lines compared to the sensitive cell lines after exposure to the Cu(II) phenanthroline-phenazine complexes demonstrated that an alternative mechanism of action to the clinical drug control, cisplatin was responsible for their cytotoxic activity with the mitochondrial being a vital component of the intrinsic apoptotic process. The work described in Chapter 5 demonstrated that increased MoMP decay was generally observed in the resistant cell lines and was coupled with increased activity of mitochondrial protease (CLPP, LON, SPG7 and YME1L1) and fission/fusion (DRP1, MFN1, MFN2 and OPA1) regulators (**Fig. 6.1**). The loss of the mitochondrial outer membrane potential is strongly associated with mitochondrial toxicity and the activation of the intrinsic apoptotic pathway. The upregulation of mitochondrial proteases (CLPP, LON, SPG7 and YME1L1) and fission/fusion (DRP1, MFN1, MFN2 and OPA1) regulators may indicate that the Cu(II) phenanthroline-phenazine complexes have a role in disrupting mitochondrial protein homeostasis through oxidative damage which resulted in cellular apoptosis. The work described in Chapter 3 characterised the resultant proteome from the exposure of the Cu(II) phenanthroline-phenazine complexes to both a cisplatin sensitive and resistant cell lines. Both sensitive and resistant cell lines induced common increases in metal sequestration (Metallothionein-2, -1X), heat shock (HSP70) and ribosomal (40S) proteins however metabolic proteins

(glycolysis/ gluconeogenesis, fatty acid synthesis, purine metabolism) tended to dominate the repertoire of the resistant cells, potentially indicating the response of the cell to its energy status brought about by exposure to the Cu(II) phenanthroline-phenazine complexes (**Fig. 6.1**). The work described in Chapter 4 used the *in-vivo* Lepidoptera model, *G. mellonella* to examine the activity of Cu-Phen (**1**), Cu-DPQ-Pen (**2**) and Cu-DPPZ-Phen (**3**). Importantly the copper complexes demonstrated higher toxicity in the larvae than cisplatin, which correlated with the results from the mammalian cell lines. The proteomics study demonstrated that metabolic (glycolysis/ gluconeogenesis and purine metabolism) and detoxification proteins (GST) were prominently expressed in the larvae exposed to the novel complex but in contrast to the *in-vitro* mammalian cells lines the toxicity did not increase with extension of the phenazine π-backbone within the complex scaffold. While this situation is contrasted to the profile of the mammalian cells, the common increase in metabolic proteins between both tests models and the addition of detoxification proteins in the *in-vivo* model may indicate that the Cu(II) phenanthroline-phenazine complexes strong DNA binding capabilities is not completely responsible for their mechanism of action.

In conclusion, this project has demonstrated that Cu(II) phenanthroline-phenazine complexes are a promising therapeutic candidate with a complex mechanism of action that is highly effective against cisplatin resistant cells. **Figure 6.2** gives an overview of the similar results across both biological models. Using both *in-vitro* mammalian cells and *in-vivo G. mellonella* models the mechanism of action of these complex has shown to be characterised by mitochondrial toxicity and subsequent activation of apoptosis and in the *in-vivo* model to be dominated by metabolic enzymes and detoxification processes which may be associated with mitochondrial action (**Fig. 6.2**). This thesis has

demonstrated for the first time the molecular mode of action of novel Cu(II) phenanthroline-phenazine complexes in both *in-vitro* and *in-vivo* biological models. Furthermore, the strong activity and mechanistic profile of this series of Cu(II) complexes against cisplatin resistant cells offers a potentially novel therapeutic avenue for treating cisplatin refractory cancers. The use of both cisplatin sensitive and resistant cell lines has evidently revealed different mechanistic pathways; however both phenotypes are highly susceptible to the Cu(II) phenanthroline-phenazine complex series.

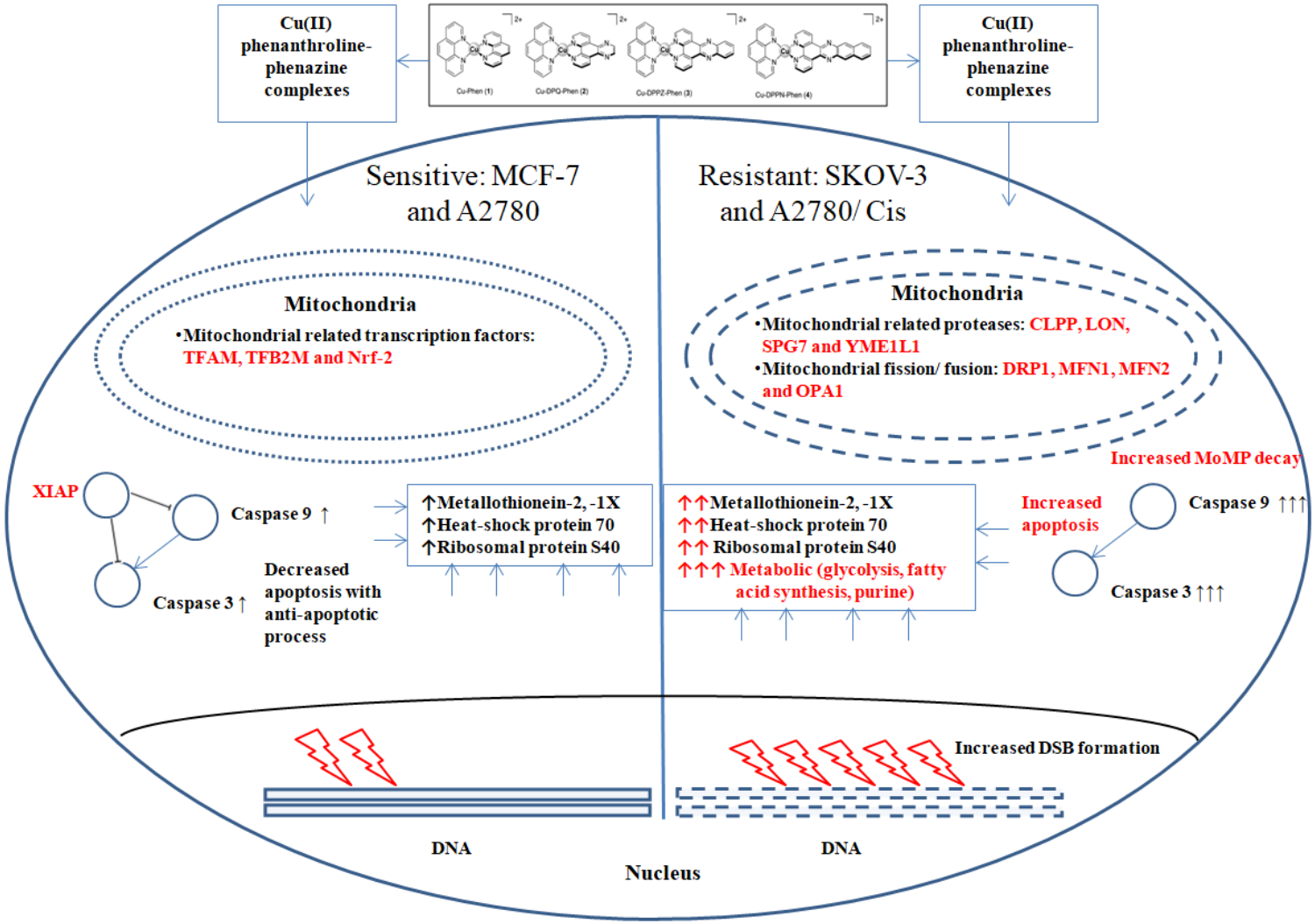

Fig. 6.1 Summary of the biological effects of the Cu(II) phenanthroline-phenazine complexes in both cisplatin sensitive (MCF-7 and A2780) and cisplatin resistant (SKOV-3 and A2780/ Cis) cells.

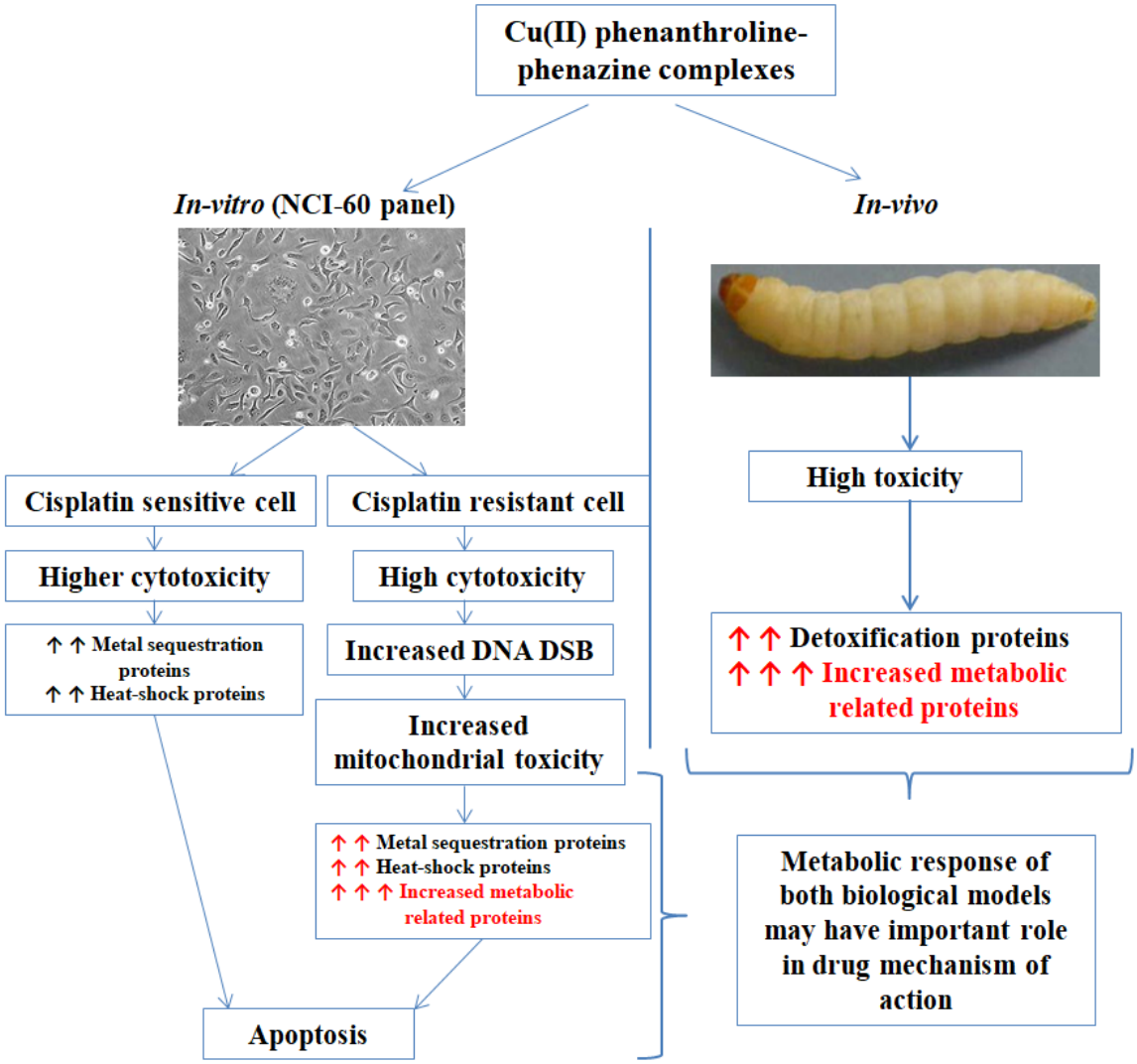

Fig. 6.2 Overview of the biological finding from both *in-vitro* and *in-vivo* models.

Chapter 7: Future Work

The work described in the preceeding Chapters demonstrated the activity of Cu(II) phenanthroline-phenazine complexes in *in-vitro* mammalian models and the *in-vivo* model, *Galleria mellonella*. These results established the high degree of therapeutic activity in cisplatin resistant cells and strong DNA damage activity, which had been previously observed by Molphy *et al.* (2014) and (2015). Gene expression and proteomic analysis indicated that apoptosis and metabolic proteins played a prominent role in the mechanism of action. Further gene expression work established that mitochondrial proteases may play a role in the mitochondrial toxicity present after exposure to the complexes. The *G. mellonella* model indicated that metabolic process may have played a strong role in the mechanism of action at an *in-vivo* level.

The future work of this project would include a more in-depth investigation of the mechanistic *in-vitro* analysis using PC-3 and A2780 cells. A major component of this is to confirm the type of apoptosis occurring (intrinsic or extrinsic). Using immundetection and flow cytometry methodologies, Annexin V (Annexin V-FITC Apoptosis Detection Kit) (Sigma, Ireland), Caspase 3 and 7 (intrinsic) (Vybrant FAM Caspase-3 and -7 Assay Kit), Caspase 8 (extrinsic) (Vybrant FAM Caspase-3 and -7 Assay Kit) (Thermo, Ireland) and the mitochondrial marker, cytochrome *c* (Anti-Cytochrome C antibody [37BA11]) (Abcam, USA) would be used to establish the nature of the apoptotic process. The proteomics work and identification of metallothioneins, heat-shock proteins and metabolic proteins would be validated using qPCR methods and western blotting to confirm gene expression and protein abundance changes. The data generated in this project demonstrated that the mitochondria may play a strong role in the mechanism of action. Based on the mitochondrial involvement, the Agilent Seahorse platform would be utilised to examine; basal respiration, ATP

production and maximal respiration using oligomycin, Carbonyl cyanide-*p*-(trifluoromethoxy)phenylhydrazone (FCCP), antimycin A and Rotenone to examine the respiratory complexes during exposure to the Cu(II) complexes. Gene expression of mitochondrial proteases (LON, CLPP, SPG7, YME1L1) and fission regulator, DRP1 demonstrated involvement in the response to the Cu(II) complexes. Western blotting and additional qPCR analysis would be used to provide additional information on their contribution to the mechanism of action. At present, the clear mechanism of action of the Cu(II) complexes centres on two process. The first is oxidative mediated DNA lesion formation (8-oxo-dG) from DNA intercalation of phenazine π-backbone extended complexes and the subsequent DSB formation and activation of p53 mediated apoptosis. The second is the generalised disruption of protein function, particularly the respiratory complex, which has consequences in cellular energy production. Mitochondrial proteases may also play a role in the eventual disruption of mitochondrial function resulting in the initiation of intrinsic apoptosis through the release of the mitochondrial permeability transition pore protein.

The Cu(II) complexes have demonstrated excellent *in-vitro* activity in cisplatin resistant cell lines and proteomic studies in the *in-vivo G. mellonella* model has provided useful pre-mammalian *in-vivo* data to support use of *in-vivo* murine models. A high degree of activity was demonstrated after exposure to the Cu(II) complexes in the PC-3 and A2780 (A2780/ Cis) cell lines compared to cisplatin treatments. Based on these finding, *in-vivo* murine models utilising xenograft tumour models of PC-3 (prostate), A2780 or SKOV-3 (ovarian) in genetically modified hosts (murine) (Nude, SCID, NOD-SCID) would provide data on *in-vivo* efficacy and valuable pre-clinical information to aid in further development.

References

Abbehausen, C., Manzano, C.M., Corbi, P.P., Farrell, N.P. (2016) 'Effects of coordination mode of 2-mercaptothiazoline on reactivity of Au(I) compounds with thiols and sulfur-containing proteins', *J. Inorg. Biochem.*, 165 , pp. 136–145.

Aggarwal, B.B., Shishodia, S., Sandur, S.K., Pandey, M.K., Sethi, G. (2006) 'Inflammation and cancer: how hot is the link?', *Biochem. Pharmacol.*, 72 , pp. 1605–1621.

Ahn, G.-O., Botting, K.J., Patterson, A. V., Ware, D.C., Tercel, M., Wilson, W.R. (2006) 'Radiolytic and cellular reduction of a novel hypoxia-activated cobalt(III) prodrug of a chloromethylbenzindoline DNA minor groove alkylator', *Biochem. Pharmacol.*, 71 (12), pp. 1683–1694.

Ahsan, A., Hiniker, S.M., Ramanand, S.G., Nyati, S., Hegde, A., Helman, A., Menawat, R., Bhojani, M.S., Lawrence, T.S., Nyati, M.K. (2010) 'Role of epidermal growth factor receptor degradation in cisplatin-induced cytotoxicity in head and neck cancer.', *Cancer Res.*, 70 (7), pp. 2862–2869.

Aida, T., Takebayashi, Y., Shimizu, T., Okamura, C., Higasimoto, M., Kanzaki, A., Nakayama, K., Terada, K., Sugiyama, T., Miyazaki, K., Ito, K., Takenoshita, S., Yaegashi, N. (2005) 'Expression of copper-transporting P-type adenosine triphosphatase (ATP7B) as a prognostic factor in human endometrial carcinoma', *Gynecol. Oncol.*, 97 (1), pp. 41–45.

Akcay, A., Turkmen, K., Lee, D., Edelstein, C.L. (2010) 'Update on the diagnosis and management of acute kidney injury', *Int. J. Nephrol. Renovasc. Dis.*, 3, pp. 129-140.

Al-Jaroudi, S.S., Altaf, M., Seliman, A.A., Yadav, S., Arjmand, F., Alhoshani, A., Korashy, H.M., Ahmad, S., Isab, A.A. (2017) 'Synthesis, characterization, in vitro cytotoxicity and DNA interaction study of phosphanegold(I) complexes with

dithiocarbamate ligands', *Inorganica Chim. Acta*, 464 , pp. 37–48.

Algra, A.M., Rothwell, P.M., Sivakumaran, R., al., et, al., et, Sandler, R. (2012) 'Effects of regular aspirin on long-term cancer incidence and metastasis: a systematic comparison of evidence from observational studies versus randomised trials', *Lancet Oncol.*, 13 (5), pp. 518–527.

Allaman, I., Bélanger, M., Magistretti, P.J. (2015) 'Methylglyoxal, the dark side of glycolysis', *Front. Neurosci.*, 9 (FEB), pp. 1–12.

Altieri, D.C. (2008) 'Survivin, cancer networks and pathway-directed drug discovery', *Nat. Rev. Cancer*, 8 (1), pp. 61–70.

André, T., Boni, C., Mounedji-Boudiaf, L., Navarro, M., Tabernero, J., Hickish, T., Topham, C., Zaninelli, M., Clingan, P., Bridgewater, J., Tabah-Fisch, I., de Gramont, A. (2004) 'Oxaliplatin, Fluorouracil, and Leucovorin as Adjuvant Treatment for Colon Cancer', *N. Engl. J. Med.*, 350 (23), pp. 2343–2351.

Andrews, P.A., Murphy, M.P., Howell, S.B. (1987) 'Metallothionein-mediated cisplatin resistance in human ovarian carcinoma cells.', *Cancer Chemother. Pharmacol.*, 19 (2), pp. 149–54.

Ang, W.H., Casini, A., Sava, G., Dyson, P.J. (2011) 'Organometallic ruthenium-based antitumor compounds with novel modes of action', *J. Organomet. Chem.*, 696 (5), pp. 989–998.

Arlington, S. (2017) *From Vision to Decision: Pharma 2020*, available: www.pwc.com/pharma2020 [accessed 1 Aug 2017].

ATCC (2017) American Type Culture Collection (ATCC) [online], *Tumor Cell Panel*, available: https://www.atcc.org/ [accessed 11 Nov 2017].

Baig, S., Seevasant, I., Mohamad, J., Mukheem, A., Huri, H.Z., Kamarul, T. (2016) 'Potential of apoptotic pathway-targeted cancer therapeutic research: Where do we

stand?', *Cell Death Dis.*, 7 (1), pp. e2058. Available at http://www.pubmedcentral.nih.gov/articlerender.fcgi?artid=PMC4816162 [accessed on 15-10-2017]

Bailey, M., Christoforidou, Z., Lewis, M.C. (2013) 'The evolutionary basis for differences between the immune systems of man, mouse, pig and ruminants', *Vet. Immunol. Immunopathol.*, 152 (1–2), pp. 13–19.

Bandmann, O., Weiss, K.H., Kaler, S.G. (2014) 'Wilson's disease and other neurological copper disorders', *Lancet Neurol.*, 14 , pp. 103–113.

Banti, C.N., Giannoulis, A.D., Kourkoumelis, N., Owczarzak, A.M., Kubicki, M., Hadjikakou, S.K. (2015) 'Silver(I) compounds of the anti-inflammatory agents salicylic acid and p-hydroxyl-benzoic acid which modulate cell function', *J. Inorg. Biochem.*, 142 , pp. 132–144.

Banti, C.N., Giannoulis, A.D., Kourkoumelis, N., Owczarzak, A.M., Poyraz, M., Kubicki, M., Charalabopoulos, K., Hadjikakou, S.K. (2012) 'Mixed ligand–silver(i) complexes with anti-inflammatory agents which can bind to lipoxygenase and calf-thymus DNA, modulating their function and inducing apoptosis', *Metallomics*, 4 (6), pp. 545-560.

Banti, C.N., Kyros, L., Geromichalos, G.D., Kourkoumelis, N., Kubicki, M., Hadjikakou, S.K. (2014) 'A novel silver iodide metalo-drug: Experimental and computational modelling assessment of its interaction with intracellular DNA, lipoxygenase and glutathione', *Eur. J. Med. Chem.*, 77 , pp. 388–399.

Banville, N., Browne, N., Kavanagh, K. (2012) 'Effect of nutrient deprivation on the susceptibility of Galleria mellonella larvae to infection.', *Virulence*, 3 (6), pp. 497–503.

Barnes, K.R., Lippard, S.J. (2004) 'Cisplatin and related anticancer drugs: recent

advances and insights.', *Met. Ions Biol. Syst.*, 42, pp. 143–77.

Barretina, J., Caponigro, G., Stransky, N., Venkatesan, K., Margolin, A.A., Kim, S., Wilson, C.J., Lehár, J., Kryukov, G. V., Sonkin, D., Reddy, A., Liu, M., Murray, L., Berger, M.F., Monahan, J.E., Morais, P., Meltzer, J., Korejwa, A., Jané-Valbuena, J., Mapa, F.A., Thibault, J., Bric-Furlong, E., Raman, P., Shipway, A., Engels, I.H., Cheng, J., Yu, G.K., Yu, J., Aspesi, P., de Silva, M., Jagtap, K., Jones, M.D., Wang, L., Hatton, C., Palescandolo, E., Gupta, S., Mahan, S., Sougnez, C., Onofrio, R.C., Liefeld, T., MacConaill, L., Winckler, W., Reich, M., Li, N., Mesirov, J.P., Gabriel, S.B., Getz, G., Ardlie, K., Chan, V., Myer, V.E., Weber, B.L., Porter, J., Warmuth, M., Finan, P., Harris, J.L., Meyerson, M., Golub, T.R., Morrissey, M.P., Sellers, W.R., Schlegel, R., Garraway, L.A. (2012) 'The Cancer Cell Line Encyclopedia enables predictive modelling of anticancer drug sensitivity', *Nature*, 483 (7391), pp. 603–307.

Barry, N.P.E., Sadler, P.J., Souvatzoglou, M., Eiber, M., Fürst, S., Ziegler, S.I., Brohl, F., Schwaiger, M., Scheidhauer, K., Humm, J.L., Brechbiel, M.W., Molinet, R., Scheinberg, D.A., Cummings, J.L., Herd, C.M., Bush, A.I., Wu, K., Fan, D., Dive, D., Biot, C. (2013) 'Exploration of the medical periodic table: towards new targets', *Chem. Commun.*, 49 (45), pp. 5106-5131.

Barsan, M.M., Pinto, E.M., Brett, C.M.A. (2008) 'Electrosynthesis and electrochemical characterisation of phenazine polymers for application in biosensors', *Electrochim. Acta*, 53, pp. 3973–3982.

Bartolini, D., Commodi, J., Piroddi, M., Incipini, L., Sancineto, L., Santi, C., Galli, F. (2015) 'Glutathione S-transferase pi expression regulates the Nrf2-dependent response to hormetic diselenides', *Free Radic Biol Med*, 88, pp. 466-480.

Bashford, A., Cooper, J. (2016) 'Analysis of Drug Resistant Properties of A2780

Ovarian Cancer Cell Lines Using Label-Free Automated Microscopy (IncuCyte ZOOM)', European Collection of Authenticated Cell Cultures.

Basu, A., Krishnamurthy, S. (2010) 'Cellular responses to Cisplatin-induced DNA damage.', *J. Nucleic Acid*. Doi: 10.4061/2010/201367 [accessed on 17-11-2017]

Beck, D.J., Brubaker, R.R. (1973) 'Effect of cis-platinum(II)diamminodichloride on wild type and deoxyribonucleic acid repair deficient mutants of Escherichia coli.', *J. Bacteriol.*, 116 (3), pp. 1247–1252.

Bellmunt, J., Paz-Ares, L., Cuello, M., Cecere, F., Albiol, S., Guillem, V., Gallardo, E., Carles, J., Mendez, P., de la Cruz, J., Taron, M., Rosell, R., Baselga, J., Spanish Oncology Genitourinary Group (2006) 'Gene expression of ERCC1 as a novel prognostic marker in advanced bladder cancer patients receiving cisplatin-based chemotherapy', *Ann. Oncol.*, 18 (3), pp. 522–528.

Del Bello, B., Toscano, M., Moretti, D., Maellaro, E., Wang, Q. (2013) 'Cisplatin-Induced Apoptosis Inhibits Autophagy, Which Acts as a Pro-Survival Mechanism in Human Melanoma Cells', *PLoS One*, 8 (2), pp. e57236. Available at http://dx.plos.org/10.1371/journal.pone.0057236 [accessed on 08-09-2017]

Bergin, D., Murphy, L., Keenan, J., Clynes, M., Kavanagh, K. (2006) 'Pre-exposure to yeast protects larvae of Galleria mellonella from a subsequent lethal infection by Candida albicans and is mediated by the increased expression of antimicrobial peptides', *Microbes Infect*, 8 (8), pp. 2105–2112.

Bergin, D., Reeves, E.P., Renwick, J., Frans, B., Kavanagh, K., Wientjes, F.B. (2005) 'Superoxide Production in Galleria mellonella Hemocytes : Identification of Proteins Homologous to the NADPH Oxidase Complex of Human Neutrophils Superoxide Production in Galleria mellonella Hemocytes : Identification of Proteins Homologous to the NADPH Ox', *Infect Immun*, 73 (7), pp. 4161–4170.

Bertrand, B., Fernandez-Cestau, J., Angulo, J., Cominetti, M.M.D., Waller, Z.A.E., Searcey, M., O'Connell, M.A., Bochmann, M. (2017) 'Cytotoxicity of Pyrazine-Based Cyclometalated (C^Npz^C)Au(III) Carbene Complexes: Impact of the Nature of the Ancillary Ligand on the Biological Properties', *Inorg. Chem.*, 56 (10), pp. 5728–5740.

Bertrand, M.J.M., Milutinovic, S., Dickson, K.M., Ho, W.C., Boudreault, A., Durkin, J., Gillard, J.W., Jaquith, J.B., Morris, S.J., Barker, P. a. (2008) 'cIAP1 and cIAP2 Facilitate Cancer Cell Survival by Functioning as E3 Ligases that Promote RIP1 Ubiquitination', *Mol. Cell*, 30 (6), pp. 689–700.

Beaufort, C, A Helmijr, J.C., Piskorz, A.M., Hoogstraat, M., Ruigrok-Ritstier, K., Besselink , N., Murtaza, M., J van IJcken, W.E., J Heine, A.A., Smid, M., Koudks, M.J., Brentonm J.D., J J Berns, E.M., Helleman, J., Pearson, R (2015) 'Ovarian Cancer Cell Line Panel (OCCP): Clinical Importance of *In Vitro* Morphological Subtypes', *PLoS One*, 10 (3). pp. e0122284. Available at https://doi.org/10.1371/journal.pone.0122284 [accessed on 24-05-2017]

Biot, C., Castro, W., Botté, C.Y., Navarro, M. (2012) 'The therapeutic potential of metal-based antimalarial agents: Implications for the mechanism of action', *Dalt. Trans*, 41 (21), pp. 6516-6527.

Blackie, M. a L., Chibale, K. (2008) 'Metallocene antimalarials: the continuing quest.', *Met. Based. Drugs*, 2008 , pp. 495123. doi: 10.1155/2008/495123 [accessed on 17-11-2017]

Bleeker-Rovers, C.P., Vos, F.J., van der Graaf, W.T.A., Oyen, W.J.G. (2011) 'Nuclear medicine imaging of infection in cancer patients (with emphasis on FDG-PET).', *Oncologist*, 16 (7), pp. 980–991.

Board, P.G., Menon, D. (2013) 'Glutathione transferases, regulators of cellular

metabolism and physiology', *Biochim. Biophys. Acta - Gen. Subj.*, 1830 , pp. 3267–3288.

Bota, D.A., Davies, K.J.A. (2016) 'Mitochondrial Lon protease in human disease and aging: Including an etiologic classification of Lon-related diseases and disorders', *Free Radic. Biol. Med.*, 100, pp. 188-198.

Bras, M., Yuste, V.J., Roué, G., Barbier, S., Sancho, P., Virely, C., Rubio, M., Baudet, S., Esquerda, J.E., Merle-Béral, H., Sarfati, M., Susin, S.A. (2007) 'Drp1 mediates caspase-independent type III cell death in normal and leukemic cells.', *Mol. Cell. Biol.*, 27 (20), pp. 7073–7088.

Breedveld, F.C. (2000) 'Therapeutic monoclonal antibodies', *Lancet*, 355, pp. 735–740.

Browne, N. (2014) *An Analysis of the Cellular and Humoral Immune Responses of Galleria Mellonella Larvae*. Unpublished PhD thesis. Maynooth University.

Browne, N., Hackenberg, F., Streciwilk, W., Tacke, M., Kavanagh, K. (2014) 'Assessment of in vivo antimicrobial activity of the carbene silver(I) acetate derivative SBC3 using Galleria mellonella larvae', *Biometals*, 27, pp. 745–752.

Browne, N., Heelan, M., Kavanagh, K. (2013) 'An analysis of the structural and functional similarities of insect hemocytes and mammalian phagocytes', *Virulence*, 4, pp. 597–603.

Browne, N., Kavanagh, K. (2013) 'Developing the potential of using Galleria mellonella larvae as models for studying brain infection by Listeria monocytogenes.', *Virulence*, 4 (4), pp. 271–272.

Browne, N., Surlis, C., Kavanagh, K. (2014) 'Thermal and physical stresses induce a short-term immune priming effect in Galleria mellonella larvae', *J. Insect Physiol*, 63 (1), pp. 21–26.

Brozovic, A., Osmak, M. (2007) 'Activation of mitogen-activated protein kinases by

cisplatin and their role in cisplatin-resistance', *Cancer Lett.*, 251 (1), pp. 1–16.

Bruijnincx, P.C., Sadler, P.J. (2008) 'New trends for metal complexes with anticancer activity', *Curr. Opin. Chem. Biol.*, 12 (2), pp. 197–206.

Bryan, R.N. and Robert N. (2010) *Introduction to the Science of Medical Imaging*, 1st edition, Cambridge University Press.

Cadet, J., Davies, K.J.A.A., Medeiros, M.H., Di Mascio, P., Wagner, J.R., Hg, M., Di, P., Wagner, J.R. (2017) 'Formation and repair of oxidatively generated damage in cellular DNA', *Free Radic. Biol. Med.*, 107, pp. 13-34.

Cai, J., Wang, J., Huang, Y., Wu, H., Xia, T., Xiao, J., Chen, X., Li, H., Qiu, Y., Wang, Y., Wang, T., Xia, H., Zhang, Q., Xiang, A.P. (2016) 'ERK/Drp1-dependent mitochondrial fission is involved in the MSC-induced drug resistance of T-cell acute lymphoblastic leukemia cells', *Cell Death Dis.*, 7 (11), pp. e2459., available at: http://www.nature.com/doifinder/10.1038/cddis.2016.370 [accessed on 17-11-2017]

Cappellini, M.-D., Cohen, A., Eleftheriou, A., Piga, A., Porter, J., Taher, A. (2008) 'Iron Overload', in *Guidelines for the Clinical Management of Thalassaemia*, Thalassaemia International Federation: Nicosia.

Carvallo-Chaigneau, F., Trejo-Solís, C., Gómez-Ruiz, C., Rodríguez-Aguilera, E., Macías-Rosales, L., Cortés-Barberena, E., Cedillo-Peláez, C., Gracia-Mora, I., Ruiz-Azuara, L., Madrid-Marina, V., Constantino-Casas, F. (2008) 'Casiopeina III-ia induces apoptosis in HCT-15 cells in vitro through caspase-dependent mechanisms and has antitumor effect in vivo', *BioMetals*, 21 (1), pp. 17–28.

Casini, A., Diawara, M.C., Scopelliti, R., Zakeeruddin, S.M., Grätzel, M., Dyson, P.J., Abbott, B.J., Mayo, J.G., Shoemaker, R.H., Boyd, M.R. (2010) 'Synthesis, characterisation and biological properties of gold(iii) compounds with modified

bipyridine and bipyridylamine ligands', *Dalt. Trans.*, 39 (9), pp. 2239-2245.

Casini, A., Gabbiani, C., Sorrentino, F., Rigobello, M.P., Bindoli, A., Geldbach, T.J., Marrone, A., Re, N., Hartinger, C.G., Dyson, P.J., Messori, L. (2008) 'Emerging Protein Targets for Anticancer Metallodrugs: Inhibition of Thioredoxin Reductase and Cathepsin B by Antitumor Ruthenium(II)−Arene Compounds', *J. Med. Chem.*, 51 (21), pp. 6773–6781.

Casini, A., Karotki, A., Gabbiani, C., Rugi, F., Vašák, M., Messori, L., Dyson, P.J. (2009) 'Reactivity of an antimetastatic organometallic ruthenium compound with metallothionein-2: relevance to the mechanism of action.', *Metallomics*, 1 (5), pp. 434–441.

Casini, A., Reedijk, J., Park, J.J., Lowe, G., Schirmer, R.H., Egan, D., Marmion, C.J., Campomanes, P., Rothlisberger, U., Luca, A. De, Bello, M. Lo, Ang, W.H., Dyson, P.J., Parker, M.W. (2012) 'Interactions of anticancer Pt compounds with proteins: an overlooked topic in medicinal inorganic chemistry?', *Chem. Sci.*, 3 (11), pp. 3135-3144.

Ceppi, P., Novello, S., Cambieri, A., Longo, M., Monica, V., Lo Iacono, M., Giaj-Levra, M., Saviozzi, S., Volante, M., Papotti, M., Scagliotti, G. (2009) 'Polymerase mRNA Expression Predicts Survival of Non-Small Cell Lung Cancer Patients Treated with Platinum-Based Chemotherapy', *Clin. Cancer Res.*, 15 (3), pp. 1039–1045.

Chabner, B. a. (2010) 'Barnett Rosenberg: In Memoriam (1924-2009)', *Cancer Res.*, 70, pp. 428–429.

Chakraborty, A., Kumar, P., Ghosh, K., Roy, P. (2010) 'Evaluation of a Schiff base copper complex compound as potent anticancer molecule with multiple targets of action.', *Eur. J. Pharmacol.*, 647, pp. 1–12.

Chalovich, J.M., Eisenberg, E. (2005) 'Mitochondrial Inner Membrane Electrophysiology Assessed by Rhodamine-123 Transport and Fluorescence', *Biophys. Chem.*, 257 (5), pp. 2432–2437.

Chee, J.L.Y., Saidin, S., Lane, D.P., Leong, S.M., Noll, J.E., Neilsen, P.M., Phua, Y.T., Gabra, H., Lim, T.M. (2013) 'Wild-type and mutant p53 mediate cisplatin resistance through interaction and inhibition of active caspase-9.', *Cell Cycle*, 12 (2), pp. 278–288.

Chen, C.B., Milne, L., Landgraf, R., Perrin, D.M., Sigman, D.S. (2001) 'Artificial nucleases.', *Chembiochem*, 2 (10), pp. 735–740.

Chen, H.H.W., Kuo, M.T. (2010) 'Role of Glutathione in the Regulation of Cisplatin Resistance in Cancer Chemotherapy', *Met. Based Drugs*, 7. Available at: https://www.ncbi.nlm.nih.gov/pmc/articles/PMC2946579/pdf/MBD2010-430939.pdf [accessed 30 Aug 2017].

Chen, Z., Zhang, J., Stamler, J.S. (2002) 'Identification of the enzymatic mechanism of nitroglycerin bioactivation', *Proc. Natl. Acad. Sci. U. S. A.*, 99, pp. 8306–8311.

Chiang, Y.-Y., Chen, S.-L., Hsiao, Y.-T., Huang, C.-H., Lin, T.-Y., Chiang, I.-P., Hsu, W.-H., Chow, K.-C. (2009) 'Nuclear expression of dynamin-related protein 1 in lung adenocarcinomas.', *Mod. Pathol.*, 22 (9), pp. 1139–1150.

Chitambar, C.R. (2012) 'Gallium-containing anticancer compounds', *Future Med. Chem.*, 4 (10), pp. 1257–1272.

Chitambar, C.R., Antholine, W.E. (2013) 'Iron-Targeting Antitumor Activity of Gallium Compounds and Novel Insights Into Triapine ® -Metal Complexes', *Antioxid. Redox Signal.*, 18 (8), pp. 956–972.

Chitrakar, I., Kim-Holzapfel, D.M., Zhou, W., French, J.B. (2017) 'Higher order structures in purine and pyrimidine metabolism', *J. Struct. Biol.*, 197 (3) , pp. 354-

364.

Cho, Y.-E., Singh, T.S.K., Lee, H.-C., Moon, P.-G., Lee, J.-E., Lee, M.-H., Choi, E.-C., Chen, Y.-J., Kim, S.-H., Baek, M.-C. (2012) 'In-depth identification of pathways related to cisplatin-induced hepatotoxicity through an integrative method based on an informatics-assisted label-free protein quantitation and microarray gene expression approach.', *Mol. Cell. Proteomics,* 11 (1), pp. M111.010884. available at: http://www.pubmedcentral.nih.gov/articlerender.fcgi?artid=3270101&tool=pmcentrez&rendertype=abstract. [accessed on 17-11-2017]

Choi, C.-H., Cha, Y., An, C.-S., Kim, K.-C.K.K.K.-J., Moon, S.-P., Lee, Z.H., Min, Y.-D. (2004) 'Molecular mechanisms of heptaplatin effective against cisplatin-resistant cancer cell lines: less involvement of metallothionein', *Cancer Cell Int.,* 4 (1), pp. 6., available at: http://www.pubmedcentral.nih.gov/articlerender.fcgi?artid=533863&tool=pmcentrez&rendertype=abstract. [accessed on 17-11-2017]

Choi, Y.-M., Kim, H.-K., Shim, W., Anwar, M.A., Kwon, J.-W., Kwon, H.-K., Kim, H.J., Jeong, H., Kim, H.M., Hwang, D., Kim, H.S., Choi, S. (2015) 'Mechanism of Cisplatin-Induced Cytotoxicity Is Correlated to Impaired Metabolism Due to Mitochondrial ROS Generation.', *PLoS One*, 10 (8), pp. e0135083., available at: http://www.ncbi.nlm.nih.gov/pubmed/26247588 [accessed 13 Aug 2017].

Christodoulou, C. V, Ferry, D.R., Fyfe, D.W., Young, A., Doran, J., Sheehan, T.M., Eliopoulos, A., Hale, K., Baumgart, J., Sass, G., Kerr, D.J. (1998) 'Phase I trial of weekly scheduling and pharmacokinetics of titanocene dichloride in patients with advanced cancer.', *J. Clin. Oncol.,* 16 (8), pp. 2761–2769.

Cleare, M.J., Hoeschele, J.D. (1973a) 'Antitumour Platinum Compounds', *Cell*, 17 (1),

pp. 2–13.

Cleare, M.J., Hoeschele, J.D. (1973b) ‘Studies on the antitumor activity of group VIII transition metal complexes. Part I. Platinum (II) complexes’, *Bioinorg. Chem.*, 2 (3), pp. 187–210.

Clermont, A., Wedde, M., Seitz, V., Podsiadlowski, L., Lenze, D., Hummel, M., Vilcinskas, A. (2004) ‘Cloning and expression of an inhibitor of microbial metalloproteinases from insects contributing to innate immunity’, *Biochem J.*, 382, pp. 315–322.

Cole, A., Wang, Z., Coyaud, E., Voisin, V., Gronda, M., Jitkova, Y., Mattson, R., Hurren, R., Babovic, S., Maclean, N., Restall, I., Wang, X., Jeyaraju, D. V, Sukhai, M.A., Prabha, S., Bashir, S., Ramakrishnan, A., Leung, E., Qia, Y.H., Zhang, N., Combes, K.R., Ketela, T., Lin, F., Houry, W.A., Aman, A., Al-Awar, R., Zheng, W., Wienholds, E., Xu, C.J., Dick, J., Wang, J.C.Y., Moffat, J., Minden, M.D., Eaves, C.J., Bader, G.D., Hao, Z., Kornblau, S.M., Raught, B., Schimmer, A.D. (2015) ‘Inhibition of the mitochondrial protease, ClpP, as a therapeutic strategy for human acute myeloid leuekmia HHS Public Access’, *Cancer Cell*, 27 (6), pp. 864–876.

Coluccia, M., Natile, G. (2007) ‘Trans-platinum complexes in cancer therapy.’, *Anticancer. Agents Med. Chem.*, 7 (1), pp. 111–123.

Cook, S.M., McArthur, J.D. (2013) ‘Developing *Galleria mellonella* as a model host for human pathogens’, *Virulence*, 4 (5), pp. 350–353.

Coombs, G.S., Schmitt, A.A., Canning, C.A., Alok, A., Low, I.C.C., Banerjee, N., Kaur, S., Utomo, V., Jones, C.M., Pervaiz, S., Toone, E.J., Virshup, D.M. (2012) ‘Modulation of Wnt/β-catenin signaling and proliferation by a ferrous iron chelator with therapeutic efficacy in genetically engineered mouse models of cancer’,

Oncogene, 31 (2), pp. 213–225.

Cooper, M.D., Alder, M.N. (2006) 'The Evolution of Adaptive Immune Systems', *Cell*, 124, pp. 815–822.

Corte-Rodríguez, M., Espina, M., Sierra, L.M., Blanco, E., Ames, T., Montes-Bayón, M., Sanz-Medel, A. (2015) 'Quantitative evaluation of cellular uptake, DNA incorporation and adduct formation in cisplatin sensitive and resistant cell lines: Comparison of different Pt-containing drugs', *Biochem. Pharmacol.*, 98, pp. 69–77.

Cossarizza, A., Baccarani-Contri, M., Kalashnikova, G., Franceschi, C. (1993) 'A new method for the cytofluorimetric analysis of mitochondrial membrane potential using the J-aggregate forming lipophilic cation 5,5',6,6'-tetrachloro-1,1',3,3'-tetraethylbenzimidazolcarbocyanine iodide (JC-1).', *Biochem. Biophys. Res. Commun.*, 197 (1), pp. 40–45.

Cotter, G., Doyle, S., Kavanagh, K. (2000a) 'Development of an insect model for the in vivo pathogenecity testing of yeasts', *FEMS Immunol. Med. Microbiol.*, 27, pp. 163–169.

Cox, J., Neuhaurser, N., Michalskit, A., Scheltema, R.A., Olsen, J. V, Mann, M. (2011) 'Andromeda: A peptide Search Engine Integrated into the MaxQuant Environment', *J. Proteome Res.*, 10 (4), pp. 1794–1805.

Coyle, B., McCann, M., Kavanagh, K., Devereux, M., McKee, V., Kayal, N., Egan, D., Deegan, C., Finn, G.J. (2004) 'Synthesis, X-ray crystal structure, anti-fungal and anti-cancer activity of [Ag2(NH3)2(salH)2] (salH2=salicylic acid).', *J. Inorg. Biochem.*, 98 (8), pp. 1361–1366.

Craig, E.A., Marszalek, J. (2002) 'A specialized mitochondrial molecular chaperone system: a role in formation of Fe/S centers.', *Cell. Mol. Life Sci.*, 59 (10), pp.

1658–1665.

Creaven, B.S., Devereux, M., Karcz, D., Kellett, A., McCann, M., Noble, A., Walsh, M. (2009) ‘Copper(II) complexes of coumarin-derived Schiff bases and their anti-Candida activity’, *J. Inorg. Biochem.,* 103 (9), pp. 1196–1203.

Crisponi, G., Nurchi, V.M., Fanni, D., Gerosa, C., Nemolato, S., Faa, G. (2010) ‘Copper-related diseases: From chemistry to molecular pathology’, *Coord. Chem. Rev.,* 254 , pp. 876–889.

Dada, L.., Sznajder, J.. (2011) ‘Mitochondrial Ca2+and ROS take center stage to orchestrate TNF-α-mediated inflammatory responses’, *J. Clin. Invest.,* 121 , pp. 1683–1685.

Daiber, A. (2004) ‘Oxidative Stress and Mitochondrial Aldehyde Dehydrogenase Activity: A Comparison of Pentaerythritol Tetranitrate with Other Organic Nitrates’, *Mol. Pharmacol.,* 66 (6), pp. 1372–1382.

Dan Dunn, J., Alvarez, L.A., Zhang, X., Soldati, T. (2015) ‘Reactive oxygen species and mitochondria: A nexus of cellular homeostasis’, *Redox Biol.,* 6 , pp. 472–485.

Dasari, S., Tchounwou, P.B. (2014) ‘Cisplatin in cancer therapy: Molecular mechanisms of action’, *Eur. J. Pharmacol.,* 740 , pp. 364–378.

Davis, R., Spallholz, J., Pence, B. (1998) ‘Inhibition of selenite-induced cytotoxicity and apoptosis in human colonic carcinoma (HT-29) cells by copper’, *Nutr. Cancer,* 32 , pp. 181–189.

Deally, A., Hackenberg, F., Lally, G., Tacke, M. (2012) ‘Synthesis and Biological Evaluation of Achiral Indole-Substituted Titanocene Dichloride Derivatives’, *Int J Med Chem,* 2012 , pp. 1–13.

Delbridge, A.R.D., Grabow, S., Strasser, A., Vaux, D.L. (2016) ‘Thirty years of BCL-2: translating cell death discoveries into novel cancer therapies’, *Nat. Rev. Cancer,* 16

(2), pp. 99–109.

Dertinger, S.D., Avlasevich, S.L., Torous, D.K., Bemis, J.C., Phonethepswath, S., Labash, C., Carlson, K., Mereness, J., Cottom, J., Palis, J., MacGregor, J.T. (2014) 'Persistence of Cisplatin-Induced Mutagenicity in Hematopoietic Stem Cells: Implications for Secondary Cancer Risk Following Chemotherapy', *Toxicol. Sci.*, 140 (2), pp. 307–314.

Desoize, B. (2004) 'Metals and metal compounds in cancer treatment.', *Anticancer Res.*, 24 (3a), pp. 1529–1544.

Devereux, M., McCann, M., O'shea, D., O'connor, M., Kiely, E., McKee, V., Naughton, D., Fisher, A., Kellett, A., Walsh, M., Egan, D., Deegan, C. (2006) 'Synthesis, Superoxide Dismutase Mimetic and Anticancer Activities of Metal Complexes of 2,2-Dimethylpentanedioic Acid(2dmepdaH(2)) and 3,3-Dimethylpentanedioic acid(3dmepdaH(2)): X-Ray Crystal Structures of [Cu(3dmepda)(bipy)](2). 6H(2)O and [Cu(2dmepda)(bipy)(EtOH)](2). 4EtOH (bipy = 2,2 Bipyridine)', *Bioinorg. Chem. Appl.*, 2006, pp. 80283. doi: 10.1155/BCA/2006/80283. [accessed on 17-11-2017]

Dias, M.H., Kitano, E.S., Zelanis, A., Iwai, L.K. (2016) 'Proteomics and drug discovery in cancer', *Drug Discov. Today*, 21 (2), pp. 264–277.

Dittrich, C., Scheulen, M.E., Jaehde, U., Kynast, B., Gneist, M., Richly, H., Schaad, S., Arion, V., Keppler, B.K. (2005) 'Phase I and pharmacokinetic study of sodium trans-[tetrachlorobis(1H-indazole)ruthenate(III)] / indazolehydrochloride (1:1.1) (FFC14A, KP1019) in patients with solid tumors - a study of the CESAR Central European Society for Anticancer Drug Research - EWIV', *Cancer Res.*, 65 (9), pp. 110.

Douer, D., Hu, W., Giralt, S., Lill, M., DiPersio, J. (2003) 'Arsenic trioxide (trisenox)

therapy for acute promyelocytic leukemia in the setting of hematopoietic stem cell transplantation.', *Oncologist,* 8 (2), pp. 132–140.

Du, C., Fang, M., Li, Y., Li, L., Wang, X. (2000) 'Smac, a mitochondrial protein that promotes cytochrome c-dependent caspase activation by eliminating IAP inhibition.', *Cell,* 102 (1), pp. 33–42.

Dunphy, G.B., Morton, D.B., Kropinski, A., Chadwick, J.M. (1986) 'Pathogenicity of lipopolysaccharide mutants of Pseudomonas aeruginosa for larvae of Galleria mellonella: Bacterial properties associated with virulence', *J Invert Path,* 47 , pp. 48–55.

Eastman, A. (1983) 'Characterization of the adducts produced in DNA by cis-diamminedichloroplatinum(II) and cis-dichloro(ethylenediamine)platinum(II).', *Biochemistry,* 22 (16), pp. 3927–3933.

Eastman, A. (1986) 'Reevaluation of interaction of cis-dichloro(ethylenediamine)platinum(II) with DNA.', *Biochemistry,* 25 (13), pp. 3912–3915.

ECACC (2017) European Collection of Authenticated Cell Cultures (ECACC) [online], *Aunthenticated Cell Cult.*, available: https://www.phe-culturecollections.org.uk [accessed 11 Nov 2017].

Elias, K. M., Emori, M. M., Papp, E., MacDuffie, E., Konecny, G. E., Velculescu V. E. and Drapkin, R. (2015) 'Beyond genomics: Critical evaluation of cell line utility for ovarian cancer research', *Gynecol. Oncol.*, 139 (1), pp. 97-103.

Elzinga, R.J. (2004) *Fundamentals of Entomology,* 6th edition, Pearson/Prentice Hall.

Enayati, A.A., Ranson, H., Hemingway, J. (2005) 'Insect glutathione transferases and insecticide resistance', *Insect Mol. Biol.*, 14 (1), pp. 3–8.

Espina, M., Corte-Rodrguez, M., Aguado, L., Montes-Bayn, M., Sierra, M.I., Mart?nez-

Camblor, P., Blanco-Gonz?lez, E., Sierra, L.M. (2017) ‘Cisplatin resistance in cell models: evaluation of metallomic and biological predictive biomarkers to address early therapy failure’, *Metallomics*, 9 (5), pp. 564–574.

Estornes, Y., Bertrand, M.J.M. (2014) ‘IAPs, regulators of innate immunity and inflammation.’, *Semin. Cell Dev. Biol.*, 39 , pp. 1–9.

Failes, T.W., Cullinane, C., Diakos, C.I., Yamamoto, N., Lyons, J.G., Hambley, T.W. (2007) ‘Studies of a Cobalt(III) Complex of the MMP Inhibitor Marimastat: A Potential Hypoxia-Activated Prodrug’, *Chem. - A Eur. J.*, 13 (10), pp. 2974–2982.

Fan, L., Tian, M., Liu, Y., Deng, Y., Liao, Z., Xu, J. (2017) ‘Salicylate •Phenanthroline copper (II) complex induces apoptosis in triple-negative breast cancer cells.’, *Oncotarget*, 8 (18), pp. 29823–29832.

Fanning, T. (2017) Bio Pharmaceuticals FDI Opportunities [online], *IDA*, available: http://www.idaireland.com/business-in-ireland/industry-sectors/bio-pharmaceuticals/ [accessed 1 Aug 2017].

Farber, S., Diamond, L.K., Mercer, R.D., Sylvester, R.F., Wolff, J.A. (1948) ‘Temporary Remissions in Acute Leukemia in Children Produced by Folic Acid Antagonist, 4-Aminopteroyl-Glutamic Acid (Aminopterin)’, *N. Engl. J. Med.*, 238 (23), pp. 787–793.

Farrell, N. (2015), ‘Multi-platinum anti-cancer agents. Substitution-inert compounds for tumor selectivity and new targets’, *Chem. Soc. Rev.*, 44 (24), pp. 8773-8785.

Feldman, D.R., Bosl, G.J., Sheinfeld, J., Motzer, R.J. (2008) ‘Medical Treatment of Advanced Testicular Cancer’, *JAMA*, 299 (6), pp. 672-684.

Fernández, R., Melchart, M., Habtemariam, A., Parsons, S., Sadler, P.J. (2004) ‘Use of Chelating Ligands to Tune the Reactive Site of Half-Sandwich Ruthenium(II)–Arene Anticancer Complexes’, *Chem. - A Eur. J.*, 10 (20), pp. 5173–5179.

Ferreira, J.A., Peixoto, A., Neves, M., Gaiteiro, C., Reis, C.A., Assaraf, Y.G., Santos, L.L. (2015) 'Mechanisms of cisplatin resistance and targeting of cancer stem cells: Adding glycosylation to the equation', *Drug Resist. Updat.*, 24 , pp. 34–54.

Festa, R.A., Thiele, D.J. (2011) 'Copper: An essential metal in biology', *CURBIO*, 21 (21) , pp. 877–883.

FDA, (2015), 'Drug Development Process Infographic', *Drug Approval Process*. Available at: http://www.phrma.org/advocacy/research-development/clinical-trials [accessed on 18-11-2017]

Filomeni, G., Piccirillo, S., Graziani, I., Cardaci, S., Da, A.M., Ferreira, C., Rotilio, G., Ciriolo, M.R. (2009) 'The isatin-Schiff base copper(II) complex Cu(isaepy) 2 acts as delocalized lipophilic cation, yields widespread mitochondrial oxidative damage and induces AMP-activated protein kinase-dependent apoptosis', *Carcinogenesis*, 30 (7), pp. 1115–1124.

Fischer-Fodor, E., Vălean, A.-M., Virag, P., Ilea, P., Tatomir, C., Imre-Lucaci, F., Schrepler, M.P., Krausz, L.T., Tudoran, L.B., Precup, C.G., Lupan, I., Hey-Hawkins, E., Silaghi-Dumitrescu, L., Chenevix-Trench, G. (2014) 'Gallium phosphinoarylbisthiolato complexes counteract drug resistance of cancer cells', *Metallomics*, 6 (4), pp. 833-844.

Florea, A.-M., Büsselberg, D. (2011) 'Cisplatin as an Anti-Tumor Drug: Cellular Mechanisms of Activity, Drug Resistance and Induced Side Effects', *Cancers (Basel)*, 3, pp. 1351–1371.

Fontaine, S. La, Mercer, J.F.B. (2007) 'Trafficking of the copper-ATPases, ATP7A and ATP7B: Role in copper homeostasis', *Arch. Biochem. Biophys.*, 463, pp. 149–167.

Fornari, F.A., Randolph, J.K., Yalowich, J.C., Ritke, M.K., Gewirtz, D.A. (1994) 'Interferance by doxorubicin with DNA unwinding in MCF-7 breast tumour cells',

Mol. Pharmacol., 45 (4), pp. 649-656.

Fraval, H.N.A., Rawlings, C.J., Roberts, J.J. (1978), 'Increased sensitivity of UV-repair-deficient human cells to DNA bound platinum products which unlike thymine dimers are not recognized by an endonuclease extracted from Micrococcus luteus', *Mutat. Res. Mol. Mech. Mutagen.*, 51 (1), pp. 121–132.

Frelon, S., Douki, T., Favier, A., Cadet, J. (2003), 'Hydroxyl Radical Is Not the Main Reactive Species Involved in the Degradation of DNA Bases by Copper in the Presence of Hydrogen Peroxide', *Chem. Res. Toxicol.*, 16 (2), pp. 191-198.

Fries, J.F., Bloch, D., Spitz, P., Mitchell, D.M. (1985) 'Cancer in rheumatoid arthritis: A prospective long-term study of mortality', *Am. J. Med.*, 78 (1), pp. 56–59.

Gabbiani, C., Casini, A., Messori, L. (2007) 'Gold(III) compounds as anticancer drugs', *Gold Bull.*, 40 (1), pp. 73–81.

Galindo-Murillo, R., Garcia-Ramos, J.C., Ruiz-Azuara, L., Cheatham, T.E., Cortes-Guzman, F. (2015) 'Intercalation processes of copper complexes in DNA', *Nucleic Acids Res.*, 1, pp. 1–13.

Galluzzi, L., Senovilla, L., Vitale, I., Michels, J., Martins, I., Kepp, O., Castedo, M., Kroemer, G. (2012) 'Molecular mechanisms of cisplatin resistance', *Oncogene*, 31 (15), pp. 1869–1883.

Gamberi, T., Massai, L., Magherini, F., Landini, I., Fiaschi, T., Scaletti, F., Gabbiani, C., Bianchi, L., Bini, L., Nobili, S., Perrone, G., Mini, E., Messori, L., Modesti, A. (2014) 'Proteomic analysis of A2780/S ovarian cancer cell response to the cytotoxic organogold(III) compound Aubipyc', *J. Proteomics*, 103 , pp. 103–120.

Ganellin, C.R., Roberts, S., Jefferis, R. (2013) *Introduction to Biological and Small Molecule Drug Research and Development : Theory and Case Studies*, 1st edition Academic Press.

Garnett, M.J., Edelman, E.J., Heidorn, S.J., Greenman, C.D., Dastur, A., Lau, K.W., Greninger, P., Thompson, I.R., Luo, X., Soares, J., Liu, Q., Iorio, F., Surdez, D., Chen, L., Milano, R.J., Bignell, G.R., Tam, A.T., Davies, H., Stevenson, J.A., Barthorpe, S., Lutz, S.R., Kogera, F., Lawrence, K., McLaren-Douglas, A., Mitropoulos, X., Mironenko, T., Thi, H., Richardson, L., Zhou, W., Jewitt, F., Zhang, T., O'Brien, P., Boisvert, J.L., Price, S., Hur, W., Yang, W., Deng, X., Butler, A., Choi, H.G., Chang, J.W., Baselga, J., Stamenkovic, I., Engelman, J.A., Sharma, S. V., Delattre, O., Saez-Rodriguez, J., Gray, N.S., Settleman, J., Futreal, P.A., Haber, D.A., Stratton, M.R., Ramaswamy, S., McDermott, U., Benes, C.H. (2012) 'Systematic identification of genomic markers of drug sensitivity in cancer cells', *Nature*, 483 (7391), pp. 570–575.

Gasche, C. (2013) 'Iron Physiology and Pathophysiology in Humans', *Gastroenterology*, 144 (2), pp. 464–465.

Gava, B., Zorzet, S., Spessotto, P., Cocchietto, M., Sava, G. (2006) 'Inhibition of B16 Melanoma Metastases with the Ruthenium Complex Imidazolium trans-Imidazoledimethylsulfoxide-tetrachlororuthenate and Down-Regulation of Tumor Cell Invasion', *J. Pharmacol. Exp. Ther.*, 317 (1), pp. 284–291.

Gelasco, A., Lippard, S.J. (1998) 'NMR solution structure of a DNA dodecamer duplex containing a cis-diammineplatinum(II) d(GpG) intrastrand cross-link, the major adduct of the anticancer drug cisplatin', *Biochemistry*, 37 (26), pp. 9230–9239.

Geraghty, R.J., Capes-Davis, A., Davis, J.M., Downward, J., Freshney, R.I., Knezevic, I., Lovell-Badge, R., Masters, J.R.W., Meredith, J., Stacey, G.N., Thraves, P., Vias, M. (2014) 'Guidelines for the use of cell lines in biomedical research', *Br. J. Cancer*, 111, pp. 1021-1046.

Giaccone, G. (2000) 'Clinical perspectives on platinum resistance.', *Drugs*, 59 Suppl

(4), pp. 9-38.

Gibson, S.B. (2013) ‘Chapter Thirteen – Investigating the Role of Reactive Oxygen Species in Regulating Autophagy’, in *Methods in Enzymology.*, 217–235.

Gifford, G., Paul, J., Vasey, P.A., Kaye, S.B., Brown, R. (2004) ‘The Acquisition of hMLH1 Methylation in Plasma DNA after Chemotherapy Predicts Poor Survival for Ovarian Cancer Patients’, *Clin. Cancer Res.*, 10 (13), pp. 4420–4426.

Gilman, A. (1946) ‘Symposium on advances in pharmacology resulting from war research: therapeutic applications of chemical warfare agents’, *Fed. Proc.*, 5, pp. 285-292.

Giner Martínez-Sierra, J., Galilea San Blas, O., Marchante Gayón, J., García Alonso, J. (2015) ‘Sulfur analysis by inductively coupled plasma-mass spectrometry: A review’, *Spectrochim. Acta Part B At. Spectrosc.*, 108, pp. 35–52.

Gleyzer, N., Vercauteren, K., Scarpulla, R.C. (2005) ‘Control of Mitochondrial Transcription Specificity Factors (TFB1M and TFB2M) by Nuclear Respiratory Factors (NRF-1 and NRF-2) and PGC-1 Family Coactivators’, *Mol. Cell. Biol.*, 25 (4), pp. 1354–1366.

Glišić, B., Rychlewska, U., Djuran, M. I. (2012), ‘Reactions and structural characterization of gold(iii) complexes with amino acids, peptides and proteins, *Dalt. Trans.*, 41 (23), pp. 6887-6901.

Goodman, L., Wintrobe, M., Dameshek, W., Goodman, M., J., Gilman, A., Mclennan, M. T., (1946) ‘Nitrogen Mustard Therapy’, J Amer. Med. Assoc., 132 (3), pp. 126-132.

Gratteri, P., Massai, L., Michelucci, E., Rigo, R., Messori, L., Cinellu, M.A., Musetti, C., Sissi, C., Bazzicalupi, C. (2015) ‘Interactions of selected gold(iii) complexes with DNA G quadruplexes’, *Dalt. Trans.*, 44 (8), pp. 3633–3639.

Green, D.R. (2011) *Means to an End: Apoptosis and Other Cell Death Mechanisms*, Cold Spring Harbor Laboratory Press.

Groner, B., Weiss, A. (2014) 'Targeting Survivin in Cancer: Novel Drug Development Approaches', *BioDrugs*, 28 (1), pp. 27–39.

Gross, A. (2016) 'BCL-2 family proteins as regulators of mitochondria metabolism', *Biochim. Biophys. Acta - Bioenerg.*, 1857 (8), pp. 10–13.

Gross, R., Wulf, G. (1959) 'Klinische und experimentelle Erfahrungen mit zyk lischen und nichtzyklischen Phosphamidestern des N-Losl in der Chemotherapie von Tumoren', *Strahlentherapie*, 41 , pp. 361–367.

Gu, M., Cooper, J.M., Butler, P., Walker, A.P., Mistry, P.K., Dooley, J.S., Schapira, A.H. (2000) 'Oxidative-phosphorylation defects in liver of patients with Wilson's disease.', *Lancet (London, England)*, 356 (9228), pp. 469–474.

Gullo, J.J., Litterst, C.L., Maguire, P.J., Sikic, B.I., Hoth, D.F., Woolley, P. V. (1980) 'Pharmacokinetics and protein binding of cis-dichlorodiammine platinum (II) administered as a one hour or as a twenty hour infusion', *Cancer Chemother. Pharmacol.*, 5 (1), pp. 21–26.

Gumulec, J., Balvan, J. a N., Sztalmachova, M., Raudenska, M., Dvorakova, V., Knopfova, L., Polanska, H., Hudcova, K., Ruttkay-Nedecky, B., Babula, P., Adam, V., Kizek, R., Stiborova, M., Masarik, M. (2014) 'Cisplatin-resistant prostate cancer model: Differences in antioxidant system, apoptosis and cell cycle', *Int J Oncol*, 44, pp. 923–933.

Guo, W., Zheng, W., Luo, Q., Li, X., Zhao, Y., Xiong, S., Wang, F. (2013) 'Transferrin Serves As a Mediator to Deliver Organometallic Ruthenium(II) Anticancer Complexes into Cells', *Inorg. Chem.*, 52 (9), pp. 5328–5338.

Gupta, A., Lutsenko, S. (2009) 'Human copper transporters: mechanism, role in human

diseases and therapeutic potential', *Futur. Med Chem*, 1 (6), pp. 1125–1142.

Haagenson, K.K., Wu, G.S. (2010) 'Mitogen activated protein kinase phosphatases and cancer', *Cancer Biol. Ther.*, 9 (5), pp. 337–340.

Hadrup, N., Lam, H.R. (2014) 'Oral toxicity of silver ions, silver nanoparticles and colloidal silver – A review', *Regul. Toxicol. Pharmacol.*, 68 (1), pp. 1–7.

Hagenbuchner, J., Kiechl-Kohlendorfer, U., Obexer, P., Ausserlechner, M.J. (2016) 'BIRC5/Survivin as a target for glycolysis inhibition in high-stage neuroblastoma', *Oncogene*, 35 (16), pp. 2052–2061.

Hait, W.N. (2010) 'Anticancer drug development: the grand challenges', *Nat. Rev. Drug Discov.*, 9 (4), pp. 253–254.

Hall, J., Cook, D., Morte, S., McIntyre, P., Buchner, K., Beer, H., Cardin, D., Brazier, J., Winter, G., Kelly, J., Cardin, C. (2013) 'X-ray crystal structure of rac-[Ru(phen)2dppz]2+ with d(ATGCAT)2 shows enantiomer orientations and water ordering', *J Am Chem Soc*, 135 , pp. 12652–12659.

Han, D., Antunes, F., Canali, R., Rettori, D., Cadenas, E. (2003) 'Voltage-dependent Anion Channels Control the Release of the Superoxide Anion from Mitochondria to Cytosol', *J. Biol. Chem.*, 278 (8), pp. 5557–5563.

Hanahan, D., Weinberg, R.A. (2000) 'The hallmarks of cancer.', *Cell*, 100 (1), pp. 57–70.

Hanahan, D., Weinberg, R.A., Pan, K.H., Shay, J.W., Cohen, S.N., Taylor, M.B., Clarke, N.W., Jayson, G.C., Eshleman, J.R., Nowak, M.A., al., et (2011) 'Hallmarks of Cancer: The Next Generation', *Cell*, 144 (5), pp. 646–674.

Harrington, C.F., Le Pla, R.C., Jones, G.D.D., Thomas, A.L., Farmer, P.B. (2010) 'Determination of Cisplatin 1,2-Intrastrand Guanine−Guanine DNA Adducts in Human Leukocytes by High-Performance Liquid Chromatography Coupled to

Inductively Coupled Plasma Mass Spectrometry', *Chem. Res. Toxicol.*, 23 (8), pp. 1313–1321.

Hartinger, C.G., Zorbas-Seifried, S., Jakupec, M.A., Kynast, B., Zorbas, H., Keppler, B.K. (2006) 'From bench to bedside – preclinical and early clinical development of the anticancer agent indazolium trans-[tetrachlorobis(1H-indazole)ruthenate(III)] (KP1019 or FFC14A)', *J. Inorg. Biochem.*, 100 (5–6), pp. 891–904.

Hartmann, B., Wai, T., Hu, H., MacVicar, T., Musante, L., Fischer-Zirnsak, B., Stenzel, W., Gräf, R., van den Heuvel, L., Ropers, H.-H., Wienker, T.F., Hübner, C., Langer, T., Kaindl, A.M. (2016) 'Homozygous YME1L1 mutation causes mitochondriopathy with optic atrophy and mitochondrial network fragmentation.', *elife*, 5, pp. e16078. Available at: http://www.ncbi.nlm.nih.gov/pubmed/27495975 [accessed 31 May 2017].

Hassan, M., Watari, H., AbuAlmaaty, A., Ohba, Y., Sakuragi, N. (2014) 'Apoptosis and molecular targeting therapy in cancer.', *Biomed Res. Int.*, pp. 150845., available: http://www.ncbi.nlm.nih.gov/pubmed/25013758 [accessed 15 Oct 2017].

Hayashi, R., Nakatsui, K., Sugiyama, D., Kitajima, T., Oohara, N., Sugiya, M., Osada, S., Kodama, H. (2014) 'Anti-tumor activities of Au(I) complexed with bisphosphines in HL-60 cells', *J. Inorg. Biochem.*, 137 , pp. 109–114.

Hayward, R.L., Schornagel, Q.C., Tente, R., Macpherson, J.S., Aird, R.E., Guichard, S., Habtemariam, A., Sadler, P., Jodrell, D.I. (2005) 'Investigation of the role of Bax, p21/Waf1 and p53 as determinants of cellular responses in HCT116 colorectal cancer cells exposed to the novel cytotoxic ruthenium(II) organometallic agent, RM175', *Cancer Chemother. Pharmacol.*, 55 (6), pp. 577–583.

Heidelberger, C., Chaudhuri, N.K., Danneberg, P., Mooren, D., Griesbach, L., Duschinsky, R., Schnitzer, R.J., Pleven, E., Scheiner, J. (1957) 'Fluorinated

Pyrimidines, A New Class of Tumour-Inhibitory Compounds', *Nature*, 179, pp. 663–666.

Hickey, J.L., Ruhayel, R.A., Barnard, P.J., Baker, M. V., Berners-Price, S.J., Filipovska, A. (2008) 'Mitochondria-Targeted Chemotherapeutics: The Rational Design of Gold(I) N-Heterocyclic Carbene Complexes That Are Selectively Toxic to Cancer Cells and Target Protein Selenols in Preference to Thiols', *J. Am. Chem. Soc.*, 130 (38), pp. 12570–12571.

Hoffmann, J. a. (1995) 'Innate immunity of insects', *Curr. Opin. Immunol.*, 7, pp. 4–10.

Holzer, A.K., Howell, S.B. (2006) 'The Internalization and Degradation of Human Copper Transporter 1 following Cisplatin Exposure', *Cancer Res.*, 66 (22), pp. 10944–10952.

Hsu, S.-C., Miller, S.A., Wang, Y., Hung, M.-C. (2009) 'Nuclear EGFR is required for cisplatin resistance and DNA repair.', *Am. J. Transl. Res.*, 1 (3), pp. 249–258.

Human Genome Sequencing Consortium, I. (2004) 'Finishing the euchromatic sequence of the human genome', *Nature*, 431, pp. 931–945.

Ichim, G., Tait, S.W.G. (2016) 'A fate worse than death: apoptosis as an oncogenic process', *Nat. Rev. Cancer*, 16 (8), pp. 539–548.

Idan Valencia-Cruz, A., Uribe-Figueroa, L.I., Galindo-Murillo, R., Baca-Ló Pez, K., Gutié Rrez, A.G., Vá Zquez-Aguirre, A., Ruiz-Azuara, L., Herná Ndez-Lemus, E., Mejía, C. (2013) 'Whole Genome Gene Expression Analysis Reveals Casiopeína-Induced Apoptosis Pathways', *PLoS One*, 8 (1), pp. e54664. Available at: http://journals.plos.org/plosone/article/file?id=10.1371/journal.pone.0054664&type=printable [accessed 21 Jul 2017].

Iglesias-Osma, C., Gonzalez-Villaron, L., San Miguel, J.F., Caballero, M.D., Vazquez, L., de Castro, S. (1995) 'Iron metabolism and fungal infections in patients with

haematological malignancies.', *J Clin Path*, 48 (3), pp. 223–225.

Jain, H. V., Meyer-Hermann, M. (2011) 'The Molecular Basis of Synergism between Carboplatin and ABT-737 Therapy Targeting Ovarian Carcinomas', *Cancer Res.*, 71 (3), pp. 705–715.

Jamieson, E., Lippard, S. (1999) 'Structure, Recognition, and Processing of Cisplatin – DNA Adducts', *Chem. Rev.*, 99, pp. 2467-2498.

Janson, V., Johansson, A., Grankvist, K. (2010) 'Resistance to caspase-8 and -9 fragments in a malignant pleural mesothelioma cell line with acquired cisplatin-resistance.', *Cell Death Dis.*, 1 (9), pp. e78., available: http://www.ncbi.nlm.nih.gov/pubmed/21364680 [accessed 31 Aug 2017].

Jennings, B.H. (2011) 'Drosophila - a versatile model in biology & medicine', *Mater. Today*, 14 (5), pp. 190–195.

Ji, H., Wang, J., Guo, J., Li, Y., Lian, S., Guo, W., Yang, H., Kong, F., Zhen, L., Guo, L., Liu, Y. (2016) 'Progress in the biological function of alpha-enolase', *Anim. Nutr.*, 2 (1), pp. 12–17.

Jovaisaite, V., Mouchiroud, L., Auwerx, J. (2014) 'The mitochondrial unfolded protein response, a conserved stress response pathway with implications in health and disease.', *J. Exp. Biol.*, 217 (1), pp. 137–143.

Jun, H.J., Ahn, M.J., Kim, H.S., Yi, S.Y., Han, J., Lee, S.K., Ahn, Y.C., Jeong, H.-S., Son, Y.-I., Baek, J.-H., Park, K. (2008) 'ERCC1 expression as a predictive marker of squamous cell carcinoma of the head and neck treated with cisplatin-based concurrent chemoradiation', *Br. J. Cancer*, 99 (1), pp. 167–172.

Jungwirth, U., Kowol, C.R., Keppler, B.K., Christian, G. (2012) 'Anticancer Activity of Metal Complexes : Involvement of Redox Processes', *Antioxid. Redox Signal.*, 15 (4), pp. 1085–1127.

Kaeser, A., Mohankumar, M., Mohanraj, J., Monti, F., Holler, M., Cid, J.-J., Moudam, O., Nierengarten, I., Karmazin-Brelot, L., Duhayon, C., Delavaux-Nicot, B., Armaroli, N., Nierengarten, J.-F. (2013) 'Heteroleptic Copper(I) Complexes Prepared from Phenanthroline and Bis-Phosphine Ligands', *Inorg. Chem.*, 52 (20), pp. 12140–12151.

Kalayda, G. V, Wagner, C.H., Jaehde, U. (2012) 'Relevance of copper transporter 1 for cisplatin resistance in human ovarian carcinoma cells', *J. Inorg. Biochem.*, 116, pp. 1–10.

Kalinowska-Lis, U., Ochocki, J., Matlawska-Wasowska, K. (2008) 'Trans geometry in platinum antitumor complexes', *Coord. Chem. Rev.*, 252 , pp. 1328–1345.

Kamal, N.S., Soria, J.-C., Mendiboure, J., Planchard, D., Olaussen, K.A., Rousseau, V., Popper, H., Pirker, R., Bertrand, P., Dunant, A., Le Chevalier, T., Filipits, M., Fouret, P., International Adjuvant Lung Trial-Bio investigators (2010) 'MutS Homologue 2 and the Long-term Benefit of Adjuvant Chemotherapy in Lung Cancer', *Clin. Cancer Res.*, 16 (4), pp. 1206–1215.

Kameyama, Y., Okazaki, N., Nakagawa, M., Koshida, H., Nakamura, M., Gemba, M. (1990) 'Nephrotoxicity of a new platinum compound, 254-S, evaluated with rat kidney cortical slices', *Toxicol. Lett.*, 52 (1), pp. 15–24.

Kansanen, E., Jyrkkänen, H.-K., Levonen, A.-L. (2012) 'Activation of stress signaling pathways by electrophilic oxidized and nitrated lipids', *Free Radic. Biol. Med.*, 52 (6), pp. 973–982.

Kansanen, E., Kuosmanen, S.M., Leinonen, H., Levonenn, A.L. (2013) 'The Keap1-Nrf2 pathway: Mechanisms of activation and dysregulation in cancer', *Redox Biol.*, 1, pp. 45–49.

Kaplan, J.H., Lutsenko, S. (2009) 'Copper Transport in Mammalian Cells: Special Care

for a Metal with Special Needs * Dietary Acquisition and Excretion of Copper', *J. Biol. Chem.*, 284 (38), pp. 25461–25465.

Karasawa, T., Steyger, P.S. (2015) 'An integrated view of cisplatin-induced nephrotoxicity and ototoxicity', *Toxicol. Lett.*, 237 (3), pp. 219–227.

Karotki, A. V., Vašák, M. (2009b) 'Reaction of human metallothionein-3 with cisplatin and transplatin', *J. Biol. Inorg. Chem.*, 14 (7), pp. 1129–1138.

Kashatus, J.A., Nascimento, A., Myers, L.J., Sher, A., Byrne, F.L., Hoehn, K.L., Counter, C.M., Kashatus, D.F. (2015) 'Erk2 phosphorylation of Drp1 promotes mitochondrial fission and MAPK-driven tumor growth', *Mol. Cell*, 57 (3), pp. 537–552.

Kasherman, Y., Sturup, S., Gibson, D. (2009) 'Is Glutathione the Major Cellular Target of Cisplatin? A Study of the Interactions of Cisplatin with Cancer Cell Extracts', *J. Med. Chem.*, 52 (14), pp. 4319–4328.

Kavanagh, K., Fallon, J.P. (2010) 'Galleria mellonella larvae as models for studying fungal virulence', *Fungal Biol. Rev.*, 24, pp. 79–83.

Kavanagh, K., Reeves, E.P. (2004) 'Exploiting the potential of insects for in vivo pathogenicity testing of microbial pathogens', *FEMS Microbiol. Rev.*, 28, pp. 101–112.

Keeler, B., Brookes, M. (2013) 'Iron chelation: a potential therapeutic strategy in oesophageal cancer', *Br. J. Pharmacol.*, 168 (6), pp. 1313–1315.

Kellett, A., Howe, O., O'Connor, M., McCann, M., Creaven, B.S., McClean, S., Foltyn-Arfa Kia, A., Casey, A., Devereux, M. (2012) 'Radical-induced DNA damage by cytotoxic square-planar copper(II) complexes incorporating o-phthalate and 1,10-phenanthroline or 2,2'-dipyridyl', *Free Radic. Biol. Med.*, 53, pp. 564–576.

Kellett, A., O'Connor, M., McCann, M., Howe, O., Casey, A., McCarron, P.,

Kavanagh, K., McNamara, M., Kennedy, S., May, D.D., Skell, P.S., O'Shea, D., Devereux, M. (2011a) 'Water-soluble bis(1,10-phenanthroline) octanedioate Cu2+ and Mn2+ complexes with unprecedented nano and picomolar in vitro cytotoxicity: promising leads for chemotherapeutic drug development', *Medchemcomm*, 2 (7), pp. 579-584.

Kellett, A., O'Connor, M., McCann, M., McNamara, M., Lynch, P., Rosair, G., McKee, V., Creaven, B., Walsh, M., McClean, S., Foltyn, A., O'Shea, D., Howe, O., Devereux, M. (2011b) 'Bis-phenanthroline copper(II) phthalate complexes are potent in vitro antitumour agents with "self-activating" metallo-nuclease and DNA binding properties', *Dalt. Trans.*, 40, pp. 1024–1027.

Kelly, J., Kavanagh, K. (2011) 'Caspofungin primes the immune response of the larvae of Galleria mellonella and induces a non-specific antimicrobial response', *J. Med. Micro.*, 60 (2), pp. 189–196.

Kemp, M., Massey, R.C. (2007) 'The use of insect models to study human pathogens', *Drug Discov. Today*, 4, pp. 105–110.

Khalaila, I., Allardyce, C.S., Verma, C.S., Dyson, P.J. (2005) 'A Mass Spectrometric and Molecular Modelling Study of Cisplatin Binding to Transferrin', *ChemBioChem*, 6 (10), pp. 1788–1795.

Kilkenny, C., Browne, W.J., Cuthill, I.C., Emerson, M., Altman, D.G. (2010) 'Improving Bioscience Research Reporting: The ARRIVE Guidelines for Reporting Animal Research', *PLoS Biol.*, 8 (6), pp. e1000412., available at: http://dx.plos.org/10.1371/journal.pbio.1000412 [accessed 11 Nov 2017].

Kim, J.S., Lee, J.H.J.M., Chwae, Y.J., Kim, Y.H., Lee, J.H.J.M., Kim, K., Lee, T.H., Kim, S.J., Park, J.H. (2004) 'Cisplatin-induced apoptosis in Hep3B cells: Mitochondria-dependent and -independent pathways', *Biochem. Pharmacol.*, 67

(8), pp. 1459–1468.

Kim, M.K., Cho, K.-J., Kwon, G.Y., Park, S.-I., Kim, Y.H., Kim, J.H., Song, H.-Y., Shin, J.H., Jung, H.Y., Lee, G.H., Choi, K.D., Kim, S.-B. (2008) 'Patients with ERCC1-Negative Locally Advanced Esophageal Cancers May Benefit from Preoperative Chemoradiotherapy', *Clin. Cancer Res.*, 14 (13), pp. 4225–4231.

Knipp, M., Karotki, A.V., Chesnov, S., Natile, G., Sadler, P.J., Brabec, V., Vašák, M., (2007) 'Reaction of Zn7Metallothionein with cis- and trans-[Pt(N-donor)2Cl2] Anticancer Complexes: trans-PtII Complexes Retain Their N-Donor Ligands', *J. Med. Chem.*, 50 (17), pp. 4075-4086.

Köberle, B., Tomicic, M.T., Usanova, S., Kaina, B. (2010) 'Cisplatin resistance: Preclinical findings and clinical implications', *Biochim. Biophys. Acta - Rev. Cancer*, 1806 (2), pp. 172–182.

Koch, M., Krieger, M.L., Stö Lting, D., Brenner, N., Beier, M., Jaehde, U., Wiese, M., Royer, H.-D., Bendas, G. (2013) 'Overcoming chemotherapy resistance of ovarian cancer cells by liposomal cisplatin: Molecular mechanisms unveiled by gene expression profiling', *Biochem. Pharmacol.*, 85 , pp. 1077–1090.

Kong, L.R., Chua, K.N., Sim, W.J., Ng, H.C., Bi, C., Ho, J., Nga, M.E., Pang, Y.H., Ong, W.R., Soo, R.A., Huynh, H., Chng, W.J., Thiery, J.-P., Goh, B.C. (2015) 'MEK Inhibition Overcomes Cisplatin Resistance Conferred by SOS/MAPK Pathway Activation in Squamous Cell Carcinoma', *Mol. Cancer Ther.*, 14 (7), pp. 1750–1760.

Kovacevic, Z., Richardson, D.R. (2012) 'Targeting Iron in Cancer Cells: A New Strategy to Inhibit Metastatic Progression', *Vitam. Trace Elem.*, 1 (3), pp. e114., available at: http://www.omicsgroup.org/journals/targeting-iron-in-cancer-cells-a-new-strategy-to-inhibit-metastatic-progression-vms.1000e114.php?aid=5766

[accessed 8 Aug 2017].

Kramer, K.J., Childs, C.N. (1977) ‘Interaction of juvenile hormone with carrier proteins and hydrolases from insect haemolymph’, *J Insect Biochem*, 7, pp. 397–403.

Kraus, W.L., Hottiger, M.O. (2013) ‘PARP-1 and gene regulation: progress and puzzles.’, *Mol Asp. Med*, 34 , pp. 1109–1123.

Kroemer, G., Galluzzi, L., Brenner, C. (2007) ‘Mitochondrial Membrane Permeabilization in Cell Death’, *Physiol. Rev.*, 87 (1), pp. 99–163.

Kröller-Schön, S., Steven, S., Kossmann, S., Scholz, A., Daub, S., Oelze, M., Xia, N., Hausding, M., Mikhed, Y., Zinßius, E., Mader, M., Stamm, P., Treiber, N., Scharffetter-Kochanek, K., Li, H., Schulz, E., Wenzel, P., Münzel, T., Daiber, A. (2014) ‘Molecular Mechanisms of the Crosstalk Between Mitochondria and NADPH Oxidase Through Reactive Oxygen Species—Studies in White Blood Cells and in Animal Models’, *Antioxid. Redox Signal.*, 20 (2), pp. 247–266.

Kröning, R., Lichtenstein, A.K., Nagami, G.T. (2000) ‘Sulfur-containing amino acids decrease cisplatin cytotoxicity and uptake in renal tubule epithelial cell lines’, *Cancer Chemother. Pharmacol.*, 45 (1), pp. 43–49.

Krumbhaar, E.B., Krumbhaar, H.D. (1919) ‘The Blood and Bone Marrow in Yelloe Cross Gas (Mustard Gas) Poisoning: Changes produced in the Bone Marrow of Fatal Cases.’, *J. Med. Res.*, 40 (3), pp. 497–508.

Kullmann, M., Kalayda, G. V, Hellwig, M., Kotz, S., Hilger, R.A., Metzger, S., Jaehde, U. (2015) ‘Assessing the contribution of the two protein disulfide isomerases PDIA1 and PDIA3 to cisplatin resistance’, *J. Inorg. Biochem.*, 153 , pp. 247–252.

Kurnik, R. (2007) ‘Rotation Algorithm for Determining Cycle Thresholds in Real-Time Polymerase Chain Reactions’, *Conf Proc IEEE Eng Med Biol Soc*, 2007 , pp. 1977–1980.

Lammering, G., Carl, U.M., Pape, H., Hartmann, K.A. (1999) ‘Änderungen der Hämoglobinkonzentration bei kombinierter Radio- und Chemotherapie lokal fortgeschrittener HNO-Tumoren’, *Strahlentherapie und Onkol.*, 175 (11), pp. 559–562.

Lange, T.S., Kim, K.K., Singh, R.K., Strongin, R.M., McCourt, C.K., Brard, L. (2008) ‘Iron(III)-Salophene: An Organometallic Compound with Selective Cytotoxic and Anti-Proliferative Properties in Platinum-Resistant Ovarian Cancer Cells’, *PLoS One*, 3 (5), pp. e2303., available at: http://www.ncbi.nlm.nih.gov/pubmed/18509533 [accessed 8 Aug 2017].

Lazarevi, T., Rilak, A., Bugar Ci, Z.D. (2017) ‘Platinum, palladium, gold and ruthenium complexes as anticancer agents: Current clinical uses, cytotoxicity studies and future perspectives’, *Eur. J. Med. Chem*. doi: 10.1016/j.ejmech.2017.04.007. [accessed on 17-11-2017]

Le Bivic, A, Hirn, M., Reggio, H. (1988) ‘HT-29 cells are an in vitro model for the generation of cell polarity in epithelia during embryonic differentiation.’, *Proc. Natl. Acad. Sci. U. S. A.*, 85 (1), pp. 136–140.

Lee, K.H., Hyun, M.S., Kim, H.-K., Jin, H.M., Yang, J., Song, H.S., Do, Y.R., Ryoo, H.M., Chung, J.S., Zang, D.Y., Lim, H.-Y., Jin, J.Y., Yim, C.Y., Park, H.S., Kim, J.S., Sohn, C.H., Lee, S.N. (2009) ‘Randomized, multicenter, phase III trial of heptaplatin 1-hour infusion and 5-fluorouracil combination chemotherapy comparing with cisplatin and 5-fluorouracil combination chemotherapy in patients with advanced gastric cancer.’, *Cancer Res. Treat.*, 41 (1), pp. 12–18.

Leijen, S., Burgers, S.A., Baas, P., Pluim, D., Tibben, M., van Werkhoven, E., Alessio, E., Sava, G., Beijnen, J.H., Schellens, J.H.M. (2015) ‘Phase I/II study with ruthenium compound NAMI-A and gemcitabine in patients with non-small cell

lung cancer after first line therapy', *Invest. New Drugs*, 33 (1), pp. 201–214.

Leung, C.-H., Liu, L.-J., Leung, K.-H., Ma, D.-L. (2016) 'Epigenetic modulation by inorganic metal complexes', *Coord. Chem. Rev.*, 319, pp. 25–34.

Ley, T.J., Mardis, E.R., Ding, L., Fulton, B., McLellan, M.D., Chen, K., Dooling, D., Dunford-Shore, B.H., McGrath, S., Hickenbotham, M., Cook, L., Abbott, T., Larson, D.E., Koboldt, D.C., Pohl, C., Smith, S., Hawkins, A., Abbott, S., Locke, D., Hillier, L.W., Miner, T., Fulton, L., Magrini, V., Wylie, T., Glasscock, J., Conyers, J., Sanders, N., Shi, X., Osborne, J.R., Minx, P., Gordon, D., Chinwalla, A., Zhao, T., Ries, R.E., Payton, J.E., Westervelt, P., Tomasson, M.H., Watson, M., Baty, J., Ivanovich, J., Heath, S., Shannon, W.D, Nagarajan, R., Walter, M.J., Link, D.C., Graubert, T.A., DiPersio, J.F., Wilson, R.K., (2008) 'DNA Sequencing of cytogenetically normal acute myeloid leukemia', *Nature*, 456 (7218), pp. 66-72.

Li, J., Feng, Q., Kim, J.-M., Schneiderman, D., Liston, P., Li, M., Vanderhyden, B., Faught, W., Fung, M.F.K., Senterman, M., Korneluk, R.G., Tsang, B.K. (2001) 'Human Ovarian Cancer and Cisplatin Resistance: Possible Role of Inhibitor of Apoptosis Proteins 1', *Endocrinology*, 142 (1), pp. 370–380.

Li, L., Ishdorj, G., Gibson, S.B. (2012) 'Reactive oxygen species regulation of autophagy in cancer: Implications for cancer treatment', *Free Radic Biol Med*, 53 , pp. 1399–1410.

Li, W., Melton, D.W. (2012) 'Cisplatin regulates the MAPK kinase pathway to induce increased expression of DNA repair gene ERCC1 and increase melanoma chemoresistance', *Oncogene*, 31 (19), pp. 2412–2422.

Liang, X., Guo, Y., Figg, W.D., Fojo, A.T., Mueller, M.D., Yu, J.J. (2011) 'The Role of Wild-Type p53 in Cisplatin-Induced Chk2 Phosphorylation and the Inhibition of Platinum Resistance with a Chk2 Inhibitor', *Chemother. Res. Pract.*, 2011, pp. 1–

8. doi: 10.1155/2011/715469. [accessed on 31-08-2017]

Lin, M., Cao, Y., Pei, H., Chen, Y., Wu, J., Li, Y., Liu, W. (2014) 'Titanium isopropoxide complexes supported by pyrrolyl Schiff base ligands: syntheses, structures, and antitumor activity', *RSC Adv.*, 4 (18), pp. 9255-9260.

Litonin, D., Sologub, M., Shi, Y., Savkina, M., Anikin, M., Falkenberg, M., Gustafsson, C.M., Temiakov, D. (2010) 'Human Mitochondrial Transcription Revisited ony TFAM and TFB2M are required for transcription of the mitochondrial genes in vitro', *J. Biol. Chem.*, 285 (24), pp. 18129–18133.

Liu, Z., Delavan, B., Roberts, R., Tong, W. (2017) 'Lessons Learned from Two Decades of Anticancer Drugs', *Trends Pharmacol. Sci.*, 38 (10), pp. 852-872.

Livak, K.J., Schmittgen, T.D. (2001) 'Analysis of relative gene expression data using real-time quantitative PCR and the 2(-Delta Delta C(T)) Method', *Methods*, 25 , pp. 402–408.

Lovejoy, K.S., Lippard, S.J. (2009) 'Non-Traditional Platinum Compounds for Improved Accumulation, Oral Bioavailability, and Tumor Targeting', *Dalt. Trans*, 9, pp. 10651–10659.

Lu, G.-L., Stevenson, R.J., Chang, J.Y.-C., Brothers, P.J., Ware, D.C., Wilson, W.R., Denny, W.A., Tercel, M. (2011) 'N-alkylated cyclen cobalt(III) complexes of 1-(chloromethyl)-3-(5,6,7-trimethoxyindol-2-ylcarbonyl)-2,3-dihydro-1H-pyrrolo[3,2-f]quinolin-5-ol DNA alkylating agent as hypoxia-activated prodrugs', *Bioorg. Med. Chem.*, 19 (16), pp. 4861–4867.

Lümmen, G., Sperling, H., Luboldt, H., Otto, T., Rübben, H. (1998) 'Phase II trial of titanocene dichloride in advanced renal-cell carcinoma', *Cancer Chemother. Pharmacol.*, 42 (5), pp. 415–417.

Maguire, R., Kunc, M., Hyrsl, P., Kavanagh, K. (2017) 'Analysis of the acute response

of Galleria mellonella larvae to potassium nitrate', *Comp. Biochem. Physiol. Part C Toxicol. Pharmacol.*, 195, pp. 44–51.

Majumder, S., Dutta, P., Mookerjee, A., Choudhuri, S.K. (2006) 'The role of a novel copper complex in overcoming doxorubicin resistance in Ehrlich ascites carcinoma cells in vivo', *Chem. Biol. Interact.*, 159 (2), pp. 90–103.

Małecki, J.G., Łakomska, I., Maroń, A., Szala, M., Fandzloch, M., Nycz, J.E. (2015) 'Phosphorescent emissions of phosphine copper(I) complexes bearing 8-hydroxyquinoline carboxylic acid analogue ligands', *J. Lumin.*, 161 , pp. 382–388.

Mandic, R., Rodgarkia-Dara, C.J., Krohn, V., Wiegand, S., Grénman, R., Werner, J.A. (2009) 'Cisplatin resistance of the HNSCC cell line UT-SCC-26A can be overcome by stimulation of the EGF-receptor.', *Anticancer Res.*, 29 (4), pp. 1181–1187.

Martín-Santos, C., Michelucci, E., Marzo, T., Messori, L., Szumlas, P., Bednarski, P.J., Mas-Ballesté, R., Navarro-Ranninger, C., Cabrera, S., Alemán, J. (2015) 'Gold(III) complexes with hydroxyquinoline, aminoquinoline and quinoline ligands: Synthesis, cytotoxicity, DNA and protein binding studies. *J. Inorg. Biochem.*, 153, pp. 399-345.

MASCOT (2017) Mascot Database Search: Scoring [online], available at: http://www.matrixscience.com/help/scoring_help.html [accessed 13 Sep 2017].

Masters, J.R. (2002) 'HeLa cells 50 years on: the good, the bad and the ugly', *Nat. Rev. Cancer*. 2 (4), pp. 315-319.

Matha, V., Acek, Z. (1984) 'Changes in Haemocyte Counts in Galleria Mellonella (L.) (Lepidoptera: Galleriidae) Larvae Infected With Steinernema Sp. (Nematoda: Steinernematidae)', *Nematologica*, 30 (1), pp. 86-89.

Matulis, S.M., Morales, A.A., Yehiayan, L., Croutch, C., Gutman, D., Cai, Y., Lee,

K.P., Boise, L.H. (2009) ‘Darinaparsin induces a unique cellular response and is active in an arsenic trioxide-resistant myeloma cell line’, *Mol. Cancer Ther.*, 8 (5), pp. 1197–1206.

Mayer, R.J. (2012) ‘Oxaliplatin as part of adjuvant therapy for colon cancer: more complicated than once thought.’, *J. Clin. Oncol.*, 30 (27), pp. 3325–3327.

Mc Namara, L., Carolan, J.C., Griffin, C.T., Fitzpatrick, D., Kavanagh, K. (2017) ‘The effect of entomopathogenic fungal culture filtrate on the immune response of the greater wax moth, Galleria mellonella’, *J. Insect Physiol.*, 100, pp. 82–92.

McCann, M., Curran, R., Ben-Shoshan, M., McKee, V., Devereux, M., Kavanagh, K., Kellett, A. (2013) ‘Synthesis, structure and biological activity of silver(I) complexes of substituted imidazoles’, *Polyhedron*, 56, pp. 180–188.

McCann, M., Kellett, a., Kavanagh, K., Devereux, M., L.S. Santos, a. (2012) ‘Deciphering the Antimicrobial Activity of Phenanthroline Chelators’, *Curr. Med. Chem.*, 19 (17), pp. 2703–2714.

McCann, M., Santos, A.L.S., da Silva, B. a., Teresa, M., Romanos, M.T. V., Pyrrho, A.S., Devereux, M., Kavanagh, K., Fichtner, I., Kellett, A. (2012) ‘In vitro and in vivo studies into the biological activities of 1,10-phenanthroline, 1,10-phenanthroline-5,6-dione and its copper(ii) and silver(i) complexes’, *Toxicol. Res.*, 1, pp. 47-54.

McCord, J.., Fridovich, I. (1988) ‘Superoxide dismutase: the first twenty years (1968-1988)’, *Free Radic Biol Med*, 5 (5–6), pp. 363–369.

McGinley, J., McCann, M., Ni, K., Tallon, T., Kavanagh, K., Devereux, M., Ma, X., McKee, V. (2013) ‘Imidazole Schiff base ligands: Synthesis, coordination complexes and biological activities’, *Polyhedron*, 55, pp. 169–178.

McIlwain, D.R., Berger, T., Mak, T.W. (2013) ‘Caspase functions in cell death and

disease', *Perspect Biol*, 5 (4), pp. 1–28.

McKeage, M.J. (2001) 'Lobaplatin: a new antitumour platinum drug', *Expert Opin. Investig. Drugs*, 10 (1), pp. 119–128.

Medici, S., Peana, M., Crisponi, G., Nurchi, V.M., Lachowicz, J.I., Remelli, M., Zoroddu, M.A. (2016) 'Silver coordination compounds: A new horizon in medicine', *Coord. Chem. Rev.*, 327–328, pp. 349–359.

Mejia, C., Ruiz-Azuara, L. (2008) 'Casiopeinas IIgly and IIIia Induce Apoptosis in Medulloblastoma Cells', *Pathol. Oncol. Res.*, 14 (4), pp. 467–472.

Melendez, E. (2012) 'Bioorganometallic Chemistry of Molybdemocene Dichloride and Its Derivatives', *J Organomet Chem.*, 29, pp. 997–1003.

Mena, M.L., Moreno-Gordaliza, E., Gómez-Gómez, M.M. (2013) 'TCEP-based rSDS–PAGE AND nLC–ESI-LTQ-MS/MS for oxaliplatin metalloproteomic analysis', *Talanta*, 116, pp. 581–592.

Meng, X., Leyva, M.L., Jenny, M., Gross, I., Benosman, S., Fricker, B., Harlepp, S., Hébraud, P., Boos, A., Wlosik, P., Bischoff, P., Sirlin, C., Pfeffer, M., Loeffler, J.-P., Gaiddon, C. (2009) 'A Ruthenium-Containing Organometallic Compound Reduces Tumor Growth through Induction of the Endoplasmic Reticulum Stress Gene CHOP', *Cancer Res.*, 69 (13), pp. 5458-5466.

Messori, L., Merlino, A. (2016) 'Cisplatin binding to proteins: A structural perspective', *Coord. Chem. Rev.*, 315, pp. 67–89.

Michaud, W.A., Nichols, A.C., Mroz, E.A., Faquin, W.C., Clark, J.R., Begum, S., Westra, W.H., Wada, H., Busse, P.M., Ellisen, L.W., Rocco, J.W. (2009) 'Bcl-2 Blocks Cisplatin-Induced Apoptosis and Predicts Poor Outcome Following Chemoradiation Treatment in Advanced Oropharyngeal Squamous Cell Carcinoma', *Clin. Cancer Res.*, 15 (5), pp. 1645–1654.

Mikuš, P., Melník, M., Forgácsová, A., Krajčiová, D., Havránek, E. (2014) 'Gallium compounds in nuclear medicine and oncology', *Main Gr. Met. Chem.*, 37 (3–4), pp. 53–65.

Milacic, V., Dou, Q.P. (2009) 'The tumor proteasome as a novel target for gold(III) complexes: implications for breast cancer therapy.', *Coord. Chem. Rev.*, 253 (11–12), pp. 1649–1660.

Milaeva, E.R., Shpakovsky, D.B., Dyadchenko, V.P., Gryzlov, A.I., Gracheva, Y.A., Antonenko, T.A., Parulava, M.J., Albov, D.V., Aslanov, L.A., Dubova, L.G., Shevtsov, P.N., Neganova, M.E., Shevtsova, E.F. (2017) 'Synthesis and biological activity of novel Au(I) complexes with a protective antioxidant 2,6-di-tert-butylphenol group', *Polyhedron*, 127, pp. 512–519.

Molphy, Z., Prisecaru, A., Slator, C., Barron, N., McCann, M., Colleran, J., Chandran, D., Gathergood, N., Kellett, A. (2014) 'Copper phenanthrene oxidative chemical nucleases', *Inorg. Chem.*, 53, pp. 5392–5404.

Molphy, Z., Slator, C., Chatgilialoglu, C., Kellett, A. (2015) 'DNA oxidation profiles of copper phenanthrene chemical nucleases', *Front. Chem.*, 3, doi: 10.3389/fchem.2015.00028. [accessed on 17-11-2017]

Monneret, C. (2011) 'Platinum anticancer drugs. From serendipity to rational design', *Ann. Pharm. Françaises*, 69 (6), pp. 286–295.

Montagner, D., Gandin, V., Marzano, C., Erxleben, A. (2015) 'DNA damage and induction of apoptosis in pancreatic cancer cells by a new dinuclear bis(triazacyclonane) copper complex', *J. Inorg. Biochem.*, 145 (3), pp. 101–107.

Moraleja, I., Moreno-Gordaliza, E., Mena, M.L., Gómez-Gómez, M.M. (2014) 'Combining TBP-based rOFFGEL-IEF with FASP and nLC–ESI-LTQ-MS/MS for the analysis of cisplatin-binding proteins in rat kidney', *Talanta*, 120 , pp. 433–

442.

Mosmann, T. (1983) ‘Rapid colorimetric assay for cellular growth and survival: application to proliferation and cytotoxicity assays’, *J. Immunol. Methods,* 65 , pp. 55–63.

Mowlds, P., Barron, A., Kavanagh, K. (2008) ‘Physical stress primes the immune response of Galleria mellonella larvae to infection by Candida albicans’, *Microbes. Infect.,* 10 (6), pp. 628–634.

Mowlds, P., Kavanagh, K. (2008) ‘Effect of pre-incubation temperature on susceptibility of Galleria mellonella larvae to infection by Candida albicans’, *Mycopathologia,* 165, pp. 5–12.

Muller, F.L., Roberts, A.G., Bowman, M.K., Kramer, D.M. (2003) ‘Architecture of the Q_o Site of the Cytochrome bc_1 Complex Probed by Superoxide Production’, *Biochemistry,* 42 (21), pp. 6493–6499.

Nazarewicz, R.R., Dikalova, A.E., Bikineyeva, A., Dikalov, S.I. (2013) ‘Nox2 as a potential target of mitochondrial superoxide and its role in endothelial oxidative stress’, *Am. J. Physiol. - Hear. Circ. Physiol.,* 305 (8), pp. 1131-1140.

Neri, C. (2011) *Value of Invertebrate Genetics and Biology to Develop Neuroprotective and Preventive Medicine in Huntington’s Disease*, Neurobiology of Huntington’s Disease: Applications to Drug Discovery, Ch. 6, CRC Press/Taylor & Francis.

Niioka, T., Uno, T., Yasui-Furukori, N., Takahata, T., Shimizu, M., Sugawara, K., Tateishi, T. (2007) ‘Pharmacokinetics of low-dose nedaplatin and validation of AUC prediction in patients with non-small-cell lung carcinoma’, *Cancer Chemother. Pharmacol.,* 59 (5), pp. 575–580.

Niyazi, H., Hall, J., O’Sullivan, K., Winter, G., Sorensen, T., Kelly, J., Cardin, C. (2012a) ‘Crystal structures of Λ-$[Ru(phen)_2dppz]^{2+}$ with oligonucleotides

containing TA/TA and AT/AT steps show two intercalation modes', *Nat. Chem.*, 4, pp. 621–628.

Nomura, T., Yamasaki, M., Nomura, Y., Mimata, H. (2005) 'Expression of the inhibitors of apoptosis proteins in cisplatin-resistant prostate cancer cells.', *Oncol. Rep.*, 14 (4), pp. 993–997.

Nordgård, O., Kvaløy, J.T., Farmen, R.K., Heikkilä, R. (2006) 'Error propagation in relative real-time reverse transcription polymerase chain reaction quantification models: The balance between accuracy and precision', *Anal. Biochem.*, 356 (2), pp. 182–193.

Notta, F., Koropatnick, D.J. (2006) 'Chapter 13 / Metallothioneins in Drug Resistance', in *Cancer Drug Discovery and Development: Cancer Drug Resistance*, 223–239.

O'Connor, P.M., Jackman, J., Bae, I., Myers, T.G., Fan, S., Mutoh, M., Scudiero, D. a., Monks, A., Sausville, E. a., Weinstein, J.N., Friend, S., Fornace, A.J., Kohn, K.W. (1997) 'Characterization of the p53 tumor suppressor pathway in cell lines of the National Cancer Institute anticancer drug screen and correlations with the growth-inhibitory potency of 123 anticancer agents', *Cancer Res.*, 57 (19), pp. 4285–4300.

O'Neill, C.F., Koberle, B., Masters, J.R., Kelland, L.R. (1999) 'Gene-specific repair of Pt/DNA lesions and induction of apoptosis by the oral platinum drug JM216 in three human ovarian carcinoma cell lines sensitive and resistant to cisplatin.', *Br. J. Cancer*, 81 (8), pp. 1294–1303.

Olaussen, K.A., Dunant, A., Fouret, P., Brambilla, E., André, F., Haddad, V., Taranchon, E., Filipits, M., Pirker, R., Popper, H.H., Stahel, R., Sabatier, L., Pignon, J.-P., Tursz, T., Le Chevalier, T., Soria, J.-C., IALT Bio Investigators (2006) 'DNA Repair by ERCC1 in Non–Small-Cell Lung Cancer and Cisplatin-Based Adjuvant Chemotherapy', *N. Engl. J. Med.*, 355 (10), pp. 983–991.

Ott, I., Schmidt, K., Kircher, B., Schumacher, P., Wiglenda, T., Gust, R. (2005) 'Antitumor-Active Cobalt−Alkyne Complexes Derived from Acetylsalicylic Acid: Studies on the Mode of Drug Action', *J. Med. Chem.*, 48 (2), pp. 622-629.

Palanimuthu, D., Shinde, S.V., Somasundaram, K., Samuelson, A.G. (2013) 'In Vitro and in Vivo Anticancer Activity of Copper Bis(thiosemicarbazone) Complexes', *J. Med. Chem.*, 56 (3), pp. 722–734.

Park, G.Y., Wilson, J.J., Song, Y., Lippard, S.J. (2012) 'Phenanthriplatin, a monofunctional DNA-binding platinum anticancer drug candidate with unusual potency and cellular activity profile.', *Proc. Natl. Acad. Sci. U. S. A.*, 109 (30), pp. 11987–11992.

Paterson, R.R.., Simmonds, M.S.., Blaney, W.. (1987) 'Mycopesticidal effects of characterized extracts of Penicillium isolates and purified secondary metabolites (including mycotoxins) on Drosophila melanogaster and Spodoptora littoralis', *J. Invert. Path.*, 50, pp. 124–133.

Patten, D.A., Wong, J., Khacho, M., Soubannier, V., Mailloux, R.J., Pilon-Larose, K., MacLaurin, J.G., Park, D.S., McBride, H.M., Trinkle-Mulcahy, L., Harper, M.-E., Germain, M., Slack, R.S. (2014) 'OPA1-dependent cristae modulation is essential for cellular adaptation to metabolic demand.', *EMBO J.*, 33 (22), pp. 2676–2691.

Pedley, A.M., Benkovic, S.J. (2017) 'A new View into the regulation of purine metabolism: The Purinosome', *Trends Biomed. Sci.*, 42 (2), pp. 141–154.

Peisach, J., Blumberg, W.E. (1969) 'A mechanism for the action of penicillamine in the treatment of Wilson's disease.', *Mol. Pharmacol.*, 5 (2), pp. 200–209.

Pellei, M., Gandin, V., Marinelli, M., Marzano, C., Yousufuddin, M., Dias, H.V.R., Santini, C. (2012) 'Synthesis and Biological Activity of Ester- and Amide-Functionalized Imidazolium Salts and Related Water-Soluble Coinage Metal N-

Heterocyclic Carbene Complexes', *Inorg. Chem.*, 51 (18), pp. 9873–9882.

Peres, L.A.B., Cunha Júnior, A.D. da (2013) 'Acute nephrotoxicity of cisplatin: Molecular mechanisms', *J. Bras. Nefrol.*, 35 (4), pp. 332–340.

Pérez, C., Díaz-García, C.V., Agudo-López, A., del Solar, V., Cabrera, S., Agulló-Ortuño, M.T., Navarro-Ranninger, C., Alemán, J., López-Martín, J.A. (2014) 'Evaluation of novel trans-sulfonamide platinum complexes against tumor cell lines', *Eur. J. Med. Chem.*, 76, pp. 360–368.

Peyrone, M. (1844) 'Ueber die Einwirkung des Ammoniaks auf Platinchlorür', *Ann. der Chemie und Pharm.*, 51 (1), pp. 1–29.

di Pietro, A., Koster, R., Boersma-van Eck, W., Dam, W.A., Mulder, N.H., Gietema, J.A., de Vries, E.G.E., de Jong, S. (2012) 'Pro- and anti-apoptotic effects of p53 in cisplatin-treated human testicular cancer are cell context-dependent.', *Cell Cycle*, 11 (24), pp. 4552–4562.

Pinho, M.B., Costas, F., Sellos, J., Dienstmann, R., Andrade, P.B., Herchenhorn, D., Peixoto, F.A., Santos, V.O., Small, I.A., Guimarães, D.P., Ferreira, C.G. (2009) 'XAF1 mRNA expression improves progression-free and overall survival for patients with advanced bladder cancer treated with neoadjuvant chemotherapy', *Urol. Oncol. Semin. Orig. Investig.*, 27 (4), pp. 382–390.

Plenchette, S., Cheung, H.H., Fong, W.G., LaCasse, E.C., Korneluk, R.G. (2007) 'The role of XAF1 in cancer.', *Curr. Opin. Investig. Drugs*, 8 (6), pp. 469–476.

Prisecaru, A., Devereux, M., Barron, N., McCann, M., Colleran, J., Casey, A., McKee, V., Kellett, A. (2012a) 'Potent oxidative DNA cleavage by the di-copper cytotoxin: [Cu2(μ-terephthalate)(1,10-phen)4]2+', *ChemComm*, 48, pp. 6906–6908.

Prisecaru, A., Devereux, M., Barron, N., McCann, M., Colleran, J., Casey, A., McKee, V., Kellett, A. (2012b) 'Potent oxidative DNA cleavage by the di-copper

cytotoxin: [Cu2([μ-terephthalate)(1,10-phen)4]$^{2+}$', *Chem. Commun.*, 48 (55), pp. 6906–6908.

Prisecaru, A., Mckee, V., Howe, O., Rochford, G., McCann, M., Colleran, J., Pour, M., Barron, N., Gathergood, N., Kellett, A. (2013) 'Regulating Bioactivity of Cu 2 + Bis-1 , 10-phenanthroline Artificial Metallonucleases with Sterically Functionalized Pendant Carboxylates', *J. Med. Chem.*, 56 (21), pp. 8599–8615.

Quinlan, C.L., Goncalves, R.L.S., Hey-Mogensen, M., Yadava, N., Bunik, V.I., Brand, M.D. (2014) 'The 2-oxoacid dehydrogenase complexes in mitochondria can produce superoxide/hydrogen peroxide at much higher rates than complex I', *J. Biol. Chem.*, 289 (12), pp. 8312–8325.

Quirós, P.M., Langer, T., López-Otín, C. (2015) 'New roles for mitochondrial proteases in health, ageing and disease', *Nat. Rev. Mol. Cell Biol.*, 16 (6), pp. 345–359.

Rabik, C.A., Dolan, M.E., Dolan, M.E. (2007) 'Molecular mechanisms of resistance and toxicity associated with platinating agents', *Cancer Treat. Rev.*, 33 , pp. 9–23.

Rafique, S., Idrees, M., Nasim, A., Akbar, H., Athar, A. (2010) 'Transition metal complexes as potential therapeutic agents', *Biotechnol. Mol. Biol. Rev.*, 5 (2), pp. 38–45.

Rang, H.P., Hill, R.G. (2013) 'Section 2: Drug Discovery', in Hill, R.G. and Rang, Humphery, P., eds., *Drug Discovery & Development: Technology in Transition*, Elsevier, 43–189.

Reddy, P.H. (2014) 'Inhibitors of mitochondrial fission as a therapeutic strategy for diseases with oxidative stress and mitochondrial dysfunction.', *J. Alzheimers. Dis.*, 40 (2), pp. 245–256.

Reddy, T.S., Priver, S.H., Mirzadeh, N., Bhargava, S.K. (2017) 'Anti-cancer gold(I) phosphine complexes: Cyclic trimers and tetramers containing the P-Au-P moiety',

J. Inorg. Biochem., 175, pp. 1–8.

Ren, J.-H., He, W.-S., Nong, L., Zhu, Q.-Y., Hu, K., Zhang, R.-G., Huang, L.-L., Zhu, F., Wu, G. (2010) 'Acquired Cisplatin Resistance in Human Lung Adenocarcinoma Cells Is Associated with Enhanced Autophagy', *Cancer Biother. Radiopharm.*, 25 (1), pp. 75–80.

Renwick, J., Kavanagh, K. (2007) 'Insects as models for studying the virulence of fungal pathogens of humans', in *New Insights in Medical Mycology*, 45–67.

Renwick, J., Reeves, E.P., Wientjes, F.B., Kavanagh, K. (2007) 'Translocation of proteins homologous to human neutrophil p47phox and p67phox to the cell membrane in activated hemocytes of Galleria mellonella', *Dev Comp Immunol*, 31, pp. 347–359.

Rho, J.K., Choi, Y.J., Choi, Y.R., Kim, S.Y., Choi, S.J., Choi, C.-M., Na, I. Il, Lee, J.C. (2011) 'The effect of acquired cisplatin resistance on sensitivity to EGFR tyrosine kinase inhibitors in EGFR mutant lung cancer cells.', *Oncol. Res.*, 19 (10–11), pp. 471–478.

Richardson, A., Kovacevic, Z., Richardson, D.R. (2013) 'Iron Chelation: Inhibition of Key Signaling Pathways in the Induction of the Epithelial Mesenchymal Transition in Pancreatic Cancer and Other Tumors', *Crit. Rev. Oncog.*, 18 (5), pp. 409–434.

Říha, M., Karlíčková, J., Filipský, T., Macáková, K., Hrdina, R., Mladěnka, P. (2013) 'Novel method for rapid copper chelation assessment confirmed low affinity of D-penicillamine for copper in comparison with trientine and 8-hydroxyquinolines', *J. Inorg. Biochem.*, 123, pp. 80–87.

Rodriguez, V., Hart, J.S., Freireich, E.J., Bodey, G.P., McCredie, K.B., Whitecar, J.P., Coltman, C.A. (1973) 'POMP combination chemotherapy of adult acute leukemia', *Cancer*, 32 (1), pp. 69–75.

Ronconi, L., Marzano, C., Zanello, P., Corsini, M., Miolo, G., Maccà, C., Trevisan, A., Fregona, D., (2006) 'Gold(III) Dithiocarbamate Derivatives for the Treatment of Cancer: Solution Chemistry, DNA Binding, and Hemolytic Properties', *J. Med. Chem.*, 49 (5), pp. 1648-1657.

Roos, W.P., Tsaalbi-Shtylik, A., Tsaryk, R., Guvercin, F., de Wind, N., Kaina, B. (2009) 'The Translesion Polymerase Rev3L in the Tolerance of Alkylating Anticancer Drugs', *Mol. Pharmacol.*, 76 (4), pp. 927–934.

Rosenberg, B., Van Camp, L. (1970) 'The successful regression of large solid S180 tumors by platinum compounds', *Cancer Res.*, 30, pp. 1799–1802.

Rosenberg, B., Camp, L. Van, Grimley, E.B., Thohlson, A.J. (1967) 'The Inhibition of Growth or Cell Division in Escherichia coli by Different Ionic Species of Platinum(IV) Complexes*', *J. Biol. Chem.*, 242 (6), pp. 1347–1352.

Rosenberg, B., Van Camp, L., Krigas, T. (1965) 'Inhibition of Cell Division in Escherichia coli by Electrolysis Products from a Platinum Electrode', *Nature*, 205, pp. 698–99.

Rosenberg, B., Renshaw, E., Vancamp, L., Hartwick, J., Drobnik, J. (1967) 'Platinum-Induiced Filamentous Growth in Escherichia coli', *J. Bacteriol.*, 93 (2), pp. 716–721.

Rosic, G., Joksimovic, J., Selakovic, D., Jakovljevic, V., Zivkovic, V., Srejovic, I., Djuric, M., Djuric, D. (2017) 'The beneficial effects of sulfur-containing amino acids on cisplatin-induced cardiotoxicity and neurotoxicity in rodents.', *Curr. Med. Chem.*, In-press, available: http://www.ncbi.nlm.nih.gov/pubmed/28685675 [accessed 4 Aug 2017].

Rowan, R., Moran, C., McCann, M., Kavanagh, K. (2009) 'Use of Galleria mellonella larvae to evaluate the in vivo anti-fungal activity of [Ag2(mal)(phen)3]',

Biometals, 22, pp. 461–467.

Ruttkay-Nedecky, B., Nejdl, L., Gumulec, J., Zitka, O., Masarik, M., Eckschlager, T., Stiborova, M., Adam, V., Kizek, R. (2013) 'The role of metallothionein in oxidative stress', *Int. J. Mol. Sci.*, 14 (3), pp. 6044–6066.

Ryan, B.M., O'Donovan, N., Duffy, M.J. (2009) 'Survivin: A new target for anti-cancer therapy', *Cancer Treat. Rev.*, 35 (7), pp. 553–562.

Safaei, R., Holzer, A.K., Katano, K., Samimi, G., Howell, S.B. (2004) 'The role of copper transporters in the development of resistance to Pt drugs', *J. Inorg. Biochem.*, 98, pp. 1607–1613.

Sakai, W., Swisher, E.M., Karlan, B.Y., Agarwal, M.K., Higgins, J., Friedman, C., Villegas, E., Jacquemont, C., Farrugia, D.J., Couch, F.J., Urban, N., Taniguchi, T. (2008) 'Secondary mutations as a mechanism of cisplatin resistance in BRCA2-mutated cancers.', *Nature*, 451 (7182), pp. 1116–1120.

Santini, C., Pellei, M., Gandin, V., Porchia, M., Tisato, F., Marzano, C. (2014) 'Advances in Copper Complexes as Anticancer Agents', *Chem. Rev.*, 114 (1), pp. 815–862.

Sava, G., Zorzet, S., Turrin, C., Vita, F., Soranzo, M., Zabucchi, G., Cocchietto, M., Bergamo, A., DiGiovine, S., Pezzoni, G., Sartor, L., Garbisa, S. (2003) 'Dual Action of NAMI-A in inhibition of solid tumor metastasis: selective targeting of metastatic cells and binding to collagen.', *Clin. Cancer Res.*, 9 (5), pp. 1898–1905.

Scherer, W.F., Syverton, J.T., Gey, G.O. (1953) 'Studies on the Propagation in Vitro of Poliomyelitis Viruses: Iv. Viral Multiplication in a Stable Strain of Human Malignant Epithelial Cells (Strain Hela) Derived From an Epidermoid Carcinoma of the Cervix', *J. Exp. Med.*, 97 (5), pp. 695–710.

Serment-Guerrero, Ò.J., Cano-Sanchez, P., Reyes-Perez, E., Velazquez-Garcia, F.,

Bravo-Gomez, M.E., Ruiz-Azuara, L. (2011) ‘Genotoxicity of the copper antineoplastic coordination complexes casiopeinasÂ®’, *Toxicol. Vitr.*, 25, pp. 1376–1384.

Sever, R., Brugge, J.S. (2015) ‘Signal Transduction in Cancer’, *Cold Spring Harb. Perspect. Med.*, 5, pp. a006098., available at: https://www.ncbi.nlm.nih.gov/pmc/articles/PMC4382731/pdf/cshperspectmed-SIG-a006098.pdf [accessed 29 Aug 2017].

Shachar, S., Ziv, O., Avkin, S., Adar, S., Wittschieben, J., Reißner, T., Chaney, S., Friedberg, E.C., Wang, Z., Carell, T., Geacintov, N., Livneh, Z. (2009) ‘Two-polymerase mechanisms dictate error-free and error-prone translesion DNA synthesis in mammals’, *EMBO J.*, 28 (4), pp. 383–393.

Shaloam, D., Tchounwou, P.B. (2014) ‘Cisplatin in cancer therapy: Molecular mechanisms of action’, *Eur. J. Pharmacol.*, 740 , pp. 364–378.

Shanmughapriya, S., Rajan, S., Hoffman, N.E., Higgins, A.M., Tomar, D., Nemani, N., Hines, K.J., Smith, D.J., Eguchi, A., Vallem, S., Shaikh, F., Cheung, M., Leonard, N.J., Stolakis, R.S., Wolfers, M.P., Ibetti, J., Chuprun, J.K., Jog, N.R., Houser, S.R., Koch, W.J., Elrod, J.W., Madesh, M. (2015) ‘SPG7 is an Essential and Conserved Component of the Mitochondrial Permeability Transition Pore HHS Public Access’, *Mol Cell*, 60 (1), pp. 47–62.

Shen, D.-W., Pouliot, L.M., Hall, M.D., Gottesman, M.M. (2012) ‘Cisplatin resistance: a cellular self-defense mechanism resulting from multiple epigenetic and genetic changes.’, *Pharmacol. Rev.*, 64 (3), pp. 706–721.

Shevchenko, A., Tomas, H., Havlis, J., Olsen, J. V, Mann, M. (2006) ‘In-gel digestion for mass spectrometric characterization of proteins and proteomes.’, *Nat. Protoc.*, 1 (6), pp. 2856–2860.

Shi, Y., Dierckx, A., Wanrooij, P.H., Wanrooij, S., Larsson, N.-G., Wilhelmsson, L.M., Falkenberg, M., Gustafsson, C.M. (2012) 'Mammalian transcription factor A is a core component of the mitochondrial transcription machinery', *Proc Natl Acad Sci USA*, 109 (41), pp. 16510–16515.

Shimada, M., Itamochi, H., Kigawa, J. (2013) 'Nedaplatin: a cisplatin derivative in cancer chemotherapy.', *Cancer Manag. Res.*, 5 , pp. 67–76.

Shoemaker, R. (2006) 'The NCI60 human tumour cell line anticancer drug screen', *Nat Rev Cancer*, 6 (10), pp. 813–823.

Shoshan-Barmatz, V., De Pinto, V., Zweckstetter, M., Raviv, Z., Keinan, N., Arbel, N. (2010) 'VDAC, a multi-functional mitochondrial protein regulating cell life and death', *Mol. Aspects Med.*, 31 (3), pp. 227–285.

Sigman, D.S., Graham, D.R., D'Aurora, V., Stern, A.M. (1979) 'Oxygen-dependent cleavage of DNA by the 1,10-phenathroline cuporous complex. Inhibition of Escherichia coli DNA polymerase I', *J. Biol. Chem.*, 254 (24), pp. 12269–12272.

Sigman, D.S., Mazumder, A., Perrin, D.M. (1993) 'Chemical Nucleases', *Chem. Rev.*, 93 (6), pp. 2295–2316.

Silva, J., Rodrigues, A.S., Videira, P.A., Lasri, J., Charmier, A.J., Pombeiro, A.J.L., Fernandes, A.R. (2014) 'Characterization of the antiproliferative potential and biological targets of a trans ketoimine platinum complex', *Inorganica Chim. Acta*, 423, pp. 156–167.

Sîrbu, A., Palamarciuc, O., Babak, M. V., Lim, J.M., Ohui, K., Enyedy, E.A., Shova, S., Darvasiová, D., Rapta, P., Ang, W.H., Arion, V.B., McDevitt, M.A. (2017) 'Copper(ii) thiosemicarbazone complexes induce marked ROS accumulation and promote nrf2-mediated antioxidant response in highly resistant breast cancer cells', *Dalt. Trans.*, 46 (12), pp. 3833–3847.

Slator, C., Barron, N., Howe, O., Kellett, A. (2016) '[Cu(o-phthalate)(phenanthroline)] Exhibits Unique Superoxide-Mediated NCI-60 Chemotherapeutic Action through Genomic DNA Damage and Mitochondrial Dysfunction', *ACS Chem. Biol.*, 11 (1), pp. 159–171.

Slator, C., Molphy, Z., McKee, V., Kellett, A. (2017) 'Triggering Autophagic Cell Death with a di-Manganese(II) Developmental Therapeutic', *Redox Biol.*, 12, pp. 150–161.

Spiers, A.S.D., Roberts, P.D., Marsh, G.W., Parekh, S.J., Franklin, A.J., Galton, G., Szur, Z.L., Paul, E.A., Husband, P., Wiltshaw, E. (1975) 'Acute lymphoblastic leukaemia: cyclical chemotherapy with three combinations of four drugs (COAP-POMP-CART regimen)', *Br. Med. J.*, 4, pp. 614–617.

Spreckelmeyer, S., Orvig, C., Casini, A. (2014) 'Cellular Transport Mechanisms of Cytotoxic Metallodrugs: An Overview beyond Cisplatin', *Molecules*, 19 (10), pp. 15584–15610.

St-Pierre, J., Buckingham, J.A., Roebuck, S.J., Brand, M.D. (2002) 'Topology of Superoxide Production from Different Sites in the Mitochondrial Electron Transport Chain', *J. Biol. Chem.*, 277 (47), pp. 44784–44790.

St Germain, C., Niknejad, N., Ma, L., Garbuio, K., Hai, T., Dimitroulakos, J. (2010) 'Cisplatin induces cytotoxicity through the mitogen-activated protein kinase pathways and activating transcription factor 3.', *Neoplasia*, 12 (7), pp. 527–538.

Stope, M.B., Koensgen, D., Burchardt, M., Concin, N., Zygmunt, M., Mustea, A. (2016) 'Jump in the fire — heat shock proteins and their impact on ovarian cancer therapy', *Crit. Rev. Oncol.*, 97, pp. 152–156.

Strohfeldt, K., Muller-Bunz, G., Pampillon, C., Tacke, M. (2007) 'Proliferative and anti proliferative effects in substituted titanocene anticancer drugs', *Transit. Met.*

Chem., 32, pp. 971–980.

Tai, S., Sun, Y., Squires, J.M., Zhang, H., Oh, W.K., Liang, C.-Z., Huang, J. (2011) 'PC3 is a cell line characteristic of prostatic small cell carcinoma', *Prostate*, 71, pp. 1668–79.

Tajeddine, N., Galluzzi, L., Kepp, O., Hangen, E., Morselli, E., Senovilla, L., Araujo, N., Pinna, G., Larochette, N., Zamzami, N., Modjtahedi, N., Harel-Bellan, A., Kroemer, G. (2008) 'Hierarchical involvement of Bak, VDAC1 and Bax in cisplatin-induced cell death', *Oncogene*, 27 (30), pp. 4221–4232.

Takahara, P., Rosenzweig, A., Frederich, C., Lippard, S. (1995) 'Crystal structure of double-stranded DNA containing the major adduct of the anticancer drug cisplatin', *Nature*, 377, pp. 649–652.

Tavares, T.T., Azevedo, G.C., Garcia, A., Carpanez, A.G., Lewer, P.M., Paschoal, D., Müller, B.L., Dos Santos, H.F., Matos, R.C., Silva, H., Grazul, R.M., Fontes, A.P.S. (2017) 'Gold(I) complexes with aryl-thiosemicarbazones: Molecular modeling, synthesis, cytotoxicity and TrxR inhibition', *Polyhedron*, 132, pp. 95–104.

Tebay, L.E., Robertson, H., Durant, S.T., Vitale, S.R., Penning, T.M., Dinkova-Kostova, A.T., Hayes, J.D. (2015) 'Mechanisms of activation of the transcription factor Nrf2 by redox stressors, nutrient cues, and energy status and the pathways through which it attenuates degenerative disease', *Free Radic. Biol. Med.*, 88, pp. 108–146.

Telford, W.G., Hawley, T., Subach, F., Verkhusha, V., Hawley, R.G. (2012) 'Flow cytometry of fluorescent proteins', *Methods*, 57, pp. 318–330.

Thati, B., Noble, A., Creaven, B.S., Walsh, M., Kavanagh, K., Egan, D. a (2007) 'An in vitro investigation of the induction of apoptosis and modulation of cell cycle

events in human cancer cells by bisphenanthroline-coumarin-6,7-dioxacetatocopper(II) complex', *Chem. Biol. Interact.*, 168, pp. 143–58.

Thomas, K.J., Jacobson, M.R. (2012) 'Defects in Mitochondrial Fission Protein Dynamin-Related Protein 1 Are Linked to Apoptotic Resistance and Autophagy in a Lung Cancer Model', *PLoS One*, 7 (9), pp. e45319, doi: 10.1371/journal.pone.0045319 [accessed on 17-11-2017]

Thompson, L.H. (2012) 'Recognition, signaling, and repair of DNA double-strand breaks produced by ionizing radiation in mammalian cells: the molecular choreography', *Mutat. Res.*, 751 (2), pp. 158–246.

Thompson, L.M., Marsh, J.L. (2003) 'Invertebrate models of neurologic disease: Insights into pathogenesis and therapy', *Curr. Neurol. Neurosci. Rep.*, 3 (5), pp. 442–448.

Thornton, L., Dixit, V., Assad, L.O.N., Ribeiro, T.P., Queiroz, D.D., Kellett, A., Casey, A., Colleran, J., Pereira, M.D., Rochford, G., McCann, M., O'Shea, D., Dempsey, R., McClean, S., Kia, A.F.-A., Walsh, M., Creaven, B., Howe, O., Devereux, M. (2016) 'Water-soluble and photo-stable silver(I) dicarboxylate complexes containing 1,10-phenanthroline ligands: Antimicrobial and anticancer chemotherapeutic potential, DNA interactions and antioxidant activity', *J. Inorg. Biochem.*, 159, pp. 120–132.

Timerbaev, A.R., Pawlak, K., Aleksenko, S.S., Foteeva, L.S., Matczuk, M., Jarosz, M. (2012) 'Advances of CE-ICP-MS in speciation analysis related to metalloproteomics of anticancer drugs', *Talanta*, 102, pp. 164–170.

Timme, S., Ihde, S., Fichter, C.D., Waehle, V., Bogatyreva, L., Atanasov, K., Kohler, I., Schöpflin, a, Geddert, H., Faller, G., Klimstra, D., Tang, L., Reinheckel, T., Hauschke, D., Busch, H., Boerries, M., Werner, M., Lassmann, S. (2013) 'STAT3

expression, activity and functional consequences of STAT3 inhibition in esophageal squamous cell carcinomas and Barrett's adenocarcinomas.', *Oncogene*, 33, pp. 3256–3266.

Tomé, M., López, C., González, A., Ozay, B., Quirante, J., Font-Bardía, M., Calvet, T., Calvis, C., Messeguer, R., Baldomá, L., Badía, J. (2013) 'Trans- and cis-2-phenylindole platinum(II) complexes as cytotoxic agents against human breast adenocarcinoma cell lines', *J. Mol. Struct.*, 1048, pp. 88–97.

Torti, S. V., Torti, F.M. (2013) 'Cellular Iron Metabolism in Prognosis and Therapy of Breast Cancer', *Crit. Rev. Oncog.*, 18 (5), pp. 435–448.

Townsend, D.M., Tew, K.D. (2003) 'The role of glutathione-S-transferase in anti-cancer drug resistance', *Oncogene*, 22 (47), pp. 7369–7375.

Trejo-Solís, C., Palencia, G., Zú Ñ Iga, S., Rodríguez-Ropon, A., Osorio-Rico, L., Luvia, S.T., Gracia-Mora, I., Marquez-Rosado, L., Sá Nchez, A., Moreno-García, M.E., Cruz, A., Bravo-Gó Mez, E., Ruiz-Ramírez, L., Rodríguez-Enriquez, S., Sotelo, J. (2005) 'Cas IIgly Induces Apoptosis in Glioma C6 Cells In Vitro and In Vivo through Caspase-Dependent and Caspase-Independent Mechanisms 1', *Neoplasia*, 7, pp. 563–574.

Trudu, F., Amato, F., Vanhara, P., Pivetta, T., Pena-Mendez, E.M., Havel, J. (2015) 'Coordination compounds in cancer: Past, present and perspectives', *J. Appl. Biomed.*, 13 (2), pp. 79–103.

Tuncer, S., Banerjee, S. (2015) 'Eicosanoid pathway in colorectal cancer: Recent updates', *World J. Gastroenterol.*, 21 (41), pp. 11748–11766.

Turel, I., Kljun, J. (2011) 'Interactions of Metal Ions with DNA, Its Constituents and Derivatives, which may be Relevant for Anticancer Research', *Curr. Top. Med. Chem.*, 11 (21), pp. 2661–2687.

Turrens, J.F. (1997) ‘Superoxide production by the mitochondrial respiratory chain.’, *Biosci. Rep.*, 17 (1), pp. 3–8.

Valiahdi, S.M., Heffeter, P., Jakupec, M.A., Marculescu, R., Berger, W., Rappersberger, K., Keppler, B.K. (2009) ‘The gallium complex KP46 exerts strong activity against primary explanted melanoma cells and induces apoptosis in melanoma cell lines’, *Melanoma Res.*, 19 (5), pp. 283–293.

Vandesompele, J., De Preter, K., Pattyn, ilip, Poppe, B., Van Roy, N., De Paepe, A., Speleman, rank (2002) ‘Accurate normalization of real-time quantitative RT-PCR data by geometric averaging of multiple internal control genes’, *Genome Biol.*, 3 (7), PMC126239. Avaliable at http://genomebiology.com/2002/3/7/research/0034.1 [accessed on 17-11-2017]

Vega-Avila, E., Pugsley, M.K. (2011) ‘An Overview of Colorimetric Assay Methods Used to Assess Survival or Proliferation of Mammalian Cells’, *Proc . West . Pharmacol . Soc*, 54, pp. 10–14.

Vertyporokh, L., Wojda, I. (2017) ‘Expression of the insect metalloproteinase inhibitor IMPI in the fat body of Galleria mellonella exposed to infection with Beauveria bassiana’, *Acta Biochim. Pol.*, 63 (2), pp. 273-278.

Vessières, A., Top, S., Beck, W., Hillard, E., Jaouen, G. (2006) ‘Metal complex SERMs (selective oestrogen receptor modulators). The influence of different metal units on breast cancer cell antiproliferative effects.’, *Dalton Trans.*, (4), pp. 529–541.

Viljakainen, L. (2015) ‘Evolutionary genetics of insect innate immunity.’, *Brief. Funct. Genomics*, 14 (6), pp. 407–412.

Villarreal, W., Colina-Vegas, L., Visbal, G., Corona, O., Corrêa, R.S., Ellena, J., Cominetti, M.R., Batista, A.A., Navarro, M. (2017) ‘Copper(I)–Phosphine Polypyridyl Complexes: Synthesis, Characterization, DNA/HSA Binding Study,

and Antiproliferative Activity', *Inorg. Chem.*, 56 (7), pp. 3781–3793.

Vilmos, P., Kurucz, E. (1998) 'Insect immunity: evolutionary roots of the mammalian innate immune system', *Immunol Lett*, 62, pp. 59–66.

Vogel, H., Altincicek, B., Glöckner, G., Vilcinskas, A. (2011) 'A comprehensive transcriptome and immune- gene repertoire of the lepidopteran model host Galleria mellonella', *BMC Genomics*, 12. doi: 10.1186/1471-2164-12-308 [accessed on 17-11-2017]

Volkoff, A.N., Rocher, J., D'Alençon, E., Bouton, M., Landais, I., Quesada-Moraga, E., Vey, A., Fournier, P., Mita, K., Devauchelle, G. (2003) 'Characterization and transcriptional profiles of three Spodoptera frugiperda genes encoding cysteine-rich peptides. A new class of defensin-like genes from lepidopteran insects?', *Gene*, 319 (1–2), pp. 43–53.

Vuong, N.Q., Goegan, P., Mohottalage, S., Breznan, D., Ariganello, M., Williams, A., Elisma, F., Karthikeyan, S., Vincent, R., Kumarathasan, P. (2016) 'Proteomic changes in human lung epithelial cells (A549) in response to carbon black and titanium dioxide exposures', *J. Proteomics*, 149, pp. 53–63.

Walters, J.B., Ratcliffe, N.. (1983) 'Studies on the in vivo cellular reactions of insects: Fate of pathogenic and non-pathogenic bacteria in Galleria mellonella nodules', *J. Insect Physiol.*, 29 , pp. 417–424.

Wang, N.X., von Recum, H.A. (2011) 'Affinity-Based Drug Delivery', *Macromol. Biosci.*, 11 (3), pp. 321–332.

Wang, Z., Qian, H., Yiu, S.-M., Sun, J., Zhu, G. (2014) 'Multi-targeted organometallic ruthenium(II)–arene anticancer complexes bearing inhibitors of poly(ADP-ribose) polymerase-1: A strategy to improve cytotoxicity', *J. Inorg. Biochem.*, 131, pp. 47–55.

Wedde, M., Weise, C., Kopacek, P., Franke, P., Vilcinskas, A. (1998) ‘Purification and characterization of an inducible metalloprotease inhibitor from the hemolymph of greater wax moth larvae, Galleria mellonella’, *Eur J Biochem*, 255 (3), pp. 535–43.

Wee, N.K.Y., Weinstein, D.C., Fraser, S.T., Assinder, S.J. (2013) ‘The mammalian copper transporters CTR1 and CTR2 and their roles in development and disease’, *Int. J. Biochem. Cell Biol.*, 45, pp. 960–963.

Wenzel, M., Casini, A. (2017), ‘Mass spectrometry as a powerful tool to study therapeutic metallodrugs speciation mechanisms: Current frontiers and perspectives’, *Coordin. Chem. Rev.*, In press. Available at: https://www.sciencedirect.com/science/article/pii/S0010854516304404 [accessed on 18-11-2017]

Wheate, N.J., Walker, S., Craig, G.E., Oun, R., Tsoutsou, P., Abatzoglou, I., Panteliadou, M., Sismanidou, K., Sivridis, E., Boulikas, T., Gianni, L., Pasini, G., Braud, F. De, Camboni, G., Marsoni, S., Pierpont, C., Lee, S.N. (2010) ‘The status of platinum anticancer drugs in the clinic and in clinical trials’, *Dalt. Trans.*, 39 (35), pp. 8113-8127.

Wilmes, A., Limonciel, A., Aschauer, L., Moenks, K., Bielow, C., Leonard, M.O., Hamon, J., Carpi, D., Ruzek, S., Handler, A., Schmal, O., Herrgen, K., Bellwon, P., Burek, C., Truisi, G.L., Hewitt, P., Di Consiglio, E., Testai, E., Blaauboer, B.J., Guillou, C., Huber, C.G., Lukas, A., Pfaller, W., Mueller, S.O., Bois, F.Y., Dekant, W., Jennings, P. (2013) ‘Application of integrated transcriptomic, proteomic and metabolomic profiling for the delineation of mechanisms of drug induced cell stress’, *J. Proteomics*, 79 (3), pp. 180–194.

Wilson-Sanders, S.E. (2011) ‘Invertebrate Models for Biomedical Research, Testing, and Education’, *ILAL J.*, 52 (2), pp. 126–152.

Winter, C., Albers, P. (2011) ‘Testicular germ cell tumors: pathogenesis, diagnosis and treatment’, *Nat. Rev. Endocrinol.*, 7 (1), pp. 43–53.

Wojda, I., Jakubowicz, T. (2007) ‘Humoral immune response upon mild heat-shock conditions in Galleria mellonella larvae’, *J. Insect Physiol.*, 53 (11), pp. 1134–1144.

Wreszinski, W. (1937) *The Papyrus Ebers, the Greatest Egyptian Medical Document*, Oxford University Press: Copenhagen.

Würstle, M.L., Laussmann, M. a., Rehm, M. (2012) ‘The central role of initiator caspase-9 in apoptosis signal transduction and the regulation of its activation and activity on the apoptosome’, *Exp. Cell Res.*, 318, pp. 1213–1220.

Xia, M., Yu, H., Gu, S., Xu, Y., Su, J., Li, H., Kang, J., Cui, M. (2014) ‘p62/SQSTM1 is involved in cisplatin resistance in human ovarian cancer cells via the Keap1-Nrf2-ARE system’, *Int. J. Oncol.*, 45 (6), pp. 2341–2348.

Yamasaki, M., Makino, T., Masuzawa, T., Kurokawa, Y., Miyata, H., Takiguchi, S., Nakajima, K., Fujiwara, Y., Matsuura, N., Mori, M., Doki, Y. (2011) ‘Role of multidrug resistance protein 2 (MRP2) in chemoresistance and clinical outcome in oesophageal squamous cell carcinoma’, *Br. J. Cancer*, 104 (4), pp. 707–713.

Yang, Y., Sauve, A.A. (2016) ‘NAD+ metabolism: Bioenergetics, signaling and manipulation for therapy’, *Biochim. Biophys. Acta - Proteins Proteomics*, 1864 (12), pp. 1787–1800.

Yoshiga, T., Georgieva, T., Dunkov, B.C., Harizanova, N., Ralchev, K., Law, J.H. (1999) ‘Drosophila melanogaster transferrin: Cloning, deduced protein sequence, expression during the life cycle, gene localization and up-regulation on bacterial infection’, *Eur J Biochem*, 260 (2), pp. 414–420.

Yu, C., Mannan, A.M., Yvone, G.M., Ross, K.N., Zhang, Y.-L., Marton, M.A., Taylor,

B.R., Crenshaw, A., Gould, J.Z., Tamayo, P., Weir, B.A., Tsherniak, A., Wong, B., Garraway, L.A., Shamji, A.F., Palmer, M.A., Foley, M.A., Winckler, W., Schreiber, S.L., Kung, A.L., Golub, T.R. (2016) 'High-throughput identification of genotype-specific cancer vulnerabilities in mixtures of barcoded tumor cell lines', *Nat. Biotechnol.*, 34 (4), pp. 419–423.

Yu, H., Chen, Y., Yu, L., Hao, Z., Zhou, L. (2012) 'Synthesis, visible light photocleavage, antiproliferative and cellular uptake properties of ruthenium complex [Ru(phen)2(mitatp)]2+', *Eur. J. Med. Chem.*, 55, pp. 146–154.

Yu, H., Su, J., Xu, Y., Kang, J., Li, H., Zhang, L., Yi, H., Xiang, X., Liu, F., Sun, L. (2011) 'p62/SQSTM1 involved in cisplatin resistance in human ovarian cancer cells by clearing ubiquitinated proteins', *Eur. J. Cancer*, 47 (10), pp. 1585–1594.

Zalewska, M., Kochman, A., Estève, J.-P., Lopez, F., Chaoui, K., Susini, C., Ożyhar, A., Kochman, M. (2009) 'Juvenile hormone binding protein traffic — Interaction with ATP synthase and lipid transfer proteins', *BBA - Biomembr.*, 1788, pp. 1695–1705.

Zhang, L.J., Hao, Y.Z., Hu, C.S., Ye, Y., Xie, Q.P., Thorne, R.F., Hersey, P., Zhang, X.D. (2008) 'Inhibition of apoptosis facilitates necrosis induced by cisplatin in gastric cancer cells', *Anticancer. Drugs*, 19 (2), pp. 159–166.

Zhao, Y.-Y., Mandal, R., Li, X.-F. (2005) 'Intact human holo-transferrin interaction with oxaliplatin', *Rapid Commun. Mass Spectrom.*, 19 (14), pp. 1956–1962.

Zischka, H., Lichtmannegger, J., Schmitt, S., Jägemann, N., Schulz, S., Wartini, D., Jennen, L., Rust, C., Larochette, N., Galluzzi, L., Chajes, V., Bandow, N., Gilles, V.S., DiSpirito, A.A., Esposito, I., Goettlicher, M., Summer, K.H., Kroemer, G. (2011) 'Liver mitochondrial membrane crosslinking and destruction in a rat model of Wilson disease', *J. Clin. Invest.*, 121 (4), pp. 1508–1518.

Zuo, J., Bi, C., Fan, Y., Buac, D., Nardon, C., Daniel, K.G., Ping Dou, Q. (2013) 'Cellular and computational studies of proteasome inhibition and apoptosis induction in human cancer cells by amino acid Schiff base–copper complexes', *J. Inorg. Biochem.*, 118, pp. 83–93.

Appendices

Appendix I: Reagents, solution constituents and experimental templates

1.1 Cell Culture and MTT cytotoxicity assay

1.1.1 Cell Culture Media:

Roswell Park Memorial Institute (RPMI-1640) (Sigma, Ireland) (Cat# R8758) 500 ml solution supplemented with:

- 60 ml Foetal Bovine Serum (Cat# F2442) (Sigma, Ireland)
- 5 ml L-Glutamine (Cat# G7513) (Sigma, Ireland)

1.1.2 Versene / EDTA (0.02 %) and trypsin solution

- 0.1 g of EDTA added to PBS (500 ml) and autoclaved prior to use.

Trypsin 2.5 % v/v (100 ml) (Thermo, Ireland) (Cat# 15090046) added to Hank's Balanced salt solution (HBSS) (Sigma, Ireland) (Cat# 9394) (1L). Solution aliquoted into 10ml and frozen to -20 °C until required. Upon thawing 10 ml aliquot combined with 10 ml Versene solution prior to application to cell culture.

1.1.3 Freeze down procedure

After each experiment was finished the cells were frozen down. This was performed to preserve the cells and protect them from genetic drift. The act of freezing cells down also limits the consumable necessary for the continuous culturing. They are preserved in the cryoprotectant DMSO (Sigma, Ireland) (cat# 276855) in cell culture media which was filtered prior to use with the cells. The initial procedure is performed at 4 °C with a stepwise decrease in temperature down to liquid nitrogen storage. This stepwise process protects the cells and limits the incidences of ice crystal formation.

1.1.4 Cu(II) phenanthroline-phenazine complexes stock and solutions

Cu(II) complex	Molecular weight (M.W)	Stock concentration (mM)	Stock volume (ml)
Cu-Phen (**1**)	547.97	9.12	2
Cu-DPQ-Phen (**2**)	609.01	8.21	2
Cu-DPPZ-Phen (**3**)	650.06	7.69	2
Cu-DPPN-Phen (**4**)	736.15	6.79	2

DMSO used as stock solvent. Solution stored in air tight sterile glass container.

1.1.5 Cisplatin (Sigma, Ireland) (*cis*-Diamineplatinum(II) dichloride, CAS: 15663-27-1) (Cat# P4394)

- Reconstituted to a stock concentration of 16.6 mM in DMSO wherein a working stock of 200 µM in RPMI-1640 cell culture media is generated.

1.1.6 Doxorubicin (Sigma, Ireland) (Doxorubicin hydrochloride, CAS: 25316-40-9) (Cat# D2975000)

- Reconstituted in 1 ml water (1 mM) and diluted to a stock of 20 µM in RPMI-1640 cell culture media.

1.1.7 Working solution make-up (Cu(II) phenanthroline-phenazine complexes)
Make-up of working solutions of the Cu(II) phenanthroline-phenazine complexes for the MCF-7, OE-33, SKOV-3, HeLa, HT-29 and SKOV-3 cell lines.

Complex stock concentration in (DMSO) (mM)	Volume (20 ml) for working solution (10 µM)	Volume (µM) from working stock made up in 5 ml cell culture media. Volume represented in µl					
		10 (µM)	5 (µM)	2.5 (µM)	1 (µM)	0.5 (µM)	0.25 (µM)
Cu-Phen (**1**)	21.92 µl	5000 µl	2500 µl	1250 µl	500 µl	250 µl	125 µl
Cu-DPQ-Phen (**2**)	24.36 µl						
Cu-DPPZ-Phen (**3**)	26.007 µl						
Cu-DPPN-Phen (**4**)	29.45 µl						

1.1.8 96-well plate set-up template

96-well plate template for the Cu(II) phenanthroline-phenazine complexes exposure for MTT cytotoxicity test. “Neg” refers to the negative control (no exposure). Concentration range of the test Cu(II) complexes 0.25-10 μM replicated down multiple rows.

	1	2	3	4	5	6	7	8	9	10	11	12
A	**Blank**											
B		Neg	0.25	0.5	1	2.5	5	10	Neg	Neg	Neg	
C		Neg	0.25	0.5	1	2.5	5	10	Neg	Neg	Neg	
D		Neg	0.25	0.5	1	2.5	5	10	Neg	Neg	Neg	
E	**Blank**	Neg	0.25	0.5	1	2.5	5	10	Neg	Neg	Neg	**Blank**
F		Neg	0.25	0.5	1	2.5	5	10	Neg	Neg	Neg	
G		Neg	0.25	0.5	1	2.5	5	10	Neg	Neg	Neg	
H		**Blank**										

1.1.9 Working solution make-up (cisplatin)

Make-up of working solutions of cisplatin for the MCF-7, OE-33, SKOV-3, HeLa, HT-29 and SKOV-3 cell line exposures.

	Volume required for working stock concentration (200 μM) (20 ml)	Volume (μM) from working stock made up in 5 ml cell culture media. Volume represented in μl						
		200	100	50	10	5	1	0.5
Cisplatin (16.6 mM)	240.96 μl	5000 μl	2500 μl	1250μl	250 μl	125 μl	25 μl	12.5 μl

1.1.10 96-well plate set-up template

96-well plate template for cisplatin exposure for MTT cytotoxicity test. “Neg” refers to the negative control (no exposure). Concentration range of cisplatin 0.5-200 μM replicated down multiple rows.

	1	2	3	4	5	6	7	8	9	10	11	12
A	**Blank**											
B		Neg	0.5	1	5	10	50	100	200	Neg	Neg	
C		Neg	0.5	1	5	10	50	100	200	Neg	Neg	
D		Neg	0.5	1	5	10	50	100	200	Neg	Neg	
E	**Blank**	Neg	0.5	1	5	10	50	100	200	Neg	Neg	**Blank**
F		Neg	0.5	1	5	10	50	100	200	Neg	Neg	
G		Neg	0.5	1	5	10	50	100	200	Neg	Neg	
H		**Blank**										

1.1.11 Working solution make-up

Make-up of Cu(II) phenanthroline-phenazine complexes and doxorubicin working solutions for A2780 and A2780/ Cis cell lines

stock concentration in DMSO (mM)	Volume required for 20 ml of working solution (10 µM)	Volume (µM) from working stock made up in 5 ml cell culture media. Volume represented in µl							
		20 (µM)	10 (µM)	5 (µM)	2.5 (µM)	1.25 (µM)	0.625 (µM)	0.312 (µM)	0.156 (µM)
Doxorubicin (1)	400 µl (20 µM)	5000 µl	2500 µl	1250 µl	625 µl	312.5µl	156.25µl	78µl	N.A
Cu-Phen (**1**) (9.12)	21.92 µl	N.A	5000 µl	2500 µl	1250 µl	625 µl	312.5µl	156 µl	78 µl
Cu-DPQ-Phen (**2**) (8.21)	24.36 µl	N.A	5000 µl	2500 µl	1250 µl	625 µl	312.5µl	156 µl	78 µl
Cu-DPPZ-Phen (**3**) (7.69)	26.007 µl	N.A	5000 µl	2500 µl	1250 µl	625 µl	312.5µl	156 µl	78 µl
Cu-DPPN-Phen (**4**) (6.79)	29.45 µl	N.A	5000 µl	2500 µl	1250 µl	625 µl	312.5µl	156 µl	78 µl

1.1.12 Working solution make-up (cisplatin)

Make-up of working solutions of cisplatin for the A2780 and A2780/ Cis cell line exposures.

	Volume required for working stock concentration (200 µM) (20 ml)	Volume (µM) from working stock made up in 5 ml cell culture media. Volume represented in µl						
		200	100	50	25	12.5	6.25	3.125
Cisplatin (16.6 mM)	240.96 µl	5000 µl	2500 µl	1250µl	625 µl	312.5 µl	156.25 µl	78.125 µl

1.1.13 96-well plate set-up template

96-well plate template for the Cu(II) phenanthroline-phenazine complexes exposure for MTT cytotoxicity test. “Neg” refers to the negative control (no exposure). Concentration range of the test Cu(II) complexes 0.156-10 μM replicated down multiple rows.

	1	2	3	4	5	6	7	8	9	10	11	12
A	**Blank**											
B		Neg	0.156	0.312	0.625	1.25	2.5	5	10	Neg	Neg	
C		Neg	0.156	0.312	0.625	1.25	2.5	5	10	Neg	Neg	
D		Neg	0.156	0.312	0.625	1.25	2.5	5	10	Neg	Neg	
E	**Blank**	Neg	0.156	0.312	0.625	1.25	2.5	5	10	Neg	Neg	**Blank**
F		Neg	0.156	0.312	0.625	1.25	2.5	5	10	Neg	Neg	
G		Neg	0.156	0.312	0.625	1.25	2.5	5	10	Neg	Neg	
H		**Blank**										

1.1.14 96-well plate set-up template

96-well plate template for cisplatin exposure for the MTT cytotoxicity test. “Neg” refers to the negative control (no exposure). Concentration range of cisplatin 3.125-200 μM replicated down multiple rows.

	1	2	3	4	5	6	7	8	9	10	11	12
A	**Blank**											
B		Neg	3.125	6.25	12.5	25	50	100	200	Neg	Neg	
C		Neg	3.125	6.25	12.5	25	50	100	200	Neg	Neg	
D		Neg	3.125	6.25	12.5	25	50	100	200	Neg	Neg	
E	**Blank**	Neg	3.125	6.25	12.5	25	50	100	200	Neg	Neg	**Blank**
F		Neg	3.125	6.25	12.5	25	50	100	200	Neg	Neg	
G		Neg	3.125	6.25	12.5	25	50	100	200	Neg	Neg	
H		**Blank**										

1.1.15 96-well plate set-up template

96-well plate template for doxorubicin exposure for the MTT cytotoxicity test. “Neg” refers to the negative control (no exposure). Concentration range 0.312-20 μM replicated down multiple rows.

	1	2	3	4	5	6	7	8	9	10	11	12
A	**Blank**											
B		Neg	0.312	0.625	1.25	2.5	5	10	20	Neg	Neg	
C		Neg	0.312	0.625	1.25	2.5	5	10	20	Neg	Neg	
D		Neg	0.312	0.625	1.25	2.5	5	10	20	Neg	Neg	
E	**Blank**	Neg	0.312	0.625	1.25	2.5	5	10	20	Neg	Neg	**Blank**
F		Neg	0.312	0.625	1.25	2.5	5	10	20	Neg	Neg	
G		Neg	0.312	0.625	1.25	2.5	5	10	20	Neg	Neg	
H		**Blank**										

1.1.16 MTT (Sigma, Ireland) (Cat# M5655) working solution (5 μg per 1 ml PBS) (100 μl per well):

- For 56 wells (one 96-well plate with 56 inoculated wells)
- 28 μg of 3-(4,5-dimethylthiazol-2-yl)-2,5-diphenyltetrazolium bromide (CAS 298-93-1) (Sigma, Ireland) in 5.6 ml PBS (Sigma, Ireland) (Cat# 806544)

- 1:10 dilution of PBS solution with cell culture media for working MTT solution.

1.1.17 Working protocol for MTT viability assay

1. Cells were inoculated onto 24- and 48- h plates as described above.
2. Cells were incubated as per usual conditions for 24 h to allow them to attach to the bottom of each well.
3. Individual universal were made up of the specific copper complexes concentrations along with cisplatin concentrations.
4. After the 24 h attachment and growth period the media is removed from the wells and 100 µl of the prepared copper complexes or cisplatin are added to the relevant wells. The plates were then incubated for 24 or 48 h.
5. Prior to the 24 or 48 h timepoint completion a suitable volume of working MTT solution is made up at a concentration of 5 mg/ml in PBS (Sigma, Ireland) (Cat# 806544). The working solution is then sterilised by being passed through a 0.2 µm nalgene filter (Thermo, Ireland) (Cat# 724-2020).
6. At the 24- or 48-hour timepoint the cell culture media/ compound solution is carefully removed from the wells. 100 µl of the MTT working solution is then added to each well and the plate is incubated for 3 h.
7. After the 3-hour incubation the MTT working solution is removed and each well is washed with sterile PBS (Sigma, Ireland) (Cat# 806544) solution 3 times. At the end of the last wash the residual liquid is carefully removed by tilting the plate and using the pipette from the corner of the cell taking care not to disturb the cells.
8. 100 µl of DMSO is added to each well and the plate is placed on a plate shaker for 15 min.

9. The absorbance of the cells is read on spectrophotometer/ multiplate reader at 595 nm wavelength to record viability.

1.2 H_2DCFDA assay (ROS assay)

1.2.1 96-well plate template for set-up of H_2DCFDA assay

Blank	Auto ctrl	Neg ctrl	0.156 µM	0.312 µM	0.625 µM	1.25 µM	2.5 µM	5 µM	10 µM	20 µM	H_2O_2 (pos)
Blank	Auto ctrl	Neg ctrl	0.156 µM	0.312 µM	0.625 µM	1.25 µM	2.5 µM	5 µM	10 µM	20 µM	H_2O_2 (pos)
Blank	Auto ctrl	Neg ctrl	0.156 µM	0.312 µM	0.625 µM	1.25 µM	2.5 µM	5 µM	10 µM	20 µM	H_2O_2 (pos)
Blank	Auto ctrl	Neg ctrl	0.156 µM	0.312 µM	0.625 µM	1.25 µM	2.5 µM	5 µM	10 µM	20 µM	H_2O_2 (pos)
Blank	Auto ctrl	Neg ctrl	0.156 µM	0.312 µM	0.625 µM	1.25 µM	2.5 µM	5 µM	10 µM	20 µM	H_2O_2 (pos)
Blank	Auto ctrl	Neg ctrl	0.156 µM	0.312 µM	0.625 µM	1.25 µM	2.5 µM	5 µM	10 µM	20 µM	H_2O_2 (pos)
Blank	Auto ctrl	Neg ctrl	0.156 µM	0.312 µM	0.625 µM	1.25 µM	2.5 µM	5 µM	10 µM	20 µM	H_2O_2 (pos)
Blank	Auto ctrl	Neg ctrl	0.156 µM	0.312 µM	0.625 µM	1.25 µM	2.5 µM	5 µM	10 µM	20 µM	H_2O_2 (pos)

Cu(II) phenanthroline-phenazine complexes and cisplatin made up to 20 µM in supplemented RPMI-1640 cell culture media and double diluted in plate as above.

1.3 γH2AX staining protocol constituents:

1.3.1 Fixing solution:

2 % v/v paraformaldehyde (Sigma, Ireland) (Cat# F8775) in PBS

1.3.2 Triton X-100 solution (0.25%):

- 2.5 µl of Triton X-100 (Sigma, Ireland) (Cat# T8787)
- 9997.5 µl of PBS.

1.3.3 Blocking Solution:

2 % Bovine Serum Albumin (w/v) (Sigma, Ireland) (Cat# A9418) in PBS

1.3.4 Primary antibody (Milipore, Ireland) (Anti-phospho-Histone H2A.X (Ser 139), clone JBW301) (Cat. # 05-636) (Lot # 2068177)):

1:500 dilution made up in blocking solution

1.3.5 Secondary antibody (Milipore, Ireland) (goat anti-mouse IgG Antibody, Alexa fluor 488 FITC conjugate)):

1:200 dilution made up in blocking solution

1.3.6 Counterstaining solution (1:1000):

- 1 µl of Propidium Iodide solution (1µg/ µl) (Sigma, Ireland) (Cat# P4864)
- 1000 µl of PBS

1.3.7 Zeiss LSM510 Meta scanning and recording parameters:

Images recorded at a resolution of 2048x2048 and sampled at 12-bit:

- Green; pin hole 76, gain 573, amplifier offset -0.226, amplifier gain 1.01
- Red; pin hole 80, gain 589, Amplifier offset 0.1, amplifier gain 2.81
- Brightfield recorded

1.4 Gene expression analysis of molecular targets:

1.4.1 cDNA synthesis kit constituents (20 µl per reaction) (Quanta Biosciences, USA) (Cat# 733-1173)

- 1 µl qScript Reverse Transcriptase
- 4 µl qScript Reaction Mix
- 10 µl Nuclear-free water

Final 5 µl is sample RNA. All samples should have the same concentration of RNA before cDNA synthesis.

1.5 Label-free quantitative whole cell proteomic analysis:

1.5.1 Constituent solutions for the In-solution digestion protocol using ProteaseMax™

- Cell lysis buffer: 6 M Urea, 2 M Thiourea, 0.1 M Tris-HCl (pH 8.0) (Cat# U5378, Cat# T8656, Cat# T3038): Prepare using MilliQ water. Aprotinin (10 mg/mL) (Cat# A6106), Leupeptin (Cat# L5793), Pepstatin (Cat# P5318) and TLCK (Cat# T7254) were added to the cell lysis buffer (10 µl of each protease inhibitor per 1ml of cell lysis buffer).
- 50 mM ammonium bicarbonate (Sigma, Ireland) (Cat# 09830): Prepare fresh before use in MilliQ water
- 0.5 M DTT (Sigma, Ireland) (Cat# D0632): Prepare fresh before use in 50 mM ammonium bicarbonate (38.56 mg in 500 µl)
- 0.55 M IAA (Sigma, Ireland) (Cat# I4386): Prepare fresh before use in 50 mM ammonium bicarbonate and protect from light (101.728 mg in 1 ml)
- ProteaseMAX stock (1 % (w/v)) (Promega, USA) (Cat# V2071): Resuspend 1 mg in 100 µl of 50 mM ammonium bicarbonate immediately before use and keep on ice prior to use. For storage, snap freeze 20 µl aliquots in liquid nitrogen and store at -20 °C.
- Trypsin (0.5 µg/µl) (Promega, USA) (Cat# V5111): Resuspend sequencing grade trypsin vial (20 µg; V5111 Promega) with 40 µl of trypsin resuspension buffer. Keep on ice until ready for use. Snap-freeze any remaining trypsin and store at -20 °C for later use.

1.5.2 Bradford assay

Bovine Serum Albumin standards (5-60 µg/ml) (Bio-Rad Munich, Germany) (Cat# G-250), were made in 800 µl deionised water and 200 µl Biorad Bradford protein assay reagent (Bio-Rad Munich, Germany) (Cat# G-250) and read on a spectrophotometer at 595 nm (Eppendorf Biophotometer). A standard curve was prepared. Bradford protein assay reagent was prepared by diluting the stock 1:5 using deionised water. Protein samples were added (20 µl) to 980 µl of Bradford protein assay reagent. The samples were inverted, allowed to stand for 5 min and read spectrophotometrically.

1.5.3 In-solution digestion working protocol using ProteaseMax™

1. Removed 60 µg of sample from lysate and perform an acetone, TCA/acetone (Sigma, Ireland) (Cat# T6399)/ (Cat# V800023) precipitation or 2D Clean up.
2. Re-suspend samples (25 µl; 60 µg) in cell lysis buffer. Note try to keep volume at 15 µl even if conc. is lower than 60 µg. The pellet may take time to re-suspend. Assist with vortex or pipetting.
3. Ammonium bicarbonate (125 µl; 50 mM) (Sigma, Ireland) (Cat# 09830) was added to the samples.
4. DTT (1 µl) (Sigma, Ireland) (Cat# D0632) was added to the samples, followed by incubation at 56 °C for 20 min.
5. Samples were allowed to cool to room temperature and 2.7 µl of IAA (Sigma, Ireland) (Cat# I4386) was added, followed by incubation at room temperature for 15 min in the dark.
6. Following reduction and alkylation 1 µl of ProteaseMAX stock and 1 µl (1 % (w/v)) (Promega, USA) (Cat# V2071) of trypsin were added to each of the samples, followed by incubation at 37 °C overnight.

7. The next day samples were spun briefly to collect any condensate and acidified by adding 1 µl of TFA (Sigma, Ireland) (Cat# 8.08260), vortexed briefly, and incubated at room temperature for 5 min (Some cloudiness can be visible at this point).
8. Samples were centrifuged at 13,000 g for 10 min at room temperature. The supernatant was removed to a new tube.
    - Each sample was divided into 2 aliquots (the removal of 77.5 µl should yield c.30 µg). One aliquot for C18 clean up and the remaining aliquot was stored at -20 °C.

1.5.4 C18 spin-column buffer constituents:

Sample Buffer 1 (Urea/Protease Max procedure):

- 2 % TFA (Sigma, Ireland) (Cat# 8.08260) in 20 % Acetonitrile (ACN) (Sigma, Ireland) (Cat# 271004); Need 1 µl for every 3 µl of sample
- 200 µl ACN, 20 µl TFA and 780 µl ddH_2O

Activation Solution: 50% ACN, 50% ddH_2O (2.5 ml ACN and 2.5 ml ddH_2O)

Equilibration Buffer: 0.5 % TFA in 5 % Acetonitrile; Need 400 µl per sample

- 4.725 ml ddH_2O, 25 µl TFA and 250 µl Acetonitrile

Wash Buffer: same as equilibration buffer; Need 600 µl per sample

Elution Buffer: 70 % Acetonitrile; Need 60 µl per sample

- 700 µl ACN, 300 µl ddH_2O

Loading Buffer for Q Exactive: 0.05 % TFA in 2 % Acetonitrile (obtain from LCMS room); Need 20 µl per sample

Activation Solution: 50% ACN, 50% ddH_2O

1.5.5 C18 spin-column (Thermo, USA) (Cat# 89870) working protocol:

1. Columns were tapped to settle the resin and the caps were removed from either end. Columns were placed in 1.5 ml Eppendorfs.
2. Urea/Protease Max Procedure: Samples were mixed with Sample Buffer 1 (3 parts sample: 1 part Sample Buffer 1; e.g. 50 µl Sample + 18 µl Sample Buffer 1) to obtain a final 0.5 % TFA in 5 % acetonitrile.
2. Activation Solution (200 µl) was added to the columns to rinse the walls of the column and wet the resin. Columns were centrifuged at 1500 g for 1 min and flow-through was discarded. Step was repeated.
3. Equilibration Solution (200 µl) was added to the columns, centrifuged at 1500 g for 1 min and flow-through was discarded. Step was repeated.
4. Samples (10-150 µl; up to 30 µg) were loaded to the top of the resin bed and the columns were placed in new receiver tubes. Samples were centrifuged at 1500 g for 1 min, the flow-through was recovered and re-applied to the column. This step was repeated twice more to ensure complete sample binding.
5. Columns were transferred into new receiver tubes and 200 µl of Wash Buffer was added. The columns were centrifuged at 1500 g for 1 min and the flow-through was discarded. This step was repeated twice more to remove high levels of contaminants.
6. The columns were placed in new receiver tubes and 25 µl of Elution Buffer was applied to the top of the resin bed. The columns were centrifuged at 1500 g for 1 min. This step was repeated twice more using the same receiver tube to collect a total ~75 µl of eluant.
7. Samples were dried in the SpeedyVac (Thermo, USA), (Run setting, medium heat)

8. Samples were re-suspend in 32 µl of Loading Buffer for Q Exactive (2 % acetonitrile, 0.05 % TFA). Samples were placed in the sonication bath for 5 min to aid peptide re-suspension prior to MS/MS injection.
9. Samples were centrifuged at 13,400 g for 5 min at room temperature to pellet any insoluble material, and the supernatants were transferred to vials for LC MS/MS analysis by the Q Exactive.

1.5.6 MASCOT and SEQUEST search parameters:

- Peptide mass tolerance at 20 ppm
- Fragment mass tolerance at 0.02 Da
- Up to 2 missed cleavages
- Cysteine carboxymethylation set at static modification
- Methionine oxidation at dynamic modification
- MASCOT ion score at minimum of 40

SEQUEST HT XCorr set at minimum 1.5 and FDR for PSMs and peptides set for strict at 0.01 and relaxed at 0.05

1.6 Rhodamine 123 MMP assay
1.6.1 96-well plate template for the MMP assay using rhodamine 123 (Sigma, Ireland) (Cat# R8004)

Blank	Neg Ctrl	1/256 IC_{50}	1/128 IC_{50}	1/64 IC_{50}	1/32 IC_{50}	1/16 IC_{50}	1/8 IC_{50}	1/4 IC_{50}	1/2 IC_{50}	IC_{50}	Pos Ctrl
Blank	Neg Ctrl	1/256 IC_{50}	1/128 IC_{50}	1/64 IC_{50}	1/32 IC_{50}	1/16 IC_{50}	1/8 IC_{50}	1/4 IC_{50}	1/2 IC_{50}	IC_{50}	Pos Ctrl
Blank	Neg Ctrl	1/256 IC_{50}	1/128 IC_{50}	1/64 IC_{50}	1/32 IC_{50}	1/16 IC_{50}	1/8 IC_{50}	1/4 IC_{50}	1/2 IC_{50}	IC_{50}	Pos Ctrl
Blank	Neg Ctrl	1/256 IC_{50}	1/128 IC_{50}	1/64 IC_{50}	1/32 IC_{50}	1/16 IC_{50}	1/8 IC_{50}	1/4 IC_{50}	1/2 IC_{50}	IC_{50}	Pos Ctrl
Blank	Neg Ctrl	1/256 IC_{50}	1/128 IC_{50}	1/64 IC_{50}	1/32 IC_{50}	1/16 IC_{50}	1/8 IC_{50}	1/4 IC_{50}	1/2 IC_{50}	IC_{50}	Pos Ctrl
Blank	Neg Ctrl	1/256 IC_{50}	1/128 IC_{50}	1/64 IC_{50}	1/32 IC_{50}	1/16 IC_{50}	1/8 IC_{50}	1/4 IC_{50}	1/2 IC_{50}	IC_{50}	Pos Ctrl
Blank	Neg Ctrl	1/256 IC_{50}	1/128 IC_{50}	1/64 IC_{50}	1/32 IC_{50}	1/16 IC_{50}	1/8 IC_{50}	1/4 IC_{50}	1/2 IC_{50}	IC_{50}	Pos Ctrl
Blank	Neg Ctrl	1/256 IC_{50}	1/128 IC_{50}	1/64 IC_{50}	1/32 IC_{50}	1/16 IC_{50}	1/8 IC_{50}	1/4 IC_{50}	1/2 IC_{50}	IC_{50}	Pos Ctrl
Blank	Neg Ctrl	1/256 IC_{50}	1/128 IC_{50}	1/64 IC_{50}	1/32 IC_{50}	1/16 IC_{50}	1/8 IC_{50}	1/4 IC_{50}	1/2 IC_{50}	IC_{50}	Pos Ctrl

1.7 *Galleria mellonella* study

1.7.1 Make-up of working solutions for *G. mellonella* inoculation

Dose (µg) (20 µl inoculation)	Cisplatin inoculation make-up	Cu(II) complex inoculation make-up
Stock	(5000 µg/ml H_2O)	(1500 µg/ml H_2O)
100 (Cisplatin only)	1ml of stock + 0 ml H_2O	N.A
30	N.A	1ml stock + 0 ml H_2O
20	N.A	0.666 ml stock + 0.334 ml H_2O
12	N.A	0.400 ml stock + 0.600 ml H_2O
10	0.1 ml stock + 0.9 ml H_2O	0.333 ml stock + 0.666 ml H_2O
8	0.08 ml stock + 0.92 ml H_2O	0.266 ml stock + 0.734 ml H_2O
6	0.06 ml stock + 0.94 ml H_2O	0.200 ml stock + 0.600 ml H_2O
4	0.04 ml stock + 0.96 ml H_2O	0.133 ml stock + 0.867 ml H_2O
2	0.02 ml stock + 0.98 ml H_2O	0.066 ml stock + 0.934 ml H_2O

100 mg of cisplatin was weighed and dissolved in 1 ml DMSO. This was added to 19 ml H_2O to make cisplatin stock. For Cu-Phen (**1**), Cu-DPQ-Phen (**2**), Cu-DPPZ-Phen (**3**) and Cu-DPPN-Phen (**4**) 15 mg was dissolved in 1 ml DMSO and then added to 9 ml H_2O to make Cu-Phen (**1**), Cu-DPQ-Phen (**2**), Cu-DPPZ-Phen (**3**) and Cu-DPPN-Phen (**4**) stock solutions.

1.7.2 *G. Mellonella* 2D SDS-PAGE analysis of protein expression

1-Dimension gel set-up and IEF buffer constituents

The following constituents were added and dissolved in deionised water and stored in 2 ml aliquots at -20 ºC until required.

- Urea 8 M (Sigma, Ireland) (Cat# U5378)
- Triton X-100 (BDH) 1 % (v/v) (Sigma, Ireland) (Cat# T8787)
- CHAPS 4 % (w/v) (Sigma, Ireland) (Cat# C9426)
- Tris-HCl 10 mM (Sigma, Ireland) (Cat# T3038)
- Thiourea 2 mM (Sigma, Ireland) (Cat# T8656)

Prior to use DTT (65 mM) (Sigma, Ireland) (Cat# D0632) was added to the buffer and solubilised by vortexing.

IEF rig program (EttanIPGphore II)

1. 50 Volts, step and hold for 10 h
2. 250 Volts, step and hold for 15 min
3. 8000 Volts, gradient for 5 h
4. 8000 Volts, step and hold for 8 h

1.7.3 2-Dimension PAGE set-up

Equilibration Buffer

- Tris-base 50 mM (Sigma, Ireland) (Cat# TRIS-RO ROCHE)
- Urea 6 M (Sigma, Ireland) (Cat# U5378)
- SDS 2 % (w/v) (Sigma, Ireland) (Cat# 862010)
- Glycerol 30 % (v/v) (Sigma, Ireland) (Cat# G5516)

The solution was adjusted to pH 6.8 and aliquoted in 40 ml volumes prior to storage at -20 ºC. For equilibration the buffer was modified as either reducing or alkylating. For reduction, DTT (0.01 g/ml) was added and dissolved thoroughly. For alkylation, IAA (0.025 g/ml) (Sigma, Ireland) (Cat# I4386) was dissolved thoroughly in the buffer.

1.7.4 Separating gel composition

- 12.5 % Bis-Acrylamide solution (Sigma, Ireland) (Cat# A3574)
- 1.5 M Tris-HCl (pH 8.9) 3 ml (Sigma, Ireland) (Cat# T3038)
- Deionised water 3.8 ml
- 30% Bis-Acrylamide 5 ml (Sigma, Ireland) (Cat# A2917)

- 10% v/v SDS 120 µl (Sigma, Ireland) (Cat# 862010)
- 10% v/v APS 75 µl (Sigma, Ireland) (Cat# A3678)
- TEMED 3 µl (Sigma, Ireland) (Cat# T9281)

These volumes were sufficient to make 3 mini-gels and volumes were adjusted accordingly where a larger volume was required.

1.7.5 5X Solubilisation Buffer for 1-D SDS–PAGE

Solubilisation buffer was prepared by dissolving the following constituents to solubility.

- Glycerol 8 ml (Sigma, Ireland) (Cat# G5516)
- Deionised water 4 ml
- 10 % (w/v) SDS 1.6 ml (Sigma, Ireland) (Cat# 862010)
- 0.5 M Tris – HCl 1 ml (Sigma, Ireland) (Cat# T3038)
- Bromophenol Blue (0.5 % w/v) 200 µl (Sigma, Ireland) (Cat# B8026)
- 2 – Mercaptoethanol 400 µl (Sigma, Ireland) (Cat# M6250)

The buffer was gently mixed for 1 h at 4 ºC and aliquoted in 500 µl volumes prior to storage at -20 ºC.

1.7.6 10 X electrode Running Buffer

Running buffer (10 X), (electrode buffer), was prepared by adding; Tris Base 30 g/l, Glycine (Sigma, Ireland) 144 g/l and SDS 10 g/l dissolved using distilled water filled up to 1000 ml mark and the mixture was stirred until the solution was solubilised. Electrode running buffer (10 X) stock was diluted to 1 X concentration by making 1/10 dilution with distilled water when required.

1.7.7 Coomassie Brilliant blue

- 0.25 % Coomassie blue (Sigma, Ireland) (Cat# B6529)
- 50 % MeOH (Sigma, Ireland) (Cat# 322415)
- 10 % HoAC (Sigma, Ireland) (Cat# A6283)
- 40 % H_2O

Leave gel in solution for 1 h followed by destaining for 1 h. Background will appear clear.

1.7.8 Destaining solution

- 5 % MeOH (Sigma, Ireland) (Cat# 322415)
- 7.5 % HoAC (Sigma, Ireland) (Cat# A6283)
- 87.5 % H_2O

1.7.9 MASCOT program searching parameters

MASCOT MS/MS Ions Search

- Database – NCBInr/ Swissprot
- Enzyme – Trypsin
- Allow up to 2 missed cleavages
- Quantitation – none
- Taxonomy – Other Metazoa
- Fixed Modifications – Carboxymethyl (C)
- Variable Modifications – Oxidation (M)
- Peptide tol. ± 2 Da #^{13}C=0
- MS/MS tol. ± 1 Da
- Peptide charge – 1+, 2+ and 3+

- Monoisotopic
- Data format – Mascot generic
- Instrument – ESI-TRAP
- Report top - AUTO

Appendix II: Equipment

2.1 Beckman COULTERTM Z1 coulter® particle counter (Beckman-Coulter, USA)

2.2 1420 Multilabel Counter Victor^{3}V spectrophotometer (PerkinElmer, USA)

2.3 SpectraMax M3 Multi-Mode Microplate Reader (Molecular Devices, USA)

2.4 MaestroNano™ spectrophotometer (Maestrogen, USA)

2.5 Prime Thermal Cycler (Techne, UK)

2.6 7500 fast Real-Time PCR System (Applied Biosystems, USA)

2.7 Accuri C6 Plus (Beckman-Dickenson Bioscience, USA)

2.7 LSM510 Meta (Zeiss, Germany)

2.8 Q Exactive™ Hybrid Quadrupole-Orbitrap Mass Spectrometer (Thermo Fisher Scientific, USA)

2.9 SpeedyVac (Thermo Fisher Scientific, USA)

2.10 EttanIPGphore II (Amersham Biosciences, USA)

2.11 6340 Ion Trap (Agilent, USA)

Appendix III: Raw data

The following data refers to the MTT viability assay with raw data from the spectrophotometer normalized to the negative control. Each table represents normalized percentage values averaged from 3 independent assays.

3.1.1 **SKOV-3 24 h exposure**

Cisplatin:

Concentration (µM)	Negative	0.5	1	5	10	50	100	200
Mean (Normalized) (%)	100	97.86041	93.17747	89.84769	88.8096	65.49721	50.80334	42.90763

Cisplatin:

Concentration (µM)	Negative	0.5	1	5	10	50	100	200
Mean (Normalized) (%)	100	95.6801	90.59057	81.46038	82.87151	85.62479	87.18415	81.11278

Cisplatin:

Concentration (µM)	Negative	0.5	1	5	10	50	100	200
Mean (Normalized) (%)	100	97.43009	94.74355	89.1221	89.8611	87.67019	89.27135	87.09333

1:

Concentration (µM)	Negative	0.25	0.5	1	2.5	5	10
Mean (Normalized) (%)	100	95.97582	88.93391	85.15331	68.04039	12.0359	8.793683

1:

Concentration (µM)	Negative	0.25	0.5	1	2.5	5	10
Mean (Normalized) (%)	100	93.73804	87.40713	84.6436	75.58633	12.94864	9.971858

1:

Concentration (µM)	Negative	0.25	0.5	1	2.5	5	10
Mean (Normalized) (%)	100	92.62858	91.85719	90.80279	74.03709	14.66592	11.24925

2:

Concentration (µM)	Negative	0.25	0.5	1	2.5	5	10

Mean (Normalized) (%)	100	96.53517	89.36107	87.08867	67.21983	10.094	8.832035

2:

Concentration (μM)	Negative	0.25	0.5	1	2.5	5	10
Mean (Normalized) (%)	100	92.10836	88.45205	84.02857	73.22263	11.26152	10.00362

2:

Concentration (μM)	Negative	0.25	0.5	1	2.5	5	10
Mean (Normalized) (%)	100	94.16484	89.16714	86.47044	71.5547	13.00472	11.60154

3:

Concentration (μM)	Negative	0.25	0.5	1	2.5	5	10
Mean (Normalized) (%)	100	89.43355	84.45206	83.04639	63.70595	7.736132	7.436689

3:

Concentration (μM)	Negative	0.25	0.5	1	2.5	5	10
Mean (Normalized) (%)	100	93.64273	92.41384	88.83005	14.16387	9.60941	9.965572

3:

Concentration (μM)	Negative	0.25	0.5	1	2.5	5	10
Mean (Normalized) (%)	100	96.25298	94.21353	79.56997	12.75276	11.6072	11.92091

4:

Concentration (μM)	Negative	0.25	0.5	1	2.5	5	10
Mean (Normalized) (%)	100	91.4319	86.17494	83.02828	82.0491	77.59611	59.51903

4:

Concentration (μM)	Negative	0.25	0.5	1	2.5	5	10
Mean (Normalized) (%)	100	92.75296	90.30353	90.13127	88.17447	80.35404	22.46599

4:

Concentration (µM)	Negative	0.25	0.5	1	2.5	5	10
Mean (Normalized) (%)	100	94.75555	94.4948	93.89969	92.81869	76.9958	18.25622

3.1.2 **SKOV-3 48 h exposure**

Cisplatin:

Concentration (µM)	Negative	0.5	1	5	10	50	100	200
Mean (Normalized) (%)	100	90.29874	84.61898	71.82421	53.21039	33.93293	31.22933	28.30161

Cisplatin:

Concentration (µM)	Negative	0.5	1	5	10	50	100	200
Mean (Normalized) (%)	100	93.34969	88.31572	84.15349	81.85864	78.7003	72.94659	64.8029

Cisplatin:

Concentration (µM)	Negative	0.5	1	5	10	50	100	200
Mean (Normalized) (%)	100	101.8218	97.35485	95.64739	94.20672	91.93487	87.67305	74.76569

1:

Concentration (µM)	Negative	0.25	0.5	1	2.5	5	10
Mean (Normalized) (%)	100	93.86481	90.73359	85.41637	51.08111	7.95897	7.758586

1:

Concentration (µM)	Negative	0.25	0.5	1	2.5	5	10
Mean (Normalized) (%)	100	93.754	92.6005	87.3097	52.98101	9.311646	9.489863

1:

Concentration (µM)	Negative	0.25	0.5	1	2.5	5	10
Mean (Normalized) (%)	100	97.02619	94.63298	88.09551	40.47344	11.41295	11.64516

2:

Concentration (µM)	Negative	0.25	0.5	1	2.5	5	10
Mean (Normalized) (%)	100	97.55172	93.31115	92.01271	61.11208	7.996761	8.199303

2:

Concentration (µM)	Negative	0.25	0.5	1	2.5	5	10
Mean (Normalized) (%)	100	90.67059	88.213	86.25801	42.91792	9.268754	9.727623

2:

Concentration (µM)	Negative	0.25	0.5	1	2.5	5	10
Mean (Normalized) (%)	100	102.9404	93.88349	91.98565	47.36876	11.62545	11.76515

3:

Concentration (µM)	Negative	0.25	0.5	1	2.5	5	10
Mean (Normalized) (%)	100	95.8996	92.62705	88.93872	8.46316	7.987409	8.345073

3:

Concentration (µM)	Negative	0.25	0.5	1	2.5	5	10
Mean (Normalized) (%)	100	89.07935	86.18738	71.76261	9.258514	9.035735	9.460964

3:

Concentration (µM)	Negative	0.25	0.5	1	2.5	5	10
Mean (Normalized) (%)	100	94.12671	88.03433	23.99019	10.18244	9.918588	10.07934

4:

Concentration (µM)	Negative	0.25	0.5	1	2.5	5	10
Mean (Normalized) (%)	100	91.08877	89.922	89.83264	94.00465	86.59244	12.91109

4:

Concentration (µM)	Negative	0.25	0.5	1	2.5	5	10
Mean (Normalized) (%)	100	91.19547	89.2356	87.51367	86.7474	34.61149	8.468885

4:

Concentration (µM)	Negative	0.25	0.5	1	2.5	5	10
Mean (Normalized) (%)	100	99.37206	95.5219	95.22162	82.6582	40.39509	10.00621

3.1.3 **PC-3 24 h exposure**

Cisplatin:

Concentration (µM)	Negative	0.5	1	5	10	50	100	200
Mean (Normalized) (%)	100	96.34771	97.7674	93.43795	94.37062	92.88649	93.90378	92.28548

Cisplatin:

Concentration (µM)	Negative	0.5	1	5	10	50	100	200
Mean (Normalized) (%)	100	89.25787	88.93958	86.6472	85.07684	76.5579	69.38236	63.51909

Cisplatin:

Concentration (µM)	Negative	0.5	1	5	10	50	100	200
Mean (Normalized) (%)	100	90.39035	92.42106	94.15695	98.87745	87.27382	83.38805	86.98496

1:

Concentration (µM)	Negative	0.25	0.5	1	2.5	5	10
Mean (Normalized) (%)	100	92.43062	92.9721	93.86121	94.45098	80.12121	59.35015

1:

Concentration (µM)	Negative	0.25	0.5	1	2.5	5	10
Mean (Normalized) (%)	100	90.93809	88.01336	90.7831	94.4711	83.53327	69.17471

1:

Concentration (µM)	Negative	0.25	0.5	1	2.5	5	10
Mean (Normalized) (%)	100	96.97557	95.53938	98.5084	102.3717	81.32744	46.21208

2:

Concentration (µM)	Negative	0.25	0.5	1	2.5	5	10
Mean (Normalized) (%)	100	92.39017	90.6362	91.54076	90.61389	72.45679	48.06606

2:

Concentration (µM)	Negative	0.25	0.5	1	2.5	5	10
Mean (Normalized) (%)	100	92.82576	89.90796	87.37021	88.50858	61.85174	38.96705

2:

Concentration (µM)	Negative	0.25	0.5	1	2.5	5	10
Mean (Normalized) (%)	100	90.72959	88.36826	82.74659	85.30403	50.10399	36.22314

3:

Concentration (µM)	Negative	0.25	0.5	1	2.5	5	10
Mean (Normalized) (%)	100	89.66077	87.1301	81.49134	46.2304	39.08511	37.71994

3:

Concentration (µM)	Negative	0.25	0.5	1	2.5	5	10
Mean (Normalized) (%)	100	90.43842	88.37507	75.27677	36.71501	29.31631	27.70235

3:

Concentration (µM)	Negative	0.25	0.5	1	2.5	5	10
Mean (Normalized) (%)	100	95.50159	96.40074	79.24688	36.90785	29.9203	29.30476

4:

Concentration (µM)	Negative	0.25	0.5	1	2.5	5	10
Mean (Normalized) (%)	100	95.50126	95.9396	91.84072	89.72771	82.52452	64.36637

4:

Concentration (µM)	Negative	0.25	0.5	1	2.5	5	10
Mean (Normalized) (%)	100	97.40188	96.56912	96.27549	93.35218	84.49471	57.87264

4:

Concentration (µM)	Negative	0.25	0.5	1	2.5	5	10
Mean (Normalized) (%)	100	99.89362	99.6043	88.33814	84.97194	71.28656	48.02778

3.1.4 **PC-3 48 h exposure**

Cisplatin:

Concentration (µM)	Negative	0.5	1	5	10	50	100	200
Mean (Normalized) (%)	100	100.4888	98.61385	98.09661	99.81848	97.8848	98.66545	93.93268

Cisplatin:

Concentration (µM)	Negative	0.5	1	5	10	50	100	200
Mean (Normalized) (%)	100	99.07198	97.72346	92.15195	88.70879	66.74982	57.61798	48.84762

Cisplatin:

Concentration (µM)	Negative	0.5	1	5	10	50	100	200
Mean (Normalized) (%)	100	78.64905	91.89447	87.86956	85.68883	72.3873	70.09817	67.9052

1:

Concentration (µM)	Negative	0.25	0.5	1	2.5	5	10
Mean (Normalized) (%)	100	92.68463	94.63625	96.77982	81.08889	60.59814	51.87435

1:

Concentration (µM)	Negative	0.25	0.5	1	2.5	5	10
Mean (Normalized) (%)	100	96.61408	96.71811	99.51628	46.23155	25.383	15.63699

1:

Concentration (µM)	Negative	0.25	0.5	1	2.5	5	10
Mean (Normalized) (%)	100	96.46511	97.39194	102.3961	77.50745	44.6905	33.30829

2:

Concentration (µM)	Negative	0.25	0.5	1	2.5	5	10
Mean (Normalized) (%)	100	92.90166	92.5282	90.39795	94.5946	57.60424	53.68285

2:

Concentration (µM)	Negative	0.25	0.5	1	2.5	5	10
Mean (Normalized) (%)	100	96.3832	93.88316	94.81814	98.31173	38.55885	28.84244

2:

Concentration (µM)	Negative	0.25	0.5	1	2.5	5	10
Mean (Normalized) (%)	100	94.38681	101.0893	92.33077	98.01181	42.15402	32.66468

3:

Concentration (µM)	Negative	0.25	0.5	1	2.5	5	10
Mean (Normalized) (%)	100	89.27144	90.57137	85.12956	55.33454	51.94949	54.09989

3:

Concentration (µM)	Negative	0.25	0.5	1	2.5	5	10
Mean (Normalized) (%)	100	90.54204	87.50935	72.40314	32.24061	28.83265	29.60639

3:

Concentration (µM)	Negative	0.25	0.5	1	2.5	5	10
Mean (Normalized) (%)	100	84.088	83.59276	60.83442	28.94409	26.20559	27.1848

4:

Concentration (µM)	Negative	0.25	0.5	1	2.5	5	10
Mean (Normalized) (%)	100	99.33918	100.1575	97.09041	92.68357	87.11181	71.5279

4:

Concentration (µM)	Negative	0.25	0.5	1	2.5	5	10
Mean (Normalized) (%)	100	94.14312	94.52576	92.5021	85.20838	68.36034	42.71255

4:

Concentration (µM)	Negative	0.25	0.5	1	2.5	5	10
Mean (Normalized) (%)	100	93.93065	91.40233	88.37948	84.22677	65.71552	37.50704

3.1.5 **OE-33 24 h exposure**

Cisplatin:

Concentration (µM)	Negative	0.5	1	5	10	50	100	200
Mean (Normalized) (%)	100	99.05012	94.68332	93.61847	88.10879	86.18838	84.06355	67.56755

Cisplatin:

Concentration (µM)	Negative	0.5	1	5	10	50	100	200
Mean (Normalized) (%)	100	101.1664	95.80555	92.36449	83.50925	83.16757	82.96213	79.32003

Cisplatin:

Concentration (µM)	Negative	0.5	1	5	10	50	100	200
Mean (Normalized) (%)	100	92.70852	90.67557	83.24087	75.66866	71.80223	69.75214	64.75196

1:

Concentration (µM)	Negative	0.25	0.5	1	2.5	5	10
Mean (Normalized) (%)	100	93.54031	89.06235	84.2935	36.16583	15.10018	11.33098

1:

Concentration (µM)	Negative	0.25	0.5	1	2.5	5	10
Mean (Normalized) (%)	100	97.77682	95.04133	93.03605	62.83079	28.60519	16.91353

1:

Concentration (µM)	Negative	0.25	0.5	1	2.5	5	10
Mean (Normalized) (%)	100	95.86788	94.44938	92.96852	64.46666	31.6388	16.55521

2:

Concentration (µM)	Negative	0.25	0.5	1	2.5	5	10
Mean (Normalized) (%)	100	93.79205	85.98112	78.03622	22.87566	11.68346	10.8837

2:

Concentration (µM)	Negative	0.25	0.5	1	2.5	5	10
Mean (Normalized) (%)	100	96.04994	93.58244	89.63625	81.9523	20.159	13.25597

2:

Concentration (µM)	Negative	0.25	0.5	1	2.5	5	10
Mean (Normalized) (%)	100	93.41833	87.08595	81.04975	75.94951	19.81809	13.15891

3:

Concentration (µM)	Negative	0.25	0.5	1	2.5	5	10
Mean (Normalized) (%)	100	96.10454	85.34502	74.72461	14.09381	9.833146	9.916219

3:

Concentration (µM)	Negative	0.25	0.5	1	2.5	5	10
Mean (Normalized) (%)	100	96.03962	82.99179	77.01749	13.4274	10.53016	10.46623

3:

Concentration (µM)	Negative	0.25	0.5	1	2.5	5	10
Mean (Normalized) (%)	100	92.20391	84.49257	71.99808	14.56886	10.05302	10.0151

4:

Concentration (µM)	Negative	0.25	0.5	1	2.5	5	10
Mean (Normalized) (%)	100	100.3991	96.97613	88.92099	69.84164	55.04	11.25414

4:

Concentration (µM)	Negative	0.25	0.5	1	2.5	5	10
Mean (Normalized) (%)	100	102.2673	95.19575	88.44111	71.60656	57.89885	11.84289

4:

Concentration (µM)	Negative	0.25	0.5	1	2.5	5	10
Mean (Normalized) (%)	100	100.6671	100.2722	95.48418	72.27852	55.0193	11.54096

3.1.6 **OE-33 48 h exposure**

Cisplatin:

Concentration (µM)	Negative	0.5	1	5	10	50	100	200
Mean (Normalized) (%)	100	93.91773	87.0817	75.58335	48.56533	30.7764	30.73177	27.26194

Cisplatin:

Concentration (μM)	Negative	0.5	1	5	10	50	100	200
Mean (Normalized) (%)	100	91.22598	82.8889	68.21368	47.32417	29.02275	28.76993	26.22796

Cisplatin:

Concentration (μM)	Negative	0.5	1	5	10	50	100	200
Mean (Normalized) (%)	100	96.13886	82.37578	77.59951	48.10703	32.18034	30.72721	26.84709

1:

Concentration (μM)	Negative	0.25	0.5	1	2.5	5	10
Mean (Normalized) (%)	100	97.31289	95.55495	91.23378	20.41621	12.46363	11.99318

1:

Concentration (μM)	Negative	0.25	0.5	1	2.5	5	10
Mean (Normalized) (%)	100	90.37446	86.21907	82.28502	21.39279	14.50389	13.59481

1:

Concentration (μM)	Negative	0.25	0.5	1	2.5	5	10
Mean (Normalized) (%)	100	97.35642	96.98491	92.38888	20.7202	13.50271	12.99567

2:

Concentration (μM)	Negative	0.25	0.5	1	2.5	5	10
Mean (Normalized) (%)	100	94.44873	91.93797	87.51699	37.18919	12.3384	12.30784

2:

Concentration (μM)	Negative	0.25	0.5	1	2.5	5	10
Mean (Normalized) (%)	100	92.42473	92.08641	85.44259	35.28852	12.46289	12.40829

2:

Concentration (μM)	Negative	0.25	0.5	1	2.5	5	10
Mean (Normalized) (%)	100	90.98416	89.86011	83.86447	34.28025	13.09684	12.67501

3:

Concentration (μM)	Negative	0.25	0.5	1	2.5	5	10
Mean (Normalized) (%)	100	98.28797	78.83183	37.05249	5.459748	5.064379	5.194013

3:

Concentration (μM)	Negative	0.25	0.5	1	2.5	5	10
Mean (Normalized) (%)	100	99.60475	77.38576	32.40458	6.054869	5.884915	6.074938

3:

Concentration (μM)	Negative	0.25	0.5	1	2.5	5	10
Mean (Normalized) (%)	100	93.4445	81.27073	34.56344	6.025351	5.907264	6.056953

4:

Concentration (μM)	Negative	0.25	0.5	1	2.5	5	10
Mean (Normalized) (%)	100	95.60365	95.81863	81.94021	52.37515	23.14789	7.178998

4:

Concentration (μM)	Negative	0.25	0.5	1	2.5	5	10
Mean (Normalized) (%)	100	96.95944	92.07313	74.23166	51.27134	20.94706	9.454846

4:

Concentration (μM)	Negative	0.25	0.5	1	2.5	5	10
Mean (Normalized) (%)	100	85.78616	84.39235	68.48527	50.7659	20.50854	6.917803

3.1.7 **HeLa 24 h exposure**

Cisplatin:

Concentration (µM)	Negative	0.5	1	5	10	50	100	200
Mean (Normalized) (%)	100	93.8426	82.89067	56.37877	32.30621	14.61619	12.92734	10.38945

Cisplatin:

Concentration (µM)	Negative	0.5	1	5	10	50	100	200
Mean (Normalized) (%)	100	93.28692	87.99112	69.74231	55.88778	21.66432	17.20322	14.66121

Cisplatin:

Concentration (µM)	Negative	0.5	1	5	10	50	100	200
Mean (Normalized) (%)	100	86.56804	81.88749	53.042	37.88466	13.8642	11.63805	9.657503

1:

Concentration (µM)	Negative	0.25	0.5	1	2.5	5	10
Mean (Normalized) (%)	100	100.0992	97.17668	92.16029	44.37012	13.93345	8.921111

1:

Concentration (µM)	Negative	0.25	0.5	1	2.5	5	10
Mean (Normalized) (%)	100	92.93808	90.26704	86.36142	40.31755	7.66424	6.184759

1:

Concentration (µM)	Negative	0.25	0.5	1	2.5	5	10
Mean (Normalized) (%)	100	96.91012	96.85775	95.43129	51.38179	11.53606	7.896907

2:

Concentration (µM)	Negative	0.25	0.5	1	2.5	5	10
Mean (Normalized) (%)	100	100.9541	98.02223	94.75863	45.67312	8.773055	8.644912

2:

Concentration (μM)	Negative	0.25	0.5	1	2.5	5	10
Mean (Normalized) (%)	100	92.66523	89.34643	87.31822	28.80301	6.108731	6.371246

2:

Concentration (μM)	Negative	0.25	0.5	1	2.5	5	10
Mean (Normalized) (%)	100	98.44376	98.41879	96.39179	58.52306	7.079081	6.629754

3:

Concentration (μM)	Negative	0.25	0.5	1	2.5	5	10
Mean (Normalized) (%)	100	95.99052	91.90524	76.19763	8.854877	8.318109	8.369734

3:

Concentration (μM)	Negative	0.25	0.5	1	2.5	5	10
Mean (Normalized) (%)	100	96.10922	90.36041	62.71801	7.324774	5.807573	5.987861

3:

Concentration (μM)	Negative	0.25	0.5	1	2.5	5	10
Mean (Normalized) (%)	100	97.43343	95.21573	72.81516	9.168402	7.00188	6.247791

4:

Concentration (μM)	Negative	0.25	0.5	1	2.5	5	10
Mean (Normalized) (%)	100	93.29714	87.39399	86.08605	82.07308	57.32977	9.414637

4:

Concentration (μM)	Negative	0.25	0.5	1	2.5	5	10
Mean (Normalized) (%)	100	96.45812	93.99861	91.53124	89.48174	74.96046	8.523633

4:

Concentration (µM)	Negative	0.25	0.5	1	2.5	5	10
Mean (Normalized) (%)	100	94.99154	81.46438	71.01594	77.22821	57.29152	10.60494

3.1.8 **HeLa 48 h exposure**

Cisplatin:

Concentration (µM)	Negative	0.5	1	5	10	50	100	200
Mean (Normalized) (%)	100	88.18665	72.84548	32.69294	13.72991	8.682486	8.476628	7.564164

Cisplatin:

Concentration (µM)	Negative	0.5	1	5	10	50	100	200
Mean (Normalized) (%)	100	80.71459	65.33866	32.87673	15.6022	7.705407	7.454121	6.792665

Cisplatin:

Concentration (µM)	Negative	0.5	1	5	10	50	100	200
Mean (Normalized) (%)	100	64.12087	54.64239	17.19445	10.73244	7.249577	6.922494	6.446763

1:

Concentration (µM)	Negative	0.25	0.5	1	2.5	5	10
Mean (Normalized) (%)	100	96.0891	86.41333	67.16693	11.24871	6.915954	6.899395

1:

Concentration (µM)	Negative	0.25	0.5	1	2.5	5	10
Mean (Normalized) (%)	100	92.18144	86.00664	82.84032	8.951934	5.710367	5.910533

1:

Concentration (µM)	Negative	0.25	0.5	1	2.5	5	10
Mean (Normalized) (%)	100	85.49835	80.39503	77.63067	12.94536	6.356769	6.350479

2:

Concentration (μM)	Negative	0.25	0.5	1	2.5	5	10
Mean (Normalized) (%)	100	98.65784	91.17604	77.04691	9.522702	6.530132	6.658732

2:

Concentration (μM)	Negative	0.25	0.5	1	2.5	5	10
Mean (Normalized) (%)	100	99.97629	99.68064	94.68064	8.151527	5.730078	5.789814

2:

Concentration (μM)	Negative	0.25	0.5	1	2.5	5	10
Mean (Normalized) (%)	100	94.94625	89.47348	83.14134	12.28046	6.992408	7.004282

3:

Concentration (μM)	Negative	0.25	0.5	1	2.5	5	10
Mean (Normalized) (%)	100	91.73124	76.72072	29.4089	6.276505	6.107685	6.229911

3:

Concentration (μM)	Negative	0.25	0.5	1	2.5	5	10
Mean (Normalized) (%)	100	97.31975	89.58344	8.065179	5.585266	5.471552	5.572273

3:

Concentration (μM)	Negative	0.25	0.5	1	2.5	5	10
Mean (Normalized) (%)	100	93.32019	90.15593	12.85724	7.468402	7.211128	7.307014

4:

Concentration (μM)	Negative	0.25	0.5	1	2.5	5	10
Mean (Normalized) (%)	100	102.209	97.14043	87.35867	66.44215	14.02664	6.334434

4:

Concentration (µM)	Negative	0.25	0.5	1	2.5	5	10
Mean (Normalized) (%)	100	95.90405	91.18835	90.79708	82.75496	17.49385	5.936537

4:

Concentration (µM)	Negative	0.25	0.5	1	2.5	5	10
Mean (Normalized) (%)	100	93.32276	71.41645	65.8557	56.5206	8.22556	6.627475

3.1.9 **HT-29 24 h exposure**

Cisplatin:

Concentration (µM)	Negative	0.5	1	5	10	50	100	200
Mean (Normalized) (%)	100	89.28681	89.83001	84.6868	86.18984	94.71167	91.61178	99.80575

Cisplatin:

Concentration (µM)	Negative	0.5	1	5	10	50	100	200
Mean (Normalized) (%)	100	90.93857	93.27319	95.95355	94.94789	100.7654	97.6495	94.49022

Cisplatin:

Concentration (µM)	Negative	0.5	1	5	10	50	100	200
Mean (Normalized) (%)	100	87.51452	88.88353	91.83185	86.68712	92.57277	90.97118	79.82445

1:

Concentration (µM)	Negative	0.25	0.5	1	2.5	5	10
Mean (Normalized) (%)	100	79.64604	82.03226	81.01017	80.72521	29.80194	25.06974

1:

Concentration (µM)	Negative	0.25	0.5	1	2.5	5	10
Mean (Normalized) (%)	100	92.29689	91.53018	87.49536	78.5834	35.47965	27.90695

1:

Concentration (μM)	Negative	0.25	0.5	1	2.5	5	10
Mean (Normalized) (%)	100	91.65199	87.06099	84.14951	53.71887	23.18119	12.4504

2:

Concentration (μM)	Negative	0.25	0.5	1	2.5	5	10
Mean (Normalized) (%)	100	99.06247	98.50713	95.6251	95.83483	35.21188	31.92175

2:

Concentration (μM)	Negative	0.25	0.5	1	2.5	5	10
Mean (Normalized) (%)	100	87.72481	89.27902	85.5072	68.84698	31.25515	28.42141

2:

Concentration (μM)	Negative	0.25	0.5	1	2.5	5	10
Mean (Normalized) (%)	100	98.25272	95.12991	89.79293	66.63609	15.60067	11.27575

3:

Concentration (μM)	Negative	0.25	0.5	1	2.5	5	10
Mean (Normalized) (%)	100	94.85664	91.18655	88.928	39.47061	37.17098	38.00671

3:

Concentration (μM)	Negative	0.25	0.5	1	2.5	5	10
Mean (Normalized) (%)	100	90.39094	89.06334	68.49534	32.31922	29.75504	30.7262

3:

Concentration (μM)	Negative	0.25	0.5	1	2.5	5	10
Mean (Normalized) (%)	100	96.49273	88.68684	56.1353	20.84964	10.23814	10.747

4:

Concentration (µM)	Negative	0.25	0.5	1	2.5	5	10
Mean (Normalized) (%)	100	94.70965	95.65224	96.09806	92.44616	53.2142	35.67207

4:

Concentration (µM)	Negative	0.25	0.5	1	2.5	5	10
Mean (Normalized) (%)	100	103.8363	107.5251	98.05099	101.5301	75.16795	37.68956

4:

Concentration (µM)	Negative	0.25	0.5	1	2.5	5	10
Mean (Normalized) (%)	100	89.5575	82.17032	80.64837	74.00164	61.26983	23.44599

3.1.10 **HT-29 48 h exposure**

Cisplatin:

Concentration (µM)	Negative	0.5	1	5	10	50	100	200
Mean (Normalized) (%)	100	83.92471	87.57517	79.36249	80.28891	94.11616	88.72132	70.57786

Cisplatin:

Concentration (µM)	Negative	0.5	1	5	10	50	100	200
Mean (Normalized) (%)	100	102.0815	88.48884	85.72174	89.37538	90.38257	80.40664	71.33552

Cisplatin:

Concentration (µM)	Negative	0.5	1	5	10	50	100	200
Mean (Normalized) (%)	100	88.447	83.2912	88.66759	86.63325	94.82659	90.8559	85.09975

1:

Concentration (µM)	Negative	0.25	0.5	1	2.5	5	10
Mean (Normalized) (%)	100	98.42289	98.38232	84.71292	33.24125	14.62347	14.70472

1:

Concentration (μM)	Negative	0.25	0.5	1	2.5	5	10
Mean (Normalized) (%)	100	90.43529	87.8405	79.49102	18.51762	8.070776	8.447783

1:

Concentration (μM)	Negative	0.25	0.5	1	2.5	5	10
Mean (Normalized) (%)	100	91.74481	87.95369	82.99506	20.17361	6.124201	4.776367

2:

Concentration (μM)	Negative	0.25	0.5	1	2.5	5	10
Mean (Normalized) (%)	100	94.36907	88.73512	89.14942	42.78091	9.403565	9.520086

2:

Concentration (μM)	Negative	0.25	0.5	1	2.5	5	10
Mean (Normalized) (%)	100	88.6509	85.77782	75.92037	20.2426	7.906325	8.223675

2:

Concentration (μM)	Negative	0.25	0.5	1	2.5	5	10
Mean (Normalized) (%)	100	90.83448	86.3538	84.12051	34.61698	6.165813	5.816937

3:

Concentration (μM)	Negative	0.25	0.5	1	2.5	5	10
Mean (Normalized) (%)	100	95.26412	89.05792	35.96643	13.09963	12.69253	13.33814

3:

Concentration (μM)	Negative	0.25	0.5	1	2.5	5	10
Mean (Normalized) (%)	100	99.78784	80.22057	32.78229	21.22446	11.43533	9.580867

3:

Concentration (µM)	Negative	0.25	0.5	1	2.5	5	10
Mean (Normalized) (%)	100	88.2203	84.05777	32.07815	5.47552	4.978397	5.473467

4:

Concentration (µM)	Negative	0.25	0.5	1	2.5	5	10
Mean (Normalized) (%)	100	94.84544	94.71235	84.1411	44.03714	21.12515	18.56558

4:

Concentration (µM)	Negative	0.25	0.5	1	2.5	5	10
Mean (Normalized) (%)	100	90.45487	82.20921	72.34153	55.12946	16.98797	10.25924

4:

Concentration (µM)	Negative	0.25	0.5	1	2.5	5	10
Mean (Normalized) (%)	100	96.03157	85.36413	78.55079	56.22409	21.87502	6.311856

3.1.11 **MCF-7 24 h exposure**

Cisplatin:

Concentration (µM)	Negative	0.5	1	5	10	50	100	200
Mean (Normalized) (%)	100	89.58957	90.46593	91.6505	90.73077	89.37792	84.49905	75.38803

Cisplatin:

Concentration (µM)	Negative	0.5	1	5	10	50	100	200
Mean (Normalized) (%)	100	88.56388	85.54209	86.04712	88.70854	87.11608	81.13191	75.15272

Cisplatin:

Concentration (µM)	Negative	0.5	1	5	10	50	100	200
Mean (Normalized) (%)	100	96.7208	95.06523	90.05926	94.61173	86.74914	71.38405	73.30466

1:

Concentration (μM)	Negative	0.25	0.5	1	2.5	5	10
Mean (Normalized) (%)	100	96.45689	92.92163	77.25166	45.61462	27.6379	23.64984

1:

Concentration (μM)	Negative	0.25	0.5	1	2.5	5	10
Mean (Normalized) (%)	100	99.63284	96.04806	81.09726	51.66538	26.3357	21.80111

1:

Concentration (μM)	Negative	0.25	0.5	1	2.5	5	10
Mean (Normalized) (%)	100	97.43649	96.92764	78.15243	50.28274	37.02686	25.42677

2:

Concentration (μM)	Negative	0.25	0.5	1	2.5	5	10
Mean (Normalized) (%)	100	100.7968	98.40866	88.22379	62.64324	25.02131	21.20461

2:

Concentration (μM)	Negative	0.25	0.5	1	2.5	5	10
Mean (Normalized) (%)	100	96.86897	87.4923	76.77568	44.60707	22.60156	22.15854

2:

Concentration (μM)	Negative	0.25	0.5	1	2.5	5	10
Mean (Normalized) (%)	100	95.09331	93.09606	79.93903	44.69655	25.28078	21.29795

3:

Concentration (μM)	Negative	0.25	0.5	1	2.5	5	10
Mean (Normalized) (%)	100	97.36947	87.48614	62.77843	31.14445	24.00153	24.53338

3:

Concentration (µM)	Negative	0.25	0.5	1	2.5	5	10
Mean (Normalized) (%)	100	81.53685	65.4534	45.90027	35.55886	16.32778	15.52787

3:

Concentration (µM)	Negative	0.25	0.5	1	2.5	5	10
Mean (Normalized) (%)	100	96.52137	89.4048	54.65021	23.5699	11.8581	12.26177

4:

Concentration (µM)	Negative	0.25	0.5	1	2.5	5	10
Mean (Normalized) (%)	100	96.85758	88.83457	78.01594	59.68105	36.55267	27.38062

4:

Concentration (µM)	Negative	0.25	0.5	1	2.5	5	10
Mean (Normalized) (%)	100	97.59807	96.05061	86.09357	63.26763	34.58072	26.12075

4:

Concentration (µM)	Negative	0.25	0.5	1	2.5	5	10
Mean (Normalized) (%)	100	97.33768	97.47567	90.70269	62.01643	37.59161	25.61939

3.1.12 **MCF-7 48 h exposure**

Cisplatin:

Concentration (µM)	Negative	0.5	1	5	10	50	100	200
Mean (Normalized) (%)	100	89.47049	85.84271	83.70825	80.41215	81.252	72.47033	65.60606

Cisplatin:

Concentration (µM)	Negative	0.5	1	5	10	50	100	200
Mean (Normalized) (%)	100	94.65653	93.9916	94.59401	89.98152	88.3358	84.32331	63.61681

Cisplatin:

Concentration (μM)	Negative	0.5	1	5	10	50	100	200
Mean (Normalized) (%)	100	97.31331	98.12768	99.62618	100.2509	93.85828	84.86598	66.70621

1:

Concentration (μM)	Negative	0.25	0.5	1	2.5	5	10
Mean (Normalized) (%)	100	94.01463	84.97095	62.72285	25.04415	12.28324	12.64557

1:

Concentration (μM)	Negative	0.25	0.5	1	2.5	5	10
Mean (Normalized) (%)	100	81.92201	68.44926	48.45887	14.25381	8.389825	8.275862

1:

Concentration (μM)	Negative	0.25	0.5	1	2.5	5	10
Mean (Normalized) (%)	100	96.83907	93.85102	64.20099	23.57751	13.39366	13.2866

2:

Concentration (μM)	Negative	0.25	0.5	1	2.5	5	10
Mean (Normalized) (%)	100	92.07604	86.41203	70.23458	40.05151	15.53315	15.8196

2:

Concentration (μM)	Negative	0.25	0.5	1	2.5	5	10
Mean (Normalized) (%)	100	98.23504	86.18557	65.42548	17.17626	9.051641	9.205625

2:

Concentration (μM)	Negative	0.25	0.5	1	2.5	5	10
Mean (Normalized) (%)	100	94.69195	90.60458	68.15737	25.18179	12.84035	12.66854

3:

Concentration (µM)	Negative	0.25	0.5	1	2.5	5	10
Mean (Normalized) (%)	100	94.89119	76.15285	35.5295	19.6627	19.08728	18.9402

3:

Concentration (µM)	Negative	0.25	0.5	1	2.5	5	10
Mean (Normalized) (%)	100	74.53503	55.92762	24.48477	10.80037	10.21332	10.63211

3:

Concentration (µM)	Negative	0.25	0.5	1	2.5	5	10
Mean (Normalized) (%)	100	91.19874	74.22266	26.91121	11.98839	11.29552	11.72016

4:

Concentration (µM)	Negative	0.25	0.5	1	2.5	5	10
Mean (Normalized) (%)	100	83.80044	77.5155	64.32329	35.1347	17.36439	16.64617

4:

Concentration (µM)	Negative	0.25	0.5	1	2.5	5	10
Mean (Normalized) (%)	100	84.22339	73.21164	52.67045	23.87646	12.91476	10.86407

4:

Concentration (µM)	Negative	0.25	0.5	1	2.5	5	10
Mean (Normalized) (%)	100	88.77194	78.41505	50.60406	23.34288	12.56878	12.50928

3.1.13 **A2780 24 h exposure**

Cisplatin

Concentration (µM)	Negative	3.125	6.25	12.5	25	50	100	200
Mean (Normalized) (%)	100	86.0136	84.28985	81.96583	76.80628	73.5489	63.57957	52.0032

Cisplatin:

Concentration (µM)	Negative	3.125	6.25	12.5	25	50	100	200
Mean (Normalized) (%)	100	84.70421	83.72907	81.92764	78.39385	74.77359	68.03609	57.98637

Cisplatin:

Concentration (µM)	Negative	3.125	6.25	12.5	25	50	100	200
Mean (Normalized) (%)	100	93.51511	92.46109	89.25803	79.76107	69.66864	61.18069	44.63108

Doxorubicin

Concentration (µM)	Negative	0.312	0.625	1.25	2.5	5	10	20
Mean (Normalized) (%)	100	78.07563	71.60782	65.53741	49.62532	41.91255	37.0627	31.01838

Doxorubicin

Concentration (µM)	Negative	0.312	0.625	1.25	2.5	5	10	20
Mean (Normalized) (%)	100	73.42166	69.28459	68.32046	53.21431	46.12058	45.06187	37.8352

Doxorubicin

Concentration (µM)	Negative	0.312	0.625	1.25	2.5	5	10	20
Mean (Normalized) (%)	100	73.67354	69.44108	67.80434	52.48246	45.06255	42.21385	35.35306

Cu-Phen (**1**)

Concentration (µM)	negative	0.156	0.312	0.625	1.25	2.5	5	10
Mean (Normalized) (%)	100	89.8571	80.56236	51.96169	26.25193	29.99624	22.09984	12.16952

Cu-Phen (**1**)

Concentration (µM)	negative	0.156	0.312	0.625	1.25	2.5	5	10
Mean (Normalized) (%)	100	90.43287	87.84067	57.63039	25.7298	29.42586	20.76481	10.91753

Cu-Phen (**1**)

Concentration (μM)	negative	0.156	0.312	0.625	1.25	2.5	5	10
Mean (Normalized) (%)	100	90.46866	75.94975	42.2625	18.07865	26.25287	19.36644	11.21463

Cu-DPQ-Phen (**2**)

Concentration (μM)	negative	0.156	0.312	0.625	1.25	2.5	5	10
Mean (Normalized) (%)	100	88.96052	78.8581	55.18052	32.37589	25.40919	12.17749	8.356541

Cu-DPQ-Phen (**2**)

Concentration (μM)	negative	0.156	0.312	0.625	1.25	2.5	5	10
Mean (Normalized) (%)	100	93.16556	81.01865	56.98839	29.86552	24.48301	11.40657	8.024622

Cu-DPQ-Phen (**2**)

Concentration (μM)	negative	0.156	0.312	0.625	1.25	2.5	5	10
Mean (Normalized) (%)	100	90.91186	86.28479	66.22094	47.26337	44.64396	44.86395	43.07975

Cu-DPPZ-Phen (**3**)

Concentration (μM)	negative	0.156	0.312	0.625	1.25	2.5	5	10
Mean (Normalized) (%)	100	91.74461	78.35336	34.89576	17.89117	13.25982	12.90997	12.72405

Cu-DPPZ-Phen (**3**)

Concentration (μM)	negative	0.156	0.312	0.625	1.25	2.5	5	10
Mean (Normalized) (%)	100	84.56129	69.91539	29.68706	17.0547	11.74842	11.59394	11.54404

Cu-DPPZ-Phen (**3**)

Concentration (μM)	negative	0.156	0.312	0.625	1.25	2.5	5	10
Mean (Normalized) (%)	100	87.74823	64.79867	29.62454	16.18112	11.80608	11.9697	11.91605

Cu-DPPN-Phen (**4**)

Concentration (µM)	negative	0.156	0.312	0.625	1.25	2.5	5	10
Mean (Normalized) (%)	100	122.1309	88.19275	69.91857	46.71827	44.21084	41.16831	40.11735

Cu-DPPN-Phen (**4**)

Concentration (µM)	negative	0.156	0.312	0.625	1.25	2.5	5	10
Mean (Normalized) (%)	100	119.3118	80.94195	63.02589	48.22756	46.40628	44.2687	41.44615

Cu-DPPN-Phen (**4**)

Concentration (µM)	negative	0.156	0.312	0.625	1.25	2.5	5	10
Mean (Normalized) (%)	100	123.9198	83.35665	63.4717	45.88444	43.42787	40.50047	37.91486

3.1.14 **A2780 48 h exposure**

Cisplatin

Concentration (µM)	Negative	3.125	6.25	12.5	25	50	100	200
Mean (Normalized) (%)	100	68.69937	59.1543	51.51677	39.70137	34.41973	33.40726	29.99638

Cisplatin:

Concentration (µM)	Negative	3.125	6.25	12.5	25	50	100	200
Mean (Normalized) (%)	100	77.1265	66.37324	60.18469	48.6095	40.9341	39.46909	35.98827

Cisplatin:

Concentration (µM)	Negative	3.125	6.25	12.5	25	50	100	200
Mean (Normalized) (%)	100	67.17897	55.75265	50.73205	36.62424	31.92125	30.2406	26.79419

Doxorubicin

Concentration (µM)	Negative	0.312	0.625	1.25	2.5	5	10	20
Mean (Normalized) (%)	100	30.39566	23.98099	9.976851	11.99326	12.25435	11.75837	10.45477

Doxorubicin

Concentration (µM)	Negative	0.312	0.625	1.25	2.5	5	10	20
Mean (Normalized) (%)	100	29.44782	25.70118	10.20702	12.42645	12.26666	12.08716	10.67504

Doxorubicin

Concentration (µM)	Negative	0.312	0.625	1.25	2.5	5	10	20
Mean (Normalized) (%)	100	31.43463	23.51924	10.90803	13.4452	12.57145	12.24259	11.52067

Cu-Phen (**1**)

Concentration (µM)	negative	0.156	0.312	0.625	1.25	2.5	5	10
Mean (Normalized) (%)	100	56.39173	21.24871	9.807663	6.529908	5.688463	5.204484	5.111699

Cu-Phen (**1**)

Concentration (µM)	negative	0.156	0.312	0.625	1.25	2.5	5	10
Mean (Normalized) (%)	100	61.42499	26.60169	9.370534	5.738302	4.900029	4.434066	4.317715

Cu-Phen (**1**)

Concentration (µM)	negative	0.156	0.312	0.625	1.25	2.5	5	10
Mean (Normalized) (%)	100	30.41239	14.59959	8.075465	6.920378	6.640573	6.209389	6.290557

Cu-DPQ-Phen (**2**)

Concentration (µM)	negative	0.156	0.312	0.625	1.25	2.5	5	10
Mean (Normalized) (%)	100	67.66213	31.9252	23.31917	22.4376	21.74468	21.99541	22.17123

Cu-DPQ-Phen (**2**)

Concentration (µM)	negative	0.156	0.312	0.625	1.25	2.5	5	10
Mean (Normalized) (%)	100	69.81788	33.17956	22.40614	21.84817	20.89013	21.25015	21.06911

Cu-DPQ-Phen (**2**)

Concentration (μM)	negative	0.156	0.312	0.625	1.25	2.5	5	10
Mean (Normalized) (%)	100	73.83998	33.68693	23.1974	22.22003	20.56333	20.93666	20.64279

Cu-DPPZ-Phen (**3**)

Concentration (μM)	negative	0.156	0.312	0.625	1.25	2.5	5	10
Mean (Normalized) (%)	100	33.40588	16.99817	9.475746	6.568533	6.109246	6.294818	6.135008

Cu-DPPZ-Phen (**3**)

Concentration (μM)	negative	0.156	0.312	0.625	1.25	2.5	5	10
Mean (Normalized) (%)	100	27.38817	14.55444	7.534133	5.790769	5.703323	5.734983	5.682239

Cu-DPPZ-Phen (**3**)

Concentration (μM)	negative	0.156	0.312	0.625	1.25	2.5	5	10
Mean (Normalized) (%)	100	28.88255	15.01421	8.154757	6.082699	5.981984	5.969394	5.929535

Cu-DPPN-Phen (**4**)

Concentration (μM)	negative	0.156	0.312	0.625	1.25	2.5	5	10
Mean (Normalized) (%)	100	72.10352	49.34685	41.13761	35.11289	34.29365	33.22471	31.84663

Cu-DPPN-Phen (**4**)

Concentration (μM)	negative	0.156	0.312	0.625	1.25	2.5	5	10
Mean (Normalized) (%)	100	64.40225	45.58899	40.48785	35.13951	34.75161	34.06629	32.44158

Cu-DPPN-Phen (**4**)

Concentration (μM)	negative	0.156	0.312	0.625	1.25	2.5	5	10
Mean (Normalized) (%)	100	57.00043	38.42484	32.01786	25.6252	24.77957	24.88013	23.74944

3.1.15 **A2780/ Cis 24 h exposure**

Cisplatin

Concentration (µM)	Negative	3.125	6.25	12.5	25	50	100	200
Mean (Normalized) (%)	100	96.79406	95.42927	93.57896	92.3235	91.71796	86.40837	78.64246

Cisplatin:

Concentration (µM)	Negative	3.125	6.25	12.5	25	50	100	200
Mean (Normalized) (%)	100	95.79164	94.7964	91.03643	89.28413	87.51002	80.17222	73.56594

Cisplatin:

Concentration (µM)	Negative	3.125	6.25	12.5	25	50	100	200
Mean (Normalized) (%)	100	97.13019	92.76964	91.00487	89.86895	89.16163	90.27624	87.5866

Doxorubicin

Concentration (µM)	Negative	0.312	0.625	1.25	2.5	5	10	20
Mean (Normalized) (%)	100	96.08352	93.24853	88.06882	78.12409	61.16687	60.47438	61.88654

Doxorubicin

Concentration (µM)	Negative	0.312	0.625	1.25	2.5	5	10	20
Mean (Normalized) (%)	100	92.78243	89.2121	84.11847	74.01145	59.8129	57.49154	58.57357

Doxorubicin

Concentration (µM)	Negative	0.312	0.625	1.25	2.5	5	10	20
Mean (Normalized) (%)	100	94.73333	85.71354	80.15855	71.20819	50.9182	46.08549	47.14541

Cu-Phen (**1**)

Concentration (µM)	negative	0.156	0.312	0.625	1.25	2.5	5	10
Mean (Normalized) (%)	100	88.56257	86.38342	85.52876	55.76933	49.65739	52.42417	41.71884

Cu-Phen (**1**)

Concentration (μM)	negative	0.156	0.312	0.625	1.25	2.5	5	10
Mean (Normalized) (%)	100	90.19982	85.34586	86.09951	57.29428	51.50486	56.34147	42.75582

Cu-Phen (**1**)

Concentration (μM)	negative	0.156	0.312	0.625	1.25	2.5	5	10
Mean (Normalized) (%)	100	94.34402	90.78114	89.86486	68.44409	46.07153	56.64278	48.24644

Cu-DPQ-Phen (**2**)

Concentration (μM)	negative	0.156	0.312	0.625	1.25	2.5	5	10
Mean (Normalized) (%)	100	90.64853	88.21814	85.79552	60.32728	47.37261	46.87532	32.76106

Cu-DPQ-Phen (**2**)

Concentration (μM)	negative	0.156	0.312	0.625	1.25	2.5	5	10
Mean (Normalized) (%)	100	95.31071	95.36203	88.73944	57.5385	45.73549	44.89347	27.97214

Cu-DPQ-Phen (**2**)

Concentration (μM)	negative	0.156	0.312	0.625	1.25	2.5	5	10
Mean (Normalized) (%)	100	90.94537	87.10868	90.89382	51.53488	39.33676	49.01895	40.1014

Cu-DPPZ-Phen (**3**)

Concentration (μM)	negative	0.156	0.312	0.625	1.25	2.5	5	10
Mean (Normalized) (%)	100	90.19643	85.19449	66.69042	51.2784	43.178	27.84648	24.29672

Cu-DPPZ-Phen (**3**)

Concentration (μM)	negative	0.156	0.312	0.625	1.25	2.5	5	10
Mean (Normalized) (%)	100	88.80044	87.47091	68.64746	49.24638	39.46049	23.14759	20.38817

Cu-DPPZ-Phen (**3**)

Concentration (µM)	negative	0.156	0.312	0.625	1.25	2.5	5	10
Mean (Normalized) (%)	100	92.66057	89.7463	69.37967	50.10512	39.77236	22.27015	20.17048

Cu-DPPN-Phen (**4**)

Concentration (µM)	negative	0.156	0.312	0.625	1.25	2.5	5	10
Mean (Normalized) (%)	100	101.9759	101.6125	90.14355	73.79762	66.65084	55.88511	50.06256

Cu-DPPN-Phen (**4**)

Concentration (µM)	negative	0.156	0.312	0.625	1.25	2.5	5	10
Mean (Normalized) (%)	100	103.0607	103.5656	90.29798	71.69352	66.24111	56.0994	52.80249

Cu-DPPN-Phen (**4**)

Concentration (µM)	negative	0.156	0.312	0.625	1.25	2.5	5	10
Mean (Normalized) (%)	100	116.308	117.5269	106.5628	82.38795	80.59868	63.26679	59.63331

3.1.16 **A2780/ Cis 48 h exposure**

Cisplatin

Concentration (µM)	Negative	3.125	6.25	12.5	25	50	100	200
Mean (Normalized) (%)	100	106.378	104.2978	100.8838	97.16887	87.4708	67.67525	55.21944

Cisplatin:

Concentration (µM)	Negative	3.125	6.25	12.5	25	50	100	200
Mean (Normalized) (%)	100	96.85894	96.78431	89.11808	78.58975	61.73598	43.80373	36.55824

Cisplatin:

Concentration (µM)	Negative	3.125	6.25	12.5	25	50	100	200
Mean (Normalized) (%)	100	90.23113	92.75227	87.31199	82.01134	69.11017	50.58679	37.55823

Doxorubicin

Concentration (µM)	Negative	0.312	0.625	1.25	2.5	5	10	20
Mean (Normalized) (%)	100	48.3148	39.95782	23.54233	11.75002	14.96108	16.56175	16.54591

Doxorubicin

Concentration (µM)	Negative	0.312	0.625	1.25	2.5	5	10	20
Mean (Normalized) (%)	100	47.68309	39.50753	25.97486	12.69497	15.10008	16.59638	16.60912

Doxorubicin

Concentration (µM)	Negative	0.312	0.625	1.25	2.5	5	10	20
Mean (Normalized) (%)	100	50.49902	42.9278	27.33233	13.60463	15.56752	16.61158	16.67926

Cu-Phen (**1**)

Concentration (µM)	negative	0.156	0.312	0.625	1.25	2.5	5	10
Mean (Normalized) (%)	100	95.45415	91.47398	31.44901	16.05698	12.69516	9.785707	7.145044

Cu-Phen (**1**)

Concentration (µM)	negative	0.156	0.312	0.625	1.25	2.5	5	10
Mean (Normalized) (%)	100	96.44916	93.41096	39.67404	14.21901	12.07862	8.891609	5.894316

Cu-Phen (**1**)

Concentration (µM)	negative	0.156	0.312	0.625	1.25	2.5	5	10
Mean (Normalized) (%)	100	93.05105	91.70988	45.21435	15.26252	12.39828	11.80875	9.584598

Cu-DPQ-Phen (**2**)

Concentration (µM)	negative	0.156	0.312	0.625	1.25	2.5	5	10
Mean (Normalized) (%)	100	97.34	90.59566	36.80488	13.96364	12.54757	10.69703	7.837751

Cu-DPQ-Phen (**2**)

Concentration (µM)	negative	0.156	0.312	0.625	1.25	2.5	5	10
Mean (Normalized) (%)	100	95.48244	91.6412	33.60882	14.49112	12.76355	10.6971	7.260566

Cu-DPQ-Phen (**2**)

Concentration (µM)	negative	0.156	0.312	0.625	1.25	2.5	5	10
Mean (Normalized) (%)	100	94.34085	93.60421	34.38856	14.47789	12.3534	10.47433	7.560114

Cu-DPPZ-Phen (**3**)

Concentration (µM)	negative	0.156	0.312	0.625	1.25	2.5	5	10
Mean (Normalized) (%)	100	94.95579	91.82204	23.2029	10.95948	10.12968	10.27628	10.28932

Cu-DPPZ-Phen (**3**)

Concentration (µM)	negative	0.156	0.312	0.625	1.25	2.5	5	10
Mean (Normalized) (%)	100	91.18941	89.96624	26.59223	12.73604	10.85382	11.00052	10.49494

Cu-DPPZ-Phen (**3**)

Concentration (µM)	negative	0.156	0.312	0.625	1.25	2.5	5	10
Mean (Normalized) (%)	100	93.46595	86.457	26.0408	12.45995	10.76561	10.89159	10.56313

Cu-DPPN-Phen (**4**)

Concentration (µM)	negative	0.156	0.312	0.625	1.25	2.5	5	10
Mean (Normalized) (%)	100	123.1062	100.4649	54.10155	41.72951	37.23335	35.85628	33.77236

Cu-DPPN-Phen (**4**)

Concentration (µM)	negative	0.156	0.312	0.625	1.25	2.5	5	10
Mean (Normalized) (%)	100	123.7448	104.514	57.77794	39.46855	35.6267	34.12154	31.94567

Cu-DPPN-Phen (**4**)

Concentration (μM)	negative	0.156	0.312	0.625	1.25	2.5	5	10
Mean (Normalized) (%)	100	126.3607	106.3315	61.55356	39.83999	35.27868	34.16648	32.38828

3.1.17 Dose-inhibition graphs

HT-29 24 h exposures to complexes **1-4**

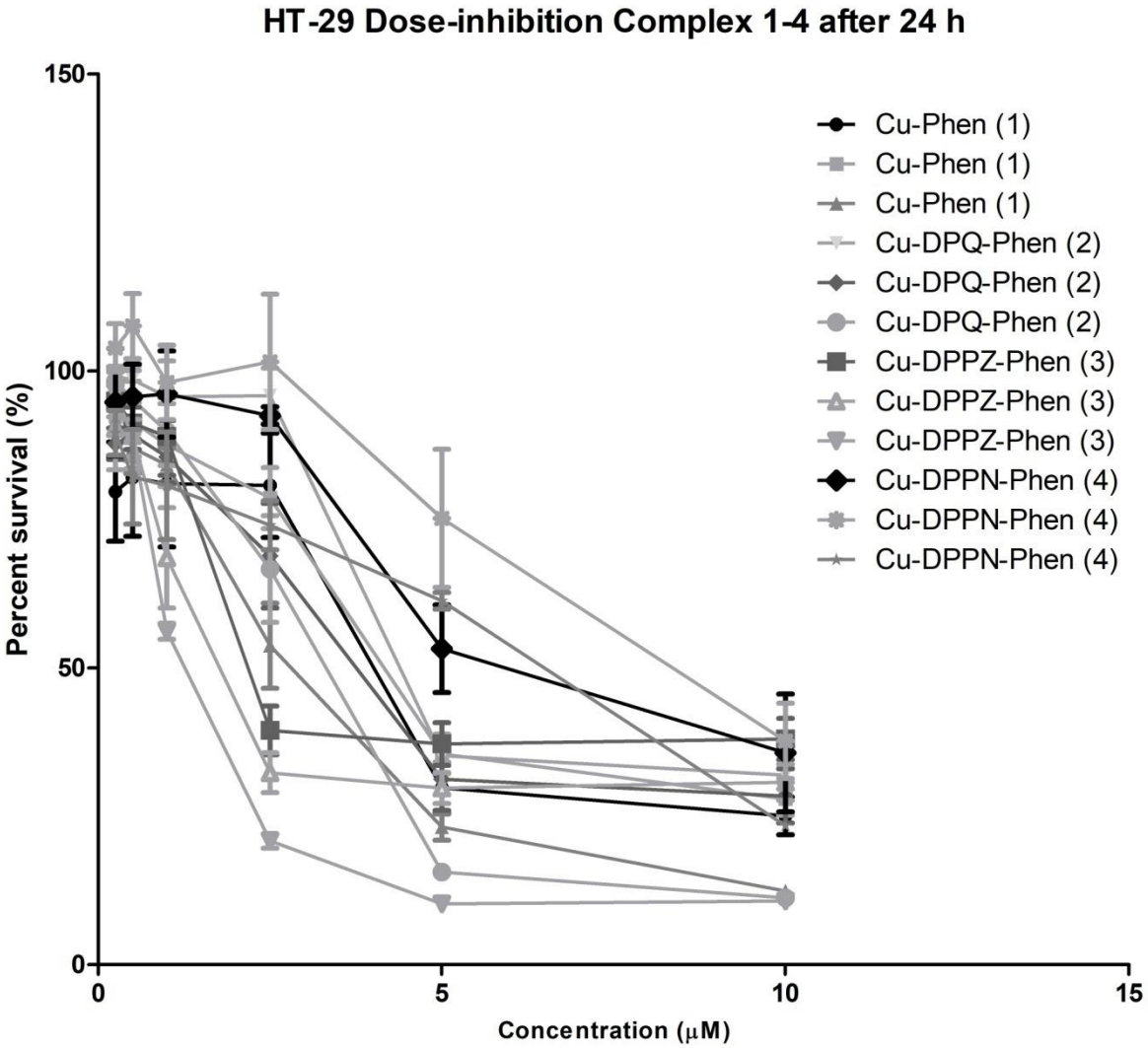

HT-29 48 h exposures to complex **1-4**

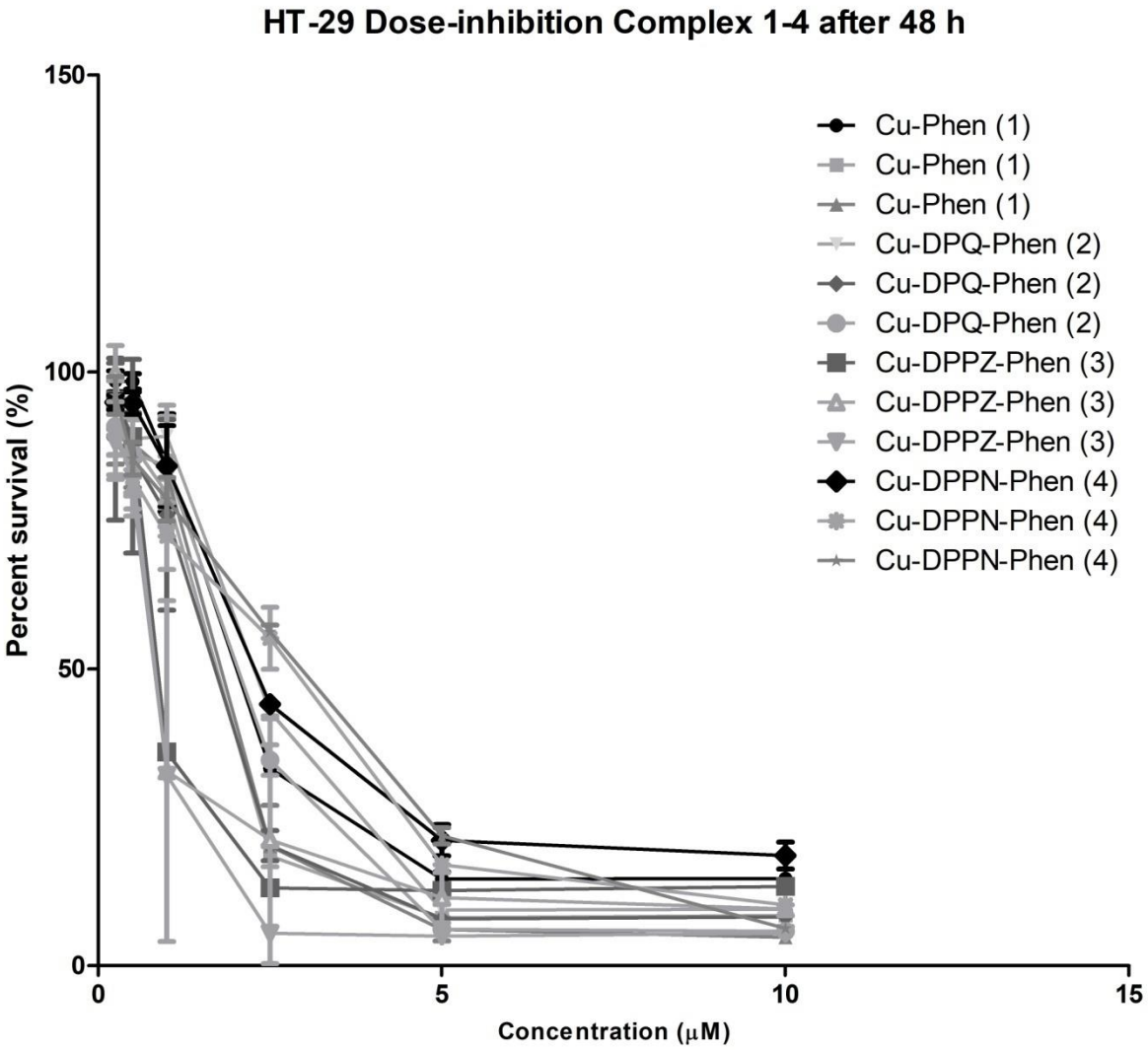

HT-29 24 and 48 h exposure to cisplatin

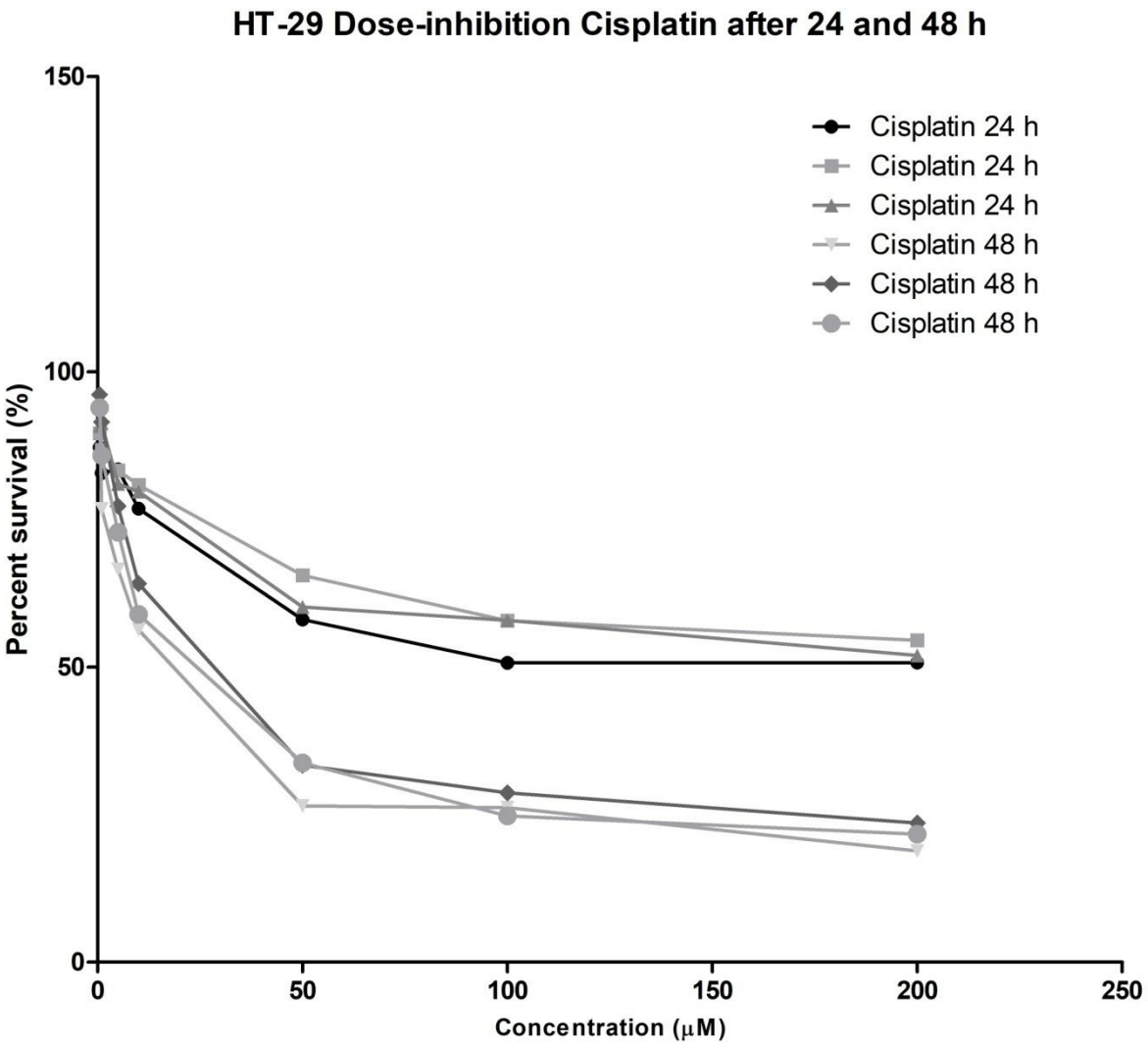

MCF-7 24 h exposure to complex **1-4**

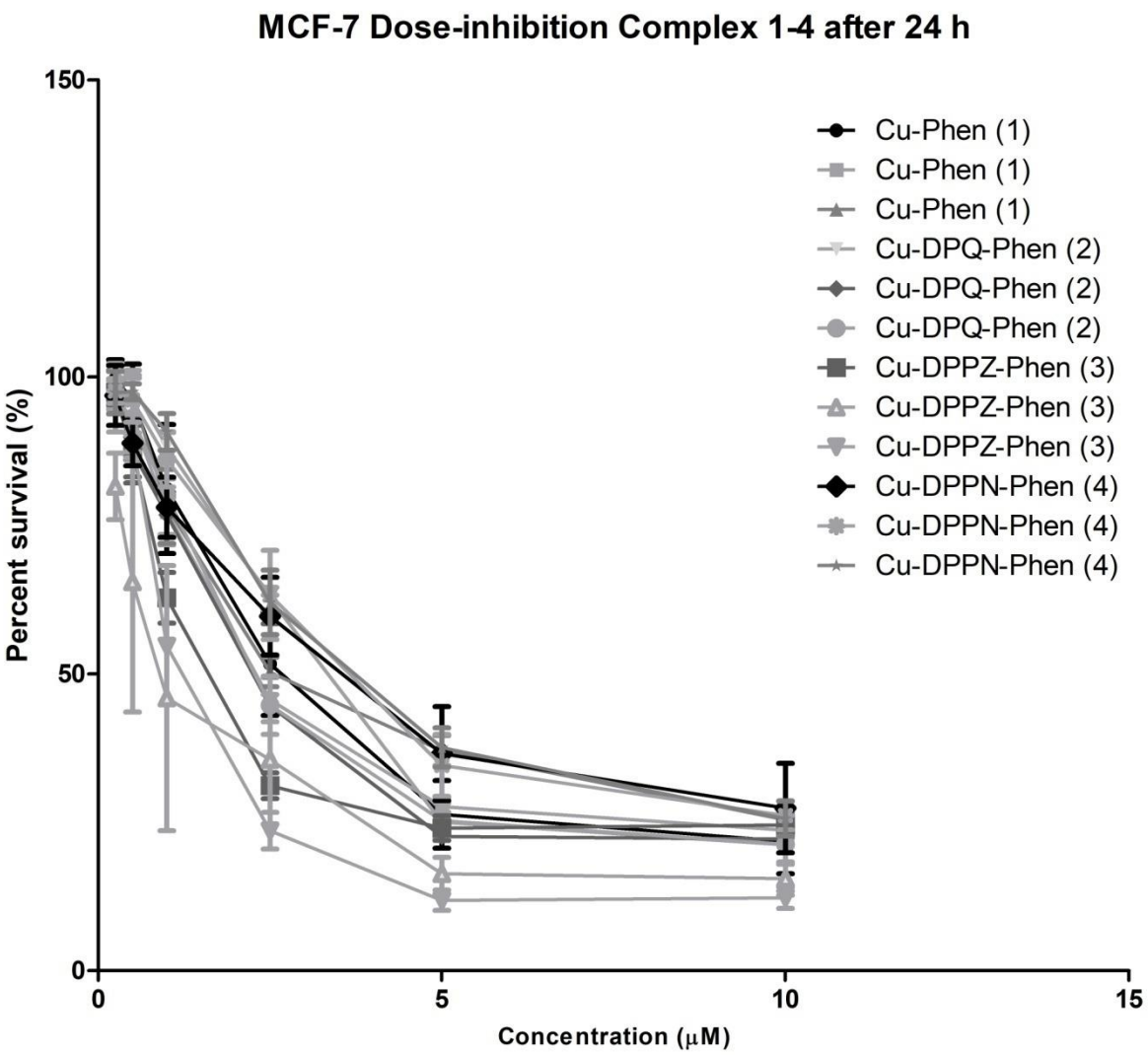

MCF-7 48 h exposure to complex **1-4**

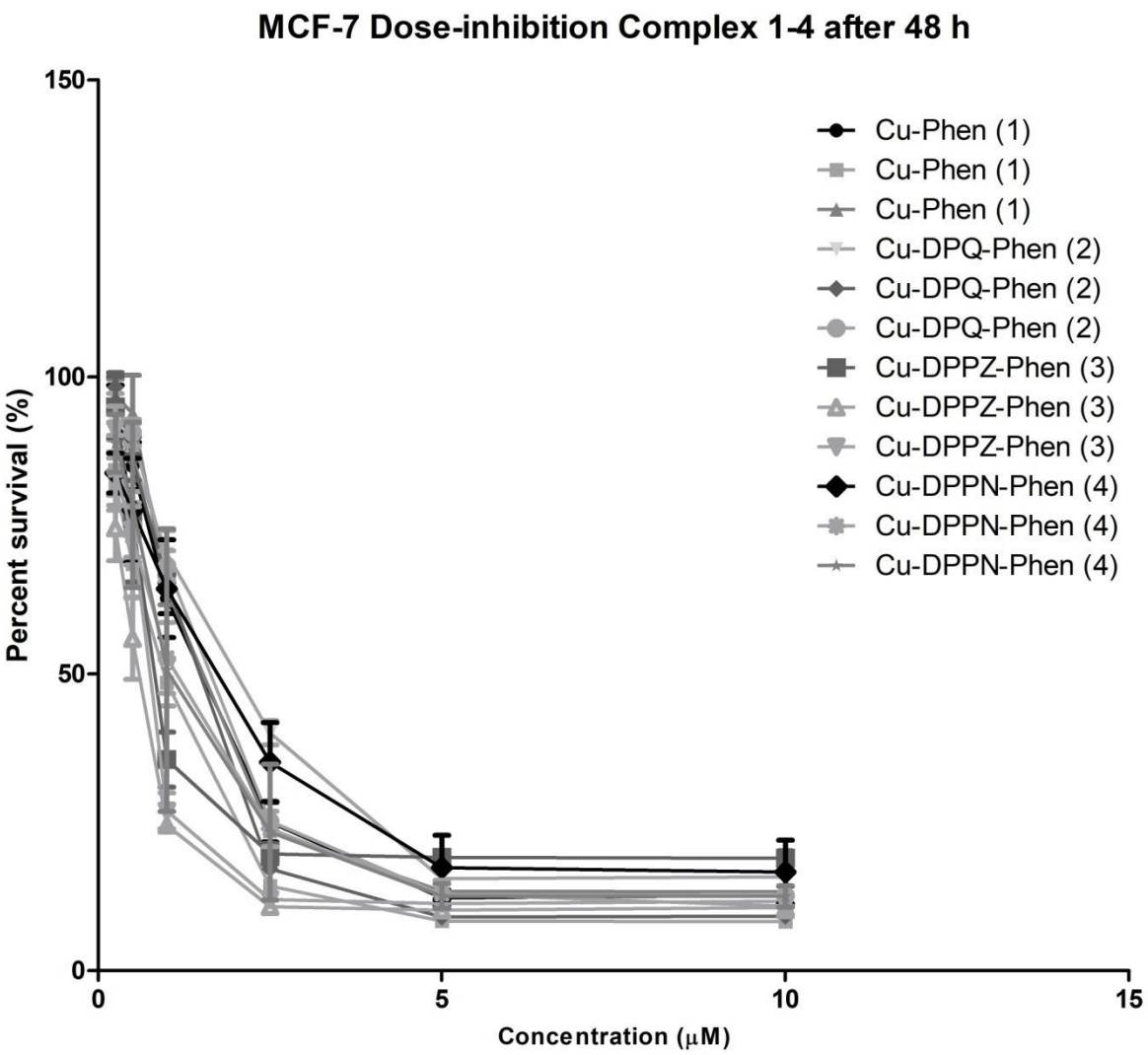

MCF-7 24 and 48 h exposure to cisplatin

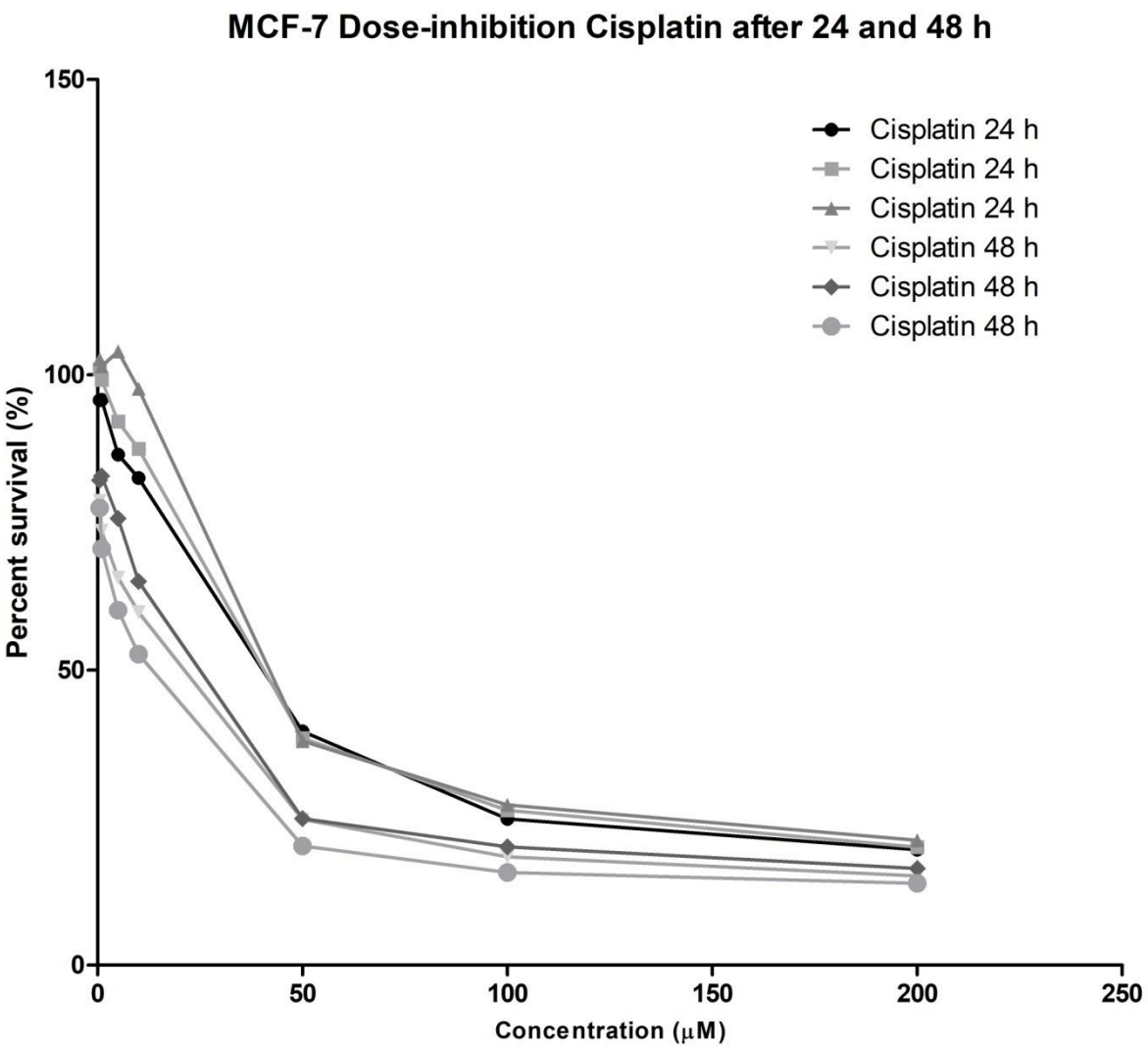

PC-3 24 h exposure to complexes **1-4**

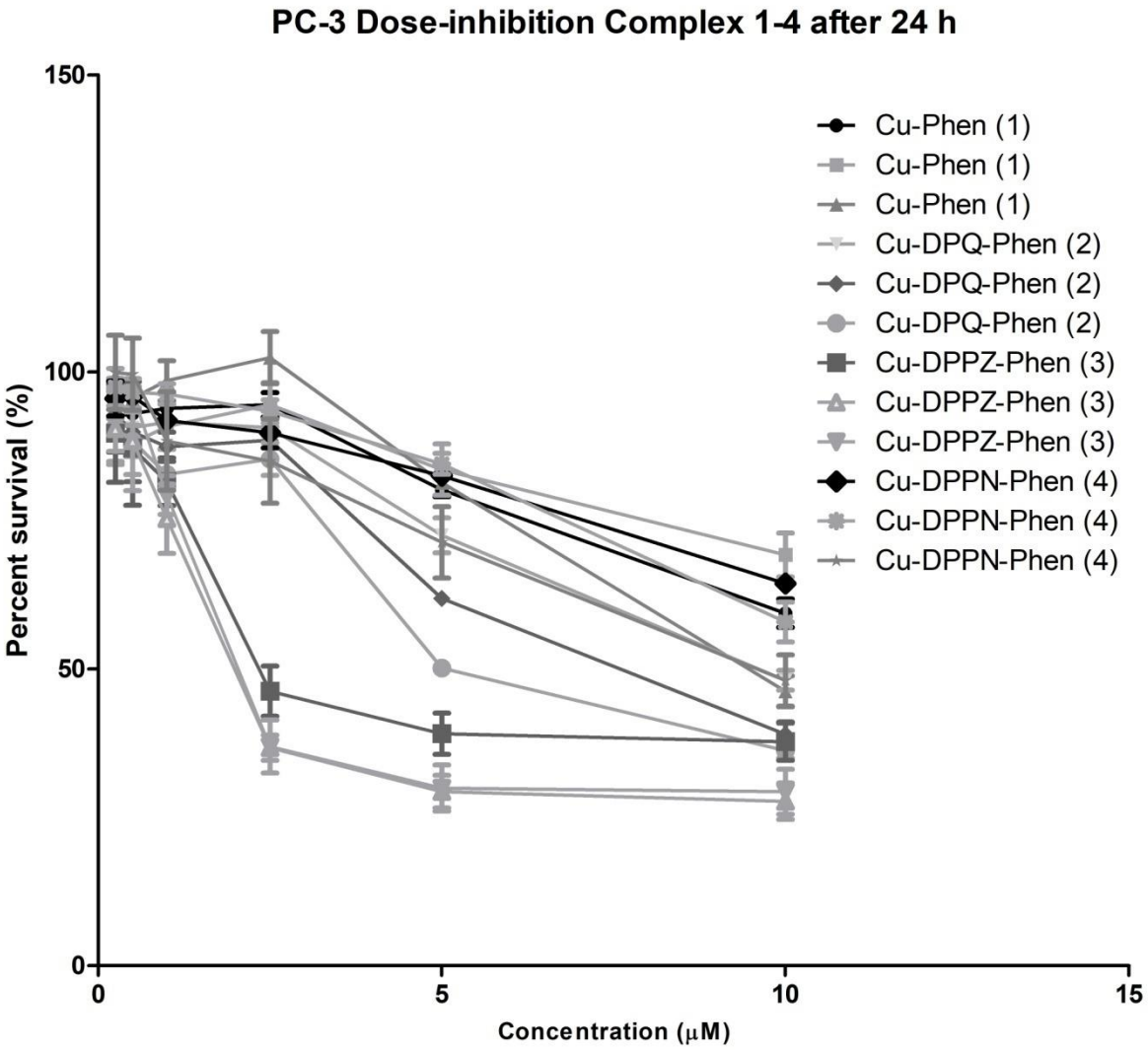

PC-3 48 h exposure to complexes **1-4**

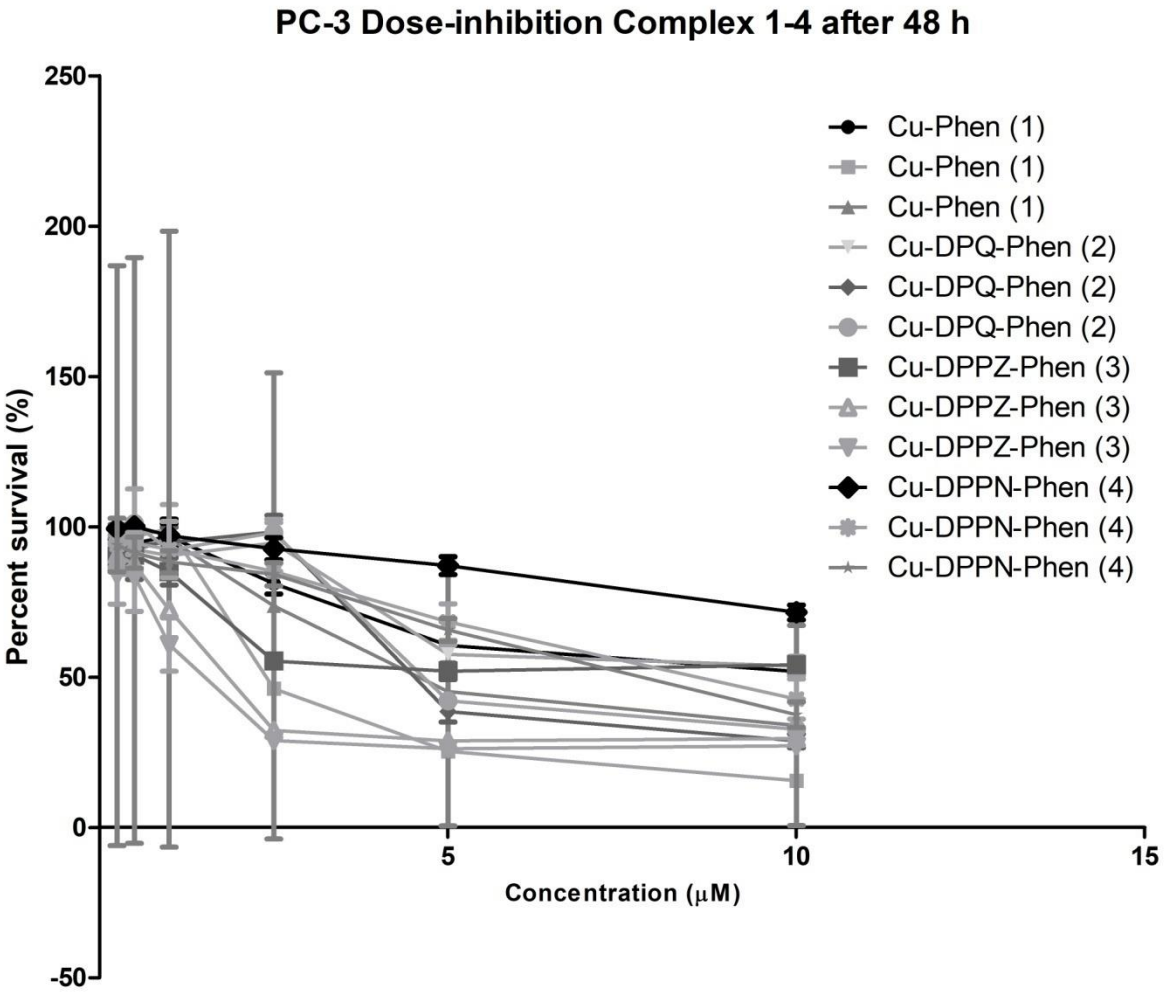

PC-3 24 and 48 h exposure to cisplatin

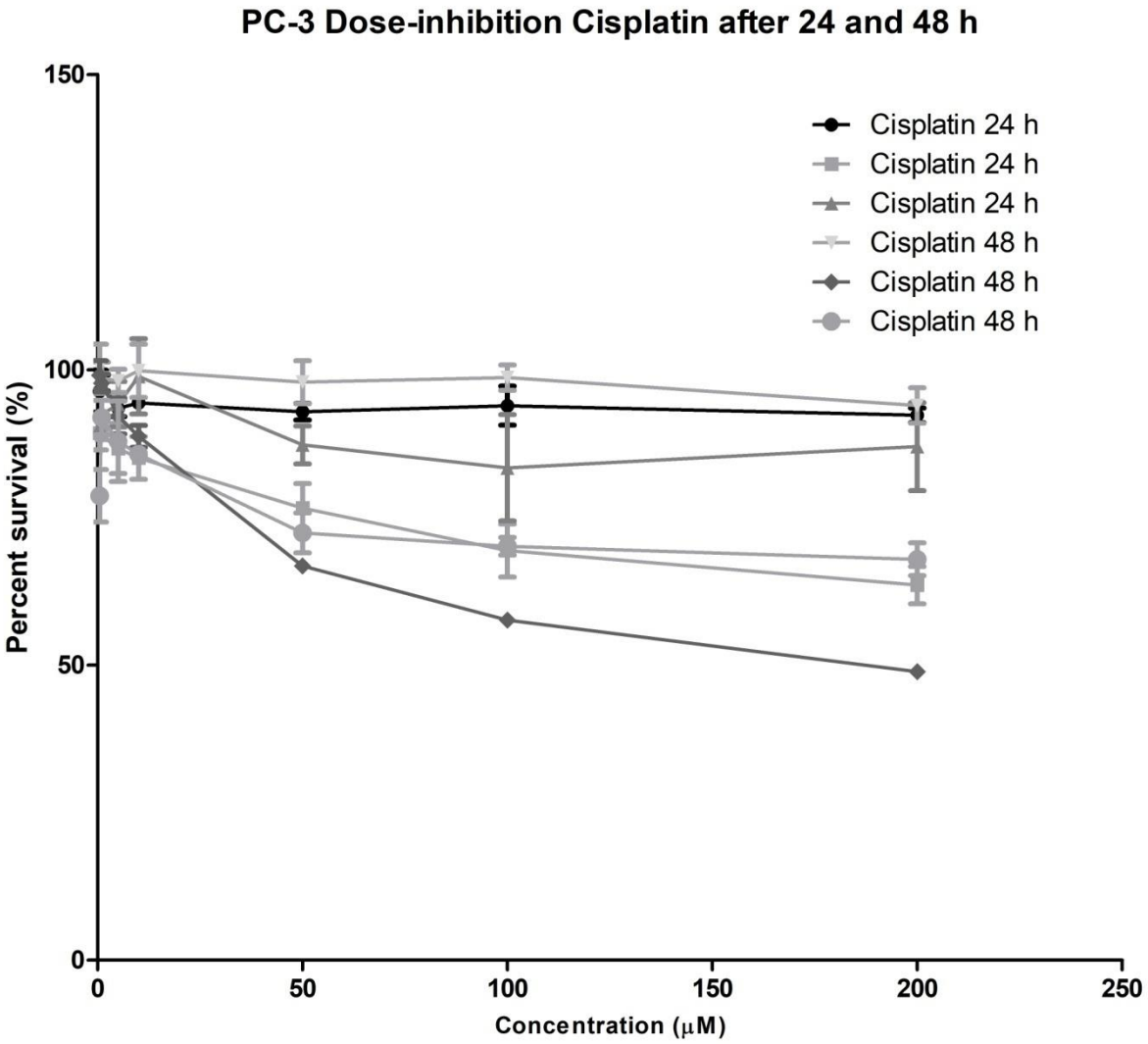

OE-33 24 h exposure to complexes **1-4**

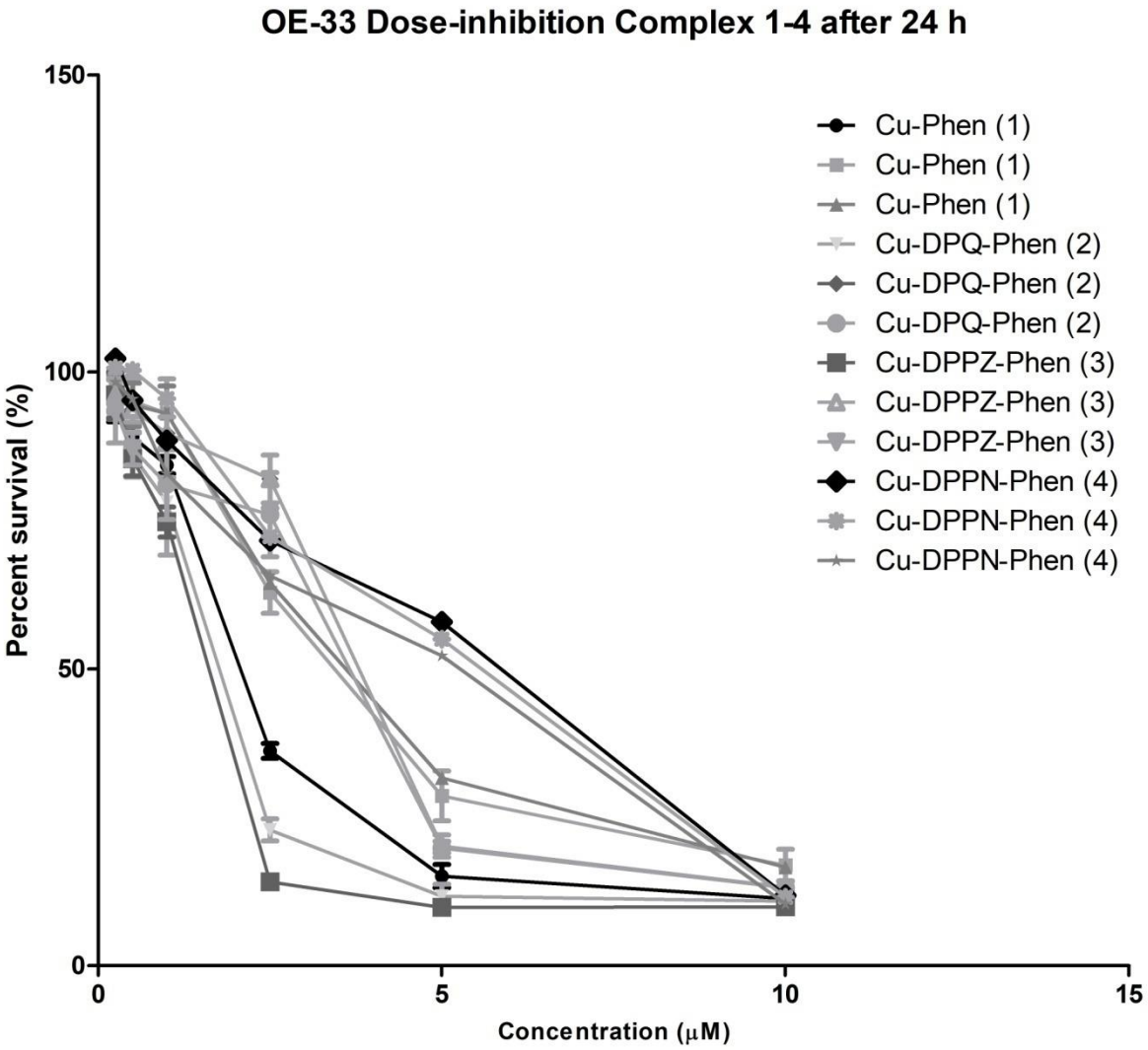

OE-33 48 h exposure to complexes **1-4**

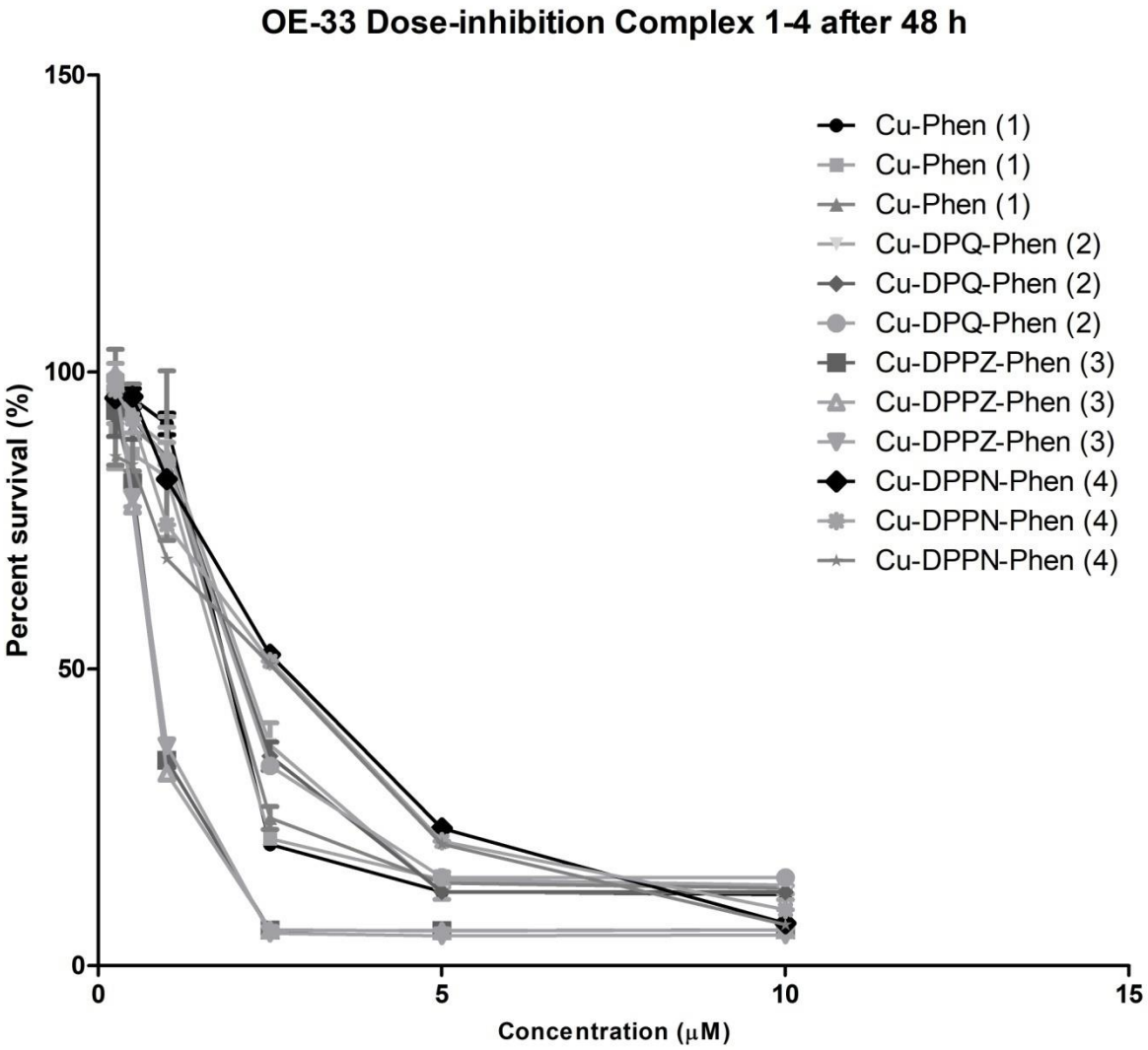

OE-33 24 and 48 h exposure to cisplatin

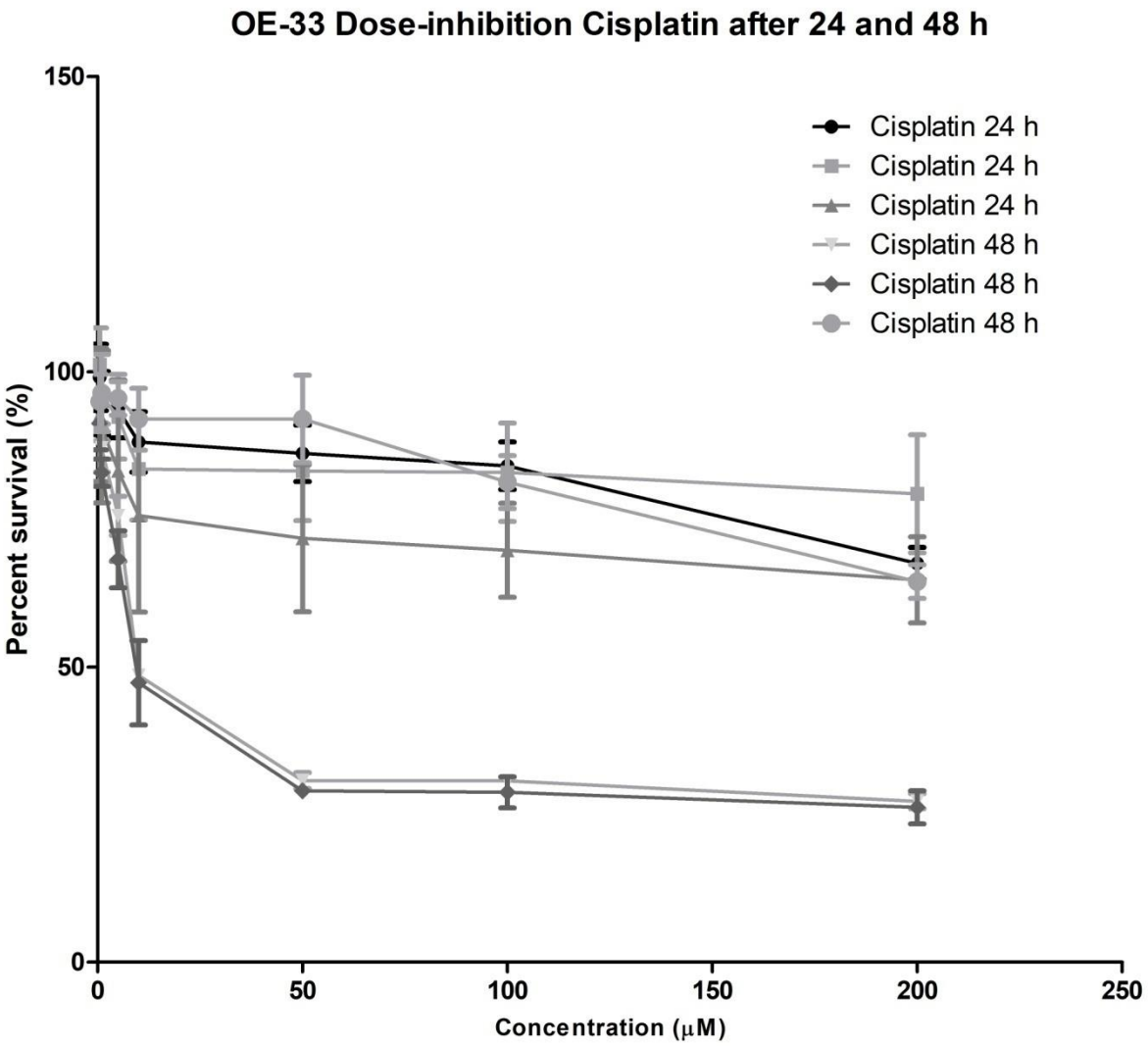

SKOV-3 24 h exposure to complexes **1-4**

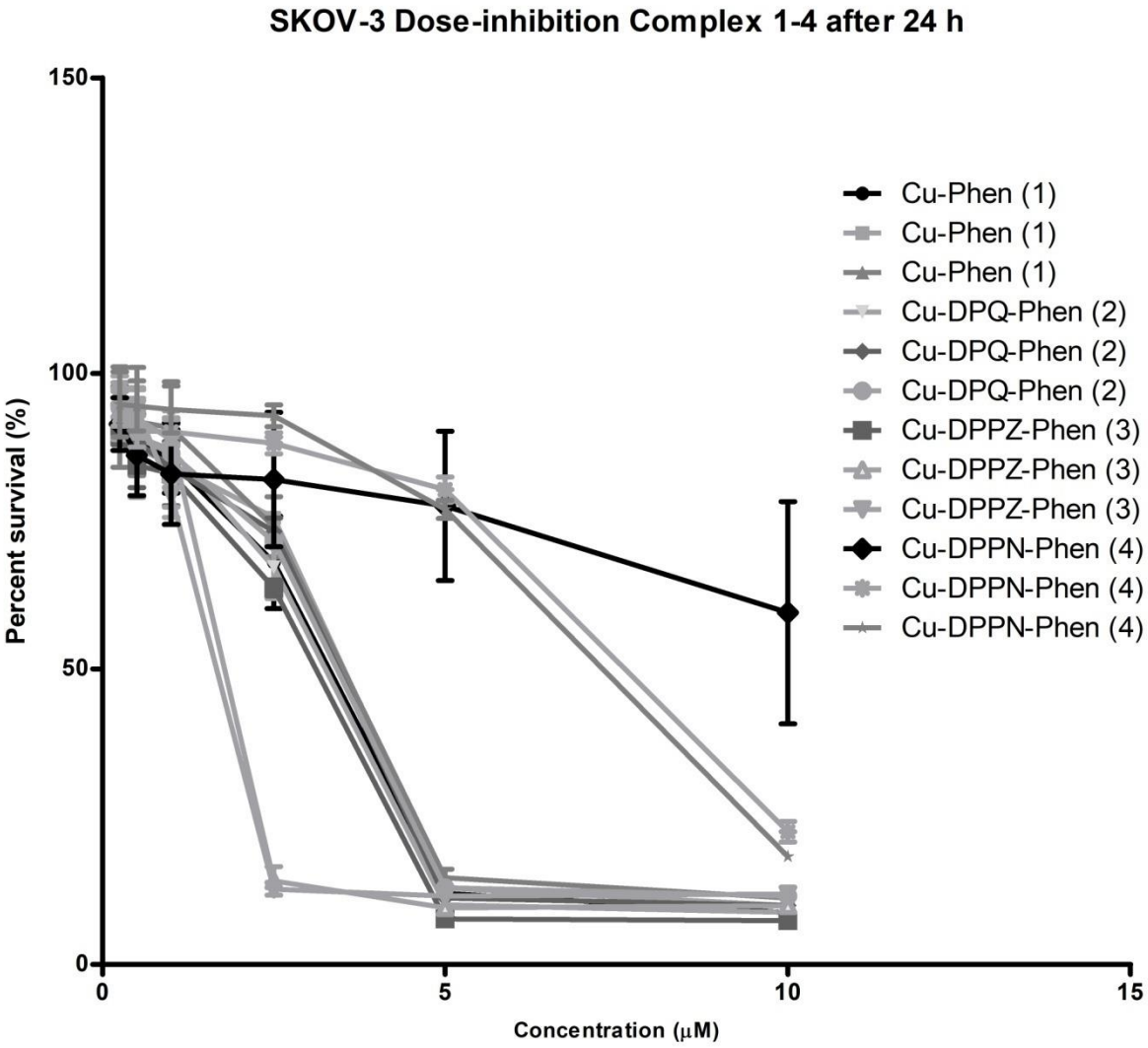

SKOV-3 48 h exposure to complexes **1-4**

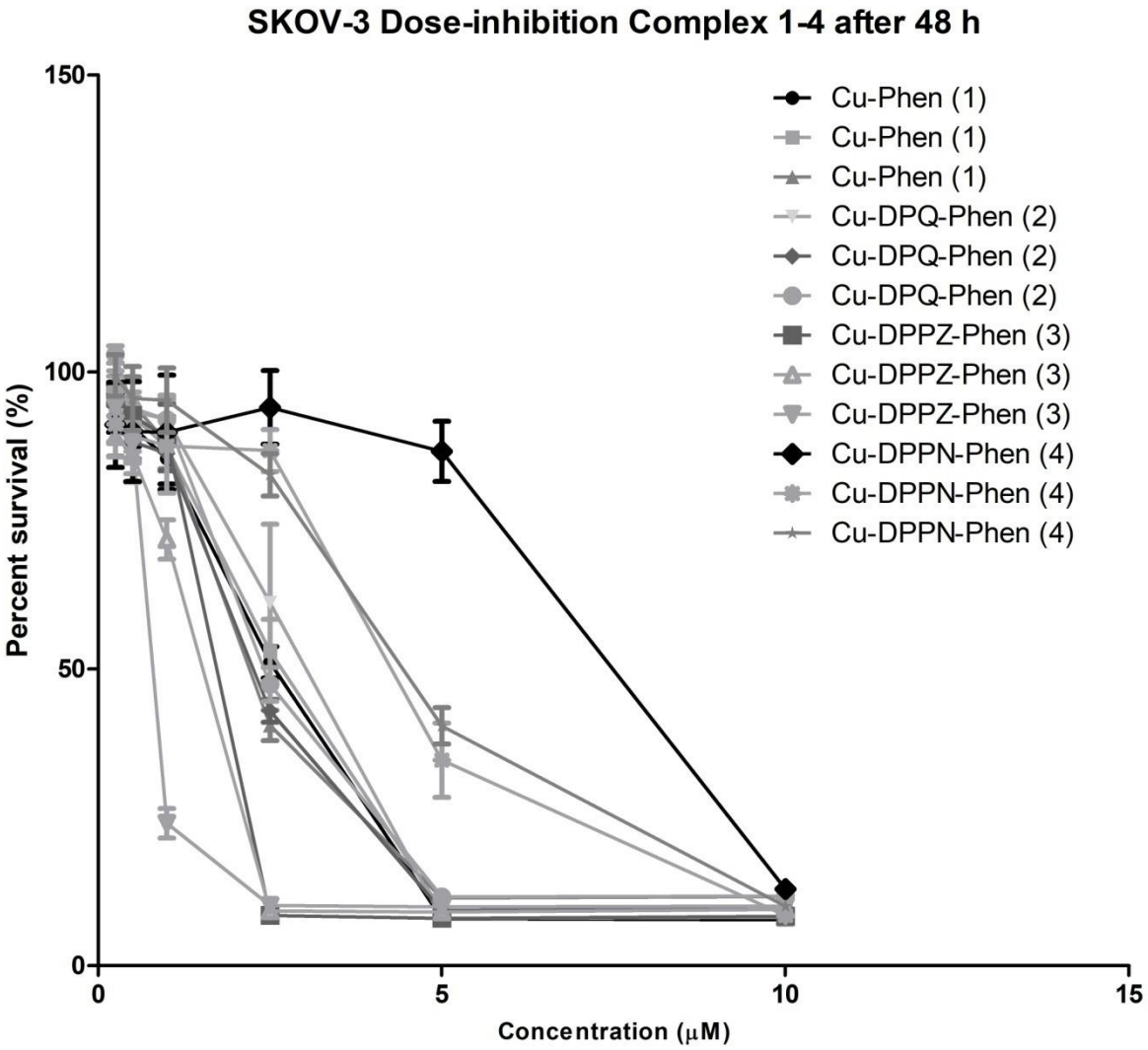

SKOV-3 24 and 48 h exposures to cisplatin

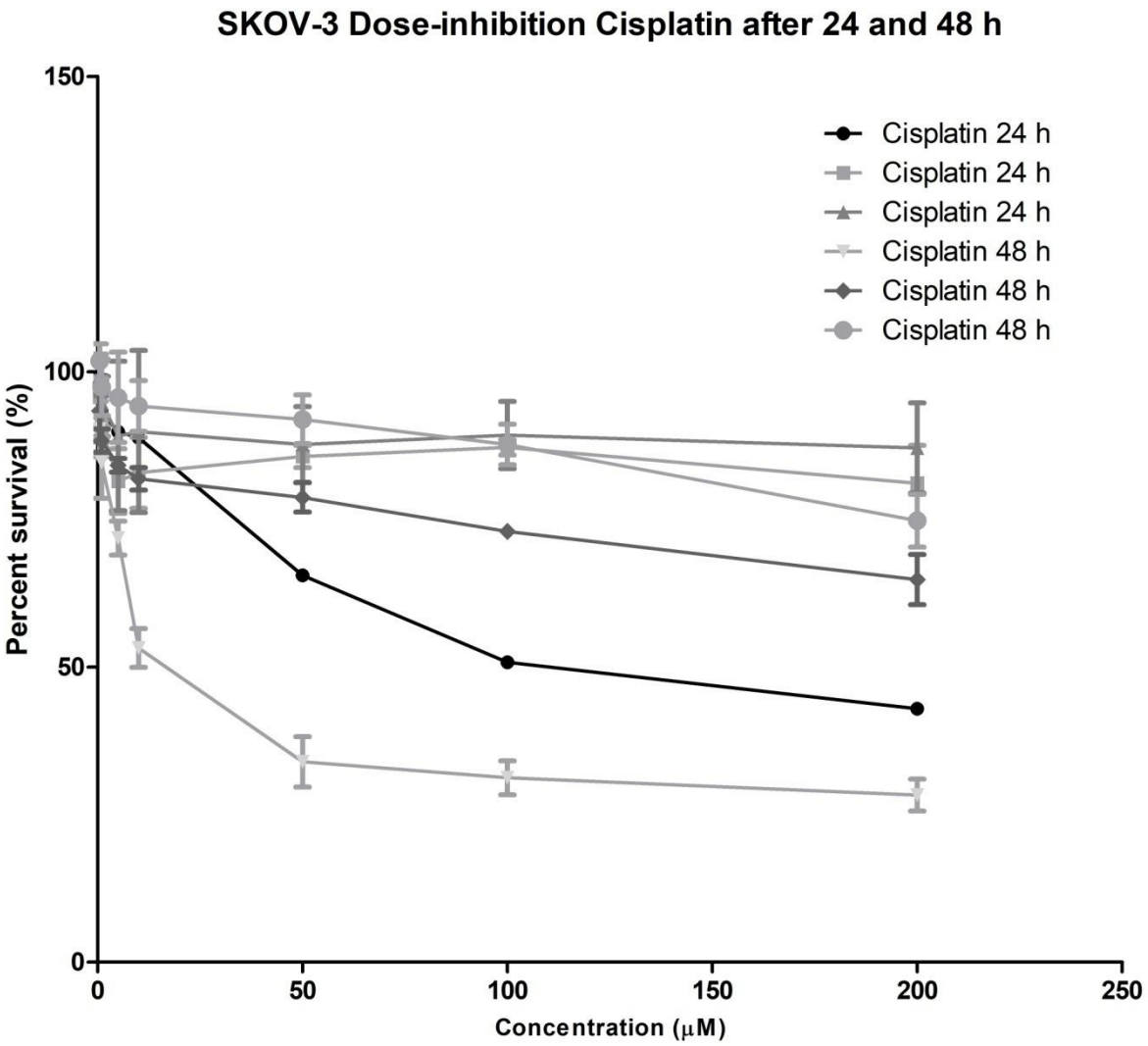

HeLa 24 h exposure to complexes **1-4**

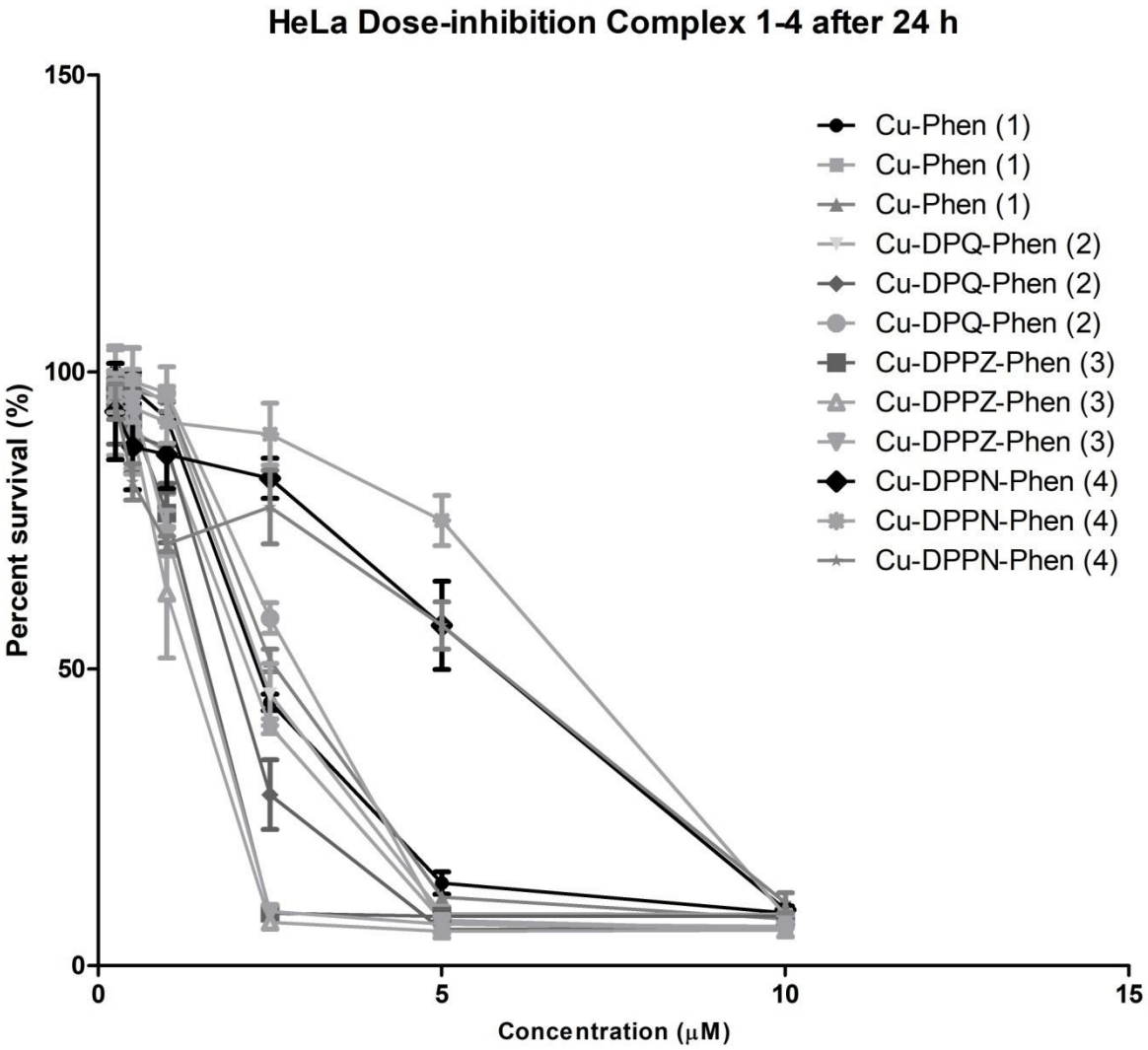

HeLa 48 h exposures to complexes **1-4**

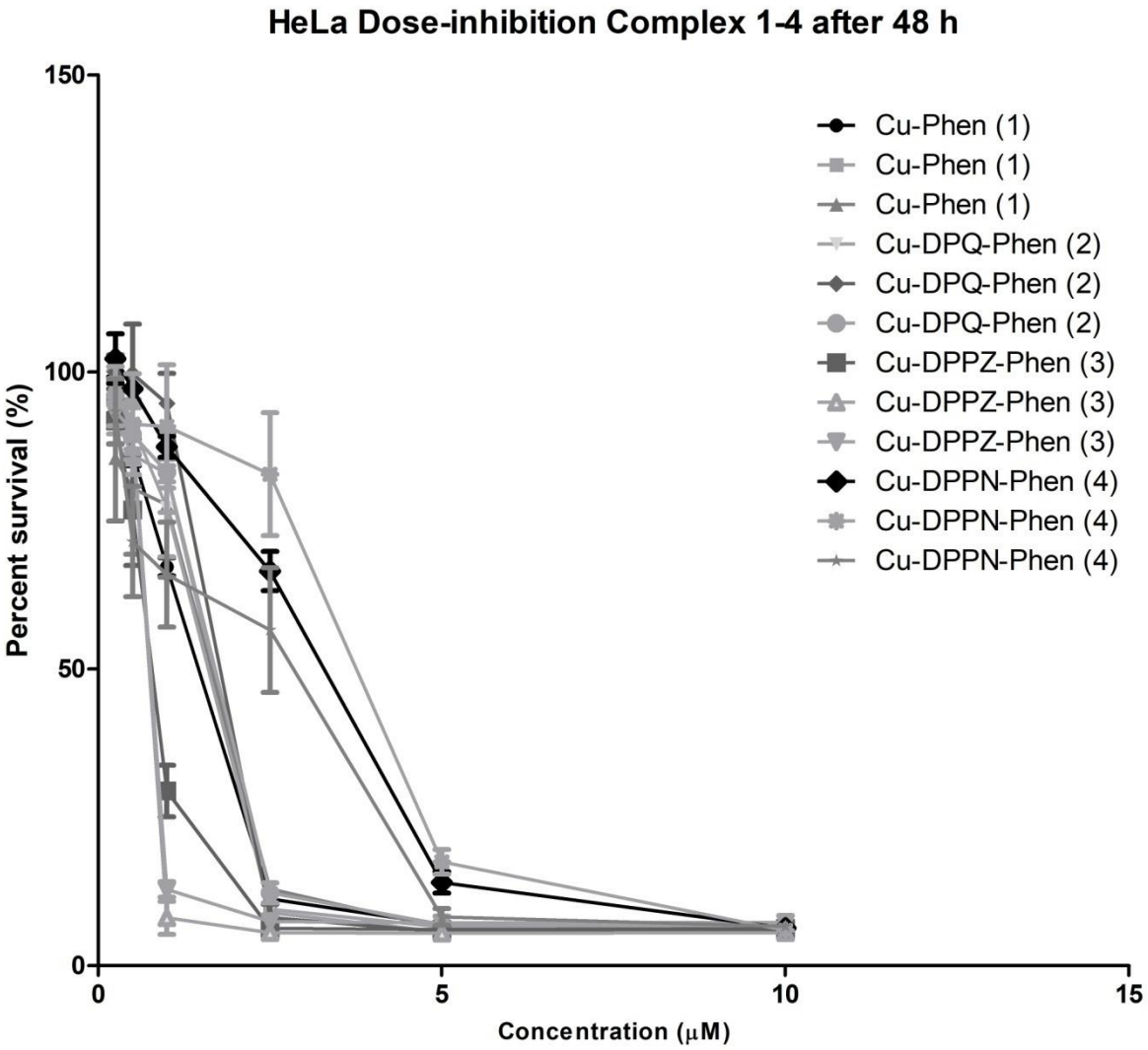

HeLa 24 and 48 h exposures to cisplatin

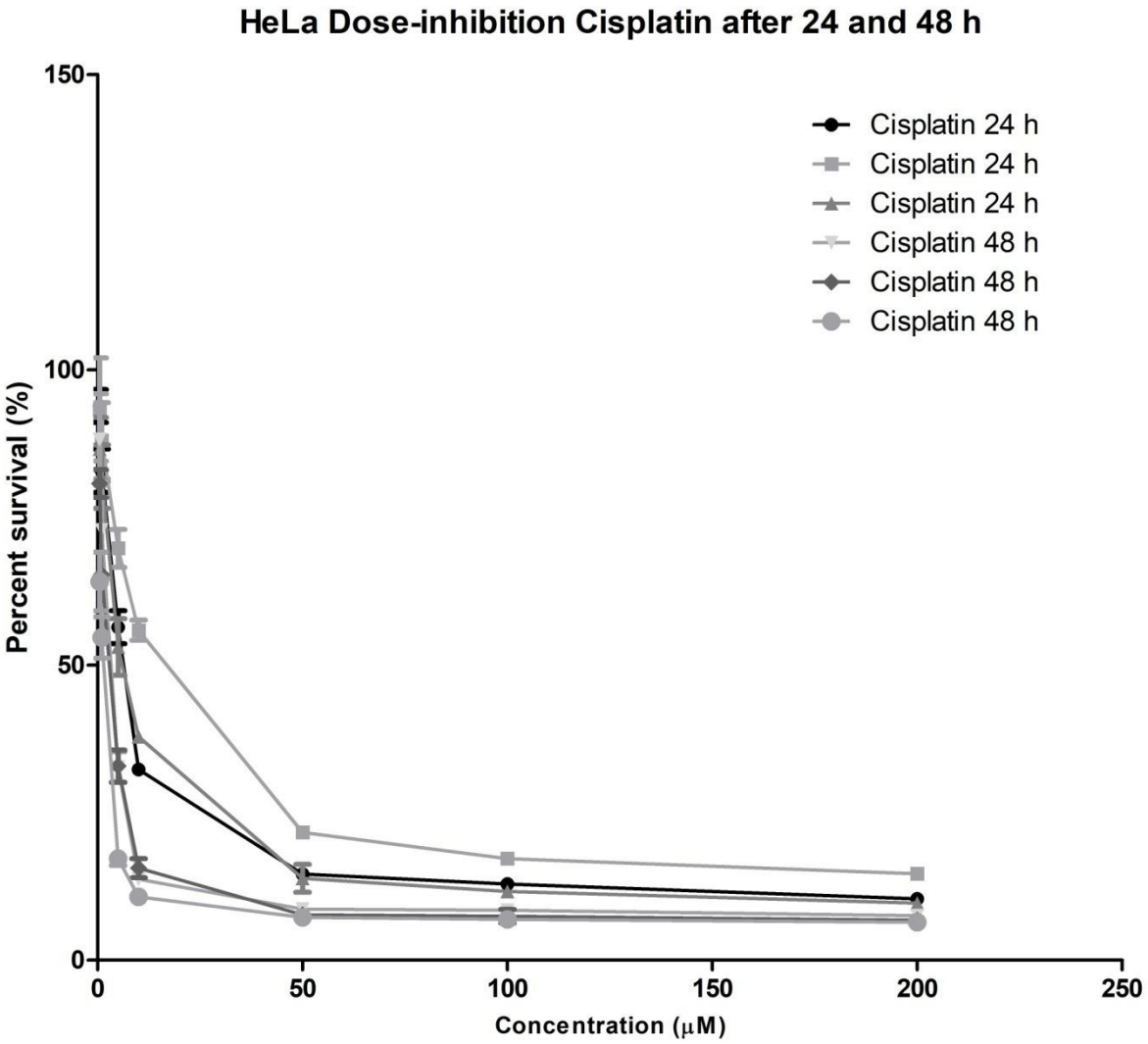

A2780 24 h exposures to complexes **1-4**

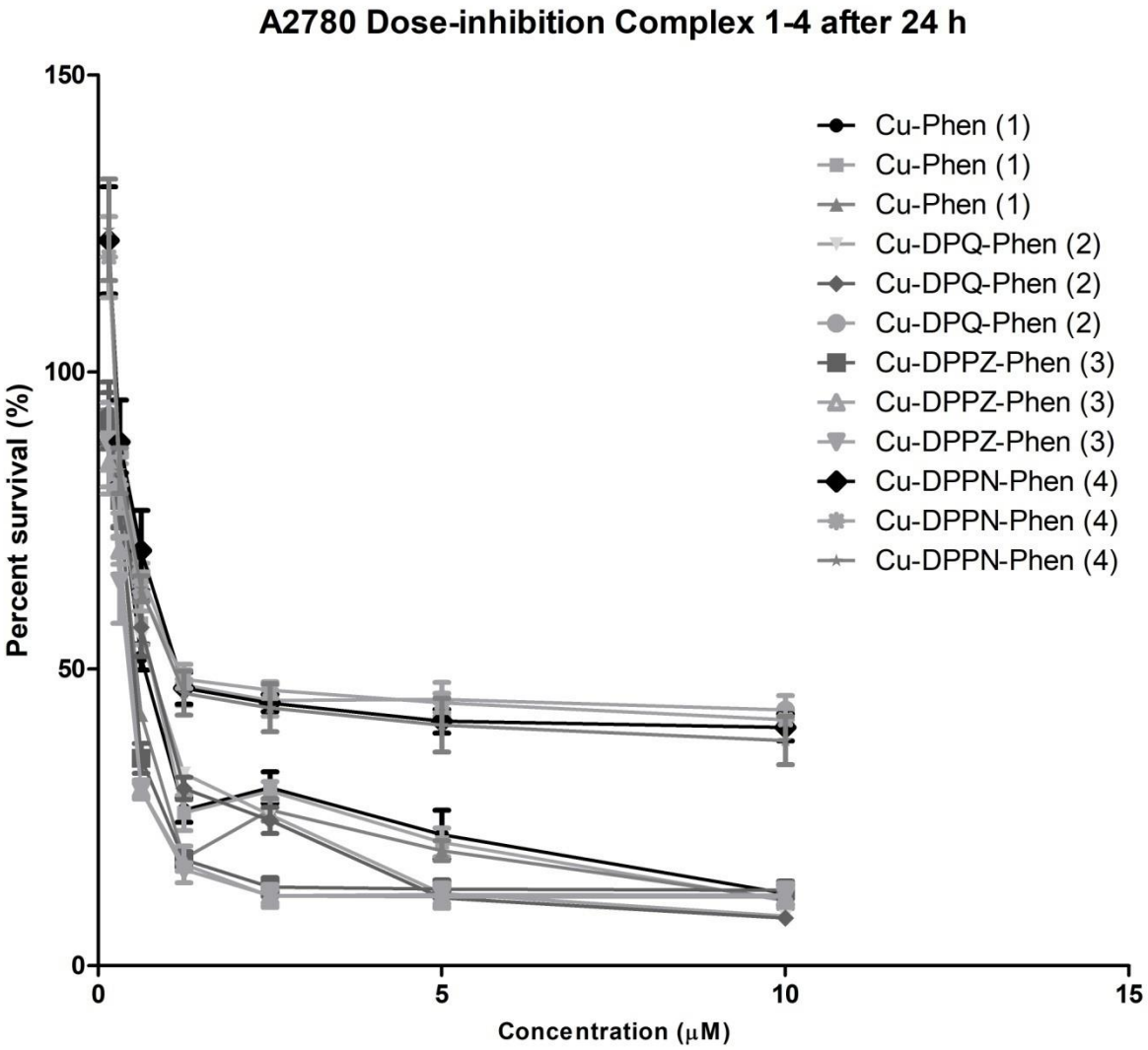

A2780 48 h exposures to complexes **1-4**

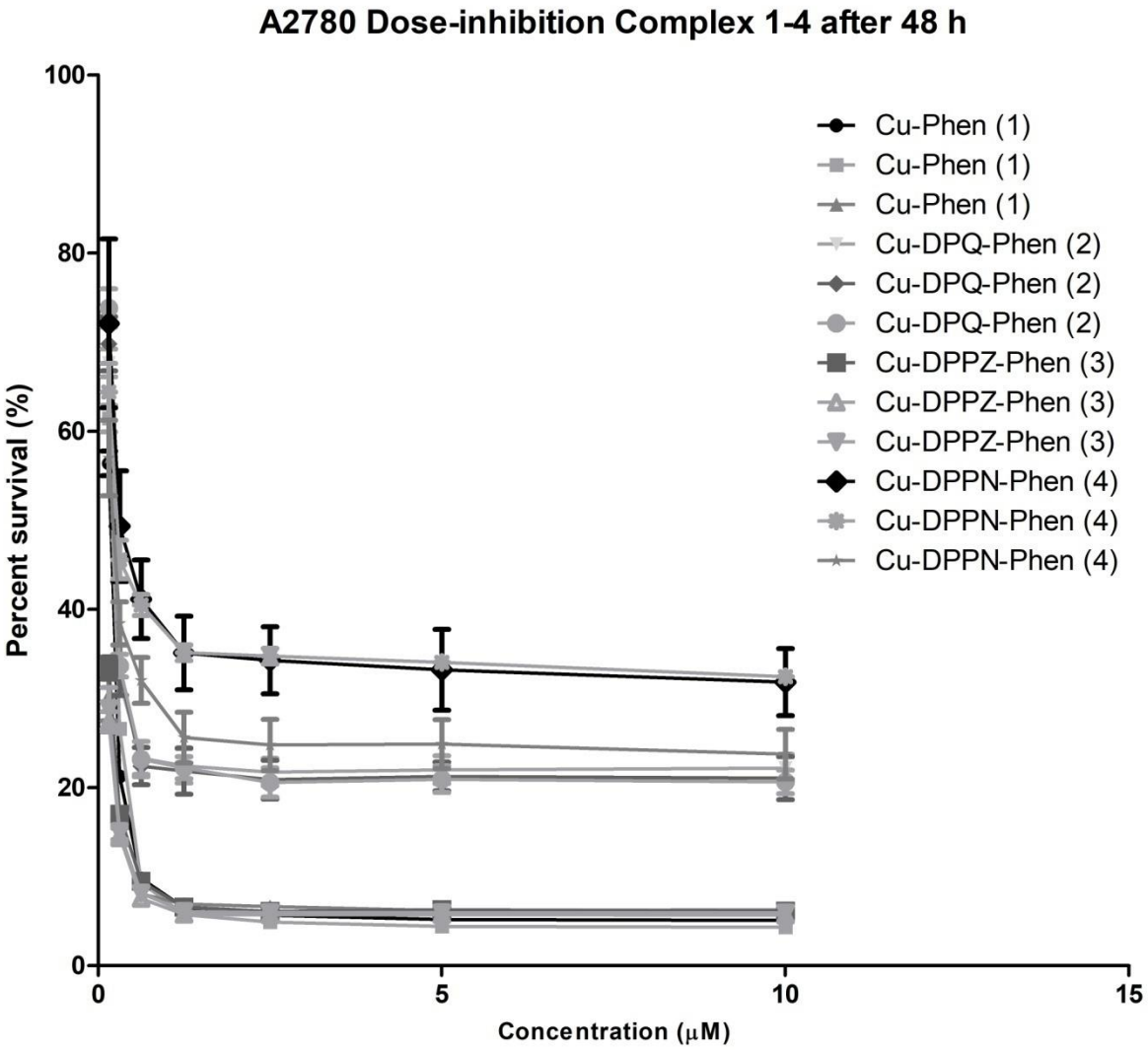

A2780 24 and 48 h exposure to doxorubicin

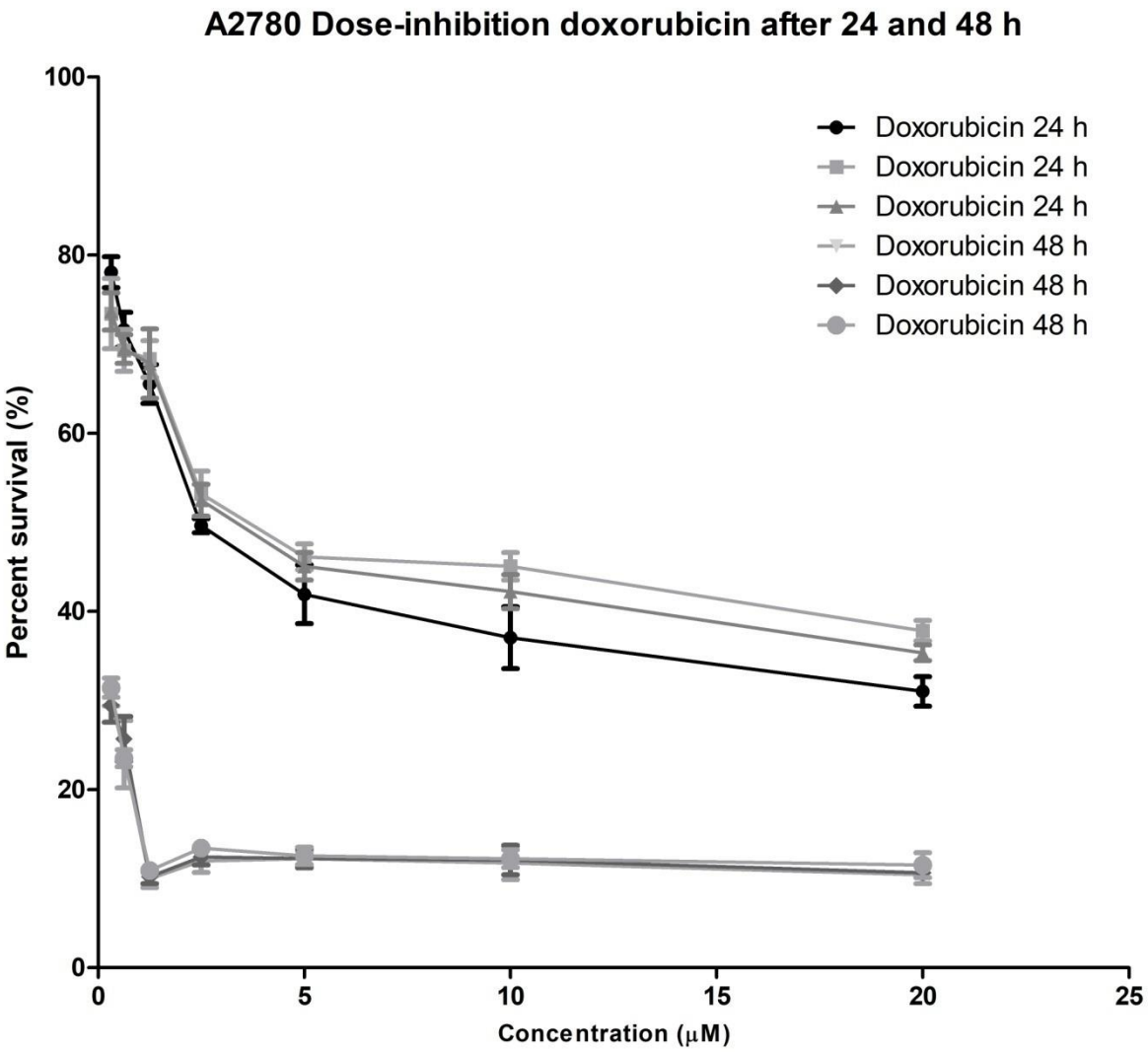

A2780 24 and 48 h exposure to cisplatin

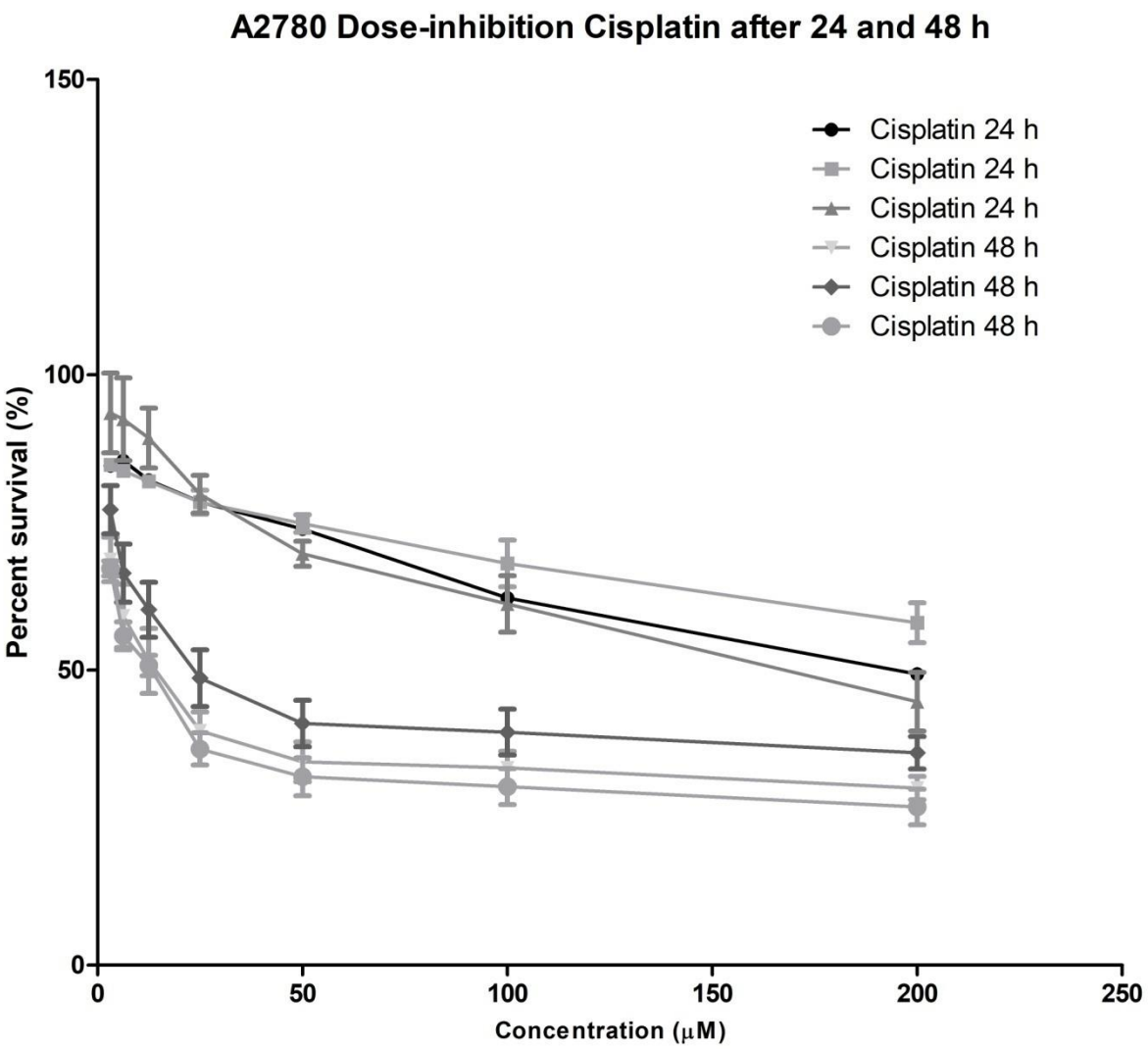

A2780/ Cis 24 h exposures to complexes **1-4**

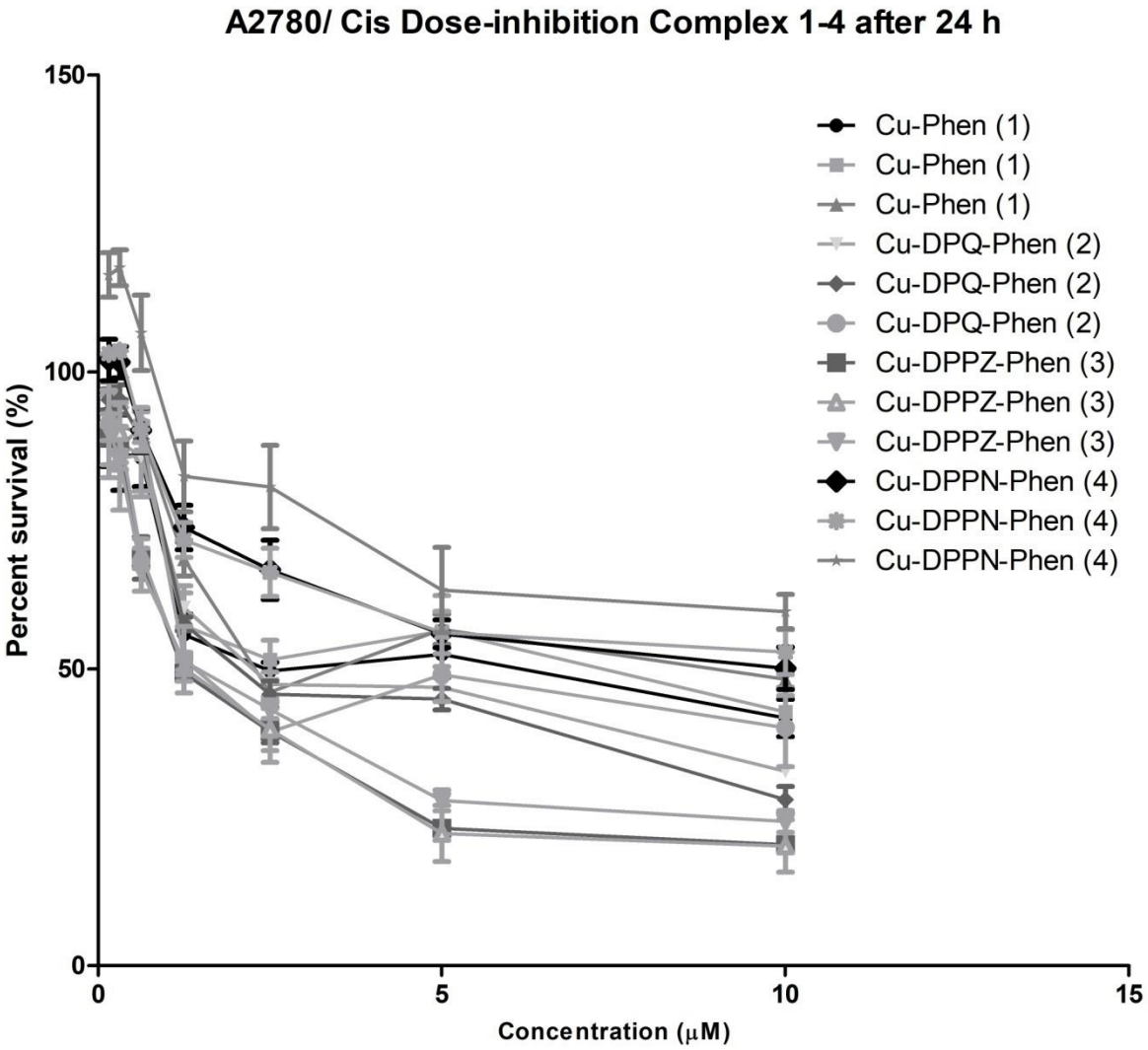

A2780/ Cis 48 h exposures to complexes **1-4**

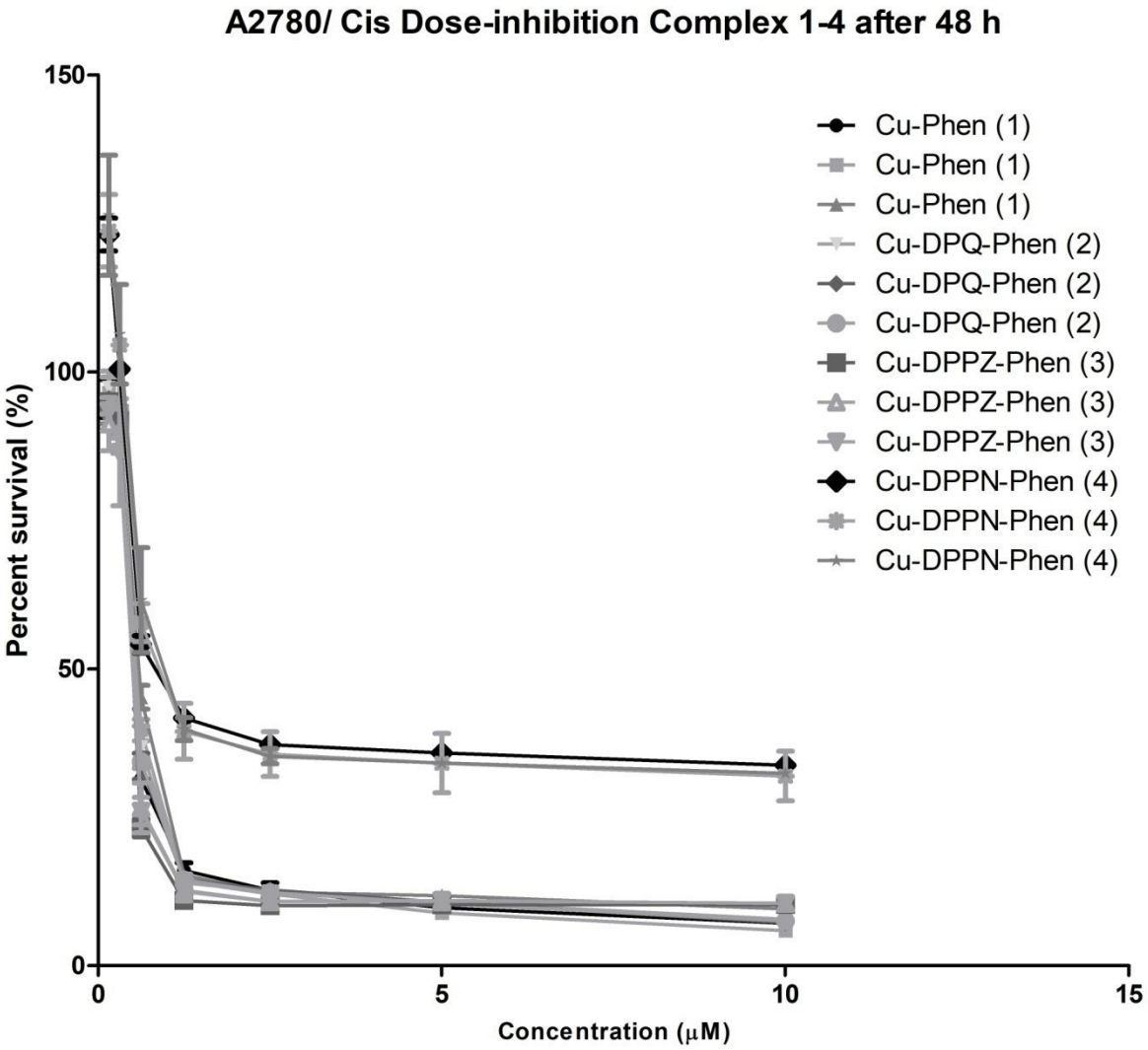

A2780/ Cis 24 and 48 h exposure to doxorubicin

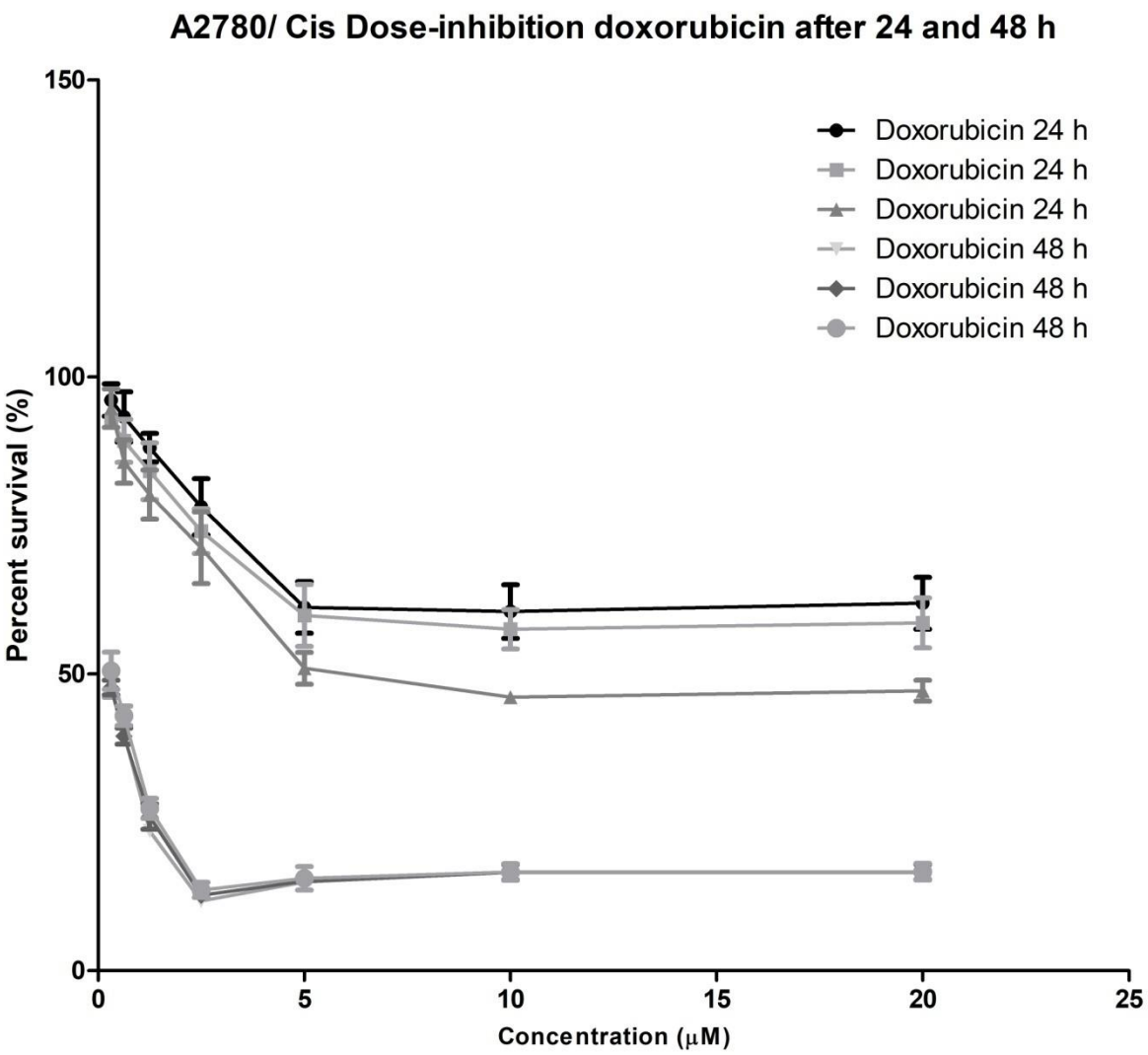

A2780/ Cis 24 and 48 h exposure to cisplatin

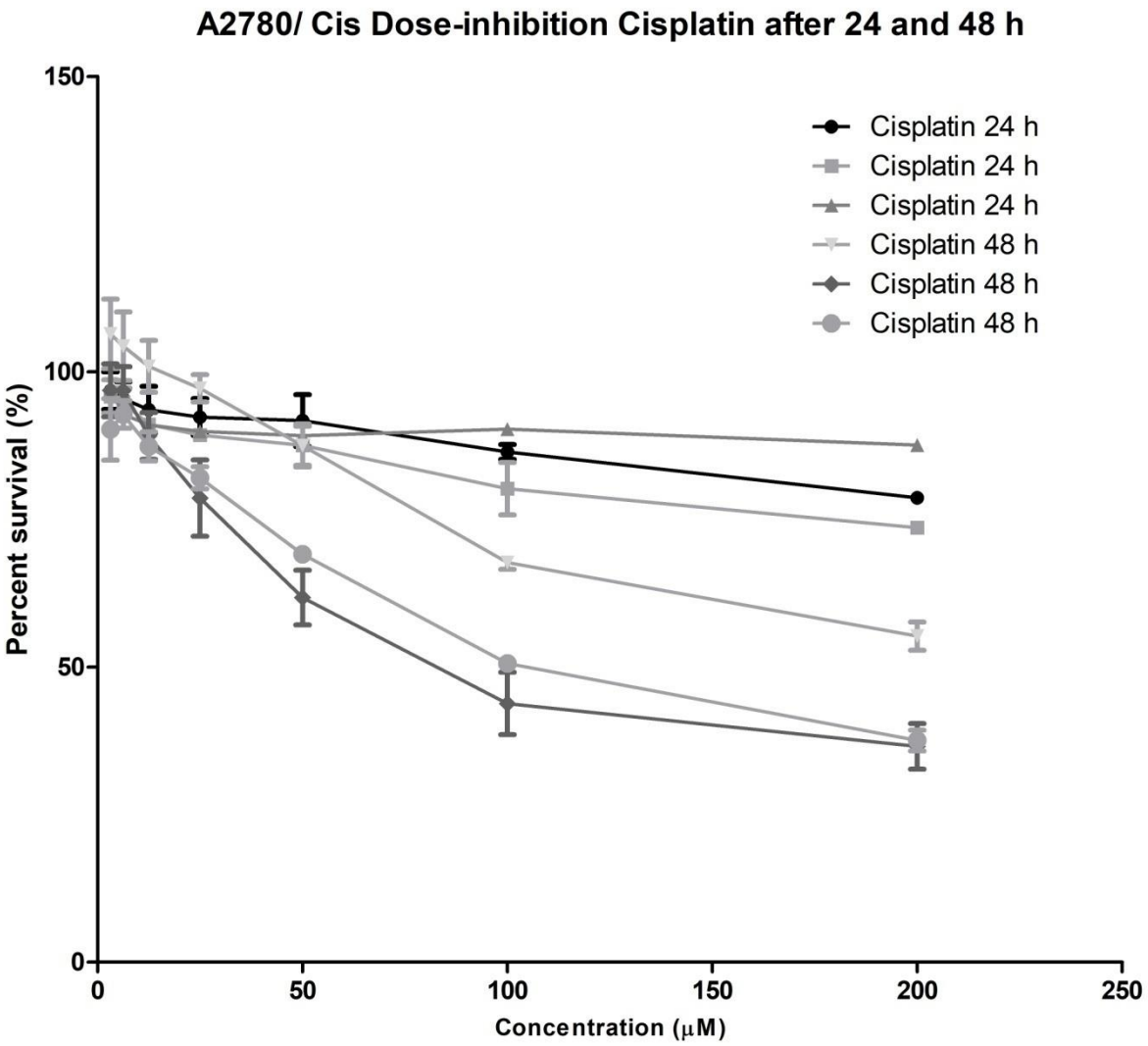

3.2 ROS assay

3.2.1 **Cu-Phen (1)**

15 min

average	121.1348	101.4963	94.294	97.69913	114.8624	141.3595	118.0984	118.1439	136.5731	124.185	147.4313	180.3421
average	79.95613	83.28388	105.3664	115.9991	98.03313	147.4684	100.2623	135.278	119.481	131.4189	170.8783	174.3163
average	105.5665	83.85525	89.69825	71.3125	98.13388	94.46325	141.0623	108.7895	123.0773	131.3106	157.4071	182.14
overall average	102.2191	89.54513	96.45288	95.00358	103.6765	127.7637	119.8076	120.7371	126.3771	128.9715	158.5722	178.9328
overall SD	20.79239	10.35392	8.054073	22.46493	9.687419	29.00034	20.45363	13.43331	9.011219	4.145584	11.76684	4.097857

30min

average	110.0398	101.776	92.52938	90.718	116.5149	140.8198	119.2631	118.8458	133.9674	121.7103	146.3926	185.1674
average	75.552	82.48088	105.9848	111.2246	97.356	145.9494	104.3244	138.6104	124.5111	141.3373	171.3948	188.8118
average	108.307	83.52688	84.99113	69.77425	105.023	87.90963	139.1546	108.1693	121.9414	128.627	153.7306	182.5896
overall average	97.96625	89.26125	94.50175	90.57229	106.298	124.8929	120.914	121.8751	126.8066	130.5582	157.1727	185.5229
overall SD	19.43063	10.8507	10.63488	20.72557	9.642861	32.131	17.47372	15.44501	6.3331	9.95499	12.85155	3.126263

1 h

average	107.4285	102.7613	84.94825	93.39713	112.7989	122.7925	108.2698	113.0388	132.4901	123.1878	143.8204	208.7564
average	71.01313	76.25438	86.71575	89.421	91.70363	133.5073	99.33825	135.8478	126.1514	141.3625	174.3131	194.4601
average	87.95525	76.70425	77.75775	77.11125	89.95175	90.71575	124.5776	113.7665	135.7283	144.357	157.4351	187.0983
overall average	88.79896	85.23996	83.14058	86.64313	98.15142	115.6718	110.7285	120.8843	131.4566	136.3024	158.5229	196.7716
overall SD	18.22234	15.17555	4.744701	8.49087	12.71528	22.2667	12.79808	12.96381	4.871375	11.4559	15.27545	11.01253

2 h

average	106.931	102.8121	84.4585	90.4155	117.8286	114.8108	116.0065	116.6624	132.977	123.2165	155.809	255.485
average	63.54425	67.98525	88.704	88.359	89.44313	134.7441	101.6381	130.1498	122.9449	138.9124	225.0075	214.9149
average	79.39213	63.67463	69.20725	69.38625	77.407	74.96225	109.5808	101.3938	126.5811	127.6436	144.3373	189.2729
overall average	83.28913	78.15733	80.78992	82.72025	94.89292	108.1724	109.0751	116.0686	127.501	129.9242	175.0513	219.8909
overall SD	21.95433	21.46018	10.25303	11.59327	20.75457	30.43878	7.19752	14.38719	5.078928	8.092637	43.64196	33.38536

3 h

average	99.916	94.26738	79.41425	85.25988	127.4288	112.612	108.4329	112.2628	130.5068	119.6244	175.5276	295.49
average	57.7585	65.89088	82.81525	84.26363	87.08363	129.5861	99.294	128.5849	122.0179	139.5968	269.4139	233.6704

average	78.81038	63.96075	69.64938	69.25825	81.44625	73.19888	112.3955	97.40438	133.4861	123.7778	145.9046	220.7283
overall average	78.82829	74.70633	77.29296	79.59392	98.65288	105.1323	106.7075	112.7507	128.6703	127.6663	196.9487	249.9629
overall SD	21.07876	16.96783	6.83447	8.9648	25.07954	28.92818	6.719012	15.59598	5.950608	10.53871	64.48086	39.95515

4 h

average	107.2695	95.32675	85.80475	89.74638	140.6806	107.3375	113.4578	115.4274	137.6036	128.8513	197.5668	368.5008
average	55.99788	66.251	83.50188	89.7745	87.60138	129.3325	100.6245	135.8879	123.1118	146.92	335.4594	277.1723
average	79.53488	64.96813	69.31913	68.2635	83.81813	69.7925	116.1639	99.64038	129.7683	126.5633	149.6695	234.7899
overall average	80.93408	75.51529	79.54192	82.59479	104.0334	102.1542	110.082	116.9852	130.1612	134.1115	227.5652	293.4876
overall SD	25.66443	17.16921	8.927761	12.41127	31.79377	30.10653	8.301482	18.17389	7.253925	11.15132	96.45932	68.33223

5 h

average	106.7855	93.415	84.0115	86.9925	155.6355	108.5354	111.0435	117.6736	138.652	132.6128	227.7604	441.7873
average	55.09813	67.17563	84.63225	84.21875	87.09388	124.4093	103.2115	137.8234	128.9338	150.7011	371.4639	310.6699
average	78.8865	65.08113	70.78113	69.66213	84.56638	69.83975	116.0663	105.4303	130.9108	133.8205	156.8821	261.3494
overall average	80.25671	75.22392	79.80829	80.29113	109.0986	100.9281	110.1071	120.3091	132.8322	139.0448	252.0355	337.9355
overall SD	25.87092	15.78871	7.823914	9.308875	40.32196	28.06885	6.478334	16.35658	5.136144	10.11273	109.3311	93.2578

3.2.2 **Cu-DPQ-Phen (1)**

15 min

average	116.3279	76.11788	80.79725	103.2093	143.265	168.642	105.5439	120.7408	129.948	158.9608	195.076	169.8499
average	132.9123	74.904	67.41288	80.56063	93.81575	82.89925	123.7205	121.1486	142.6211	137.3926	169.6883	179.0626
average	91.58063	61.75675	113.646	77.70875	108.85	71.62025	93.05163	121.647	129.2323	174.5751	182.7473	198.162
overall average	113.6069	70.92621	87.28538	87.15954	115.3103	107.7205	107.4387	121.1788	133.9338	156.9762	182.5038	182.3582
overall SD	20.79972	7.964145	23.78965	13.97241	25.34972	53.06012	15.42199	0.453878	7.531958	18.67053	12.69563	14.4409

30 min

average	107.8736	72.47963	74.23013	109.104	140.1339	150.1705	109.8148	124.4971	133.1759	159.4139	195.861	178.585
average	122.0039	72.46538	67.62463	76.404	93.756	79.65413	120.9475	127.313	144.4811	141.2036	169.0836	185.4018
average	89.09225	61.31063	107.55778	75.2515	100.7569	71.29375	92.22488	124.4329	126.9528	174.3481	179.5568	200.8559
overall average	106.3233	68.75188	83.14417	86.91983	111.5489	100.3728	107.6624	125.4143	134.8699	158.3219	181.5005	188.2809
overall SD	16.5105	6.444315	21.41631	19.22069	25.00156	43.3282	14.48178	1.644607	8.886131	16.59921	13.49409	11.41118

1 h

average	81.96463	63.38263	66.77825	85.76613	106.9129	117.5796	97.78225	109.9908	121.5034	152.5414	187.6648	174.997
average	97.97438	62.75438	58.90588	68.28125	82.95225	71.1505	106.5761	113.5138	133.9178	131.7944	171.4915	179.7405
average	84.53213	56.00888	100.46	72.93525	97.32088	68.47788	88.37738	118.6298	116.6756	163.322	176.92	197.2488
overall average	88.15704	60.71529	75.38138	75.66088	95.72867	85.736	97.57858	114.0448	124.0323	149.2193	178.6921	183.9954
overall SD	8.598432	4.087963	22.07253	9.055495	12.0594	27.60975	9.101084	4.34391	8.894893	16.02421	8.230961	11.72021

2 h

average	78.30925	56.7805	62.10538	86.63188	82.076	88.9365	93.39375	99.20338	114.6121	152.1583	184.8775	168.943
average	92.17875	58.19188	55.82913	64.20213	76.47525	69.37688	106.4508	103.2446	128.9935	127.6809	167.457	183.9906
average	83.32163	56.1805	101.9224	73.89825	98.2675	66.80838	87.54125	113.982	123.2253	170.6291	169.3938	212.8666
overall average	84.60321	57.05096	73.28563	74.91075	85.60625	75.04058	95.79525	105.4767	122.277	150.1561	173.9094	188.6001
overall SD	7.023005	1.032603	24.99791	11.2491	11.31691	12.10255	9.68079	7.637961	7.237433	21.54401	9.547874	22.32166

3 h

average	58.524	46.84563	51.12763	91.42788	75.499	97.56738	77.66963	85.62788	97.413	129.1531	168.2775	165.1851
average	81.0195	55.83413	53.33188	60.83125	71.76263	65.14675	95.122	97.34675	120.8526	120.8691	149.8219	186.6195
average	69.698	45.29913	76.96038	61.18125	71.25588	58.73038	72.74363	115.6745	106.9968	149.855	167.5974	183.7031
overall average	69.74717	49.32629	60.47329	71.14679	72.83917	73.81483	81.84508	99.54971	108.4208	133.2924	161.8989	178.5026
overall SD	11.24783	5.688746	14.32071	17.56481	2.317377	20.81898	11.75899	15.14397	11.78452	14.92969	10.46455	11.62507

4 h

average	61.87375	50.04138	54.50225	97.62075	84.78413	123.5028	88.89613	94.34563	110.3638	138.0859	180.0783	181.3024
average	77.01063	57.48963	53.40613	61.50988	72.15188	65.22313	94.71463	97.56813	120.6631	125.8658	156.8238	193.5919
average	71.92775	44.608	63.01513	57.35563	65.77238	62.0955	75.3255	115.9048	118.0614	152.7539	164.8841	204.5558
overall average	70.27071	50.713	56.9745	72.16208	74.23613	83.60713	86.31208	102.6062	116.3628	138.9018	167.262	193.15
overall SD	7.703284	6.467022	5.259965	22.14548	9.675729	34.586	9.949497	11.62907	5.355677	13.46262	11.80821	11.63298

5 h

average	59.71875	49.23025	53.68438	88.00563	77.091	102.8566	81.53875	90.68313	105.028	139.3104	177.5296	183.8006
average	79.26763	52.6205	54.60413	61.73438	71.21888	66.215	99.7235	97.18688	125.7238	124.7016	166.9633	195.7084
average	73.75438	44.51088	65.32925	59.0265	71.432	57.467	73.65025	112.0141	111.3919	148.4673	171.7913	199.8406
overall average	70.91358	48.78721	57.87258	69.58883	73.24729	75.51288	84.97083	99.96138	114.0479	137.4931	172.0947	193.1165
overall SD	10.0793	4.072925	6.474017	16.00677	3.330454	24.08095	13.37116	10.93281	10.60044	11.98658	5.28972	8.328181

3.2.3 Cu-DPPZ-Phen (3)

15 min

average	87.6115	64.486	73.13613	56.03475	78.76	66.3545	90.25263	94.24725	102.3129	126.51	148.8425	174.3548
average	82.80675	65.38113	73.5225	74.14425	101.3189	86.91313	115.7144	106.4958	112.4111	121.481	145.025	181.1304
average	84.70313	69.26675	71.01875	72.59625	89.496	78.8165	105.3326	107.4595	116.077	111.6905	141.7309	186.6878
overall average	85.04046	66.37796	72.55913	67.59175	89.85829	77.36138	103.7665	102.7342	110.267	119.8938	145.1995	180.7243
overall SD	2.420073	2.541486	1.34792	10.03854	11.2838	10.35627	12.80292	7.365665	7.128165	7.536161	3.559021	6.17652

30 min

average	90.72088	63.12	71.5235	54.61463	78.79763	66.82063	94.39275	94.46988	102.7086	126.9849	155.2663	182.2213
average	82.00575	66.17163	72.48525	74.3215	101.5106	86.3315	116.5769	109.2995	111.7514	122.3845	146.7204	178.7116
average	83.49363	68.67775	67.72838	68.00688	86.08313	79.84863	103.2489	100.7413	119.0586	109.3856	138.9304	178.34
overall average	85.40675	65.98979	70.57904	65.64767	88.79713	77.66692	104.7395	101.5035	111.1729	119.585	146.9723	179.7576
overall SD	4.661908	2.783333	2.515147	10.06303	11.59717	9.936722	11.16693	7.444143	8.190337	9.127502	8.170852	2.141638

1 h

average	83.5515	61.7835	65.60775	52.593	75.30975	62.1345	85.887	90.47688	98.48463	128.3425	161.07	190.6906
average	81.86425	64.15875	71.50663	74.01213	101.52504	88.39188	113.824	107.4743	110.6823	120.5506	143.3664	184.5169
average	79.72338	64.16138	66.86838	70.7495	79.54488	82.52213	106.2416	103.7898	117.6186	112.6196	141.0654	182.0895
overall average	81.71304	63.36788	67.99425	65.78488	85.36833	77.68283	101.9842	100.5803	108.9285	120.5043	148.5006	185.7657
overall SD	1.918537	1.37211	3.106425	11.54038	13.9163	13.78138	14.44691	8.941653	9.686806	7.86154	10.94606	4.434461

2 h

average	85.6885	62.59438	69.97538	53.23763	77.98713	65.40575	90.011	96.55975	105.9814	132.397	196.4709	206.574
average	71.26675	62.22538	69.20338	71.05575	98.80025	84.69788	108.0316	104.9298	107.4524	121.3771	145.6418	186.6914
average	81.31288	64.80763	67.677	74.38875	82.13975	84.38175	108.6746	106.5604	122.6625	118.7403	147.2305	202.7988
overall average	79.42271	63.20913	68.95192	66.22738	86.30904	78.16179	102.2391	102.6833	112.0321	124.1715	163.1144	198.688
overall SD	7.39434	1.396582	1.169639	11.37222	11.01516	11.04819	10.59471	5.36545	9.235544	7.24451	28.8985	10.5595

3 h

average	85.821	63.244	71.59475	55.95913	82.58913	69.45525	99.98425	100.9688	110.797	138.1641	232.272	222.8466
average	78.64713	64.823	70.39388	73.20863	101.7396	88.71138	108.3565	110.5215	107.7339	122.2306	151.6459	201.9883
average	78.39425	67.0535	66.8515	66.86863	82.78325	84.30325	109.0406	105.1409	122.498	120.3593	149.8856	226.4305
overall average	80.95413	65.04017	69.61338	65.34546	89.03733	80.82329	105.7938	105.5437	113.6763	126.918	177.9345	217.0885
overall SD	4.216733	1.914012	2.466068	8.725041	11.00094	10.08871	5.042825	4.789098	7.791828	9.784273	47.06589	13.19937

4 h

average	67.46413	52.16363	57.87925	45.51925	64.65488	56.78313	77.4365	80.00413	86.5505	114.1185	230.8238	198.1663
average	70.53013	57.853	62.47363	63.99663	93.04863	78.4885	94.65325	98.8185	93.90575	109.0118	140.0231	183.8066
average	61.95838	56.405	55.45638	56.68325	67.6195	70.64888	88.73588	84.97363	99.52338	101.0655	127.3876	213.0355
overall average	66.65088	55.47388	58.60308	55.39971	75.10767	68.64017	86.94188	87.93208	93.32654	108.0653	166.0782	198.3361
overall SD	4.343358	2.956771	3.564183	9.305319	15.60787	10.99122	8.747454	9.749848	6.505804	6.577773	56.42612	14.61518

5 h

average	65.86263	53.75013	61.314	49.27175	66.95538	57.22588	76.80013	84.43413	91.56013	122.0168	238.1313	211.0398
average	68.834	57.53813	62.73138	65.11388	94.04713	78.84438	95.88363	98.78063	94.95963	112.3585	143.212	188.2195
average	64.12163	52.80313	57.97325	58.88575	67.73588	67.976	86.60588	82.92588	98.16813	97.53675	129.3491	224.4069
overall average	66.27275	54.69713	60.67288	57.75713	76.24613	68.01542	86.42988	88.71354	94.89596	110.6373	170.2308	207.8887
overall SD	2.382807	2.505526	2.442994	7.981139	15.42106	10.8093	9.542967	8.750905	3.30446	12.33043	59.21063	18.29831

3.2.4 Cu-DPPN-Phen (4)

15 min

average 1	93.0075	71.06013	69.85188	61.564	73.698	72.63125	99.54875	104.5646	113.9465	125.678	151.8369	182.6935
average 2	99.036	64.32775	81.75613	69.71163	83.32475	101.003	117.417	125.7413	130.8913	130.7868	157.5288	261.3234
average 3	62.80575	77.07938	85.68788	79.93763	103.0185	91.51688	116.0648	106.5531	133.7285	122.388	156.0066	224.6785
overall average	84.94975	70.82242	79.09863	70.40442	86.68042	88.38371	111.0102	112.2863	126.1888	126.2843	155.1241	222.8985
overall S.D	19.41271	6.379135	8.245693	9.206383	14.94551	14.44305	9.948879	11.69464	10.69659	4.232069	2.946781	39.34515

30 min

average 1	101.6153	67.62513	69.05175	58.7605	71.708	69.64425	100.2485	100.5724	111.2576	120.5999	144.4935	177.4166
average 2	96.2455	64.4205	75.73488	71.679	84.936	100.9188	118.6794	124.8351	126.9881	122.0663	159.7194	278.6899
average 3	134.3758	77.61638	89.39838	77.62925	103.3458	92.41025	117.1506	110.1046	135.0776	124.6178	161.2724	237.014
overall average	110.7455	69.88733	78.06167	69.35625	86.66325	87.65775	112.0262	111.8374	124.4411	122.428	155.1618	231.0402
overall S.D	20.63977	6.882657	10.37096	9.64644	15.88944	16.16983	10.22836	12.22383	12.11254	2.033213	9.271549	50.90022

1 h

average 1	76.37188	53.752	55.10275	47.1375	57.48475	55.3815	79.32838	79.30688	85.822	95.62475	118.7374	157.797
average 2	77.382	51.23813	62.109	57.43025	69.092	84.77075	95.34738	101.1735	111.4599	99.61538	136.0716	313.1693
average 3	110.3233	61.9915	74.62325	62.8395	84.65775	73.40863	94.63875	91.43175	108.1794	98.33	130.3054	219.5124
overall average	88.02571	55.66054	63.945	55.80242	70.4115	71.18696	89.7715	90.63738	101.8204	97.85671	128.3715	230.1595
overall S.D	19.31684	5.625004	9.888916	7.976565	13.63447	14.82005	9.050949	10.95493	13.95179	2.036977	8.827462	78.23142

2 h

average 1	76.99413	57.91	57.90263	49.73425	59.5185	57.68213	85.01138	83.0775	93.96713	107.3186	131.2813	191.6808
average 2	84.24925	55.296	71.656	62.31688	78.48663	93.56975	107.3594	114.3399	120.6939	116.3595	163.977	392.0216
average 3	103.0339	70.58275	80.484	70.76563	91.55188	82.22688	99.16575	96.38338	115.4911	108.7041	140.9241	247.1878
overall average	88.09242	61.26292	70.01421	60.93892	76.5519	77.82625	97.17883	97.93358	110.0507	110.7941	145.3941	276.9634
overall S.D	13.43855	8.176351	11.37986	10.58318	16.10708	18.34406	11.30571	15.68873	14.16963	4.869322	16.79996	103.4362

3 h

average 1	71.24513	55.39925	56.49375	49.58888	59.04125	55.68425	78.79213	77.14813	87.99663	101.6889	131.3758	209.2605
average 2	78.74463	56.25325	70.9025	60.9065	78.62513	91.34888	105.904	115.4011	122.4365	118.7776	190.0664	452.7523
average 3	118.244	72.04625	81.959	72.244	93.46525	82.71225	101.9933	99.0795	118.9474	112.9591	149.1729	281.1395
overall average	89.41125	61.23292	69.78508	60.91313	77.04388	76.58179	95.56313	97.20958	109.7935	111.1419	156.8717	314.3841
overall S.D	25.24988	9.374351	12.76935	11.32756	17.26639	18.60587	14.65515	19.19493	18.95709	8.688103	30.0932	125.1038

4 h

average 1	71.57563	56.91975	58.96038	50.85488	63.27925	57.57838	86.66375	81.8375	95.9305	107.7958	145.7165	241.7764
average 2	76.513	55.82125	69.37663	59.90375	74.6645	83.11488	102.0065	112.1086	113.1775	116.6979	219.5583	514.7801
average 3	94.94613	69.77238	83.06975	70.8395	95.79463	83.61513	102.523	102.2064	121.1145	114.1234	157.6814	329.1156
overall average	81.01158	60.83779	70.46892	60.53271	77.91279	74.76946	97.06442	98.7175	110.0742	112.8723	174.3187	361.8907
overall S.D	12.31759	7.757046	12.09175	10.00715	16.49927	14.89002	9.010943	15.4342	12.87562	4.581025	39.63271	139.4217

5 h

average 1	70.31563	59.43	59.513	52.11213	64.99763	59.29188	85.75425	82.9115	96.19325	107.0675	147.9321	247.2293
average 2	81.765	60.21675	70.60338	63.22763	80.75963	82.67263	108.5994	121.5629	129.9368	116.7038	226.5816	516.393
average 3	79.88613	66.66475	82.82663	68.958	94.5165	82.863	105.2218	102.879	118.5659	115.4044	162.2516	342.3465
overall average	77.32225	62.10383	70.9081	61.43258	80.09125	74.9425	99.85846	102.4511	114.8986	113.0585	178.9218	368.6563
overall S.D	6.140207	3.96941	11.6614	8.565192	14.77078	13.55417	12.3308	19.32924	17.16807	5.228913	41.89101	136.497

3.2.5 Cisplatin

15 min

average	104.382	74.501	68.1175	71.03375	78.18513	82.19163	106.7043	117.3806	109.4129	115.4	159.4791	192.4573
average	147.5389	81.761	71.3765	76.92888	90.82275	88.55938	118.9281	113.1848	128.604	129.436	183.7751	200.9878
average	100.1893	72.90838	65.91938	65.784	80.86175	105.5155	108.2779	108.275	118.72	123.2548	160.868	192.4998
overall average	117.37	76.39013	68.47113	71.24888	83.28988	92.08883	111.3034	112.9468	118.9123	122.6969	168.0408	195.3149
overall SD	26.21095	4.718987	2.745695	5.575551	6.659522	12.05585	6.649903	4.557474	9.597007	7.034608	13.64405	4.912864

30 min

average	103.8544	68.677	69.808	68.00638	77.73625	80.587	104.4905	114.6466	108.2538	116.1194	153.2649	196.7166
average	115.6744	78.28663	72.366	76.5325	85.38625	88.91575	119.2426	115.7841	126.4719	128.9825	176.7378	212.1075
average	100.3348	74.47175	66.56213	65.5575	81.80688	91.73938	107.4026	110.2561	118.9311	123.798	156.5999	189.245
overall average	106.6212	73.81179	69.57871	70.03213	81.64313	87.08071	110.3786	113.5623	117.8856	122.9666	162.2008	199.3564
overall SD	8.035383	4.838686	2.908723	5.761111	3.827628	5.798224	7.813357	2.919166	9.153955	6.471737	12.69929	11.6576

1 h

average	95.18525	63.50813	66.90288	63.721	75.75888	79.91713	101.4426	114.4734	110.5811	115.8093	156.2116	200.7998
average	115.1245	76.564	70.2675	76.74025	89.25788	91.0715	119.4081	119.4654	129.745	138.4349	174.7018	222.5378
average	88.41525	73.65463	63.75263	65.43963	80.235	88.487	103.3653	106.1145	118.5279	125.6943	152.9571	191.9903
overall average	99.575	71.24225	66.97433	68.63363	81.75058	86.49188	108.072	113.3511	119.618	126.6461	161.2902	205.1093
overall SD	13.88519	6.854096	3.258025	7.072937	6.875936	5.8387	9.864326	6.745822	9.628333	11.34281	11.72821	15.72311

2 h

average	91.24863	65.67475	65.8195	62.69375	76.01588	82.16975	106.9736	112.5498	112.803	119.0713	156.7694	238.5026
average	101.9895	73.43413	63.402	74.77675	84.67575	84.85013	112.8769	109.8498	123.7103	132.0609	170.0205	279.0011
average	88.77275	79.51975	66.08063	66.6415	80.71388	86.09613	104.2031	104.6834	120.3905	122.761	151.513	208.4858
overall average	94.00363	72.87621	65.10071	68.03733	80.4685	84.372	108.0179	109.0276	118.9679	124.631	159.4343	241.9965
overall SD	7.025891	6.939341	1.476907	6.161249	4.335149	2.006379	4.430161	3.997109	5.591049	6.693682	9.537202	35.38728

3 h

average	89.96588	73.41975	64.75863	65.26813	73.74875	82.25563	108.9149	117.1276	112.6718	126.2691	167.2274	274.4806
average	101.2378	72.71525	66.531	75.7885	85.581	86.88563	114.0823	113.2056	128.06	136.7788	174.0779	334.8594
average	81.91163	79.1665	69.4885	66.96963	84.646	83.845	106.252	107.5268	126.3105	128.6918	152.9133	225.6094
overall average	91.03842	75.1005	66.92604	69.34208	81.32525	84.32875	109.7497	112.62	122.3474	130.5799	164.7395	278.3165
overall SD	9.707602	3.538834	2.389555	5.647211	6.578075	2.352602	3.981321	4.827154	8.424908	5.503346	10.79942	54.72592

4 h

average	94.414	71.50913	68.79	64.81113	75.65475	87.60588	108.4454	117.7246	116.083	132.2198	173.7979	314.8485
average	99.20963	72.47075	66.83075	78.02238	88.89388	91.06538	118.5908	118.9459	131.422	141.247	173.9151	372.2539
average	83.07013	80.75775	75.29575	69.43875	90.803	83.203	107.8671	110.2376	128.01	128.368	157.1053	248.9383
overall average	92.23125	74.91254	70.3055	70.75742	85.11721	87.29142	111.6344	115.636	125.1717	133.9449	168.2728	312.0135
overall SD	8.288194	5.084882	4.431322	6.703614	8.250138	3.940609	6.031295	4.714874	8.053778	6.610545	9.671516	61.70667

5 h

average	90.53713	75.7685	66.76125	65.82138	73.22175	85.155	111.726	118.8535	117.2648	134.1099	174.8896	351.1676
average	102.6719	74.40713	68.70375	81.93725	93.02575	89.70388	119.4141	115.8015	129.1305	139.5123	173.9649	437.8226
average	80.57363	72.97175	65.09175	66.94188	82.80175	80.6685	103.4008	108.7395	125.1568	128.6525	154.2598	267.2998
overall average	91.26088	74.38246	66.85225	71.56683	83.01642	85.17579	111.5136	114.4648	123.8507	134.0915	167.7048	352.0967
overall SD	11.06689	1.398538	1.807719	8.998502	9.903745	4.517723	8.0088	5.187799	6.039735	5.429898	11.65289	85.26523

3.3 γH2AX flow cytometry data

3.3.1 MCF-7 24 MFI

24 hour	1	2	3	minus unstained			average	S.D
unstained	279,596.00				279,596.00			
negative	490,851.49	389,595.39	397,909.57	211,255.49	109,999.39	118,313.57	146,522.82	56,214.06
Cu-Phen	861,215.04	750,444.70	723,451.46	581,619.04	470,848.70	443,855.46	498,774.40	73,004.00
Cu-DPQ-Phen	647,679.50	813,437.19	763,463.05	368,083.50	533,841.19	483,867.05	461,930.58	85,028.29
Cu-DPPZ-Phen	446,059.81	665,598.85	987,079.58	166,463.81	386,002.85	707,483.58	546,743.22	227,321.20
Cu-DPPN-Phen	714,708.66	637,517.87	812,723.98	435,112.66	357,921.87	533,127.98	442,054.17	87,809.08
Cisplatin	736,047.01	734,048.62	685,885.84	456,451.01	454,452.62	406,289.84	439,064.49	28,401.26

3.3.2 MCF-7 48 MFI

48 hour	1.00	2.00	3.00	minus unstained			average	S.D
unstained	317,230.50	391,989.33			354,609.92			
negative	637,858.54	402,906.67	610,808.77	283,248.63	48,296.75	256,198.86	195,914.75	128,554.37
Cu-Phen	638,822.79	859,698.62	691,462.37	284,212.88	505,088.71	336,852.46	375,384.68	115,369.33
Cu-DPQ-Phen	717,208.48	749,028.43	654,020.94	362,598.57	394,418.52	299,411.03	352,142.70	48,359.07
Cu-DPPZ-Phen	883,372.51	694,466.48	840,278.02	528,762.60	339,856.57	485,668.11	451,429.09	98,998.00
Cu-DPPN-Phen	894,070.38	1,005,348.67	938,015.30	539,460.47	650,738.76	583,405.39	591,201.54	56,047.30
Cisplatin	795,995.61	1,020,455.70	704,715.98	441,385.70	665,845.79	350,106.07	485,779.18	162,483.78

3.3.3 MCF-7 24 % positive

24 hour	1.00	2.00	3.00	minus unstained			average	S.D
unstained	0.02				0.02			
negative	7.14	2.49	1.16	7.12	2.47	1.14	1.81	0.94
Cu-Phen	25.84	25.99	33.35	25.82	25.97	33.33	28.37	4.29
Cu-DPQ-Phen	34.32	28.07	34.81	34.30	28.05	34.79	32.38	3.76
Cu-DPPZ-Phen	6.48	31.83	27.61	6.46	31.81	27.59	29.70	2.98
Cu-DPPN-Phen	18.26	26.39	40.25	18.24	26.37	40.23	28.28	11.12
Cisplatin	18.54	36.51	27.98	18.52	36.49	27.96	27.66	8.99

3.3.4 MCF-7 48 % positive

48 hour	1.00	2.00	3.00	minus unstained		average	S.D
unstained	0.05	0.08			0.07		
negative	3.92	2.09	2.93	3.86	2.03	2.87	2.92	0.92
Cu-Phen	17.39	24.41	24.28	17.33	24.35	24.22	21.96	4.02
Cu-DPQ-Phen	18.02	23.67	19.11	17.96	23.61	19.05	20.20	3.00
Cu-DPPZ-Phen	15.34	39.99	39.43	15.28	39.93	39.37	39.65	0.40
Cu-DPPN-Phen	26.11	42.66	49.38	26.05	42.60	49.32	39.32	11.98
Cisplatin	15.77	22.79	19.79	15.71	22.73	19.73	19.39	3.52

3.3.5 SKOV-3 24 MFI

24 hour	1	2	3	minus unstained		average	S.D
unstained	224,793.20				224,793.20		
negative	384,258.69	331,680.12	291,577.67	159,465.49	106,886.92	66,784.47	111,045.63	46,480.25
Cu-Phen	892,763.94	1,629,239.25	1,048,159.18	785,877.02	1,404,446.05	823,365.98	804,621.50	26,508.70
Cu-DPQ-Phen	3,545,402.48	2,591,848.30	3,263,657.20	3,320,609.28	2,367,055.10	3,038,864.00	3,179,736.64	199,224.00
Cu-DPPZ-Phen	448,971.04	1,418,586.71	796,652.27	224,177.84	1,193,793.51	571,859.07	398,018.46	245,847.76
Cu-DPPN-Phen	1,776,284.64	2,221,018.81	2,403,559.35	1,551,491.44	1,996,225.61	2,178,766.15	1,908,827.73	322,640.95
Cisplatin	661,100.80	481,911.07	478,746.83	436,307.60	257,117.87	253,953.63	315,793.03	104,380.67

3.3.6 SKOV-3 48 MFI

48 hour	1.00	2.00	3.00	minus unstained		average	S.D
unstained	165,113.67				165,113.67		
negative	327,805.08	292,748.46	321,728.97	162,691.41	127,634.79	156,615.30	148,980.50	18,733.91
Cu-Phen	1,052,929.57	1,320,156.72	958,401.93	925,294.78	1,155,043.05	793,288.26	957,875.36	183,064.89
Cu-DPQ-Phen	1,552,887.33	1,220,135.32	1,507,947.72	1,387,773.66	1,055,021.65	1,342,834.05	1,261,876.45	180,545.21
Cu-DPPZ-Phen	346,399.52	352,252.59	480,414.86	181,285.85	187,138.92	315,301.19	227,908.65	75,740.72
Cu-DPPN-Phen	536,471.79	470,761.76	532,279.75	371,358.12	305,648.09	367,166.08	348,057.43	36,787.33
Cisplatin	410,063.89	550,775.45	395,338.29	244,950.22	385,661.78	230,224.62	286,945.54	85,807.24

3.3.7 SKOV-3 24 % positive

24 hour	1.00	2.00	3.00	minus unstained			average	S.D
unstained	0.03				0.03			
negative	6.43	7.70	6.79	6.40	7.67	6.76	6.94	0.65
Cu-Phen	89.57	90.83	86.84	81.90	90.80	86.81	86.50	4.46
Cu-DPQ-Phen	87.71	89.15	88.14	87.68	89.12	88.11	88.30	0.74
Cu-DPPZ-Phen	51.60	84.10	62.13	51.57	84.07	62.10	56.84	7.45
Cu-DPPN-Phen	91.83	94.90	95.62	91.80	94.87	95.59	94.09	2.01
Cisplatin	74.18	60.14	59.88	74.15	60.11	59.85	64.70	8.18

3.3.8 SKOV-3 48 % positive

48 hour	1.00	2.00	3.00	minus unstained			average	S.D
unstained	0.04				0.04			
negative	6.41	11.59	10.00	6.37	11.55	9.96	9.29	2.65
Cu-Phen	70.54	72.02	56.52	58.99	71.98	56.48	62.48	8.32
Cu-DPQ-Phen	70.42	74.66	77.27	70.38	74.62	77.23	74.08	3.46
Cu-DPPZ-Phen	41.62	38.61	33.87	41.58	38.57	33.83	37.99	3.91
Cu-DPPN-Phen	70.88	69.27	71.51	70.84	69.23	71.47	70.51	1.16
Cisplatin	34.61	35.21	41.69	34.57	35.17	41.65	37.13	3.93

3.4 Gene expression data (Ct values and processing)

3.4.1 HT-29 24 h

Negative

	Actin	Tubulin				Target genes										
	Ref gene 1	Ref gene 2	Ref gene 3	Ref gene 4		IL-6	NF-KB	PARP	Casp9	Casp3	SMAC	BCL-2	BAX	XIAP	IAP1	IAP2
Ct 1	11.24	11.81				29.18	20.96	16.5	24.42	38.87	25.87			33.23	25.64	32.4
Ct 2	11.71	11.61				29.3	20.66	21.71	23.93	41.99	25.33			34.21	27.29	31.99
Ct 3	22.73															
Ct 4	22.26															
Ct 5																
Ct 6																
Ref Geometric mean	14.45734				Target mean	29.24	20.81	19.105	24.175	40.43	25.6	#DIV/0!	#DIV/0!	33.72	26.465	32.195
Ref S.D	5.635284				Target S.D	0.084853	0.212132	3.684026	0.346482	2.206173	0.381838	#DIV/0!	#DIV/0!	0.692965	1.166726	0.289914
					error propagated S.D	5.635923	5.639275	6.732643	5.645926	6.051746	5.648206	#DIV/0!	#DIV/0!	5.677731	5.754796	5.642737
					delta Ct	14.78266	6.352662	4.647662	9.717662	25.97266	11.14266	#DIV/0!	#DIV/0!	19.26266	12.00766	17.73766
					delta delta Ct	0	0	0	0	0	0	#DIV/0!	#DIV/0!	0	0	0
					Normalized ddCt	1	1	1	1	1	1	#DIV/0!	#DIV/0!	1	1	1
					positive error	5.635923	5.639275	6.732643	5.645926	6.051746	5.648206	#DIV/0!	#DIV/0!	5.677731	5.754796	5.642737
					negative error	-5.63592	-5.63928	-6.73264	-5.64593	-6.05175	-5.64821	#DIV/0!	#DIV/0!	-5.67773	-5.7548	-5.64274
					Normalized positive error	0.020111	0.020064	0.009403	0.019971	0.015075	0.01994	#DIV/0!	#DIV/0!	0.019536	0.01852	0.020016
					Normalized negative error	49.72581	49.84149	106.3475	50.07177	66.33718	50.15097	#DIV/0!	#DIV/0!	51.18789	53.99657	49.96121

Cisplatin

	Actin	Tubulin														
	Ref gene 1	Ref gene 2	Ref gene 3	Ref gene 4		IL-6	NF-KB	PARP	Casp9	Casp3	SMAC	BCL-2	BAX	XIAP	IAP1	IAP2
Ct 1	11.56	13.54				31.55	21.32	17.84	19.71	31.58	24.55			28.61	28.57	32.86
Ct 2	11.96	13.37				32.72	21.5	19.66	16.91	31.8	24.46			30.69	28.82	32.5
Ct 3	22.43															
Ct 4	21.92															
Ct 5																
Ct 6																
Ref Geometric mean	15.19444				Target mean	32.135	21.41	18.75	18.31	31.69	24.505	#DIV/0!	#DIV/0!	29.65	28.695	32.68
Ref S.D	5.002938				target S.D	0.827315	0.127279	1.286934	1.979899	0.155563	0.06364	#DIV/0!	#DIV/0!	1.470782	0.176777	0.254558
					error propagated S.D	5.070881	5.004557	5.165809	5.380463	5.005356	5.003343	#DIV/0!	#DIV/0!	5.214651	5.00606	5.00941
					delta Ct	16.94056	6.215556	3.555556	3.115556	16.49556	9.310556	#DIV/0!	#DIV/0!	14.45556	13.50056	17.48556
					delta delta Ct	2.157893	-0.13711	-1.09211	-6.60211	-9.47711	-1.83211	#DIV/0!	#DIV/0!	-4.80711	1.492893	-0.25211
					Normalized ddCt	0.224083	1.099697	2.131851	97.14761	712.678	3.560566	#DIV/0!	#DIV/0!	27.99518	0.355299	1.190945
					positive error	7.228775	4.86745	4.073703	-1.22164	-4.47175	3.171236	#DIV/0!	#DIV/0!	0.407544	6.498953	4.757303
					negative error	-2.91299	-5.14166	-6.25792	-11.9826	-14.4825	-6.83545	#DIV/0!	#DIV/0!	-10.0218	-3.51317	-5.26152
					Normalized positive error	0.006667	0.034257	0.059387	2.332122	22.18866	0.11101	#DIV/0!	#DIV/0!	0.753905	0.011057	0.036975
					Normalized negative error	7.531765	35.30164	76.52801	4046.812	22890.52	114.2024	#DIV/0!	#DIV/0!	1039.56	11.41743	38.35962

Cu-Phen (**1**)

	Actin	Tubulin														
	Ref gene 1	Ref gene 2	Ref gene 3	Ref gene 4		IL-6	NF-KB	PARP	Casp9	Casp3	SMAC	BCL-2	BAX	XIAP	IAP1	IAP2
Ct 1	20.49	22.23				32.11	33.69	31.68	31.35	30.06	14.6				42.42	17.51
Ct 2	21.26	21.79				31.16	32.92	31.5	31.06	31.02	14.7				42.35	17.69
Ct 3	11.66															
Ct 4	11.2															
Ct 5																
Ct 6																
Ref Geometric mean	17.37947				Target mean	31.635	33.305	31.59	31.205	30.54	14.65	#DIV/0!	#DIV/0!	#DIV/0!	42.385	17.6
Ref S.D	5.204885				target S.D	0.671751	0.544472	0.127279	0.205061	0.678823	0.070711	#DIV/0!	#DIV/0!	#DIV/0!	0.049497	0.127279
					error propagated S.D	5.248055	5.233286	5.206441	5.208923	5.248965	5.205366	#DIV/0!	#DIV/0!	#DIV/0!	5.205121	5.206441
					delta Ct	14.25553	15.92553	14.21053	13.82553	13.16053	-2.72947	#DIV/0!	#DIV/0!	#DIV/0!	25.00553	0.220535
					delta delta Ct	-0.52713	9.572872	9.562872	4.107872	-12.8121	-13.8721	#DIV/0!	#DIV/0!	#DIV/0!	12.99787	-17.5171
					Normalized ddCt	1.441058	0.001313	0.001322	0.057997	7191.754	14994.31	#DIV/0!	#DIV/0!	#DIV/0!	0.000122	187577.6
					positive error	4.720927	14.80616	14.76931	9.316795	-7.56316	-8.66676	#DIV/0!	#DIV/0!	#DIV/0!	18.20299	-12.3107
					negative error	-5.77518	4.339586	4.356431	-1.10105	-18.0611	-19.0775	#DIV/0!	#DIV/0!	#DIV/0!	7.792752	-22.7236
					Normalized positive error	0.037919	3.49E-05	3.58E-05	0.001568	189.1207	406.4016	#DIV/0!	#DIV/0!	#DIV/0!	3.31E-06	5080.26
					Normalized negative error	54.76502	0.049392	0.048818	2.145109	27348.2	55321 9.9	#DIV/0!	#DIV/0!	#DIV/0!	0.00451	6925895

Cu-DPQ-Phen (**2**)

	Actin	Tubulin														
	Ref gene 1	Ref gene 2	Ref gene 3	Ref gene 4		IL-6	NF-KB	PARP	Casp9	Casp3	SMAC	BCL-2	BAX	XIAP	IAP1	IAP2
Ct 1	12.68	13.81				29.01	21.87	20.54	25.17	39.79	25.79			35.64	27.64	33.5
Ct 2	13.12	13.41				29.89	23.53	22.44	26.31	42.25	25.98			35.44	26.66	3.7
Ct 3	23.99															
Ct 4	23.53															
Ct 5																
Ct 6																
Ref Geometric mean	16.09612				Target mean	29.45	22.7	21.49	25.74	41.02	25.885	#DIV/0!	#DIV/0!	35.54	27.15	18.6
Ref S.D	5.439241				target S.D	0.622254	1.173797	1.343503	0.806102	1.739483	0.13435	#DIV/0!	#DIV/0!	0.141421	0.692965	21.07178
					error propagated S.D	5.474719	5.564454	5.602709	5.49865	5.710617	5.4409	#DIV/0!	#DIV/0!	5.44108	5.483206	21.76248
					delta Ct	13.35388	6.603877	5.393877	9.643877	24.92388	9.788877	#DIV/0!	#DIV/0!	19.44388	11.05388	2.503877
					delta delta Ct	-1.42879	0.251214	0.746214	-0.07379	-1.04879	-1.35379	#DIV/0!	#DIV/0!	0.181214	-0.95379	-15.2338
					Normalized ddCt	2.6922	0.840189	0.596166	1.052475	2.068788	2.555819	#DIV/0!	#DIV/0!	0.88196	1.936949	38532.43
					positive error	4.045933	5.815668	6.348923	5.424864	4.661831	4.087115	#DIV/0!	#DIV/0!	5.622294	4.52942	6.52869
					negative error	-6.9035	-5.31324	-4.85649	-5.57244	-6.7594	-6.79469	#DIV/0!	#DIV/0!	-5.25987	-6.43699	-36.9963
					Normalized positive error	0.060541	0.017755	0.012268	0.023278	0.039505	0.058838	#DIV/0!	#DIV/0!	0.020301	0.043302	0.010831
					Normalized negative error	119.7187	39.75983	28.97014	47.58501	108.3385	111.0208	#DIV/0!	#DIV/0!	38.31574	86.64181	1.37E+11

3.4.2 HT-29 48 h

Negative

	Actin	Tubulin				Target genes										
	Ref gene 1	Ref gene 2	Ref gene 3	Ref gene 4		IL-6	NF-KB	PARP	Casp9	Casp3	SMAC	BCL-2	BAX	XIAP	IAP1	IAP2
Ct 1	14.75	14				31.36	24.84	20.48	21.84	36.84	23.67			32.28	20.76	33.75
Ct 2	14.58	14.25				32.68	24.95	18.48	21.6	38.83	23.45			32.97	21.31	32.6
Ct 3	17.43															
Ct 4	18.54															
Ct 5																
Ct 6																
Ref Geometric mean	15.49946				Target mean	32.02	24.895	19.48	21.72	37.835	23.56	#DIV/0!	#DIV/0!	32.625	21.035	33.175
Ref S.D	1.904599				Target S.D	0.933381	0.077782	1.414214	0.169706	1.407142	0.155563	#DIV/0!	#DIV/0!	0.487904	0.388909	0.813173
					error propagated S.D	2.121013	1.906186	2.372235	1.912145	2.368026	1.910941	#DIV/0!	#DIV/0!	1.966099	1.9439	2.070929
					delta Ct	16.52054	9.395539	3.980539	6.220539	22.33554	8.060539	#DIV/0!	#DIV/0!	17.12554	5.535539	17.67554
					delta delta Ct	0	0	0	0	0	0	#DIV/0!	#DIV/0!	0	0	0
					Normalized ddCt	1	1	1	1	1	1	#DIV/0!	#DIV/0!	1	1	1
					positive error	2.121013	1.906186	2.372235	1.912145	2.368026	1.910941	#DIV/0!	#DIV/0!	1.966099	1.9439	2.070929
					negative error	-2.12101	-1.90619	-2.37223	-1.91214	-2.36803	-1.91094	#DIV/0!	#DIV/0!	-1.9661	-1.9439	-2.07093
					Normalized positive error	0.229885	0.266797	0.193146	0.265697	0.193711	0.265919	#DIV/0!	#DIV/0!	0.255944	0.259913	0.238006
					Normalized negative error	4.349993	3.74817	5.177424	3.763681	5.162343	3.760544	#DIV/0!	#DIV/0!	3.907103	3.847443	4.201571

Cisplatin

	Actin	Tubulin														
	Ref gene 1	Ref gene 2	Ref gene 3	Ref gene 4		IL-6	NF-KB	PARP	Casp9	Casp3	SMAC	BCL-2	BAX	XIAP	IAP1	IAP2
Ct 1	12.85	12.92				31.21	23.7	20.31	22.34	37.73	20.26			33.57	23	32.33
Ct 2	12.92	13.12				29.12	23.3	20	22.57	37.45	19.92			33.3	23.93	31.91
Ct 3	14.67															
Ct 4	15.51															
Ct 5																
Ct 6																
Ref Geometric mean	13.62701				Target mean	30.165	23.5	20.155	22.455	37.59	20.09	#DIV/0!	#DIV/0!	33.435	23.465	32.12
Ref S.D	1.13889				target S.D	1.477853	0.282843	0.219203	0.162635	0.19799	0.240416	#DIV/0!	#DIV/0!	0.190919	0.657609	0.296985
					error propagated S.D	1.865776	1.173486	1.159793	1.150443	1.155971	1.163989	#DIV/0!	#DIV/0!	1.154781	1.315112	1.176975
					delta Ct	16.53799	9.872988	6.527988	8.827988	23.96299	6.462988	#DIV/0!	#DIV/0!	19.80799	9.837988	18.49299
					delta delta Ct	0.017449	0.477449	2.547449	2.607449	1.627449	-1.59755	#DIV/0!	#DIV/0!	2.682449	4.302449	0.817449
					Normalized ddCt	0.987978	0.718247	0.171057	0.164089	0.32366	3.026293	#DIV/0!	#DIV/0!	0.155777	0.05068	0.567445
					positive error	1.883225	1.650935	3.707242	3.757892	2.78342	-0.43356	#DIV/0!	#DIV/0!	3.83723	5.617561	1.994423
					negative error	-1.84833	-0.69604	1.387655	1.457005	0.471477	-2.76154	#DIV/0!	#DIV/0!	1.527667	2.987336	-0.35953
					Normalized positive error	0.271077	0.318434	0.076561	0.07392	0.145247	1.350565	#DIV/0!	#DIV/0!	0.069965	0.020368	0.250968
					Normalized negative error	3.600825	1.620049	0.382185	0.364248	0.721226	6.781199	#DIV/0!	#DIV/0!	0.346838	0.126102	1.283005

Cu-Phen (**1**)

	Actin	Tubulin														
	Ref gene 1	Ref gene 2	Ref gene 3	Ref gene 4		IL-6	NF-KB	PARP	Casp9	Casp3	SMAC	BCL-2	BAX	XIAP	IAP1	IAP2
Ct 1	12.91	13.62				27.59	23.42	21.25	19.67	35.62	22.42			28.33	19	30.52
Ct 2	13.52	13.42				27.94	23.6	18.82	19.79	36.48	22.85			28.6	19.51	30.21
Ct 3	17.66															
Ct 4	18.4															
Ct 5																
Ct 6																
Ref Geometric mean	14.76636				Target mean	27.765	23.51	20.035	19.73	36.05	22.635	#DIV/0!	#DIV/0!	28.465	19.255	30.365
Ref S.D	2.431382				target S.D	0.247487	0.127279	1.718269	0.084853	0.608112	0.304056	#DIV/0!	#DIV/0!	0.190919	0.360624	0.219203
					error propagated S.D	2.443945	2.434711	2.977258	2.432862	2.506275	2.45032	#DIV/0!	#DIV/0!	2.438866	2.45798	2.441243
					delta Ct	12.99864	8.743638	5.268638	4.963638	21.28364	7.868638	#DIV/0!	#DIV/0!	13.69864	4.488638	15.59864
					delta delta Ct	-3.5219	-0.6519	1.288099	-1.2569	-1.0519	-0.1919	#DIV/0!	#DIV/0!	-3.4269	-1.0469	-2.0769
					Normalized ddCt	11.48677	1.571237	0.40949	2.389819	2.07326	1.142268	#DIV/0!	#DIV/0!	10.75474	2.066087	4.219
					positive error	-1.07796	1.78281	4.265357	1.175961	1.454374	2.258419	#DIV/0!	#DIV/0!	-0.98804	1.411079	0.364342
					negative error	-5.96585	-3.08661	-1.68916	-3.68976	-3.55818	-2.64222	#DIV/0!	#DIV/0!	-5.86577	-3.50488	-4.51814
					Normalized positive error	2.111043	0.290617	0.052	0.442589	0.364913	0.209001	#DIV/0!	#DIV/0!	1.983482	0.37603	0.776823
					Normalized negative error	62.50268	8.494988	3.224688	12.90415	11.77926	6.242919	#DIV/0!	#DIV/0!	58.31386	11.35205	22.91379

Cu-DPQ-Phen (**2**)

	Actin	Tubulin														
	Ref gene 1	Ref gene 2	Ref gene 3	Ref gene 4		IL-6	NF-KB	PARP	Casp9	Casp3	SMAC	BCL-2	BAX	XIAP	IAP1	IAP2
Ct 1	15.91	15.88				28.4	26.23	22.44	22.94	37.74	23.35			21.61	21.61	31.51
Ct 2	16.16	18.88				28.47	26.64	20.79		39.18	23.99			20.98	20.98	32.1
Ct 3	17.8															
Ct 4	17.58															
Ct 5																
Ct 6																
Ref Geometric mean	16.9981				Target mean	28.435	26.435	21.615	22.94	38.46	23.67	#DIV/0!	#DIV/0!	21.295	21.295	31.805
Ref S.D	1.237057				target S.D	0.049497	0.289914	1.166726	#DIV/0!	1.018234	0.452548	#DIV/0!	#DIV/0!	0.445477	0.445477	0.417193
					error propagated S.D	1.238047	1.270575	1.700459	#DIV/0!	1.60222	1.317236	#DIV/0!	#DIV/0!	1.314823	1.314823	1.305511
					delta Ct	11.4369	9.436896	4.616896	5.941896	21.4619	6.671896	#DIV/0!	#DIV/0!	4.296896	4.296896	14.8069
					delta delta Ct	-5.08364	0.041357	0.636357	-0.27864	-0.87364	-1.38864	#DIV/0!	#DIV/0!	-12.8286	-1.23864	-2.86864
					Normalized ddCt	33.9101	0.971741	0.643335	1.213053	1.832284	2.618323	#DIV/0!	#DIV/0!	7274.554	2.359765	7.303779
					positive error	-3.8456	1.311932	2.336816	#DIV/0!	0.728577	-0.0714	#DIV/0!	#DIV/0!	-11.5138	0.07618	-1.56313
					negative error	-6.32169	-1.22922	-1.0641	#DIV/0!	-2.47586	-2.70588	#DIV/0!	#DIV/0!	-14.1435	-2.55347	-4.17415
					Normalized positive error	14.37606	0.402781	0.197947	#DIV/0!	0.603499	1.050741	#DIV/0!	#DIV/0!	2924.187	0.948566	2.954946
					Normalized negative error	79.9868	2.344398	2.090868	#DIV/0!	5.563001	6.524552	#DIV/0!	#DIV/0!	18097.04	5.87043	18.05285

3.4.3 PC-3 24 h

Negative

	Actin	Tubulin				Target genes										
	Ref gene 1	Ref gene 2	Ref gene 3	Ref gene 4		IL-6	NF-KB	PARP	Casp9	Casp3	SMAC	BCL-2	BAX	XIAP	IAP1	IAP2
Ct 1	13.5	12.76				23.43	22.6	17.55	21.23	36.62	18.15			35.93	21.73	23.53
Ct 2	14.9	13.52				22.76	23.87	17.85	21.78	41.85	18.21			30.7	22.2	22.81
Ct 3	14.92															
Ct 4	14.73															
Ct 5																
Ct 6																
Ref Geometric mean	14.02985				Target mean	23.095	23.235	17.7	21.505	39.235	18.18	#DIV/0!	#DIV/0!	33.315	21.965	23.17
Ref S.D	0.915331				Target S.D	0.473762	0.898026	0.212132	0.388909	3.698168	0.042426	#DIV/0!	#DIV/0!	3.698168	0.33234	0.509117
					error propagated S.D	1.03067	1.282295	0.93959	0.994525	3.809761	0.916313	#DIV/0!	#DIV/0!	3.809761	0.973797	1.047392
					delta Ct	9.065146	9.205146	3.670146	7.475146	25.20515	4.150146	#DIV/0!	#DIV/0!	19.28515	7.935146	9.140146
					delta delta Ct	0	0	0	0	0	0	#DIV/0!	#DIV/0!	0	0	0
					Normalized ddCt	1	1	1	1	1	1	#DIV/0!	#DIV/0!	1	1	1
					positive error	1.03067	1.282295	0.93959	0.994525	3.809761	0.916313	#DIV/0!	#DIV/0!	3.809761	0.973797	1.047392
					negative error	-1.03067	-1.28229	-0.93959	-0.99453	-3.80976	-0.91631	#DIV/0!	#DIV/0!	-3.80976	-0.9738	-1.04739
					Normalized positive error	0.489483	0.411141	0.521381	0.501901	0.07131	0.529861	#DIV/0!	#DIV/0!	0.07131	0.509164	0.483842
					Normalized negative error	2.042972	2.432256	1.917984	1.992424	14.02337	1.887286	#DIV/0!	#DIV/0!	14.02337	1.964002	2.06679

Cisplatin

	Actin	Tubulin														
	Ref gene 1	Ref gene 2	Ref gene 3	Ref gene 4		IL-6	NF-KB	PARP	Casp9	Casp3	SMAC	BCL-2	BAX	XIAP	IAP1	IAP2
Ct 1	15.13	13.8				21.41	22.91	17.99	20.7	37.79	18.29			39.54	22.72	22.5
Ct 2	13.98	14.82				21.67	23.33	17.73	20.87	38.99	18.48			37.4	23.55	22.39
Ct 3	16.97															
Ct 4	16.36															
Ct 5																
Ct 6																
Ref Geometric mean	15.13293				Target mean	21.54	23.12	17.86	20.785	38.39	18.385	#DIV/0!	#DIV/0!	38.47	23.135	22.445
Ref S.D	1.270664				target S.D	0.183848	0.296985	0.183848	0.120208	0.848528	0.13435	#DIV/0!	#DIV/0!	1.513209	0.586899	0.077782
					error propagated S.D	1.283895	1.304909	1.283895	1.276337	1.527935	1.277747	#DIV/0!	#DIV/0!	1.975952	1.399656	1.273042
					delta Ct	6.407068	7.987068	2.727068	5.652068	23.25707	3.252068	#DIV/0!	#DIV/0!	23.33707	8.002068	7.312068
					delta delta Ct	-2.6808	-1.2188	-0.9438	-1.8238	-1.9488	-0.8988	#DIV/0!	#DIV/0!	4.051922	0.066922	-1.8288
					Normalized ddCt	6.311916	2.326366	1.922626	3.538353	3.858601	1.863582	#DIV/0!	#DIV/0!	0.060291	0.954673	3.550637
					positive error	-1.3741	0.086831	0.340817	-0.5467	-0.4201	0.379669	#DIV/0!	#DIV/0!	6.027874	1.466578	-0.5550
					negative error	-3.9419	-2.5229	-2.2269	-3.0994	-3.4760	-2.1758	#DIV/0!	#DIV/0!	2.07597	-1.3327	-3.1011
					Normalized positive error	2.592221	0.941589	0.789594	1.460782	1.33806	0.768614	#DIV/0!	#DIV/0!	0.015326	0.36184	1.469205
					Normalized negative error	15.36923	5.747707	4.681507	8.570713	11.12716	4.51844	#DIV/0!	#DIV/0!	0.237176	2.518795	8.580848

Cu-Phen (**1**)

	Actin	Tubulin														
	Ref gene 1	Ref gene 2	Ref gene 3	Ref gene 4		IL-6	NF-KB	PARP	Casp9	Casp3	SMAC	BCL-2	BAX	XIAP	IAP1	IAP2
Ct 1	15.1	16.97				23.78	26.78	21.55	23.59	42.39	20.73			36.25	25.5	24.36
Ct 2	17.65	17.01				23.94	26.36	21.77	22.97		20.94			34.67	25.17	24.01
Ct 3	17.18															
Ct 4	17.22															
Ct 5																
Ct 6																
Ref Geometric mean	16.83426				Target mean	23.86	26.57	21.66	23.28	42.39	20.835	#DIV/0!	#DIV/0!	35.46	25.335	24.185
Ref S.D	0.893101				target S.D	0.113137	0.296985	0.155563	0.438406	#DIV/0!	0.148492	#DIV/0!	#DIV/0!	1.117229	0.233345	0.247487
					error propagated S.D	0.900239	0.941185	0.906548	0.994902	#DIV/0!	0.905362	#DIV/0!	#DIV/0!	1.430325	0.923082	0.926758
					delta Ct	7.02574	9.73574	4.82574	6.44574	25.55574	4.00074	#DIV/0!	#DIV/0!	18.62574	8.50074	7.35074
					delta delta Ct	-2.03941	0.530595	1.155595	-1.02941	0.350595	-0.14941	#DIV/0!	#DIV/0!	-0.65941	0.565595	-1.78941
					Normalized ddCt	4.110716	0.692269	0.448881	2.041183	0.784261	1.109112	#DIV/0!	#DIV/0!	1.579431	0.675677	3.456724
					positive error	-1.13917	1.47178	2.062143	-0.0345	#DIV/0!	0.755957	#DIV/0!	#DIV/0!	0.77092	1.488677	-0.86265
					negative error	-2.93964	-0.41059	0.249046	-2.02431	#DIV/0!	-1.05477	#DIV/0!	#DIV/0!	-2.08973	-0.35749	-2.71616
					Normalized positive error	2.202537	0.360537	0.23946	1.024204	#DIV/0!	0.592154	#DIV/0!	#DIV/0!	0.586044	0.356339	1.818372
					Normalized negative error	7.67222	1.32923	0.841452	4.067965	#DIV/0!	2.077383	#DIV/0!	#DIV/0!	4.256685	1.281192	6.571228

Cu-DPQ-Phen (**2**)

	Actin	Tubulin														
	Ref gene 1	Ref gene 2	Ref gene 3	Ref gene 4		IL-6	NF-KB	PARP	Casp9	Casp3	SMAC	BCL-2	BAX	XIAP	IAP1	IAP2
Ct 1	13.87	14.19				20.82	24.9	19.96	20.45	36.77	18.03			33.83	21.9	21.56
Ct 2	13.64	13.62				21.04	25.91	19.65	20.65	37.58	18.28			32.78	22.01	20.86
Ct 3	14.93															
Ct 4	14.66															
Ct 5																
Ct 6																
Ref Geometric mean	14.14297				Target mean	20.93	25.405	19.805	20.55	37.175	18.155	#DIV/0!	#DIV/0!	33.305	21.955	21.21
Ref S.D	0.545799				target S.D	0.155563	0.714178	0.219203	0.141421	0.572756	0.176777	#DIV/0!	#DIV/0!	0.742462	0.077782	0.494975
					error propagated S.D	0.567536	0.898859	0.588172	0.563823	0.791168	0.573713	#DIV/0!	#DIV/0!	0.921492	0.551314	0.736815
					delta Ct	6.787028	11.26203	5.662028	6.407028	23.03203	4.012028	#DIV/0!	#DIV/0!	19.16203	7.812028	7.067028
					delta delta Ct	-2.2781 2	2.056882	1.991882	-1.0681 2	-2.1731 2	-0.1381 2	#DIV/0!	#DIV/0!	-0.1231 2	-0.1231 2	-2.0731 2
					Normalized ddCt	4.850447	0.240335	0.251411	2.096696	4.50997	1.100468	#DIV/0!	#DIV/0!	1.089086	1.089086	4.207951
					positive error	-1.7105 8	2.955741	2.580055	-0.5042 9	-1.3819 5	0.435595	#DIV/0!	#DIV/0!	0.798374	0.428196	-1.3363
					negative error	-2.8456 5	1.158024	1.40371	-1.6319 4	-2.9642 9	-0.7118 3	#DIV/0!	#DIV/0!	-1.0446 1	-0.6744 3	-2.8099 3
					Normalized positive error	3.272929	0.128894	0.167235	1.41843	2.606204	0.739389	#DIV/0!	#DIV/0!	0.574997	0.743191	2.525034
					Normalized negative error	7.188314	0.448126	0.377956	3.099297	7.804389	1.637881	#DIV/0!	#DIV/0!	2.062808	1.595968	7.01252

3.4.4 PC-3 48 h

Negative

	Actin	Tubulin				Target genes										
	Ref gene 1	Ref gene 2	Ref gene 3	Ref gene 4		IL-6	NF-KB	PARP	Casp9	Casp3	SMAC	BCL-2	BAX	XIAP	IAP1	IAP2
Ct 1	16.24	14.25				25.31	24.29	19.7	21.38	36.41	19.49			30.75	22.83	25.7
Ct 2	15.02	14.33				25.39	24.31	19.34	22.07	36.33	19.71			30.52	22.97	24.48
Ct 3	16.61															
Ct 4	16.78															
Ct 5																
Ct 6																
Ref Geometric mean	15.50291				Target mean	25.35	24.3	19.52	21.725	36.37	19.6	#DIV/0!	#DIV/0!	30.635	22.9	25.09
Ref S.D	1.146393				Target S.D	0.056569	0.014142	0.254558	0.487904	0.056569	0.155563	#DIV/0!	#DIV/0!	0.162635	0.098995	0.86267
					error propagated S.D	1.147788	1.14648	1.174315	1.2459	1.147788	1.1569	#DIV/0!	#DIV/0!	1.157872	1.150659	1.434718
					delta Ct	9.847094	8.797094	4.017094	6.222094	20.86709	4.097094	#DIV/0!	#DIV/0!	15.13209	7.397094	9.587094
					delta delta Ct	0	0	0	0	0	0	#DIV/0!	#DIV/0!	0	0	0
					Normalized ddCt	1	1	1	1	1	1	#DIV/0!	#DIV/0!	1	1	1
					positive error	1.147788	1.14648	1.174315	1.2459	1.147788	1.1569	#DIV/0!	#DIV/0!	1.157872	1.150659	1.434718
					negative error	-1.14779	-1.14648	-1.17432	-1.2459	-1.14779	-1.1569	#DIV/0!	#DIV/0!	-1.15787	-1.15066	-1.43472
					Normalized positive error	0.451317	0.451726	0.443094	0.421645	0.451317	0.448475	#DIV/0!	#DIV/0!	0.448173	0.450419	0.369919
					Normalized negative error	2.215739	2.213731	2.256858	2.371665	2.215739	2.229777	#DIV/0!	#DIV/0!	2.23128	2.220153	2.703294

Cisplatin

	Actin	Tubulin														
	Ref gene 1	Ref gene 2	Ref gene 3	Ref gene 4		IL-6	NF-KB	PARP	Casp9	Casp3	SMAC	BCL-2	BAX	XIAP	IAP1	IAP2
Ct 1	16.82	16.25				23.68	24.39	21.64	22.44	37.06	21.47			32.31	23.83	24.09
Ct 2	16.54	16.36				23.75	24.29	20.84	22.5	37.93	21.73			30.71	23.79	24.84
Ct 3	18.92															
Ct 4	18.36															
Ct 5																
Ct 6																
Ref Geometric mean	17.17771				Target mean	23.715	24.34	21.24	22.47	37.495	21.6	#DIV/0!	#DIV/0!	31.51	23.81	24.465
Ref S.D	1.139446				target S.D	0.049497	0.070711	0.565685	0.042426	0.615183	0.183848	#DIV/0!	#DIV/0!	1.131371	0.028284	0.53033
					error propagated S.D	1.140552	1.141638	1.272139	1.140235	1.294908	1.154182	#DIV/0!	#DIV/0!	1.605772	1.139797	1.256816
					delta Ct	6.537288	7.162288	4.062288	5.292288	20.31729	4.422288	#DIV/0!	#DIV/0!	14.33229	6.632288	7.287288
					delta delta Ct	-3.30981	-1.63481	0.045193	-0.92981	-0.54981	0.325193	#DIV/0!	#DIV/0!	-0.79981	-0.76481	-2.29981
					Normalized ddCt	9.916334	3.10546	0.96916	1.905021	1.46389	0.798192	#DIV/0!	#DIV/0!	1.740868	1.699143	4.923919
					positive error	-2.16929	-0.49317	1.317332	0.210428	0.745101	1.479375	#DIV/0!	#DIV/0!	0.805913	0.37499	-1.04299
					negative error	-4.45033	-2.77644	-1.22695	-2.07004	-1.84471	-0.82899	#DIV/0!	#DIV/0!	-2.40553	-1.9046	-3.55662
					Normalized positive error	4.498009	1.407533	0.401276	0.864281	0.596626	0.358644	#DIV/0!	#DIV/0!	0.572	0.771111	2.060495
					Normalized negative error	21.8616	6.851618	2.340709	4.19899	3.59182	1.77644	#DIV/0!	#DIV/0!	5.29829	3.74406	11.76658

Cu-Phen (**1**)

	Actin	Tubulin														
	Ref gene 1	Ref gene 2	Ref gene 3	Ref gene 4		IL-6	NF-KB	PARP	Casp9	Casp3	SMAC	BCL-2	BAX	XIAP	IAP1	IAP2
Ct 1	12.32	12.81				22.44	21.5	17.46	19.81	34.71	17.72			26.73	19.78	23.54
Ct 2	12.24	12.74				22.68	21.18	17.48	20.39	33.85	17.8			26.1	19.76	23.81
Ct 3	14.23															
Ct 4	13.79															
Ct 5																
Ct 6																
Ref Geometric mean	13.0011				Target mean	22.56	21.34	17.47	20.1	34.28	17.76	#DIV/0!	#DIV/0!	26.415	19.77	23.675
Ref S.D	0.809677				target S.D	0.169706	0.226274	0.014142	0.410122	0.608112	0.056569	#DIV/0!	#DIV/0!	0.445477	0.014142	0.190919
					error propagated S.D	0.827271	0.8407	0.8098	0.907621	1.012609	0.811651	#DIV/0!	#DIV/0!	0.924136	0.8098	0.831881
					delta Ct	9.558904	8.338904	4.468904	7.098904	21.2789	4.758904	#DIV/0!	#DIV/0!	13.4139	6.768904	10.6739
					delta delta Ct	-0.28819	-0.45819	0.451809	0.876809	0.411809	0.661809	#DIV/0!	#DIV/0!	-1.71819	-0.62819	1.086809
					Normalized ddCt	1.221108	1.373818	0.731125	0.544571	0.75168	0.632085	#DIV/0!	#DIV/0!	3.290235	1.545625	0.470801
					positive error	0.53908	0.382509	1.26161	1.784431	1.424418	1.47346	#DIV/0!	#DIV/0!	-0.79406	0.18161	1.918691
					negative error	-1.11546	-1.29889	-0.35799	-0.03081	-0.6008	-0.14984	#DIV/0!	#DIV/0!	-2.64233	-1.43799	0.254928
					Normalized positive error	0.68821	0.767102	0.417078	0.290291	0.37257	0.360118	#DIV/0!	#DIV/0!	1.733941	0.881719	0.264494
					Normalized negative error	2.166643	2.460397	1.28164	1.021587	1.516557	1.109447	#DIV/0!	#DIV/0!	6.243376	2.709433	0.838029

Cu-DPQ-Phen (**2**)

	Actin	Tubulin														
	Ref gene 1	Ref gene 2	Ref gene 3	Ref gene 4		IL-6	NF-KB	PARP	Casp9	Casp3	SMAC	BCL-2	BAX	XIAP	IAP1	IAP2
Ct 1	13.34	14.82				20.87	23.95	19.53	19.81	36.96	19.53			30.52	22.16	22.44
Ct 2	12.97	14.89				21.63	24.27	19.81	19.91	35.78	19.92			30.67	22.23	22.7
Ct 3	15.87															
Ct 4	15.4															
Ct 5																
Ct 6																
Ref Geometric mean	14.50962				Target mean	21.25	24.11	19.67	19.86	36.37	19.725	#DIV/0!	#DIV/0!	30.595	22.195	22.57
Ref S.D	1.15012				target S.D	0.537401	0.226274	0.19799	0.070711	0.834386	0.275772	#DIV/0!	#DIV/0!	0.106066	0.049497	0.183848
					error propagated S.D	1.269479	1.172168	1.167038	1.152292	1.420907	1.18272	#DIV/0!	#DIV/0!	1.155001	1.151185	1.164722
					delta Ct	6.740379	9.600379	5.160379	5.350379	21.86038	5.215379	#DIV/0!	#DIV/0!	16.08538	7.685379	8.060379
					delta delta Ct	-3.10672	0.803285	1.143285	-0.87172	0.993285	1.118285	#DIV/0!	#DIV/0!	0.953285	0.288285	-1.52672
					Normalized ddCt	8.614119	0.573043	0.452728	1.829837	0.502333	0.460641	#DIV/0!	#DIV/0!	0.516455	0.818875	2.881291
					positive error	-1.83724	1.975452	2.310322	0.280577	2.414192	2.301005	#DIV/0!	#DIV/0!	2.108286	1.43947	-0.36199
					negative error	-4.37619	-0.36888	-0.02375	-2.02401	-0.42762	-0.06444	#DIV/0!	#DIV/0!	-0.20172	-0.8629	-2.69144
					Normalized positive error	3.573249	0.25429	0.201615	0.823262	0.18761	0.202922	#DIV/0!	#DIV/0!	0.231922	0.368703	1.285201
					Normalized negative error	20.76661	1.291352	1.0166	4.067119	1.345015	1.045675	#DIV/0!	#DIV/0!	1.150065	1.818691	6.459564

3.4.5 OE-33 24 h

Negative

	Actin	Tubulin				Target genes										
	Ref gene 1	Ref gene 2	Ref gene 3	Ref gene 4		IL-6	NF-KB	PARP	Casp9	Casp3	SMAC	BCL-2	BAX	XIAP	IAP1	IAP2
Ct 1	20.95	20.5				22.28	36.96	30.86	22.24	36.54	22.58			42.7	26.71	21.66
Ct 2	21.52	25.82				22.14	42.14	31.44	22.77	37.25	22.67			37.71	28.47	22.4
Ct 3	21.21															
Ct 4	20.38															
Ct 5																
Ct 6																
Ref Geometric mean	21.6561				Target mean	22.21	39.55	31.15	22.505	36.895	22.625	#DIV/0!	#DIV/0!	40.205	27.59	22.03
Ref S.D	2.048726				Target S.D	0.098995	3.662813	0.410122	0.374767	0.502046	0.06364	#DIV/0!	#DIV/0!	3.528463	1.244508	0.523259
					error propagated S.D	2.051117	4.196842	2.089373	2.082722	2.109343	2.049715	#DIV/0!	#DIV/0!	4.080114	2.397098	2.114493
					delta Ct	0.553902	17.8939	9.493902	0.848902	15.2389	0.968902	#DIV/0!	#DIV/0!	18.5489	5.933902	0.373902
					delta delta Ct	0	0	0	0	0	0	#DIV/0!	#DIV/0!	0	0	0
					Normalized ddCt	1	1	1	1	1	1	#DIV/0!	#DIV/0!	1	1	1
					positive error	2.051117	4.196842	2.089373	2.082722	2.109343	2.049715	#DIV/0!	#DIV/0!	4.080114	2.397098	2.114493
					negative error	-2.05112	-4.19684	-2.08937	-2.08222	-2.10934	-2.04971	#DIV/0!	#DIV/0!	-4.08011	-2.3971	-2.11449
					Normalized positive error	0.241297	0.054529	0.234983	0.236069	0.231752	0.241532	#DIV/0!	#DIV/0!	0.059124	0.189846	0.230927
					Normalized negative error	4.144266	18.33898	4.255631	4.236056	4.314949	4.140241	#DIV/0!	#DIV/0!	16.91362	5.267426	4.330378

Cisplatin

	Actin	Tubulin														
	Ref gene 1	Ref gene 2	Ref gene 3	Ref gene 4		IL-6	NF-KB	PARP	Casp9	Casp3	SMAC	BCL-2	BAX	XIAP	IAP1	IAP2
Ct 1	28.7	42.52				23.6	41.39	36.35	28.91							33.02
Ct 2	2.83	29.3						33		7					31.76	
Ct 3																
Ct 4																
Ct 5																
Ct 6																
Ref Geometric mean	17.83538				Target mean	23.6	41.39	34.675	28.91	7	#DIV/0!	#DIV/0!	#DIV/0!	#DIV/0!	31.76	33.02
Ref S.D	16.61158				target S.D	#DIV/0!	#DIV/0!	2.368808	#DIV/0!	#DIV/0!	#DIV/0!	#DIV/0!	#DIV/0!	#DIV/0!	#DIV/0!	#DIV/0!
					error propagated S.D	#DIV/0!	#DIV/0!	16.77962	#DIV/0!	#DIV/0!	#DIV/0!	#DIV/0!	#DIV/0!	#DIV/0!	#DIV/0!	#DIV/0!
					delta Ct	5.764623	23.55462	16.83962	11.07462	-10.8354	#DIV/0!	#DIV/0!	#DIV/0!	#DIV/0!	13.92462	15.18462
					delta delta Ct	5.210721	5.660721	7.345721	10.22572	-26.0743	#DIV/0!	#DIV/0!	#DIV/0!	#DIV/0!	7.990721	14.81072
					Normalized ddCt	0.027003	0.019768	0.006148	0.000835	70654563	#DIV/0!	#DIV/0!	#DIV/0!	#DIV/0!	0.003931	3.48E-05
					positive error	#DIV/0!	#DIV/0!	24.12535	#DIV/0!	#DIV/0!	#DIV/0!	#DIV/0!	#DIV/0!	#DIV/0!	#DIV/0!	#DIV/0!
					negative error	#DIV/0!	#DIV/0!	-9.4339	#DIV/0!	#DIV/0!	#DIV/0!	#DIV/0!	#DIV/0!	#DIV/0!	#DIV/0!	#DIV/0!
					Normalized positive error	#DIV/0!	#DIV/0!	5.46E-08	#DIV/0!	#DIV/0!	#DIV/0!	#DIV/0!	#DIV/0!	#DIV/0!	#DIV/0!	#DIV/0!
					Normalized negative error	#DIV/0!	#DIV/0!	691.6528	#DIV/0!	#DIV/0!	#DIV/0!	#DIV/0!	#DIV/0!	#DIV/0!	#DIV/0!	#DIV/0!

Cu-Phen (**1**)

	Actin	Tubulin														
	Ref gene 1	Ref gene 2	Ref gene 3	Ref gene 4		IL-6	NF-KB	PARP	Casp9	Casp3	SMAC	BCL-2	BAX	XIAP	IAP1	IAP2
Ct 1	24.45	24.69				25.33	41.44	37.39	26.54	7.82	25.25				33.83	25.86
Ct 2	23.78	23.48				24.82		35.49	25.83	41.37	25.07				31.83	25.55
Ct 3	26.16															
Ct 4	26.46															
Ct 5																
Ct 6																
Ref Geometric mean	24.81168				Target mean	25.075	41.44	36.44	26.185	24.595	25.16	#DIV/0!	#DIV/0!	#DIV/0!	32.83	25.705
Ref S.D	1.225931				target S.D	0.360624	#DIV/0!	1.343503	0.502046	23.72343	0.127279	#DIV/0!	#DIV/0!	#DIV/0!	1.414214	0.219203
					error propagated S.D	1.277872	#DIV/0!	1.818765	1.324748	23.75509	1.23252	#DIV/0!	#DIV/0!	#DIV/0!	1.871605	1.245374
					delta Ct	0.263316	16.62832	11.62832	1.373316	-0.21668	0.348316	#DIV/0!	#DIV/0!	#DIV/0!	8.018316	0.893316
					delta delta Ct	-0.29059	-1.26559	2.134414	0.524414	-15.4556	-0.62059	#DIV/0!	#DIV/0!	#DIV/0!	2.084414	0.519414
					Normalized ddCt	1.223137	2.404249	0.22776	0.695242	44936.07	1.5375	#DIV/0!	#DIV/0!	#DIV/0!	0.235792	0.697655
					positive error	0.987286	#DIV/0!	3.953179	1.849161	8.299501	0.611934	#DIV/0!	#DIV/0!	#DIV/0!	3.956019	1.764788
					negative error	-1.5684 6	#DIV/0!	0.315649	-0.80033	-39.2107	-1.85311	#DIV/0!	#DIV/0!	#DIV/0!	0.212808	-0.72596
					Normalized positive error	0.504426	#DIV/0!	0.064562	0.277554	0.003174	0.654319	#DIV/0!	#DIV/0!	#DIV/0!	0.064435	0.29427
					Normalized negative error	2.965876	#DIV/0!	0.80349	1.741504	6.36E+11	3.612773	#DIV/0!	#DIV/0!	#DIV/0!	0.862856	1.654001

Cu-DPQ-Phen (**2**)

	Actin	Tubulin														
	Ref gene 1	Ref gene 2	Ref gene 3	Ref gene 4		IL-6	NF-KB	PARP	Casp9	Casp3	SMAC	BCL-2	BAX	XIAP	IAP1	IAP2
Ct 1	24.46	23.91				24.68	41.63	37.49	25.4	15.93	27.4			37.69	32.78	28.47
Ct 2	24.34	23.88				24.7	39.16	36.42	25.41		26.77			26.12	35.52	28.35
Ct 3	27.93															
Ct 4	26.75															
Ct 5																
Ct 6																
Ref Geometric mean	25.16504				Target mean	24.69	40.395	36.955	25.405	15.93	27.085	#DIV/0!	#DIV/0!	31.905	34.15	28.41
Ref S.D	1.705772				target S.D	0.014142	1.746554	0.756604	0.007071	#DIV/0!	0.445477	#DIV/0!	#DIV/0!	8.181225	1.937473	0.084853
					error propagated S.D	1.70583	2.441333	1.86604	1.705786	#DIV/0!	1.762982	#DIV/0!	#DIV/0!	8.357159	2.581367	1.707881
					delta Ct	-0.47504	15.22996	11.78996	0.239961	-9.23504	1.919961	#DIV/0!	#DIV/0!	6.739961	8.984961	3.244961
					delta delta Ct	-1.02894	-2.66394	2.296059	-0.60894	-24.4739	0.951059	#DIV/0!	#DIV/0!	-11.8089	3.051059	2.871059
					Normalized ddCt	2.040526	6.33762	0.203619	1.525139	23301848	0.517253	#DIV/0!	#DIV/0!	3587.943	0.120653	0.136686
					positive error	0.676889	-0.22261	4.162099	1.096845	#DIV/0!	2.714041	#DIV/0!	#DIV/0!	-3.45178	5.632426	4.57894
					negative error	-2.73477	-5.10527	0.430019	-2.31473	#DIV/0!	-0.81192	#DIV/0!	#DIV/0!	-20.1661	0.469692	1.163178
					Normalized positive error	0.625513	1.166841	0.055858	0.467538	#DIV/0!	0.152403	#DIV/0!	#DIV/0!	10.94183	0.020159	0.041841
					Normalized negative error	6.656534	34.42236	0.742252	4.975106	#DIV/0!	1.75555	#DIV/0!	#DIV/0!	1176525	0.722119	0.446528

3.4.6 OE-33 48 h

Negative

	Actin	Tubulin				Target genes										
	Ref gene 1	Ref gene 2	Ref gene 3	Ref gene 4		IL-6	NF-KB	PARP	Casp9	Casp3	SMAC	BCL-2	BAX	XIAP	IAP1	IAP2
Ct 1	21.59	21.32				22.54	34.98	30	22.72	42.98	23.47			40.7	27.7	22.73
Ct 2	20.89	21.07				22.58	35.41	29.48	22.74	36.75	23.34				28.62	22.92
Ct 3	22.29															
Ct 4	22															
Ct 5																
Ct 6																
Ref Geometric mean	21.52101				Target mean	22.56	35.195	29.74	22.73	39.865	23.405	#DIV/0!	#DIV/0!	40.7	28.16	22.825
Ref S.D	0.541726				Target S.D	0.028284	0.304056	0.367696	0.014142	4.405275	0.091924	#DIV/0!	#DIV/0!	#DIV/0!	0.650538	0.13435
					error propagated S.D	0.542464	0.621222	0.654726	0.54191	4.438459	0.549469	#DIV/0!	#DIV/0!	#DIV/0!	0.846562	0.558137
					delta Ct	1.038993	13.67399	8.218993	1.208993	18.34399	1.883993	#DIV/0!	#DIV/0!	19.17899	6.638993	1.303993
					delta delta Ct	0	0	0	0	0	0	#DIV/0!	#DIV/0!	0	0	0
					Normalized ddCt	1	1	1	1	1	1	#DIV/0!	#DIV/0!	1	1	1
					positive error	0.542464	0.621222	0.654726	0.54191	4.438459	0.549469	#DIV/0!	#DIV/0!	#DIV/0!	0.846562	0.558137
					negative error	-0.54246	-0.62122	-0.65473	-0.54191	-4.43846	-0.54947	#DIV/0!	#DIV/0!	#DIV/0!	-0.84656	-0.55814
					Normalized positive error	0.686597	0.650122	0.635196	0.686861	0.04612	0.683271	#DIV/0!	#DIV/0!	#DIV/0!	0.556109	0.679179
					Normalized negative error	1.456457	1.538177	1.574317	1.455899	21.68249	1.463547	#DIV/0!	#DIV/0!	#DIV/0!	1.79821	1.472366

Cisplatin

	Actin	Tubulin														
	Ref gene 1	Ref gene 2	Ref gene 3	Ref gene 4		IL-6	NF-KB	PARP	Casp9	Casp3	SMAC	BCL-2	BAX	XIAP	IAP1	IAP2
Ct 1	20.07	24.22				25.35	36.34							26.68	30.09	24.61
Ct 2	18.64	28.53				24.03	37.67	33.6	26.95					11.36		28.56
Ct 3																
Ct 4																
Ct 5																
Ct 6																
Ref Geometric mean	22.54848				Target mean	24.69	37.005	33.6	26.95	#DIV/0!	#DIV/0!	#DIV/0!	#DIV/0!	19.02	30.09	26.585
Ref S.D	4.456864				target S.D	0.933381	0.940452	#DIV/0!	#DIV/0!	#DIV/0!	#DIV/0!	#DIV/0!	#DIV/0!	10.83288	#DIV/0!	2.793072
					error propagated S.D	4.553552	4.555006	#DIV/0!	#DIV/0!	#DIV/0!	#DIV/0!	#DIV/0!	#DIV/0!	11.71387	#DIV/0!	5.259742
					delta Ct	2.141519	14.45652	11.05152	4.401519	#DIV/0!	#DIV/0!	#DIV/0!	#DIV/0!	-3.52848	7.541519	4.036519
					delta delta Ct	1.102526	0.782526	2.832526	3.192526	#DIV/0!	#DIV/0!	#DIV/0!	#DIV/0!	-22.7075	0.902526	2.732526
					Normalized ddCt	0.4657	0.581348	0.140386	0.109384	#DIV/0!	#DIV/0!	#DIV/0!	#DIV/0!	6849058	0.534949	0.150462
					positive error	5.656078	5.337532	#DIV/0!	#DIV/0!	#DIV/0!	#DIV/0!	#DIV/0!	#DIV/0!	-10.9936	#DIV/0!	7.992268
					negative error	-3.45103	-3.77248	#DIV/0!	#DIV/0!	#DIV/0!	#DIV/0!	#DIV/0!	#DIV/0!	-34.4213	#DIV/0!	-2.52722
					Normalized positive error	0.019831	0.024731	#DIV/0!	#DIV/0!	#DIV/0!	#DIV/0!	#DIV/0!	#DIV/0!	2038.936	#DIV/0!	0.003927
					Normalized negative error	10.9361	13.66563	#DIV/0!	#DIV/0!	#DIV/0!	#DIV/0!	#DIV/0!	#DIV/0!	2.3E+10	#DIV/0!	5.764581

Cu-Phen (**1**)

	Actin	Tubulin														
	Ref gene 1	Ref gene 2	Ref gene 3	Ref gene 4		IL-6	NF-KB	PARP	Casp9	Casp3	SMAC	BCL-2	BAX	XIAP	IAP1	IAP2
Ct 1	24.28	25.05				26.18	37.94	32.54	23.53	38.42	24.38			36.6	33.41	25.69
Ct 2	24	24.4				26.18	39.99	32.59	23.98		24.46			37.23	33.31	25.25
Ct 3	24.6															
Ct 4	24.57															
Ct 5																
Ct 6																
Ref Geometric mean	24.48121				Target mean	26.18	38.965	32.565	23.755	38.42	24.42	#DIV/0!	#DIV/0!	36.915	33.36	25.47
Ref S.D	0.353308				target S.D	0	1.449569	0.035355	0.318198	#DIV/0!	0.056569	#DIV/0!	#DIV/0!	0.445477	0.070711	0.311127
					error propagated S.D	0.353308	1.492004	0.355073	0.475475	#DIV/0!	0.357808	#DIV/0!	#DIV/0!	0.568574	0.360315	0.470772
					delta Ct	1.698786	14.48379	8.083786	-0.72621	13.93879	-0.06121	#DIV/0!	#DIV/0!	12.43379	8.878786	0.988786
					delta delta Ct	0.659793	0.809793	-0.13521	-1.93521	-4.40521	-1.94521	#DIV/0!	#DIV/0!	-6.74521	2.239793	-0.31521
					Normalized ddCt	0.632969	0.570464	1.09825	3.82433	21.18846	3.850931	#DIV/0!	#DIV/0!	107.2778	0.211717	1.244119
					positive error	1.013101	2.301797	0.219866	-1.45973	#DIV/0!	-1.5874	#DIV/0!	#DIV/0!	-6.17663	2.600108	0.155565
					negative error	0.306485	-0.68221	-0.49028	-2.41068	#DIV/0!	-2.30302	#DIV/0!	#DIV/0!	-7.31378	1.879478	-0.78598
					Normalized positive error	0.49548	0.20281	0.858645	2.750572	#DIV/0!	3.005071	#DIV/0!	#DIV/0!	72.33555	0.164926	0.897781
					Normalized negative error	0.80861	1.604597	1.404717	5.317257	#DIV/0!	4.934881	#DIV/0!	#DIV/0!	159.099	0.271782	1.724263

Cu-DPQ-Phen (**2**)

	Actin	Tubulin														
	Ref gene 1	Ref gene 2	Ref gene 3	Ref gene 4		IL-6	NF-KB	PARP	Casp9	Casp3	SMAC	BCL-2	BAX	XIAP	IAP1	IAP2
Ct 1	23.72	23.98				24.99	38.93	31.91	24.55		24.72			40.85	32.26	25.44
Ct 2	23.63	24.32				25.26	38.22	32.31	24.43		25.23				33.37	25.38
Ct 3	23.45															
Ct 4	24.47															
Ct 5																
Ct 6																
Ref Geometric mean	23.92552				Target mean	25.125	38.575	32.11	24.49	#DIV/0!	24.975	#DIV/0!	#DIV/0!	40.85	32.815	25.41
Ref S.D	0.402662				target S.D	0.190919	0.502046	0.282843	0.084853	#DIV/0!	0.360624	#DIV/0!	#DIV/0!	#DIV/0!	0.784889	0.042426
					error propagated S.D	0.445631	0.643573	0.492074	0.411505	#DIV/0!	0.540543	#DIV/0!	#DIV/0!	#DIV/0!	0.882149	0.404891
					delta Ct	1.199483	14.64948	8.184483	0.564483	#DIV/0!	1.049483	#DIV/0!	#DIV/0!	16.92448	8.889483	1.484483
					delta delta Ct	0.16049	0.97549	-0.03451	-0.64451	#DIV/0!	-0.83451	#DIV/0!	#DIV/0!	-2.25451	2.25049	0.18049
					Normalized ddCt	0.894721	0.508567	1.024209	1.563208	#DIV/0!	1.783251	#DIV/0!	#DIV/0!	4.771721	0.210153	0.882403
					positive error	0.606121	1.619064	0.457564	-0.233	#DIV/0!	-0.29397	#DIV/0!	#DIV/0!	#DIV/0!	3.132639	0.585381
					negative error	-0.28514	0.331917	-0.52658	-1.05601	#DIV/0!	-1.37505	#DIV/0!	#DIV/0!	#DIV/0!	1.368342	-0.2244
					Normalized positive error	0.656961	0.325547	0.728215	1.17528	#DIV/0!	1.226007	#DIV/0!	#DIV/0!	#DIV/0!	0.11402	0.666473
					Normalized negative error	1.218529	0.79448	1.440514	2.07918	#DIV/0!	2.593774	#DIV/0!	#DIV/0!	#DIV/0!	0.387336	1.168292

3.4.7 HeLa 24 h

Negative

	Actin	Tubulin				Target genes										
	Ref gene 1	Ref gene 2	Ref gene 3	Ref gene 4		IL-6	NF-KB	PARP	Casp9	Casp3	SMAC	BCL-2	BAX	XIAP	IAP1	IAP2
Ct 1	21.48	22.58				33.66	30.64	27.14	29.45	32.71	29.79			34.46	33.23	30.54
Ct 2	21.68	22.88				32.73	30.97	27.57	29.74	32.48	31.37			35.32	33.19	36.38
Ct 3																
Ct 4																
Ct 5																
Ct 6																
Ref Geometric mean	22.14718				Target mean	33.195	30.805	27.355	29.595	32.595	30.58	#DIV/0!	#DIV/0!	34.89	33.21	33.46
Ref S.D	0.680074				Target S.D	0.657609	0.233345	0.304056	0.205061	0.162635	1.117229	#DIV/0!	#DIV/0!	0.608112	0.028284	4.129504
					error propagated S.D	0.946018	0.718992	0.74495	0.710317	0.69925	1.307937	#DIV/0!	#DIV/0!	0.912305	0.680661	4.185128
					delta Ct	11.04782	8.657823	5.207823	7.447823	10.44782	8.432823	#DIV/0!	#DIV/0!	12.74282	11.06282	11.31282
					delta delta Ct	0	0	0	0	0	0	#DIV/0!	#DIV/0!	0	0	0
					Normalized ddCt	1	1	1	1	1	1	#DIV/0!	#DIV/0!	1	1	1
					positive error	0.946018	0.718992	0.74495	0.710317	0.69925	1.307937	#DIV/0!	#DIV/0!	0.912305	0.680661	4.185128
					negative error	-0.94602	-0.71899	-0.74495	-0.71032	-0.69925	-1.30794	#DIV/0!	#DIV/0!	-0.9123	-0.68066	-4.18513
					Normalized positive error	0.519063	0.607522	0.596689	0.611186	0.615892	0.403898	#DIV/0!	#DIV/0!	0.531336	0.623879	0.054973
					Normalized negative error	1.926548	1.646032	1.675916	1.636163	1.62366	2.475873	#DIV/0!	#DIV/0!	1.88205	1.602874	18.19069

Cisplatin

	Actin	Tubulin														
	Ref gene 1	Ref gene 2	Ref gene 3	Ref gene 4		IL-6	NF-KB	PARP	Casp9	Casp3	SMAC	BCL-2	BAX	XIAP	IAP1	IAP2
Ct 1	23.93	25.31				32.97	32.26	28.97	32.99	32.38	32.01			36.52	33.93	36.29
Ct 2	23.92	24.93				33.35	32.32	29.36	32.88		32.11			35.33	34.62	31.6
Ct 3																
Ct 4																
Ct 5																
Ct 6																
Ref Geometric mean	24.51487				Target mean	33.16	32.29	29.165	32.935	32.38	32.06	#DIV/0!	#DIV/0!	35.925	34.275	33.945
Ref S.D	0.707172				target S.D	0.268701	0.042426	0.275772	0.077782	#DIV/0!	0.070711	#DIV/0!	#DIV/0!	0.841457	0.487904	3.316331
					error propagated S.D	0.7565	0.708443	0.75904	0.711436	#DIV/0!	0.710698	#DIV/0!	#DIV/0!	1.099155	0.859152	3.390891
					delta Ct	8.645131	7.775131	4.650131	8.420131	7.865131	7.545131	#DIV/0!	#DIV/0!	11.41013	9.760131	9.430131
					delta delta Ct	-2.40269	-0.88269	-0.55769	0.972308	-2.58269	-0.88769	#DIV/0!	#DIV/0!	-1.33269	-1.30269	-1.88269
					Normalized ddCt	5.287889	1.843812	1.471912	0.50969	5.990564	1.850214	#DIV/0!	#DIV/0!	2.518722	2.466887	3.687625
					positive error	-1.64619	-0.17425	0.201348	1.683745	#DIV/0!	-0.17699	#DIV/0!	#DIV/0!	-0.23354	-0.44354	1.508199
					negative error	-3.15919	-1.59113	-1.31673	0.260872	#DIV/0!	-1.59839	#DIV/0!	#DIV/0!	-2.43185	-2.16184	-5.27358
					Normalized positive error	3.130064	1.128377	0.869737	0.311274	#DIV/0!	1.130526	#DIV/0!	#DIV/0!	1.175714	1.359937	0.35155
					Normalized negative error	8.933289	3.012863	2.491012	0.834583	#DIV/0!	3.028052	#DIV/0!	#DIV/0!	5.395837	4.474863	38.68179

Cu-Phen (**1**)

	Actin	Tubulin														
	Ref gene 1	Ref gene 2	Ref gene 3	Ref gene 4		IL-6	NF-KB	PARP	Casp9	Casp3	SMAC	BCL-2	BAX	XIAP	IAP1	IAP2
Ct 1	20.37	21.35				32.61	30.14	25.97	26.41	30.8	27.61			34.24	32.35	29.97
Ct 2	20.35	22.2				33.29	30.51	25.94	26.41	8.58	27.63			33.43	30.75	30.1
Ct 3																
Ct 4																
Ct 5																
Ct 6																
Ref Geometric mean	21.05361				Target mean	32.95	30.325	25.955	26.41	19.69	27.62	#DIV/0!	#DIV/0!	33.835	31.55	30.035
Ref S.D	0.887633				target S.D	0.480833	0.26163	0.021213	0	15.71191	0.014142	#DIV/0!	#DIV/0!	0.572756	1.131371	0.091924
					error propagated S.D	1.009501	0.925387	0.887886	0.887633	15.73697	0.887745	#DIV/0!	#DIV/0!	1.056381	1.438017	0.89238
					delta Ct	11.89639	9.27139	4.90139	5.35639	-1.36361	6.56639	#DIV/0!	#DIV/0!	12.78139	10.49639	8.98139
					delta delta Ct	0.848567	0.613567	-0.30643	-2.09143	-11.8114	-1.86643	#DIV/0!	#DIV/0!	0.038567	-0.56643	-2.33143
					Normalized ddCt	0.555336	0.653579	1.236646	4.261712	3594.145	3.646299	#DIV/0!	#DIV/0!	0.973622	1.480858	5.03305
					positive error	1.858068	1.538954	0.581453	-1.2038	3.925533	-0.97869	#DIV/0!	#DIV/0!	1.094948	0.871584	-1.43905
					negative error	-0.16093	-0.31182	-1.19432	-2.97907	-27.5484	-2.75418	#DIV/0!	#DIV/0!	-1.01781	-2.00445	-3.22381
					Normalized positive error	0.275845	0.344135	0.66829	2.303456	0.065811	1.970672	#DIV/0!	#DIV/0!	0.468153	0.546547	2.711429
					Normalized negative error	1.11801	1.241273	2.288368	7.884753	1.96E+08	6.746682	#DIV/0!	#DIV/0!	2.024849	4.012356	9.342526

Cu-DPQ-Phen (**2**)

	Actin	Tubulin														
	Ref gene 1	Ref gene 2	Ref gene 3	Ref gene 4		IL-6	NF-KB	PARP	Casp9	Casp3	SMAC	BCL-2	BAX	XIAP	IAP1	IAP2
Ct 1	24.87	26.91				35.2	32.97	30.15	33.15	5.54	34.32			37.08	33.93	31.04
Ct 2	24.74	26.03				35.79	32.32	29.93	33.88		32.84			36.44	33.45	31.15
Ct 3																
Ct 4																
Ct 5																
Ct 6																
Ref Geometric mean	25.62217				Target mean	35.495	32.645	30.04	33.515	5.54	33.58	#DIV/0!	#DIV/0!	36.76	33.69	31.095
Ref S.D	1.027598				target S.D	0.417193	0.459619	0.155563	0.516188	#DIV/0!	1.046518	#DIV/0!	#DIV/0!	0.452548	0.339411	0.077782
					error propagated S.D	1.109057	1.125703	1.039307	1.14996	#DIV/0!	1.466683	#DIV/0!	#DIV/0!	1.122835	1.082201	1.030538
					delta Ct	9.872834	7.022834	4.417834	7.892834	-20.0822	7.957834	#DIV/0!	#DIV/0!	11.13783	8.067834	5.472834
					delta delta Ct	-1.17499	-1.63499	-0.78999	0.445011	-30.53	-0.47499	#DIV/0!	#DIV/0!	-1.60499	-2.99499	-5.83999
					Normalized ddCt	2.257911	3.105851	1.729061	0.734579	1.55E+09	1.389907	#DIV/0!	#DIV/0!	3.041934	7.97226	57.28116
					positive error	-0.06593	-0.50929	0.249318	1.594971	#DIV/0!	0.991694	#DIV/0!	#DIV/0!	-0.48215	-1.91279	-4.80945
					negative error	-2.28405	-2.76069	-1.8293	-0.70495	#DIV/0!	-1.94167	#DIV/0!	#DIV/0!	-2.72782	-4.07719	-6.87053
					Normalized positive error	1.04676	1.423345	0.841294	0.331029	#DIV/0!	0.502887	#DIV/0!	#DIV/0!	1.396827	3.76536	28.04071
					Normalized negative error	4.87042	6.777213	3.553635	1.630087	#DIV/0!	3.841505	#DIV/0!	#DIV/0!	6.624555	16.87937	117.0131

3.4.8 HeLa 48 h

Negative

	Actin	Tubulin				Target genes										
	Ref gene 1	Ref gene 2	Ref gene 3	Ref gene 4		IL-6	NF-KB	PARP	Casp9	Casp3	SMAC	BCL-2	BAX	XIAP	IAP1	IAP2
Ct 1	31.31	29.86				34.31	31.16	28.75	32.21	28.42	34.77			28.99	31.73	27.68
Ct 2	30.27	30.67				35.49	31.68	28.91	31.92	30.72	34.5			30.11	30.78	27.95
Ct 3																
Ct 4																
Ct 5																
Ct 6																
Ref Geometric mean	30.52283				Target mean	34.9	31.42	28.83	32.065	29.57	34.635	#DIV/0!	#DIV/0!	29.55	31.255	27.815
Ref S.D	0.61765				Target S.D	0.834386	0.367696	0.113137	0.205061	1.626346	0.190919	#DIV/0!	#DIV/0!	0.79196	0.671751	0.190919
					error propagated S.D	1.038119	0.718813	0.627926	0.650801	1.739681	0.646484	#DIV/0!	#DIV/0!	1.004336	0.912547	0.646484
					delta Ct	4.377172	0.897172	-1.69283	1.542172	-0.95283	4.112172	#DIV/0!	#DIV/0!	-0.97283	0.732172	-2.70783
					delta delta Ct	0	0	0	0	0	0	#DIV/0!	#DIV/0!	0	0	0
					Normalized ddCt	1	1	1	1	1	1	#DIV/0!	#DIV/0!	1	1	1
					positive error	1.038119	0.718813	0.627926	0.650801	1.739681	0.646484	#DIV/0!	#DIV/0!	1.004336	0.912547	0.646484
					negative error	-1.03812	-0.71881	-0.62793	-0.6508	-1.73968	-0.64648	#DIV/0!	#DIV/0!	-1.00434	-0.91255	-0.64648
					Normalized positive error	0.486962	0.607597	0.647106	0.636927	0.299436	0.638835	#DIV/0!	#DIV/0!	0.498499	0.531246	0.638835
					Normalized negative error	2.053549	1.645827	1.545342	1.570039	3.339614	1.565349	#DIV/0!	#DIV/0!	2.006021	1.882366	1.565349

Cisplatin

	Actin	Tubulin														
	Ref gene 1	Ref gene 2	Ref gene 3	Ref gene 4		IL-6	NF-KB	PARP	Casp9	Casp3	SMAC	BCL-2	BAX	XIAP	IAP1	IAP2
Ct 1	25.86	27.73				35.98	32.78	28.34	32.98	26.13	32.45			31.24	30.6	28.93
Ct 2	26.04	27.69				34.88	32.91	28.9	32.7	29.79	33.69			29.99	30.42	32.86
Ct 3																
Ct 4																
Ct 5																
Ct 6																
Ref Geometric mean	26.81548				Target mean	35.43	32.845	28.62	32.84	27.96	33.07	#DIV/0!	#DIV/0!	30.615	30.51	30.895
Ref S.D	1.018921				target S.D	0.777817	0.091924	0.39598	0.19799	2.588011	0.876812	#DIV/0!	#DIV/0!	0.883883	0.127279	2.77893
					error propagated S.D	1.281874	1.023059	1.093161	1.037979	2.781367	1.344247	#DIV/0!	#DIV/0!	1.34887	1.02684	2.95984
					delta Ct	8.61452	6.02952	1.80452	6.02452	1.14452	6.25452	#DIV/0!	#DIV/0!	3.79952	3.69452	4.07952
					delta delta Ct	4.237347	5.132347	3.497347	4.482347	2.097347	2.142347	#DIV/0!	#DIV/0!	4.772347	2.962347	6.787347
					Normalized ddCt	0.053019	0.028511	0.088551	0.044738	0.233688	0.226511	#DIV/0!	#DIV/0!	0.036592	0.128305	0.009053
					positive error	5.519221	6.155407	4.590508	5.520326	4.878714	3.486594	#DIV/0!	#DIV/0!	6.121217	3.989187	9.747187
					negative error	2.955474	4.109288	2.404187	3.444369	-0.68402	0.7981	#DIV/0!	#DIV/0!	3.423478	1.935508	3.827508
					Normalized positive error	0.021805	0.014029	0.041507	0.021788	0.033991	0.089213	#DIV/0!	#DIV/0!	0.014366	0.06297	0.001164
					Normalized negative error	0.128918	0.05794	0.188916	0.091863	1.606609	0.575106	#DIV/0!	#DIV/0!	0.093203	0.261429	0.070438

Cu-Phen (**1**)

	Actin	Tubulin														
	Ref gene 1	Ref gene 2	Ref gene 3	Ref gene 4		IL-6	NF-KB	PARP	Casp9	Casp3	SMAC	BCL-2	BAX	XIAP	IAP1	IAP2
Ct 1	30.4	30.92				35.85	34.51	29.37	32.14	1.75	35.52			9.37	30.42	29.97
Ct 2	30.92	30.94				34.81	30.94	29.24	32.27	31.62	35.16			30.49	32.67	29.58
Ct 3																
Ct 4																
Ct 5																
Ct 6																
Ref Geometric mean	30.79415				Target mean	35.33	32.725	29.305	32.205	16.685	35.34	#DIV/0!	#DIV/0!	19.93	31.545	29.775
Ref S.D	0.263502				target S.D	0.735391	2.524371	0.091924	0.091924	21.12128	0.254558	#DIV/0!	#DIV/0!	14.9341	1.59099	0.275772
					error propagated S.D	0.781174	2.538087	0.279076	0.279076	21.12292	0.366379	#DIV/0!	#DIV/0!	14.93642	1.612663	0.381423
					delta Ct	4.53585	1.93085	-1.48915	1.41085	-14.1091	4.54585	#DIV/0!	#DIV/0!	-10.8641	0.75085	-1.01915
					delta delta Ct	0.158678	1.033678	0.203678	-0.13132	-13.1563	0.433678	#DIV/0!	#DIV/0!	-9.89132	0.018678	1.688678
					Normalized ddCt	0.895845	0.488463	0.868334	1.095297	9129.511	0.740372	#DIV/0!	#DIV/0!	949.6959	0.987137	0.310211
					positive error	0.939853	3.571765	0.482754	0.147754	7.966601	0.800057	#DIV/0!	#DIV/0!	5.045098	1.631342	2.070101
					negative error	-0.6225	-1.5044	-0.0754	-0.4104	-34.2792	0.0673	#DIV/0!	#DIV/0!	-24.827	-1.59399	1.307255
					Normalized positive error	0.521286	0.084099	0.71561	0.902655	0.003998	0.574327	#DIV/0!	#DIV/0!	0.030288	0.322788	0.238143
					Normalized negative error	1.539537	2.837083	1.053651	1.329052	2.08E+10	0.954423	#DIV/0!	#DIV/0!	29777958	3.018821	0.404089

Cu-DPQ-Phen (**2**)

	Actin	Tubulin														
	Ref gene 1	Ref gene 2	Ref gene 3	Ref gene 4		IL-6	NF-KB	PARP	Casp9	Casp3	SMAC	BCL-2	BAX	XIAP	IAP1	IAP2
Ct 1	26.83	28.31				34.09	31.78	28.77	32.86	31.87	32.66			32.34	30.75	31.04
Ct 2	26.52	27.05				34.55	31	29.35	32.6	27.59	34.61			31.05	31.43	31.15
Ct 3																
Ct 4																
Ct 5																
Ct 6																
Ref Geometric mean	27.16911				Target mean	34.32	31.39	29.06	32.73	29.73	33.635	#DIV/0!	#DIV/0!	31.695	31.09	31.095
Ref S.D	0.785679				target S.D	0.325269	0.551543	0.410122	0.183848	3.026417	1.378858	#DIV/0!	#DIV/0!	0.912168	0.480833	0.077782
					error propagated S.D	0.850348	0.959944	0.88628	0.806903	3.126738	1.586991	#DIV/0!	#DIV/0!	1.203886	0.921136	0.78952
					delta Ct	7.150895	4.220895	1.890895	5.560895	2.560895	6.465895	#DIV/0!	#DIV/0!	4.525895	3.920895	3.925895
					delta delta Ct	2.773723	3.323723	3.583723	4.018723	3.513723	2.353723	#DIV/0!	#DIV/0!	5.498723	3.188723	6.633723
					Normalized ddCt	0.146227	0.099876	0.083405	0.061694	0.087552	0.195641	#DIV/0!	#DIV/0!	0.022117	0.109673	0.01007
					positive error	3.624071	4.283666	4.470002	4.825625	6.640461	3.940714	#DIV/0!	#DIV/0!	6.702609	4.109859	7.423243
					negative error	1.923375	2.363779	2.697443	3.21182	0.386985	0.766731	#DIV/0!	#DIV/0!	4.294837	2.267587	5.844203
					Normalized positive error	0.081105	0.051344	0.045123	0.035265	0.010024	0.065122	#DIV/0!	#DIV/0!	0.009601	0.057917	0.005826
					Normalized negative error	0.263637	0.194282	0.154166	0.107931	0.764726	0.587748	#DIV/0!	#DIV/0!	0.050948	0.207677	0.017407

3.4.9 MCF-7 24 h

Negative

	Actin	Tubulin				Target genes										
	Ref gene 1	Ref gene 2	Ref gene 3	Ref gene 4		IL-6	NF-KB	PARP	Casp9	Casp3	SMAC	BCL-2	BAX	XIAP	IAP1	IAP2
Ct 1	18.47	15.48				26.75	28.07	23.3	21.38	40.81	17.74	27.755	22.754	31.14	23.02	26.85
Ct 2	18.67	15.6				26.51	28.43	19.51	22.28		17.53	27.755	23.477	32.64	23.54	23.81
Ct 3	15.615	17.58						35.95	22.151	38.867	22.103	27.702	22.43	32.373	25.994	30.939
Ct 4	15.615	17.58							22.151	38.867	22.545	27.69	22.839	32.373	25.994	30.939
Ct 5	15.99															
Ct 6	13.88															
Ref Geometric mean	16.38274				Target mean	26.63	28.25	26.25333	21.9905	39.51467	19.9795	27.7255	22.875	32.1315	24.637	28.1345
Ref S.D	1.543334				Target S.D	0.169706	0.254558	8.608718	0.411518	1.121792	2.714557	0.034414	0.438317	0.672877	1.581244	3.468029
					error propagated S.D	1.552636	1.564186	8.745965	1.597256	1.907956	3.122611	1.543717	1.604369	1.683639	2.209573	3.795933
					delta Ct	10.24726	11.86726	9.870589	5.607756	23.13192	3.596756	11.34276	6.492256	15.74876	8.254256	11.75176
					delta delta Ct	0	0	0	0	0	0	0	0	0	0	0
					Normalized ddCt	1	1	1	1	1	1	1	1	1	1	1
					positive error	1.552636	1.564186	8.745965	1.597256	1.907956	3.122611	1.543717	1.604369	1.683639	2.209573	3.795933
					negative error	-1.55264	-1.56419	-8.74597	-1.59726	-1.90796	-3.12261	-1.54372	-1.60437	-1.68364	-2.20957	-3.79593
					Normalized positive error	0.340887	0.338168	0.002329	0.330505	0.26647	0.114816	0.343001	0.328879	0.311296	0.216198	0.071996
					Normalized negative error	2.933527	2.957107	429.3366	3.025672	3.75277	8.709625	2.915447	3.040628	3.212373	4.625382	13.8896

Cisplatin

	Actin	Tubulin														
	Ref gene 1	Ref gene 2	Ref gene 3	Ref gene 4		IL-6	NF-KB	PARP	Casp9	Casp3	SMAC	BCL-2	BAX	XIAP	IAP1	IAP2
Ct 1	14.71	14.01				25.15	23.3	20.22	26.54		22.16	26.754	22.225	36.89	23.46	29.85
Ct 2	14.76	13.55				26.24	24.37	21.29	23.88		21.94	27.044	22.633	33.62	24.53	29.79
Ct 3	16.353	16.96				33	42.15		22.334	39.135	22.524	27.311	22.225	32.334	26.855	30.265
Ct 4	14.927	17.24				26.02		32.31	20.596	38.685	27.227	26.85	21.818	32.759	26.855	30.11
Ct 5	16.19															
Ct 6	15.9															
Ref Geometric mean	15.41435				Target mean	27.6025	29.94	24.60667	23.3375	38.91	23.46275	26.98975	22.22525	33.90075	25.425	30.00375
Ref S.D	1.248534				target S.D	3.628979	10.5877	6.6927	2.521451	0.318198	2.521029	0.2458	0.332722	2.06339	1.708025	0.222762
					error propagated S.D	3.837751	10.66106	6.808162	2.813637	1.288444	2.813258	1.2725	1.292108	2.411725	2.1157	1.268251
					delta Ct	12.18815	14.52565	9.192312	7.923145	23.49565	8.048395	11.5754	6.810895	18.4864	10.01065	14.5894
					delta delta Ct	1.940889	2.658389	-0.67828	2.315389	0.363722	4.451639	0.232639	0.318639	2.737639	1.756389	2.837639
					Normalized ddCt	0.260456	0.158396	1.600228	0.200909	0.777157	0.045701	0.851077	0.801826	0.14993	0.295988	0.139889
					positive error	5.77864	13.31945	6.129884	5.129026	1.652166	7.264897	1.505139	1.610747	5.149364	3.872089	4.10589
					negative error	-1.89686	-8.00267	-7.48644	-0.49825	-0.92472	1.638381	-1.03986	-0.97347	0.325914	-0.35931	1.569388
					Normalized positive error	0.018216	9.78E-05	0.01428	0.028577	0.318162	0.006502	0.352296	0.327429	0.028177	0.068294	0.058077
					Normalized negative error	3.724022	256.4739	179.3259	1.412497	1.898318	0.321217	2.056029	1.963556	0.797793	1.282813	0.336951

Cu-Phen (**1**)

	Actin	Tubulin														
	Ref gene 1	Ref gene 2	Ref gene 3	Ref gene 4		IL-6	NF-KB	PARP	Casp9	Casp3	SMAC	BCL-2	BAX	XIAP	IAP1	IAP2
Ct 1	13.96	12.94				23.62	22.9	20.63	23.58	42.54	22.6	27.244	23.173	34.28	25.23	26.37
Ct 2	14.27	13.2				22.38	23.96	21.55	23.52		22.9	27.819	23.015	36.1	26.62	26.37
Ct 3	15.504	17.135				26.94	24.02		21.285	40.645	22.792	27.587	23.39	32.504	25.855	25.88
Ct 4	17.975	16.942				26.17			6.034	40.645	22.229	27.026	23.267	33.842	26.7	25.277
Ct 5	14.48															
Ct 6	14.44															
Ref Geometric mean	14.99724				Target mean	24.7775	23.62667	21.09	18.60475	41.27667	22.63025	27.419	23.21125	34.1815	26.10125	25.97425
Ref S.D	1.733486				target S.D	2.137231	0.630026	0.650538	8.44828	1.094079	0.29487	0.35275	0.158153	1.485442	0.694579	0.519062
					error propagated S.D	2.75186	1.844426	1.851533	8.624291	2.049874	1.758386	1.769013	1.740685	2.282873	1.867462	1.80953
					delta Ct	9.780255	8.629422	6.092755	3.607505	26.27942	7.633005	12.42176	8.214005	19.18426	11.10401	10.97701
					delta delta Ct	-0.467	-3.23783	-3.77783	-2.00025	3.147499	4.036249	1.078999	1.721749	3.435499	2.849749	-0.77475
					Normalized ddCt	1.382233	9.433769	13.71644	4.000696	0.112852	0.060949	0.473357	0.303181	0.09243	0.13872	1.710895
					positive error	2.284859	-1.39341	-1.9263	6.624041	5.197373	5.794635	2.848012	3.462434	5.718372	4.717211	1.034779
					negative error	-3.21886	-5.08226	-5.62937	-10.6245	1.097626	2.277863	-0.69001	-0.01894	1.152626	0.982288	-2.58428
					Normalized positive error	0.205205	2.626986	3.800796	0.010138	0.027254	0.018015	0.138887	0.09072	0.018993	0.038017	0.488091
					Normalized negative error	9.310512	33.87761	49.50035	1578.723	0.467285	0.206203	1.613299	1.013212	0.449806	0.506177	5.997166

Cu-DPQ-Phen (**2**)

	Actin	Tubulin														
	Ref gene 1	Ref gene 2	Ref gene 3	Ref gene 4		IL-6	NF-KB	PARP	Casp9	Casp3	SMAC	BCL-2	BAX	XIAP	IAP1	IAP2
Ct 1	15.31	14.19				26.62	24.81	21.25	21.87		20.27	27.731	22.844	36.63	25.94	29.91
Ct 2	17.3	13.7				26.56	24.83	21.18	21.64		20.46	27.537	21.832	31.25	24.33	29.81
Ct 3	30.19	18.938				26.43	21.78		20.324	39.934	23.819	28.056	22.969	32.279	26.406	30.345
Ct 4	15.28						37.59	34.71	20.324	39.934	21.617	27.812	23.731	30.35	26.406	30.599
Ct 5	15.88															
Ct 6	15.82															
Ref Geometric mean	16.90918				Target mean	26.53667	27.2525	25.71333	21.0395	39.934	21.5415	27.784	22.844	32.62725	25.7705	30.166
Ref S.D	5.045083				target S.D	0.097125	7.039093	7.79142	0.831507	0	1.630855	0.214931	0.780286	2.782443	0.985138	0.370496
					error propagated S.D	5.046018	8.660352	9.282193	5.113147	5.045083	5.302127	5.04966	5.105067	5.761498	5.140366	5.058669
					delta Ct	9.627491	10.34332	8.804158	4.130325	23.02482	4.632325	10.87482	5.934825	15.71807	8.861325	13.25682
					delta delta Ct	-0.61976	-1.52393	-1.06643	-1.47743	-0.1071	1.035569	-0.46793	-0.55743	-0.03068	0.607069	1.505069
					Normalized ddCt	1.536624	2.875736	2.094247	2.784525	1.07706	0.487824	1.383125	1.471647	1.021494	0.656529	0.352313
					positive error	4.426254	7.13642	8.215761	3.635716	4.937985	6.337696	4.581728	4.547636	5.730817	5.747435	6.563738
					negative error	-5.66578	-10.1843	-10.3486	-6.59058	-5.15218	-4.26656	-5.51759	-5.6625	-5.79218	-4.5333	-3.5536
					Normalized positive error	0.046512	0.007108	0.003364	0.080453	0.032623	0.012364	0.04176	0.042759	0.01883	0.018614	0.010571
					Normalized negative error	50.76573	1163.522	1303.906	96.37441	35.55995	19.24696	45.81001	50.65029	55.41402	23.15573	11.74195

3.4.10 MCF-7 48 h

Negative

	Actin	Tubulin				Target genes																							
	Ref gene 1	Ref gene 2	Ref gene 3	Ref gene 4		IL-6	NF-KB	PARP	Casp9	Casp3	SMAC	BCL-2	BAX	XIAP	IAP1	IAP2	HMOX	TFAM	TFB1M	TFB2M	NRF-2	CLPP	LON	SPG7	YME1L1	DRP1	MFN1	MFN2	OPA1
Ct 1	29.62	29.64				31.87	36.57	34.2	31.46		31.63	32.475			37.87	34.24	27.21	25.69	35.49	33.68	24.66	42.12	33.61		29.58				26.23
Ct 2	28.94	29.54				32.46	38.12	33.25	31.27		30.9	32.674			38.73	34.39	26.25		35.53	42.94	22.36		34.21		32.76		18.2	24.86	23.95
Ct 3	25.83	29.74						30.09	21.8	6.637	33.16	34.933	35.99		28.43	28.26													
Ct 4	26.468	22.97				24.16		30.87		6.637	32.204	31.277	34.27			31.85													
Ct 5	28.64																												
Ct 6	27.66																												
Ref Geometric mean	27.81983				Target mean	29.49667	37.345	32.1025	28.17667	6.637	31.9735	32.83975	35.13	#DIV/0!	35.01	32.185	26.73	25.69	35.51	38.31	23.51	42.12	33.91	#DIV/0!	31.17	#DIV/0!	18.2	24.86	25.09
Ref S.D	2.220816				Target S.D	4.631094	1.096016	1.939542	5.523172	0	0.954168	1.525822	1.216224	#DIV/0!	5.714648	2.863733	0.678823	#DIV/0!	0.028284	6.547809	1.626346	#DIV/0!	0.424264	#DIV/0!	2.2486	#DIV/0!	#DIV/0!	#DIV/0!	1.612203
					error propagated S.D	5.136054	2.476544	2.948533	5.952937	2.220816	2.417118	2.694467	2.532039	#DIV/0!	6.131005	3.623946	2.322245	#DIV/0!	2.209096	6.914175	2.752639	#DIV/0!	2.260978	#DIV/0!	3.160415	#DIV/0!	#DIV/0!	#DIV/0!	2.744307
					delta Ct	1.676835	9.525168	4.282668	0.356835	-21.1828	4.153668	5.019918	7.310168	#DIV/0!	7.190168	4.365168	-1.08983	-2.12983	7.690168	10.49017	-4.30983	14.30017	6.090168	#DIV/0!	3.350168	#DIV/0!	-9.61983	-2.95983	-2.72983
					delta delta Ct	0	0	0	0	0	0	0	0	#DIV/0!	0	0	0	0	0	0	0	0	0	#DIV/0!	0	#DIV/0!	0	0	0
					Normalized ddCt	1	1	1	1	1	1	1	1	#DIV/0!	1	1	1	1	1	1	1	1	1	#DIV/0!	1	#DIV/0!	1	1	1
					positive error	5.136054	2.476544	2.948533	5.952937	2.220816	2.417118	2.694467	2.532039	#DIV/0!	6.131005	3.623946	2.322245	#DIV/0!	2.209096	6.914175	2.752639	#DIV/0!	2.260978	#DIV/0!	3.160415	#DIV/0!	#DIV/0!	#DIV/0!	2.744307
					negative error	-5.13605	-2.47654	-2.94853	-5.95294	-2.22082	-2.41712	-2.69447	-2.53204	#DIV/0!	-6.131	-3.62395	-2.32224	#DIV/0!	-2.2221	-6.91418	-2.75264	#DIV/0!	-2.26098	#DIV/0!	-3.16041	#DIV/0!	#DIV/0!	#DIV/0!	-2.74431
					Normalized positive error	0.028438	0.179674	0.12954	0.016143	0.21452	0.18723	0.154484	0.172894	#DIV/0!	0.014269	0.081112	0.199956	#DIV/0!	0.014493	0.008291	0.148379	#DIV/0!	0.208631	#DIV/0!	0.011846	#DIV/0!	#DIV/0!	#DIV/0!	0.149239

					Normalized negative error	35.16466	5.565627	7.719637	61.94589	4.661569	5.341028	6.473147	5.783886	#DIV/0!	70.0836	12.32868	5.010098	#DIV/0!	4.662151	120.6075	6.739488	#DIV/0!	4.793163	#DIV/0!	8.940867	#DIV/0!	#DIV/0!	#DIV/0!	6.700678

Cisplatin

	Actin	Tubulin																											
	Refgene 1	Refgene 2	Refgene 3	Ref gene 4		IL-6	NF-KB	PARP	Casp9	Casp3	SMAC	BCL-2	BAX	XIAP	IAP1	IAP2	HMOX	TFAM	TFB1M	TFB2M	NRF-2	CLPP	LON	SPG7	YME1L1	DRP1	MFN1	MFN2	OPA1
Ct 1	19.99	18.42				27.64	30.31	25.88	22.62	36.59	18.82	25.713		30.96	23.79	28.7	24.25	18.18	31.6	28	24.53		34.79	39.23	29.5	23.43		18.27	22.95
Ct 2	19.93	18.22				27.69	30.62	21.4	22.63	35.29	19.52	26.001		30.24	23.79	28.55	23.66	4.18		28.76	24.82	17.49	31.4						
Ct 3	13.196	22.88				25.12	40.23	31.05	25.87	18.118	21.711	26.499	41.37																
Ct 4	15.065	23.21				11.4	37.78	30.95	21.65	15.154	22.054	25.612	42.37		28.29	41.2													
Ct 5	16.56																												
Ct 6	16.79																												
Ref Geometric mean	18.1711				Target mean	22.9625	34.735	27.32	23.1925	26.288	20.52625	25.95625	41.87	30.6	25.29	32.81667	23.955	11.18	31.6	28.38	24.675	17.49	33.095	39.23	29.5	23.43	#DIV/0!	18.27	22.95
Ref S.D	3.202135				target S.D	7.801164	5.03259	4.626366	1.843229	11.22322	1.5980 7	0.397601	0.707107	0.509117	2.598076	7.260567	0.417193	9.899495	#DIV/0!	0.537401	0.205061	#DIV/0!	2.397092	#DIV/0!	#DIV/0!	#DIV/0!	#DIV/0!	#DIV/0!	#DIV/0!
					error propagated S.D	8.432783	5.964951	5.626645	3.694748	11.67109	3.578756	3.226725	3.279279	3.242356	4.123551	7.953333	3.229198	10.4045	#DIV/0!	3.246917	3.208694	#DIV/0!	3.999965	#DIV/0!	#DIV/0!	#DIV/0!	#DIV/0!	#DIV/0!	#DIV/0!
					delta Ct	4.791402	16.5639	9.148902	5.021402	8.116902	2.355152	7.785152	23.6989	12.4289	7.118902	14.64557	5.783902	-6.9911	13.4289	10.2089	6.503902	-0.6811	14.9239	21.0589	11.3289	5.258902	#DIV/0!	0.098902	4.789702
					delta delta Ct	3.114567	7.038733	4.866233	4.664567	29.29973	-1.79852	2.765233	16.38873	#DIV/0!	-0.07127	10.2804	6.873733	-4.86127	5.738733	-0.28127	10.81373	-14.9813	8.833733	#DIV/0!	7.978733	#DIV/0!	#DIV/0!	3.058733	7.508733
					Normalized ddCt	0.115457	0.007606	0.034286	0.00393	1.51E-09	3.478624	0.14709	1.17E-05	#DIV/0!	1.050639	0.000804	0.008527	29.06612	0.018727	1.215261	0.000556	32345.26	0.002192	#DIV/0!	0.003964	#DIV/0!	#DIV/0!	0.120013	0.005491
					positive error	11.54735	13.00368	10.49268	8.359315	40.97082	1.78024	5.991959	19.66801	#DIV/0!	4.052284	18.21573	10.10293	5.543236	#DIV/0!	2.965 6 5	14.02243	#DIV/0!	12.8337	#DIV/0!	#DIV/0!	#DIV/0!	#DIV/0!	#DIV/0!	#DIV/0!
					negative error	-5.31822	1.073783	-0.76022	0.969819	17.62864	-5.37727	-0.46149	13.10945	#DIV/0!	-4.19482	2.345068	3.644535	-15.2658	#DIV/0!	-3.52818	7.605039	#DIV/0!	4.833768	#DIV/0!	#DIV/0!	#DIV/0!	#DIV/0!	#DIV/0!	#DIV/0!

					Normalized positive error	0.000334	0.000122	0.000694	0.000305	4.64E-13	0.291135	0.000157	1.2E-06	#DIV/0!	0.000276	3.28E-06	0.000909	0.000214	#DIV/0!	0.128012	6.01E-05	#DIV/0!	0.000137	#DIV/0!	#DIV/0!	#DIV/0!	#DIV/0!	#DIV/0!	#DIV/0!
					Normalized negative error	39.89722	0.475072	1.693745	0.51057	4.93E-06	41.5643	1.376965	0.000113	#DIV/0!	18.31327	0.196818	0.000799	39396.2	#DIV/0!	11.5369	0.005136	#DIV/0!	0.000350	#DIV/0!	#DIV/0!	#DIV/0!	#DIV/0!	#DIV/0!	#DIV/0!

Cu-Phen (**1**)

	Actin	Tubulin																										
	Refgene 1	Refgene 2	Refgene 3	Ref gene 4		IL-6	NF-KB	PARP	Casp9	Casp3	SMAC	BCL-2	BAX	XIAP	IAP1	IAP2	HMOX	TFAM	TFB1M	TFB2M	NRF-2	CLPP	LON	SPG7	YME1L1	DRP1	MFN1	MFN2	OPA1
Ct 1	12.92	12.86				21.47	18.62	18.35	21.48	36.39	17.15	24.973		28.97	21.89	23.87	2.48	15.33	33.33	31.7	22.39	28.42	31.15	32.87	27.8	8.1	22.91		21.07
Ct 2	12.66	12.87				21.83	20.99	19.22	21.35	37.29	16.66	25.766		30.24	22.21	23.03			31.32	38.63			30.98	33.6				25.12	
Ct 3	15.333					25.48		27.42			21.679	25.142	10.2		29.55	28.35													
Ct 4	17.711	22.6				26.12	38.01	28.3	24.82		21.457	24.923	6.75		28.17														
Ct 5	14.48																												
Ct 6	14.44																												
Ref Geometric mean	14.83212				Target mean	23.725	25.87333	23.3225	22.55	36.84	19.2365	25.201	8.475	29.605	25.455	25.08333	2.48	15.33	32.325	35.165	22.39	28.42	31.065	33.235	27.8	8.1	22.91	25.12	21.07
Ref S.D	3.252653				target S.D	2.414684	10.57725	5.263753	1.966952	0.636396	2.701127	0.388147	2.439518	0.898026	3.974062	2.860023	#DIV/0!	#DIV/0!	1.421285	4.900025	#DIV/0!	#DIV/0!	0.120208	0.516188	#DIV/0!	#DIV/0!	#DIV/0!	#DIV/0!	#DIV/0!
					error propagated S.D	4.050982	11.06607	6.187637	3.801139	3.314326	4.227983	3.275731	4.065834	3.374345	5.135457	4.331222	#DIV/0!	#DIV/0!	3.549622	5.881514	#DIV/0!	#DIV/0!	3.254874	3.293358	#DIV/0!	#DIV/0!	#DIV/0!	#DIV/0!	#DIV/0!
					delta Ct	8.892876	11.04121	8.490376	7.717876	22.00788	4.404376	10.36888	-6.35712	14.77288	10.62288	10.25121	-12.3521	0.497876	17.49288	20.33288	7.557876	13.58788	16.23288	18.40288	12.96788	-6.73212	8.077876	10.28788	6.237876
					delta delta Ct	7.216041	1.516041	4.207707	7.361041	43.19071	0.250707	5.348957	-13.6673	#DIV/0!	3.432707	5.886041	-11.2623	2.627707	9.802707	9.842707	11.86771	-0.71229	10.14271	#DIV/0!	9.617707	#DIV/0!	17.69771	13.24771	8.967707
					Normalized ddCt	0.006726	0.349644	0.005412	0.006083	9.96E-14	0.840484	0.002453	13009.63	#DIV/0!	0.092609	0.016909	2456.337	0.161801	0.001112	0.001089	0.000268	1.638406	0.000885	#DIV/0!	0.001273	#DIV/0!	4.7E-06	0.000103	0.001997
					positive error	11.26702	12.58211	10.39534	11.16218	46.50503	4.478691	8.624688	-9.60146	#DIV/0!	8.568165	10.21726	#DIV/0!	#DIV/0!	13.35233	15.72422	#DIV/0!	#DIV/0!	13.39758	#DIV/0!	#DIV/0!	#DIV/0!	#DIV/0!	#DIV/0!	#DIV/0!

					negative error	3.16505959	-9.5500303	-1.979933	3.5599002	39.87638	-3.977228	2.073227	-17.7331	#DIV/0!	-1.702775	1.554818	#DIV/0!	#DIV/0!	6.253087	3.961194	#DIV/0!	#DIV/0!	6.878833	#DIV/0!	#DIV/0!	#DIV/0!	#DIV/0!	#DIV/0!	#DIV/0!	#DIV/0!
					Normalized positive error	0.000406	0.000163	0.000742	0.000436	1E-14	0.044852	0.002533	776.832	#DIV/0!	0.002635	0.000884	#DIV/0!	#DIV/0!	9.56E-05	1.85E-05	#DIV/0!	#DIV/0!	9.27E-05	#DIV/0!	#DIV/0!	#DIV/0!	#DIV/0!	#DIV/0!	#DIV/0!	#DIV/0!
					Normalized negative error	0.111487	749.629	3.944737	0.084794	9.91E-13	15.74995	0.237627	217872.8	#DIV/0!	3.255208	0.340371	#DIV/0!	#DIV/0!	0.013111	0.064204	#DIV/0!	#DIV/0!	0.008444	#DIV/0!	#DIV/0!	#DIV/0!	#DIV/0!	#DIV/0!	#DIV/0!	#DIV/0!

Cu-DPQ-Phen (**2**)

	Actin	Tubulin																										
	Refgene 1	Refgene 2	Refgene 3	Ref gene 4		IL-6	NF-KB	PARP	Casp9	Casp3	SMAC	BCL-2	BAX	XIAP	IAP1	IAP2	HMOX	TFAM	TFB1M	TFB2M	NRF-2	CLPP	LON	SPG7	YME1L1	DRP1	MFN1	MFN2	OPA1
Ct 1	14.62	13.98				25.93	24.53	20.61	21.52	35.94	21.97	24.26		29.55	23.47	30.12	25.99		30.77	28.58	27	26.85	30.72	33.89	30	23.52	23.73	23.91	
Ct 2	14.81	13.89				26.66	24.72	19.28	21.66	35.88	22.46	27.722		28.87	23.53	29.7	24.45	14.75	33.22	39.54	22.52	28.31	29.82	33.88	28.15		24.7	26.08	22.64
Ct 3	15.588						33.62		22.29		22.889	24.972	10.01		27.78														
Ct 4	15.768					25.5	36.58				21.733	23.658	11.01		29.88														
Ct 5	15.28																												
Ct 6	15.85																												
Ref Geometric mean	14.9556				Target mean	26.03	29.8625	19.945	21.82333	35.91	22.263	25.153	10.51	29.21	26.165	29.91	25.22	14.75	31.995	34.06	24.76	27.58	30.27	33.885	29.075	23.52	24.215	24.995	22.64
Ref S.D	0.773096				target S.D	0.58643	6.167779	0.940452	0.410163	0.042426	0.515569	1.7949	0.707107	0.480833	3.194563	0.296985	1.088944	#DIV/0!	1.732412	7.74989	3.167838	1.032376	0.636396	0.007071	1.308148	#DIV/0!	0.685894	1.534422	#DIV/0!
					error propagated S.D	0.970349	6.216041	1.217427	0.875163	0.074259	0.929241	1.954314	1.047701	0.910427	3.286778	0.828177	1.335469	#DIV/0!	1.897084	7.788355	3.260809	1.289759	1.001338	0.773128	1.519516	#DIV/0!	1.033503	1.718176	#DIV/0!
					delta Ct	11.0744	14.9069	4.989397	6.86773	20.9544	7.307397	10.1974	-4.4456	14.2544	11.2094	14.9544	10.2644	-0.2056	17.0394	19.1044	9.804397	12.6244	15.3144	18.9294	14.1194	8.564397	9.259397	10.0394	7.684397
					delta delta Ct	9.397562	5.381728	0.706728	6.510895	42.13723	3.153728	5.177478	-11.7558	#DIV/0!	4.019228	10.58923	11.35423	1.924228	9.349228	8.614228	14.11423	-1.67577	9.224228	#DIV/0!	10.76923	#DIV/0!	18.87923	12.99923	10.41423
					Normalized ddCt	0.001483	0.023985	0.612708	0.010965	2.07E-13	0.112366	0.027633	3458.119	#DIV/0!	0.061673	0.000649	0.000382	0.263481	0.001533	0.002552	5.64E-05	3.194902	0.001672	#DIV/0!	0.000573	#DIV/0!	2.07E-06	0.000122	0.000733

					positive error	10.36791	11.59777	1.924155	7.386058	42.91149	4.082969	7.131792	-10.7081	#DIV/0!	7.306006	11.41741	12.6897	#DIV/0!	11.24631	16.40258	17.37504	-0.38601	10.22557	#DIV/0!	12.28874	#DIV/0!	19.91273	14.7174	#DIV/0!
					negative error	8.427212	-0.83431	-0.5107	5.635732	41.36297	2.224487	3.223164	-12.8035	#DIV/0!	0.73245	9.761051	10.01876	#DIV/0!	7.452144	0.825873	10.85342	-2.96553	8.222289	#DIV/0!	9.249713	#DIV/0!	17.84573	11.28105	#DIV/0!
					Normalized positive error	0.000757	0.000323	0.263495	0.005978	1.21E-13	0.059007	0.007113	1672.825	#DIV/0!	0.006319	0.000366	0.001051	#DIV/0!	0.000412	1.15E-05	5.88E-06	1.306777	0.000835	#DIV/0!	0.0002	#DIV/0!	1.01E-06	3.71E-05	#DIV/0!
					Normalized negative error	0.002905	1.783008	1.414744	0.020113	3.54E-13	0.213975	0.107086	7148.738	#DIV/0!	0.601881	0.001152	0.000964	#DIV/0!	0.005711	0.564141	0.000054	7.811126	0.003347	#DIV/0!	0.001643	#DIV/0!	4.25E-06	0.000402	#DIV/0!

3.4.11 SKOV-3 24 h

Negative

	Actin	Tubulin				Target genes										
	Ref gene 1	Ref gene 2	Ref gene 3	Ref gene 4		IL-6	NF-KB	PARP	Casp9	Casp3	SMAC	BCL-2	BAX	XIAP	IAP1	IAP2
Ct 1	23.79	21.67				24.66	40.5	32.13	22.73	42.54	23	26.291	31.696	33.6	28.89	23.78
Ct 2	22.74	21.61				24.46	39.53	31.97	22.51		22.94	25.961	28.365		29.26	23.99
Ct 3	21.717	22.599						33.09	22.382		25.544	25.82	26.054		24.785	26.989
Ct 4	21.283	23.151							21.412		25.633	25.717	27.037		23.825	25.895
Ct 5	23.03															
Ct 6	21.6															
Ref Geometric mean	22.30457				Target mean	24.56	40.015	32.39667	22.2585	42.54	24.27925	25.94725	28.288	33.6	26.69	25.1635
Ref S.D	0.849429				Target S.D	0.141421	0.685894	0.60575	0.582346	#DIV/0!	1.512427	0.25004	2.461446	#DIV/0!	2.785806	1.544746
					error propagated S.D	0.861121	1.091778	1.043294	1.029882	#DIV/0!	1.734637	0.885466	2.603891	#DIV/0!	2.91243	1.762887
					delta Ct	2.255433	17.71043	10.0921	-0.04607	20.23543	1.974683	3.642683	5.983433	11.29543	4.385433	2.858933
					delta delta Ct	0	0	0	0	0	0	0	0	0	0	0
					Normalized ddCt	1	1	1	1	1	1	1	1	1	1	1
					positive error	0.861121	1.091778	1.043294	1.029882	#DIV/0!	1.734637	0.885466	2.603891	#DIV/0!	2.91243	1.762887

					negative error	-0.86112	-1.09178	-1.04329	-1.02988	#DIV/0!	-1.73464	-0.88547	-2.60389	#DIV/0!	-2.91243	-1.76289
					Normalized positive error	0.550524	0.469183	0.485218	0.48975	#DIV/0!	0.300485	0.541313	0.164494	#DIV/0!	0.132822	0.294658
					Normalized negative error	1.81645	2.131366	2.060929	2.041857	#DIV/0!	3.327957	1.847361	6.079239	#DIV/0!	7.528851	3.393765

Cisplatin

	Actin	Tubulin														
	Ref gene 1	Ref gene 2	Ref gene 3	Ref gene 4		IL-6	NF-KB	PARP	Casp9	Casp3	SMAC	BCL-2	BAX	XIAP	IAP1	IAP2
Ct 1	22.77	21.53				24.72	36.58	32.37	23.22	40	25.42	24.54	24.379	32.71	30.83	26.26
Ct 2	22.75	21.6				24.79	40.87	31.94	22.87	38.81	24.55	24.7	23.941		31.07	27.31
Ct 3	20.318	21.728				22.44			19.602		23.873	24.446	23.757		22.126	24.417
Ct 4	19.676	20.243				32.81		30.5	20.153		23.873	25.057	25.437		22.126	23.69
Ct 5	19.58															
Ct 6	19.05															
Ref Geometric mean	20.88653				Target mean	26.19	38.725	31.60333	21.46125	39.405	24.429	24.68575	24.3785	32.71	26.538	25.41925
Ref S.D	1.329968				target S.D	4.546347	3.033488	0.979405	1.848072	0.841457	0.733711	0.268795	0.75235	#DIV/0!	5.095481	1.660984
					error propagated S.D	4.736885	3.31223	1.65168	2.27688	1.573806	1.518929	1.356859	1.52802	#DIV/0!	5.266188	2.127835
					delta Ct	5.303473	17.83847	10.71681	0.574723	18.51847	3.542473	3.799223	3.491973	11.82347	5.651473	4.532723
					delta delta Ct	3.04804	0.12804	0.624707	0.62079	-1.71696	1.56779	0.15654	-2.49146	0.52804	1.26604	1.67379
					Normalized ddCt	0.120906	0.915074	0.648552	0.650315	3.28743	0.337325	0.897174	5.623468	0.693496	0.4158	0.313429
					positive error	7.784925	3.44027	2.276387	2.89767	-0.14315	3.086719	1.513399	-0.96344	#DIV/0!	6.532228	3.801625
					negative error	-1.68885	-3.18419	-1.02697	-1.65609	-3.29077	0.048861	-1.20032	-4.01948	#DIV/0!	-4.00015	-0.45405
					Normalized positive error	0.004534	0.092125	0.206414	0.134188	1.104317	0.117708	0.350285	1.949954	#DIV/0!	0.010804	0.071713

					Normalized negative error	3.223985	9.089428	2.037745	3.151613	9.786315	0.966699	2.297904	16.2175	#DIV/0!	16.00165	1.369876

Cu-Phen (**1**)

	Actin	Tubulin														
	Ref gene 1	Ref gene 2	Ref gene 3	Ref gene 4		IL-6	NF-KB	PARP	Casp9	Casp3	SMAC	BCL-2	BAX	XIAP	IAP1	IAP2
Ct 1	21.89	20.22				22.85	37.98	32.9	21.2		21.97	24.723	26.98	34.78	28.84	23.83
Ct 2	21.35	20.5				22.75	41.2	32.86	21.03		21.74	24.5	24.617		30.29	23.81
Ct 3	22.93	21.667							20.721		24.712	24.795	25.545		22.532	24.83
Ct 4	22.93	21.456						41.35	19.753		24.712	24.833	29.431		23.257	24.428
Ct 5	20.62															
Ct 6	21.55															
Ref Geometric mean	21.49349				Target mean	22.8	39.59	35.70333	20.676	#DIV/0!	23.2835	24.71275	26.64325	34.78	26.22975	24.2245
Ref S.D	0.925458				target S.D	0.070711	2.276884	4.890198	0.646489	#DIV/0!	1.65216	0.148989	2.097363	#DIV/0!	3.907669	0.495137
					error propagated S.D	0.928155	2.457778	4.976998	1.128902	#DIV/0!	1.893701	0.937374	2.292467	#DIV/0!	4.015763	1.049587
					delta Ct	1.306506	18.09651	14.20984	-0.81749	#DIV/0!	1.790006	3.219256	5.149756	13.28651	4.736256	2.731006
					delta delta Ct	-0.94893	0.386073	4.117739	-0.77143	#DIV/0!	-0.18468	-0.42343	-0.83368	1.991073	0.350823	-0.12793
					Normalized ddCt	1.930437	0.76521	0.057602	1.706958	#DIV/0!	1.136563	1.34111	1.782222	0.251552	0.784137	1.092723
					positive error	-0.02077	2.84385	9.094737	0.357475	#DIV/0!	1.709024	0.513946	1.458789	#DIV/0!	4.366585	0.92166
					negative error	-1.87708	-2.07171	-0.85926	-1.90033	#DIV/0!	-2.07838	-1.3608	-3.12614	#DIV/0!	-3.66494	-1.17751
					Normalized positive error	1.014502	0.139289	0.001829	0.780529	#DIV/0!	0.305867	0.700304	0.363798	#DIV/0!	0.048476	0.527901
					Normalized negative error	3.673315	4.203833	1.814106	3.732985	#DIV/0!	4.223324	2.568278	8.730982	#DIV/0!	12.68402	2.261868

Cu-DPQ-Phen (**2**)

	Actin	Tubulin														
	Ref gene 1	Ref gene 2	Ref gene 3	Ref gene 4		IL-6	NF-KB	PARP	Casp9	Casp3	SMAC	BCL-2	BAX	XIAP	IAP1	IAP2
Ct 1	21.62	20.71				23.52		31.88	22.52	38.57	23.98	25.04	23.843	40.26	30.07	27.61
Ct 2	21.63	20.54				22.99		31.38	22.43	40.32	23.4	25.042	23.154		29.76	25.83
Ct 3	20.397	22.798						13.38	39		24.313	24.51	24.788		22.025	23.982
Ct 4	20.397	21.075							39		23.573	25.934	24.654		23.425	25.352
Ct 5	20.43															
Ct 6	20.01															
Ref Geometric mean	20.94597				Target mean	23.255	#DIV/0!	25.54667	30.7375	39.445	23.8165	25.1315	24.10975	40.26	26.32	25.6935
Ref S.D	0.838796				target S.D	0.374767	#DIV/0!	10.53961	9.540784	1.237437	0.410694	0.590664	0.761762	#DIV/0!	4.192221	1.498606
					error propagated S.D	0.91871	#DIV/0!	10.57293	9.577585	1.494934	0.933942	1.025896	1.133075	#DIV/0!	4.275312	1.717381
					delta Ct	2.309028	#DIV/0!	4.600695	9.791528	18.49903	2.870528	4.185528	3.163778	19.31403	5.374028	4.747528
					delta delta Ct	0.053595	#DIV/0!	-5.4914	9.837595	-1.7364	0.895845	0.542845	-2.81965	8.018595	0.988595	1.888595
					Normalized ddCt	0.963532	#DIV/0!	44.98602	0.001093	3.332038	0.537432	0.686416	7.059935	0.003856	0.503968	0.27007
					positive error	0.972305	#DIV/0!	5.081528	19.41518	-0.24147	1.829787	1.568741	-1.6865	#DIV/0!	5.263907	3.605976
					negative error	-0.8651	#DIV/0!	-16.0643	0.26001	-3.23134	-0.0381	-0.48305	-3.95273	#DIV/0!	-3.28672	0.171214
					Normalized positive error	0.509691	#DIV/0!	0.029533	1.43E-06	1.182197	0.281306	0.337103	3.218927	#DIV/0!	0.026026	0.082128
					Normalized negative error	1.821485	#DIV/0!	68524.77	0.835082	9.391392	1.026759	1.397696	15.48426	#DIV/0!	9.758891	0.888095

3.4.12 SKOV-3 48 h

Negative

	Actin	Tubulin				Target genes																						
	Ref gene 1	Ref gene 2	Ref gene 3	Ref gene 4		IL-6	NF-KB	PARP	Casp9	Casp3	SMAC	BCL-2	BAX	XIAP	IAP1	IAP2	HMOX	TFAM	TFB1M	TFB2M	NRF-2	CLPP	LON	SPG7	YME1L1	DRP1	MFN1	MFN2	OPA1
Ct 1	23.28	21.52				23.6	40.23	32.36	22.4		22.83	25.583		37.4	27.11	23.32	26.59		37.93		32.11	37.7			33.91		25.86		43.71
Ct 2	24.97	21.69				24.77	38.61	32.62	21.79		22.61	26.238			28.89	22.79	27.57	29.31	35.93	2.62	14.99		29.45				25.89	23.34	27.29
Ct 3	22.948								19.712	40	25.751	27.949																	
Ct 4	21.545	33.99				28.59			19.712	27.02	27.882	25.12																	
Ct 5	23.21																												
Ct 6	22.4																												
Ref Geometric mean	23.71294				Target mean	25.65333	39.42	32.49	20.9035	33.51	24.76825	26.2225	#DIV/0!	37.4	28	23.055	27.08	29.31	36.93	2.62	23.55	37.7	29.45	#DIV/0!	33.91	#DIV/0!	25.875	23.34	35.5
Ref S.D	3.921759				Target S.D	2.609642	1.145513	0.183848	1.398182	9.178246	2.521646	1.2392	#DIV/0!	#DIV/0!	1.25865	0.374767	0.692965	#DIV/0!	1.414214	#DIV/0!	12.10567	#DIV/0!	#DIV/0!	#DIV/0!	#DIV/0!	#DIV/0!	0.021213	#DIV/0!	11.61069
					error propagated S.D	4.710671	4.085632	3.926066	4.163545	9.981002	4.662498	4.112829	#DIV/0!	#DIV/0!	4.118785	3.939624	3.982511	#DIV/0!	4.168956	#DIV/0!	12.72507	#DIV/0!	#DIV/0!	#DIV/0!	#DIV/0!	#DIV/0!	3.921816	#DIV/0!	12.25514
					delta Ct	1.940391	15.70706	8.770758	-2.80944	9.770758	1.055308	2.509558	#DIV/0!	13.68706	4.287058	-0.65794	3.367058	5.597058	13.21706	-21.0929	-0.16294	13.98706	5.737058	#DIV/0!	10.19706	#DIV/0!	2.162058	-0.37294	11.78706
					delta delta Ct	0	0	0	0	0	0	0	#DIV/0!	0	0	0	0	0	0	0	0	0	0	#DIV/0!	0	#DIV/0!	0	0	0
					Normalized ddCt	1	1	1	1	1	1	1	#DIV/0!	1	1	1	1	1	1	1	1	1	1	#DIV/0!	1	#DIV/0!	1	1	1
					positive error	4.710671	4.085632	3.926066	4.163545	9.981002	4.662498	4.112829	#DIV/0!	#DIV/0!	4.118785	3.939624	3.982511	#DIV/0!	4.168956	#DIV/0!	12.72507	#DIV/0!	#DIV/0!	#DIV/0!	#DIV/0!	#DIV/0!	3.921816	#DIV/0!	12.25514
					negative error	-4.71067	-4.08563	-3.92607	-4.16354	-9.981	-4.662	-4.11283	#DIV/0!	#DIV/0!	-4.11879	-3.93962	-3.98251	#DIV/0!	-4.16896	#DIV/0!	-12.7251	#DIV/0!	#DIV/0!	#DIV/0!	#DIV/0!	#DIV/0!	-3.92182	#DIV/0!	-12.2551
					Normalized positive error	0.038119	0.058898	0.065786	0.055802	0.00099	0.039486	0.057798	#DIV/0!	#DIV/0!	0.05756	0.065171	0.063262	#DIV/0!	0.055593	#DIV/0!	0.000148	#DIV/0!	#DIV/0!	#DIV/0!	#DIV/0!	#DIV/0!	0.065981	#DIV/0!	0.000205

					Normalized negative error	26.18505	16.97844	15.2007	17.92057	1010.604	25.32514	17.30154	#DIV/0!	#DIV/0!	17.37312	15.34423	15.80721	#DIV/0!	17.98791	#DIV/0!	6770.607	#DIV/0!	#DIV/0!	#DIV/0!	#DIV/0!	#DIV/0!	#DIV/0!	15.15599	#DIV/0!	4888.369

Cisplatin

	Actin	Tubulin																											
	Ref gene 1	Ref gene 2	Ref gene 3	Ref gene 4		IL-6	NF-KB	PARP	Casp9	Casp3	SMAC	BCL-2	BAX	XIAP	IAP1	IAP2	HMOX	TFAM	TFB1M	TFB2M	NRF-2	CLPP	LON	SPG7	YME1L1	DRP1	MFN1	MFN2	OPA1
Ct 1	20.86	20.34				22.72	35.82	30.99	20.86	38.39	21.5	22.54			27.39	23.15	27.81	14.17	33.21	2.41	23.78	37.92	34.15		30.17			4.1	23.21
Ct 2	20.35	20.42				22.52	37.48	30.3	20.79	39.43	22.45	23.265			27.42	22.48	37.95		31.04		25.59	37.99	34.69		13.06		22.23		41.18
Ct 3	19.02								18.597		22.545	23.145				22.33													
Ct 4	18.078								18.597		23.352	22.757				34.64													
Ct 5	18.52																												
Ct 6	19.1																												
Ref Geometric mean	19.56208				Target mean	22.62	36.65	30.645	19.711	38.91	22.46175	22.92675	#DIV/0!	#DIV/0!	27.405	25.65	32.88	14.17	32.125	2.41	24.685	37.955	34.42	#DIV/0!	21.615	#DIV/0!	22.23	4.1	32.195
Ref S.D	1.030798				target S.D	0.141421	1.173797	0.487904	1.286654	0.735391	0.758195	0.336866	#DIV/0!	#DIV/0!	0.021213	6.039026	7.170063	#DIV/0!	1.534422	#DIV/0!	1.279863	0.049497	0.381838	#DIV/0!	12.09806	#DIV/0!	#DIV/0!	#DIV/0!	12.706771
					error propagated S.D	1.040454	1.556216	1.140436	1.648643	1.266233	1.279611	1.084446	#DIV/0!	#DIV/0!	1.031017	6.091771	7.243778	#DIV/0!	1.848512	#DIV/0!	1.643349	1.031986	1.099248	#DIV/0!	12.14243	#DIV/0!	#DIV/0!	#DIV/0!	12.748445
					delta Ct	3.057918	17.08792	11.08292	0.148918	19.34792	2.899668	3.364668	#DIV/0!	#DIV/0!	7.842918	6.087918	13.31792	-5.39208	12.56292	-17.1521	5.122918	18.39292	14.85792	#DIV/0!	2.052918	#DIV/0!	2.667918	-15.4621	12.632922
					delta delta Ct	1.117527	1.380886	2.305886	2.958386	9.508386	1.844336	0.855111	#DIV/0!	#DIV/0!	3.558386	6.745886	9.908386	-10.9891	-0.65414	3.940886	5.285886	4.405886	9.120886	#DIV/0!	-8.14414	#DIV/0!	0.505886	-15.0891	0.845886
					Normalized ddCt	0.460883	0.383939	0.202224	0.128666	0.001333	0.278479	0.552823	#DIV/0!	#DIV/0!	0.085031	0.009317	0.001011	203 2.641	1.573678	0.065115	0.025633	0.047174	0.001796	#DIV/0!	282.8984	#DIV/0!	0.704244	34856.5	0.563579
					positive error	2.157981	2.943302	3.462696	4.607003	10.81709	3.123971	1.939556	#DIV/0!	#DIV/0!	4.586877	12.83763	17.19464	#DIV/0!	1.194372	#DIV/0!	6.929209	5.437846	10.22011	#DIV/0!	3.98229	#DIV/0!	#DIV/0!	#DIV/0!	13.59431
					negative error	0.077072	-0.1813	1.165424	1.309717	8.284627	0.564749	-0.22934	#DIV/0!	#DIV/0!	2.524843	0.654089	2.707078	#DIV/0!	-2.50265	#DIV/0!	3.642511	3.373874	8.021612	#DIV/0!	-20.2866	#DIV/0!	#DIV/0!	#DIV/0!	-11.9026

					Normalized positive error	0.22407	0.130036	0.091741	0.041035	0.000554	0.114707	0.260697	#DIV/0!	#DIV/0!	0.041611	0.000137	6.67E-06	#DIV/0!	0.436977	#DIV/0!	0.008205	0.002307	0.000838	#DIV/0!	0.062574	#DIV/0!	#DIV/0!	#DIV/0!	#DIV/0!	8.09E-05
					Normalized negative error	0.947979	1.133905	0.445833	0.4034	0.003207	0.676073	1.172296	#DIV/0!	#DIV/0!	0.173759	0.635477	0.15314	#DIV/0!	5.667261	#DIV/0!	0.080075	0.009663	0.003848	#DIV/0!	1278986	#DIV/0!	#DIV/0!	#DIV/0!	#DIV/0!	3828.572

Cu-Phen (**1**)

	Actin	Tubulin																											
	Refgene 1	Refgene 2	Refgene 3	Ref gene 4		IL-6	NF-KB	PARP	Casp9	Casp3	SMAC	BCL-2	BAX	XIAP	IAP1	IAP2	HMOX	TFAM	TFB1M	TFB2M	NRF-2	CLPP	LON	SPG7	YME1L1	DRP1	MFN1	MFN2	OPA1
Ct 1	22.54	23.4				25.75	36.78	31.9	20.82	41.93	22.71	25.216			28.84	23.48		17.77	41.63	35.35		36.9			23.22		25.85	13.52	
Ct 2	22.26	21.99				24.08	39.92	31.26	20.61		22.59	26.44			27.86	23.41		39.76		2.85	24.68	41.32	37.05		6.09		27.08		38.04
Ct 3	21.091										24.964	24.303				24.66													
Ct 4	24.935					14.01	40.17				24.937	25.511																	
Ct 5	21.64																												
Ct 6	21.38																												
Ref Geometric mean	22.37492				Target mean	21.28	38.95667	31.58	20.715	41.93	23.80025	25.3675	#DIV/0!	#DIV/0!	28.35	23.85	#DIV/0!	28.765	41.63	19.1	24.68	39.11	37.05	#DIV/0!	14.655	#DIV/0!	26.465	13.52	38.04
Ref S.D	1.251562				target S.D	6.351134	1.889189	0.452548	0.148492	#DIV/0!	1.329143	0.807712	#DIV/0!	#DIV/0!	0.692965	0.702353	#DIV/0!	15.54928	#DIV/0!	22.98097	#DIV/0!	3.125412	#DIV/0!	#DIV/0!	12.11274	#DIV/0!	0.869741	#DIV/0!	#DIV/0!
					error propagated S.D	6.473276	2.266151	1.330867	1.26034	#DIV/0!	1.825658	1.530379	#DIV/0!	#DIV/0!	1.430596	1.435168	#DIV/0!	15.59957	#DIV/0!	23.01503	#DIV/0!	3.366691	#DIV/0!	#DIV/0!	12.17723	#DIV/0!	1.524092	#DIV/0!	#DIV/0!
					delta Ct	-1.09492	16.58175	9.205082	-1.65992	19.55508	1.425332	2.992582	#DIV/0!	#DIV/0!	5.975082	1.475082	#DIV/0!	6.390082	19.25508	-3.27492	2.305082	16.73508	14.67508	#DIV/0!	-7.71992	#DIV/0!	4.090082	-8.85492	15.66508
					delta delta Ct	-3.03531	0.874691	0.428024	1.149524	9.758024	0.370024	0.483024	#DIV/0!	#DIV/0!	1.688024	2.133024	#DIV/0!	0.793024	6.038024	17.81802	2.468024	2.748024	8.938024	#DIV/0!	-17.917	#DIV/0!	1.928024	-8.48198	3.878024
					Normalized ddCt	8.198212	0.545371	0.743279	0.450774	0.001155	0.773777	0.715476	#DIV/0!	#DIV/0!	0.310352	0.227979	#DIV/0!	0.577133	0.015219	4.33E-06	0.180739	0.148855	0.002039	#DIV/0!	247.484	#DIV/0!	0.262789	357.5437	0.068014
					positive error	3.437967	3.140842	1.758891	2.409864	#DIV/0!	2.195682	2.013403	#DIV/0!	#DIV/0!	3.118621	3.568192	#DIV/0!	16.39259	#DIV/0!	40.83305	#DIV/0!	6.114715	#DIV/0!	#DIV/0!	-5.73975	#DIV/0!	3.452116	#DIV/0!	#DIV/0!

					negative error	-9.50859	-1.39146	-0.90284	-0.11082	#DIV/0!	-1.45563	-1.04735	#DIV/0!	#DIV/0!	0.257428	0.697856	#DIV/0!	-14.8065	#DIV/0!	-5.197	#DIV/0!	-0.61867	#DIV/0!	#DIV/0!	-30.0942	#DIV/0!	0.439032	#DIV/0!	#DIV/0!
					Normalized positive error	0.092272	0.113374	0.295475	0.188174	#DIV/0!	0.21829	0.247688	#DIV/0!	#DIV/0!	0.115133	0.084308	#DIV/0!	1.16E-05	#DIV/0!	5.11E-13	#DIV/0!	0.014431	#DIV/0!	#DIV/0!	53.43633	#DIV/0!	0.091371	#DIV/0!	#DIV/0!
					Normalized negative error	728.3992	2.623441	1.869747	1.079839	#DIV/0!	2.742771	2.066737	#DIV/0!	#DIV/0!	0.836578	0.616488	#DIV/0!	28655.85	#DIV/0!	36.68203	#DIV/0!	1.535455	#DIV/0!	#DIV/0!	1.15E+09	#DIV/0!	0.755796	#DIV/0!	#DIV/0!

Cu-DPQ-Phen (**2**)

	Actin	Tubulin																											
	Refgene 1	Refgene 2	Refgene 3	Ref gene 4		IL-6	NF-KB	PARP	Casp9	Casp3	SMAC	BCL-2	BAX	XIAP	IAP1	IAP2	HMOX	TFAM	TFB1M	TFB2M	NRF-2	CLPP	LON	SPG7	YME1L1	DRP1	MFN1	MFN2	OPA1
Ct 1	20.67	20.6				22.63	39.56	31.25	21.24	39.01	23.29	23.438			28.78	24.78	33.88			34.88		11.11	42.06				37.69	39.82	
Ct 2	20.75	20.46				22.4	37.57	30.82	21.45	39.06	23.31	23.919			28.61	24.32	30.32	32.02							36.43		13.86		
Ct 3	19.981										23.196	24.425																	
Ct 4	19.859					19.42					24.367	25.699																	
Ct 5																													
Ct 6																													
Ref Geometric mean	20.38376				Target mean	21.48333	38.565	31.035	21.345	39.035	23.54075	24.37025	#DIV/0!	#DIV/0!	28.695	24.55	32.1	32.02	#DIV/0!	34.88	#DIV/0!	11.11	42.06	#DIV/0!	36.43	#DIV/0!	25.775	39.82	#DIV/0!
Ref S.D	0.375813				target S.D	1.790596	1.407142	0.304056	0.148492	0.035355	0.553071	0.973189	#DIV/0!	#DIV/0!	0.120208	0.325269	2.5173	#DIV/0!	#DIV/0!	#DIV/0!	#DIV/0!	#DIV/0!	#DIV/0!	#DIV/0!	#DIV/0!	#DIV/0!	#DIV/0!	16.85035	#DIV/0!	#DIV/0!
					error propagated S.D	1.829609	1.456463	0.48341	0.404085	0.037472	0.668672	1.043232	#DIV/0!	#DIV/0!	0.394569	0.497026	2.545198	#DIV/0!	#DIV/0!	#DIV/0!	#DIV/0!	#DIV/0!	#DIV/0!	#DIV/0!	#DIV/0!	#DIV/0!	#DIV/0!	16.85454	#DIV/0!	#DIV/0!
					delta Ct	1.099571	18.18124	10.65124	0.961238	18.65124	3.156988	3.986488	#DIV/0!	#DIV/0!	8.311238	4.166238	11.71624	11.63624	#DIV/0!	14.49624	#DIV/0!	-9.27376	21.67624	#DIV/0!	16.04624	#DIV/0!	5.391238	19.43624	#DIV/0!
					delta delta Ct	-0.84082	2.474178	1.874178	3.770678	8.854178	2.101678	1.476933	#DIV/0!	#DIV/0!	4.024178	4.824178	8.349178	6.039178	#DIV/0!	35.58918	#DIV/0!	-23.2608	15.93918	#DIV/0!	5.849178	#DIV/0!	3.229178	19.80918	#DIV/0!
					Normalized ddCt	1.791067	0.179969	0.272782	0.073268	0.002161	0.232987	0.359252	#DIV/0!	#DIV/0!	0.061461	0.00353	0.003067	0.015206	#DIV/0!	1.93E-11	#DIV/0!	1005088	1.59E-05	#DIV/0!	0.017347	#DIV/0!	0.106664	1.09E-06	#DIV/0!

					positive error	0.988789	3.930644	2.35759	4.174766	9.231652	2.770353	2.520162	#DIV/0!	#DIV/0!	4.41875	5.321207	10.89438	#DIV/0!	#DIV/0!	#DIV/0!	#DIV/0!	#DIV/0!	#DIV/0!	#DIV/0!	#DIV/0!	#DIV/0!	#DIV/0!	20.08373	#DIV/0!	#DIV/0!
					negative error	-2.67043	1.017717	1.390771	3.366595	8.476708	1.433008	0.433699	#DIV/0!	#DIV/0!	3.629611	4.327154	5.839382	#DIV/0!	#DIV/0!	#DIV/0!	#DIV/0!	#DIV/0!	#DIV/0!	#DIV/0!	#DIV/0!	#DIV/0!	#DIV/0!	-13.6254	#DIV/0!	#DIV/0!
					Normalized positive error	0.5039	0.065578	0.195117	0.055369	0.001663	0.146569	0.174323	#DIV/0!	#DIV/0!	0.046755	0.025013	0.000525	#DIV/0!	#DIV/0!	#DIV/0!	#DIV/0!	#DIV/0!	#DIV/0!	#DIV/0!	#DIV/0!	#DIV/0!	#DIV/0!	9E-07	#DIV/0!	#DIV/0!
					Normalized negative error	6.366182	0.493897	0.381361	0.096951	0.002807	0.370358	0.740361	#DIV/0!	#DIV/0!	0.080794	0.049819	0.017899	#DIV/0!	#DIV/0!	#DIV/0!	#DIV/0!	#DIV/0!	#DIV/0!	#DIV/0!	#DIV/0!	#DIV/0!	#DIV/0!	12636.98	#DIV/0!	#DIV/0!

3.4.13 A2780 24 h

Negative

	Actin	Tubulin				Target genes																							
	Ref gene 1	Ref gene 2	Ref gene 3	Ref gene 4		IL-6	NF-KB	PARP	Casp9	Casp3	SMAC	BCL-2	BAX	XIAP	IAP1	IAP2	HMOX	TFAM	TFB1M	TFB2M	NRF-2	CLPP	LON	SPG7	YME1L1	DRP1	MFN1	MFN2	OPA1
Ct 1	24.51	27.43							28.34			27.92	30.57	42.23			22.21	18.86	31.35	33.73	25.24	36.82	33.62	27.16					
Ct 2	24.48	27.35							28.52			28.4	30.29				22.6	19.26	28.97	34.32	24.92	37.07	23.94	25.8					
Ct 3	20.22	22.28							30.22			27.28	30.96	39.71			22.92	18.82	27.35	25.57	24.69	26.49	26.34	29.84					
Ct 4	20.63	21.25							28.76			28.25	30.32	39.38			22.04	19.23	25.13	25.99	22.02	25.74	26.26	29.5					
Ct 5																													
Ct 6																													
Ref Geometric mean	23.367462				Target mean	#DIV/0!	#DIV/0!	#DIV/0!	28.96	#DIV/0!	#DIV/0!	27.9625	30.5535	40.44	#DIV/0!	#DIV/0!	22.4425	19.0425	28.2	29.9025	24.2175	31.53	27.54	28.075	#DIV/0!	#DIV/0!	#DIV/0!	#DIV/0!	#DIV/0!
Ref S.D	2.8733078 9				Target S.D	#DIV/0!	#DIV/0!	#DIV/0!	0.857438	#DIV/0!	#DIV/0!	0.497217	0.309892	1.558942	#DIV/0!	#DIV/0!	0.395337	0.234716	2.624424	4.769426	1.482259	6.261028	4.203364	1.928618	#DIV/0!	#DIV/0!	#DIV/0!	#DIV/0!	#DIV/0!
					error propagated S.D	#DIV/0!	#DIV/0!	#DIV/0!	2.998516	#DIV/0!	#DIV/0!	2.916012	2.889971	3.268975	#DIV/0!	#DIV/0!	2.900378	2.882879	3.891465	5.568063	3.233108	6.888858	5.091578	3.460558	#DIV/0!	#DIV/0!	#DIV/0!	#DIV/0!	#DIV/0!

					delta Ct	#DIV/0!	#DIV/0!	#DIV/0!	5.592538	#DIV/0!	#DIV/0!	4.594038	7.167538	17.07254	#DIV/0!	#DIV/0!	-0.92496	-4.32496	4.832538	6.535038	0.850038	8.162538	4.172538	4.707538	#DIV/0!	#DIV/0!	#DIV/0!	#DIV/0!	#DIV/0!
					delta delta Ct	#DIV/0!	#DIV/0!	#DIV/0!	0	#DIV/0!	#DIV/0!	0	0	0	#DIV/0!	#DIV/0!	0	0	0	0	0	0	0	0	#DIV/0!	#DIV/0!	#DIV/0!	#DIV/0!	#DIV/0!
					Normalized ddCt	#DIV/0!	#DIV/0!	#DIV/0!	1	#DIV/0!	#DIV/0!	1	1	1	#DIV/0!	#DIV/0!	1	1	1	1	1	1	1	1	#DIV/0!	#DIV/0!	#DIV/0!	#DIV/0!	#DIV/0!
					positive error	#DIV/0!	#DIV/0!	#DIV/0!	2.998516	#DIV/0!	#DIV/0!	2.916012	2.888991	3.268975	#DIV/0!	#DIV/0!	2.900378	2.882879	3.891465	5.568063	3.233108	6.888858	5.095178	3.460558	#DIV/0!	#DIV/0!	#DIV/0!	#DIV/0!	#DIV/0!
					negative error	#DIV/0!	#DIV/0!	#DIV/0!	-2.99852	#DIV/0!	#DIV/0!	-2.91601	-2.88997	-3.26898	#DIV/0!	#DIV/0!	-2.90038	-2.88288	-3.89146	-5.56806	-3.23311	-6.88886	-5.09158	-3.46056	#DIV/0!	#DIV/0!	#DIV/0!	#DIV/0!	#DIV/0!
					Normalized positive error	#DIV/0!	#DIV/0!	#DIV/0!	0.125129	#DIV/0!	#DIV/0!	0.132493	0.134906	0.103739	#DIV/0!	#DIV/0!	0.133937	0.135571	0.067383	0.021079	0.10635	0.008438	0.029328	0.090838	#DIV/0!	#DIV/0!	#DIV/0!	#DIV/0!	#DIV/0!
					Normalized negative error	#DIV/0!	#DIV/0!	#DIV/0!	7.991775	#DIV/0!	#DIV/0!	7.547566	7.412555	9.639612	#DIV/0!	#DIV/0!	7.466218	7.376205	14.84047	47.44101	9.402917	118.5094	34.09712	11.0086	#DIV/0!	#DIV/0!	#DIV/0!	#DIV/0!	#DIV/0!

Doxorubicin

	Actin	Tubulin																											
	Ref gene 1	Ref gene 2	Ref gene 3	Ref gene 4		IL-6	NF-KB	PARP	Casp9	Casp3	SMAC	BCL-2	BAX	XIAP	IAP1	IAP2	HMOX	TFAM	TFB1M	TFB2M	NRF-2	CLPP	LON	SPG7	YME1L1	DRP1	MFN1	MFN2	OPA1
Ct 1	24.98	26.07							26.42			27.29	28.29				23.88	18.67		34.06	22.97	35.79	35.2						
Ct 2	23.96	25.51							27.06			26.71	28.3				23.87	18.91	26.17	32.23	21.82	35.91	35.92	36.21					
Ct 3	22.74	25.74							26.97			26.13	28.97				23.36	18.16	31.5	32.66	23.12	37.63	34.67	36.29					
Ct 4	22.5	24.93							28.9			26.16	29.32				24.89	17.91	29.22	32.06	22.01	36.03	34.27	34.73					
Ct 5																													
Ct 6																													

Ref Geometric mean	24.520497				Target mean	#DIV/0!	#DIV/0!	#DIV/0!	27.3375	#DIV/0!	#DIV/0!	26.5725	28.72	#DIV/0!	#DIV/0!	#DIV/0!	24	18.4125	28.96333	32.7525	22.48	36.34	35.015	35.74333	#DIV/0!	#DIV/0!	#DIV/0!	#DIV/0!	#DIV/0!
Ref S.D	1.3524574 2				target S.D	#DIV/0!	#DIV/0!	#DIV/0!	1.079394	#DIV/0!	#DIV/0!	0.547624	0.511143	#DIV/0!	#DIV/0!	#DIV/0!	0.641093	0.458285	2.674254	0.907501	0.659848	0.865563	0.713512	0.878484	#DIV/0!	#DIV/0!	#DIV/0!	#DIV/0!	#DIV/0!
					error propagated S.D	#DIV/0!	#DIV/0!	#DIV/0!	1.730385	#DIV/0!	#DIV/0!	1.459121	1.445824	#DIV/0!	#DIV/0!	#DIV/0!	1.49671	1.427994	2.996794	1.628711	1.504839	1.605721	1.529131	1.612723	#DIV/0!	#DIV/0!	#DIV/0!	#DIV/0!	#DIV/0!
					delta Ct	#DIV/0!	#DIV/0!	#DIV/0!	2.817	#DIV/0!	#DIV/0!	2.052	4.1995	#DIV/0!	#DIV/0!	#DIV/0!	-0.5205	-6.108	4.442834	8.232	-2.0405	11.8195	10.4945	11.22283	#DIV/0!	#DIV/0!	#DIV/0!	#DIV/0!	#DIV/0!
					delta delta Ct	#DIV/0!	#DIV/0!	#DIV/0!	-2.77554	#DIV/0!	#DIV/0!	-2.54304	-2.96804	#DIV/0!	#DIV/0!	#DIV/0!	0.404462	-1.78304	-0.3897	1.696962	-2.89054	3.656962	6.321962	6.515296	#DIV/0!	#DIV/0!	#DIV/0!	#DIV/0!	#DIV/0!
					Normalized ddCt	#DIV/0!	#DIV/0!	#DIV/0!	6.847312	#DIV/0!	#DIV/0!	5.828149	7.824712	#DIV/0!	#DIV/0!	#DIV/0!	0.755518	3.441501	1.310125	0.308435	7.415468	0.079277	0.01025	0.010932	#DIV/0!	#DIV/0!	#DIV/0!	#DIV/0!	#DIV/0!
					positive error	#DIV/0!	#DIV/0!	#DIV/0!	-1.04515	#DIV/0!	#DIV/0!	-1.08392	-1.52221	#DIV/0!	#DIV/0!	#DIV/0!	1.901172	-0.35504	2.60709	3.325673	-1.3857	5.262684	7.851093	8.128018	#DIV/0!	#DIV/0!	#DIV/0!	#DIV/0!	#DIV/0!
					negative error	#DIV/0!	#DIV/0!	#DIV/0!	-4.50592	#DIV/0!	#DIV/0!	-4.00216	-4.41386	#DIV/0!	#DIV/0!	#DIV/0!	-1.09225	-3.21103	-3.38665	0.068251	-4.39538	2.051241	4.792831	4.902573	#DIV/0!	#DIV/0!	#DIV/0!	#DIV/0!	#DIV/0!
					Normalized positive error	#DIV/0!	#DIV/0!	#DIV/0!	2.063585	#DIV/0!	#DIV/0!	2.111978 4	2.872312 4	#DIV/0!	#DIV/0!	#DIV/0!	0.267726	1.279025	0.16413	0.099741	2.612984	0.026048	0.004331	0.003575	#DIV/0!	#DIV/0!	#DIV/0!	#DIV/0!	#DIV/0!
					Normalized negative error	#DIV/0!	#DIV/0!	#DIV/0!	22.7205	#DIV/0!	#DIV/0!	16.02395	21.31596	#DIV/0!	#DIV/0!	#DIV/0!	2.13206	9.260124	10.45773	0.953793	21.04458	0.241276	0.036076	0.034333	#DIV/0!	#DIV/0!	#DIV/0!	#DIV/0!	#DIV/0!

Cisplatin

	Actin	Tubulin																										
	Ref gene 1	Ref gene 2	Ref gen	Ref gen		IL-6	NF-KB	PARP	Casp9	Casp3	SMAC	BCL-2	BAX	XIAP	IAP1	IAP2	HMOX	TFAM	TFB1M	TFB2M	NRF-2	CLPP	LON	SPG7	YME1L1	DRP1	MFN1	MFN2	OPA1

			e3	e4																									
Ct 1	12.43	17.34							23.48			23.51	22.92				22.29	18.78	24.35	20.4	20.8	20.96	19.75	26					
Ct 2	12.88	17.06							23.34			24.8	21.6	26.88			21.94	17.23	22.58	20.24	20.45	20.99	21.6	25.43					
Ct 3	12.61	19.44							25.04			24.56	22.59	29.47			22.39	18.65	24.07	22.3	23.95	22.03	21.63	26.86					
Ct 4	11.93	17.63							24.69			24.81	20.86	29.56			22.4	18.66	24.02	22.14	22.09	22.65	24.88	27.12					
Ct 5																													
Ct 6																													
Ref Geometric mean	14.909562 6				Target mean	#DIV/0!	#DIV/0!	#DIV/0!	24.1375	#DIV/0!	#DIV/0!	24.42	21.9925	28.66367	#DIV/0!	#DIV/0!	22.255	18.33	23.755	21.27	21.8225	21.6575	21.965	26.3525	#DIV/0!	#DIV/0!	#DIV/0!	#DIV/0!	#DIV/0!
Ref S.D	2.9849192 4				target S.D	#DIV/0!	#DIV/0!	#DIV/0!	0.854025	#DIV/0!	#DIV/0!	0.617576	0.940545	1.521983	#DIV/0!	#DIV/0!	0.215793	0.735708	0.796681	1.100848	1.58399	0.827823	2.132987	0.779289	#DIV/0!	#DIV/0!	#DIV/0!	#DIV/0!	#DIV/0!
					error propagated S.D	#DIV/0!	#DIV/0!	#DIV/0!	3.10469	#DIV/0!	#DIV/0!	3.048138	3.129595	3.350549	#DIV/0!	#DIV/0!	2.992709	3.074249	3.089408	3.181448	3.379167	3.097585	3.668702	3.084969	#DIV/0!	#DIV/0!	#DIV/0!	#DIV/0!	#DIV/0!
					delta Ct	#DIV/0!	#DIV/0!	#DIV/0!	9.227937	#DIV/0!	#DIV/0!	9.510437	7.082937	13.7271	#DIV/0!	#DIV/0!	7.345437	3.420437	8.845437	6.360437	6.912937	6.747937	7.055437	11.44294	#DIV/0!	#DIV/0!	#DIV/0!	#DIV/0!	#DIV/0!
					delta delta Ct	#DIV/0!	#DIV/0!	#DIV/0!	3.635399	#DIV/0!	#DIV/0!	4.915399	-0.0846	-3.34543	#DIV/0!	#DIV/0!	8.270399	7.745399	4.012899	-0.1746	6.062899	-1.4146	2.882899	6.735399	#DIV/0!	#DIV/0!	#DIV/0!	#DIV/0!	#DIV/0!
					Normalized ddCt	#DIV/0!	#DIV/0!	#DIV/0!	0.08047	#DIV/0!	#DIV/0!	0.033137	1.060394	10.16426	#DIV/0!	#DIV/0!	0.003239	0.00466	0.061944	1.128652	0.014958	2.665859	0.135569	0.009385	#DIV/0!	#DIV/0!	#DIV/0!	#DIV/0!	#DIV/0!
					positive error	#DIV/0!	#DIV/0!	#DIV/0!	6.74009	#DIV/0!	#DIV/0!	7.963537	3.044995	0.005115	#DIV/0!	#DIV/0!	11.26311	10.81965	7.102308	3.006847	9.442066	1.682985	6.551602	9.820369	#DIV/0!	#DIV/0!	#DIV/0!	#DIV/0!	#DIV/0!
					negative error	#DIV/0!	#DIV/0!	#DIV/0!	0.530709	#DIV/0!	#DIV/0!	1.867262	-3.2142	-6.69598	#DIV/0!	#DIV/0!	5.27769	4.67115	0.923491	-3.35605	2.683733	-4.51219	-0.7858	3.65043	#DIV/0!	#DIV/0!	#DIV/0!	#DIV/0!	#DIV/0!
					Normalized positive error	#DIV/0!	#DIV/0!	#DIV/0!	0.009355	#DIV/0!	#DIV/0!	0.004006	0.121162	0.996461	#DIV/0!	#DIV/0!	0.000407	0.000553	0.000727 8	0.124408	0.001438	0.311438	0.01066	0.001106	#DIV/0!	#DIV/0!	#DIV/0!	#DIV/0!	#DIV/0!
					Normalized	#DIV/0!	#DIV/0!	#DIV/0!	0.692214	#DIV/0!	#DIV/0!	0.274093	9.280458	103.6792	#DIV/0!	#DIV/0!	0.025778	0.03925	0.527232	10.23932	0.155638	22.81935	1.724051	0.079636	#DIV/0!	#DIV/0!	#DIV/0!	#DIV/0!	#DIV/0!

					negative error																							

Cu-Phen (**1**)

	Actin	Tubulin																										
	Ref gene 1	Ref gene 2	Ref gene 3	Ref gene 4		IL-6	NF-KB	PARP	Casp9	Casp3	SMAC	BCL-2	BAX	XIAP	IAP1	IAP2	HMOX	TFAM	TFB1M	TFB2M	NRF-2	CLPP	LON	SPG7	YME1L1	DRP1	MFN1	MFN2	OPA1
Ct 1	24.31	19.83							29.6			27.8	30.19	36.09			24	18.94	28.82	24.3	23.37	38.91	34.28	35.52					
Ct 2	27.94	26.28							28.12			30.95	30.85	36.09			22.64	18.53	30.03	28.94	23.4	38.87	32.72	37.85					
Ct 3	24.33	27.79							28.66			27.03	31.56				22.49	18.6	30.73	32.02	24.92	38.31	33.07	36.36					
Ct 4	23.98								28.39			26.32	30.74				22.08	19.91	30.55	32.54	24.06	39.72	34.6	35.99					
Ct 5																												
Ct 6																												
Ref Geometric mean	24.781069				Target mean	#DIV/0!	#DIV/0!	#DIV/0!	28.6925	#DIV/0!	#DIV/0!	28.025	30.835	36.09	#DIV/0!	#DIV/0!	22.8025	18.995	30.0325	29.45	23.9375	38.9525	33.6675	36.43	#DIV/0!	#DIV/0!	#DIV/0!	#DIV/0!	#DIV/0!
Ref S.D	2.7904224				target S.D	#DIV/0!	#DIV/0!	#DIV/0!	0.643914	#DIV/0!	#DIV/0!	2.041511	0.562998	0	#DIV/0!	#DIV/0!	0.832681	0.635741	0.861099	3.783103	0.728303	0.580366	0.912775	1.007141	#DIV/0!	#DIV/0!	#DIV/0!	#DIV/0!	#DIV/0!
					error propagated S.D	#DIV/0!	#DIV/0!	#DIV/0!	2.863753	#DIV/0!	#DIV/0!	3.457488	2.846651	2.790422	#DIV/0!	#DIV/0!	2.912012	2.861927	2.920265	4.700885	2.883901	2.850137	2.935918	2.966613	#DIV/0!	#DIV/0!	#DIV/0!	#DIV/0!	#DIV/0!
					delta Ct	#DIV/0!	#DIV/0!	#DIV/0!	3.911439	#DIV/0!	#DIV/0!	3.243939	6.053939	11.30894	#DIV/0!	#DIV/0!	-1.97856	-5.78606	5.251439	4.668939	-0.84356	14.17144	8.886439	11.64894	#DIV/0!	#DIV/0!	#DIV/0!	#DIV/0!	#DIV/0!
					delta delta Ct	#DIV/0!	#DIV/0!	#DIV/0!	-1.68111	#DIV/0!	#DIV/0!	-1.35111	-1.11136	-5.76136	#DIV/0!	#DIV/0!	-1.05536	-1.46111	0.418901	-1.86161	-1.69136	6.008901	4.713901	6.941401	#DIV/0!	#DIV/0!	#DIV/0!	#DIV/0!	#DIV/0!
					Normalized ddCt	#DIV/0!	#DIV/0!	#DIV/0!	3.206721	#DIV/0!	#DIV/0!	2.551064	2.163848	54.32705	#DIV/0!	#DIV/0!	2.075701	2.75318	0.747994	3.645455	3.234626	0.015529	0.038104	0.008136	#DIV/0!	#DIV/0!	#DIV/0!	#DIV/0!	#DIV/0!

					positive error	#DIV/0!	#DIV/0!	#DIV/0!	1.182654	#DIV/0!	#DIV/0!	2.106389	1.733052	-2.97318	#DIV/0!	#DIV/0!	1.858413	1.400828	3.339166	2.834786	1.190302	8.859038	7.649819	9.908014	#DIV/0!	#DIV/0!	#DIV/0!	#DIV/0!	#DIV/0!
					negative error	#DIV/0!	#DIV/0!	#DIV/0!	-4.54485	#DIV/0!	#DIV/0!	-4.80859	-3.96025	-8.55402	#DIV/0!	#DIV/0!	-3.96561	-4.32303	-2.50136	-6.56698	-4.57575	3.158764	1.777983	3.974788	#DIV/0!	#DIV/0!	#DIV/0!	#DIV/0!	#DIV/0!
					Normalized positive error	#DIV/0!	#DIV/0!	#DIV/0!	0.44054	#DIV/0!	#DIV/0!	0.232228	0.300815	7.852633	#DIV/0!	#DIV/0!	0.275779	0.378712	0.098812	0.140167	0.438211	0.002154	0.004979	0.001041	#DIV/0!	#DIV/0!	#DIV/0!	#DIV/0!	#DIV/0!
					Normalized negative error	#DIV/0!	#DIV/0!	#DIV/0!	23.34193	#DIV/0!	#DIV/0!	28.02392	15.56518	375.8521	#DIV/0!	#DIV/0!	15.62313	20.01522	5.662206	94.81112	23.87617	0.111974	0.291591	0.063602	#DIV/0!	#DIV/0!	#DIV/0!	#DIV/0!	#DIV/0!

Cu-DPQ-Phen (**2**)

	Actin	Tubulin																											
	Refgene 1	Refgene 2	Refgene 3	Refgene 4		IL-6	NF-KB	PARP	Casp9	Casp3	SMAC	BCL-2	BAX	XIAP	IAP1	IAP2	HMOX	TFAM	TFB1M	TFB2M	NRF-2	CLPP	LON	SPG7	YME1L1	DRP1	MFN1	MFN2	OPA1
Ct 1	19.72								27.76			27.96		39.08			21.13	18.57	27.28	28.06		28.39	29.85	32.49					
Ct 2	20.71	22.77							29.7			28.07	30.04	39.96			21.04	18.42	28.24	28.8	24.21	28.94	30.19	34.19					
Ct 3	18.86	18.7							27.22			29.51	26.23	36.02			29.01	19.74	23.58	27.73	22.91	24.82	27.79	31					
Ct 4	17.72	20.08							27.68			28.11	27.67	37.88			19.87	19.46	25.77	26.75	23.21	25.95	28.2	31.15					
Ct 5																													
Ct 6																													
Ref Geometric mean	19.737602 3				Target mean	#DIV/0!	#DIV/0!	#DIV/0!	28.09	#DIV/0!	#DIV/0!	28.4125	27.98	38.235	#DIV/0!	#DIV/0!	22.7625	19.0475	26.2175	27.835	23.44333	27.025	29.0075	32.2075	#DIV/0!	#DIV/0!	#DIV/0!	#DIV/0!	#DIV/0!
Ref S.D	1.6408113 6				target S.D	#DIV/0!	#DIV/0!	#DIV/0!	1.093934	#DIV/0!	#DIV/0!	0.73441	1.923824	1.705081	#DIV/0!	#DIV/0!	4.204358	0.651018	2.031098	0.85051	0.680686	1.96198	1.189184	1.481719	#DIV/0!	#DIV/0!	#DIV/0!	#DIV/0!	#DIV/0!
					error propagate	#DIV/0!	#DIV/0!	#DIV/0!	1.975077	#DIV/0!	#DIV/0!	1.797671	2.52851	2.366339	#DIV/0!	#DIV/0!	4.51319	1.765244	2.611057	1.848142	1.77464	2.557661	2.02643	2.210826	#DIV/0!	#DIV/0!	#DIV/0!	#DIV/0!	#DIV/0!

					d S.D																							
					delta Ct	#DIV/0!	#DIV/0!	#DIV/0!	8.352398	#DIV/0!	#DIV/0!	8.674898	8.242398	18.4974	#DIV/0!	#DIV/0!	3.024898	-0.69001	6.479898	8.097398	3.705731	7.287398	9.269898	12.4699	#DIV/0!	#DIV/0!	#DIV/0!	#DIV/0!	#DIV/0!
					delta delta Ct	#DIV/0!	#DIV/0!	#DIV/0!	2.75986	#DIV/0!	#DIV/0!	4.07986	1.07486	1.42486	#DIV/0!	#DIV/0!	3.94986	3.63486	1.64736	1.56236	2.855693	-0.87514	5.09736	7.76236	#DIV/0!	#DIV/0!	#DIV/0!	#DIV/0!	#DIV/0!
					Normalized ddCt	#DIV/0!	#DIV/0!	#DIV/0!	0.147638	#DIV/0!	#DIV/0!	0.059134	0.474717	0.372456	#DIV/0!	#DIV/0!	0.06471	0.08005	0.319224	0.338597	0.13815	1.834186	0.029211	0.004606	#DIV/0!	#DIV/0!	#DIV/0!	#DIV/0!	#DIV/0!
					positive error	#DIV/0!	#DIV/0!	#DIV/0!	4.734937	#DIV/0!	#DIV/0!	5.87753	3.60337	3.791199	#DIV/0!	#DIV/0!	8.46305	5.400104	4.258417	3.410502	4.632093	1.68252	7.12379	9.973186	#DIV/0!	#DIV/0!	#DIV/0!	#DIV/0!	#DIV/0!
					negative error	#DIV/0!	#DIV/0!	#DIV/0!	0.784783	#DIV/0!	#DIV/0!	2.282189	-1.45365	-0.94148	#DIV/0!	#DIV/0!	-0.56333	1.869616	-0.9637	-0.28578	1.079294	-3.43428	3.070929	5.551533	#DIV/0!	#DIV/0!	#DIV/0!	#DIV/0!	#DIV/0!
					Normalized positive error	#DIV/0!	#DIV/0!	#DIV/0!	0.037553	#DIV/0!	#DIV/0!	0.017009	0.082277	0.072233	#DIV/0!	#DIV/0!	0.002834	0.023681	0.05225	0.094045	0.040327	0.31538	0.00717	0.000995	#DIV/0!	#DIV/0!	#DIV/0!	#DIV/0!	#DIV/0!
					Normalized negative error	#DIV/0!	#DIV/0!	#DIV/0!	0.580439	#DIV/0!	#DIV/0!	0.205586	2.739002	1.920497	#DIV/0!	#DIV/0!	1.477677	0.273646	1.950302	1.219071	0.470321	10.79881	0.119003	0.021322	#DIV/0!	#DIV/0!	#DIV/0!	#DIV/0!	#DIV/0!

Cu-DPPZ-Phen (**3**)

	Actin	Tubulin																										
	Ref gene 1	Ref gene 2	Ref gene 3	Ref gene 4		IL-6	NF-KB	PARP	Casp9	Casp3	SMAC	BCL-2	BAX	XIAP	IAP1	IAP2	HMOX	TFAM	TFB1M	TFB2M	NRF-2	CLPP	LON	SPG7	YME1L1	DRP1	MFN1	MFN2	OPA1
Ct 1	15.45	24.28							28.86			28.13	25.92	28.01			21.62	18.47		30.79	28.37	32.47	29.01	28.69					
Ct 2	18.93	23.99							30.27			27.18	26.7	33.72			21.68	19.31	28.54	30.3	28.4	31.92	29.97	33.63					
Ct 3	20.07	26.81							27.91			26.39	29.21				23.16	18.33	34.38	30.17	27.62	28.54	27.52	33.29					
Ct 4	20.18	26.13							29.39			27.1	28.11				25.11	19.03	34.17	30.02	27.57	29.79	27.5	33.56					
Ct 5																												

Ct 6																												
Ref Geometric mean	21.653736 5				Target mean	#DIV/0!	#DIV/0!	#DIV/0!	29.1075	#DIV/0!	#DIV/0!	27.2	27.485	30.865	#DIV/0!	#DIV/0!	22.8925	18.785	32.33333	30.32	27.99	30.68	28.5	32.2925	#DIV/0!	#DIV/0!	#DIV/0!	#DIV/0!	#DIV/0!
Ref S.D	3.9408664 7				target S.D	#DIV/0!	#DIV/0!	#DIV/0!	0.98767	#DIV/0!	#DIV/0!	0.71447	1.464206	4.03758	#DIV/0!	#DIV/0!	1.640963	0.462565	3.312768	0.333567	0.456727	1.836065	1.208498	2.406136	#DIV/0!	#DIV/0!	#DIV/0!	#DIV/0!	#DIV/0!
					error propagated S.D	#DIV/0!	#DIV/0!	#DIV/0!	4.062748	#DIV/0!	#DIV/0!	4.005109	4.204085	5.642028	#DIV/0!	#DIV/0!	4.268862	3.967921	5.148287	3.954958	3.967244	4.343759	4.122001	4.61735	#DIV/0!	#DIV/0!	#DIV/0!	#DIV/0!	#DIV/0!
					delta Ct	#DIV/0!	#DIV/0!	#DIV/0!	7.453763	#DIV/0!	#DIV/0!	5.546263	5.831263	9.211263	#DIV/0!	#DIV/0!	1.238763	-2.86874	10.7096	8.666263	6.336263	9.026263	6.846263	10.63876	#DIV/0!	#DIV/0!	#DIV/0!	#DIV/0!	#DIV/0!
					delta delta Ct	#DIV/0!	#DIV/0!	#DIV/0!	1.861225	#DIV/0!	#DIV/0!	0.951225	-1.33627	-7.86127	#DIV/0!	#DIV/0!	2.163725	1.456225	5.877059	2.131225	5.486225	0.863725	2.673725	5.931225	#DIV/0!	#DIV/0!	#DIV/0!	#DIV/0!	#DIV/0!
					Normalized ddCt	#DIV/0!	#DIV/0!	#DIV/0!	0.275242	#DIV/0!	#DIV/0!	0.517193	2.524984	232.5302	#DIV/0!	#DIV/0!	0.223179	0.364445	0.017015	0.228264	0.022309	0.549532	0.156721	0.016388	#DIV/0!	#DIV/0!	#DIV/0!	#DIV/0!	#DIV/0!
					positive error	#DIV/0!	#DIV/0!	#DIV/0!	5.923973	#DIV/0!	#DIV/0!	4.956334	2.86781	-2.21925	#DIV/0!	#DIV/0!	6.432588	5.424146	11.02535	6.086184	9.45347	5.211318	6.795727	10.54858	#DIV/0!	#DIV/0!	#DIV/0!	#DIV/0!	#DIV/0!
					negative error	#DIV/0!	#DIV/0!	#DIV/0!	-2.20152	#DIV/0!	#DIV/0!	-3.05388	-5.54036	-13.5033	#DIV/0!	#DIV/0!	-2.10514	-2.51117	0.728772	-1.82373	1.518981	-3.48387	-1.44828	1.313876	#DIV/0!	#DIV/0!	#DIV/0!	#DIV/0!	#DIV/0!
					Normalized positive error	#DIV/0!	#DIV/0!	#DIV/0!	0.01647	#DIV/0!	#DIV/0!	0.03221	0.136994	4.656502	#DIV/0!	#DIV/0!	0.011577	0.02329	0.00048	0.014719	0.001426	0.026992	0.009001	0.000668	#DIV/0!	#DIV/0!	#DIV/0!	#DIV/0!	#DIV/0!
					Normalized negative error	#DIV/0!	#DIV/0!	#DIV/0!	4.599645	#DIV/0!	#DIV/0!	8.304442	46.53871	11611.79	#DIV/0!	#DIV/0!	4.302386	5.702898	0.603418	3.539959	0.348932	11.1879	2.728817	0.402239	#DIV/0!	#DIV/0!	#DIV/0!	#DIV/0!	#DIV/0!

Cu-DPPN-Phen (**4**)

	Actin	Tubulin																											
	Ref gene 1	Ref gene 2	Ref gene 3	Ref gene 4		IL-6	NF-KB	PARP	Casp9	Casp3	SMAC	BCL-2	BAX	XIAP	IAP1	IAP2	HMOX	TFAM	TFB1M	TFB2M	NRF-2	CLPP	LON	SPG7	YME1L1	DRP1	MFN1	MFN2	OPA1
Ct 1	16.42	22.16							32.01			29.12	27.33	33.35			23.97	20.88	29.04	26.83	27.47	28.05	26.45	31.21					
Ct 2	17.53								30.08			31.9	28.3	34.57			22.9	19.97	30.62	29.91	27.7	26.78	25.9	32.35					
Ct 3	14.12	20.73							29.73			28.41	26.57	31.45			22.24	20.86	28.45	27.45	28.49	27.26	25.8	32.45					
Ct 4	14.63	20.2							29.75			29.04	26.95	30.49			21.77	21.83	28.86	26.97	28.08	26.81	27.29	33.04					
Ct 5																													
Ct 6																													
Ref Geometric mean	17.734627 6				Target mean	#DIV/0!	#DIV/0!	#DIV/0!	30.3925	#DIV/0!	#DIV/0!	29.6175	27.2875	32.4465	#DIV/0!	#DIV/0!	22.72	20.885	29.2425	27.79	27.935	27.225	26.36	32.2625	#DIV/0!	#DIV/0!	#DIV/0!	#DIV/0!	#DIV/0!
Ref S.D	3.1283861 7				target S.D	#DIV/0!	#DIV/0!	#DIV/0!	1.09021	#DIV/0!	#DIV/0!	1.555444 3	0.7428894	1.83894	#DIV/0!	#DIV/0!	0.955355	0.759583	0.950943	1.438054	0.4474	0.592199	0.682691	0.764869	#DIV/0!	#DIV/0!	#DIV/0!	#DIV/0!	#DIV/0!
					error propagated S.D	#DIV/0!	#DIV/0!	#DIV/0!	3.312908	#DIV/0!	#DIV/0!	3.493292	3.215384	3.628843	#DIV/0!	#DIV/0!	3.270484	3.21928	3.269723	3.44308	3.160216	3.183944	3.20201	3.220532	#DIV/0!	#DIV/0!	#DIV/0!	#DIV/0!	#DIV/0!
					delta Ct	#DIV/0!	#DIV/0!	#DIV/0!	12.65787	#DIV/0!	#DIV/0!	11.88287	9.552872	14.73037	#DIV/0!	#DIV/0!	4.985372	3.150372	11.50787	10.05537	10.20037	9.490372	8.625372	14.52787	#DIV/0!	#DIV/0!	#DIV/0!	#DIV/0!	#DIV/0!
					delta delta Ct	#DIV/0!	#DIV/0!	#DIV/0!	7.065334	#DIV/0!	#DIV/0!	7.287834	2.385334	-2.34217	#DIV/0!	#DIV/0!	5.910334	7.475334	6.675334	3.520334	9.350334	1.327834	4.452834	9.820334	#DIV/0!	#DIV/0!	#DIV/0!	#DIV/0!	#DIV/0!
					Normalized ddCt	#DIV/0!	#DIV/0!	#DIV/0!	0.007467	#DIV/0!	#DIV/0!	0.006399	0.1914	5.070632	#DIV/0!	#DIV/0!	0.016627	0.00562	0.009784	0.087151	0.001532	0.398366	0.045663	0.001106	#DIV/0!	#DIV/0!	#DIV/0!	#DIV/0!	#DIV/0!
					positive error	#DIV/0!	#DIV/0!	#DIV/0!	10.37824	#DIV/0!	#DIV/0!	10.78113	5.600718	1.286677	#DIV/0!	#DIV/0!	9.180819	10.69461	9.945058	6.963414	12.51055	4.511778	7.654844	13.04087	#DIV/0!	#DIV/0!	#DIV/0!	#DIV/0!	#DIV/0!
					negative	#DIV/0	#DIV/0	#DIV/0	3.75242	#DIV/0	#DIV/0	3.79454	-0.83	-5.97	#DIV/0	#DIV/0	2.63985	4.25605	3.40561	0.07725	6.19011	-1.85	1.25082	6.59980	#DIV/0!	#DIV/0	#DIV/0	#DIV/0	#DIV/0

					error	!	!	!	7	!	!	2	005	101	!	!		4	1	4	8	611	5	3		!	!	!	!
					Normalized positive error	#DIV/0!	#DIV/0!	#DIV/0!	0.000751	#DIV/0!	#DIV/0!	0.000568	0.020607	0.409894	#DIV/0!	#DIV/0!	0.001723	0.000603	0.001014	0.000803	0.000171	0.043835	0.004962	0.000119	#DIV/0!	#DIV/0!	#DIV/0!	#DIV/0!	#DIV/0!
					Normalized negative error	#DIV/0!	#DIV/0!	#DIV/0!	0.074201	#DIV/0!	#DIV/0!	0.072066	1.777746	62.72673	#DIV/0!	#DIV/0!	0.160445	0.052336	0.094365	0.94786	0.013696	3.620301	0.420208	0.01031	#DIV/0!	#DIV/0!	#DIV/0!	#DIV/0!	#DIV/0!

3.4.14 A2780/ Cis 24 h

Negative

	Actin	Tubulin				Target genes																								
	Refgene 1	Refgene 2	Refgene 3	Ref gene 4		IL-6	NF-KB	PARP	Casp9	Casp3	SMAC	BCL-2	BAX	XIAP	IAP1	IAP2	HMOX	TFAM	TFB1M	TFB2M	NRF-2	CLPP	LON	SPG7	YME1L1	DRP1	MFN1	MFN2	OPA1
Ct 1	25.01	24.39							28.48	38.51		26.18	28.87				23.73	16.43	34.93	34.83	27.17	33.28	32.79	35	29.95	25.98	27.37	25.99	26.63
Ct 2	24.59	25.63							28.33			27.09	29.04				23.12	16.12	36.05	35.16	26.38	32.46	35.38	35.82	27.93	42.43	27.35	26.67	25.74
Ct 3																													
Ct 4																													
Ct 5																													
Ct 6																													
Ref Geometric mean	24.90051				Target mean	#DIV/0!	#DIV/0!	#DIV/0!	28.405	38.51	#DIV/0!	26.635	28.955	#DIV/0!	#DIV/0!	#DIV/0!	23.425	16.275	35.49	34.995	26.775	32.87	34.085	35.41	28.94	34.205	27.36	26.33	26.185
Ref S.D	0.548057				Target S.D	#DIV/0!	#DIV/0!	#DIV/0!	0.106066	#DIV/0!	#DIV/0!	0.643467	0.120208	#DIV/0!	#DIV/0!	#DIV/0!	0.431335	0.219203	0.791896	0.233345	0.558614	0.579828	1.831407	0.579828	1.428356	11.63191	0.014142	0.480833	0.629325
					error propagated S.D	#DIV/0!	#DIV/0!	#DIV/0!	0.558226	#DIV/0!	#DIV/0!	0.845232	0.561085	#DIV/0!	#DIV/0!	#DIV/0!	0.697436	0.590268	0.963103	0.595665	0.782571	0.797851	1.911653	0.797851	1.529891	11.64481	0.548324	0.729086	0.834516
					delta Ct	#DIV/0!	#DIV/0!	#DIV/0!	3.504495	13.60949	#DIV/0!	1.734495	4.054495	#DIV/0!	#DIV/0!	#DIV/0!	-1.47551	-8.62551	10.58949	10.09449	1.874495	7.969495	9.184495	10.50949	4.039495	9.304495	2.459495	1.429495	1.284495
					delta delta Ct	#DIV/0!	#DIV/0!	#DIV/0!	0	0	#DIV/0!	0	0	#DIV/0!	#DIV/0!	#DIV/0!	0	0	0	0	0	0	0	0	0	0	0	0	0

					Normalized ddCt	#DIV/0!	#DIV/0!	#DIV/0!	1	1	#DIV/0!	1	1	#DIV/0!	#DIV/0!	#DIV/0!	1	1	1	1	1	1	1	1	1	1	1	1	1
					positive error	#DIV/0!	#DIV/0!	#DIV/0!	0.5582 26	#DIV/0!	#DIV/0!	0.8452 32	0.5610 85	#DIV/0!	#DIV/0!	#DIV/0!	0.6974 36	0.5902 68	0.9631 03	0.5956 65	0.7825 71	0.7978 51	1.9116 53	0.7978 51	1.5298 91	11.644 81	0.5482 4	0.7290 86	0.8345 16
					negative error	#DIV/0!	#DIV/0!	#DIV/0!	-0.5583	#DIV/0!	#DIV/0!	-0.8452 3	-0.5610 9	#DIV/0!	#DIV/0!	#DIV/0!	-0.6974 4	-0.5902 7	-0.9631	-0.5956 6	-0.7825 7	-0.7978 5	-1.9116 5	-0.7978 5	-1.5298 9	-11.644 8	-0.5482 4	-0.7290 9	-0.8345 2
					Normalized positive error	#DIV/0!	#DIV/0!	#DIV/0!	0.6791 37	#DIV/0!	#DIV/0!	0.5566 21	0.6777 92	#DIV/0!	#DIV/0!	#DIV/0!	0.6166 67	0.6642 19	0.5129 53	0.6617 39	0.5813 3	0.5752 05	0.2657 88	0.5752 05	0.3463 04	0.0003 12	0.6838 54	0.6032 86	0.5607 71
					Normalized negative error	#DIV/0!	#DIV/0!	#DIV/0!	1.4724 58	#DIV/0!	#DIV/0!	1.7965 53	1.4753 79	#DIV/0!	#DIV/0!	#DIV/0!	1.6216 2	1.5055 27	1.9494 98	1.5111 69	1.7201 93	1.7385 1	3.7623 99	1.7385 1	2.8876 4	3202.1 18	1.4623	1.6575 89	1.7832 58

Doxorubicin

	Actin	Tubulin																										
	Refgene 1	Refgene 2	Refgene 3	Ref gene 4		IL-6	NF-KB	PARP	Casp9	Casp3	SMAC	BCL-2	BAX	XIAP	IAP1	IAP2	HMOX	TFAM	TFB1M	TFB2M	NRF-2	CLPP	LON	SPG7	YME1L1	DRP1	MFN1	MFN2	OPA1
Ct 1	25.32	25.91							30			27.42	29.63				23.04	11.65	35.49	35.34	27.95	34.51	34.94	35.71	30.75	27.76	28.6	27.21	27.49
Ct 2	24.9	26.66							29.03			27.49	30.78				23.46	17.24	35.75	35.84	27.78	34.08	34.47	37.53	29.49	27.98	29.99	28.02	28.21
Ct 3																													
Ct 4																													
Ct 5																													
Ct 6																													
Ref Geometric mean	25.68903				Target mean	#DIV/0!	#DIV/0!	#DIV/0!	29.515	#DIV/0!	#DIV/0!	27.455	30.205	#DIV/0!	#DIV/0!	#DIV/0!	23.25	14.445	35.62	35.59	27.865	34.295	34.705	36.62	30.12	27.87	29.295	27.615	27.85
Ref S.D	0.763779				target S.D	#DIV/0!	#DIV/0!	#DIV/0!	0.685894	#DIV/0!	#DIV/0!	0.049497	0.813173	#DIV/0!	#DIV/0!	#DIV/0!	0.296985	3.952727	0.183848	0.353553	0.120208	0.304056	0.323 4	1.286934	0.890955	0.155563	0.982878	0.572756	0.509117
					error propagated S.D	#DIV/0!	#DIV/0!	#DIV/0!	1.026552	#DIV/0!	#DIV/0!	0.765381	1.15622	#DIV/0!	#DIV/0!	#DIV/0!	0.819487	4.025843	0.785594	0.8416 4	0.773181	0.822076	0.832952	1.496515	1.173524	0.77946	1.244752	0.954677	0.917911
					delta Ct	#DIV/0!	#DIV/0!	#DIV/0!	3.825973	#DIV/0!	#DIV/0!	1.765973	4.515973	#DIV/0!	#DIV/0!	#DIV/0!	-2.43903	-11.244	9.930973	9.900973	2.175973	8.605973	9.015973	10.93097	4.430973	2.180973	3.605973	1.925973	2.160973
					delta delta Ct	#DIV/	#DIV/	#DIV/	0.3214	#DIV/	#DIV/	0.0314	0.4614	#DIV/	#DIV/	#DIV/	-0.9	-2.6	-0.6	-0.1	0.3014	0.6364	-0.1	0.4214	0.3914	-7.1	1.1464	0.4964	0.8764

						0!	0!	0!	78	0!	0!	78	78	0!	0!	0!	6352	1852	5852	9352	78	78	6852	78	78	2352	78	78	78
					Normalized ddCt	#DIV/0!	#DIV/0!	#DIV/0!	0.800249	#DIV/0!	#DIV/0!	0.978417	0.726242	#DIV/0!	#DIV/0!	#DIV/0!	1.950064	6.141205	1.578464	1.143552	0.811421	0.643281	1.123906	0.746659	0.762348	139.442	0.451727	0.708835	0.544695
					positive error	#DIV/0!	#DIV/0!	#DIV/0!	1.348003	#DIV/0!	#DIV/0!	0.796859	1.577098	#DIV/0!	#DIV/0!	#DIV/0!	-0.14404	1.407321	0.127073	0.648119	1.074659	1.458554	0.664433	1.917994	1.565002	-6.34406	2.391231	1.451155	1.794388
					negative error	#DIV/0!	#DIV/0!	#DIV/0!	-0.70507	#DIV/0!	#DIV/0!	-0.7339	-0.65414	#DIV/0!	#DIV/0!	#DIV/0!	-1.78301	-6.64436	-1.44412	-1.03516	-0.4717	-0.11856	-1.01047	-1.01754	-0.78205	-7.90298	-0.09827	-0.4582	-0.04143
					Normalized positive error	#DIV/0!	#DIV/0!	#DIV/0!	0.392828	#DIV/0!	#DIV/0!	0.575601	0.335155	#DIV/0!	#DIV/0!	#DIV/0!	1.104991	0.377011	0.915688	0.638112	0.474783	0.363858	0.630938	0.264622	0.337977	81.23679	0.190629	0.365728	0.288294
					Normalized negative error	#DIV/0!	#DIV/0!	#DIV/0!	1.630228	#DIV/0!	#DIV/0!	1.663132	1.57368	#DIV/0!	#DIV/0!	#DIV/0!	3.443143	100.0352	2.702096	2.049344	1.386745	1.137288	2.002043	2.106776	1.719567	239.3507	1.070492	1.373826	1.029134

Cisplatin

	Actin	Tubulin																										
	Refgene 1	Refgene 2	Refgene 3	Ref gene 4		IL-6	NF-KB	PARP	Casp9	Casp3	SMAC	BCL-2	BAX	XIAP	IAP1	IAP2	HMOX	TFAM	TFB1M	TFB2M	NRF-2	CLPP	LON	SPG7	YME1L1	DRP1	MFN1	MFN2	OPA1
Ct 1	26.63	17.73											35.43				23.34		36.82	38.19		37.3	37.72	37.69	35.02	25.59	26.98	26.68	25.47
Ct 2	24.75	27.9										5.24					41.23		35.19		27	34.88	37.29	39.18	34.28	25.09	26.68	26.94	25.56
Ct 3																													
Ct 4																													
Ct 5																													
Ct 6																													
Ref Geometric mean	23.89543				Target mean	#DIV/0!	#DIV/0!	#DIV/0!	#DIV/0!	#DIV/0!	#DIV/0!	5.24	35.43	#DIV/0!	#DIV/0!	#DIV/0!	32.285	#DIV/0!	36.005	38.19	27	36.09	37.505	38.435	34.65	25.34	26.83	26.81	25.515
Ref S.D	4.536786				target S.D	#DIV/0!	#DIV/0!	#DIV/0!	#DIV/0!	#DIV/0!	#DIV/0!	#DIV/0!	#DIV/0!	#DIV/0!	#DIV/0!	#DIV/0!	12.65014	#DIV/0!	1.152584	#DIV/0!	#DIV/0!	1.711198	0.304056	1.053589	0.523259	0.353553	0.212132	0.183848	0.06364
					error propagated S.D	#DIV/0!	#DIV/0!	#DIV/0!	#DIV/0!	#DIV/0!	#DIV/0!	#DIV/0!	#DIV/0!	#DIV/0!	#DIV/0!	#DIV/0!	13.43907	#DIV/0!	4.680905	#DIV/0!	#DIV/0!	4.848776	4.546963	4.657518	4.566862	4.550541	4.541743	4.540509	4.537232
					delta Ct	#DIV/0!	#DIV/0!	#DIV/0!	#DIV/0!	#DIV/0!	#DIV/0!	-18.655	11.53457	#DIV/0!	#DIV/0!	#DIV/0!	8.389571	#DIV/0!	12.10957	14.29457	3.104571	12.19457	13.60957	14.53957	10.75457	1.444571	2.934571	2.914571	1.619571

												4																
					delta delta Ct	#DIV/0!	#DIV/0!	#DIV/0!	#DIV/0!	#DIV/0!	#DIV/0!	-20.3899	7.480076	#DIV/0!	#DIV/0!	#DIV/0!	9.865076	#DIV/0!	1.520076	4.200076	1.230076	4.225076	4.425076	4.030076	6.715076	-7.85992	0.475076	1.485076	0.335076
					Normalized ddCt	#DIV/0!	#DIV/0!	#DIV/0!	#DIV/0!	#DIV/0!	#DIV/0!	1373974	0.005601	#DIV/0!	#DIV/0!	#DIV/0!	0.001072	#DIV/0!	0.348667	0.054407	0.426295	0.053472	0.046555	0.061211	0.009518	232.3126	0.719429	0.357233	0.792742
					positive error	#DIV/0!	#DIV/0!	#DIV/0!	#DIV/0!	#DIV/0!	#DIV/0!	#DIV/0!	#DIV/0!	#DIV/0!	#DIV/0!	#DIV/0!	#DIV/0!	23.30414	#DIV/0!	6.200982	#DIV/0!	#DIV/0!	9.073852	8.972044	8.687594	11.28194	-3.30938	5.016819	6.025586	4.872308
					negative error	#DIV/0!	#DIV/0!	#DIV/0!	#DIV/0!	#DIV/0!	#DIV/0!	#DIV/0!	#DIV/0!	#DIV/0!	#DIV/0!	#DIV/0!	#DIV/0!	-3.57399	#DIV/0!	-3.16083	#DIV/0!	#DIV/0!	-0.6237	-0.12189	-0.62744	2.148215	-12.4105	-4.06667	-3.05543	-4.20216
					Normalized positive error	#DIV/0!	#DIV/0!	#DIV/0!	#DIV/0!	#DIV/0!	#DIV/0!	#DIV/0!	#DIV/0!	#DIV/0!	#DIV/0!	#DIV/0!	#DIV/0!	9.66E-08	#DIV/0!	0.013593	#DIV/0!	#DIV/0!	0.001856	0.001991	0.002425	0.000402	9.913417	0.030888	0.01535	0.034142
					Normalized negative error	#DIV/0!	#DIV/0!	#DIV/0!	#DIV/0!	#DIV/0!	#DIV/0!	#DIV/0!	#DIV/0!	#DIV/0!	#DIV/0!	#DIV/0!	#DIV/0!	11.90907	#DIV/0!	8.943435	#DIV/0!	#DIV/0!	1.540821	1.088157	1.544823	0.255092	5444.051	16.7567	8.313367	18.40666

Cu-Phen (**1**)

	Actin	Tubulin																											
	Ref gene 1	Ref gene 2	Ref gene 3	Ref gene 4		IL-6	NF-KB	PARP	Casp9	Casp3	SMAC	BCL-2	BAX	XIAP	IAP1	IAP2	HMOX	TFAM	TFB1M	TFB2M	NRF-2	CLPP	LON	SPG7	YME1L1	DRP1	MFN1	MFN2	OPA1
Ct 1	24.31	24.28							27.93	42.17		25.73	28.94				24.02	15.69	34.21	33.07	26.4	32.81	32.6	35.88	26.37	26.97	26.21	26.52	26.11
Ct 2	25.88	24.34							28.39			26.22	28.22				23.93	16.81	34.63	33.19	26.69	33.8	30.65	33.21	25.7	25.71	26.06	26.3	27.03
Ct 3																													
Ct 4																													
Ct 5																													
Ct 6																													
Ref Geometric mean	24.69333				Target mean	#DIV/0!	#DIV/0!	#DIV/0!	28.16	42.17	#DIV/0!	25.975	28.58	#DIV/0!	#DIV/0!	#DIV/0!	23.975	16.25	34.42	33.13	26.545	33.305	31.625	34.545	26.035	26.34	26.135	26.41	26.57
Ref S.D	0.785382				target S.D	#DIV/0!	#DIV/0!	#DIV/0!	0.325269	#DIV/0!	#DIV/0!	0.346482	0.509117	#DIV/0!	#DIV/0!	#DIV/0!	0.006364	0.791996	0.296985	0.084853	0.205061	0.700036	1.378858	1.879475	0.473762	0.890955	0.106066	0.155563	0.650538
					error	#D	#D	#D	0.8	#D	#D	0.8	0.9	#D	#D	#D	0.7	1.1	0.8	0.7	0.8	1.0	1.5	2.0	0.9	1.1	0.7	0.8	1.0

					propagated S.D	IV/0!	IV/0!	IV/0!	50074	IV/0!	IV/0!	58414	35962	IV/0!	IV/0!	IV/0!	87956	15359	39658	89953	11711	52081	86844	44817	1721	87697	92512	0064	19816
					delta Ct	#DIV/0!	#DIV/0!	#DIV/0!	3.466672	17.47667	#DIV/0!	1.281672	3.886672	#DIV/0!	#DIV/0!	#DIV/0!	-0.71833	-8.44333	9.726672	8.436672	1.851672	8.611672	6.931672	9.851672	1.341672	1.646672	1.441672	1.716672	1.876672
					delta delta Ct	#DIV/0!	#DIV/0!	#DIV/0!	-0.03782	3.867177	#DIV/0!	-0.45282	-0.16782	#DIV/0!	#DIV/0!	#DIV/0!	0.757177	0.182177	-0.86282	-1.65782	-0.02282	0.642177	-2.25282	-0.65782	-2.69782	-7.65782	-1.01782	0.287177	0.592177
					Normalized ddCt	#DIV/0!	#DIV/0!	#DIV/0!	1.026563	0.068527	#DIV/0!	1.368716	1.123362	#DIV/0!	#DIV/0!	#DIV/0!	0.591653	0.881372	1.818593	3.1554	1.015945	0.640745	4.766145	1.5777	6.488822	201.9456	2.024861	0.819504	0.633441
					positive error	#DIV/0!	#DIV/0!	#DIV/0!	0.812251	#DIV/0!	#DIV/0!	0.405592	0.768139	#DIV/0!	#DIV/0!	#DIV/0!	1.545134	1.297536	-0.02317	-0.86787	0.788888	1.694259	-0.66598	1.386994	-1.78061	-6.47013	-0.22531	1.087818	1.611993
					negative error	#DIV/0!	#DIV/0!	#DIV/0!	-0.8879	#DIV/0!	#DIV/0!	-1.31124	-1.10378	#DIV/0!	#DIV/0!	#DIV/0!	-0.03078	-0.93318	-1.70248	-2.44778	-0.83453	-0.4099	-3.83967	-2.70264	-3.61503	-8.84552	-1.81033	-0.51346	-0.42764
					Normalized positive error	#DIV/0!	#DIV/0!	#DIV/0!	0.569493	#DIV/0!	#DIV/0!	0.754927	0.587174	#DIV/0!	#DIV/0!	#DIV/0!	0.342664	0.406802	1.016186	1.824967	0.578779	0.309013	1.586644	0.382361	3.43572	88.65471	1.169029	0.470473	0.327146
					Normalized negative error	#DIV/0!	#DIV/0!	#DIV/0!	1.850476	#DIV/0!	#DIV/0!	2.481542	2.149178	#DIV/0!	#DIV/0!	#DIV/0!	1.021564	1.909482	3.2546	5.455741	1.783281	1.328597	14.3171	6.509918	12.25275	460.0096	3.507236	1.427473	1.3450 3

Cu-DPQ-Phen (**2**)

	Actin	Tubulin																											
	Refgene 1	Refgene 2	Refgene 3	Ref gene 4		IL-6	NF-KB	PARP	Casp9	Casp3	SMAC	BCL-2	BAX	XIAP	IAP1	IAP2	HMOX	TFAM	TFB1M	TFB2M	NRF-2	CLPP	LON	SPG7	YME1L1	DRP1	MFN1	MFN2	OPA1
Ct 1	27.69	29.92								37.61			36.71				21.29	28.14	32.33	32.14	34.77	33.12	31.81		28.94	33.34	32.71	35.04	32.86
Ct 2	26.88	28.08								5.48			38.37				21.21	29.17	32.89	33.25	35.91	34.01	30.21	35.76	33.87	33.75	35.32	38.96	34.14
Ct 3																													
Ct 4																													
Ct 5																													
Ct 6																													
Ref Geometric mean	28.1208				Target mean	#DIV/0!	#DIV/0!	#DIV/0!	#DIV/0!	21.545	#DIV/0!	#DIV/0!	37.54	#DIV/0!	#DIV/0!	#DIV/0!	21.25	28.655	32.61	32.695	35.34	33.565	31.01	35.76	31.405	33.545	34.015	37	33.5

Ref S.D	1.2860 89				target S.D	#DIV/0!	#DIV/0!	#DIV/0!	#DIV/0!	22.719 34	#DIV/0!	#DIV/0!	1.1737 97	#DIV/0!	#DIV/0!	#DIV/0!	#DIV/0!	0.0565 69	0.7283 2	0.3959 8	0.7848 89	0.8061 02	0.6293 25	1.1313 71	#DIV/0!	3.4860 36	0.2899 14	1.8455 49	2.7718 59	0.9050 97
					error propagated S.D	#DIV/0!	#DIV/0!	#DIV/0!	#DIV/0!	22.755 71	#DIV/0!	#DIV/0!	1.7412 14	#DIV/0!	#DIV/0!	#DIV/0!	#DIV/0!	1.2873 33	1.4779 97	1.3456 69	1.5066 77	1.5178 36	1.4318 08	1.7129	#DIV/0!	3.7157 07	1.3183 61	2.2494 61	3.0556 87	1.5726 49
					delta Ct	#DIV/0!	#DIV/0!	#DIV/0!	#DIV/0!	-6.5758	#DIV/0!	#DIV/0!	9.4191 96	#DIV/0!	#DIV/0!	#DIV/0!	#DIV/0!	-6.8708	0.5341 96	4.4891 96	4.5741 96	7.2191 96	5.4441 96	2.8891 96	7.6391 96	3.2841 96	5.4241 96	5.8941 96	8.8791 96	5.3791 96
					delta delta Ct	#DIV/0!	#DIV/0!	#DIV/0!	#DIV/0!	-20.1853	#DIV/0!	#DIV/0!	5.3647 01	#DIV/0!	#DIV/0!	#DIV/0!	#DIV/0!	-5.3953	9.1597 01	-6.1003	-5.5203	5.3447 01	-2.5253	-6.2953	-2.8703	-0.7553	-3.8803	3.4347 01	7.4497 01	4.0947 01
					Normalized ddCt	#DIV/0!	#DIV/0!	#DIV/0!	#DIV/0!	1192286	#DIV/0!	#DIV/0!	0.0242 7	#DIV/0!	#DIV/0!	#DIV/0!	#DIV/0!	42.086 88	0.0017 48	68.607 7	45.896 07	0.0246 08	5.7569 26	78.536 89	7.3121 65	1.6879 81	14.726 05	0.0924 81	0.0057 2	0.0585 29
					positive error	#DIV/0!	#DIV/0!	#DIV/0!	#DIV/0!	2.5704 14	#DIV/0!	#DIV/0!	7.1059 15	#DIV/0!	#DIV/0!	#DIV/0!	#DIV/0!	-4.1079 7	10.637 7	-4.7546 3	-4.0136 2	6.8625 37	-1.0934 9	-4.5824	#DIV/0!	2.9604 08	-2.5619 4	5.6841 62	10.505 39	5.6673 5
					negative error	#DIV/0!	#DIV/0!	#DIV/0!	#DIV/0!	-42.941	#DIV/0!	#DIV/0!	3.6234 88	#DIV/0!	#DIV/0!	#DIV/0!	#DIV/0!	-6.6826 3	7.6817 04	-7.4459 7	-7.0269 8	3.8268 66	-3.9571 1	-8.0082	#DIV/0!	-4.4710 1	-5.1986 6	1.1852 4	4.3940 14	2.5220 52
					Normalized positive error	#DIV/0!	#DIV/0!	#DIV/0!	#DIV/0!	0.1683 56	#DIV/0!	#DIV/0!	0.0072 59	#DIV/0!	#DIV/0!	#DIV/0!	#DIV/0!	17.243 32	0.0006 628	26.995 17	16.151 79	0.0085 94	2.1338 97	23.957 39	#DIV/0!	0.1284 78	5.9050 03	0.0194 49	0.0006 88	0.0196 77
					Normalized negative error	#DIV/0!	#DIV/0!	#DIV/0!	#DIV/0!	8.44E +12	#DIV/0!	#DIV/0!	0.0811 37	#DIV/0!	#DIV/0!	#DIV/0!	#DIV/0!	102.72 41	0.0048 71	174.36 51	130.41 58	0.0704 69	15.531 3	257.45 89	#DIV/0!	22.177 2	36.724 2	0.4397 51	0.0475 63	0.1740 95

Cu-DPPZ-Phen (**3**)

	Actin	Tubulin																												
	Refgene 1	Refgene 2	Refgene 3	Ref gene 4		IL-6	NF-KB	PARP	Casp9	Casp3	SMAC	BCL-2	BAX	XIAP	IAP1	IAP2	HMOX	TFAM	TFB1M	TFB2M	NRF-2	CLPP	LON	SPG7	YME1L1	DRP1	MFN1	MFN2	OPA1
Ct 1		32.98							24.43	35		26.93					32.04		34.81		12.11	35.69	37.97	40.74	32.2	25.6	26.89	27.39	25.9
Ct 2		24.62										27.82	29.89				21.64					35.5	35.38	37.69	32.77	25.71	27.98	27.99	25.99
Ct 3																														
Ct 4																														
Ct 5																														

Ct 6																												
Ref Geometric mean	28.49505				Target mean	#DIV/0!	#DIV/0!	#DIV/0!	24.43	35	#DIV/0!	27.375	29.89	#DIV/0!	#DIV/0!	#DIV/0!	26.84	#DIV/0!	34.81	#DIV/0!	12.11	35.595	36.675	39.215	32.485	25.655	27.435	27.69	25.945
Ref S.D	5.911413				target S.D	#DIV/0!	#DIV/0!	#DIV/0!	#DIV/0!	#DIV/0!	#DIV/0!	0.629325	#DIV/0!	#DIV/0!	#DIV/0!	#DIV/0!	7.353911	#DIV/0!	#DIV/0!	#DIV/0!	#DIV/0!	0.13435	1.831407	2.156676	0.403051	0.077782	0.770746	0.424264	0.006364
					error propagated S.D	#DIV/0!	#DIV/0!	#DIV/0!	#DIV/0!	#DIV/0!	#DIV/0!	5.944817	#DIV/0!	#DIV/0!	#DIV/0!	#DIV/0!	9.435295	#DIV/0!	#DIV/0!	#DIV/0!	#DIV/0!	5.912939	6.188606	6.292539	5.925137	5.911924	5.961447	5.926618	5.911755
					delta Ct	#DIV/0!	#DIV/0!	#DIV/0!	-4.06505	6.504955	#DIV/0!	-1.12005	1.394955	#DIV/0!	#DIV/0!	#DIV/0!	-1.65505	#DIV/0!	6.314955	#DIV/0!	-16.385	7.099955	8.179955	10.71995	3.899955	-2.80405	-1.06005	-0.80505	-2.55005
					delta delta Ct	#DIV/0!	#DIV/0!	#DIV/0!	-7.56954	-7.10454	#DIV/0!	-2.85454	-2.65954	#DIV/0!	#DIV/0!	#DIV/0!	-0.17954	#DIV/0!	-4.27454	#DIV/0!	-18.2595	-0.86954	-1.00454	0.21046	-0.04954	-12.1445	-3.51954	-2.23454	-3.83454
					Normalized ddCt	#DIV/0!	#DIV/0!	#DIV/0!	189.9585	137.6194	#DIV/0!	7.232729	6.318316	#DIV/0!	#DIV/0!	#DIV/0!	1.132523	#DIV/0!	19.35373	#DIV/0!	313811.8	1.827028	2.006304	0.864262	1.034935	4527.629	11.46799	4.706126	14.26631
					positive error	#DIV/0!	#DIV/0!	#DIV/0!	#DIV/0!	#DIV/0!	#DIV/0!	3.090277	#DIV/0!	#DIV/0!	#DIV/0!	#DIV/0!	9.255755	#DIV/0!	#DIV/0!	#DIV/0!	#DIV/0!	5.043399	5.184066	6.502999	5.875597	-6.23262	2.419407	3.692078	2.077215
					negative error	#DIV/0!	#DIV/0!	#DIV/0!	#DIV/0!	#DIV/0!	#DIV/0!	-8.79936	#DIV/0!	#DIV/0!	#DIV/0!	#DIV/0!	-9.61484	#DIV/0!	#DIV/0!	#DIV/0!	#DIV/0!	-6.78248	-7.19315	-6.08208	-5.97468	-18.0565	-9.48099	-8.16116	-9.7463
					Normalized positive error	#DIV/0!	#DIV/0!	#DIV/0!	#DIV/0!	#DIV/0!	#DIV/0!	0.117418	#DIV/0!	#DIV/0!	#DIV/0!	#DIV/0!	0.001636	#DIV/0!	#DIV/0!	#DIV/0!	#DIV/0!	0.030324	0.027507	0.011026	0.017032	75.19765	0.18404	0.007737	0.236971
					Normalized negative error	#DIV/0!	#DIV/0!	#DIV/0!	#DIV/0!	#DIV/0!	#DIV/0!	445.5233	#DIV/0!	#DIV/0!	#DIV/0!	#DIV/0!	784.0683	#DIV/0!	#DIV/0!	#DIV/0!	#DIV/0!	110.0854	146.3366	67.74673	62.88645	272607.3	714.5975	286.2552	858.8696

Cu-DPPN-Phen (**4**)

	Actin	Tubulin																										
	Refgene 1	Refgene 2	Refgene 3	Ref gene 4		IL-6	NF-KB	PARP	Casp9	Casp3	SMAC	BCL-2	BAX	XIAP	IAP1	IAP2	HMOX	TFAM	TFB1M	TFB2M	NRF-2	CLPP	LON	SPG7	YME1L1	DRP1	MFN1	MFN2	OPA1
Ct 1										37.94		27.82	27						27.68		26.72	23.73	26.56	29.57	26.51	26.77	26.84	27.45	25.69
Ct 2										36.15			40.2						29.03	5.08	26.39	25.92	30.27	29.85	31.75	25.95	26.54	27.02	26.91

Ct 3																												
Ct 4																												
Ct 5																												
Ct 6																												
Ref Geometric mean	#NUM!				Target mean	#DIV/0!	#DIV/0!	#DIV/0!	#DIV/0!	37.045	#DIV/0!	27.82	33.6	#DIV/0!	#DIV/0!	#DIV/0!	#DIV/0!	#DIV/0!	#DIV/0!	28.355	5.08	26.555	24.825	28.415	29.71	29.13	26.36	26.69	27.235	26.3
Ref S.D	#DIV/0!				target S.D	#DIV/0!	#DIV/0!	#DIV/0!	#DIV/0!	1.265721	#DIV/0!	#DIV/0!	9.33381	#DIV/0!	#DIV/0!	#DIV/0!	#DIV/0!	#DIV/0!	#DIV/0!	0.954594	#DIV/0!	0.233345	1.548564	2.623366	0.19799	3.70524	0.579828	0.212132	0.304056	0.866267
					error propagated S.D	#DIV/0!	#DIV/0!	#DIV/0!	#DIV/0!	#DIV/0!	#DIV/0!	#DIV/0!	#DIV/0!	#DIV/0!	#DIV/0!	#DIV/0!	#DIV/0!	#DIV/0!	#DIV/0!	#DIV/0!	#DIV/0!	#DIV/0!	#DIV/0!	#DIV/0!	#DIV/0!	#DIV/0!	#DIV/0!	#DIV/0!	#DIV/0!	#DIV/0!
					delta Ct	#DIV/0!	#DIV/0!	#DIV/0!	#DIV/0!	#NUM!	#DIV/0!	#NUM!	#NUM!	#DIV/0!	#DIV/0!	#DIV/0!	#DIV/0!	#DIV/0!	#DIV/0!	#NUM!	#NUM!	#NUM!	#NUM!	#NUM!	#NUM!	#NUM!	#NUM!	#NUM!	#NUM!	#NUM!
					delta delta Ct	#DIV/0!	#DIV/0!	#DIV/0!	#DIV/0!	#NUM!	#DIV/0!	#NUM!	#NUM!	#DIV/0!	#DIV/0!	#DIV/0!	#DIV/0!	#DIV/0!	#DIV/0!	#NUM!	#NUM!	#NUM!	#NUM!	#NUM!	#NUM!	#NUM!	#NUM!	#NUM!	#NUM!	#NUM!
					Normalized ddCt	#DIV/0!	#DIV/0!	#DIV/0!	#DIV/0!	#NUM!	#DIV/0!	#NUM!	#NUM!	#DIV/0!	#DIV/0!	#DIV/0!	#DIV/0!	#DIV/0!	#DIV/0!	#NUM!	#NUM!	#NUM!	#NUM!	#NUM!	#NUM!	#NUM!	#NUM!	#NUM!	#NUM!	#NUM!
					positive error	#DIV/0!	#DIV/0!	#DIV/0!	#DIV/0!	#NUM!	#DIV/0!	#NUM!	#NUM!	#DIV/0!	#DIV/0!	#DIV/0!	#DIV/0!	#DIV/0!	#DIV/0!	#NUM!	#NUM!	#NUM!	#NUM!	#NUM!	#NUM!	#NUM!	#NUM!	#NUM!	#NUM!	#NUM!
					negative error	#DIV/0!	#DIV/0!	#DIV/0!	#DIV/0!	#NUM!	#DIV/0!	#NUM!	#NUM!	#DIV/0!	#DIV/0!	#DIV/0!	#DIV/0!	#DIV/0!	#DIV/0!	#NUM!	#NUM!	#NUM!	#NUM!	#NUM!	#NUM!	#NUM!	#NUM!	#NUM!	#NUM!	#NUM!
					Normalized positive error	#DIV/0!	#DIV/0!	#DIV/0!	#DIV/0!	#NUM!	#DIV/0!	#NUM!	#NUM!	#DIV/0!	#DIV/0!	#DIV/0!	#DIV/0!	#DIV/0!	#DIV/0!	#NUM!	#NUM!	#NUM!	#NUM!	#NUM!	#NUM!	#NUM!	#NUM!	#NUM!	#NUM!	#NUM!
					Normalized negative error	#DIV/0!	#DIV/0!	#DIV/0!	#DIV/0!	#NUM!	#DIV/0!	#NUM!	#NUM!	#DIV/0!	#DIV/0!	#DIV/0!	#DIV/0!	#DIV/0!	#DIV/0!	#NUM!	#NUM!	#NUM!	#NUM!	#NUM!	#NUM!	#NUM!	#NUM!	#NUM!	#NUM!	#NUM!

3.4.15 Galleria mellonella gene expression data (Ct values)

	S7e					transferrin				IMPI			
Undisturbed	13.65	12.16	12.59	13.51		17.4	19	18.11	18.63	14.57	15.15	14.31	15.73
Sham-inoculated	12.47	13.77	14			17.37	17.68	16.7	39.27	14.96	15.26	15.44	14.25
Solvent inoculated	12.93	12.38	14.03	12.56		19.41	19.86	19.49	19.53	16.22	16.65	14.96	15.83
Cu-Phen	14.01		13.3	13.37		20.43	20.74	21.57	36.86	18.29	18.92	18.73	18.5
Cu-DPQ-Phen	14.69	14.67	13.13	12.51		21.68	22.6	21.73	21.91	20.07	19.65	20.58	20.06
Cu-DPPZ-Phen	16.64	14.08	14.92			23.49	22.52	22.41	22.05	21.27	20.6	20.59	

3.5 MMP assay

3.5.1 MCF-7

Cisplatin

Blank	Neg Ctrl	1/256 IC50	1/128 IC50	1/64 IC50	1/32 IC50	1/16 IC50	1/8 IC50	1/4 IC50	1/2 IC50	IC50	Pos ctrl
9.128	506.718	453.086	542.683	607.939	608.995	568.578	851.269	970.412	743.37	926.727	813.146
9.703	552.134	536.476	550.32	599.773	631.376	576.785	631.486	701.259	794.388	743.228	755.373
8.444	499.785	552.445	557.673	556.453	617.174	561.787	551.751	599.976	647.223	745.034	808.048
8.082	511.148	534.461	597.429	564.029	575.22	633.27	580.254	665.266	841.416	892.526	723.457
8.02	470.116	530.88	521.564	497.128	593.076	659.255	623.533	880.197	750.489	853.686	631.266
6.649	493.751	460.169	519.527	587.934	498.008	599.731	544.49	604.188	646.18	673.752	574.185
6.191	474.031	496.176	521.085	522.093	503.105	497.825	561.385	600.086	657.801	653.949	598.064
6.226	447.447	515.718	500.795	510.968	513.037	550.786	542.551	620.389	984.038	733.595	1084.987

Cu-Phen (**1**)

Blank	Neg Ctrl	1/256 IC50	1/128 IC50	1/64 IC50	1/32 IC50	1/16 IC50	1/8 IC50	1/4 IC50	1/2 IC50	IC50	Pos ctrl
11.388	839.89	689.395	956.073	797.202	772.629	689.011	1261.447	1189.715	919.059	2204.209	966.239
13.087	854.739	731.065	865.002	740.393	702.219	799.086	718.64	833.483	918.437	1624.356	907.817
11.918	852.671	564.017	688.853	755.475	707.276	723.938	745.112	789.889	823.622	797.823	840.194
11.645	731.532	626.663	629.582	712.59	680.408	793.764	784.374	743.06	813.251	920.752	835.77
11.082	828.136	625.463	792.176	731.698	731.188	779.409	714.577	1054.128	890.222	1617.007	1103.628
10.204	727.958	709.082	615.908	728.683	774.234	780.161	854.278	800.422	822.52	727.638	632.898
9.703	671.485	572.677	619.99	640.363	626.622	773.172	744.566	691.116	800.63	1308.835	969.449
9.373	724.485	604.462	645.289	682.48	646.812	811.533	1058.268	866.841	843.338	823.905	844.346

Cu-DPQ-Phen (**2**)

Blank	Neg Ctrl	1/256 IC50	1/128 IC50	1/64 IC50	1/32 IC50	1/16 IC50	1/8 IC50	1/4 IC50	1/2 IC50	IC50	Pos ctrl
11.28	659.343	614.057	637.504	717.358	704.728	1548.65	878.079	1190.044	941.97	1569.782	784.065
11.032	594.24	506.477	681.614	743.946	645.391	1011.993	761.386	776.51	786.451	965.072	1133.801
11.363	580.577	501.497	611.706	611.778	643.732	695.56	698.542	712.871	804.321	918.945	842.112
10.229	567.64	585.698	503.024	513.524	706.827	721.599	765.559	624.608	887.923	718.917	907.533
8.634	541.267	522.546	610.041	569.477	707.021	715.714	759.478	823.756	705.717	946.64	852.92
8.285	534.492	579.437	593.3	651.673	606.406	587.971	700.579	618.922	648.413	689.27	692.069
7.805	525.379	496.905	526.456	552.321	547.818	620.647	625.234	637.231	720.295	666.83	987.404
10.328	505.416	637.473	489.196	616.548	552.747	636.197	540.925	673.376	799.125	722.714	856.245

Cu-DPPZ-Phen (**3**)

Blank	Neg Ctrl	1/256 IC50	1/128 IC50	1/64 IC50	1/32 IC50	1/16 IC50	1/8 IC50	1/4 IC50	1/2 IC50	IC50	Pos ctrl
10.664	762.426	897.178	566.753	730.459	710.41	1046.865	841.239	653.741	633.035	673.284	862.739
7.469	519.842	556.337	541.787	587.299	732.575	947.018	624.637	629.226	624.116	723.687	695.084
7.543	490.897	510.949	492.817	485.496	724.809	658.397	903.091	658.404	731.466	684.039	735.039
6.848	423.897	507.235	439.716	480.268	593.609	560.056	596.338	621.039	836.867	665.646	672.571
7.562	513.492	476.469	475.542	505.142	540.103	554.519	669.589	726.58	607.91	594.977	608.917
6.896	422.034	437.963	416.919	460.224	456.674	490.456	537.577	537.597	573.132	627.524	628.984
6.923	454.169	441.341	466.125	449.62	524.484	510.47	556.231	561.601	676.257	652.5	516.042
7.527	555.781	592.763	547.635	533.075	653.166	590.48	648.243	534.429	741.503	2243.404	612.715

Cu-DPPN-Phen (**4**)

Blank	Neg Ctrl	1/256 IC50	1/128 IC50	1/64 IC50	1/32 IC50	1/16 IC50	1/8 IC50	1/4 IC50	1/2 IC50	IC50	Pos ctrl
9.308	596.759	586.965	610.715	613.997	602.447	752.706	754.305	705.027	796.809	1015.209	961.697
10.115	690.972	635.233	688.418	683.725	698.452	720.535	767.632	751.985	856.462	811.534	940.854
11.378	578.837	545.578	596.401	604.855	652.217	624.474	787.984	689.815	880.405	957.708	992.58
11.133	610.3	617.47	617.425	649.549	708.163	680.764	774.363	740.888	941.216	935.544	1261.741
9.258	605.4	561.161	613.793	575.778	740.784	716.059	738.395	703.574	779.397	842.072	994.372
7.383	582.693	594.011	557.869	609.744	608.683	660.515	625.191	681.166	703.349	731.411	810.523
6.794	614.275	557.61	583.024	590.845	777.269	720.242	840.737	803.351	991.313	898.19	846.371
6.527	591.152	551.569	568.914	592.305	663.106	641.807	761.241	865.087	836.98	1331.609	1030.221

3.5.2 SKOV-3

Cisplatin

Blank	Neg Ctrl	1/256 IC50	1/128 IC50	1/64 IC50	1/32 IC50	1/16 IC50	1/8 IC50	1/4 IC50	1/2 IC50	IC50	Pos ctrl
17.631	1482.928	1541.292	1646.367	1579.823	1570.328	2113.758	1474.858	1698.752	2041.813	2436.93	1880.505
16.826	1484.648	1447.802	1607.041	1984.95	1665.978	1747.007	1681.032	1674.77	1937.778	2123.499	1944.924
17.618	1413.231	1593.239	1539.869	1767.222	1764.041	1898.922	1791.706	1878.98	2048.281	2274.302	1822.878
17.958	1452.445	1780.221	1582.973	2431.131	1782.233	2002.06	1855.115	1934.545	2076.255	2574.82	1925.265
17.49	1425.034	1694.132	1699.93	1696.706	1718.89	1950.804	1926.301	1848.778	1974.598	2522.268	2131.355
16.887	1281.278	1571.129	1503.485	1753.506	1855.109	2042.139	1874.213	2036.729	2093.132	2415.934	2000.796
17.419	1266.47	1669.301	1795.944	1743.137	1808.202	1961.658	1949.172	1917.2	1928.633	2380.801	3457.857
15.746	1460.583	1505.555	1774.461	2008.568	1684.946	1762.988	1846.589	1934.263	2249.58	2497.793	5846.842

Cu-Phen (**1**)

Blank	Neg Ctrl	1/256 IC50	1/128 IC50	1/64 IC50	1/32 IC50	1/16 IC50	1/8 IC50	1/4 IC50	1/2 IC50	IC50	Pos ctrl
12.728	1777.721	2995.407	1621.098	1644.858	2242.798	1509.021	1646.426	1687.415	1745.027	1954.098	1832.661
12.91	1720.042	1540.596	2058.084	2044.742	1511.438	1535.013	1596.237	1637.836	1764.671	1955.988	1840.632
13.498	1549.786	1371.211	1561.218	1455.596	1919.442	1592.202	1624.351	1722.277	1891.147	1917.326	1886.195
14.62	1307.888	1392.419	1641.959	1329.182	1763.412	1861.532	1652.354	1763.653	1886.445	1971.598	1888.633
16.235	1399.179	1509.693	1579.339	1545.143	1941.11	1717.979	1734.109	1696.343	1809.565	1912.115	1846.745
16.121	1464.884	1434.482	1614.998	1573.901	1709.979	1771.814	1876.762	1809.683	1856.466	1880.324	1912.261
14.871	1324.831	1393.424	1337.391	1536.543	1640.435	2057.611	1679.715	1779.501	2000.028	1816.933	1858.618
13.713	1448.826	1453.775	1567.684	1634.401	1826.988	2000.664	2614.607	1992.214	4068.493	1718.367	1855.585

Cu-DPQ-Phen (**2**)

Blank	Neg Ctrl	1/256 IC50	1/128 IC50	1/64 IC50	1/32 IC50	1/16 IC50	1/8 IC50	1/4 IC50	1/2 IC50	IC50	Pos ctrl
16.189	2039.046	1950.989	1871.576	2103.234	1905.289	1838.615	1967.228	1930.042	2076.016	2791.063	2220.892
41.994	2359.966	1953.028	1910.092	1846.731	1690.954	1758.921	1908.126	1818.468	1913.303	2174.004	1970.162
18.68	2597.347	1897.703	1879.917	1846.009	1800.287	1865.969	2053.81	1916.56	2276.002	3048.51	2101.561
16.185	1916.382	1785.829	1466.499	1574.672	1592.245	1891.44	1836.621	1920.431	1982.319	1929.022	2026.745
18.551	1928.769	1512.62	1648.526	1967.74	1997.381	1752.161	2018.466	2019.784	2140.413	2116.6	2102.961
17.87	1899.191	1615.907	1816.464	1680.714	1679.19	2009.084	2065.51	2090.162	2360.585	2255.232	2263.879
16.996	1892.651	1621.502	1935.184	1933.526	1789.007	1816.934	2063.081	1825.514	2241.732	2160.499	2190.036
16.941	1882.937	1951.04	1624.497	1922.732	1799.849	1892.854	2036.268	2123.055	2304.657	2134.791	3155.254

Cu-DPPZ-Phen (**3**)

Blank	Neg Ctrl	1/256 IC50	1/128 IC50	1/64 IC50	1/32 IC50	1/16 IC50	1/8 IC50	1/4 IC50	1/2 IC50	IC50	Pos ctrl
15.65	1485.592	1880.114	1762.333	1617.244	1627.213	1701.314	1661.698	1765.995	2713.743	2971.99	2331.586
17.229	1530.495	1536.796	1636.714	1567.798	1552.995	1493.291	1680.443	1817.546	1940.178	2076.552	2575.137
16.155	1528.67	1606.435	1411.98	1558.523	1616.592	1850.647	1747.052	1901.445	2042.482	2058.729	2828.922
17.108	1647.291	1511.568	1488.755	1612.034	1613.213	1713.184	1821.293	1898.864	2033.051	2613.176	2157.999
23.6	1545.215	1711.893	1545.375	2601.39	1664.832	1760.765	1815.903	1869.688	1895.812	2168.957	2078.533
13.919	1485.86	1603.454	1630.42	1692.92	1686.388	1787.017	1840.423	1912.968	1962.585	2039.197	2072.87
15.015	1523.869	1610.735	1608.938	1656.727	1709.19	1624.946	1853.86	1936.892	1968.521	2145.512	2176.635
14.013	1619.355	1701.322	1575.636	1698.899	1758.463	1801.728	1895.95	2048.104	2845.021	2230.076	2617.438

Cu-DPPN-Phen (**4**)

Blank	Neg Ctrl	1/256 IC50	1/128 IC50	1/64 IC50	1/32 IC50	1/16 IC50	1/8 IC50	1/4 IC50	1/2 IC50	IC50	Pos ctrl
18.774	1600.586	1610.022	2055.639	1599.684	1809.347	1857.896	1817.074	1775.634	1905.505	2663.932	1663.396
21.081	1541.753	1973.234	1735.962	1903.795	1866.891	2807.895	1711.856	1793.603	1809.71	2041.508	1937.931
22.97	1604.109	1556.548	2285.936	1698.342	1685.807	2482.175	1717.112	1872.075	1864.718	2017.506	1900.608
23.882	1613.641	1717.776	1691.271	1776.554	1674.926	1828.652	1728.352	1835.943	1853.612	1818.253	2133.085
20.66	1527.565	1730.526	1495.548	1706.165	1741.629	1751.89	1764.181	1829.585	1839.979	2078.914	2051.156
20.07	1614.848	1397.594	1587.757	1632.515	1669.488	1789.063	1804.538	1725.299	1901.525	1976.097	2045.74
20.421	1447.258	1772.861	1702.758	1768.758	1552.277	1911.01	1842.377	1970.097	2044.564	2070.486	1975.462
18.321	1734.828	1695.794	1674.927	1632.37	1848.718	1839.968	1855.664	2029.889	2009.055	2225.469	1946.013

3.5.3 A2780

Cisplatin

Blank	Neg Ctrl	1/256 IC50	1/128 IC50	1/64 IC50	1/32 IC50	1/16 IC50	1/8 IC50	1/4 IC50	1/2 IC50	IC50	Pos ctrl
10.346	816.645	793.653	897.652	1051.014	1014.806	1065.123	1089.4	1159.727	1245.414	1377.901	1020.874
8.325	844.719	941.09	940.614	1105.187	1095.068	1077.302	1179.4	1232.124	1403.57	1296.089	956.647
10.613	837.652	950.74	1004.219	1054.189	1094.885	1088.144	1180.798	1260.742	1400.018	1215.644	949.094
12.639	926.009	969.312	1095.19	1052.729	1023.67	1170.845	1129.756	1323.267	1463.214	1249.171	901.838
18.834	908.751	802.765	971.361	1032.553	1029.675	1065.355	1097.668	1148.847	1313.117	1181.723	834.281
11.445	857.412	913.485	997.807	1017.048	1048.882	1112.116	1155.424	1273.49	1307.196	1304.18	1002.721
11.507	881.393	905.523	988.365	993.062	1026.91	1053.608	1113.841	1208.345	1317.585	1251.242	913.603
29.545	862.353	879.775	979.884	1001.825	1036.604	1071.437	1132.464	1234.68	1307.022	1385.25	946.716

Doxorubicin

Blank	Neg Ctrl	1/256 IC50	1/128 IC50	1/64 IC50	1/32 IC50	1/16 IC50	1/8 IC50	1/4 IC50	1/2 IC50	IC50	Pos ctrl
12.428	262.813	276.767	290.588	378.508	416.94	350.685	311.406	398.556	479.96	360.334	804.053
11.636	233.63	243.223	277.606	317.763	361.267	332.625	385.025	471.027	579.103	356.494	434.905
10.949	274.172	285.845	279.445	324.411	369.477	367.496	419.138	418.825	479.559	332.828	433.382
10.877	287.055	283.188	265.643	352.815	378.846	381.88	458.826	417.957	500.825	357.867	482.754
10.404	270.447	278.614	274.828	319.736	360.616	362.698	418.672	401.103	489.798	342.215	301.424
11.253	266.973	259.02	263.665	365.238	350.948	410.986	431.014	454.784	471.265	437.83	335.732
9.543	276.614	278.506	269.723	343.126	291.008	345.859	452.733	467.408	413.105	370.985	370.114
10.757	351.158	327.877	370.416	336.787	353.718	350.642	403.163	424.79	413.19	360.848	315.363

Cu-Phen (**1**)

Blank	Neg Ctrl	1/256 IC50	1/128 IC50	1/64 IC50	1/32 IC50	1/16 IC50	1/8 IC50	1/4 IC50	1/2 IC50	IC50	Pos ctrl
13.048	517.155	363.904	394.961	499.872	352.516	453.192	486.589	467.579	998.633	575.888	509.54
13.498	392.516	364.705	395.109	375.583	381.761	463.353	521.865	421.832	742.271	563.051	322.179
14.169	359.882	354.351	468.497	389.709	418.62	496.449	389.201	414.79	984.622	558.713	487.754
17.307	344.236	349.569	411.084	368.916	381.41	387.19	438.711	300.218	360.466	426.508	316.089
16.207	330.977	335.811	412.714	428.753	402.555	447.323	479.229	457.462	753.636	422.799	287.238
18.556	281.126	292.182	327.514	321.325	378.158	400.374	377.532	384.837	402.606	682.274	418.345
16.156	309.777	316.012	407.624	391.524	362.5	447.18	440.225	364.315	370.12	399.081	276.656
15.232	312.966	328.225	344.942	354.089	326.517	352.887	377.802	354.359	434.698	416.278	302.665

Cu-DPQ-Phen (**2**)

Blank	Neg Ctrl	1/256 IC50	1/128 IC50	1/64 IC50	1/32 IC50	1/16 IC50	1/8 IC50	1/4 IC50	1/2 IC50	IC50	Pos ctrl
16.624	316.091	313.16	349.874	320.748	343.798	355.251	352.857	362.643	408.418	516.102	458.037
18.515	319.559	295.582	310.071	329.219	293.672	345.216	388.675	364.473	376.19	518.519	471.777
17.949	301.801	313.047	317.8	321.838	292.654	345.458	349.929	362.85	406.274	506.801	380.612
18.011	305.008	292.382	317.05	293.235	285.952	373.726	320.525	396.539	460.915	512.492	590.379
18.951	297.095	273.735	305.809	316.427	306.115	359.018	387.83	372.949	393.023	512.982	363.152
15.211	253.304	273.782	285.459	298.936	293.678	348.564	333.622	330.105	425.882	447.067	353.654
16.24	278.376	287.035	306.462	326.498	325.14	364.924	337.217	336.243	409.072	508.465	590.771
15.429	303.206	324.959	330.39	324.215	346.311	366.486	359.916	382.082	446.97	493.322	380.541

Cu-DPPZ-Phen (**3**)

Blank	Neg Ctrl	1/256 IC50	1/128 IC50	1/64 IC50	1/32 IC50	1/16 IC50	1/8 IC50	1/4 IC50	1/2 IC50	IC50	Pos ctrl
18.371	348.639	379.433	409.45	380.188	372.281	357.138	426.505	388.159	508.477	423.005	381.8
17.378	340.322	322.79	323.048	358.756	366.475	374.372	378.235	395.032	468.446	420.271	419.559
15.837	284.987	304.619	340.615	346.516	360.54	369.987	372.726	395.592	412.858	414.518	382.338
15.943	301.768	300.435	341.922	352.062	374.487	368.75	404.623	403.997	418.983	414.456	607.45
15.84	304.464	288.604	324.979	341.632	357.432	356.969	370.315	393.141	459.805	423.935	416.573
13.65	281.393	290.849	305.313	318.048	338.076	368.731	335.495	364.414	421.451	384.201	454.737
13.733	293.622	288.645	305.455	335.337	333.634	345.642	371.116	399.889	400.18	436.478	368.711
14.003	333.567	327.031	339.913	348.747	355.214	375.617	374.759	382.06	404.089	438.988	393.89

Cu-DPPN-Phen (**4**)

Blank	Neg Ctrl	1/256 IC50	1/128 IC50	1/64 IC50	1/32 IC50	1/16 IC50	1/8 IC50	1/4 IC50	1/2 IC50	IC50	Pos ctrl
10.858	225.607	249.214	255.958	242.863	261.538	288.776	305.541	331.163	352.578	418.824	357.172
10.062	237.143	219.826	247.445	232.461	390.365	322.378	282.708	339.836	396.76	481.423	271.901
10.771	241.373	245.719	249.077	243.729	264.239	262.032	293.861	319.479	371.741	458.63	362.714
9.715	222.802	235.075	251.461	236.372	256.299	305.598	289.028	317.612	406.446	396.203	343.642
10.166	258.745	252.561	242.13	265.19	276.654	313.318	298.791	370.378	473.307	405.596	339.155
9.592	254.853	272.144	260.982	260.043	278.421	301.595	290.239	355.897	401.969	420.965	381.242
9.02	344.706	246.67	280.42	295.612	322.028	337.294	309.472	408.439	395.918	425.637	331.514
11.277	280.074	287.274	291.542	338.368	307.502	324.864	370.363	417.071	440.184	418.871	388.947

3.5.4 A2780/ Cis

Cisplatin

Blank	Neg Ctrl	1/256 IC50	1/128 IC50	1/64 IC50	1/32 IC50	1/16 IC50	1/8 IC50	1/4 IC50	1/2 IC50	IC50	Pos ctrl
13.21	832.697	842.709	907.67	951.236	1140.587	1080.346	1127.531	977.185	1142.735	1248.972	904.927
13.3	805.324	873.66	875.705	968.508	1025.102	956.864	1211.278	1176.601	1078.938	1048.882	825.007
14.683	771.35	904.72	929.473	974.085	1030.214	1006.042	1042.89	1056.756	1077.315	1125.744	3654.78
15.1	766.037	820.528	807.142	950.138	905.615	977.148	1012.304	1056.895	1030.025	996.652	936.847
16.022	832.914	841.901	803.542	884.032	884.479	954.832	1031.641	1020.253	1029.603	912.835	3055.658
15.28	799.233	811.378	851.006	880.924	865.963	890.617	943.209	1574.846	889.659	977.919	838.11
14.317	795.518	836.986	777.951	855.316	891.319	943.644	933.511	982.813	992.956	992.269	2184.756
21.274	809.702	824.405	815.491	866.197	911.447	937.521	974.595	1079.587	988.667	876.517	2318.345

Doxorubicin

Blank	Neg Ctrl	1/256 IC50	1/128 IC50	1/64 IC50	1/32 IC50	1/16 IC50	1/8 IC50	1/4 IC50	1/2 IC50	IC50	Pos ctrl
14.806	1191.289	1053.188	1085.774	1199.239	1345.397	1311.426	1405.45	1402.177	1563.067	1608.051	1076.858
12.923	1020.699	1044.198	1123.277	1129.151	1313.232	1320.697	1411.045	1463.994	1413.457	1580.593	1453.219
12.642	955.496	1192.936	1088.472	1115.572	1228.922	1190.301	1213.637	1336.466	1354.801	1405.701	2075.314
55.967	935.682	1043.063	1007.394	1015.365	1192.621	1168.073	1351.424	1312.083	1226.83	1244.073	1253.189
17.576	954.984	926.237	1158.425	1277.376	1079.722	1133.398	1239.02	1200.403	1319.461	1348.531	1597.471
11.215	943.83	914.852	1261.149	920.238	1094.288	1048.44	1116.907	1217.912	1363.034	1460.652	1826.992
17.359	1058.185	915.638	972.427	973.677	977.196	1019.532	1134.309	1671.795	1179.198	1200.67	1004.709
13.376	870.639	945.429	1158.576	1043.032	1111.728	1042.439	1073.185	1042.355	1662.78	1071.253	1625.559

Cu-Phen (**1**)

Blank	Neg Ctrl	1/256 IC50	1/128 IC50	1/64 IC50	1/32 IC50	1/16 IC50	1/8 IC50	1/4 IC50	1/2 IC50	IC50	Pos ctrl
10.346	816.645	793.653	897.652	1051.014	1014.806	1065.123	1089.4	1159.727	1245.414	1377.901	1020.874
8.325	844.719	941.09	940.614	1105.187	1095.068	1077.302	1179.4	1232.124	1403.57	1296.089	956.647
10.613	837.652	950.74	1004.219	1054.189	1094.885	1088.144	1180.798	1260.742	1400.018	1215.644	949.094
12.639	926.009	969.312	1095.19	1052.729	1023.67	1170.845	1129.756	1323.267	1463.214	1249.171	901.838
18.834	908.751	802.765	971.361	1032.553	1029.675	1065.355	1097.668	1148.847	1313.117	1181.723	834.281
11.445	857.412	913.485	997.807	1017.048	1048.882	1112.116	1155.424	1273.49	1307.196	1304.18	1002.721
11.507	881.393	905.523	988.365	993.062	1026.91	1053.608	1113.841	1208.345	1317.585	1251.242	913.603
29.545	862.353	879.775	979.884	1001.825	1036.604	1071.437	1132.464	1234.68	1307.022	1385.25	946.716

Cu-DPQ-Phen (**2**)

Blank	Neg Ctrl	1/256 IC50	1/128 IC50	1/64 IC50	1/32 IC50	1/16 IC50	1/8 IC50	1/4 IC50	1/2 IC50	IC50	Pos ctrl
9.207	916.163	902.093	1097.145	1155.329	1048.008	1306.692	1304.497	1456.397	1405.894	1640.736	1215.699
10.329	909.792	1051.484	1023.504	1169.108	1215.189	1251.604	1342.53	1426.486	1495.22	1526.759	1202.239
12.5	910.944	1039.648	1148.793	1242.674	1189.062	1261.202	1315.779	1521.92	1572.269	1692.783	2351.139
13.604	972.329	1104.043	1118.444	1213.803	1250.113	1336.172	1354.101	1500.361	1574.503	1968.221	1630.182
12.388	991.31	976.227	1072.965	1071.043	1196.501	1197.146	1314.54	1420.178	1693.491	1850.69	1437.993
13.861	1005.83	991.658	1080.939	1156.473	1256.012	1292.508	1284.074	1439.942	1646.366	1944.897	1774.199
11.446	965.707	1059.672	1099.955	1177.434	1245.73	1288.667	1288.736	1431.472	1481.536	1620.751	1871.977
14.266	999.544	1068.855	1062.316	1168.054	1272.643	1311.927	1326.038	1355.693	2047.205	1791.31	1859.703

Cu-DPPZ-Phen (**3**)

Blank	Neg Ctrl	1/256 IC50	1/128 IC50	1/64 IC50	1/32 IC50	1/16 IC50	1/8 IC50	1/4 IC50	1/2 IC50	IC50	Pos ctrl
9.176	1301.744	1219.584	1307.642	1186.031	1356.654	1379.193	1369.579	1443.567	2040.051	1476.098	1398.758
10.867	1203.337	1185.302	1220.175	1288.117	1368.342	1509.722	1503.257	1470.616	1620.104	1559.354	1536.876
12.734	1095.251	1092.048	1346.877	1302.657	1391.529	1491.75	1532.654	1480.275	1637.505	1463.076	1285.775
13.353	1423.966	1187.244	1284.745	1279.284	1326.283	1524.565	1425.723	1576.742	1619.091	1557.843	1564.318
11.742	1301.969	1112.405	1205.211	1195.719	1217.198	1255.43	1396.926	1351.295	1574.221	1537.891	1280.035
13.642	1232.496	1163.313	1362.25	1258.53	1251.972	1357.241	1340.112	1592.788	1544.049	1688.169	1443.603
13.882	1197.59	1191.372	1211.805	1276.066	1338.13	1353.482	1460.046	1551.291	1464.123	1516.113	1211.712
28.884	1118.711	1230.755	1186.055	1313.897	1353.76	1333.024	1450.848	1587.075	1407.307	1569.99	1360.441

Cu-DPPN-Phen (**4**)

Blank	Neg Ctrl	1/256 IC50	1/128 IC50	1/64 IC50	1/32 IC50	1/16 IC50	1/8 IC50	1/4 IC50	1/2 IC50	IC50	Pos ctrl
20.403	884.887	1077.483	1172.274	1178.109	1093.569	1219.03	1123.791	1314.85	1223.694	1269.598	1019.248
12.738	955.92	996.323	1083.246	1145.998	1193.692	1195.987	1265.487	1178.963	1218.341	1220.061	932.414
14.886	976.193	1044.249	1090.174	1025.674	1165.207	1198.125	1257.104	1220.18	1253.411	1169.818	744.024
13.045	897.052	888.568	990.63	973.652	1085.939	1100.526	1155.792	1133.052	1172.967	1230.278	840.214
13.552	977.035	974.161	1041.26	1071.319	1055.048	1114.176	1177.203	1186.59	1223.523	1232.479	850.918
15.243	999.988	912.113	1029.778	1032.928	1082.746	1139.261	1132.343	1180.928	1259.753	1214.967	809.495
11.95	1006.231	1060.446	1059.832	1091.633	1119.473	1187.063	1213.912	1223.378	1292.823	1170.401	886.985
37.147	1052.683	1103.588	1142.551	1065.034	1140.387	1175.778	1224.922	1191.695	1279.438	1237.094	885.867

3.6 *Galleria mellonella* mortality

3.6.1 Cisplatin

		24 hours		mean % mortality	S.D		48 hour		mean % mortality	S.D		72 hours		mean % mortality	72h S.D % mortality
Compound/ exposure per larvae	plate 1 %	plate 2 %	plate 3 %			plate 1 %	plate 2 %	plate 3 %			plate 1 %	plate 2 %	plate 3 %		
Cisplatin															
100ug (0.333uM)	90	100	70	86.67	15.27525	90	100	70	86.67	15.27525	100	100	70	90.00	17.3
10ug (0.033uM)	0	0	0	0.00	0	10	10	0	6.67	5.773503	10	10	0	6.67	5.8
8ug (0.026uM)	0	0	0	0.00	0	0	0	0	0.00	0	0	0	0	0.00	0.0
6ug (0.019uM)	0	0	0	0.00	0	0	0	10	3.33	5.773503	0	0	10	3.33	5.8
4ug (0.013uM)	0	0	0	0.00	0	0	0	10	3.33	5.773503	0	0	10	3.33	5.8
2ug (0.006uM)	0	0	0	0.00	0	0	0	10	3.33	5.773503	0	0	10	3.33	5.8

3.6.2 Cu-Phen (**1**)

		4hr		mean %	S.D		24h		mean %	S.D		48h		mean %	S.D		72h		mean %	S.D
Compound/ exposure per larvae	plate 1 %	plate 2 %	plate 3 %			plate 1 %	plate 2 %	plate 3 %			plate 1 %	plate 2 %	plate 3 %			plate 1 %	plate 2 %	plate 3 %		
Cu-Phen																				
30ug	100	100	100	100.00	0	100	100	100	100.00	0	100	100	100	100.00	0	100	100	100	100.00	0.0
25ug	90	100	100	96.67	5.773503	100	100	100	100.00	0	100	100	100	100.00	0	100	100	100	100.00	0.0
20ug	80	90	90	86.67	5.773503	100	100	100	100.00	0	100	100	100	100.00	0	100	100	100	100.00	0.0
15ug	70	70	70	70.00	0	100	100	100	100.00	0	100	100	100	100.00	0	100	100	100	100.00	0.0
12ug	40	50	50	46.67	5.773503	100	100	100	100.00	0	100	100	100	100.00	0	100	100	100	100.00	0.0
10ug (0.018uM)	0	10	10	6.67	5.773503	80	70	100	83.33	15.27525	80	70	100	83.33	15.27525	80	70	100	83.33	15.3
8ug (0.014uM)	0	0	0	0.00	0	20	30	0	16.67	15.27525	20	30	0	16.67	15.27525	20	30	0	16.67	15.3
6ug (0.010uM)	0	0	0	0.00	0	0	0	0	0.00	0	0	0	0	0.00	0	0	0	0	0.00	0.0
4ug (0.007uM)	0	0	0	0.00	0	0	0	0	0.00	0	0	0	0	0.00	0	0	0	0	0.00	0.0
2ug (0.003uM)	0	0	0	0.00	0	0	0	0	0.00	0	0	0	0	0.00	0	0	0	0	0.00	0.0

3.6.3 Cu-DPQ-Phen (**2**)

Compound/ exposure per larvae	plate 1 %	plate 2 %	plate 3 %			plate 1 %	plate 2 %	plate 3 %			plate 1 %	plate 2 %	plate 3 %			plate 1 %	plate 2 %	plate 3 %		
Cu-DPQ-Phen																				
30ug	100	100	100	100.00	0	100	100	100	100.00	0	100	100		100.00	0	100	100	100	100.00	0
28ug	100	100	100	100.00	0	100	100	100	100.00	0	100	100		100.00	0	100	100	100	100.00	0
24ug	70	80	80	76.67	5.773503	100	100	100	100.00	0	100	100		100.00	0	100	100	100	100.00	0
20ug	40	40	40	40.00	0	100	100	100	100.00	0	100	100	100	100.00	0	100	100	100	100.00	0
16ug	20	20	20	20.00	0	90	90	90	90.00	0	90	90	100	93.33	5.773503	90	100	100	96.67	5.773503
14ug	0	0	0	0.00	0	80	90	80	83.33	5.773503	90	100	80	90.00	10	90	100	80	90.00	10
12ug	0	0	0	0.00	0	80	70	70	73.33	5.773503	80	70	70	73.33	5.773503	70	70	70	70.00	0
10ug (0.016uM)	0	0	0	0.00	0	30	30	50	36.67	11.54701	30	30	50	36.67	11.54701	30	30	50	36.67	11.54701
8ug (0.013uM)	0	0	0	0.00	0	0	0	0	0.00	0	0	0	0	0.00	0	0	0	0	0.00	0
6ug (0.0098uM)	0	0	0	0.00	0	0	0	0	0.00	0	0	0	0	0.00	0	0	0	0	0.00	0
4ug (0.006uM)	0	0	0	0.00	0	0	0	10	3.33	5.773503	0	0	10	3.33	5.773503	0	0	10	3.33	5.773503
2ug (0.003uM)	0	0	0	0.00	0	0	0	0	0.00	0	0	0	0	0.00	0	0	0	0	0.00	0

3.6.4 Cu-DPPZ-Phen (**3**)

		4hr		mean %	S.D		24h		mean %	S.D		48h		mean %	S.D		72h		mean %	S.D
Compound/ exposure per larvae	plate 1 %	plate 2 %	plate 3 %			plate 1 %	plate 2 %	plate 3 %			plate 1 %	plate 2 %	plate 3 %			plate 1 %	plate 2 %	plate 3 %		
Cu-DPPZ-Phen																				
40ug	100	100	100	100.00	0	100	100	100	100.00	0	100	100	100	100.00	0	100	100	100	100.00	0
30ug	100	100	100	100.00	0	100	100	100	100.00	0	100	100	100	100.00	0	100	100	100	100.00	0
20ug	100	100	100	100.00	0	100	100	100	100.00	0	100	100	100	100.00	0	100	100	100	100.00	0
12ug	100	60	70	76.67	20.81666	100	70	70	80.00	17.32051	100	70	70	80.00	17.32051	100	70	70	80.00	17.32051
11ug	80	60	80	73.33	11.54701	80	80	90	83.33	5.773503										
10ug (0.016uM)	0	0	0	0.00	0	0	0	0	0.00	0	0	0	0	0.00	0	50	40	30	40.00	10
8ug (0.013uM)	0	0	0	0.00	0	0	0	0	0.00	0	0	0	0	0.00	0	0	0	0	0.00	0
6ug (0.0098uM)	0	0	0	0.00	0	0	0	0	0.00	0	0	0	0	0.00	0	0	0	0	0.00	0
4ug (0.006uM)	0	0	0	0.00	0	0	0	0	0.00	0	0	0	0	0.00	0	10	0	0	3.33	5.773503
2ug (0.003uM)	0	0	0	0.00	0	0	0	0	0.00	0	0	0	0	0.00	0	0	0	0	0.00	0

3.6.5 Cu-DPPN-Phen (**4**)

		4hr		mean %	S.D		24h		mean %	S.D		48h		mean %	S.D		72h		mean %	S.D
Compound/ exposure per larvae	plate 1 %	plate 2 %	plate 3 %			plate 1 %	plate 2 %	plate 3 %			plate 1 %	plate 2 %	plate 3 %			plate 1 %	plate 2 %	plate 3 %		
Cu-DPPN-Phen																				
40ug	10	0	0	3.33	5.773503	30	0	20	16.67	15.27525	30	0	20	16.67	15.27525	30	0	40	23.33	20.81666
30ug	0	0	0	0.00	0	10	0	0	3.33	5.773503	20	10	20	16.67	5.773503	20	10	20	16.67	5.773503
20ug	0	0	0	0.00	0	20	0	10	10.00	10	20	0	20	13.33	11.54701	20	10	20	16.67	5.773503
12ug	0	0	0	0.00	0	0	30	30	20.00	17.32051	0	30	30	20.00	17.32051	0	30	30	20.00	17.32051
10ug (0.016uM)	0	0	0	0.00	0	0	0	0	0.00	0	0	10	10	6.67	5.773503	30	30	30	30.00	0
8ug (0.013uM)	0	0	0	0.00	0	0	0	0	0.00	0	0	0	0	0.00	0	0	0	0	0.00	0
6ug (0.0098uM)	0	0	0	0.00	0	0	0	0	0.00	0	0	0	10	3.33	5.773503	0	10	0	3.33	5.773503
4ug (0.006uM)	0	0	0	0.00	0	0	0	0	0.00	0	0	10	0	3.33	5.773503	10	0	0	3.33	5.773503
2ug (0.003uM)	0	0	0	0.00	0	0	0	0	0.00	0	0	0	0	0.00	0	0	0	0	0.00	0

3.7 *G. mellonella* haemocyte count at LD_{50} exposure after 24 h

Solvent/ negative					average	haemocyte count per ml	average	S.D
1	86	93	94	79	88	4.40E+07		
	86	79	72	99	84	4.20E+07		
2	75	65	50	65	63.75	3.19E+07		
	59	77	63	64	65.75	3.29E+07		
3	56	65	76	67	66	3.30E+07		
	66	83	86	85	80	4.00E+07		
4	75	62	43	64	61	3.05E+07		
	64	55	60	71	62.5	3.13E+07	3.57E+07	5.396E+06
Cu-Phen LD50 24h								
5	95	98	81	48	80.5	4.03E+07		
	94	104	110	109	104.25	5.21E+07		
6	92	77	77	76	80.5	4.03E+07		
	87	82	92	80	85.25	4.26E+07		
7	89	71	71	62	73.25	3.66E+07		
	53	78	92	65	72	3.60E+07		
8	69	71	72	66	69.5	3.48E+07		
	81	77	83	70	77.75	3.89E+07	4.02E+07	5.477E+06
Cu-DPQ-Phen LD50 24h								
9	121	127	119	105	118	5.90E+07		
	119	125	146	127	129.25	6.46E+07		
10	101	102	96	87	96.5	4.83E+07		
	69	83	81	79	78	3.90E+07		
11								
12	58	50	65	60	58.25	2.91E+07		
	62	66	59	60	61.75	3.09E+07	4.51E+07	1.469E+07
Cu-DPPZ-Phen LD50 24h								
13	150	113	128	84	118.75	5.94E+07		
	122	122	121	141	126.5	6.33E+07		
14	57	55	59	64	58.75	2.94E+07		
	46	37	54	56	48.25	2.41E+07		
15	96	94	84	100	93.5	4.68E+07		
	93	106	118	106	105.75	5.29E+07		
16	73	58	73	65	67.25	3.36E+07		
	80	57	73	89	74.75	3.74E+07	4.33E+07	1.439E+07
Sham inoculation								
17	85	86	79	88	84.5	4.23E+07		
	74	73	86	98	82.75	4.14E+07		
18	87	91	66	105	87.25	4.36E+07		

	97	99	79	95	92.5	4.63E+07		
19	42	49	51	63	51.25	2.56E+07		
	48	47	47	44	46.5	2.33E+07		
20	50	53	58	60	55.25	2.76E+07		
	64	76	62	83	71.25	3.56E+07	3.57E+07	9.031E+06
undisturbed								
21								
22	10	21	12	11	13.5	6.75E+06		
	13	14	10	13	12.5	6.25E+06		
23	80	78	79	86	80.75	4.04E+07		
	70	82	95	88	83.75	4.19E+07		
24	51	69	64	73	64.25	3.21E+07		
	76	66	76	68	71.5	3.58E+07	2.72E+07	1.639E+07

3.8 *G. mellonella* 2D-PAGE

3.8.1 *G. mellonella* 2D-PAGE Progenesis SameSpot analysis output

#	Anova (p)	Fold	Average Normalized Volumes			
			Negative control	Cu-Phen LD_{50} 24 h	Cu-DPQ-Phen LD_{50} 24 h	Cu-DPPZ-Phen LD_{50} 24 h
53	7.436e-004	6.4	7323.822	3935.175	1152.780	1684.348
65	0.001	4.6	7577.226	9539.601	2073.979	2339.487
8	0.006	2.4	3938.221	2922.647	1633.304	1761.574
66	0.008	3.7	587.533	583.879	288.907	159.284
29	0.011	5.1	203.019	489.475	681.113	1043.649
36	0.016	1.9	2003.462	1108.715	1058.913	1101.398
40	0.021	3.9	106.498	109.043	347.222	411.424
27	0.031	2.7	5271.907	4582.039	1981.567	2568.498
52	0.034	3.6	1036.671	1199.377	336.827	528.988
18	0.034	1.8	1.999e+004	2.211e+004	1.233e+004	1.321e+004
67	0.036	6.0	6869.326	6701.720	1375.526	1139.020
13	0.038	2.5	1848.394	1490.794	750.606	807.622
11	0.041	3.4	2122.252	3658.593	7143.887	5350.948
60	0.042	4.6	258.385	855.154	807.837	1182.532
50	0.047	2.5	2616.734	2071.074	1030.475	1352.780
47	0.051	2.0	687.285	524.745	588.299	1061.341
41	0.051	3.4	384.577	441.488	287.730	990.522
39	0.052	7.0	43.642	28.937	86.487	202.319
31	0.053	4.8	651.762	215.125	135.131	253.534
12	0.055	2.6	887.524	1255.481	1814.490	2325.213
62	0.057	21.2	69.578	101.674	1475.647	104.466
45	0.066	2.2	7532.939	6618.067	3352.145	4817.492
46	0.066	3.1	896.714	834.220	289.701	339.827
23	0.069	1.7	1.975e+004	1.455e+004	1.183e+004	1.290e+004
30	0.089	2.0	316.222	406.972	203.185	357.257

70	0.094	23.8	107.967	153.353	2565.508	170.794
72	0.100	2.7	50.138	117.981	44.135	43.222
5	0.117	4.4	627.053	1724.708	490.010	388.114
44	0.117	24.1	91.295	78.375	1890.529	159.353
4	0.128	2.1	3445.723	3441.988	1626.416	1712.553
48	0.138	2.4	4526.798	2929.349	1880.411	3001.447
56	0.138	2.5	3369.012	2270.598	1814.836	1374.868
49	0.140	2.2	2837.915	2511.156	1302.332	1834.473
34	0.142	2.0	1.977e+004	1.659e+004	9968.003	1.197e+004
59	0.162	3.1	176.401	165.412	511.368	473.533
38	0.168	5.3	67.279	65.405	151.448	343.382
20	0.188	3.1	1124.548	2790.878	917.328	891.349
33	0.219	2.0	2570.036	1486.672	3018.909	2888.208
64	0.222	2.6	4155.465	3352.677	1597.735	1990.542
57	0.222	17.6	38.441	56.343	613.663	34.918
28	0.226	12.5	133.024	136.932	790.134	1662.759
74	0.228	22.1	79.639	49.963	868.391	39.342
71	0.228	2.4	342.703	569.514	265.289	232.605
42	0.242	18.9	186.831	146.721	2766.168	1211.422
43	0.257	17.9	93.909	83.787	1501.969	731.180
9	0.258	1.6	1277.390	1199.383	1563.950	1937.297
61	0.262	16.8	116.328	213.553	1950.766	389.116
73	0.265	15.8	124.769	130.854	1977.515	166.480
51	0.275	5.0	229.887	345.178	84.987	69.432
75	0.282	19.4	143.635	43.087	837.767	72.479
58	0.288	7.2	113.472	478.690	166.975	813.537
32	0.297	22.7	35.910	27.161	588.544	615.879
7	0.300	5.2	494.238	196.970	370.351	1018.925
15	0.303	3.5	718.361	880.380	2148.315	2484.520
69	0.319	2.7	504.724	1059.895	556.446	392.397
14	0.340	13.1	246.157	3230.745	1037.657	478.838
37	0.349	25.8	147.411	63.333	1631.806	1596.772
22	0.361	2.3	524.162	275.472	517.235	645.903
21	0.384	3.9	534.690	1053.363	362.497	1397.116
68	0.402	24.7	113.215	223.228	2794.570	213.855
63	0.440	16.8	134.658	160.518	2268.669	178.954
54	0.465	2.5	725.627	495.541	284.561	449.127
16	0.505	2.7	6349.447	4948.409	7817.841	1.337e+004
35	0.526	1.9	1067.037	567.532	854.359	928.222
17	0.545	2.3	1095.678	1530.519	2481.758	2076.828
10	0.554	1.9	2919.251	4255.945	3274.193	2233.827
1	0.597	5.8	549.099	876.387	149.986	270.128
24	0.619	2.9	322.139	229.958	656.394	509.381
3	0.627	1.7	4272.990	2729.826	4752.135	2724.785
25	0.647	14.3	60.858	65.843	76.570	872.798
2	0.724	3.4	1581.201	2688.157	1970.295	790.099
6	0.829	4.1	223.799	921.343	334.794	474.664
26	0.882	1.7	1887.232	2295.809	3282.388	2088.000

19	0.896	2.0	512.918	1029.904	652.866	531.966
55	0.920	2.4	118.476	252.067	121.061	106.360

3.8.2 Spots analysed using MASCOT from Progenesis SameSpot differential expression report (3.8.1) and presented in the thesis main body.

Excised spots No.	Spots No. in thesis
53	1
65	2
8	Not included
36	Not included
27	Not included
52	Not included
67	Not included
11	3
60	4
41	Not included
45	5
23	6
4	7
48	8
56	9
49	Not included
34	10
58	Not included
54	Not included
26	Not included

3.9 *G. mellonella* LFQ proteomics

3.9.1 List of identified protein in comparisons between the negative control and Cu-Phen (**1**)

F1_contig00131_1.exp_gi|112983250|ref|NP_001037610.1|putative alcohol
F1_contig00234_1.f1.exp_gi|183979231|dbj|BAG30777.1|chitin binding
F1_contig00848_1.exp_gi|229002332|dbj|BAH57948.1|hypothetical protein
F1_contig00859_1.f1.exp_gi|170041898|ref|XP_001848684.1|apyrase
F1_contig01324_1.exp_gi|56462286|gb|AAV91426.1|putative protease
F1_contig01421_1.exp_gi|157114409|ref|XP_001652257.1|dihydropteridine
F1_contig01421_1.exp_gi|157114409|ref|XP_001652257.1|dihydropteridine
F1_contig01451_1.f1.exp_gi|158285614|ref|XP_308397.4|AGAP007475-PA
F1_contig02233_1.f1.exp_gi|112983096|ref|NP_001037054.
F1_contig02487_1.exp_gi|157833800|pdb|1SEK|AChain A, The Structure Of
F1_contig02586_1.exp_gi|56462162|gb|AAV91364.1|hypothetical protein
F1_contig02726_1.exp_gi|114050871|ref|NP_001040411.1|carboxylesterase
F1_contig02803_1.exp_gi|116791778|gb|ABK26104.1|unknown [Picea
F1_contig02961_1.f1.exp_gi|158289805|ref|XP_311447.4|AGAP010733-PA
F1_contig03361_1.exp_gi|183979284|dbj|BAG30769.1|elongation factor 1

F1_contig07944_1.exp_gi|110743533|dbj|BAE98324.1|methionine-rich
F1_contig13620_1.f1.exp_gi|109502352|gb|ABE01157.2|carboxylesterase
F1_contig15344_1.exp_gi|193704761|ref|XP_001947608.1|PREDICTED:;F1_GME-string_Contig_3474.0_gi|170030366|ref|XP_001843060.
F1_contig15714_1.exp_gi|112982880|ref|NP_001037572.1|translationally
F1_contig16332_1.exp_gi|114051702|ref|NP_001040423.1|zinc-containing
F1_contig16841_1.exp_gi|6671050|gb|AAF23078.1|AF128867_1glutathione
F1_contig17276_1.exp_gi|114051481|ref|NP_001040300.
F1_contig17506_1.exp_gi|112983070|ref|NP_001037057.1|BCP inhibitor
F1_contig18074_1.exp_gi|156551613|ref|XP_001600684.1|PREDICTED:
F1_contig18862_1.exp_gi|56462318|gb|AAV91442.1|hypothetical protein
F1_contig19578_1.f1.exp_gi|114051325|ref|NP_001040376.
F1_contig19578_1.f1.exp_gi|114051325|ref|NP_001040376.
F1_contig19579_1.exp_gi|156254836|gb|ABU62829.1|serpin-2 [Spodoptera
F1_contig19674_1.f1.exp_gi|242009020|ref|XP_002425291.1|paramyosin,
F1_contig20154_1.f1.exp_gi|34921426|sp|O96790.2|DPGN_DIPMARecName:
F1_contig21121_1.exp_gi|148266444|gb|ABQ53630.1|glutathione
F1_contig21523_1.exp_gi|162462783|ref|NP_001104822.
F1_contig21523_1.exp_gi|162462783|ref|NP_001104822.
F1_GME-string_Contig_1038.0_gi|49532918|dbj|BAD26694.1|cellular
F1_GME-string_Contig_1038.0_gi|49532918|dbj|BAD26694.1|cellular
F1_GME-string_Contig_1160.0_gi|112983082|ref|NP_001037668.1|cytosolic
F1_GME-string_Contig_1333.0_gi|241263211|ref|XP_002405507.1|CNDP
F1_GME-string_Contig_1535.0_gi|154707830|gb|AAU84716.
F1_GME-string_Contig_1831.0_gi|156547253|ref|XP_001601340.
F1_GME-string_Contig_1931.0_gi|158515746|gb|AAN06604.
F1_GME-string_Contig_1931.0_gi|158515746|gb|AAN06604.
F1_GME-string_Contig_1949.0_gi|158515746|gb|AAN06604.
F1_GME-string_Contig_1997.0_gi|121308868|dbj|BAF43531.1|serine
F1_GME-string_Contig_2092.0_gi|114050771|ref|NP_001040154.
F1_GME-string_Contig_2215.0_gi|239835734|ref|NP_001155190.1|tau-like
F1_GME-string_Contig_2311.0_gi|195107829|ref|XP_001998496.1|GI24003
F1_GME-string_Contig_337.0_gi|170058562|ref|XP_001864974.1|dimeric
F1_GME-string_Contig_374.0_gi|112983164|ref|NP_001036945.
F1_GME-string_Contig_4545.0_gi|225031010|gb|ACN79512.1|alpha
F1_GME-string_Contig_48.0_gi|15146043|gb|AAK83435.1|alpha-crystallin
F1_GME-string_Contig_5294.0_gi|112983342|ref|NP_001036965.
F1_GME-string_Contig_5500.0_gi|45330818|dbj|BAD12426.1|fructose
F1_GME-string_Contig_581.0_gi|4090964|gb|AAD09279.1|immune-related
F1_GME-string_Contig_581.0_gi|4090964|gb|AAD09279.1|immune-related
F1_GME-string_Contig_5857.0_gi|66508985|ref|XP_624902.1|PREDICTED:
F1_GME-string_Contig_6852.0_gi|219552448|gb|ACL26939.1|arginine
F1_GME-string_Contig_6852.0_gi|219552448|gb|ACL26939.1|arginine
F1_GME-string_Contig_962.0_gi|156968291|gb|ABU98617.1|unknown
F1_GME-string_Contig_962.0_gi|156968291|gb|ABU98617.1|unknown

F2_contig00391_1.exp_gi|148298770|ref|NP_001091821.1|ATPase
F2_contig00893_1.exp_gi|116087|sp|P01507.1|CECA_HYACERecName:
F2_contig01621_1.exp_gi|114052174|ref|NP_001040228.1|aminoacylase
F2_contig02236_1.exp_gi|46396271|sp|P83632.1|P27K_GALMERecName:
F2_contig02362_1.exp_gi|4753912|emb|CAB41997.1|3-dehydroecdysone
F2_contig02401_1.exp_gi|170035237|ref|XP_001845477.1|aliphatic
F2_contig02401_1.exp_gi|170035237|ref|XP_001845477.1|aliphatic
F2_contig02482_1.f1.exp_gi|91079628|ref|XP_967731.1|PREDICTED:
F2_contig02701_1.exp_gi|66517857|ref|XP_391850.2|PREDICTED: similar
F2_contig02857_1.exp_gi|73671225|gb|AAZ80044.1|diapause bioclock
F2_contig02908_1.exp_gi|183979374|dbj|BAG30739.1|Tropomyosin 2
F2_contig02932_1.f1.exp_gi|91082539|ref|XP_973726.1|PREDICTED:
F2_contig04024_1.exp_gi|186703381|gb|ACC91897.1|hemolin [Heliothis
F2_contig06283_1.exp_gi|34556399|gb|AAQ75026.1|prophenoloxidase
F2_contig07194_1.exp_gi|198452388|ref|XP_001358750.2|GA20334
F2_contig13577_1.exp_gi|183979239|dbj|BAG30781.1|similar to
F2_contig15137_1.exp_gi|58864722|emb|CAI06089.1|putative annexin IX-B
F2_contig15175_1.exp_gi|55139149|gb|AAV41247.1|hemolin [Plodia
F2_contig15383_1.exp_gi|112984026|ref|NP_001036831.1|BmP109 [Bombyx
F2_contig16122_1.f1.exp_gi|226693130|dbj|BAH56565.1|sepiapterin
F2_contig16165_1.f1.exp_gi|148298800|ref|NP_001091831.1|enolase
F2_contig16165_1.f1.exp_gi|148298800|ref|NP_001091831.1|enolase
F2_contig16750_1.f1.exp_gi|229562186|gb|ACQ78181.1|heat shock protein
F2_contig16968_1.exp_gi|159528|gb|AAA29321.1|methionine-rich storage
F2_contig17054_1.exp_gi|17901818|gb|AAL47694.1|AF329683_132 kDa
F2_contig17442_1.exp_gi|25989211|gb|AAL31707.1|prophenoloxidase
F2_contig17460_1.exp_gi|112983086|ref|NP_001037594.1|troponin C
F2_contig18014_1.exp_gi|242009020|ref|XP_002425291.1|paramyosin,
F2_contig18192_1.exp_gi|14599864|gb|AAK71137.1|AF356843_1hexamerin
F2_contig18407_1.exp_gi|170046360|ref|XP_001850736.1|conserved
F2_contig18681_1.exp_gi|112982865|ref|NP_001037108.1|profilin [Bombyx
F2_contig18979_1.exp_gi|114052677|ref|NP_001040269.1|phosphoserine
F2_contig19502_1.f1.exp_gi|183979392|dbj|BAG30748.1|hypothetical
F2_contig19502_1.f1.exp_gi|183979392|dbj|BAG30748.1|hypothetical
F2_contig20908_1.f1.exp_gi|9087198|sp|O62605.1|SI25_GALMERecName:
F2_contig21210_1.exp_gi|109119903|dbj|BAE96011.
F2_contig21210_1.exp_gi|109119903|dbj|BAE96011.
F2_contig21539_1.exp_gi|384243|prf||1905335Aarylphorin
F2_contig21568_1.exp_gi|170036627|ref|XP_001846164.1|Gelsolin [Culex
F2_GME-string_Contig_1598.0_gi|91083881|ref|XP_967558.1|PREDICTED:
F2_GME-string_Contig_186.0_gi|164459610|gb|ABY57912.1|hydroxypyruvate
F2_GME-string_Contig_2050.0_gi|60592747|dbj|BAD90848.
F2_GME-string_Contig_2064.0_gi|112983994|ref|NP_001036836.
F2_GME-string_Contig_233.0_gi|238915964|gb|ACR78449.1|growth-blocking

F2_GME-string_Contig_3629.0_gi|6919921|sp|P81906.
F2_GME-string_Contig_3762.0_gi|6560637|gb|AAF16696.
F2_GME-string_Contig_3905.0_gi|112983390|ref|NP_001036987.
F2_GME-string_Contig_4835.0_gi|112983550|ref|NP_001036879.
F2_GME-string_Contig_512.0_gi|114051966|ref|NP_001040198.
F2_GME-string_Contig_5466.0_gi|6164595|gb|AAF04457.
F2_GME-string_Contig_555.0_gi|114051738|ref|NP_001040426.1|alcohol
F2_GME-string_Contig_5601.0_gi|91078812|ref|XP_970578.1|PREDICTED:
F2_GME-string_Contig_5861.0_gi|116780375|gb|ABK21656.1|unknown [Picea
F2_GME-string_Contig_6549.0_gi|229002332|dbj|BAH57948.1|hypothetical
F2_GME-string_Contig_6549.0_gi|229002332|dbj|BAH57948.1|hypothetical
F2_GME-string_Contig_695.0_gi|114052561|ref|NP_001040257.1|cytosolic
F2_GME-string_Contig_695.0_gi|114052561|ref|NP_001040257.1|cytosolic
F3_contig00036_1.exp_gi|112983654|ref|NP_001036872.1|Bombyrin [Bombyx
F3_contig00049_1.f1.exp_gi|226342884|ref|NP_001139704.1|serpin 11
F3_contig00380_1.f1.exp_gi|159078|gb|AAA74229.1|arylphorin [Galleria
F3_contig00412_1.f1.exp_gi|14599862|gb|AAK71136.1|AF356842_1hexamerin
F3_contig00812_1.exp_gi|114050771|ref|NP_001040154.1|short-chain
F3_contig01202_1.exp_gi|14517793|gb|AAK64362.
F3_contig01621_1.exp_gi|114052174|ref|NP_001040228.1|aminoacylase
F3_contig02609_1.exp_gi|21630233|gb|AAM69353.1|AF518768_1serine
F3_contig02707_1.exp_gi|11890404|gb|AAG41120.1|26kDa ferritin subunit
F3_contig02722_1.f1.exp_gi|239938036|gb|ACS36117.1|beta-galactosidase
F3_contig04057_1.exp_gi|2498144|sp|Q25490.1|APLP_MANSERecName:
F3_contig04490_1.exp_gi|195115822|ref|XP_002002455.1|GI17397
F3_contig04490_1.exp_gi|195115822|ref|XP_002002455.1|GI17397
F3_contig05096_1.exp_gi|237874122|dbj|BAH59606.1|multicystatin and
F3_contig05096_1.exp_gi|237874122|dbj|BAH59606.1|multicystatin and
F3_contig12543_1.exp_gi|156630460|sp|P85216.1|AP2_GALMERecName:
F3_contig14928_1.exp_gi|114052472|ref|NP_001040479.1|peptidylprolyl
F3_contig15255_1.exp_gi|75906185|ref|YP_313566.1|adhesion-like
F3_contig15340_1.exp_gi|50404098|gb|AAT76806.1|apolipophorin
F3_contig15340_1.exp_gi|50404098|gb|AAT76806.1|apolipophorin
F3_contig15609_1.exp_gi|74873244|sp|O96382.1|DFP11_HYPCURecName:
F3_contig16820_1.exp_gi|164451507|gb|ABY56688.1|troponin I [Loxostege
F3_contig16921_1.f1.exp_gi|112982822|ref|NP_001037540.
F3_contig18074_1.exp_gi|156551613|ref|XP_001600684.1|PREDICTED:
F3_contig19161_1.f1.exp_gi|145286562|gb|ABP52098.1|lysozyme-like
F3_contig19165_1.exp_gi|114051866|ref|NP_001040134.1|isocitrate
F3_contig19165_1.exp_gi|114051866|ref|NP_001040134.1|isocitrate
F3_contig20116_1.exp_gi|193610917|ref|XP_001950677.1|PREDICTED:
F3_contig20343_1.exp_gi|148298833|ref|NP_001091765.1|NADP-dependent
F3_contig21439_1.exp_gi|33439712|gb|AAQ18894.1|spodoptericin
F3_contig21568_1.exp_gi|170036627|ref|XP_001846164.1|Gelsolin [Culex

F3_contig21932_1.exp_gi|91093363|ref|XP_969584.1|PREDICTED: similar
F3_contig22104_1.exp_gi|229002332|dbj|BAH57948.1|hypothetical protein
F3_GME-string_Contig_1060.0_gi|49532886|dbj|BAD26678.1|Diazepam
F3_GME-string_Contig_1065.0_gi|148298726|ref|NP_001091755.
F3_GME-string_Contig_1139.0_gi|212710319|ref|ZP_03318447.
F3_GME-string_Contig_1226.0_gi|41053309|ref|NP_956337.
F3_GME-string_Contig_1489.0_gi|23208546|gb|AAN15790.1|heat shock-like
F3_GME-string_Contig_1544.0_gi|39579195|gb|AAR28762.1|odorant-binding
F3_GME-string_Contig_1581.0_gi|114052116|ref|NP_001040454.1|ML-domain
F3_GME-string_Contig_1802.0_gi|242022233|ref|XP_002431545.1|high
F3_GME-string_Contig_190.0_gi|116782397|gb|ABK22491.1|unknown [Picea
F3_GME-string_Contig_2113.0_gi|124527|sp|Q00630.1|ICYB_MANSERecName:
F3_GME-string_Contig_2408.0_gi|229002332|dbj|BAH57948.1|hypothetical
F3_GME-string_Contig_3163.0_gi|1146408|gb|AAA85089.1|gallerin
F3_GME-string_Contig_352.0_gi|114052242|ref|NP_001040131.
F3_GME-string_Contig_45.0_gi|229002332|dbj|BAH57948.1|hypothetical
F3_GME-string_Contig_5353.0_gi|2498144|sp|Q25490.1|APLP_MANSERecName:
F3_GME-string_Contig_5382.0_gi|125629089|emb|CAL23158.2|gustatory
F3_GME-string_Contig_5682.0_gi|77415676|emb|CAJ01507.1|hypothetical
F3_GME-string_Contig_5682.0_gi|77415676|emb|CAJ01507.1|hypothetical
F3_GME-string_Contig_5764.0_gi|195119912|ref|XP_002004473.1|GI19595;R2_contig18735_1.exp_gi|158293921|ref|XP_315269.4|AGAP011516-PA
F3_GME-string_Contig_5764.0_gi|195119912|ref|XP_002004473.1|GI19595;R2_contig18735_1.exp_gi|158293921|ref|XP_315269.4|AGAP011516-PA
F3_GME-string_Contig_6108.0_gi|189239301|ref|XP_971644.2|PREDICTED:
F3_GME-string_Contig_944.0_gi|112982743|ref|NP_001037556.1|elongation
R1_contig01633_1.exp_gi|195475698|ref|XP_002090121.1|GE20538
R1_contig01804_1.f1.exp_gi|112984054|ref|NP_001037422.1|yellow1
R1_contig02674_1.f1.exp_gi|114051966|ref|NP_001040198.1|mitochondrial
R1_contig02829_1.exp_gi|117970173|dbj|BAF36817.
R1_contig03614_1.f1.exp_gi|91084675|ref|XP_968140.1|PREDICTED:
R1_contig03752_1.exp_gi|189181680|ref|NP_001121191.1|carboxylesterase
R1_contig05149_1.exp_gi|112984026|ref|NP_001036831.1|BmP109 [Bombyx
R1_contig09082_1.exp_gi|114051598|ref|NP_001040416.1|leukotriene A4
R1_contig15056_1.f1.exp_gi|162462783|ref|NP_001104822.
R1_contig16410_1.exp_gi|189237651|ref|XP_001813448.1|PREDICTED:
R1_contig17461_1.exp_gi|158962511|dbj|BAF91716.1|chemosensory protein
R1_contig17461_1.exp_gi|158962511|dbj|BAF91716.1|chemosensory protein
R1_contig18077_1.exp_gi|220902980|gb|ACL83459.1|carboxylesterase
R1_contig19537_1.exp_gi|47607477|gb|AAT36640.1|imaginal disc growth
R1_contig19537_1.exp_gi|47607477|gb|AAT36640.1|imaginal disc growth
R1_contig20220_1.exp_gi|242004672|ref|XP_002423204.1|conserved
R1_contig20227_1.exp_gi|23208535|gb|AAN15786.1|peptidoglycan
R1_contig20227_1.exp_gi|23208535|gb|AAN15786.1|peptidoglycan

R1_contig21466_1.exp_gi|134103857|gb|ABO60878.1|cationic peptide CP8
R1_contig21950_1.exp_gi|56462300|gb|AAV91433.1|putative serine
R1_contig22070_1.exp_gi|112983062|ref|NP_001037056.
R1_contig22148_1.exp_gi|18140733|gb|AAL60414.1|AF393489_1twelve
R1_GME-string_Contig_2259.0_gi|91092064|ref|XP_970689.1|PREDICTED:
R1_GME-string_Contig_2606.0_gi|114052613|ref|NP_001040544.
R1_GME-string_Contig_2799.0_gi|112983414|ref|NP_001036985.1|heat
R1_GME-string_Contig_2799.0_gi|112983414|ref|NP_001036985.1|heat
R1_GME-string_Contig_3773.0_gi|242003442|ref|XP_002422733.
R1_GME-string_Contig_397.0_gi|70609810|gb|AAQ63970.2|transferrin
R1_GME-string_Contig_4434.0_gi|114050871|ref|NP_001040411.
R1_GME-string_Contig_482.0_gi|158962507|dbj|BAF91714.1|chemosensory
R1_GME-string_Contig_646.0_gi|56718390|gb|AAW24481.1|prophenol
R1_GME-string_Contig_6551.0_gi|91084741|ref|XP_971031.1|PREDICTED:
R2_contig00224_1.exp_gi|2498144|sp|Q25490.1|APLP_MANSERecName:
R2_contig00936_1.exp_gi|148298796|ref|NP_001091804.1|thioredoxin-like
R2_contig03613_1.f1.exp_gi|195391648|ref|XP_002054472.1|GJ22788
R2_contig04543_1.f1.exp_gi|91079020|ref|XP_974879.1|PREDICTED:
R2_contig07154_1.exp_gi|85726208|gb|ABC79625.1|imaginal disc growth
R2_contig07154_1.exp_gi|85726208|gb|ABC79625.1|imaginal disc growth
R2_contig07952_1.exp_gi|157927723|gb|ABW03225.1|beta actin [Mamestra
R2_contig07952_1.exp_gi|157927723|gb|ABW03225.1|beta actin [Mamestra
R2_contig14020_1.exp_gi|238667031|emb|CAZ37422.1|tubulin alpha chain,
R2_contig14853_1.exp_gi|182509208|ref|NP_001116815.1|carboxylesterase
R2_contig15056_1.f1.exp_gi|162462783|ref|NP_001104822.
R2_contig16833_1.f1.exp_gi|153791206|ref|NP_001093269.1|scolexin
R2_contig17849_1.exp_gi|194759166|ref|XP_001961820.1|GF15158
R2_contig18685_1.exp_gi|114052150|ref|NP_001040220.1|triacylglycerol
R2_contig19592_1.exp_gi|183979239|dbj|BAG30781.1|similar to
R2_contig19736_1_exp_NA
R2_contig19736_1_exp_NA
R2_contig20011_1.r1.exp_gi|118789328|ref|XP_001237914.1|AGAP008115-PA
R2_contig20268_1.exp_gi|116245495|ref|XP_001230506.1|AGAP012658-PA
R2_contig21524_1.exp_gi|91091270|ref|XP_969358.1|PREDICTED: similar
R2_GME-string_Contig_1207.0_gi|192763882|gb|ACF05615.1|actin 3
R2_GME-string_Contig_1307.0_gi|162462783|ref|NP_001104822.
R2_GME-string_Contig_1861.0_gi|91091728|ref|XP_967315.1|PREDICTED:
R2_GME-string_Contig_2266.0_gi|157108606|ref|XP_001650307.1|AMP
R2_GME-string_Contig_3472.0_gi|189181680|ref|NP_001121191.
R2_GME-string_Contig_3720.0_gi|112983052|ref|NP_001037068.
R2_GME-string_Contig_4671.0_gi|56418411|gb|AAV91013.1|hemolymph
R2_GME-string_Contig_4865.0_gi|114052484|ref|NP_001040250.
R2_GME-string_Contig_6634.0_gi|39579195|gb|AAR28762.1|odorant-binding
R3_contig01012_1.exp_gi|229556834|ref|ZP_04444623.1|NADPH:quinone

R3_contig02658_1.f1.exp_gi|159078|gb|AAA74229.1|arylphorin [Galleria
R3_contig09410_1.exp_gi|183979372|dbj|BAG30738.1|troponin T [Papilio
R3_contig12733_1.exp_gi|2498144|sp|Q25490.1|APLP_MANSERecName:
R3_contig14894_1.exp_gi|239787860|ref|NP_001155183.1|multiple
R3_contig15438_1.exp_gi|151301198|ref|NP_001093087.1|mobility group
R3_contig15747_1.f1.exp_gi|189181680|ref|NP_001121191.
R3_contig16309_1.exp_gi|87248109|gb|ABD36107.1|enoyl-CoA hydratase
R3_contig16410_1.exp_gi|189237651|ref|XP_001813448.1|PREDICTED:
R3_contig16578_1.exp_gi|110649240|emb|CAL25129.1|gloverin [Manduca
R3_contig17104_1.exp_gi|169646838|ref|NP_001112375.1|heat shock
R3_contig18934_1.exp_gi|91080775|ref|XP_968281.1|PREDICTED: similar
R3_contig19564_1.exp_gi|91091664|ref|XP_971445.1|PREDICTED: similar
R3_contig20216_1.exp_gi|46396271|sp|P83632.1|P27K_GALMERecName:;F1_GME-string_Contig_4258.0_gi|156968297|gb|ABU98620.1|unknown
R3_GME-string_Contig_1320.0_gi|114052783|ref|NP_001040279.1|serine
R3_GME-string_Contig_135.0_gi|183979237|dbj|BAG30780.1|muscle protein
R3_GME-string_Contig_1961.0_gi|153791847|ref|NP_001093284.1|abnormal
R3_GME-string_Contig_1961.0_gi|153791847|ref|NP_001093284.1|abnormal
R3_GME-string_Contig_211.0_gi|114051191|ref|NP_001040386.
R3_GME-string_Contig_317.0_gi|91088191|ref|XP_972764.1|PREDICTED:
R3_GME-string_Contig_3809.0_gi|112983816|ref|NP_001037386.
R3_GME-string_Contig_3809.0_gi|112983816|ref|NP_001037386.
R3_GME-string_Contig_398.0_gi|157118472|ref|XP_001659123.
R3_GME-string_Contig_528.0_gi|114050827|ref|NP_001040323.
R3_GME-string_Contig_534.0_gi|149898901|gb|ABR27951.1|ubiquitin
R3_GME-string_Contig_5769.0_gi|148719710|gb|ABR08302.1|putative
R3_GME-string_Contig_6082.0_gi|114649525|emb|CAK22401.1|beta-1,
R3_GME-string_Contig_6634.0_gi|39579195|gb|AAR28762.1|odorant-binding
R3_GME-string_Contig_6732.0_gi|9087200|sp|O76192.1|SERO_GALMERecName:
R3_GME-string_Contig_6732.0_gi|9087200|sp|O76192.1|SERO_GALMERecName:

3.9.2 List of identified protein in comparison between the negative control and Cu-DPQ-Phen (**2**)

F1_contig00131_1.exp_gi|112983250|ref|NP_001037610.1|putative alcohol
F1_contig00234_1.f1.exp_gi|183979231|dbj|BAG30777.1|chitin binding
F1_contig00848_1.exp_gi|229002332|dbj|BAH57948.1|hypothetical protein
F1_contig00859_1.f1.exp_gi|170041898|ref|XP_001848684.1|apyrase
F1_contig01324_1.exp_gi|56462286|gb|AAV91426.1|putative protease
F1_contig01421_1.exp_gi|157114409|ref|XP_001652257.1|dihydropteridine
F1_contig01421_1.exp_gi|157114409|ref|XP_001652257.1|dihydropteridine
F1_contig01451_1.f1.exp_gi|158285614|ref|XP_308397.4|AGAP007475-PA
F1_contig02233_1.f1.exp_gi|112983096|ref|NP_001037054.
F1_contig02487_1.exp_gi|157833800|pdb|1SEK|AChain A, The Structure Of
F1_contig02586_1.exp_gi|56462162|gb|AAV91364.1|hypothetical protein
F1_contig02726_1.exp_gi|114050871|ref|NP_001040411.1|carboxylesterase

F1_contig02803_1.exp_gi|116791778|gb|ABK26104.1|unknown [Picea
F1_contig02961_1.f1.exp_gi|158289805|ref|XP_311447.4|AGAP010733-PA
F1_contig02961_1.f1.exp_gi|158289805|ref|XP_311447.4|AGAP010733-PA
F1_contig03361_1.exp_gi|183979284|dbj|BAG30769.1|elongation factor 1
F1_contig07944_1.exp_gi|110743533|dbj|BAE98324.1|methionine-rich
F1_contig13620_1.f1.exp_gi|109502352|gb|ABE01157.2|carboxylesterase
F1_contig15344_1.exp_gi|193704761|ref|XP_001947608.1|PREDICTED:;F1_GME-string_Contig_3474.0_gi|170030366|ref|XP_001843060.
F1_contig15714_1.exp_gi|112982880|ref|NP_001037572.1|translationally
F1_contig16332_1.exp_gi|114051702|ref|NP_001040423.1|zinc-containing
F1_contig16841_1.exp_gi|6671050|gb|AAF23078.1|AF128867_1glutathione
F1_contig17276_1.exp_gi|114051481|ref|NP_001040300.
F1_contig17506_1.exp_gi|112983070|ref|NP_001037057.1|BCP inhibitor
F1_contig18074_1.exp_gi|156551613|ref|XP_001600684.1|PREDICTED:
F1_contig18862_1.exp_gi|56462318|gb|AAV91442.1|hypothetical protein
F1_contig19578_1.f1.exp_gi|114051325|ref|NP_001040376.
F1_contig19578_1.f1.exp_gi|114051325|ref|NP_001040376.
F1_contig19579_1.exp_gi|156254836|gb|ABU62829.1|serpin-2 [Spodoptera
F1_contig19674_1.f1.exp_gi|242009020|ref|XP_002425291.1|paramyosin,
F1_contig20154_1.f1.exp_gi|34921426|sp|O96790.2|DPGN_DIPMARecName:
F1_contig21121_1.exp_gi|148266444|gb|ABQ53630.1|glutathione
F1_contig21523_1.exp_gi|162462783|ref|NP_001104822.
F1_contig21523_1.exp_gi|162462783|ref|NP_001104822.
F1_GME-string_Contig_1038.0_gi|49532918|dbj|BAD26694.1|cellular
F1_GME-string_Contig_1038.0_gi|49532918|dbj|BAD26694.1|cellular
F1_GME-string_Contig_1160.0_gi|112983082|ref|NP_001037668.1|cytosolic
F1_GME-string_Contig_1333.0_gi|241263211|ref|XP_002405507.1|CNDP
F1_GME-string_Contig_1535.0_gi|154707830|gb|AAU84716.
F1_GME-string_Contig_1831.0_gi|156547253|ref|XP_001601340.
F1_GME-string_Contig_1931.0_gi|158515746|gb|AAN06604.
F1_GME-string_Contig_1949.0_gi|158515746|gb|AAN06604.
F1_GME-string_Contig_1997.0_gi|121308868|dbj|BAF43531.1|serine
F1_GME-string_Contig_2092.0_gi|114050771|ref|NP_001040154.
F1_GME-string_Contig_2215.0_gi|239835734|ref|NP_001155190.1|tau-like
F1_GME-string_Contig_2311.0_gi|195107829|ref|XP_001998496.1|GI24003
F1_GME-string_Contig_337.0_gi|170058562|ref|XP_001864974.1|dimeric
F1_GME-string_Contig_374.0_gi|112983164|ref|NP_001036945.
F1_GME-string_Contig_4545.0_gi|225031010|gb|ACN79512.1|alpha
F1_GME-string_Contig_48.0_gi|15146043|gb|AAK83435.1|alpha-crystallin
F1_GME-string_Contig_5294.0_gi|112983342|ref|NP_001036965.
F1_GME-string_Contig_5500.0_gi|45330818|dbj|BAD12426.1|fructose
F1_GME-string_Contig_581.0_gi|4090964|gb|AAD09279.1|immune-related
F1_GME-string_Contig_581.0_gi|4090964|gb|AAD09279.1|immune-related
F1_GME-string_Contig_5857.0_gi|66508985|ref|XP_624902.1|PREDICTED:
F1_GME-string_Contig_6852.0_gi|219552448|gb|ACL26939.1|arginine

F1_GME-string_Contig_6852.0_gi|219552448|gb|ACL26939.1|arginine
F1_GME-string_Contig_962.0_gi|156968291|gb|ABU98617.1|unknown
F1_GME-string_Contig_962.0_gi|156968291|gb|ABU98617.1|unknown
F2_contig00391_1.exp_gi|148298770|ref|NP_001091821.1|ATPase
F2_contig00893_1.exp_gi|116087|sp|P01507.1|CECA_HYACERecName:
F2_contig01621_1.exp_gi|114052174|ref|NP_001040228.1|aminoacylase
F2_contig02236_1.exp_gi|46396271|sp|P83632.1|P27K_GALMERecName:
F2_contig02362_1.exp_gi|4753912|emb|CAB41997.1|3-dehydroecdysone
F2_contig02401_1.exp_gi|170035237|ref|XP_001845477.1|aliphatic
F2_contig02401_1.exp_gi|170035237|ref|XP_001845477.1|aliphatic
F2_contig02482_1.f1.exp_gi|91079628|ref|XP_967731.1|PREDICTED:
F2_contig02701_1.exp_gi|66517857|ref|XP_391850.2|PREDICTED: similar
F2_contig02857_1.exp_gi|73671225|gb|AAZ80044.1|diapause bioclock
F2_contig02908_1.exp_gi|183979374|dbj|BAG30739.1|Tropomyosin 2
F2_contig02932_1.f1.exp_gi|91082539|ref|XP_973726.1|PREDICTED:
F2_contig04024_1.exp_gi|186703381|gb|ACC91897.1|hemolin [Heliothis
F2_contig06283_1.exp_gi|34556399|gb|AAQ75026.1|prophenoloxidase
F2_contig07194_1.exp_gi|198452388|ref|XP_001358750.2|GA20334
F2_contig13577_1.exp_gi|183979239|dbj|BAG30781.1|similar to
F2_contig15137_1.exp_gi|58864722|emb|CAI06089.1|putative annexin IX-B
F2_contig15175_1.exp_gi|55139149|gb|AAV41247.1|hemolin [Plodia
F2_contig15383_1.exp_gi|112984026|ref|NP_001036831.1|BmP109 [Bombyx
F2_contig16122_1.f1.exp_gi|226693130|dbj|BAH56565.1|sepiapterin
F2_contig16165_1.f1.exp_gi|148298800|ref|NP_001091831.1|enolase
F2_contig16165_1.f1.exp_gi|148298800|ref|NP_001091831.1|enolase
F2_contig16750_1.f1.exp_gi|229562186|gb|ACQ78181.1|heat shock protein
F2_contig16968_1.exp_gi|159528|gb|AAA29321.1|methionine-rich storage
F2_contig17054_1.exp_gi|17901818|gb|AAL47694.1|AF329683_132 kDa
F2_contig17442_1.exp_gi|25989211|gb|AAL31707.1|prophenoloxidase
F2_contig17460_1.exp_gi|112983086|ref|NP_001037594.1|troponin C
F2_contig18014_1.exp_gi|242009020|ref|XP_002425291.1|paramyosin,
F2_contig18192_1.exp_gi|14599864|gb|AAK71137.1|AF356843_1hexamerin
F2_contig18407_1.exp_gi|170046360|ref|XP_001850736.1|conserved
F2_contig18681_1.exp_gi|112982865|ref|NP_001037108.1|profilin [Bombyx
F2_contig18979_1.exp_gi|114052677|ref|NP_001040269.1|phosphoserine
F2_contig19502_1.f1.exp_gi|183979392|dbj|BAG30748.1|hypothetical
F2_contig19502_1.f1.exp_gi|183979392|dbj|BAG30748.1|hypothetical
F2_contig20908_1.f1.exp_gi|9087198|sp|O62605.1|SI25_GALMERecName:
F2_contig21210_1.exp_gi|109119903|dbj|BAE96011.
F2_contig21210_1.exp_gi|109119903|dbj|BAE96011.
F2_contig21539_1.exp_gi|384243|prf||1905335Aarylphorin
F2_contig21568_1.exp_gi|170036627|ref|XP_001846164.1|Gelsolin [Culex
F2_contig21568_1.exp_gi|170036627|ref|XP_001846164.1|Gelsolin [Culex
F2_GME-string_Contig_1598.0_gi|91083881|ref|XP_967558.1|PREDICTED:

F2_GME-string_Contig_186.0_gi|164459610|gb|ABY57912.1|hydroxypyruvate
F2_GME-string_Contig_186.0_gi|164459610|gb|ABY57912.1|hydroxypyruvate
F2_GME-string_Contig_2050.0_gi|60592747|dbj|BAD90848.
F2_GME-string_Contig_2064.0_gi|112983994|ref|NP_001036836.
F2_GME-string_Contig_2064.0_gi|112983994|ref|NP_001036836.
F2_GME-string_Contig_233.0_gi|238915964|gb|ACR78449.1|growth-blocking
F2_GME-string_Contig_3629.0_gi|6919921|sp|P81906.
F2_GME-string_Contig_3629.0_gi|6919921|sp|P81906.
F2_GME-string_Contig_3762.0_gi|6560637|gb|AAF16696.
F2_GME-string_Contig_3905.0_gi|112983390|ref|NP_001036987.
F2_GME-string_Contig_4835.0_gi|112983550|ref|NP_001036879.
F2_GME-string_Contig_512.0_gi|114051966|ref|NP_001040198.
F2_GME-string_Contig_5466.0_gi|6164595|gb|AAF04457.
F2_GME-string_Contig_555.0_gi|114051738|ref|NP_001040426.1|alcohol
F2_GME-string_Contig_5601.0_gi|91078812|ref|XP_970578.1|PREDICTED:
F2_GME-string_Contig_5861.0_gi|116780375|gb|ABK21656.1|unknown [Picea
F2_GME-string_Contig_5861.0_gi|116780375|gb|ABK21656.1|unknown [Picea
F2_GME-string_Contig_6549.0_gi|229002332|dbj|BAH57948.1|hypothetical
F2_GME-string_Contig_6549.0_gi|229002332|dbj|BAH57948.1|hypothetical
F2_GME-string_Contig_695.0_gi|114052561|ref|NP_001040257.1|cytosolic
F2_GME-string_Contig_695.0_gi|114052561|ref|NP_001040257.1|cytosolic
F3_contig00036_1.exp_gi|112983654|ref|NP_001036872.1|Bombyrin [Bombyx
F3_contig00049_1.f1.exp_gi|226342884|ref|NP_001139704.1|serpin 11
F3_contig00380_1.f1.exp_gi|159078|gb|AAA74229.1|arylphorin [Galleria
F3_contig00412_1.f1.exp_gi|14599862|gb|AAK71136.1|AF356842_1hexamerin
F3_contig00812_1.exp_gi|114050771|ref|NP_001040154.1|short-chain
F3_contig01202_1.exp_gi|14517793|gb|AAK64362.
F3_contig01621_1.exp_gi|114052174|ref|NP_001040228.1|aminoacylase
F3_contig02609_1.exp_gi|21630233|gb|AAM69353.1|AF518768_1serine
F3_contig02609_1.exp_gi|21630233|gb|AAM69353.1|AF518768_1serine
F3_contig02707_1.exp_gi|11890404|gb|AAG41120.1|26kDa ferritin subunit
F3_contig02722_1.f1.exp_gi|239938036|gb|ACS36117.1|beta-galactosidase
F3_contig04057_1.exp_gi|2498144|sp|Q25490.1|APLP_MANSERecName:
F3_contig04490_1.exp_gi|195115822|ref|XP_002002455.1|GI17397
F3_contig04490_1.exp_gi|195115822|ref|XP_002002455.1|GI17397
F3_contig05096_1.exp_gi|237874122|dbj|BAH59606.1|multicystatin and
F3_contig12543_1.exp_gi|156630460|sp|P85216.1|AP2_GALMERecName:
F3_contig12543_1.exp_gi|156630460|sp|P85216.1|AP2_GALMERecName:
F3_contig14928_1.exp_gi|114052472|ref|NP_001040479.1|peptidylprolyl
F3_contig15255_1.exp_gi|75906185|ref|YP_313566.1|adhesion-like
F3_contig15340_1.exp_gi|50404098|gb|AAT76806.1|apolipophorin
F3_contig15340_1.exp_gi|50404098|gb|AAT76806.1|apolipophorin
F3_contig15609_1.exp_gi|74873244|sp|O96382.1|DFP11_HYPCURecName:
F3_contig16820_1.exp_gi|164451507|gb|ABY56688.1|troponin I [Loxostege

F3_contig16921_1.f1.exp_gi|112982822|ref|NP_001037540.
F3_contig18074_1.exp_gi|156551613|ref|XP_001600684.1|PREDICTED:
F3_contig19161_1.f1.exp_gi|145286562|gb|ABP52098.1|lysozyme-like
F3_contig19165_1.exp_gi|114051866|ref|NP_001040134.1|isocitrate
F3_contig20116_1.exp_gi|193610917|ref|XP_001950677.1|PREDICTED:
F3_contig20343_1.exp_gi|148298833|ref|NP_001091765.1|NADP-dependent
F3_contig21439_1.exp_gi|33439712|gb|AAQ18894.1|spodoptericin
F3_contig21568_1.exp_gi|170036627|ref|XP_001846164.1|Gelsolin [Culex
F3_contig21932_1.exp_gi|91093363|ref|XP_969584.1|PREDICTED: similar
F3_contig22104_1.exp_gi|229002332|dbj|BAH57948.1|hypothetical protein
F3_contig22104_1.exp_gi|229002332|dbj|BAH57948.1|hypothetical protein
F3_GME-string_Contig_1060.0_gi|49532886|dbj|BAD26678.1|Diazepam
F3_GME-string_Contig_1065.0_gi|148298726|ref|NP_001091755.
F3_GME-string_Contig_1139.0_gi|212710319|ref|ZP_03318447.
F3_GME-string_Contig_1226.0_gi|41053309|ref|NP_956337.
F3_GME-string_Contig_1489.0_gi|23208546|gb|AAN15790.1|heat shock-like
F3_GME-string_Contig_1544.0_gi|39579195|gb|AAR28762.1|odorant-binding
F3_GME-string_Contig_1544.0_gi|39579195|gb|AAR28762.1|odorant-binding
F3_GME-string_Contig_1581.0_gi|114052116|ref|NP_001040454.1|ML-domain
F3_GME-string_Contig_1802.0_gi|242022233|ref|XP_002431545.1|high
F3_GME-string_Contig_190.0_gi|116782397|gb|ABK22491.1|unknown [Picea
F3_GME-string_Contig_2113.0_gi|124527|sp|Q00630.1|ICYB_MANSERecName:
F3_GME-string_Contig_2408.0_gi|229002332|dbj|BAH57948.1|hypothetical
F3_GME-string_Contig_2408.0_gi|229002332|dbj|BAH57948.1|hypothetical
F3_GME-string_Contig_3163.0_gi|1146408|gb|AAA85089.1|gallerin
F3_GME-string_Contig_352.0_gi|114052242|ref|NP_001040131.
F3_GME-string_Contig_45.0_gi|229002332|dbj|BAH57948.1|hypothetical
F3_GME-string_Contig_5353.0_gi|2498144|sp|Q25490.1|APLP_MANSERecName:
F3_GME-string_Contig_5382.0_gi|125629089|emb|CAL23158.2|gustatory
F3_GME-string_Contig_5682.0_gi|77415676|emb|CAJ01507.1|hypothetical
F3_GME-string_Contig_5764.0_gi|195119912|ref|XP_002004473.1|GI19595;R2_contig18735_1.exp_gi|158293921|ref|XP_315269.4|AGAP011516-PA
F3_GME-string_Contig_5764.0_gi|195119912|ref|XP_002004473.1|GI19595;R2_contig18735_1.exp_gi|158293921|ref|XP_315269.4|AGAP011516-PA
F3_GME-string_Contig_6108.0_gi|189239301|ref|XP_971644.2|PREDICTED:
F3_GME-string_Contig_944.0_gi|112982743|ref|NP_001037556.1|elongation
R1_contig01633_1.exp_gi|195475698|ref|XP_002090121.1|GE20538
R1_contig01804_1.f1.exp_gi|112984054|ref|NP_001037422.1|yellow1
R1_contig02674_1.f1.exp_gi|114051966|ref|NP_001040198.1|mitochondrial
R1_contig02829_1.exp_gi|117970173|dbj|BAF36817.
R1_contig03614_1.f1.exp_gi|91084675|ref|XP_968140.1|PREDICTED:
R1_contig03752_1.exp_gi|189181680|ref|NP_001121191.1|carboxylesterase
R1_contig05149_1.exp_gi|112984026|ref|NP_001036831.1|BmP109 [Bombyx
R1_contig09082_1.exp_gi|114051598|ref|NP_001040416.1|leukotriene A4

R1_contig15056_1.f1.exp_gi|162462783|ref|NP_001104822.
R1_contig16410_1.exp_gi|189237651|ref|XP_001813448.1|PREDICTED:
R1_contig17461_1.exp_gi|158962511|dbj|BAF91716.1|chemosensory protein
R1_contig17461_1.exp_gi|158962511|dbj|BAF91716.1|chemosensory protein
R1_contig18077_1.exp_gi|220902980|gb|ACL83459.1|carboxylesterase
R1_contig19537_1.exp_gi|47607477|gb|AAT36640.1|imaginal disc growth
R1_contig19537_1.exp_gi|47607477|gb|AAT36640.1|imaginal disc growth
R1_contig20220_1.exp_gi|242004672|ref|XP_002423204.1|conserved
R1_contig20220_1.exp_gi|242004672|ref|XP_002423204.1|conserved
R1_contig20227_1.exp_gi|23208535|gb|AAN15786.1|peptidoglycan
R1_contig21466_1.exp_gi|134103857|gb|ABO60878.1|cationic peptide CP8
R1_contig21466_1.exp_gi|134103857|gb|ABO60878.1|cationic peptide CP8
R1_contig21950_1.exp_gi|56462300|gb|AAV91433.1|putative serine
R1_contig22070_1.exp_gi|112983062|ref|NP_001037056.
R1_contig22148_1.exp_gi|18140733|gb|AAL60414.1|AF393489_1twelve
R1_GME-string_Contig_2259.0_gi|91092064|ref|XP_970689.1|PREDICTED:
R1_GME-string_Contig_2606.0_gi|114052613|ref|NP_001040544.
R1_GME-string_Contig_2799.0_gi|112983414|ref|NP_001036985.1|heat
R1_GME-string_Contig_2799.0_gi|112983414|ref|NP_001036985.1|heat
R1_GME-string_Contig_3773.0_gi|242003442|ref|XP_002422733.
R1_GME-string_Contig_397.0_gi|70609810|gb|AAQ63970.2|transferrin
R1_GME-string_Contig_4434.0_gi|114050871|ref|NP_001040411.
R1_GME-string_Contig_482.0_gi|158962507|dbj|BAF91714.1|chemosensory
R1_GME-string_Contig_646.0_gi|56718390|gb|AAW24481.1|prophenol
R1_GME-string_Contig_6551.0_gi|91084741|ref|XP_971031.1|PREDICTED:
R2_contig00224_1.exp_gi|2498144|sp|Q25490.1|APLP_MANSERecName:
R2_contig00224_1.exp_gi|2498144|sp|Q25490.1|APLP_MANSERecName:
R2_contig00936_1.exp_gi|148298796|ref|NP_001091804.1|thioredoxin-like
R2_contig03613_1.f1.exp_gi|195391648|ref|XP_002054472.1|GJ22788
R2_contig04543_1.f1.exp_gi|91079020|ref|XP_974879.1|PREDICTED:
R2_contig07154_1.exp_gi|85726208|gb|ABC79625.1|imaginal disc growth
R2_contig07154_1.exp_gi|85726208|gb|ABC79625.1|imaginal disc growth
R2_contig07952_1.exp_gi|157927723|gb|ABW03225.1|beta actin [Mamestra
R2_contig07952_1.exp_gi|157927723|gb|ABW03225.1|beta actin [Mamestra
R2_contig14020_1.exp_gi|238667031|emb|CAZ37422.1|tubulin alpha chain,
R2_contig14853_1.exp_gi|182509208|ref|NP_001116815.1|carboxylesterase
R2_contig15056_1.f1.exp_gi|162462783|ref|NP_001104822.
R2_contig16833_1.f1.exp_gi|153791206|ref|NP_001093269.1|scolexin
R2_contig17849_1.exp_gi|194759166|ref|XP_001961820.1|GF15158
R2_contig18685_1.exp_gi|114052150|ref|NP_001040220.1|triacylglycerol
R2_contig19592_1.exp_gi|183979239|dbj|BAG30781.1|similar to
R2_contig19736_1_exp_NA
R2_contig19736_1_exp_NA
R2_contig20011_1.r1.exp_gi|118789328|ref|XP_001237914.1|AGAP008115-PA

R2_contig20268_1.exp_gi|116245495|ref|XP_001230506.1|AGAP012658-PA
R2_contig21524_1.exp_gi|91091270|ref|XP_969358.1|PREDICTED: similar
R2_GME-string_Contig_1207.0_gi|192763882|gb|ACF05615.1|actin 3
R2_GME-string_Contig_1307.0_gi|162462783|ref|NP_001104822.
R2_GME-string_Contig_1307.0_gi|162462783|ref|NP_001104822.
R2_GME-string_Contig_1861.0_gi|91091728|ref|XP_967315.1|PREDICTED:
R2_GME-string_Contig_2266.0_gi|157108606|ref|XP_001650307.1|AMP
R2_GME-string_Contig_3472.0_gi|189181680|ref|NP_001121191.
R2_GME-string_Contig_3720.0_gi|112983052|ref|NP_001037068.
R2_GME-string_Contig_4671.0_gi|56418411|gb|AAV91013.1|hemolymph
R2_GME-string_Contig_4671.0_gi|56418411|gb|AAV91013.1|hemolymph
R2_GME-string_Contig_4865.0_gi|114052484|ref|NP_001040250.
R2_GME-string_Contig_6634.0_gi|39579195|gb|AAR28762.1|odorant-binding
R3_contig01012_1.exp_gi|229556834|ref|ZP_04444623.1|NADPH:quinone
R3_contig02658_1.f1.exp_gi|159078|gb|AAA74229.1|arylphorin [Galleria
R3_contig09410_1.exp_gi|183979372|dbj|BAG30738.1|troponin T [Papilio
R3_contig12733_1.exp_gi|2498144|sp|Q25490.1|APLP_MANSERecName:
R3_contig14894_1.exp_gi|239787860|ref|NP_001155183.1|multiple
R3_contig15438_1.exp_gi|151301198|ref|NP_001093087.1|mobility group
R3_contig15747_1.f1.exp_gi|189181680|ref|NP_001121191.
R3_contig16309_1.exp_gi|87248109|gb|ABD36107.1|enoyl-CoA hydratase
R3_contig16410_1.exp_gi|189237651|ref|XP_001813448.1|PREDICTED:
R3_contig16578_1.exp_gi|110649240|emb|CAL25129.1|gloverin [Manduca
R3_contig17104_1.exp_gi|169646838|ref|NP_001112375.1|heat shock
R3_contig18934_1.exp_gi|91080775|ref|XP_968281.1|PREDICTED: similar
R3_contig19564_1.exp_gi|91091664|ref|XP_971445.1|PREDICTED: similar
R3_contig20216_1.exp_gi|46396271|sp|P83632.1|P27K_GALMERecName:;F1_GME-string_Contig_4258.0_gi|156968297|gb|ABU98620.1|unknown
R3_GME-string_Contig_1320.0_gi|114052783|ref|NP_001040279.1|serine
R3_GME-string_Contig_135.0_gi|183979237|dbj|BAG30780.1|muscle protein
R3_GME-string_Contig_1961.0_gi|153791847|ref|NP_001093284.1|abnormal
R3_GME-string_Contig_1961.0_gi|153791847|ref|NP_001093284.1|abnormal
R3_GME-string_Contig_211.0_gi|114051191|ref|NP_001040386.
R3_GME-string_Contig_317.0_gi|91088191|ref|XP_972764.1|PREDICTED:
R3_GME-string_Contig_3809.0_gi|112983816|ref|NP_001037386.
R3_GME-string_Contig_3809.0_gi|112983816|ref|NP_001037386.
R3_GME-string_Contig_398.0_gi|157118472|ref|XP_001659123.
R3_GME-string_Contig_528.0_gi|114050827|ref|NP_001040323.
R3_GME-string_Contig_534.0_gi|149898901|gb|ABR27951.1|ubiquitin
R3_GME-string_Contig_5769.0_gi|148719710|gb|ABR08302.1|putative
R3_GME-string_Contig_6082.0_gi|114649525|emb|CAK22401.1|beta-1,
R3_GME-string_Contig_6082.0_gi|114649525|emb|CAK22401.1|beta-1,
R3_GME-string_Contig_6634.0_gi|39579195|gb|AAR28762.1|odorant-binding
R3_GME-string_Contig_6732.0_gi|9087200|sp|O76192.1|SERO_GALMERecName:
R3_GME-string_Contig_6732.0_gi|9087200|sp|O76192.1|SERO_GALMERecName:

3.9.3 List of identified protein in comparison between the negative control and Cu-DPPZ-Phen (**3**)

F1_GME-string_Contig_1949.0_gi|158515746|gb|AAN06604.
F1_contig00131_1.exp_gi|112983250|ref|NP_001037610.1|putative alcohol
F1_contig00234_1.f1.exp_gi|183979231|dbj|BAG30777.1|chitin binding
F1_contig00848_1.exp_gi|229002332|dbj|BAH57948.1|hypothetical protein
F1_contig00859_1.f1.exp_gi|170041898|ref|XP_001848684.1|apyrase
F1_contig01324_1.exp_gi|56462286|gb|AAV91426.1|putative protease
F1_contig01421_1.exp_gi|157114409|ref|XP_001652257.1|dihydropteridine
F1_contig01421_1.exp_gi|157114409|ref|XP_001652257.1|dihydropteridine
F1_contig01451_1.f1.exp_gi|158285614|ref|XP_308397.4|AGAP007475-PA
F1_contig02233_1.f1.exp_gi|112983096|ref|NP_001037054.
F1_contig02487_1.exp_gi|157833800|pdb|1SEK|AChain A, The Structure Of
F1_contig02586_1.exp_gi|56462162|gb|AAV91364.1|hypothetical protein
F1_contig02726_1.exp_gi|114050871|ref|NP_001040411.1|carboxylesterase
F1_contig02803_1.exp_gi|116791778|gb|ABK26104.1|unknown [Picea
F1_contig02961_1.f1.exp_gi|158289805|ref|XP_311447.4|AGAP010733-PA
F1_contig03361_1.exp_gi|183979284|dbj|BAG30769.1|elongation factor 1
F1_contig07944_1.exp_gi|110743533|dbj|BAE98324.1|methionine-rich
F1_contig13620_1.f1.exp_gi|109502352|gb|ABE01157.2|carboxylesterase
F1_contig15344_1.exp_gi|193704761|ref|XP_001947608.1|PREDICTED:;F1_GME-string_Contig_3474.0_gi|170030366|ref|XP_001843060.
F1_contig15714_1.exp_gi|112982880|ref|NP_001037572.1|translationally
F1_contig16332_1.exp_gi|114051702|ref|NP_001040423.1|zinc-containing
F1_contig16841_1.exp_gi|6671050|gb|AAF23078.1|AF128867_1glutathione
F1_contig17276_1.exp_gi|114051481|ref|NP_001040300.
F1_contig17506_1.exp_gi|112983070|ref|NP_001037057.1|BCP inhibitor
F1_contig18074_1.exp_gi|156551613|ref|XP_001600684.1|PREDICTED:
F1_contig18862_1.exp_gi|56462318|gb|AAV91442.1|hypothetical protein
F1_contig19578_1.f1.exp_gi|114051325|ref|NP_001040376.
F1_contig19578_1.f1.exp_gi|114051325|ref|NP_001040376.
F1_contig19579_1.exp_gi|156254836|gb|ABU62829.1|serpin-2 [Spodoptera
F1_contig19674_1.f1.exp_gi|242009020|ref|XP_002425291.1|paramyosin,
F1_contig20154_1.f1.exp_gi|34921426|sp|O96790.2|DPGN_DIPMARecName:
F1_contig20154_1.f1.exp_gi|34921426|sp|O96790.2|DPGN_DIPMARecName:
F1_contig21121_1.exp_gi|148266444|gb|ABQ53630.1|glutathione
F1_contig21523_1.exp_gi|162462783|ref|NP_001104822.
F1_contig21523_1.exp_gi|162462783|ref|NP_001104822.
F1_GME-string_Contig_1038.0_gi|49532918|dbj|BAD26694.1|cellular
F1_GME-string_Contig_1038.0_gi|49532918|dbj|BAD26694.1|cellular
F1_GME-string_Contig_1160.0_gi|112983082|ref|NP_001037668.1|cytosolic
F1_GME-string_Contig_1333.0_gi|241263211|ref|XP_002405507.1|CNDP
F1_GME-string_Contig_1535.0_gi|154707830|gb|AAU84716.
F1_GME-string_Contig_1831.0_gi|156547253|ref|XP_001601340.
F1_GME-string_Contig_1931.0_gi|158515746|gb|AAN06604.

F1_GME-string_Contig_1931.0_gi|158515746|gb|AAN06604.
F1_GME-string_Contig_1997.0_gi|121308868|dbj|BAF43531.1|serine
F1_GME-string_Contig_1997.0_gi|121308868|dbj|BAF43531.1|serine
F1_GME-string_Contig_2092.0_gi|114050771|ref|NP_001040154.
F1_GME-string_Contig_2215.0_gi|239835734|ref|NP_001155190.1|tau-like
F1_GME-string_Contig_2311.0_gi|195107829|ref|XP_001998496.1|GI24003
F1_GME-string_Contig_337.0_gi|170058562|ref|XP_001864974.1|dimeric
F1_GME-string_Contig_374.0_gi|112983164|ref|NP_001036945.
F1_GME-string_Contig_4545.0_gi|225031010|gb|ACN79512.1|alpha
F1_GME-string_Contig_48.0_gi|15146043|gb|AAK83435.1|alpha-crystallin
F1_GME-string_Contig_5294.0_gi|112983342|ref|NP_001036965.
F1_GME-string_Contig_5500.0_gi|45330818|dbj|BAD12426.1|fructose
F1_GME-string_Contig_581.0_gi|4090964|gb|AAD09279.1|immune-related
F1_GME-string_Contig_581.0_gi|4090964|gb|AAD09279.1|immune-related
F1_GME-string_Contig_5857.0_gi|66508985|ref|XP_624902.1|PREDICTED:
F1_GME-string_Contig_6852.0_gi|219552448|gb|ACL26939.1|arginine
F1_GME-string_Contig_6852.0_gi|219552448|gb|ACL26939.1|arginine
F1_GME-string_Contig_962.0_gi|156968291|gb|ABU98617.1|unknown
F1_GME-string_Contig_962.0_gi|156968291|gb|ABU98617.1|unknown
F2_contig00391_1.exp_gi|148298770|ref|NP_001091821.1|ATPase
F2_contig00893_1.exp_gi|116087|sp|P01507.1|CECA_HYACERecName:
F2_contig01621_1.exp_gi|114052174|ref|NP_001040228.1|aminoacylase
F2_contig02236_1.exp_gi|46396271|sp|P83632.1|P27K_GALMERecName:
F2_contig02236_1.exp_gi|46396271|sp|P83632.1|P27K_GALMERecName:
F2_contig02362_1.exp_gi|4753912|emb|CAB41997.1|3-dehydroecdysone
F2_contig02401_1.exp_gi|170035237|ref|XP_001845477.1|aliphatic
F2_contig02401_1.exp_gi|170035237|ref|XP_001845477.1|aliphatic
F2_contig02482_1.f1.exp_gi|91079628|ref|XP_967731.1|PREDICTED:
F2_contig02701_1.exp_gi|66517857|ref|XP_391850.2|PREDICTED: similar
F2_contig02857_1.exp_gi|73671225|gb|AAZ80044.1|diapause bioclock
F2_contig02908_1.exp_gi|183979374|dbj|BAG30739.1|Tropomyosin 2
F2_contig02932_1.f1.exp_gi|91082539|ref|XP_973726.1|PREDICTED:
F2_contig04024_1.exp_gi|186703381|gb|ACC91897.1|hemolin [Heliothis
F2_contig06283_1.exp_gi|34556399|gb|AAQ75026.1|prophenoloxidase
F2_contig07194_1.exp_gi|198452388|ref|XP_001358750.2|GA20334
F2_contig13577_1.exp_gi|183979239|dbj|BAG30781.1|similar to
F2_contig15137_1.exp_gi|58864722|emb|CAI06089.1|putative annexin IX-B
F2_contig15175_1.exp_gi|55139149|gb|AAV41247.1|hemolin [Plodia
F2_contig15383_1.exp_gi|112984026|ref|NP_001036831.1|BmP109 [Bombyx
F2_contig16122_1.f1.exp_gi|226693130|dbj|BAH56565.1|sepiapterin
F2_contig16165_1.f1.exp_gi|148298800|ref|NP_001091831.1|enolase
F2_contig16165_1.f1.exp_gi|148298800|ref|NP_001091831.1|enolase
F2_contig16750_1.f1.exp_gi|229562186|gb|ACQ78181.1|heat shock protein
F2_contig16968_1.exp_gi|159528|gb|AAA29321.1|methionine-rich storage

F2_contig16968_1.exp_gi|159528|gb|AAA29321.1|methionine-rich storage
F2_contig17054_1.exp_gi|17901818|gb|AAL47694.1|AF329683_132 kDa
F2_contig17442_1.exp_gi|25989211|gb|AAL31707.1|prophenoloxidase
F2_contig17460_1.exp_gi|112983086|ref|NP_001037594.1|troponin C
F2_contig18014_1.exp_gi|242009020|ref|XP_002425291.1|paramyosin,
F2_contig18192_1.exp_gi|14599864|gb|AAK71137.1|AF356843_1hexamerin
F2_contig18192_1.exp_gi|14599864|gb|AAK71137.1|AF356843_1hexamerin
F2_contig18407_1.exp_gi|170046360|ref|XP_001850736.1|conserved
F2_contig18681_1.exp_gi|112982865|ref|NP_001037108.1|profilin [Bombyx
F2_contig18979_1.exp_gi|114052677|ref|NP_001040269.1|phosphoserine
F2_contig19502_1.f1.exp_gi|183979392|dbj|BAG30748.1|hypothetical
F2_contig19502_1.f1.exp_gi|183979392|dbj|BAG30748.1|hypothetical
F2_contig20908_1.f1.exp_gi|9087198|sp|O62605.1|SI25_GALMERecName:
F2_contig21210_1.exp_gi|109119903|dbj|BAE96011.
F2_contig21210_1.exp_gi|109119903|dbj|BAE96011.
F2_contig21539_1.exp_gi|384243|prf||1905335Aarylphorin
F2_contig21539_1.exp_gi|384243|prf||1905335Aarylphorin
F2_contig21568_1.exp_gi|170036627|ref|XP_001846164.1|Gelsolin [Culex
F2_contig21568_1.exp_gi|170036627|ref|XP_001846164.1|Gelsolin [Culex
F2_GME-string_Contig_1598.0_gi|91083881|ref|XP_967558.1|PREDICTED:
F2_GME-string_Contig_186.0_gi|164459610|gb|ABY57912.1|hydroxypyruvate
F2_GME-string_Contig_186.0_gi|164459610|gb|ABY57912.1|hydroxypyruvate
F2_GME-string_Contig_2050.0_gi|60592747|dbj|BAD90848.
F2_GME-string_Contig_2064.0_gi|112983994|ref|NP_001036836.
F2_GME-string_Contig_2064.0_gi|112983994|ref|NP_001036836.
F2_GME-string_Contig_233.0_gi|238915964|gb|ACR78449.1|growth-blocking
F2_GME-string_Contig_3629.0_gi|6919921|sp|P81906.
F2_GME-string_Contig_3629.0_gi|6919921|sp|P81906.
F2_GME-string_Contig_3762.0_gi|6560637|gb|AAF16696.
F2_GME-string_Contig_3905.0_gi|112983390|ref|NP_001036987.
F2_GME-string_Contig_4835.0_gi|112983550|ref|NP_001036879.
F2_GME-string_Contig_4835.0_gi|112983550|ref|NP_001036879.
F2_GME-string_Contig_512.0_gi|114051966|ref|NP_001040198.
F2_GME-string_Contig_5466.0_gi|6164595|gb|AAF04457.
F2_GME-string_Contig_555.0_gi|114051738|ref|NP_001040426.1|alcohol
F2_GME-string_Contig_5601.0_gi|91078812|ref|XP_970578.1|PREDICTED:
F2_GME-string_Contig_5861.0_gi|116780375|gb|ABK21656.1|unknown [Picea
F2_GME-string_Contig_5861.0_gi|116780375|gb|ABK21656.1|unknown [Picea
F2_GME-string_Contig_6549.0_gi|229002332|dbj|BAH57948.1|hypothetical
F2_GME-string_Contig_6549.0_gi|229002332|dbj|BAH57948.1|hypothetical
F2_GME-string_Contig_695.0_gi|114052561|ref|NP_001040257.1|cytosolic
F2_GME-string_Contig_695.0_gi|114052561|ref|NP_001040257.1|cytosolic
F3_contig00036_1.exp_gi|112983654|ref|NP_001036872.1|Bombyrin [Bombyx
F3_contig00049_1.f1.exp_gi|226342884|ref|NP_001139704.1|serpin 11

F3_contig00380_1.f1.exp_gi|159078|gb|AAA74229.1|arylphorin [Galleria
F3_contig00412_1.f1.exp_gi|14599862|gb|AAK71136.1|AF356842_1hexamerin
F3_contig00812_1.exp_gi|114050771|ref|NP_001040154.1|short-chain
F3_contig01202_1.exp_gi|14517793|gb|AAK64362.
F3_contig01621_1.exp_gi|114052174|ref|NP_001040228.1|aminoacylase
F3_contig02609_1.exp_gi|21630233|gb|AAM69353.1|AF518768_1serine
F3_contig02707_1.exp_gi|11890404|gb|AAG41120.1|26kDa ferritin subunit
F3_contig02722_1.f1.exp_gi|239938036|gb|ACS36117.1|beta-galactosidase
F3_contig04057_1.exp_gi|2498144|sp|Q25490.1|APLP_MANSERecName:
F3_contig04057_1.exp_gi|2498144|sp|Q25490.1|APLP_MANSERecName:
F3_contig04490_1.exp_gi|195115822|ref|XP_002002455.1|GI17397
F3_contig04490_1.exp_gi|195115822|ref|XP_002002455.1|GI17397
F3_contig05096_1.exp_gi|237874122|dbj|BAH59606.1|multicystatin and
F3_contig12543_1.exp_gi|156630460|sp|P85216.1|AP2_GALMERecName:
F3_contig14928_1.exp_gi|114052472|ref|NP_001040479.1|peptidylprolyl
F3_contig15255_1.exp_gi|75906185|ref|YP_313566.1|adhesion-like
F3_contig15340_1.exp_gi|50404098|gb|AAT76806.1|apolipophorin
F3_contig15340_1.exp_gi|50404098|gb|AAT76806.1|apolipophorin
F3_contig15609_1.exp_gi|74873244|sp|O96382.1|DFP11_HYPCURecName:
F3_contig16820_1.exp_gi|164451507|gb|ABY56688.1|troponin I [Loxostege
F3_contig16921_1.f1.exp_gi|112982822|ref|NP_001037540.
F3_contig18074_1.exp_gi|156551613|ref|XP_001600684.1|PREDICTED:
F3_contig19161_1.f1.exp_gi|145286562|gb|ABP52098.1|lysozyme-like
F3_contig19165_1.exp_gi|114051866|ref|NP_001040134.1|isocitrate
F3_contig19165_1.exp_gi|114051866|ref|NP_001040134.1|isocitrate
F3_contig20116_1.exp_gi|193610917|ref|XP_001950677.1|PREDICTED:
F3_contig20343_1.exp_gi|148298833|ref|NP_001091765.1|NADP-dependent
F3_contig21439_1.exp_gi|33439712|gb|AAQ18894.1|spodoptericin
F3_contig21568_1.exp_gi|170036627|ref|XP_001846164.1|Gelsolin [Culex
F3_contig21932_1.exp_gi|91093363|ref|XP_969584.1|PREDICTED: similar
F3_contig22104_1.exp_gi|229002332|dbj|BAH57948.1|hypothetical protein
F3_contig22104_1.exp_gi|229002332|dbj|BAH57948.1|hypothetical protein
F3_GME-string_Contig_1060.0_gi|49532886|dbj|BAD26678.1|Diazepam
F3_GME-string_Contig_1065.0_gi|148298726|ref|NP_001091755.
F3_GME-string_Contig_1139.0_gi|212710319|ref|ZP_03318447.
F3_GME-string_Contig_1226.0_gi|41053309|ref|NP_956337.
F3_GME-string_Contig_1489.0_gi|23208546|gb|AAN15790.1|heat shock-like
F3_GME-string_Contig_1544.0_gi|39579195|gb|AAR28762.1|odorant-binding
F3_GME-string_Contig_1581.0_gi|114052116|ref|NP_001040454.1|ML-domain
F3_GME-string_Contig_1802.0_gi|242022233|ref|XP_002431545.1|high
F3_GME-string_Contig_190.0_gi|116782397|gb|ABK22491.1|unknown [Picea
F3_GME-string_Contig_2113.0_gi|124527|sp|Q00630.1|ICYB_MANSERecName:
F3_GME-string_Contig_2408.0_gi|229002332|dbj|BAH57948.1|hypothetical
F3_GME-string_Contig_2408.0_gi|229002332|dbj|BAH57948.1|hypothetical

F3_GME-string_Contig_3163.0_gi|1146408|gb|AAA85089.1|gallerin
F3_GME-string_Contig_352.0_gi|114052242|ref|NP_001040131.
F3_GME-string_Contig_45.0_gi|229002332|dbj|BAH57948.1|hypothetical
F3_GME-string_Contig_5353.0_gi|2498144|sp|Q25490.1|APLP_MANSERecName:
F3_GME-string_Contig_5353.0_gi|2498144|sp|Q25490.1|APLP_MANSERecName:
F3_GME-string_Contig_5382.0_gi|125629089|emb|CAL23158.2|gustatory
F3_GME-string_Contig_5682.0_gi|77415676|emb|CAJ01507.1|hypothetical
F3_GME-string_Contig_5764.0_gi|195119912|ref|XP_002004473.1|GI19595;R2_contig18735_1.exp_gi|158293921|ref|XP_315269.4|AGAP011516-PA
F3_GME-string_Contig_5764.0_gi|195119912|ref|XP_002004473.1|GI19595;R2_contig18735_1.exp_gi|158293921|ref|XP_315269.4|AGAP011516-PA
F3_GME-string_Contig_6108.0_gi|189239301|ref|XP_971644.2|PREDICTED:
F3_GME-string_Contig_944.0_gi|112982743|ref|NP_001037556.1|elongation
R1_contig01633_1.exp_gi|195475698|ref|XP_002090121.1|GE20538
R1_contig01804_1.f1.exp_gi|112984054|ref|NP_001037422.1|yellow1
R1_contig02674_1.f1.exp_gi|114051966|ref|NP_001040198.1|mitochondrial
R1_contig02829_1.exp_gi|117970173|dbj|BAF36817.
R1_contig03614_1.f1.exp_gi|91084675|ref|XP_968140.1|PREDICTED:
R1_contig03752_1.exp_gi|189181680|ref|NP_001121191.1|carboxylesterase
R1_contig05149_1.exp_gi|112984026|ref|NP_001036831.1|BmP109 [Bombyx
R1_contig09082_1.exp_gi|114051598|ref|NP_001040416.1|leukotriene A4
R1_contig15056_1.f1.exp_gi|162462783|ref|NP_001104822.
R1_contig16410_1.exp_gi|189237651|ref|XP_001813448.1|PREDICTED:
R1_contig17461_1.exp_gi|158962511|dbj|BAF91716.1|chemosensory protein
R1_contig17461_1.exp_gi|158962511|dbj|BAF91716.1|chemosensory protein
R1_contig18077_1.exp_gi|220902980|gb|ACL83459.1|carboxylesterase
R1_contig19537_1.exp_gi|47607477|gb|AAT36640.1|imaginal disc growth
R1_contig19537_1.exp_gi|47607477|gb|AAT36640.1|imaginal disc growth
R1_contig20220_1.exp_gi|242004672|ref|XP_002423204.1|conserved
R1_contig20220_1.exp_gi|242004672|ref|XP_002423204.1|conserved
R1_contig20227_1.exp_gi|23208535|gb|AAN15786.1|peptidoglycan
R1_contig21466_1.exp_gi|134103857|gb|ABO60878.1|cationic peptide CP8
R1_contig21466_1.exp_gi|134103857|gb|ABO60878.1|cationic peptide CP8
R1_contig21950_1.exp_gi|56462300|gb|AAV91433.1|putative serine
R1_contig22070_1.exp_gi|112983062|ref|NP_001037056.
R1_contig22148_1.exp_gi|18140733|gb|AAL60414.1|AF393489_1twelve
R1_GME-string_Contig_2259.0_gi|91092064|ref|XP_970689.1|PREDICTED:
R1_GME-string_Contig_2606.0_gi|114052613|ref|NP_001040544.
R1_GME-string_Contig_2799.0_gi|112983414|ref|NP_001036985.1|heat
R1_GME-string_Contig_2799.0_gi|112983414|ref|NP_001036985.1|heat
R1_GME-string_Contig_3773.0_gi|242003442|ref|XP_002422733.
R1_GME-string_Contig_397.0_gi|70609810|gb|AAQ63970.2|transferrin
R1_GME-string_Contig_397.0_gi|70609810|gb|AAQ63970.2|transferrin
R1_GME-string_Contig_4434.0_gi|114050871|ref|NP_001040411.

R1_GME-string_Contig_482.0_gi|158962507|dbj|BAF91714.1|chemosensory
R1_GME-string_Contig_646.0_gi|56718390|gb|AAW24481.1|prophenol
R1_GME-string_Contig_6551.0_gi|91084741|ref|XP_971031.1|PREDICTED:
R2_contig00224_1.exp_gi|2498144|sp|Q25490.1|APLP_MANSERecName:
R2_contig00224_1.exp_gi|2498144|sp|Q25490.1|APLP_MANSERecName:
R2_contig00936_1.exp_gi|148298796|ref|NP_001091804.1|thioredoxin-like
R2_contig03613_1.f1.exp_gi|195391648|ref|XP_002054472.1|GJ22788
R2_contig04543_1.f1.exp_gi|91079020|ref|XP_974879.1|PREDICTED:
R2_contig07154_1.exp_gi|85726208|gb|ABC79625.1|imaginal disc growth
R2_contig07154_1.exp_gi|85726208|gb|ABC79625.1|imaginal disc growth
R2_contig07952_1.exp_gi|157927723|gb|ABW03225.1|beta actin [Mamestra
R2_contig07952_1.exp_gi|157927723|gb|ABW03225.1|beta actin [Mamestra
R2_contig14020_1.exp_gi|238667031|emb|CAZ37422.1|tubulin alpha chain,
R2_contig14853_1.exp_gi|182509208|ref|NP_001116815.1|carboxylesterase
R2_contig15056_1.f1.exp_gi|162462783|ref|NP_001104822.
R2_contig15056_1.f1.exp_gi|162462783|ref|NP_001104822.
R2_contig16833_1.f1.exp_gi|153791206|ref|NP_001093269.1|scolexin
R2_contig17849_1.exp_gi|194759166|ref|XP_001961820.1|GF15158
R2_contig18685_1.exp_gi|114052150|ref|NP_001040220.1|triacylglycerol
R2_contig19592_1.exp_gi|183979239|dbj|BAG30781.1|similar to
R2_contig19736_1_exp_NA
R2_contig19736_1_exp_NA
R2_contig20011_1.r1.exp_gi|118789328|ref|XP_001237914.1|AGAP008115-PA
R2_contig20268_1.exp_gi|116245495|ref|XP_001230506.1|AGAP012658-PA
R2_contig21524_1.exp_gi|91091270|ref|XP_969358.1|PREDICTED: similar
R2_GME-string_Contig_1207.0_gi|192763882|gb|ACF05615.1|actin 3
R2_GME-string_Contig_1307.0_gi|162462783|ref|NP_001104822.
R2_GME-string_Contig_1307.0_gi|162462783|ref|NP_001104822.
R2_GME-string_Contig_1861.0_gi|91091728|ref|XP_967315.1|PREDICTED:
R2_GME-string_Contig_2266.0_gi|157108606|ref|XP_001650307.1|AMP
R2_GME-string_Contig_3472.0_gi|189181680|ref|NP_001121191.
R2_GME-string_Contig_3472.0_gi|189181680|ref|NP_001121191.
R2_GME-string_Contig_3720.0_gi|112983052|ref|NP_001037068.
R2_GME-string_Contig_4671.0_gi|56418411|gb|AAV91013.1|hemolymph
R2_GME-string_Contig_4865.0_gi|114052484|ref|NP_001040250.
R2_GME-string_Contig_4865.0_gi|114052484|ref|NP_001040250.
R2_GME-string_Contig_6634.0_gi|39579195|gb|AAR28762.1|odorant-binding
R2_GME-string_Contig_6634.0_gi|39579195|gb|AAR28762.1|odorant-binding
R3_contig01012_1.exp_gi|229556834|ref|ZP_04444623.1|NADPH:quinone
R3_contig02658_1.f1.exp_gi|159078|gb|AAA74229.1|arylphorin [Galleria
R3_contig09410_1.exp_gi|183979372|dbj|BAG30738.1|troponin T [Papilio
R3_contig12733_1.exp_gi|2498144|sp|Q25490.1|APLP_MANSERecName:
R3_contig14894_1.exp_gi|239787860|ref|NP_001155183.1|multiple
R3_contig15438_1.exp_gi|151301198|ref|NP_001093087.1|mobility group

R3_contig15747_1.f1.exp_gi|189181680|ref|NP_001121191.
R3_contig16309_1.exp_gi|87248109|gb|ABD36107.1|enoyl-CoA hydratase
R3_contig16410_1.exp_gi|189237651|ref|XP_001813448.1|PREDICTED:
R3_contig16578_1.exp_gi|110649240|emb|CAL25129.1|gloverin [Manduca
R3_contig17104_1.exp_gi|169646838|ref|NP_001112375.1|heat shock
R3_contig18934_1.exp_gi|91080775|ref|XP_968281.1|PREDICTED: similar
R3_contig19564_1.exp_gi|91091664|ref|XP_971445.1|PREDICTED: similar
R3_contig20216_1.exp_gi|46396271|sp|P83632.1|P27K_GALMERecName:;F1_GME-string_Contig_4258.0_gi|156968297|gb|ABU98620.1|unknown
R3_GME-string_Contig_1320.0_gi|114052783|ref|NP_001040279.1|serine
R3_GME-string_Contig_135.0_gi|183979237|dbj|BAG30780.1|muscle protein
R3_GME-string_Contig_1961.0_gi|153791847|ref|NP_001093284.1|abnormal
R3_GME-string_Contig_1961.0_gi|153791847|ref|NP_001093284.1|abnormal
R3_GME-string_Contig_211.0_gi|114051191|ref|NP_001040386.
R3_GME-string_Contig_317.0_gi|91088191|ref|XP_972764.1|PREDICTED:
R3_GME-string_Contig_3809.0_gi|112983816|ref|NP_001037386.
R3_GME-string_Contig_3809.0_gi|112983816|ref|NP_001037386.
R3_GME-string_Contig_398.0_gi|157118472|ref|XP_001659123.
R3_GME-string_Contig_528.0_gi|114050827|ref|NP_001040323.
R3_GME-string_Contig_534.0_gi|149898901|gb|ABR27951.1|ubiquitin
R3_GME-string_Contig_5769.0_gi|148719710|gb|ABR08302.1|putative
R3_GME-string_Contig_6082.0_gi|114649525|emb|CAK22401.1|beta-1,
R3_GME-string_Contig_6634.0_gi|39579195|gb|AAR28762.1|odorant-binding
R3_GME-string_Contig_6634.0_gi|39579195|gb|AAR28762.1|odorant-binding
R3_GME-string_Contig_6732.0_gi|9087200|sp|O76192.1|SERO_GALMERecName:
R3_GME-string_Contig_6732.0_gi|9087200|sp|O76192.1|SERO_GALMERecName:

3.10 Progenesis QI for Proteomics output of mammalian *in-vitro* proteomics

3.10.1 Exposure of MCF-7 cells at 24 h to Cu-Phen (**1**) and Cu-DPQ-Phen (**2**) against the negative control

									Neg ctrl			Cu-Phen			Cu-DPQ-Phen		
Accession	Peptide count	Unique peptides	Confidence score	Anova (p)	Max fold change	Highest mean condition	Lowest mean condition	Description	1 2	1 3	average	2 1	2 3	average	3 2	3 3	average
P04733	2	2	2.555315614	0.000209	121.1664671	Cu-Phen	Neg ctrl	Metallothionein-1F OS=Homo sapiens GN=MT1F PE=1 SV=1 [MASS=6086]	6696.379	4458.347	5577.363	699361.9	652216.8	675789.4	521402.9	434066.1	477734.5
P80297	4	4	12.66441011	8.01E-06	75.31655295	Cu-DPQ-Phen	Neg ctrl	Metallothionein-1X OS=Homo sapiens GN=MT1X PE=1 SV=1 [MASS=6068]	57546.51	57375.45	57460.98	4487136	4084866	4286001	4555106	4100417	4327762
P02795	3	3	12.68113565	0.000166	25.653942 78	Cu-Phen	Neg ctrl	Metallothionein-2 OS=Homo sapiens GN=MT2A PE=1 SV=1 [MASS=6042]	311882.7	273794.1	292838.4	8125883	6899037	7512460	6992238	5766130	6379184
P22392	3	3	93.7048763	0.000107	11.7224999	Neg ctrl	Cu-Phen	Nucleoside diphosphate kinase B OS=Homo sapiens GN=NME2 PE=1 SV=1	762382.2	903590	832986.1	70056.47	72061.01	71058.74	592599.3	623783.6	608191.4
Q92597	2	2	59.94046591	0.000355	3.600229191	Cu-Phen	Neg ctrl	Protein NDRG1 OS=Homo sapiens GN=NDRG1 PE=1 SV=1	70120.04	63738.52	66929.28	253624.9	228296.6	240960.8	68404.07	65546.1	66975.09
P07237	2	2	108.5906362	0.000228	3.302235255	Cu-Phen	Cu-DPQ-Phen	Protein disulfide-isomerase OS=Homo sapiens GN=P4HB PE=1 SV=3 [MASS=57116]	603167.5	668092.9	635630.2	760979.8	739605	750292.4	223165.4	231249.5	227207.4
Q9H0H5	2	2	2.165493011	0.001772	3.281684305	Neg ctrl	Cu-Phen	Rac GTPase-activating protein 1 OS=Homo sapiens GN=RACGAP1 PE=1 SV=1 [MASS=71026]	101977.4	114613	108295.2	34795.52	31204.25	32999.89	44426.68	50896.93	47661.81
Q8NBS9	3	3	3.522167504	8.59E-05	3.169788333	Cu-Phen	Cu-DPQ-Phen	Thioredoxin domain-containing protein 5 OS=Homo sapiens GN=TXNDC5 PE=1 SV=2	120389.2	120800.9	120595	147744.9	137929.3	142837.1	45880.01	44244.07	45062.04
P04908	4	4	110.1025574	0.00011	3.127401308	Cu-DPQ-Phen	Cu-Phen	Histone H2A type 1-B/E OS=Homo sapiens GN=HIST1H2AB PE=1 SV=2 [MASS=14135]	311534 8	319099 8	315317 3	203090 2	190535 8	196813 0	627088 5	603937 7	615513 1
P08758	2	2	50.29293829	0.002173	3.108439447	Neg ctrl	Cu-Phen	Annexin A5 OS=Homo sapiens GN=ANXA5 PE=1 SV=2	297823	315518	306670.5	91070.11	106244.7	98657.39	148132.8	169021.3	158577
P00491	2	2	2.625335455	0.003508	2.602427962	Neg ctrl	Cu-Phen	Purine nucleoside phosphorylase OS=Homo sapiens GN=PNP PE=1 SV=2	491867.4	479431.8	485649.6	176970.5	196257.6	186614	260806.8	312045.7	286426.2
P62851	4	4	71.90551483	6.49E-05	2.511886924	Cu-DPQ-Phen	Cu-Phen	40S ribosomal protein S25 OS=Homo sapiens GN=RPS25 PE=1 SV=1	602902.9	617636.2	610269.5	516604.9	491722.8	504163.8	127040 7	126239 8	126640 3
P50914	2	2	2.969927669	0.0236	2.474609798	Cu-DPQ-Phen	Neg ctrl	60S ribosomal protein L14 OS=Homo sapiens GN=RPL14 PE=1 SV=4 [MASS=23432]	24946.	25608	25277.	47045.	51871.	49458.	74264	50839.	62551.

				28					66		33	96	6	78		07	53
P02768	3	3	5.715718865	6.01E-05	2.423990541	Cu-Phen	Cu-DPQ-Phen	Serum albumin OS=Homo sapiens GN=ALB PE=1 SV=2 [MASS=69366]	3835783	3885216	3860500	6064969	5812055	5938512	2424500	2475282	2449891
P05387	3	3	4.234240532	0.000372	2.386879561	Neg ctrl	Cu-DPQ-Phen	60S acidic ribosomal protein P2 OS=Homo sapiens GN=RPLP2 PE=1 SV=1	593538.6	591247.9	592393.3	441756.8	398784.1	420270.4	268757.3	227617.3	248187.3
P62917	4	4	9.268190861	0.012489	2.377837184	Cu-DPQ-Phen	Cu-Phen	60S ribosomal protein L8 OS=Homo sapiens GN=RPL8 PE=1 SV=2 [MASS=28024]	712409.6	647549.9	679979.8	592696.7	518162.8	555429.8	1487983	1153460	1320722
Q92879	2	2	2.765305042	0.000043	2.376253424	Neg ctrl	Cu-Phen	CUGBP Elav-like family member 1 OS=Homo sapiens GN=CELF1 PE=1 SV=2	201112.4	204576.9	202844.7	89653.83	81072.64	85363.24	192995.8	197722.7	195359.2
P09382	3	3	7.469929457	0.000959	2.348016311	Cu-Phen	Cu-DPQ-Phen	Galectin-1 OS=Homo sapiens GN=LGALS1 PE=1 SV=2 [MASS=14716]	593603.1	542897.2	568250.1	649416.4	589623.9	619520.1	263979	263717.7	263848.3
Q9BSV6	2	2	2.066867173	0.002227	2.323709585	Neg ctrl	Cu-Phen	tRNA-splicing endonuclease subunit Sen34 OS=Homo sapiens GN=TSEN34 PE=1 SV=1	76777.86	86373.51	81575.68	33118.48	37093.12	35105.8	68613.17	71102.46	69857.81
P58876	15	15	270.8635308	0.012	2.319849 34	Cu-DPQ-Phen	Cu-Phen	Histone H2B type 1-D OS=Homo sapiens GN=HIST1H2BD PE=1 SV=2 [MASS=13936]	91138921	98816228	94977575	50248089	45453305	47850697	1.09E+08	1.13E+08	1.11E+08
O95817	2	2	53.89916581	0.001627	2.274193152	Cu-Phen	Neg ctrl	BAG family molecular chaperone regulator 3 OS=Homo sapiens GN=BAG3 PE=1 SV=3 [MASS=61594]	164835	180218.7	172526.9	414438.9	370279.9	392359.4	194709.2	186492.6	190600.9
P68431	4	4	159.986363	0.000101	2.268229794	Cu-DPQ-Phen	Neg ctrl	Histone H3.1 OS=Homo sapiens GN=HIST1H3A PE=1 SV=2 [MASS=15404]	884085.4	907588.7	895837	968193.7	917314.3	942754	2023837	2040091	2031964
P15924	3	3	4.273333907	0.003172	2.241619693	Neg ctrl	Cu-DPQ-Phen	Desmoplakin OS=Homo sapiens GN=DSP PE=1 SV=3	191994	183311	187652.5	151569.1	138529	145049	89613.07	77812.73	83712.9
Q14694	2	2	64.73455347	0.013135	2.225654 65	Neg ctrl	Cu-DPQ-Phen	Ubiquitin carboxyl-terminal hydrolase 10 OS=Homo sapiens GN=USP10 PE=1 SV=2	263799.7	257241.1	260520.4	196736.8	222593.1	209665	102040.2	132066.5	117053.4
Q15050	2	2	3.116464615	7.88E-06	2.212552 52	Neg ctrl	Cu-Phen	Ribosome biogenesis regulatory protein homolog OS=Homo sapiens GN=RRS1 PE=1 SV=2	510145.4	509563	509854.2	228315	232559.2	230437.1	340114.7	344430.9	342272.8
Q16881	3	3	5.619893 67	0.003966	2.209611141	Cu-Phen	Neg ctrl	Thioredoxin reductase 1, cytoplasmic OS=Homo sapiens GN=TXNRD1 PE=1 SV=3	383669.4	430997	407333.2	845611.7	954484.3	900048	607943.9	648625.4	628284.6
P50402	2	2	1.474200875	0.011279	2.208602385	Neg ctrl	Cu-DPQ-Phen	Emerin OS=Homo sapiens GN=EMD PE=1 SV=1 [MASS=28994]	169712.8	172891.7	171302.2	121824.2	105827.1	113825.7	85966.4	69156.34	77561.37
P19012	1	1	1.884904861	0.008947	2.170638294	Cu-DPQ-Phen	Neg ctrl	Keratin, type I cytoskeletal 15 OS=Homo sapiens GN=KRT15 PE=1 SV=3	82471.17	91058.46	86764.82	118380.5	139616.6	128998.6	200577.8	176092.3	188335

P62750	3	3	46.53425916	0.000162	2.135121701	Cu-DPQ-Phen	Cu-Phen	60S ribosomal protein L23a OS=Homo sapiens GN=RPL23A PE=1 SV=1 [MASS=17695]	3023680	3011117	3017399	2469589	2329662	2399626	5087277	5159708	5123493
P22087	2	2	3.204127312	0.004545	2.131527519	Neg ctrl	Cu-DPQ-Phen	rRNA 2'-O-methyltransferase fibrillarin OS=Homo sapiens GN=FBL PE=1 SV=2 [MASS=33784]	72694.01	75841.01	74267.51	74297.54	62180.28	68238.91	33586.54	36098.24	34842.39
P18077	4	4	91.42913613	0.000692	2.131461921	Cu-DPQ-Phen	Cu-Phen	60S ribosomal protein L35a OS=Homo sapiens GN=RPL35A PE=1 SV=2 [MASS=12538]	676700.6	640254.8	658477.7	508754	470461.5	489607.8	104399 5	104316 6	104358 0
P55795	3	3	50.96020674	0.000232	2.100656271	Neg ctrl	Cu-DPQ-Phen	Heterogeneous nuclear ribonucleoprotein H2 OS=Homo sapiens GN=HNRNPH2 PE=1 SV=1 [MASS=49263]	816821.5	795130.5	805976	538892.3	508384.5	523638.4	385547.9	381808.5	383678.2
P00338	10	10	164.7280651	6.11E-05	2.051002799	Cu-Phen	Cu-DPQ-Phen	L-lactate dehydrogenase A chain OS=Homo sapiens GN=LDHA PE=1 SV=2	2628797	2692228	2660513	5268969	5093103	5181036	2505245	2546953	2526099
Q9BUF5	5	5	61.56546287	0.000168	2.046160257	Neg ctrl	Cu-Phen	Tubulin beta-6 chain OS=Homo sapiens GN=TUBB6 PE=1 SV=1 [MASS=49857]	3011532	3093493	3052512	1453462	1530187	1491825	2611739	2588806	2600273
P62753	4	4	119.663771	0.010185	2.015768092	Cu-DPQ-Phen	Cu-Phen	40S ribosomal protein S6 OS=Homo sapiens GN=RPS6 PE=1 SV=1 [MASS=28680]	2836237	2898755	2867496	1786684	1945666	1866175	3382142	4141409	3761776
O60814	1	1	3.628651381	0.002291	2.012450333	Cu-DPQ-Phen	Cu-Phen	Histone H2B type 1-K OS=Homo sapiens GN=HIST1H2BK PE=1 SV=3	619402.1	621354.6	620378.4	521821.2	600909.1	561365.2	111833 9	114110 0	112972 0
Q14847	2	2	4.001458883	0.000683	1.997938078	Cu-Phen	Cu-DPQ-Phen	LIM and SH3 domain protein 1 OS=Homo sapiens GN=LASP1 PE=1 SV=2	116185.2	110269.3	113227.2	158785.6	156428	157606.8	81543.87	76225.58	78884.72
Q32MZ4	1	1	1.636516571	0.003479	1.978125508	Cu-Phen	Cu-DPQ-Phen	Leucine-rich repeat flightless-interacting protein 1 OS=Homo sapiens GN=LRRFIP1 PE=1 SV=2	54332.38	53662.63	53997.51	57112.48	58685.32	57898.9	26921.65	31617.51	29269.58
P98179	4	4	212.0843164	0.011407	1.945576584	Neg ctrl	Cu-Phen	RNA-binding protein 3 OS=Homo sapiens GN=RBM3 PE=1 SV=1	5303037	5688673	5495855	2799196	2850394	2824795	4200186	5206681	4703434
P83916	1	1	0.993197978	0.013724	1.944348925	Cu-DPQ-Phen	Cu-Phen	Chromobox protein homolog 1 OS=Homo sapiens GN=CBX1 PE=1 SV=1 [MASS=21418]	288206.4	299627.5	293916.9	186373.1	205654.1	196013.6	341821.5	420416.2	381118.9
P09467	4	4	61.3734225	0.007766	1.938918875	Neg ctrl	Cu-DPQ-Phen	Fructose-1,6-bisphosphatase 1 OS=Homo sapiens GN=FBP1 PE=1 SV=5 [MASS=36842]	1004210	1063646	1033928	875187.4	918347.3	896767.4	483831.3	582668.3	533249.8
P09429	4	4	60.73044674	0.000123	1.93156846	Neg ctrl	Cu-DPQ-Phen	High mobility group protein B1 OS=Homo sapiens GN=HMGB1 PE=1 SV=3	3011513	3019987	3015750	2814356	2715920	2765138	1533572	1589020	1561296
Q9UHX1	4	4	76.0082928	0.003854	1.927635743	Neg ctrl	Cu-DPQ-Phen	Poly(U)-binding-splicing factor PUF60 OS=Homo sapiens GN=PUF60 PE=1 SV=1	1822046	1897021	1859534	981272.4	958230	969751.2	886091.9	1043250	964670.7
O43175	2	2	4.951719999	0.004855	1.925818793	Cu-DPQ-Phen	Cu-Phen	D-3-phosphoglycerate dehydrogenase OS=Homo sapiens GN=PHGDH PE=1 SV=4 [MASS=56650]	328309.9	372124.3	350217.1	278974.2	272146.6	275560.4	504718.7	556640	530679.3

Q9UHV9	2	2	55.1966523	0.013107	1.916280768	Neg ctrl	Cu-DPQ-Phen	Prefoldin subunit 2 OS=Homo sapiens GN=PFDN2 PE=1 SV=1	472710	517628.5	495169.3	456561.7	469773	463167.4	228963	287839.4	258401.2
P62081	6	6	59.37182954	0.00753	1.91515707	Cu-DPQ-Phen	Cu-Phen	40S ribosomal protein S7 OS=Homo sapiens GN=RPS7 PE=1 SV=1 [MASS=22127]	2849865	2861292	2855579	1871909	1601342	1736626	3138310	3513512	3325911
P52209	2	2	3.024845481	0.00202208	1.91234507	Cu-Phen	Cu-DPQ-Phen	6-phosphogluconate dehydrogenase, decarboxylating OS=Homo sapiens GN=PGD PE=1 SV=3 [MASS=53140]	335217.1	363275.6	349246.4	474004.6	513470.1	493737.3	252957.4	263411	258184.2
P05455	3	3	7.624866724	0.00005526	1.908777426	Neg ctrl	Cu-DPQ-Phen	Lupus La protein OS=Homo sapiens GN=SSB PE=1 SV=2 [MASS=46837]	633647.5	648157.8	640902.7	528644.5	563428.8	546036.6	341983.4	329548.7	335766.1
P62140	1	1	1.325521708	0.018051	1.903373701	Cu-Phen	Cu-DPQ-Phen	Serine/threonine-protein phosphatase PP1-beta catalytic subunit OS=Homo sapiens GN=PPP1CB PE=1 SV=3 [MASS=37187]	81212.64	82341.63	81777.14	97222.77	121333	109277.9	54361.99	60463.49	57412.74
Q02878	4	4	144.5667752	0.00138	1.891550875	Cu-DPQ-Phen	Cu-Phen	60S ribosomal protein L6 OS=Homo sapiens GN=RPL6 PE=1 SV=3	1225860	1277896	1251878	904215.5	834406.1	869310.8	160662.8	168206.3	164434.6
P62987	3	3	78.67881227	0.00031616	1.890722887	Cu-Phen	Neg ctrl	Ubiquitin-60S ribosomal protein L40 OS=Homo sapiens GN=UBA52 PE=1 SV=2	1501392	1526670	1514031	2783983	2941242	2862612	1838069	1884851	1861460
P26599	4	4	6.007434726	0.00009965	1.889361222	Neg ctrl	Cu-Phen	Polypyrimidine tract-binding protein 1 OS=Homo sapiens GN=PTBP1 PE=1 SV=1	1138419	1125331	1131875	619008.5	579147.6	599078	864514.5	815229.4	839871.9
Q15181	5	5	50.09401792	0.00300305	1.877949957	Neg ctrl	Cu-DPQ-Phen	Inorganic pyrophosphatase OS=Homo sapiens GN=PPA1 PE=1 SV=2	1027025	1091773	1059399	878844.2	886548	882696.1	563196	565054.3	564125.2
Q9BX40	2	2	53.75191876	0.00027785	1.875515014	Cu-DPQ-Phen	Cu-Phen	Protein LSM14 homolog B OS=Homo sapiens GN=LSM14B PE=1 SV=1	349942.4	327811.3	338876.9	310293	281736.2	296014.6	573033.9	537325.7	555179.8
O43765	2	2	2.908461928	0.00030909	1.874649581	Cu-Phen	Cu-DPQ-Phen	Small glutamine-rich tetratricopeptide repeat-containing protein alpha OS=Homo sapiens GN=SGTA PE=1 SV=1 [MASS=34063]	180989.6	190278.2	185633.9	218334	239412.5	228873.3	126981.5	117195.7	122088.6
Q99729	7	7	67.88360565	0.00076262	1.868306186	Neg ctrl	Cu-DPQ-Phen	Heterogeneous nuclear ribonucleoprotein A/B OS=Homo sapiens GN=HNRNPAB PE=1 SV=2 [MASS=36225]	1253087	1350043	1301565	1187901	1201657	1194779	680948.8	712364.6	696656.7
Q13501	4	4	68.14238884	2.80E-06	1.862554101	Cu-Phen	Neg ctrl	Sequestosome-1 OS=Homo sapiens GN=SQSTM1 PE=1 SV=1 [MASS=47687]	848687.9	850898.6	849793.2	159277.4	157279.8	158278.6	990734.8	991495.1	991114.9
P07108	2	2	5.618388951	0.00004415	1.861220763	Neg ctrl	Cu-DPQ-Phen	Acyl-CoA-binding protein OS=Homo sapiens GN=DBI PE=1 SV=2 [MASS=10044]	2093223	2239528	2166375	1909451	1881857	1895654	1163645	1164263	1163954
O00515	3	3	5.23459065	0.00301138	1.857159764	Cu-DPQ-Phen	Cu-Phen	Ladinin-1 OS=Homo sapiens GN=LAD1 PE=1 SV=2 [MASS=57131]	193984.1	204540.3	199262.2	108270.2	122567.2	115418.7	244215.6	184486.4	214351
Q92890	2	2	3.283143163	0.00010283	1.843580402	Neg ctrl	Cu-Phen	Ubiquitin fusion degradation protein 1 homolog OS=Homo sapiens GN=UFD1L PE=1 SV=3 [MASS=34500]	638473.2	666300.1	652386.6	340876.7	366862.1	353869.4	554268.5	672915.7	613592.1

P06748	11	11	526.3506037	0.001133	1.833304576	Cu-DPQ-Phen	Cu-Phen	Nucleophosmin OS=Homo sapiens GN=NPM1 PE=1 SV=2	44885569	44984404	44934987	27494883	30163223	28829053	53119120	52585750	52852435
O15231	2	2	2.337854505	0.007292	1.832440424	Neg ctrl	Cu-DPQ-Phen	Zinc finger protein 185 OS=Homo sapiens GN=ZNF185 PE=1 SV=3	217002.5	191548	204275.2	159881.9	143066	151474	112808	110146.3	111477.1
P25205	2	2	3.309811473	0.008222	1.832209424	Cu-DPQ-Phen	Neg ctrl	DNA replication licensing factor MCM3 OS=Homo sapiens GN=MCM3 PE=1 SV=3	96071.03	110859.2	103465.1	162273.3	151259.7	156766.5	181453.8	197685.8	189569.8
P62910	3	3	101.8140203	0.00598	1.830545284	Cu-DPQ-Phen	Cu-Phen	60S ribosomal protein L32 OS=Homo sapiens GN=RPL32 PE=1 SV=2	1062225	999869.8	1031047	936592.4	829840.6	883216.5	169175.8	154177.8	161676.8
P46779	4	4	10.82278156	0.006067	1.827645342	Cu-DPQ-Phen	Neg ctrl	60S ribosomal protein L28 OS=Homo sapiens GN=RPL28 PE=1 SV=3 [MASS=15747]	661498.1	681636.2	671567.1	756530.9	780070.8	768300.9	112970.3	132507.0	122738.7
P50395	6	6	74.25755175	0.0083	1.826179194	Cu-DPQ-Phen	Cu-Phen	Rab GDP dissociation inhibitor beta OS=Homo sapiens GN=GDI2 PE=1 SV=2	1544124	1600173	1572149	978259.3	1033193	1005726	1680907	1992365	1836636
P49023	2	2	3.122792125	0.000467	1.815348316	Cu-Phen	Cu-DPQ-Phen	Paxillin OS=Homo sapiens GN=PXN PE=1 SV=3 [MASS=64505]	159895.2	168188.4	164041.8	269453.6	262406.1	265929.9	143556.6	149422.9	146489.7
Q07955	2	2	3.783863664	0.003348	1.789775776	Neg ctrl	Cu-DPQ-Phen	Serine/arginine-rich splicing factor 1 OS=Homo sapiens GN=SRSF1 PE=1 SV=2	687084.5	748893.6	717989	667813	616897.2	642355.1	388883	413439.9	401161.4
P27797	2	2	41.07159074	0.00514	1.788705865	Cu-Phen	Cu-DPQ-Phen	Calreticulin OS=Homo sapiens GN=CALR PE=1 SV=1	288313.3	262829.6	275571.5	348476.3	323917.2	336196.7	196123.1	179787.5	187955.3
Q15785	2	2	62.13948697	0.006597	1.788325649	Cu-DPQ-Phen	Cu-Phen	Mitochondrial import receptor subunit TOM34 OS=Homo sapiens GN=TOMM34 PE=1 SV=2	297109.3	273360.9	285235.1	173166.5	183096.5	178131.5	297455.1	339659	318557.1
P48735	2	2	5.641456008	0.001984	1.782789158	Cu-Phen	Cu-DPQ-Phen	Isocitrate dehydrogenase [NADP], mitochondrial OS=Homo sapiens GN=IDH2 PE=1 SV=2 [MASS=50909]	146729.8	146052.2	146391	191548.8	183613.4	187581.1	110211.2	100224.3	105217.8
P55209	2	2	55.15697287	0.00852	1.775931524	Cu-Phen	Cu-DPQ-Phen	Nucleosome assembly protein 1-like 1 OS=Homo sapiens GN=NAP1L1 PE=1 SV=1 [MASS=45374]	493752.3	547331.9	520542.1	627674.1	688203.4	657938.8	351994.1	388956.6	370475.3
P30086	3	3	6.13757062	3.46E-05	1.771733113	Neg ctrl	Cu-Phen	Phosphatidylethanolamine-binding protein 1 OS=Homo sapiens GN=PEBP1 PE=1 SV=3 [MASS=21057]	1930366	1964741	1947554	109201.3	110646.0	109923.7	109548.1	111850.4	110699.3
P38646	8	8	282.465249	0.001375	1.771398142	Cu-Phen	Cu-DPQ-Phen	Stress-70 protein, mitochondrial OS=Homo sapiens GN=HSPA9 PE=1 SV=2 [MASS=73680]	1977814	2070432	2024123	265994.2	251548.3	258771.2	142065.5	150100.6	146083.0
Q13838	1	1	60.79	0.002406	1.769105989	Neg ctrl	Cu-DPQ-Phen	Spliceosome RNA helicase DDX39B OS=Homo sapiens GN=DDX39B PE=1 SV=1	285887.8	312772.5	299330.2	214348.2	216571.6	215459.9	163995.8	174401.3	169198.5
Q9Y230	3	3	46.27136041	0.006894	1.764435435	Cu-DPQ-Phen	Cu-Phen	RuvB-like 2 OS=Homo sapiens GN=RUVBL2 PE=1 SV=3 [MASS=51156]	607098.8	646807.8	626953.3	426197.9	439867.4	433032.7	710411.9	817704.5	764058.2

Q86YP4	2	2	55.99532264	7.35E-05	1.758238048	Cu-Phen	Cu-DPQ-Phen	Transcriptional repressor p66-alpha OS=Homo sapiens GN=GATAD2A PE=1 SV=1	126962.8	126851.9	126907.4	159899.5	156233.6	158066.6	91001.07	88800.02	89900.55
Q00610	3	3	55.27548661	0.000124	1.756275249	Cu-Phen	Cu-DPQ-Phen	Clathrin heavy chain 1 OS=Homo sapiens GN=CLTC PE=1 SV=5 [MASS=191613]	193273.4	192480.7	192877.1	300184.6	299510.7	299847.6	174274.5	167184.1	170729.3
Q01518	2	2	2.257493764	0.00565	1.746515494	Neg ctrl	Cu-DPQ-Phen	Adenylyl cyclase-associated protein 1 OS=Homo sapiens GN=CAP1 PE=1 SV=5 [MASS=51901]	216862.5	236012.4	226437.4	193805.7	180404.2	187105	135719.5	123582.4	129651
P26368	2	2	4.642561316	0.001447	1.745489738	Neg ctrl	Cu-DPQ-Phen	Splicing factor U2AF 65 kDa subunit OS=Homo sapiens GN=U2AF2 PE=1 SV=4	520809.6	513528	517168.8	482075.6	449646.2	465860.9	305715.2	286862.1	296288.7
P52292	5	5	209.2361139	0.002996	1.740640699	Neg ctrl	Cu-Phen	Importin subunit alpha-1 OS=Homo sapiens GN=KPNA2 PE=1 SV=1	197258.8	206170.3	201714.6	110767.4	121003.1	115885.2	124938.4	133973.8	129456.1
O60506	5	5	167.9670476	0.002006	1.739513934	Neg ctrl	Cu-DPQ-Phen	Heterogeneous nuclear ribonucleoprotein Q OS=Homo sapiens GN=SYNCRIP PE=1 SV=2 [MASS=69602]	193466.6	196804.5	195135.6	129800.8	140726.4	135263.6	108885.9	115470.5	112178.2
Q14103	4	4	6.4397012	0.000747	1.735845692	Cu-Phen	Cu-DPQ-Phen	Heterogeneous nuclear ribonucleoprotein D0 OS=Homo sapiens GN=HNRNPD PE=1 SV=1	672348.1	698160.4	685254.3	720012	673652.5	696832.2	396207.2	406666.2	401436.7
P06396	3	3	45.64031177	0.001013	1.733358468	Neg ctrl	Cu-Phen	Gelsolin OS=Homo sapiens GN=GSN PE=1 SV=1	144218.1	151824.2	148021.2	870639.6	837272.4	853956	105360.1	123647.4	114503.7
P10644	2	2	4.792080402	0.003457	1.729914956	Cu-Phen	Neg ctrl	cAMP-dependent protein kinase type I-alpha regulatory subunit OS=Homo sapiens GN=PRKAR1A PE=1 SV=1 [MASS=42981]	120255.4	112689.1	116472.2	196703.7	206270.4	201487.1	205943.8	185190	195566.9
P32969	2	2	2.980671525	0.006314	1.727641011	Cu-DPQ-Phen	Cu-Phen	60S ribosomal protein L9 OS=Homo sapiens GN=RPL9 PE=1 SV=1	855581.1	935522.5	895551.8	688503.5	697822.7	693163.1	112962.2	126545.2	119753.7
P45880	4	4	56.73005418	0.011583	1.727036489	Neg ctrl	Cu-DPQ-Phen	Voltage-dependent anion-selective channel protein 2 OS=Homo sapiens GN=VDAC2 PE=1 SV=2 [MASS=31566]	153483.7	151338.9	152411.3	157082.8	131367.9	144225.3	846205.3	918798.5	882501.9
P30040	3	3	57.8457856	0.003396	1.726624019	Neg ctrl	Cu-DPQ-Phen	Endoplasmic reticulum resident protein 29 OS=Homo sapiens GN=ERP29 PE=1 SV=4 [MASS=28993]	389427.4	399767.2	394597.3	328564.1	356409.3	342486.7	218588.5	238485.3	228536.9
Q14789	2	2	2.149471939	0.016998	1.724802237	Cu-Phen	Neg ctrl	Golgin subfamily B member 1 OS=Homo sapiens GN=GOLGB1 PE=1 SV=2 [MASS=376017]	152562	138429.9	145496	261664.5	240239.1	250951.8	190490.2	224204	207347.1
P08195	3	3	53.29711726	0.009416	1.713513838	Cu-DPQ-Phen	Cu-Phen	4F2 cell-surface antigen heavy chain OS=Homo sapiens GN=SLC3A2 PE=1 SV=3	806364.2	850054.8	828209.5	581718.7	600060.6	590889.6	934809	1090186	1012498
P62136	2	2	3.378300162	0.003429	1.711218216	Neg ctrl	Cu-DPQ-Phen	Serine/threonine-protein phosphatase PP1-alpha catalytic subunit OS=Homo sapiens GN=PPP1CA PE=1 SV=1 [MASS=37512]	145786.5	151662	148724.3	142389.6	127502.3	134945.9	85246.65	88576.01	86911.33
P04075	19	19	449.8006871	0.000194	1.708350046	Cu-Phen	Cu-DPQ-Phen	Fructose-bisphosphate aldolase A OS=Homo sapiens GN=ALDOA PE=1 SV=2 [MASS=39420]	15590912	15664808	15627860	22572105	22246551	22409328	12841629	13393419	13117524

P60981	3	3	76.58752676	0.000327	1.707357038	Cu-Phen	Cu-DPQ-Phen	Destrin OS=Homo sapiens GN=DSTN PE=1 SV=3 [MASS=18506]	555659.8	576050.1	565855	587246.5	562808	575027.3	333326.3	340261.3	336793.8
P21796	3	3	75.88414212	0.002414	1.703375811	Neg ctrl	Cu-DPQ-Phen	Voltage-dependent anion-selective channel protein 1 OS=Homo sapiens GN=VDAC1 PE=1 SV=2	2818530	3036938	2927734	2598709	2615906	2607307	1652808	1784759	1718783
P14854	5	5	14.22238809	0.003521	1.703037469	Neg ctrl	Cu-Phen	Cytochrome c oxidase subunit 6B1 OS=Homo sapiens GN=COX6B1 PE=1 SV=2	3808836	3760673	3784754	2265886	2178825	2222355	3067762	3431291	3249526
Q9NR45	4	4	5.960805416	0.000465	1.700014993	Neg ctrl	Cu-DPQ-Phen	Sialic acid synthase OS=Homo sapiens GN=NANS PE=1 SV=2 [MASS=40307]	594763.5	586087.9	590425.7	408650.4	387935.3	398292.9	342572.7	352039.6	347306.2
Q9UJY1	3	3	50.92363057	0.000669	1.699700351	Cu-DPQ-Phen	Neg ctrl	Heat shock protein beta-8 OS=Homo sapiens GN=HSPB8 PE=1 SV=1	313609.7	332158	322883.8	363703.1	372109.6	367906.3	556989.6	540621.8	548805.7
P28066	2	2	105.4358072	0.012263	1.697336262	Cu-DPQ-Phen	Cu-Phen	Proteasome subunit alpha type-5 OS=Homo sapiens GN=PSMA5 PE=1 SV=3 [MASS=26411]	3048756	3234894	3141825	2869727	3128923	2999325	4672212	5509514	5090863
Q0184	2	2	45.55177347	0.005072	1.695923971	Neg ctrl	Cu-DPQ-Phen	RNA-binding protein EWS OS=Homo sapiens GN=EWSR1 PE=1 SV=1 [MASS=68478]	959681.4	1047230	1003455	826692.6	750736.9	788714.8	589682.1	593691	591686.6
P51858	3	3	4.655085802	0.012399	1.691852444	Neg ctrl	Cu-DPQ-Phen	Hepatoma-derived growth factor OS=Homo sapiens GN=HDGF PE=1 SV=1 [MASS=26788]	935257.1	935890.5	935573.8	700190.6	752616.2	726403.4	508078.1	597897.5	552987.8
P17980	6	6	111.5673554	0.011929	1.688381568	Cu-Phen	Neg ctrl	26S protease regulatory subunit 6A OS=Homo sapiens GN=PSMC3 PE=1 SV=3	719839.8	738813.4	729326.6	1126324	1336439	1231382	1005584	1032306	1018945
Q15366	6	6	86.62331831	2.05E-05	1.687683295	Cu-Phen	Cu-DPQ-Phen	Poly(rC)-binding protein 2 OS=Homo sapiens GN=PCBP2 PE=1 SV=1	3444265	3490594	3467429	4024240	3984732	4004486	2357633	2387909	2372771
P23528	7	7	123.8621402	6.34E-05	1.683800454	Cu-Phen	Cu-DPQ-Phen	Cofilin-1 OS=Homo sapiens GN=CFL1 PE=1 SV=3	5747619	5563873	5655746	5777542	5814872	5796207	3445670	3439002	3442336
P46777	2	2	49.37921958	0.001548	1.682545488	Neg ctrl	Cu-DPQ-Phen	60S ribosomal protein L5 OS=Homo sapiens GN=RPL5 PE=1 SV=3 [MASS=34362]	1331385	1381127	1356256	1089197	1008233	1048715	8082185	8039295	8060740
P12004	3	3	6.891806245	0.002029	1.681713242	Cu-DPQ-Phen	Cu-Phen	Proliferating cell nuclear antigen OS=Homo sapiens GN=PCNA PE=1 SV=1 [MASS=28769]	1414190	1454172	1434181	986553.6	982655.8	984604.7	1578427	1733219	1655823
Q6KB66	2	2	2.412766218	0.039421	1.672982836	Cu-DPQ-Phen	Cu-Phen	Keratin, type II cytoskeletal 80 OS=Homo sapiens GN=KRT80 PE=1 SV=2	1051344.4	1115582.2	1083463.3	88494.67	80691.27	84592.97	1248876.6	1581575.5	1415226.6
P25685	3	3	5.031237721	0.001511	1.672422515	Cu-Phen	Cu-DPQ-Phen	DnaJ homolog subfamily B member 1 OS=Homo sapiens GN=DNAJB1 PE=1 SV=4	3070891.1	3062913.3	3066902.2	3736826.6	3725257.7	3731042.2	2325492.2	2136349.9	2230920
Q14683	2	2	2.22154057	0.003388	1.663367177	Neg ctrl	Cu-Phen	Structural maintenance of chromosomes protein 1A OS=Homo sapiens GN=SMC1A PE=1 SV=2	531722.8	510431	521076.9	329885.2	296647.4	313266.3	356779.2	354103.2	355441.2

P45973	3	3	46.59716193	0.001779	1.662394728	Cu-Phen	Cu-DPQ-Phen	Chromobox protein homolog 5 OS=Homo sapiens GN=CBX5 PE=1 SV=1	144501.2	156017.5	150259.3	187458.1	191316.5	189387.3	116099.3	111749.4	113924.4
P23396	3	3	126.4354308	0.002629	1.656502926	Cu-Phen	Cu-DPQ-Phen	40S ribosomal protein S3 OS=Homo sapiens GN=RPS3 PE=1 SV=2	776971.2	749486.4	763228.8	768483.1	786015	777249	444637.6	493784	469210.8
P39687	2	2	5.582118 75	0.00305	1.656411041	Cu-Phen	Cu-DPQ-Phen	Acidic leucine-rich nuclear phosphoprotein 32 family member A OS=Homo sapiens GN=ANP32A PE=1 SV=1 [MASS=28585]	327889.7	362036.3	344963	356770.9	343906.1	350338.5	217271.4	205737.7	211504.6
P62906	2	2	3.680121899	0.01662	1.653655059	Neg ctrl	Cu-DPQ-Phen	60S ribosomal protein L10a OS=Homo sapiens GN=RPL10A PE=1 SV=2 [MASS=24831]	344700.2	353964.4	349332.3	236995.8	271882.1	254439	197579	224918.3	211248.6
Q09666	6	6	237.888389	0.018799	1.649023248	Neg ctrl	Cu-DPQ-Phen	Neuroblast differentiation-associated protein AHNAK OS=Homo sapiens GN=AHNAK PE=1 SV=2	902161.9	101688 2	959522	789090.1	717780.7	753435.4	546530.1	617215.7	581872.9
P31153	2	2	3.682513118	0.00816 1	1.64883776	Cu-Phen	Cu-DPQ-Phen	S-adenosylmethionine synthase isoform type-2 OS=Homo sapiens GN=MAT2A PE=1 SV=1 [MASS=43660]	156946.1	135862.4	146404.3	167053.6	173148.5	170101.1	102666.1	103662.3	103164.2
P78406	3	3	3.874538898	0.03983 7	1.64532319	Neg ctrl	Cu-DPQ-Phen	mRNA export factor OS=Homo sapiens GN=RAE1 PE=1 SV=1	370083	306850.7	338466.9	283033	336182.9	309608	215349	196080	205714.5
P14174	6	6	192.7639766	0.003443	1.64479769	Cu-DPQ-Phen	Cu-Phen	Macrophage migration inhibitory factor OS=Homo sapiens GN=MIF PE=1 SV=4	20472231	21393025	20932628	16317794	15814093	16065944	25200100	27650353	26425227
Q9BWF3	4	4	144.9100616	0.004571	1.643942578	Neg ctrl	Cu-DPQ-Phen	RNA-binding protein 4 OS=Homo sapiens GN=RBM4 PE=1 SV=1	1208727	1290154	1249441	888709	868654.6	878681.8	721939	798115	760027
P18669	7	7	153.3572601	0.00044	1.643360932	Cu-Phen	Cu-DPQ-Phen	Phosphoglycerate mutase 1 OS=Homo sapiens GN=PGAM1 PE=1 SV=2 [MASS=28804]	2640774	2765466	2703120	2963974	3044494	3004234	1810827	1845380	1828104
Q15056	2	2	4.481635213	0.003064	1.643038 74	Cu-DPQ-Phen	Cu-Phen	Eukaryotic translation initiation factor 4H OS=Homo sapiens GN=EIF4H PE=1 SV=5 [MASS=27385]	1994146	2039848	2016997	1321622	1180337	1250980	2033839	2076976	2055408
Q9Y446	3	3	116.5504042	0.046494	1.641306362	Cu-DPQ-Phen	Cu-Phen	Plakophilin-3 OS=Homo sapiens GN=PKP3 PE=1 SV=1 [MASS=87082]	1225057	1257683	1241370	976188.4	928069.6	952129	1360869	1764602	1562735
Q01813	2	2	42.68882101	0.004083	1.638961732	Cu-Phen	Neg ctrl	ATP-dependent 6-phosphofructokinase, platelet type OS=Homo sapiens GN=PFKP PE=1 SV=2 [MASS=85596]	117671.5	124486	121078.8	198428.4	198458.6	198443.5	167637.9	151907	159772.5
P53582	2	2	5.023619533	0.012917	1.637323035	Neg ctrl	Cu-Phen	Methionine aminopeptidase 1 OS=Homo sapiens GN=METAP1 PE=1 SV=2	634596.1	673179.4	653887.7	433888.9	364838.9	399363.9	656002.5	620999	638500.8
Q92688	2	2	46.767 2238	0.025626	1.629843801	Neg ctrl	Cu-Phen	Acidic leucine-rich nuclear phosphoprotein 32 family member B OS=Homo sapiens GN=ANP32B PE=1 SV=1	387523.4	426899.2	407211.3	245806	253887.6	249846.8	259875.1	315595.8	287735.5
P49207	3	3	6.210760713	0.0049	1.628035198	Cu-DPQ-Phen	Cu-Phen	60S ribosomal protein L34 OS=Homo sapiens GN=RPL34 PE=1 SV=3	338666	342902	340784	264497	262751	263624	403933	454446	429190

				28						.2	.1	.9	.1	.5	.5	.5	
P45974	2	2	3.541555159	0.009077	1.622815676	Cu-Phen	Cu-DPQ-Phen	Ubiquitin carboxyl-terminal hydrolase 5 OS=Homo sapiens GN=USP5 PE=1 SV=2 [MASS=95786]	168470.2	175302.8	171886.5	225529.1	257321.4	241425.2	153062.6	144476.1	148769.3
P06576	7	7	355.9068607	0.000693	1.620474468	Cu-Phen	Cu-DPQ-Phen	ATP synthase subunit beta, mitochondrial OS=Homo sapiens GN=ATP5B PE=1 SV=3	3290276	3344356	3317316	3526608	3482059	3504333	2094227	2230843	2162535
Q15046	2	2	4.455866694	0.017491	1.620319176	Neg ctrl	Cu-DPQ-Phen	Lysine--tRNA ligase OS=Homo sapiens GN=KARS PE=1 SV=3 [MASS=68048]	254332.4	253657.2	253994.8	245186	227447	236316.5	142299	171213	156756
P35232	6	6	329.7814474	0.001523	1.618625681	Cu-DPQ-Phen	Cu-Phen	Prohibitin OS=Homo sapiens GN=PHB PE=1 SV=1 [MASS=29804]	3512491	3523991	3518241	2765773	2827500	2796636	4355739	4697676	4526708
Q13243	4	4	65.31810094	0.011149	1.618424978	Neg ctrl	Cu-Phen	Serine/arginine-rich splicing factor 5 OS=Homo sapiens GN=SRSF5 PE=1 SV=1	588249.7	661466.5	624858.1	395533.6	376646.9	386090.3	523715.6	578515.9	551115.8
P54578	4	4	119.6135534	0.001442	1.616906502	Cu-DPQ-Phen	Neg ctrl	Ubiquitin carboxyl-terminal hydrolase 14 OS=Homo sapiens GN=USP14 PE=1 SV=3	600010.9	593874.2	596942.6	643561.9	692255.9	667908.9	981291	949109.6	965200.3
Q9UKY7	2	2	3.616181612	0.006124	1.616565494	Neg ctrl	Cu-DPQ-Phen	Protein CDV3 homolog OS=Homo sapiens GN=CDV3 PE=1 SV=1 [MASS=27335]	1670823	1700101	1685462	1617862	1420060	1518961	1033148	1052090	1042619
P62241	4	4	78.71486284	0.00456	1.615313477	Cu-DPQ-Phen	Cu-Phen	40S ribosomal protein S8 OS=Homo sapiens GN=RPS8 PE=1 SV=2 [MASS=24205]	1333791	1325489	1329640	956982.7	1038506	997744.5	1546946	1676395	1611670
P13693	3	3	45.6539606	0.018888	1.61502051	Cu-Phen	Cu-DPQ-Phen	Translationally-controlled tumor protein OS=Homo sapiens GN=TPT1 PE=1 SV=1	306868.4	257129.7	281999.1	350865.3	344046	347455.7	221623.8	208656.4	215140.1
P61160	2	2	4.551150441	0.001089	1.614880913	Cu-DPQ-Phen	Neg ctrl	Actin-related protein 2 OS=Homo sapiens GN=ACTR2 PE=1 SV=1 [MASS=44760]	184110.5	185336.9	184723.7	200301.9	211579.1	205940.5	305545.5	291067.9	298306.7
P07437	11	11	508.8837404	0.017249	1.612682996	Neg ctrl	Cu-Phen	Tubulin beta chain OS=Homo sapiens GN=TUBB PE=1 SV=2 [MASS=49671]	36450505	35654160	36052333	22980656	21730341	22355499	27131215	32207529	29669372
P17987	2	2	50.68206149	0.01463	1.611388409	Cu-DPQ-Phen	Neg ctrl	T-complex protein 1 subunit alpha OS=Homo sapiens GN=TCP1 PE=1 SV=1	1067917	1107914	1087916	1285753	1481830	1383792	1677825	1828284	1753055
Q9UK76	4	4	90.42429374	0.000827	1.608883025	Neg ctrl	Cu-Phen	Hematological and neurological expressed 1 protein OS=Homo sapiens GN=HN1 PE=1 SV=3 [MASS=16014]	4479527	4647877	4563702	2904483	2768648	2836566	3869995	3960723	3915359
P08238	16	16	559.2415663	0.007644	1.608023351	Cu-DPQ-Phen	Neg ctrl	Heat shock protein HSP 90-beta OS=Homo sapiens GN=HSP90AB1 PE=1 SV=4	21803912	22577400	22190656	22522187	22258690	22390438	33028785	38337401	35683093
P25787	3	3	91.38072838	0.027346	1.607288593	Cu-DPQ-Phen	Cu-Phen	Proteasome subunit alpha type-2 OS=Homo sapiens GN=PSMA2 PE=1 SV=2	1776813	1892130	1834472	1360997	1428245	1394621	2023088	2460030	2241559

Q13283	2	2	3.170634985	0.007223	1.597046299	Cu-Phen	Neg ctrl	Ras GTPase-activating protein-binding protein 1 OS=Homo sapiens GN=G3BP1 PE=1 SV=1	139442.7	125285.9	132364.3	205642.3	217141.5	211391.9	144208	133207.1	138707.5
P30153	3	3	8.040452361	0.002406	1.588280649	Cu-DPQ-Phen	Cu-Phen	Serine/threonine-protein phosphatase 2A 65 kDa regulatory subunit A alpha isoform OS=Homo sapiens GN=PPP2R1A PE=1 SV=4	768561.4	803088.7	785825	707537.1	658768.4	683152.8	1066109	1103967	1085038
P37837	2	2	48.07770297	0.002913	1.584751197	Cu-DPQ-Phen	Neg ctrl	Transaldolase OS=Homo sapiens GN=TALDO1 PE=1 SV=2 [MASS=37540]	105415.8	112499.3	108957.5	148329.2	178914.1	163621.6	182582.9	162758.2	172670.6
Q9NR46	3	3	5.924301863	0.001844	1.584356261	Cu-Phen	Cu-DPQ-Phen	Endophilin-B2 OS=Homo sapiens GN=SH3GLB2 PE=1 SV=1 [MASS=43974]	181911.8	172079	176995.4	205217.3	210505.6	207861.5	134748.6	127643.7	131196.2
P10768	4	4	6.047174901	0.005357	1.582801353	Neg ctrl	Cu-DPQ-Phen	S-formylglutathione hydrolase OS=Homo sapiens GN=ESD PE=1 SV=2 [MASS=31463]	585773.8	655179.3	620476.6	431844.5	411839.8	421842.1	387685.6	396337.7	392011.6
P10809	8	8	143.6137379	0.001038	1.580893823	Cu-Phen	Neg ctrl	60 kDa heat shock protein, mitochondrial OS=Homo sapiens GN=HSPD1 PE=1 SV=2	1574300	1656700	1615500	2508444	2599425	2553934	1710269	1768991	1739630
Q14980	4	4	63.88655664	0.003165	1.580159678	Cu-DPQ-Phen	Cu-Phen	Nuclear mitotic apparatus protein 1 OS=Homo sapiens GN=NUMA1 PE=1 SV=2 [MASS=238258]	521775.1	569929	545852	420849.5	402679.7	411764.6	588427.7	712879.9	650653.8
P07900	16	14	451.6550597	0.002684	1.577867935	Cu-DPQ-Phen	Neg ctrl	Heat shock protein HSP 90-alpha OS=Homo sapiens GN=HSP90AA1 PE=1 SV=5	21869984	22819005	22344494	27905682	28428292	28166987	33888974	36624348	35256661
Q9H910	5	5	54.37261577	0.000532	1.574328105	Cu-DPQ-Phen	Cu-Phen	Hematological and neurological expressed 1-like protein OS=Homo sapiens GN=HN1L PE=1 SV=1 [MASS=20063]	1743795	1768332	1756064	1538119	1586163	1562141	2407262	2511384	2459323
P46778	4	4	48.07353099	0.000648	1.571774864	Cu-DPQ-Phen	Cu-Phen	60S ribosomal protein L21 OS=Homo sapiens GN=RPL21 PE=1 SV=2 [MASS=18565]	2644104	2650630	2647367	1915319	1997938	1956629	3017556	3133204	3075380
Q13151	2	2	69.90514934	0.004872	1.566495641	Cu-Phen	Cu-DPQ-Phen	Heterogeneous nuclear ribonucleoprotein A0 OS=Homo sapiens GN=HNRNPA0 PE=1 SV=1 [MASS=30840]	203900.5	208942.7	206421.6	283571	297235.6	290403.3	176016.9	194751.3	185384.1
P30101	6	6	200.9636838	0.001927	1.565835746	Cu-Phen	Cu-DPQ-Phen	Protein disulfide-isomerase A3 OS=Homo sapiens GN=PDIA3 PE=1 SV=4	2354845	2390623	2372734	2911077	3074996	2993036	1964658	1858267	1911462
P04406	20	20	711.7931999	0.00167	1.564565603	Cu-Phen	Cu-DPQ-Phen	Glyceraldehyde-3-phosphate dehydrogenase OS=Homo sapiens GN=GAPDH PE=1 SV=3	58046934	59099466	58573200	62247359	59996196	61121777	37643595	40488990	39066292
O00299	11	11	64.05288076	0.001881	1.56452109	Neg ctrl	Cu-DPQ-Phen	Chloride intracellular channel protein 1 OS=Homo sapiens GN=CLIC1 PE=1 SV=4 [MASS=26923]	3217208	3431590	3324399	2888041	2970353	2929197	2167783	2081950	2124867
P09525	2	2	56.25140424	0.003194	1.559836767	Cu-DPQ-Phen	Neg ctrl	Annexin A4 OS=Homo sapiens GN=ANXA4 PE=1 SV=4	240112.9	208203.7	224158.3	318294.1	291853.6	305073.8	373533.1	325767.7	349650.4
P63244	5	5	53.52324968	3.05E-05	1.559635038	Cu-Phen	Cu-DPQ-Phen	Guanine nucleotide-binding protein subunit beta-2-like 1 OS=Homo sapiens GN=GNB2L1 PE=1 SV=3 [MASS=35076]	1482303	1506068	1494186	1972666	1949651	1961159	1258374	1256520	1257447

P83731	4	4	151.370769	0.000582	1.558393955	Cu-DPQ-Phen	Cu-Phen	60S ribosomal protein L24 OS=Homo sapiens GN=RPL24 PE=1 SV=1 [MASS=17779]	665134.2	698907.2	682020.7	464764.1	458124.4	461444.3	710045.2	728178.7	719112
P39748	2	2	3.680451870	0.002061	1.55812746	Neg ctrl	Cu-Phen	Flap endonuclease 1 OS=Homo sapiens GN=FEN1 PE=1 SV=1 [MASS=42593]	284258.2	303139.2	293698.7	193384.7	183604.6	188494.7	211125.4	213297.9	212211.6
Q8N257	3	3	5.151692152	0.005632	1.55812309	Neg ctrl	Cu-Phen	Histone H2B type 3-B OS=Homo sapiens GN=HIST3H2BB PE=1 SV=3	410994.4	391569.3	401281.8	263251.2	251832.4	257541.8	277880.5	248999.8	263440.2
P50995	4	4	92.82739638	0.001063	1.556398659	Neg ctrl	Cu-Phen	Annexin A11 OS=Homo sapiens GN=ANXA11 PE=1 SV=1	404707.3	382497.2	393602.3	250128.8	255657.1	252893	330098.4	322915.5	326506.9
P41227	2	2	2.837938190	0.000579	1.555100402	Cu-Phen	Cu-DPQ-Phen	N-alpha-acetyltransferase 10 OS=Homo sapiens GN=NAA10 PE=1 SV=1	91776.05	92632.72	92204.39	97150.11	97077.23	97113.67	60687.99	64208.99	62448.49
O95994	4	4	71.32430869	0.003383	1.552446685	Neg ctrl	Cu-DPQ-Phen	Anterior gradient protein 2 homolog OS=Homo sapiens GN=AGR2 PE=1 SV=1 [MASS=19979]	1685526	1780606	1733066	1099651	1147519	1123585	1069996	1162694	1116345
P49327	3	3	51.90390673	0.003248	1.551094288	Cu-DPQ-Phen	Cu-Phen	Fatty acid synthase OS=Homo sapiens GN=FASN PE=1 SV=3 [MASS=273425]	424921.5	417505	421213.2	418274	399955.3	409114.6	605434.5	663716.3	634575.4
P17174	2	2	3.389299512	0.001716	1.545797535	Cu-DPQ-Phen	Cu-Phen	Aspartate aminotransferase, cytoplasmic OS=Homo sapiens GN=GOT1 PE=1 SV=3 [MASS=46247]	296831.8	305445	301138.4	280970.3	261563.5	271266.9	417363.8	421283.6	419323.7
P46781	2	2	4.897615433	0.001001 2	1.545089745	Cu-Phen	Cu-DPQ-Phen	40S ribosomal protein S9 OS=Homo sapiens GN=RPS9 PE=1 SV=3 [MASS=22591]	110946.6	111333.6	111140.1	127304.3	116371.2	121837.7	83259.71	74449.86	78854.78
Q9NYF8	2	2	51.3534041	0.005011	1.544791036	Cu-Phen	Neg ctrl	Bcl-2-associated transcription factor 1 OS=Homo sapiens GN=BCLAF1 PE=1 SV=2 [MASS=106121]	121214.8	116190.9	118702.9	175415.4	191326.9	183371.1	137802.7	130761.7	134282.2
P23526	3	3	68.09453972	0.011359	1.542919441	Cu-DPQ-Phen	Neg ctrl	Adenosylhomocysteinase OS=Homo sapiens GN=AHCY PE=1 SV=4 [MASS=47716]	1219326	1246861	1233093	1208761	1350982	1279871	1800044	2005084	1902564
P62805	4	4	173.7480936	0.001259	1.54290579	Cu-DPQ-Phen	Cu-Phen	Histone H4 OS=Homo sapiens GN=HIST1H4A PE=1 SV=2 [MASS=11367]	899546.6	100298 8	951267.4	839196.8	883825.1	861510.9	1266050	1392411	1329230
P63220	10	10	220.9136952	0.005032	1.542634213	Cu-DPQ-Phen	Cu-Phen	40S ribosomal protein S21 OS=Homo sapiens GN=RPS21 PE=1 SV=1 [MASS=9111]	12081831	12222379	12152105	882229 6	8503382	8662839	12662552	14064631	13363592
P25398	3	3	59.47168091	0.005148	1.541062634	Cu-Phen	Cu-DPQ-Phen	40S ribosomal protein S12 OS=Homo sapiens GN=RPS12 PE=1 SV=3	701345.8	683805.4	692575.6	783875.7	752861.9	768368.8	473280.5	523913	498596.7
Q01130	2	2	44.28210039	0.009691	1.533962 54	Cu-Phen	Cu-DPQ-Phen	Serine/arginine-rich splicing factor 2 OS=Homo sapiens GN=SRSF2 PE=1 SV=4 [MASS=25476]	520825.5	537115.8	528970.7	612442.5	613390.3	612916.4	373370.8	425757.5	399564.1
P52943	2	2	3.219120264	0.000200 47	1.531074029	Cu-Phen	Cu-DPQ-Phen	Cysteine-rich protein 2 OS=Homo sapiens GN=CRIP2 PE=1 SV=1	678138.7	799420	738779.4	771399.1	800392.1	785895.6	531818.2	494775.7	513296.9

P62195	5	5	132.9412926	0.001523	1.526835395	Cu-DPQ-Phen	Cu-Phen	26S protease regulatory subunit 8 OS=Homo sapiens GN=PSMC5 PE=1 SV=1 [MASS=45626]	490657.6	504396.1	497526.8	463032.4	479482	471257.2	697657.1	741407.3	719532.2
P61224	3	3	49.4068516	0.001757	1.524275944	Cu-Phen	Cu-DPQ-Phen	Ras-related protein Rap-1b OS=Homo sapiens GN=RAP1B PE=1 SV=1 [MASS=20825]	213247.7	199175.4	206211.5	224434.7	216961.6	220698.1	145911	143666.7	144788.8
P62879	2	2	2.673986673	0.000921	1.523569027	Neg ctrl	Cu-DPQ-Phen	Guanine nucleotide-binding protein G(I)/G(S)/G(T) subunit beta-2 OS=Homo sapiens GN=GNB2 PE=1 SV=3 [MASS=37331]	218151.4	228184.9	223168.2	159313.9	158529	158921.5	143400.4	149554	146477.2
P62937	16	16	447.5828699	0.000521	1.523001005	Neg ctrl	Cu-DPQ-Phen	Peptidyl-prolyl cis-trans isomerase A OS=Homo sapiens GN=PPIA PE=1 SV=2 [MASS=18012]	35746653	37034906	36390779	28691402	27768709	28230056	23944290	23843964	23894127
P26373	5	5	108.4427043	0.00054	1.521558015	Cu-DPQ-Phen	Cu-Phen	60S ribosomal protein L13 OS=Homo sapiens GN=RPL13 PE=1 SV=4 [MASS=24261]	991093.7	1036416	1013755	928053.3	943671.9	935862.6	1437753	1410185	1423969
Q9Y266	2	2	3.133537412	0.003316	1.52126868	Cu-Phen	Cu-DPQ-Phen	Nuclear migration protein nudC OS=Homo sapiens GN=NUDC PE=1 SV=1 [MASS=38243]	154484.1	154772.9	154628.5	239284	216929.7	228106.9	151173.4	148716.9	149945.2
O95336	2	2	3.318991661	0.006652	1.515981277	Cu-DPQ-Phen	Cu-Phen	6-phosphogluconolactonase OS=Homo sapiens GN=PGLS PE=1 SV=2	269573.9	295284.7	282429.3	228954.9	214682.5	221818.7	332966.6	339579.5	336273
P62979	2	2	6.748395801	0.000455	1.515705222	Neg ctrl	Cu-DPQ-Phen	Ubiquitin-40S ribosomal protein S27a OS=Homo sapiens GN=RPS27A PE=1 SV=2	1301951	1260553	1281252	1265474	1246794	1256134	860872.2	829762.8	845317.5
P11021	14	14	581.5513644	0.000495	1.512399303	Cu-Phen	Cu-DPQ-Phen	78 kDa glucose-regulated protein OS=Homo sapiens GN=HSPA5 PE=1 SV=2	8610270	8838310	8724290	9070454	8935812	9003133	5827836	6077926	5952881
P62266	2	2	4.268333197	0.001667	1.51199537	Neg ctrl	Cu-DPQ-Phen	40S ribosomal protein S23 OS=Homo sapiens GN=RPS23 PE=1 SV=3	245812.9	251776.2	248794.5	248998.4	238341.5	243669.9	159537.7	169556.6	164547.2
P50454	4	4	241.3570866	0.003086	1.511993489	Neg ctrl	Cu-DPQ-Phen	Serpin H1 OS=Homo sapiens GN=SERPINH1 PE=1 SV=2	1847601	1920292	1883946	1553879	1669368	1611623	1227135	1264869	1246002
P62249	3	3	154.4446077	0.007016	1.510730706	Cu-DPQ-Phen	Cu-Phen	40S ribosomal protein S16 OS=Homo sapiens GN=RPS16 PE=1 SV=2	1431177	1389047	1410112	1198493	1081724	1140108	1687674	1757119	1722397
P60660	6	6	109.0200595	0.000912	1.509574856	Neg ctrl	Cu-DPQ-Phen	Myosin light polypeptide 6 OS=Homo sapiens GN=MYL6 PE=1 SV=2 [MASS=16930]	223492.9	235398.3	229445.6	209140.7	213093.7	211117.2	153781.8	150205.2	151993.5
P38919	2	2	47.04104536	0.017894	1.506219981	Cu-DPQ-Phen	Cu-Phen	Eukaryotic initiation factor 4A-III OS=Homo sapiens GN=EIF4A3 PE=1 SV=4 [MASS=46871]	516688.7	572893.1	544790.9	495525.4	527068.4	511296.9	724708.9	815542.2	770125.5
P61604	8	8	144.2026424	0.003332	1.504505998	Cu-Phen	Cu-DPQ-Phen	10 kDa heat shock protein, mitochondrial OS=Homo sapiens GN=HSPE1 PE=1 SV=2	2137008	2321405	2229207	2625979	2555863	2590921	1734280	1709935	1722108
P49411	4	4	8.791793942	0.000731	1.502121543	Cu-Phen	Cu-DPQ-Phen	Elongation factor Tu, mitochondrial OS=Homo sapiens GN=TUFM PE=1 SV=2	389486.3	396078.6	392782.5	503056.7	479127.9	491092.3	325706.7	328158.2	326932.4

Q9BR76	5	5	134.7579319	0.001497	1.496020276	Cu-DPQ-Phen	Cu-Phen	Coronin-1B OS=Homo sapiens GN=CORO1B PE=1 SV=1	1205753	1205242	1205498	923991.1	890350.9	907171	1318961	1395331	1357146
P30041	5	5	215.5329451	0.00435	1.494106898	Cu-DPQ-Phen	Cu-Phen	Peroxiredoxin-6 OS=Homo sapiens GN=PRDX6 PE=1 SV=3	3711339	3859843	3785591	3770299	3541978	3656138	4861312	6064011	5462661
Q9HB71	6	6	51.37886147	0.00269	1.494050746	Cu-Phen	Cu-DPQ-Phen	Calcyclin-binding protein OS=Homo sapiens GN=CACYBP PE=1 SV=2 [MASS=26210]	995908.4	986649.5	991278.9	1144268	1125135	1134702	789459.5	729500.4	759479.9
O14745	5	5	9.988047123	0.009721	1.493663519	Neg ctrl	Cu-DPQ-Phen	Na(+)/H(+) exchange regulatory cofactor NHE-RF1 OS=Homo sapiens GN=SLC9A3R1 PE=1 SV=4 [MASS=38868]	988992.2	957818.2	973405.2	892130.3	829833.7	860982	619201.9	684177.6	651689.8
P37802	7	7	167.4361701	7.37E-05	1.492255402	Neg ctrl	Cu-DPQ-Phen	Transgelin-2 OS=Homo sapiens GN=TAGLN2 PE=1 SV=3 [MASS=22391]	2876546	2898875	2887710	2721063	2657390	2689226	1930592	1939670	1935131
P0DMV9	17	17	848.556057	0.003134	1.48516479	Cu-Phen	Neg ctrl	Heat shock 70 kDa protein 1B OS=Homo sapiens GN=HSPA1B PE=1 SV=1	17095309	17351051	17223180	25774719	25383801	25579260	21659212	23506575	22582893
Q14011	4	4	45.83568261	0.006554	1.481980708	Cu-DPQ-Phen	Cu-Phen	Cold-inducible RNA-binding protein OS=Homo sapiens GN=CIRBP PE=1 SV=1 [MASS=18648]	1480115	1488212	1484163	1085128	1002510	1043819	1612885	1480953	1546919
O43707	12	12	260.2619242	0.016515	1.481837352	Cu-DPQ-Phen	Cu-Phen	Alpha-actinin-4 OS=Homo sapiens GN=ACTN4 PE=1 SV=2	5710401	5875734	5793067	4702799	4584359	4643579	6397107	7364951	6881029
P11413	9	9	189.2614992	9.15E-05	1.471205207	Cu-Phen	Neg ctrl	Glucose-6-phosphate 1-dehydrogenase OS=Homo sapiens GN=G6PD PE=1 SV=4 [MASS=59256]	6189722	6315633	6252677	9151644	9246299	9198972	7364422	7290489	7327456
P25786	5	5	13.81284559	0.000238	1.458927712	Cu-DPQ-Phen	Neg ctrl	Proteasome subunit alpha type-1 OS=Homo sapiens GN=PSMA1 PE=1 SV=1 [MASS=29555]	2282835	2317252	2300043	2349597	2426178	2387887	3340425	3370770	3355597
P04792	7	7	478.930298	0.003204	1.451542664	Cu-DPQ-Phen	Cu-Phen	Heat shock protein beta-1 OS=Homo sapiens GN=HSPB1 PE=1 SV=2	53199088	56734517	54966803	46289548	50535396	48412472	65303051	75242485	70272768
P22626	9	9	73.96374882	0.006081	1.42592239	Cu-DPQ-Phen	Cu-Phen	Heterogeneous nuclear ribonucleoproteins A2/B1 OS=Homo sapiens GN=HNRNPA2B1 PE=1 SV=2	4598065	4809740	4703903	3967398	4298370	4132884	5828725	5957619	5893172
P55072	16	16	275.4490522	0.01164	1.408828387	Neg ctrl	Cu-Phen	Transitional endoplasmic reticulum ATPase OS=Homo sapiens GN=VCP PE=1 SV=4 [MASS=89321]	8732249	9381878	9057063	6689093	6168489	6428791	7583091	7831242	7707167
Q15233	10	10	340.9270171	5.59E-06	1.37959721	Neg ctrl	Cu-DPQ-Phen	Non-POU domain-containing octamer-binding protein OS=Homo sapiens GN=NONO PE=1 SV=4	4337910	4331426	4334668	3893617	3864180	3878899	3137681	3146281	3141981
Q99832	7	7	197.691467	0.004734	1.379199743	Cu-DPQ-Phen	Cu-Phen	T-complex protein 1 subunit eta OS=Homo sapiens GN=CCT7 PE=1 SV=2 [MASS=59366]	3359047	3439932	3399489	2773125	2718988	2746057	3650381	3924340	3787361
P61978	10	10	235.5741868	0.0032	1.367758438	Neg ctrl	Cu-Phen	Heterogeneous nuclear ribonucleoprotein K OS=Homo sapiens GN=HNRNPK PE=1 SV=1 [MASS=50976]	106963	113616	110289	815887	796822	806355	105327	108980	107154

				45					76	00	88	9	0	0	94	44	19
Q13509	16	15	374.14084466	0.011164	1.34492708	Cu-DPQ-Phen	Cu-Phen	Tubulin beta-3 chain OS=Homo sapiens GN=TUBB3 PE=1 SV=2	22183207	22378704	22280956	17487519	16723025	17105272	21913774	24096912	23005343
Q15365	7	7	76.03269608	0.010485	1.306748864	Cu-Phen	Cu-DPQ-Phen	Poly(rC)-binding protein 1 OS=Homo sapiens GN=PCBP1 PE=1 SV=2	22979628	23033988	23006800	23415007	23336003	23375533	17034366	18742226	17888831
P06733	21	21	551.2854683	0.001839	1.304829257	Cu-Phen	Cu-DPQ-Phen	Alpha-enolase OS=Homo sapiens GN=ENO1 PE=1 SV=2	18652318	18282395	18467356	18973563	18069280	18521421	14141348	14247687	14194517
P35579	6	6	13.40317863	0.004029	1.291358206	Neg ctrl	Cu-Phen	Myosin-9 OS=Homo sapiens GN=MYH9 PE=1 SV=4	11894496	12271888	12083422	956756.4	914671.8	935714.1	1026258	1048162	1037210

3.10.2 Exposure of MCF-7 cells at 48 h to Cu-Phen (**1**) and Cu-DPQ-Phen (**2**) against the negative control

									neg ctrl			Cu Phen				Cu DPQ Phen			
Accession	Peptide count	Uniqu e peptides	Confidence score	Anova (p)	Max fold change	Highest mean condition	Lowest mean condition	Description	4 1	4 3	average	5 1	5 2	5 3	average	6 1	6 2	6 3	average
P62826	2	2	70.74315	1.31E-05	1.716406	Cu Phen	neg ctrl	GTP-binding nuclear protein Ran OS=Homo sapiens GN=RAN PE=1 SV=3	6425583	6216231	6320907	1086260	1064693	1103821	1084925	7983872	8049888	8553692	8195817
P02795	3	3	11.2133	2.35E-05	58.50562	Cu DPQ Phen	neg ctrl	Metallothionein-2 OS=Homo sapiens GN=MT2A PE=1 SV=1 [MASS=6042]	10653.12	12037.93	11345.53	3528872	5827424	5131235	4829177	4605866	8253367	7054076	6637777
Q13509	3	3	125.0539	3.29E-05	1.778542	Cu Phen	neg ctrl	Tubulin beta-3 chain OS=Homo sapiens GN=TUBB3 PE=1 SV=2	6182333	6564215	6373274	1130844	1142223	1127474	1133514	7155576	6405167	7005895	6855607
P00558	3	3	85.90375	0.0000164	1.918641	Cu Phen	neg ctrl	Phosphoglycerate kinase 1 OS=Homo sapiens GN=PGK1 PE=1 SV=3 [MASS=44614]	5896113	6825428	6360773	1286379	1171915	1202917	1220404	6833255	5950859	6419746	6401286
P07437	2	2	132.8479	0.0000302	1.87079	Cu Phen	neg ctrl	Tubulin beta chain OS=Homo sapiens GN=TUBB PE=1 SV=2 [MASS=49671]	1202531	1196916	1199724	2119858	2368975	2244461	2244431	1518684	1347058	1264553	1376765
P04350	2	2	189.78	0.000	1.948131	Cu Phen	neg ctrl	Tubulin beta-4A chain OS=Homo sapiens GN=TUBB4A PE=1 SV=2	3220	3134	3177	6937	5516	6117	6190	4172	3557	3751	3827

				925				[MASS=49585]	821	580	701	071	752	912	578	779	434	669	294
P07355	2	2	100.857	0.001364	1.606623	Cu Phen	neg ctrl	Annexin A2 OS=Homo sapiens GN=ANXA2 PE=1 SV=2 [MASS=38604]	190992.7	220666.3	205829.5	300161.9	351098.1	340811.1	330690.4	226666.7	209186.1	221808	219220.3
Q9BUF5	1	1	213.83	0.003377	1.873073	Cu Phen	neg ctrl	Tubulin beta-6 chain OS=Homo sapiens GN=TUBB6 PE=1 SV=1 [MASS=49857]	938847.7	740705.9	839776.8	142704	178549	151268	157264	953222.1	815792.7	753685.5	840900.1
P62979	2	2	49.74613	0.009225	2.07619	Cu DPQ Phen	Cu Phen	Ubiquitin-40S ribosomal protein S27a OS=Homo sapiens GN=RPS27A PE=1 SV=2	132316	1089947	1206554	1316453	870220.76	1034031	1073564	1821926	2514319	2350522	2228922
O60814	1	1	5.154781	0.013344	2.135498	Cu DPQ Phen	Cu Phen	Histone H2B type 1-K OS=Homo sapiens GN=HIST1H2BK PE=1 SV=3	199713 5	193510 4	196611 9	134554 7	970411.8	107262 2	112952 7	179852 6	302412 1	241365 8	241210 2
P62081	2	2	57.87473	0.014061	3.595101	Cu Phen	neg ctrl	40S ribosomal protein S7 OS=Homo sapiens GN=RPS7 PE=1 SV=1 [MASS=22127]	604333.24	39586.7	500009.97	117047.5	243428.3	178897	179790.9	795550.12	109697.5	106690.3	986485.98
P14618	5	5	97.52064	0.014983	1.585147	Cu Phen	neg ctrl	Pyruvate kinase PKM OS=Homo sapiens GN=PKM PE=1 SV=4 [MASS=57937]	843821.6	788087.8	815954.7	104469	132315 7	151240 0	129340 8	898096.5	778355.8	813886.2	830112.8
P02768	3	3	89.44949	0.015447	2.221727	neg ctrl	Cu Phen	Serum albumin OS=Homo sapiens GN=ALB PE=1 SV=2 [MASS=69366]	114517 6	165659 3	140088 4	681377	502252.5	707985.8	630538.4	979358.9	145364 9	146642 5	129981 1
Q14011	2	2	4.10287	0.017185	1.928592	neg ctrl	Cu Phen	Cold-inducible RNA-binding protein OS=Homo sapiens GN=CIRBP PE=1 SV=1 [MASS=18648]	344486.4	444486.1	394486.2	189975.2	219522.8	204140.8	204546.2	267167.3	415336.9	401337.9	361280.7
Q9P258	2	2	90	0.019778	1.591395	Cu DPQ Phen	Cu Phen	Protein RCC2 OS=Homo sapiens GN=RCC2 PE=1 SV=2 [MASS=56084]	999311.25	1175816	1087564	961856.7	674413.6	692822.5	776365.1	121940.4	129151.8	119558.9	123550.3
P0DMV9	1	1	61.82	0.025529	1.999333	Cu Phen	neg ctrl	Heat shock 70 kDa protein 1B OS=Homo sapiens GN=HSPA1B PE=1 SV=1	966053.5	1040741	1003397	146213 3	201535 2	254089 0	200612 5	113721 5	115029 6	139784 4	122845 2
P25786	2	2	4.038128	0.028276	1.555136	Cu DPQ Phen	Cu Phen	Proteasome subunit alpha type-1 OS=Homo sapiens GN=PSMA1 PE=1 SV=1 [MASS=29555]	215825.7	199645.5	207735.6	135016.6	141260.1	149216.8	141831.2	169692	248076.9	243931.3	220566.7
P05388	2	2	4.160388	0.029	2.154607	Cu Phen	neg ctrl	60S acidic ribosomal protein P0 OS=Homo sapiens GN=RPLP0	5108	4935	5022	7435	1290	1212	1082	4795	6540	6827	6054

				841				PE=1 SV=1 [MASS=34273]	82.2	99.7	41	07.4	593	296	132	70.6	37.9	21.9	43.5
Q15149	2	2	41.67123	0.031353	1.745964	Cu DPQ Phen	Cu Phen	Plectin OS=Homo sapiens GN=PLEC PE=1 SV=3	5838 4.1	6824 9.65	6331 6.87	4990 3.96	4981 8.41	4505 2.39	4825 8.25	6199 5.07	9183 7.58	9893 8.8	8425 7.15
P21333	3	3	97.47057	0.035525	2.612624	Cu Phen	neg ctrl	Filamin-A OS=Homo sapiens GN=FLNA PE=1 SV=4	3569 90.4	3862 33.7	3716 12.1	6459 88	7929 97.7	1473 662	9708 82.4	4764 78.8	5029 73.6	5405 05.2	5066 52.5

3.10.3 Exposure of SKOV-3 cells at 24 h to Cu-Phen (**1**) and Cu-DPQ-Phen (**2**) against the negative control

Accession	Peptide count	Unique peptides	Confidence score	Anova (p)	Max fold change	Highest mean condition	Lowest mean condition	Description	7 2	7 3	average	8 1	8 3	average	9 1	9 2	average
P80297	5	5	17.18442	0.0028222	17.62856	SKOV-3 24 hr Cu-DPQ-Phen	SKOV-3 24 hr Neg	Metallothionein-1X OS=Homo sapiens GN=MT1X PE=1 SV=1 [MASS=6068]	256602.6	227899.1	242250.9	270954 2	442389 4	3566718	3427973	5113096	4270534
P02795	5	5	23.61522	0.003971	5.872623	SKOV-3 24 hr Cu-DPQ-Phen	SKOV-3 24 hr Neg	Metallothionein-2 OS=Homo sapiens GN=MT2A PE=1 SV=1 [MASS=6042]	1756431	1647780	1702106	669175 4	955979 1	8125772	8786702	1120495 1	9995826
P17066	9	9	56.29835	0.000625	4.561281	SKOV-3 24 hr Cu-Phen	SKOV-3 24 hr Neg	Heat shock 70 kDa protein 6 OS=Homo sapiens GN=HSPA6 PE=1 SV=2	552407.6	552657.8	552532.7	239078 0	264973 4	2520257	1038951	1210391	1124671
P0DMV9	11	11	584.9433	0.002073	4.036755	SKOV-3 24 hr Cu-Phen	SKOV-3 24 hr Neg	Heat shock 70 kDa protein 1B OS=Homo sapiens GN=HSPA1B PE=1 SV=1	3349767	3685774	3517770	129779 11	154228 46	14200379	6221569	7293979	6757774
P00558	4	4	47.26452	0.005269	1.500938	SKOV-3 24 hr Cu-Phen	SKOV-3 24 hr Neg	Phosphoglycerate kinase 1 OS=Homo sapiens GN=PGK1 PE=1 SV=3 [MASS=44614]	504822.3	566029.2	535425.8	794894.3	812387.5	8036 40.9	5322 75.7	5395 46.2	5359 10.9
P62979	2	2	78.96194	0.007836	1.599998	SKOV-3 24 hr Cu-Phen	SKOV-3 24 hr Neg	Ubiquitin-40S ribosomal protein S27a OS=Homo sapiens GN=RPS27A PE=1 SV=2	747589.7	751159.1	749374.4	120708 0	119091 5	1198997	8331 77.9	9540 43.8	8936 10.9
O43399	2	2	76.76597	0.010363	1.681286	SKOV-3 24 hr Cu-Phen	SKOV-3 24 hr Neg	Tumor protein D54 OS=Homo sapiens GN=TPD52L2 PE=1 SV=2	752124.9	758452.2	755288.6	120680 7	133290 5	1269856	1032783	1184831	1108807
P36578	2	2	54.78042	5.83E-05	1.73107	SKOV-3 24 hr Neg	SKOV-3 24 hr Cu-DPQ-Phen	60S ribosomal protein L4 OS=Homo sapiens GN=RPL4 PE=1 SV=5	445230.4	446522.7	445876.6	272992.2	281216.5	2771 04.4	2592 99.8	2558 45.7	2575 72.8
P22392	1	1	55.1	0.000145	3.096555	SKOV-3 24 hr Neg	SKOV-3 24 hr Cu-Phen	Nucleoside diphosphate kinase B OS=Homo sapiens GN=NME2 PE=1 SV=1	340998.8	336539.1	338768.9	105021.1	113782.6	1094 01.9	1718 50.8	1677 20.5	1697 85.7
P35	3	3	155.	0.00	1.69	SKOV-3 24	SKOV-3 24	Myosin-9 OS=Homo sapiens GN=MYH9 PE=1	124	128	126	757	737	747	788	745	767

579			8751	0594	5001	hr Neg	hr Cu-Phen	SV=4	6913	7173	7043	846.8	187.5	517.2	989.5	168.2	078.8
P16152	2	2	3.237441	0.001074	1.758111	SKOV-3 24 hr Neg	SKOV-3 24 hr Cu-Phen	Carbonyl reductase [NADPH] 1 OS=Homo sapiens GN=CBR1 PE=1 SV=3	225537.4	210715.2	218126.3	126802.5	121334.6	124068.6	122657.6	128586.3	125621.9
Q04695	4	4	63.18959	0.001174	2.06492	SKOV-3 24 hr Neg	SKOV-3 24 hr Cu-Phen	Keratin, type I cytoskeletal 17 OS=Homo sapiens GN=KRT17 PE=1 SV=2	503965.5	548104.7	526035.1	261264.2	248232.6	254748.4	279250.8	297159.4	288205.1
Q9Y490	2	2	3.718414	0.001237	1.707421	SKOV-3 24 hr Neg	SKOV-3 24 hr Cu-DPQ-Phen	Talin-1 OS=Homo sapiens GN=TLN1 PE=1 SV=3 [MASS=269765]	432862.1	412243.5	422552.8	283772	288634.5	286203.2	239209.1	255751.2	247480.1
Q15149	5	5	115.4087	0.00214	1.943558	SKOV-3 24 hr Neg	SKOV-3 24 hr Cu-Phen	Plectin OS=Homo sapiens GN=PLEC PE=1 SV=3	543201	575867	559534	298041	277742.1	287891.6	353437.7	383969	368703.3
P68363	2	2	64.16891	0.002746	29.43665	SKOV-3 24 hr Neg	SKOV-3 24 hr Cu-Phen	Tubulin alpha-1B chain OS=Homo sapiens GN=TUBA1B PE=1 SV=1	752722.1	959065.6	855893.9	38844.44	19307.13	29075.79	41083.89	45319.35	43201.62
P58876	7	7	140.7897	0.003123	2.183503	SKOV-3 24 hr Neg	SKOV-3 24 hr Cu-Phen	Histone H2B type 1-D OS=Homo sapiens GN=HIST1H2BD PE=1 SV=2 [MASS=13936]	18635193	16836740	17735966	8050366	8195059	8122713	10958331	9606130	10282230
P22626	3	3	75.79218	0.003691	1.559121	SKOV-3 24 hr Neg	SKOV-3 24 hr Cu-DPQ-Phen	Heterogeneous nuclear ribonucleoproteins A2/B1 OS=Homo sapiens GN=HNRNPA2B1 PE=1 SV=2	2217279	2010832	2114055	1404313	1446829	1425571	1378224	1333631	1355928
P52292	2	2	211.42	0.005035	2.115807	SKOV-3 24 hr Neg	SKOV-3 24 hr Cu-Phen	Importin subunit alpha-1 OS=Homo sapiens GN=KPNA2 PE=1 SV=1	638426.6	672754.1	655590.3	309582.3	310124.9	309853.6	353785.7	424333.7	389059.7
P13639	6	6	143.408	0.005238	1.507959	SKOV-3 24 hr Neg	SKOV-3 24 hr Cu-Phen	Elongation factor 2 OS=Homo sapiens GN=EEF2 PE=1 SV=4	1237590	1129347	1183469	771975.8	797654.3	784815	888705.2	921612.9	905159
P06576	2	2	46.89017	0.005629	1.729273	SKOV-3 24 hr Neg	SKOV-3 24 hr Cu-Phen	ATP synthase subunit beta, mitochondrial OS=Homo sapiens GN=ATP5B PE=1 SV=3	441669.8	495983.2	468826.5	271978.3	270245.6	271112	369460.8	341938.4	355699.6
P26599	2	2	60.80959	0.005943	1.614739	SKOV-3 24 hr Neg	SKOV-3 24 hr Cu-DPQ-Phen	Polypyrimidine tract-binding protein 1 OS=Homo sapiens GN=PTBP1 PE=1 SV=1	209505.1	196861.1	203183.1	127738.7	137776.2	132757.5	131844	119816.5	125830.3
P38646	2	2	4.023734	0.007217	1.744696	SKOV-3 24 hr Neg	SKOV-3 24 hr Cu-Phen	Stress-70 protein, mitochondrial OS=Homo sapiens GN=HSPA9 PE=1 SV=2 [MASS=73680]	257206.8	270670.1	263938.5	162559.2	140001.8	151280.5	184246.3	183177.6	183712
P04350	2	2	11.31024	0.009558	1.719389	SKOV-3 24 hr Neg	SKOV-3 24 hr Cu-Phen	Tubulin beta-4A chain OS=Homo sapiens GN=TUBB4A PE=1 SV=2 [MASS=49585]	2725091	2843533	2784312	1763750	1474972	1619361	1678446	1592382	1635414
P16402	3	3	140.4852	0.01111	2.243415	SKOV-3 24 hr Neg	SKOV-3 24 hr Cu-Phen	Histone H1.3 OS=Homo sapiens GN=HIST1H1D PE=1 SV=2	860065	831292.7	845678.8	341984.9	411936.3	376960.6	515650.9	618945.7	567298.3
P12814	2	2	68.28382	0.011112	1.788792	SKOV-3 24 hr Neg	SKOV-3 24 hr Cu-Phen	Alpha-actinin-1 OS=Homo sapiens GN=ACTN1 PE=1 SV=2	957671.1	979376.9	968524	519809.7	563070.9	541440.3	574414.5	685933.8	630174.2

P15531	2	2	5.475556	0.011527	1.937117	SKOV-3 24 hr Neg	SKOV-3 24 hr Cu-Phen	Nucleoside diphosphate kinase A OS=Homo sapiens GN=NME1 PE=1 SV=1	397590.7	463227.8	430409.2	217658	226723.3	222190.6	254416.3	212008.3	233212.3
O43396	2	2	55.53893	0.011941	1.923953	SKOV-3 24 hr Neg	SKOV-3 24 hr Cu-Phen	Thioredoxin-like protein 1 OS=Homo sapiens GN=TXNL1 PE=1 SV=3 [MASS=32251]	326980	359203.6	343091.8	187134.1	169518.9	178326.5	238382.6	282619	260500.8
P83731	2	2	66.17481	0.016525	1.532224	SKOV-3 24 hr Neg	SKOV-3 24 hr Cu-DPQ-Phen	60S ribosomal protein L24 OS=Homo sapiens GN=RPL24 PE=1 SV=1 [MASS=17779]	244998.4	275052.5	260025.4	228985.1	239349.7	234167.4	160366	179043.2	169704.6
O60814	1	1	5.461892	0.017438	2.281502	SKOV-3 24 hr Neg	SKOV-3 24 hr Cu-Phen	Histone H2B type 1-K OS=Homo sapiens GN=HIST1H2BK PE=1 SV=3	223828 0	194936 9	209382 5	976318.1	859161	917739.5	141407 1	109649 4	125528 2
P06748	6	6	100.6096	0.019783	1.631587	SKOV-3 24 hr Neg	SKOV-3 24 hr Cu-DPQ-Phen	Nucleophosmin OS=Homo sapiens GN=NPM1 PE=1 SV=2	411592 9	397564 2	404578 6	263031 5	247879 3	255455 4	273714 8	222217 9	247966 3
P49915	3	3	3.719249	0.022672	1.577997	SKOV-3 24 hr Neg	SKOV-3 24 hr Cu-Phen	GMP synthase [glutamine-hydrolyzing] OS=Homo sapiens GN=GMPS PE=1 SV=1	964119	108849 5	102630 7	626958.7	673812.9	650385.8	670121.5	771509.1	720815.3
P62081	2	2	3.558209	0.023447	1.745811	SKOV-3 24 hr Neg	SKOV-3 24 hr Cu-DPQ-Phen	40S ribosomal protein S7 OS=Homo sapiens GN=RPS7 PE=1 SV=1 [MASS=22127]	121757 5	136551 1	129154 3	779202.2	710263.6	744732.9	655922.3	823668.8	739795.6
P47914	2	2	4.668583	0.024961	1.817085	SKOV-3 24 hr Neg	SKOV-3 24 hr Cu-DPQ-Phen	60S ribosomal protein L29 OS=Homo sapiens GN=RPL29 PE=1 SV=2 [MASS=17752]	483190.7	441383.5	462287.1	315402.9	368101.1	341752	278247.4	230575.3	254411.4
P60174	2	2	4.178611	0.025416	1.55732	SKOV-3 24 hr Neg	SKOV-3 24 hr Cu-Phen	Triosephosphate isomerase OS=Homo sapiens GN=TPI1 PE=1 SV=3 [MASS=30791]	746787.2	699898.8	723343	433595.3	495363.4	464479.4	451846.3	525734.2	488790.2
P15311	2	2	6.177118	0.031335	1.566759	SKOV-3 24 hr Neg	SKOV-3 24 hr Cu-DPQ-Phen	Ezrin OS=Homo sapiens GN=EZR PE=1 SV=4 [MASS=69412]	171845 2	154153 0	162999 1	109571 5	108822 1	109196 8	114682 1	933896.1	104035 9

3.10.4 Exposure of SKOV-3 cells at 48 h to Cu-Phen (**1**) and Cu-DPQ-Phen (**2**) against the negative control

									SKOV-3 48 hr neg			SKOV-3 48 hr Cu-Phen			SKOV-3 48 hr Cu-DPQ-Phen		
Accession	Peptide count	Unique peptides	Confidence score	Anova (p)	Max fold change	Highest mean condition	Lowest mean condition	Description	102	103	average	112	113	average	122	123	average
P04406	6	6	190.7604	3.50E-06	1.591744	SKOV-3 48 hr Cu-Phen	SKOV-3 48 hr Cu-DPQ-Phen	Glyceraldehyde-3-phosphate dehydrogenase OS=Homo sapiens GN=GAPDH PE=1 SV=3	4581113	4563752	4572433	6903104	6863176	6883140	4306101	4342449	4324275
P80297	5	5	17.36828	1.37E-05	32.1166	SKOV-3 48 hr Cu-DPQ-Phen	SKOV-3 48 hr neg	Metallothionein-1X OS=Homo sapiens GN=MT1X PE=1 SV=1 [MASS=6068]	139105.6	124668.4	131887	4195316	4275982	4235649	4400736	4070788	4235762
Q0	6	6	177.91	1.7	1.785	SKOV-3	SKOV-3	Elongation factor 1-alpha 2 OS=Homo sapiens	343	344	343	194	190	192	298	296	297

5639			67	5E-05	811	48 hr neg	48 hr Cu-Phen	GN=EEF1A2 PE=1 SV=1	0253	7698	8976	6058	5386	5722	1463	8371	4917
O60493	2	2	89.02	2.35E-05	2.023513	SKOV-3 48 hr neg	SKOV-3 48 hr Cu-DPQ-Phen	Sorting nexin-3 OS=Homo sapiens GN=SNX3 PE=1 SV=3	173877.5	173065.8	173471.6	152178.4	153767	152972.7	84516.25	86939.7	85727.97
Q13435	3	3	54.43092	2.42E-05	1.586723	SKOV-3 48 hr neg	SKOV-3 48 hr Cu-Phen	Splicing factor 3B subunit 2 OS=Homo sapiens GN=SF3B2 PE=1 SV=2 [MASS=100227]	788088.1	795341.1	791714.6	494476.3	503447.7	498962	738517.3	736631.5	737574.4
P06748	8	8	335.8957	2.53E-05	1.744022	SKOV-3 48 hr Cu-DPQ-Phen	SKOV-3 48 hr neg	Nucleophosmin OS=Homo sapiens GN=NPM1 PE=1 SV=2	4114575	4027604	4071090	6716779	6782927	6749853	7135655	7061448	7100068
P00558	16	16	478.1443	2.69E-05	2.300324	SKOV-3 48 hr Cu-Phen	SKOV-3 48 hr neg	Phosphoglycerate kinase 1 OS=Homo sapiens GN=PGK1 PE=1 SV=3 [MASS=44614]	4173274	4323637	4248455	9676858	9868786	9772822	4289785	4277860	4283822
P62979	3	3	84.0875	2.93E-05	1.620134	SKOV-3 48 hr Cu-DPQ-Phen	SKOV-3 48 hr Cu-Phen	Ubiquitin-40S ribosomal protein S27a OS=Homo sapiens GN=RPS27A PE=1 SV=2	1488379	1465366	1476873	929660.5	927860.1	928760.3	1518220	1491212	1504716
O43707	2	2	62.85283	3.30E-05	2.261426	SKOV-3 48 hr Cu-Phen	SKOV-3 48 hr neg	Alpha-actinin-4 OS=Homo sapiens GN=ACTN4 PE=1 SV=2	1827264	1810761	1819013	4068098	4159026	4113562	2457240	2528761	2493001
P0DMV9	9	9	386.5659	4.30E-05	1.772115	SKOV-3 48 hr Cu-Phen	SKOV-3 48 hr neg	Heat shock 70 kDa protein 1B OS=Homo sapiens GN=HSPA1B PE=1 SV=1	2653346	2596498	2624922	4673078	4630246	4651662	3195703	3142410	3169056
P02768	2	2	42.58599	5.02E-05	1.969546	SKOV-3 48 hr Cu-DPQ-Phen	SKOV-3 48 hr Cu-Phen	Serum albumin OS=Homo sapiens GN=ALB PE=1 SV=2 [MASS=69366]	487842.4	478603.7	483223.1	248154.5	254700.5	251427.5	489300	501096.1	495198.1
P23246	5	5	158.0942	5.12E-05	1.896888	SKOV-3 48 hr neg	SKOV-3 48 hr Cu-Phen	Splicing factor, proline- and glutamine-rich OS=Homo sapiens GN=SFPQ PE=1 SV=2	858495.4	878556.1	868525.8	451766.2	463971.5	457868.9	840423.7	829291.8	834857.8
P30101	4	4	100.3245	0.000109	1.799068	SKOV-3 48 hr Cu-Phen	SKOV-3 48 hr Cu-DPQ-Phen	Protein disulfide-isomerase A3 OS=Homo sapiens GN=PDIA3 PE=1 SV=4	746921.3	737962.7	742442	1036400	1075451	1055925	584171.2	589687.2	586929.2
P25786	2	2	7.89099	0.000136	1.966534	SKOV-3 48 hr Cu-Phen	SKOV-3 48 hr Cu-DPQ-Phen	Proteasome subunit alpha type-1 OS=Homo sapiens GN=PSMA1 PE=1 SV=1 [MASS=29555]	724193.8	705916.7	715055.3	1370428	1424679	1397554	699217	722120.1	710668.5
P14625	7	7	132.8844	0.000139	1.973994	SKOV-3 48 hr Cu-Phen	SKOV-3 48 hr Cu-DPQ-Phen	Endoplasmin OS=Homo sapiens GN=HSP90B1 PE=1 SV=1 [MASS=92468]	2112263	2191964	2152113	3468929	3593412	3531170	1782846	1794943	1788895
P04350	3	2	77.35044	0.000139	2.076134	SKOV-3 48 hr Cu-Phen	SKOV-3 48 hr Cu-DPQ-Phen	Tubulin beta-4A chain OS=Homo sapiens GN=TUBB4A PE=1 SV=2 [MASS=49585]	2074555	2182745	2128650	2563640	2605383	2584511	1254444	1235290	1244867
P60174	7	7	221.1072	0.000152	1.829474	SKOV-3 48 hr Cu-Phen	SKOV-3 48 hr neg	Triosephosphate isomerase OS=Homo sapiens GN=TPI1 PE=1 SV=3 [MASS=30791]	1281272	1332192	1306732	2414932	2366333	2390632	1491976	1519990	1505983
P14174	8	8	240.6552	0.000152	1.834063	SKOV-3 48 hr Cu-Phen	SKOV-3 48 hr neg	Macrophage migration inhibitory factor OS=Homo sapiens GN=MIF PE=1 SV=4	8293877	8453061	8373469	15202663	15512268	15357465	8207844	8585401	8396622

P11021	9	9	519.8589	0.000116	1.736337	SKOV-3 48 hr Cu-Phen	SKOV-3 48 hr Cu-DPQ-Phen	78 kDa glucose-regulated protein OS=Homo sapiens GN=HSPA5 PE=1 SV=2	2740861	2733592	2737227	3746492	3907339	3826916	2196307	2211727	2204017
Q9UQ80	4	4	9.384492	0.000169	2.100517	SKOV-3 48 hr Cu-DPQ-Phen	SKOV-3 48 hr Cu-Phen	Proliferation-associated protein 2G4 OS=Homo sapiens GN=PA2G4 PE=1 SV=3 [MASS=43787]	1381062	1466907	1423985	712838.5	713078.4	712958.5	1479670	1515492	1497581
P04075	12	12	400.9881	0.000173	1.993099	SKOV-3 48 hr Cu-Phen	SKOV-3 48 hr Cu-DPQ-Phen	Fructose-bisphosphate aldolase A OS=Homo sapiens GN=ALDOA PE=1 SV=2 [MASS=39420]	20663712	21117699	20890705	35857479	37408196	36632837	18077383	18682286	18379834
P07437	3	3	218.8649	0.000184	3.265984	SKOV-3 48 hr Cu-Phen	SKOV-3 48 hr neg	Tubulin beta chain OS=Homo sapiens GN=TUBB PE=1 SV=2 [MASS=49671]	1720913	1595407	1658160	55463752	52846722	54155523	3517615	3397515	3457565
Q9H6Z4	2	2	56.1516	0.00021	1.658414	SKOV-3 48 hr Cu-DPQ-Phen	SKOV-3 48 hr Cu-Phen	Ran-binding protein 3 OS=Homo sapiens GN=RANBP3 PE=1 SV=1 [MASS=60210]	255460.1	256339.9	255900	151677.2	158817.7	155247.5	259563.3	255365.8	257464.5
Q92597	6	6	170.3254	0.00028	6.507291	SKOV-3 48 hr Cu-Phen	SKOV-3 48 hr neg	Protein NDRG1 OS=Homo sapiens GN=NDRG1 PE=1 SV=1	180511.9	151444.1	165978	10772069	10829297	10800677	215639.3	212836.1	214237.7
P48643	6	6	55.86385	0.00033	1.627698	SKOV-3 48 hr Cu-DPQ-Phen	SKOV-3 48 hr Cu-Phen	T-complex protein 1 subunit epsilon OS=Homo sapiens GN=CCT5 PE=1 SV=1	295030.5	308461.7	301746.1	195002.8	194333.2	194668	314670.4	319051.1	316860.8
Q9Y266	2	2	52.54356	0.00072	2.357033	SKOV-3 48 hr Cu-DPQ-Phen	SKOV-3 48 hr Cu-Phen	Nuclear migration protein nudC OS=Homo sapiens GN=NUDC PE=1 SV=1 [MASS=38243]	150556.7	162202.8	156379.7	74660.65	73511.03	74085.84	171200.2	178045.3	174622.8
P16949	4	4	147.2034	0.00279	1.860592	SKOV-3 48 hr neg	SKOV-3 48 hr Cu-Phen	Stathmin OS=Homo sapiens GN=STMN1 PE=1 SV=3 [MASS=17302]	389274	369058.3	379166.1	203632.9	203942.8	203787.8	326878.1	318302.1	322590.1
O60814	11	11	290.0382	0.00295	2.214836	SKOV-3 48 hr Cu-Phen	SKOV-3 48 hr neg	Histone H2B type 1-K OS=Homo sapiens GN=HIST1H2BK PE=1 SV=3	8247668	8486894	8367281	18846725	18217592	18532158	18371342	17100563	17735953
P02795	5	5	26.11894	0.00317	5.452212	SKOV-3 48 hr Cu-DPQ-Phen	SKOV-3 48 hr neg	Metallothionein-2 OS=Homo sapiens GN=MT2A PE=1 SV=1 [MASS=6042]	2532709	2150728	2341718	11220834	11843033	11531933	13184200	12350891	12767545
Q96AE4	4	4	97.49044	0.00329	1.653407	SKOV-3 48 hr neg	SKOV-3 48 hr Cu-Phen	Far upstream element-binding protein 1 OS=Homo sapiens GN=FUBP1 PE=1 SV=3	428833.2	423313.7	426073.5	250891.4	264497.2	257694.3	425424.9	419194	422309.4
P16401	3	3	142.5295	0.00035	2.624016	SKOV-3 48 hr Cu-DPQ-Phen	SKOV-3 48 hr Cu-Phen	Histone H1.5 OS=Homo sapiens GN=HIST1H1B PE=1 SV=3 [MASS=22580]	224025.8	220926.7	222476.3	93739.52	87098.22	90418.87	246487.3	228059.9	237273.6
P02545	8	8	443.0467	0.00353	1.505093	SKOV-3 48 hr Cu-DPQ-Phen	SKOV-3 48 hr Cu-Phen	Prelamin-A/C OS=Homo sapiens GN=LMNA PE=1 SV=1	2102874	2073448	2088161	14551449	15049496	14800466	22564066	22012866	22288846
P26373	2	2	111.81	0.00379	1.765328	SKOV-3 48 hr Cu-DPQ-Phen	SKOV-3 48 hr Cu-Phen	60S ribosomal protein L13 OS=Homo sapiens GN=RPL13 PE=1 SV=4 [MASS=24261]	472243.2	486781.4	479512.3	279998.4	280848.1	280423.3	509389.8	480688	495038.9
Q07955	2	2	41.72075	0.00416	2.037121	SKOV-3 48 hr neg	SKOV-3 48 hr Cu-Phen	Serine/arginine-rich splicing factor 1 OS=Homo sapiens GN=SRSF1 PE=1 SV=2	479336.8	500400.8	489868.8	233055.1	247887.2	240471.1	432559.3	445958.5	439258.9

P14618	9	9	429.5825	0.000421	1.560538	SKOV-3 48 hr Cu-Phen	SKOV-3 48 hr Cu-DPQ-Phen	Pyruvate kinase PKM OS=Homo sapiens GN=PKM PE=1 SV=4 [MASS=57937]	11439757	11971838	11705797	14758038	14944861	14851449	9535812	9497949	9516880
P18206	4	4	55.95852	0.000492	1.590687	SKOV-3 48 hr Cu-Phen	SKOV-3 48 hr Cu-DPQ-Phen	Vinculin OS=Homo sapiens GN=VCL PE=1 SV=4 [MASS=123799]	501741.8	512345.8	507043.8	723073.9	737188.9	730131.4	448268.4	469739.5	459003.9
P40227	3	3	91.38595	0.000518	1.628871	SKOV-3 48 hr Cu-DPQ-Phen	SKOV-3 48 hr Cu-Phen	T-complex protein 1 subunit zeta OS=Homo sapiens GN=CCT6A PE=1 SV=3	357560.6	378725.2	368142.9	226004.8	231798	228901.4	374349.8	371351.9	372850.9
P13639	11	11	437.9142	0.000564	1.568412	SKOV-3 48 hr neg	SKOV-3 48 hr Cu-Phen	Elongation factor 2 OS=Homo sapiens GN=EEF2 PE=1 SV=4	358625.0	355601.5	357113.2	222593.3	232788.5	227690.9	288852.3	281254.6	285053.5
Q07666	2	2	126.92	0.00058	1.948866	SKOV-3 48 hr Cu-DPQ-Phen	SKOV-3 48 hr Cu-Phen	KH domain-containing, RNA-binding, signal transduction-associated protein 1 OS=Homo sapiens GN=KHDRBS1 PE=1 SV=1	361886.2	345571.8	353729	193966	202078.1	198022.1	397424.7	374412.4	385918.6
Q15149	16	16	348.9228	0.000609	1.614467	SKOV-3 48 hr neg	SKOV-3 48 hr Cu-Phen	Plectin OS=Homo sapiens GN=PLEC PE=1 SV=3	134184.0	139165.0	136674.5	829431.1	863690.9	846561	121975.6	119017.0	120496.3
P61978	4	4	187.6851	0.000634	1.636442	SKOV-3 48 hr neg	SKOV-3 48 hr Cu-Phen	Heterogeneous nuclear ribonucleoprotein K OS=Homo sapiens GN=HNRNPK PE=1 SV=1 [MASS=50976]	925046.4	871353.7	898200.1	550499.9	547247.6	548873.7	858609.1	885052.2	871830.7
P68371	1	1	48.8	0.000635	2.023779	SKOV-3 48 hr Cu-DPQ-Phen	SKOV-3 48 hr Cu-Phen	Tubulin beta-4B chain OS=Homo sapiens GN=TUBB4B PE=1 SV=1	92828.86	92176.58	92502.72	44636.97	48684.88	46660.93	92311.09	96551.72	94431.41
P06396	2	2	2.208626	0.000648	1.989964	SKOV-3 48 hr Cu-Phen	SKOV-3 48 hr Cu-DPQ-Phen	Gelsolin OS=Homo sapiens GN=GSN PE=1 SV=1	168233.7	160973.4	164603.5	207871.8	221748.7	214810.3	109765	106128.7	107946.8
P31689	2	2	3.991654	0.000653	2.358789	SKOV-3 48 hr Cu-DPQ-Phen	SKOV-3 48 hr Cu-Phen	DnaJ homolog subfamily A member 1 OS=Homo sapiens GN=DNAJA1 PE=1 SV=2	65980.46	64350.94	65165.7	27340.35	30696.92	29018.63	68805.35	68092.35	68448.85
P18669	6	6	103.9907	0.000696	2.006999	SKOV-3 48 hr Cu-Phen	SKOV-3 48 hr Cu-DPQ-Phen	Phosphoglycerate mutase 1 OS=Homo sapiens GN=PGAM1 PE=1 SV=2 [MASS=28804]	3314196	3633676	3473936	6500909	6715266	6608088	3293894	3292150	3292522
P55010	2	2	63.40357	0.000702	1.664043	SKOV-3 48 hr neg	SKOV-3 48 hr Cu-Phen	Eukaryotic translation initiation factor 5 OS=Homo sapiens GN=EIF5 PE=1 SV=2 [MASS=49222]	282867	289830.1	286348.6	174823.4	169336.6	172080	237780.8	226047.8	231914.3
P47914	2	2	3.449145	0.000711	2.837057	SKOV-3 48 hr neg	SKOV-3 48 hr Cu-Phen	60S ribosomal protein L29 OS=Homo sapiens GN=RPL29 PE=1 SV=2	157214.5	165958.1	161586.3	54048.25	59862.96	56955.6	165609.8	150276.3	157943
P06744	3	3	132.409	0.000717	2.455567	SKOV-3 48 hr Cu-Phen	SKOV-3 48 hr neg	Glucose-6-phosphate isomerase OS=Homo sapiens GN=GPI PE=1 SV=4 [MASS=63147]	316366.8	352302.2	334334.5	799151.6	842878.9	821015.2	404155.7	398870.5	401513.1
P62857	2	2	6.132586	0.000748	1.521865	SKOV-3 48 hr Cu-Phen	SKOV-3 48 hr Cu-DPQ-Phen	40S ribosomal protein S28 OS=Homo sapiens GN=RPS28 PE=1 SV=1 [MASS=7841]	1131262	1070498	1100880	1525640	1508024	1516832	994499.8	998885.3	996692.6
Q8N257	1	1	2.751464	0.000847	1.827475	SKOV-3 48 hr neg	SKOV-3 48 hr Cu-Phen	Histone H2B type 3-B OS=Homo sapiens GN=HIST3H2BB PE=1 SV=3	131989	125451.7	128720.4	69297.52	71574.89	70436.2	123486.5	115749.6	119618

P07237	2	2	79.92049	0.000861	2.548912	SKOV-3 48 hr Cu-Phen	SKOV-3 48 hr Cu-DPQ-Phen	Protein disulfide-isomerase OS=Homo sapiens GN=P4HB PE=1 SV=3 [MASS=57116]	1317328	1302068	1309698	2200817	2317977	2259397	937578	835254.2	886416.1
P52292	5	5	292.7578	0.000915	1.637491	SKOV-3 48 hr neg	SKOV-3 48 hr Cu-Phen	Importin subunit alpha-1 OS=Homo sapiens GN=KPNA2 PE=1 SV=1	1355263	1340737	1348000	8512847	7951368	8232107	1141608	1136087	1138848
Q13185	3	3	4.816595	0.001032	1.90529	SKOV-3 48 hr neg	SKOV-3 48 hr Cu-Phen	Chromobox protein homolog 3 OS=Homo sapiens GN=CBX3 PE=1 SV=4 [MASS=20811]	289073.2	292304.3	290688.7	155853.8	149284.8	152569.3	213035.1	196382.8	204709
Q14974	3	3	76.3131	0.00112	3.390856	SKOV-3 48 hr neg	SKOV-3 48 hr Cu-Phen	Importin subunit beta-1 OS=Homo sapiens GN=KPNB1 PE=1 SV=2 [MASS=97170]	83043.09	73948	78495.54	276861.7	255472.6	266167.1	155416.9	174285.1	164851
P55072	9	9	136.2619	0.001135	1.561608	SKOV-3 48 hr Cu-Phen	SKOV-3 48 hr Cu-DPQ-Phen	Transitional endoplasmic reticulum ATPase OS=Homo sapiens GN=VCP PE=1 SV=4 [MASS=89321]	2981721	3155251	3068486	4373873	4475152	4424512	2783162	2883448	2833305
P35268	2	2	115.6531	0.001163	2.094354	SKOV-3 48 hr Cu-DPQ-Phen	SKOV-3 48 hr Cu-Phen	60S ribosomal protein L22 OS=Homo sapiens GN=RPL22 PE=1 SV=2 [MASS=14787]	400008.4	416336.9	408172.6	203791.7	220098.7	211945.2	462627.1	425149.5	443888.3
P06899	1	1	4.735424	0.001171	2.27991	SKOV-3 48 hr neg	SKOV-3 48 hr Cu-Phen	Histone H2B type 1-J OS=Homo sapiens GN=HIST1H2BJ PE=1 SV=3	517845.6	551121	534483.3	222101.5	246762	234431.7	359150.1	365925.8	362538
P62263	3	3	138.3183	0.001206	1.724141	SKOV-3 48 hr Cu-DPQ-Phen	SKOV-3 48 hr Cu-Phen	40S ribosomal protein S14 OS=Homo sapiens GN=RPS14 PE=1 SV=3 [MASS=16273]	533561.7	500216.1	516888.9	325443.4	342265	333854.2	584376.5	566847	575611.8
Q13509	4	4	107.4256	0.001208	1.959416	SKOV-3 48 hr Cu-Phen	SKOV-3 48 hr neg	Tubulin beta-3 chain OS=Homo sapiens GN=TUBB3 PE=1 SV=2	1080379	1116736	1098558	2080432	2224630	2152531	1397810	1299576	1348693
Q15084	2	2	131.61	0.001245	2.103471	SKOV-3 48 hr Cu-Phen	SKOV-3 48 hr Cu-DPQ-Phen	Protein disulfide-isomerase A6 OS=Homo sapiens GN=PDIA6 PE=1 SV=1	170986.6	155938.1	163462.3	212120.7	198205.5	205163.1	98612.57	96458.36	97535.47
P09972	2	2	3.038664	0.00126	14.89492	SKOV-3 48 hr Cu-Phen	SKOV-3 48 hr neg	Fructose-bisphosphate aldolase C OS=Homo sapiens GN=ALDOC PE=1 SV=2 [MASS=39456]	6493.699	5446.825	5970.262	94864.91	82988.29	88926.6	75900.05	11179.28	9384.665
P62081	4	4	10.84917	0.001299	2.019081	SKOV-3 48 hr Cu-Phen	SKOV-3 48 hr neg	40S ribosomal protein S7 OS=Homo sapiens GN=RPS7 PE=1 SV=1 [MASS=22127]	659365	735643.4	697504.2	138259.2	143404.4	140831.8	125133.9	128139.1	126636.5
Q14697	5	5	49.6196	0.001301	2.449889	SKOV-3 48 hr Cu-Phen	SKOV-3 48 hr Cu-DPQ-Phen	Neutral alpha-glucosidase AB OS=Homo sapiens GN=GANAB PE=1 SV=3 [MASS=106873]	296260.2	287990.2	292125.2	730146.7	647337.5	688742.1	267504.1	294759.7	281131.9
Q9H6S3	2	2	47.36045	0.001337	1.698721	SKOV-3 48 hr Cu-Phen	SKOV-3 48 hr Cu-DPQ-Phen	Epidermal growth factor receptor kinase substrate 8-like protein 2 OS=Homo sapiens GN=EPS8L2 PE=1 SV=2 [MASS=80620]	423260.7	444367.3	433814	582925.2	549784.7	566355	327877.1	338924.7	333400.9
Q15366	4	4	6.186841	0.001341	1.736804	SKOV-3 48 hr Cu-DPQ-Phen	SKOV-3 48 hr Cu-Phen	Poly(rC)-binding protein 2 OS=Homo sapiens GN=PCBP2 PE=1 SV=1	475899.7	511124	493511.9	314610	331540.7	323075.3	566563.2	555674	561118.6
Q9UMS	2	2	68.00023	0.001392	3.482387	SKOV-3 48 hr Cu-DPQ-Phen	SKOV-3 48 hr neg	Pre-mRNA-processing factor 19 OS=Homo sapiens GN=PRPF19 PE=1 SV=1	32674.6	38545.37	35609.98	91805.8	101128.3	96467.04	129378	118637.4	124007.7

4																		
P00338	10	10	124.362	0.001413	2.522489	SKOV-3 48 hr Cu-Phen	SKOV-3 48 hr neg	L-lactate dehydrogenase A chain OS=Homo sapiens GN=LDHA PE=1 SV=2	3298881	3553064	3425973	8033008	9250951	8641979	3676601	3799056	3737829
P35579	4	4	210.1079	0.001422	1.532251	SKOV-3 48 hr Cu-Phen	SKOV-3 48 hr neg	Myosin-9 OS=Homo sapiens GN=MYH9 PE=1 SV=4	916234.7	929397.7	922816.2	138142.9	144654.3	141398.6	116972.7	122865.1	119918.9
O14818	2	2	44.12967	0.001473	2.048886	SKOV-3 48 hr neg	SKOV-3 48 hr Cu-Phen	Proteasome subunit alpha type-7 OS=Homo sapiens GN=PSMA7 PE=1 SV=1 [MASS=27887]	71689.81	74858.12	73273.96	34160.17	37365.5	35762.83	73124.48	67222.74	70173.61
Q9Y617	3	3	5.130463	0.001566	1.613932	SKOV-3 48 hr Cu-Phen	SKOV-3 48 hr neg	Phosphoserine aminotransferase OS=Homo sapiens GN=PSAT1 PE=1 SV=2 [MASS=40422]	210077.8	219055.2	214566.5	335065.8	357525.7	346295.8	210981.9	221251.4	216116.7
Q9NYF8	2	2	3.996529	0.001616	2.251225	SKOV-3 48 hr Cu-DPQ-Phen	SKOV-3 48 hr Cu-Phen	Bcl-2-associated transcription factor 1 OS=Homo sapiens GN=BCLAF1 PE=1 SV=2 [MASS=106121]	148093.5	163690.9	155892.2	68351.34	76639.59	72495.46	164184.1	162223	163203.6
P22392	2	2	62.38913	0.001638	1.927317	SKOV-3 48 hr Cu-Phen	SKOV-3 48 hr neg	Nucleoside diphosphate kinase B OS=Homo sapiens GN=NME2 PE=1 SV=1	281765.2	273103.4	277434.3	564296.6	505111.2	534703.9	458966.7	461654.6	460310.7
P15531	2	2	3.176337	0.001855	1.965457	SKOV-3 48 hr Cu-DPQ-Phen	SKOV-3 48 hr neg	Nucleoside diphosphate kinase A OS=Homo sapiens GN=NME1 PE=1 SV=1	81061.51	82416.43	81738.97	149862.9	168931.8	159397.3	165586.6	155722.3	160654.4
Q99733	2	2	103.12	0.001946	1.577429	SKOV-3 48 hr Cu-DPQ-Phen	SKOV-3 48 hr Cu-Phen	Nucleosome assembly protein 1-like 4 OS=Homo sapiens GN=NAP1L4 PE=1 SV=1	177779	183539.4	180659.2	112289.5	122311.3	117300.4	185633.5	184432.6	185033.1
Q13885	14	14	463.9918	0.001973	1.639589	SKOV-3 48 hr Cu-Phen	SKOV-3 48 hr neg	Tubulin beta-2A chain OS=Homo sapiens GN=TUBB2A PE=1 SV=1 [MASS=49907]	11833434	12233372	12033403	19170445	20289236	19729840	13833492	14705438	14269465
P30153	4	4	67.32709	0.002024	1.961934	SKOV-3 48 hr Cu-Phen	SKOV-3 48 hr Cu-DPQ-Phen	Serine/threonine-protein phosphatase 2A 65 kDa regulatory subunit A alpha isoform OS=Homo sapiens GN=PPP2R1A PE=1 SV=4	733807.2	793177.7	763492.4	110226.6	116499.3	113362.9	599840.7	555783.5	577812.1
P16402	3	3	149.5883	0.002061	1.901412	SKOV-3 48 hr neg	SKOV-3 48 hr Cu-Phen	Histone H1.3 OS=Homo sapiens GN=HIST1H1D PE=1 SV=2	899373.1	998196	948784.5	481517.8	516461.1	498989.5	950108.5	910636.3	930372.4
P31150	2	2	44.42941	0.002076	3.656288	SKOV-3 48 hr Cu-Phen	SKOV-3 48 hr neg	Rab GDP dissociation inhibitor alpha OS=Homo sapiens GN=GDI1 PE=1 SV=2	113018.5	101269.8	107144.1	350726	432773.6	391749.8	236912.3	236528	236720.1
O00764	3	3	8.540829	0.002139	1.620236	SKOV-3 48 hr Cu-Phen	SKOV-3 48 hr Cu-DPQ-Phen	Pyridoxal kinase OS=Homo sapiens GN=PDXK PE=1 SV=1	761144.6	817353.2	789248.9	980409.2	1014700	997554.7	603346	628023.3	615684.7
Q13151	2	2	53.19447	0.002175	1.967653	SKOV-3 48 hr Cu-DPQ-Phen	SKOV-3 48 hr Cu-Phen	Heterogeneous nuclear ribonucleoprotein A0 OS=Homo sapiens GN=HNRNPA0 PE=1 SV=1 [MASS=30840]	251815.6	268968.8	260392.2	131862.7	146160.2	139011.5	282757.4	264295.3	273526.3
Q92841	2	2	76.89421	0.002393	1.736315	SKOV-3 48 hr neg	SKOV-3 48 hr Cu-Phen	Probable ATP-dependent RNA helicase DDX17 OS=Homo sapiens GN=DDX17 PE=1 SV=2 [MASS=80272]	388444.8	420576.9	404510.9	226982.5	238959.1	232970.8	394326.1	368976.8	381651.5

Q9H910	2	2	5.553971	0.002396	1.812396	SKOV-3 48 hr Cu-Phen	SKOV-3 48 hr Cu-DPQ-Phen	Hematological and neurological expressed 1-like protein OS=Homo sapiens GN=HN1L PE=1 SV=1 [MASS=20063]	737622.5	810567.8	774095.2	120828 1	130241 5	125534 8	694822.4	690469	692645.7
O14979	2	2	4.901844	0.002453	4.157707	SKOV-3 48 hr neg	SKOV-3 48 hr Cu-Phen	Heterogeneous nuclear ribonucleoprotein D-like OS=Homo sapiens GN=HNRNPDL PE=1 SV=3 [MASS=46437]	287657.5	293022.3	290339.9	597 16. 11	799 47. 36	698 31. 74	220653.4	217200.6	218927
P62826	3	3	6.740623	0.002456	1.595161	SKOV-3 48 hr neg	SKOV-3 48 hr Cu-Phen	GTP-binding nuclear protein Ran OS=Homo sapiens GN=RAN PE=1 SV=3	289837.8	274034	281935.9	169629	183859.9	176744.4	265866.4	266379.8	266123.1
Q9UKV3	3	3	3.087448	0.002477	2.132351	SKOV-3 48 hr Cu-DPQ-Phen	SKOV-3 48 hr Cu-Phen	Apoptotic chromatin condensation inducer in the nucleus OS=Homo sapiens GN=ACIN1 PE=1 SV=2	625 59. 08	672 51. 24	649 05. 16	353 28. 97	399 61. 42	376 45. 2	782 88. 4	822 57. 13	802 72. 77
P46821	2	2	4.501382	0.002499	1.558454	SKOV-3 48 hr Cu-Phen	SKOV-3 48 hr neg	Microtubule-associated protein 1B OS=Homo sapiens GN=MAP1B PE=1 SV=2 [MASS=270632]	244110.9	261398.7	252754.8	406383.5	381430.1	393906.8	260445.1	265361.2	262903.1
P43243	2	2	76.73094	0.002531	2.202025	SKOV-3 48 hr Cu-DPQ-Phen	SKOV-3 48 hr Cu-Phen	Matrin-3 OS=Homo sapiens GN=MATR3 PE=1 SV=2 [MASS=94623]	234724.4	250252.7	242488.5	102959.7	118478.3	110719	254393.4	233218.5	243806
P06733	11	11	205.5786	0.002675	1.544463	SKOV-3 48 hr Cu-Phen	SKOV-3 48 hr Cu-DPQ-Phen	Alpha-enolase OS=Homo sapiens GN=ENO1 PE=1 SV=2	585941 2	585376 5	585658 9	736144 6	798358 8	767251 7	489075 5	504476 0	496775 8
P17844	4	4	57.53803	0.002831	1.875219	SKOV-3 48 hr neg	SKOV-3 48 hr Cu-Phen	Probable ATP-dependent RNA helicase DDX5 OS=Homo sapiens GN=DDX5 PE=1 SV=1 [MASS=69148]	290805.1	286478.2	288641.6	145028.2	162820.3	153924.3	243580.3	260182	251881.2
P49327	2	2	2.334169	0.002863	1.942459	SKOV-3 48 hr neg	SKOV-3 48 hr Cu-Phen	Fatty acid synthase OS=Homo sapiens GN=FASN PE=1 SV=3 [MASS=273425]	364 00. 3	373 57. 28	368 78. 79	760 53. 09	672 17. 98	716 35. 53	506 96. 37	483 76. 77	495 36. 57
P19 40	5	5	68.38202	0.002927	1.988385	SKOV-3 48 hr neg	SKOV-3 48 hr Cu-Phen	Polyadenylate-binding protein 1 OS=Homo sapiens GN=PABPC1 PE=1 SV=2	404967.1	402371	403669	197461.2	208565.8	203013.5	314526.8	359928.7	337227.8
Q14011	2	2	6.478024	0.003008	1.9459	SKOV-3 48 hr neg	SKOV-3 48 hr Cu-Phen	Cold-inducible RNA-binding protein OS=Homo sapiens GN=CIRBP PE=1 SV=1 [MASS=18648]	129441 7	134973 1	132207 4	633153 .1	725677 .1	679415 .1	121209 8	116505 1	118857 5
P09651	5	5	126.7105	0.003156	2.939622	SKOV-3 48 hr Cu-DPQ-Phen	SKOV-3 48 hr Cu-Phen	Heterogeneous nuclear ribonucleoprotein A1 OS=Homo sapiens GN=HNRNPA1 PE=1 SV=5	108116 4	106166 6	107141 5	571494	501345 .6	536419 .8	172366 9	143007 4	157687 1
Q14764	2	2	3.808239	0.003307	1.714394	SKOV-3 48 hr Cu-Phen	SKOV-3 48 hr Cu-DPQ-Phen	Major vault protein OS=Homo sapiens GN=MVP PE=1 SV=4	538019.2	552174.6	545096.9	669016.4	726396.5	697706.5	391515.8	422423.6	406969.7
P12814	3	3	63.89795	0.003309	2.637703	SKOV-3 48 hr Cu-Phen	SKOV-3 48 hr neg	Alpha-actinin-1 OS=Homo sapiens GN=ACTN1 PE=1 SV=2	325230.7	306908.3	316069.5	884930.8	782038.9	833484.8	651235.6	775258.2	713246.9
P68104	1	1	2.16072	0.003367	4.689 89	SKOV-3 48 hr neg	SKOV-3 48 hr Cu-Phen	Elongation factor 1-alpha 1 OS=Homo sapiens GN=EEF1A1 PE=1 SV=1	854594.9	848619.3	851607.1	211554.6	151612.6	181583.6	374432.6	384759.1	379595.9
Q969G5	2	2	3.261124	0.003455	1.646687	SKOV-3 48 hr Cu-Phen	SKOV-3 48 hr Cu-DPQ-Phen	Protein kinase C delta-binding protein OS=Homo sapiens GN=PRKCDBP PE=1 SV=3 [MASS=27701]	104207.5	100641.5	102424.5	128496.6	139169.1	133832.9	838 63. 75	786 84. 3	812 74. 02

Q9Y3C0	2	2	3.667238	0.003534	1.511682	SKOV-3 48 hr Cu-Phen	SKOV-3 48 hr Cu-DPQ-Phen	WASH complex subunit CCDC53 OS=Homo sapiens GN=CCDC53 PE=1 SV=1	145803.7	152495.2	149149.5	160019	168798	164408.5	105316.4	112200.9	108758.7
Q15417	2	2	2.629979	0.003543	2.419772	SKOV-3 48 hr Cu-DPQ-Phen	SKOV-3 48 hr neg	Calponin-3 OS=Homo sapiens GN=CNN3 PE=1 SV=1 [MASS=36413]	89462.53	82756.32	86109.42	176607.3	161285.3	168946.3	191573.6	225156.8	208365.2
P06703	3	3	49.05977	0.003694	1.772696	SKOV-3 48 hr neg	SKOV-3 48 hr Cu-Phen	Protein S100-A6 OS=Homo sapiens GN=S100A6 PE=1 SV=1 [MASS=10180]	543523.9	481122.9	512323.4	279315	298701.2	289008.1	492058.6	509057	500557.8
P19338	4	4	439.8871	0.003696	1.654648	SKOV-3 48 hr neg	SKOV-3 48 hr Cu-Phen	Nucleolin OS=Homo sapiens GN=NCL PE=1 SV=3 [MASS=76614]	3077514	3420170	3248842	1927949	1998979	1963464	2633449	2623018	2628234
P49588	2	2	58.11334	0.003742	1.762044	SKOV-3 48 hr Cu-Phen	SKOV-3 48 hr Cu-DPQ-Phen	Alanine--tRNA ligase, cytoplasmic OS=Homo sapiens GN=AARS PE=1 SV=2 [MASS=106810]	486420	537660.2	512040.1	782023.8	844126.6	813075.2	450897.5	471979.8	461438.7
Q9BUF5	5	4	406.0359	0.003767	1.564868	SKOV-3 48 hr Cu-Phen	SKOV-3 48 hr Cu-DPQ-Phen	Tubulin beta-6 chain OS=Homo sapiens GN=TUBB6 PE=1 SV=1 [MASS=49857]	1728111	1624720	1676415	2505061	2719516	2612288	1627086	1711582	1669334
O00571	4	4	49.0445	0.003934	1.957075	SKOV-3 48 hr neg	SKOV-3 48 hr Cu-Phen	ATP-dependent RNA helicase DDX3X OS=Homo sapiens GN=DDX3X PE=1 SV=3	237126.9	208926	223026.4	120498.3	107419.9	113959.1	215097.5	219376.2	217236.9
Q15424	2	2	2.037627	0.003959	1.737865	SKOV-3 48 hr neg	SKOV-3 48 hr Cu-Phen	Scaffold attachment factor B1 OS=Homo sapiens GN=SAFB PE=1 SV=4	99266.85	90092.79	94679.82	55531	53430.06	54480.53	86309.39	79786.13	83047.76
P22314	2	2	168.46	0.004573	1.587489	SKOV-3 48 hr neg	SKOV-3 48 hr Cu-Phen	Ubiquitin-like modifier-activating enzyme 1 OS=Homo sapiens GN=UBA1 PE=1 SV=3 [MASS=117848]	444235.7	491649.8	467942.7	723387.9	762319.7	742853.8	498079.5	513136.4	505607.9
P61313	2	2	47.26898	0.004635	1.836966	SKOV-3 48 hr neg	SKOV-3 48 hr Cu-Phen	60S ribosomal protein L15 OS=Homo sapiens GN=RPL15 PE=1 SV=2 [MASS=24146]	93197.6	101635.3	97416.46	50499.15	55563.19	53031.17	66386.49	71080.3	68733.39
P46060	2	2	45.91207	0.005097	1.70412	SKOV-3 48 hr neg	SKOV-3 48 hr Cu-Phen	Ran GTPase-activating protein 1 OS=Homo sapiens GN=RANGAP1 PE=1 SV=1 [MASS=63542]	68515.01	74634.96	71574.98	40521.73	43480.57	42001.15	71194.12	64818.47	68006.29
P62805	2	2	163.39	0.005859	1.779491	SKOV-3 48 hr neg	SKOV-3 48 hr Cu-DPQ-Phen	Histone H4 OS=Homo sapiens GN=HIST1H4A PE=1 SV=2 [MASS=11367]	841427.8	731999.7	786713.8	574999.3	556777.3	565888.3	451584.5	432616.1	442100.3
O00151	2	2	4.229351	0.005868	1.621996	SKOV-3 48 hr Cu-Phen	SKOV-3 48 hr Cu-DPQ-Phen	PDZ and LIM domain protein 1 OS=Homo sapiens GN=PDLIM1 PE=1 SV=4	356611.9	382506.9	369559.4	522819	471918	497368.5	303151.1	310128.5	306639.8
P50995	2	2	47.61123	0.006297	1.552668	SKOV-3 48 hr Cu-Phen	SKOV-3 48 hr Cu-DPQ-Phen	Annexin A11 OS=Homo sapiens GN=ANXA11 PE=1 SV=1	173202.3	181642.6	177422.4	193817.7	191381.8	192599.8	131148.1	116938.9	124043.5
Q8IVF2	2	2	3.434687	0.006302	2.394165	SKOV-3 48 hr Cu-Phen	SKOV-3 48 hr Cu-DPQ-Phen	Protein AHNAK2 OS=Homo sapiens GN=AHNAK2 PE=1 SV=2 [MASS=616625]	128939.5	152750.5	140845	192070.5	186181.2	189125.9	72591.42	85397.6	78994.51
P60900	2	2	88.65466	0.006704	1.576345	SKOV-3 48 hr Cu-DPQ-Phen	SKOV-3 48 hr Cu-Phen	Proteasome subunit alpha type-6 OS=Homo sapiens GN=PSMA6 PE=1 SV=1	554696.6	579675.9	567186.2	357275.9	405868.9	381572.4	599764.4	603214.9	601489.6

O15460	2	2	41.70324	0.006999	13.75253	SKOV-3 48 hr Cu-Phen	SKOV-3 48 hr neg	Prolyl 4-hydroxylase subunit alpha-2 OS=Homo sapiens GN=P4HA2 PE=1 SV=1 [MASS=60902]	1582.445	3237.64	2410.043	33963.17	32325.21	33144.19	3681.511	2523.759	3102.635
P32320	4	4	13.55332	0.008685	1.603737	SKOV-3 48 hr Cu-Phen	SKOV-3 48 hr Cu-DPQ-Phen	Cytidine deaminase OS=Homo sapiens GN=CDA PE=1 SV=2 [MASS=16185]	1331637	1382996	1357317	1853686	1875132	1864409	1082386	1242696	1162541
P33993	2	2	3.752781	0.008946	1.772795	SKOV-3 48 hr neg	SKOV-3 48 hr Cu-Phen	DNA replication licensing factor MCM7 OS=Homo sapiens GN=MCM7 PE=1 SV=4 [MASS=81307]	47015.9	41130.93	44073.41	23481.84	26240.11	24860.98	36567.67	37654.77	37111.22
Q14847	3	3	66.37567	0.009699	1.873618	SKOV-3 48 hr Cu-DPQ-Phen	SKOV-3 48 hr Cu-Phen	LIM and SH3 domain protein 1 OS=Homo sapiens GN=LASP1 PE=1 SV=2	308842.4	359004.2	333923.3	191196.5	216707.2	203951.8	393286.8	370968.9	382127.8
P62888	4	4	9.635822	0.010949	1.570761	SKOV-3 48 hr Cu-DPQ-Phen	SKOV-3 48 hr Cu-Phen	60S ribosomal protein L30 OS=Homo sapiens GN=RPL30 PE=1 SV=2 [MASS=12784]	361315.6	375455.7	368385.7	238370	276483	257426.5	408437.2	400273.6	404355.4
Q8NBS9	2	2	3.005022	0.01098	1.639801	SKOV-3 48 hr Cu-Phen	SKOV-3 48 hr Cu-DPQ-Phen	Thioredoxin domain-containing protein 5 OS=Homo sapiens GN=TXNDC5 PE=1 SV=2	52332.09	48408.88	50370.49	69653.69	66512.74	68083.21	38751.94	44286.43	41519.19
P05552	2	2	2.450166	0.011265	1.689804	SKOV-3 48 hr Cu-DPQ-Phen	SKOV-3 48 hr Cu-Phen	Vasodilator-stimulated phosphoprotein OS=Homo sapiens GN=VASP PE=1 SV=3 [MASS=39829]	77740.89	71235.24	74488.07	56473.88	58870.71	57672.3	104251.5	90658.26	97454.88
P63241	2	2	48.12928	0.011605	3.275396	SKOV-3 48 hr Cu-DPQ-Phen	SKOV-3 48 hr Cu-Phen	Eukaryotic translation initiation factor 5A-1 OS=Homo sapiens GN=EIF5A PE=1 SV=2 [MASS=16832]	125385.7	120463.1	122924.4	47568.86	31922.89	39745.88	142919.4	117447.5	130183.5
P17858	1	1	1.611707	0.011964	3.120284	SKOV-3 48 hr Cu-Phen	SKOV-3 48 hr neg	ATP-dependent 6-phosphofructokinase, liver type OS=Homo sapiens GN=PFKL PE=1 SV=6	5818.881	8683.719	7251.3	21777.93	23474.3	22626.11	8518.75	8946.387	8732.569
Q92499	3	3	3.186867	0.013039	2.068442	SKOV-3 48 hr Cu-DPQ-Phen	SKOV-3 48 hr Cu-Phen	ATP-dependent RNA helicase DDX1 OS=Homo sapiens GN=DDX1 PE=1 SV=2 [MASS=82432]	43498.13	52499.98	47999.05	30560.17	27616.73	29088.45	64306	56029.56	60167.78
Q01813	2	2	111.62	0.013061	2.029268	SKOV-3 48 hr Cu-Phen	SKOV-3 48 hr neg	ATP-dependent 6-phosphofructokinase, platelet type OS=Homo sapiens GN=PFKP PE=1 SV=2 [MASS=85596]	110639.5	137027.1	123833.3	230547.6	272034.2	251290.9	129549.7	130790.9	130170.3
P40121	2	2	4.675643	0.013111	1.659966	SKOV-3 48 hr Cu-Phen	SKOV-3 48 hr Cu-DPQ-Phen	Macrophage-capping protein OS=Homo sapiens GN=CAPG PE=1 SV=2 [MASS=38498]	532430.5	628026	580228.3	830443.3	875919.5	853181.4	499888.9	528061.5	513975.2
P63104	3	3	81.12653	0.014142	1.515608	SKOV-3 48 hr neg	SKOV-3 48 hr Cu-Phen	14-3-3 protein zeta/delta OS=Homo sapiens GN=YWHAZ PE=1 SV=1	1065862	1101499	1083680	662539.9	767487.2	715013.6	965107.2	949877	957492.1
P83916	1	1	1.577531	0.015142	2.212397	SKOV-3 48 hr neg	SKOV-3 48 hr Cu-Phen	Chromobox protein homolog 1 OS=Homo sapiens GN=CBX1 PE=1 SV=1 [MASS=21418]	38597.02	47947.42	43272.22	18085.32	21032.63	19558.98	35230.43	41246	38238.22
Q14103	2	2	4.69943	0.015928	1.996752	SKOV-3 48 hr neg	SKOV-3 48 hr Cu-Phen	Heterogeneous nuclear ribonucleoprotein D0 OS=Homo sapiens GN=HNRNPD PE=1 SV=1	253326.1	194074.2	223700.1	112690.6	111373.3	112032	201723.7	194579.9	198151.8
O00469	2	2	2.963435	0.018776	4.42614	SKOV-3 48 hr Cu-Phen	SKOV-3 48 hr neg	Procollagen-lysine,2-oxoglutarate 5-dioxygenase 2 OS=Homo sapiens GN=PLOD2 PE=1 SV=2	48653.33	29349.73	39001.53	169157	176095.4	172626.2	57934.25	39348.53	48641.39

P21796	4	4	47.01698	0.020335	1.549621	SKOV-3 48 hr neg	SKOV-3 48 hr Cu-DPQ-Phen	Voltage-dependent anion-selective channel protein 1 OS=Homo sapiens GN=VDAC1 PE=1 SV=2	706723	605356.4	656039.7	459757	407355.4	433556.2	425001.3	421708.8	423355.1
P18124	2	2	4.104121	0.021194	2.065053	SKOV-3 48 hr Cu-DPQ-Phen	SKOV-3 48 hr Cu-Phen	60S ribosomal protein L7 OS=Homo sapiens GN=RPL7 PE=1 SV=1	124138.9	158579.5	141359.2	79130.06	87978.05	83554.05	185094.8	159992.3	172543.5
Q8WUW1	2	2	44.31034	0.024086	1.575044	SKOV-3 48 hr Cu-Phen	SKOV-3 48 hr Cu-DPQ-Phen	Protein BRICK1 OS=Homo sapiens GN=BRK1 PE=1 SV=1 [MASS=8745]	197059.8	204301.3	200680.5	332728.8	275635.1	304182	202114	184138	193126
P56537	2	2	51.45122	0.02607	1.642589	SKOV-3 48 hr neg	SKOV-3 48 hr Cu-Phen	Eukaryotic translation initiation factor 6 OS=Homo sapiens GN=EIF6 PE=1 SV=1 [MASS=26599]	157807.2	175612.6	166709.9	108241.4	94742.94	101492.2	136118	118774.9	127446.4
P61160	2	2	5.038398	0.028157	1.640296	SKOV-3 48 hr Cu-Phen	SKOV-3 48 hr Cu-DPQ-Phen	Actin-related protein 2 OS=Homo sapiens GN=ACTR2 PE=1 SV=1 [MASS=44760]	148760.8	145061.3	146911	194814.2	242758.1	218786.1	128320.4	138443.8	133382.1
P05388	2	2	4.761885	0.033084	1.597382	SKOV-3 48 hr neg	SKOV-3 48 hr Cu-Phen	60S acidic ribosomal protein P0 OS=Homo sapiens GN=RPLP0 PE=1 SV=1	376956	472577.2	424766.6	275422.6	256405.8	265914.2	411529.4	390232.1	400880.8
Q14980	2	2	92.46	0.033343	1.590793	SKOV-3 48 hr Cu-Phen	SKOV-3 48 hr Cu-DPQ-Phen	Nuclear mitotic apparatus protein 1 OS=Homo sapiens GN=NUMA1 PE=1 SV=2 [MASS=238258]	395453.4	405155	400304.2	495381.1	555365	525373.1	362019.4	298497.9	330258.7
Q9UBR2	2	2	4.212255	0.035868	2.962436	SKOV-3 48 hr Cu-Phen	SKOV-3 48 hr neg	Cathepsin Z OS=Homo sapiens GN=CTSZ PE=1 SV=1 [MASS=33868]	40403.6	50144.75	45274.17	156203.6	112040.1	134121.9	61575.33	39785.02	50680.17
P23526	2	2	73.98219	0.036493	1.609993	SKOV-3 48 hr Cu-Phen	SKOV-3 48 hr Cu-DPQ-Phen	Adenosylhomocysteinase OS=Homo sapiens GN=AHCY PE=1 SV=4 [MASS=47716]	607018.1	492183	549600.6	785099.7	793415.2	789257.5	457482	523004.5	490243.2
P39023	2	2	67.48181	0.037758	1.795638	SKOV-3 48 hr Cu-DPQ-Phen	SKOV-3 48 hr Cu-Phen	60S ribosomal protein L3 OS=Homo sapiens GN=RPL3 PE=1 SV=2 [MASS=46109]	80250.32	96717.21	88483.77	49433.8	63411.17	56422.49	102630	99998.77	101314.4
P35232	2	2	3.492512	0.045832	1.967714	SKOV-3 48 hr Cu-Phen	SKOV-3 48 hr Cu-DPQ-Phen	Prohibitin OS=Homo sapiens GN=PHB PE=1 SV=1 [MASS=29804]	313797.2	364578.4	339187.8	306102.8	418930.8	362516.8	202828.6	165636.4	184232.5